U-004-304 .16

5659

REMEDIAL INVESTIGATION REPORT FOR OPERABLE UNIT 2 VOLUME 2 OF 6 OVERSIZED FIGURES & APPENDIX A JUNE 1994

06/15/94

DOE-FN 394 REPORT

EPA

REMEDIAL INVESTIGATION REPORT FOR OPERABLE UNIT 2

FERNALD ENVIRONMENTAL MANAGEMENT PROJECT
FERNALD, OHIO

REMEDIAL INVESTIGATION AND FEASIBILITY STUDY

VOLUME 2 OF 6
OVERSIZED FIGURES AND APPENDIX A

JUNE 1994

U.S. DEPARTMENT OF ENERGY
FERNALD FIELD OFFICE

DRAFT

TABLE OF CONTENTS
APPENDIX A

List of Tables . . . . . A-v

List of Figures . . . . . A-xii

List of Acronyms . . . . . A-xvii

A.1.0 Surface Water Modeling A-1-1

A.1.1 Introduction A-1-1

A.1.2 Conceptual Model A-1-1

A.1.3 Technical Approach A-1-4

A.1.4 Surface Water Model Description A-1-7

A.1.4.1 Model Assumptions A-1-8

A.1.4.2 Calculation of Soil Loss from Runoff A-1-8

A.1.4.3 Calculation of Constituent Partitioning and Loading A-1-9

A.1.5 Results of Surface Water Runoff Modeling A-1-15

A.1.5.1 Solid Waste Landfill A-1-15

A.1.5.2 Lime Sludge Ponds A-1-19

A.1.5.3 Inactive Flyash Pile A-1-19

A.1.5.4 South Field A-1-23

A.1.5.5 Active Flyash Pile A-1-28

A.1.5.6 Combined Modeling Results A-1-32

A.1.6 Uncertainties in the Surface Water Model A-1-35

A.1.7 Loading to the Great Miami Aquifer A-1-37

A.1.7.1 Screening Procedure A-1-37

A.1.7.2 Solid Waste Landfill A-1-39

A.1.7.3 Inactive Flyash Pile and South Field A-1-39

A.1.7.4 Active Flyash Pile A-1-43

A.1.7.5 Combined Loading A-1-49

A.2.0 Groundwater Fate and Transport Modeling A-2-1

A.2.1 Introduction A-2-1

A.2.1.1 Technical Approach A-2-2

A.2.1.2 Approach to Screening and Modeling A-2-6

A.2.2 Hydrogeologic Setting A-2-7

TABLE OF CONTENTS
(Continued)

A.2.2.1 Geologic Setting A-2-7
A.2.2.2 Vadose Zone A-2-10
A.2.2.3 Great Miami Aquifer A-2-12
A.2.2.4 General Contaminant Hydrogeology at the FEMP A-2-13
A.2.3 Conceptual Model A-2-13
A.2.3.1 Solid Waste Landfill A-2-18
A.2.3.2 Lime Sludge Ponds A-2-18
A.2.3.3 Inactive Flyash Pile and South Field A-2-25
A.2.3.4 Active Flyash Pile A-2-31
A.2.4 Approach for Source Term Development A-2-31
A.2.4.1 Site-Specific Data A-2-31
A.2.4.2 Source Term Development A-2-34
A.2.4.3 Estimation of Leachate Concentrations A-2-36
A.2.4.4 Uncertainty in Estimating Leachate Compositions A-2-38
A.2.5 Parameters A-2-39
A.2.6 Constitutent Screening and Review - Vadose Zone Pathway A-2-45
A.2.6.1 Background Screening A-2-49
A.2.6.2 Toxicological Screening A-2-50
A.2.6.3 Vadoes Zone Model Toxicity Screening A-2-50
A.2.6.4 Great Miami Aquifer Dilution Screening A-2-51
A.2.7 Vadose Zone Modeling A-2-51
A.2.7.1 Estimating Infiltration Rates A-2-52
A.2.7.1.1 Description of HELP Model A-2-52
A.2.7.1.2 Infiltration Rate Results A-2-53
A.2.7.2 ODAST Description A-2-61
A.2.7.3 ODAST Modeling Results and Screening of CPCs A-2-65
A.2.8 Aquifer Modeling A-2-109
A.2.8.1 Background, Description, and Development of Model . . . A-2-109
A.2.8.2 SWIFT III Modeling A-2-121

000070

TABLE OF CONTENTS
(Continued)

A.2.8.2.1 Source Loading to the Great Miami Aquifer A-2-124

A.2.8.3 Results of SWIFT III Modeling A-2-126

A.2.8.3.1 Solid Waste Landfill A-2-126

A.2.8.3.2 Lime Sludge Ponds A-2-126

A.2.8.3.3 Inactive Flyash Pile/South Field A-2-130

A.2.8.3.4 Active Flyash A-2-147

A.2.8.3.5 Combined Impact of All Operable Unit 2 Subunits A-2-182

A.2.9 Modeling Results of Waste at Background Concentrations A-2-182

A.2.9.1 Solid Waste Landfill A-2-189

A.2.9.2 Lime Sludge Ponds A-2-189

A.2.9.3 Inactive Flyash Pile and South Field A-2-189

A.2.9.4 Active Flyash Pile A-2-193

A.2.10 Uncertainty in Modeling Results A-2-197

A.2.10.1 HELP Model A-2-200

A.2.10.2 ODAST Model A-2-206

A.2.10.3 SWIFT Model A-2-213

A.3.0 Air Transport Analysis A-3-1

A.3.1 Air Dispersion Modeling of Operable Unit 2 . . . . . A-3-1

A.3.2 Site Description of Operable Unit 2 . . . . . A-3-1

A.3.3 Conceptual Air Model Source Scenarios A-3-3

A.3.4 Air Dispersion Model A-3-4

A.3.5 Input Parameters A-3-5

TABLE OF CONTENTS
(Continued)

A.3.5.1 Meteorological Data A-3-5

A.3.5.2 Source Data A-3-9

A.3.5.3 Emission Rates A-3-20

A.3.5.4 Receptor Data A-3-28

A.3.6 Air Dispersion Modeling Results A-3-28

A.3.6.1 Current Scenario - Concentrations Estimations A-3-32

A.3.6.2 Current Scenario - Deposition Rate Estimations A-3-32

A.3.6.3 Future Scenario - Concentrations Estimations A-3-33

A.3.6.4 Future Scenario - Deposition Rate Estimations A-3-33

Attachment A.3-I A.3-I-1

Attachment A.3-II A.3-II-1

Attachment A.3-III A.3-III-1

References R-A-1

LIST OF TABLES

Table	Title	Page No.
A.1-1	Variables Used in the Surface Water Runoff Model	A-1-13
A.1-2A	Runoff Effluent and Sediment Loading to Surface Water From the Solid Waste Landfill	A-1-16
A.1-2B	Contaminant Loading to the Great Miami River From the Solid Waste Landfill	A-1-18
A.1-3A	Runoff Effluent and Sediment Loading to Surface Water From the Inactive Flyash Pile	A-1-20
A.1-3B	Contaminant Loading to the Great Miami River from the Inactive Flyash Pile	A-1-22
A.1-4A	Runoff Effluent and Sediment Loading From the South Field	A-1-24
A.1-4B	Contaminant Loading to the Great Miami River from the South Field	A-1-26
A.1-5A	Runoff Effluent and Sediment Loading From the Active Flyash Pile	A-1-29
A.1-5B	Contaminant Loading to the Great Miami River from the Active Flyash Pile	A-1-30
A.1-6	Comparison of Modeled Results to Measured Surface Water Concentrations in Storm Sewer Outfall Ditch	A-1-33
A.1-7	Impact of all Operable Unit 2 Submunits on Paddys Run and the Great Miami River	A-1-34
A.1-8	Comparison of Modeled Results to Measured Surface Water Concentrations in Paddys Run	A-1-36
A.1-9	Loading to the Great Miami Aquifer from Paddys Run and CPC Screening for Groundwater Modeling, Solid Waste Landfill	A-1-42
A.1-10A	Loading to the Great Miami Aquifer from Paddys Run and CPC Screening (First Step) for Groundwater Modeling, Inactive Flyash Pile/South Field	A-1-44
A.1-10B	CPC Screening For Groundwater Modeling Using Full SWIFT Cell Dilution Inactive Flyash Pile/South Field	A-1-45
A.1-11	Loading to the Great Miami Aquifer from the Storm Sewer Outfall Ditch and CPC Screening (First Step) for Groundwater Modeling, Active Flyash Pile	A-1-47
A.1-12	CPC Screening for Groundwater Modeling Using Full Swift Cell Dilution, Active Flyash Pile	A-1-48
A.1-13	Comparison of Great Miami Aquifer and Modeled Results from Surface Runoff Pathway, Active Flyash Pile	A-1-50

LIST OF TABLES
(Continued)

Table	Title	Page No.
A.1-14	Summary of Constituents of Concern for Groundwater from Surface Water Pathway	A-1-51
A.2-1	Physical Parameters for the SWIFT III Cells Impacted by the Solid Waste Landfill	A-2-23
A.2-2	Physical Parameters for the SWIFT III Grid Cells Impacted by the Lime Sludge Ponds	A-2-24
A.2-3	Physical Parameters for the SWIFT III Grid Cells Impacted by the Inactive Flyash Pile and South Field	A-2-27
A.2-4	Physical Parameters for the SWIFT III Grid Cells Impacted by the Active Flyash Pile	A-2-33
A.2-5	Summary of Source Areas and Physical Parameters for Operable Unit 2 Aquifer Model	A-2-35
A.2-6	Media Parameters for Vadose Zone Model	A-2-40
A.2-7	Vadose Zone Model Input Parameters	A-2-42
A.2-8	Distribution of Coefficients, K_{ow} and Decay Half Lives for Constituents of Potential Concern	A-2-47
A.2-9	Media Parameters for HELP Model	A-2-54
A.2-10	HELP Model Results for the Solid Waste Landfill	A-2-55
A.2-11	HELP Model Results for the Lime Sludge Pond	A-2-56
A.2-12	HELP Model Results for the Inactive Flyash Pile and South Field	A-2-57
A.2-13	HELP Model Results for the Active Flyash Pile	A-2-60
A.2-14	List of Constituents of Potential Concern for Vadose Zone Modeling for the Solid Waste Landfill	A-2-66
A.2-15	Retardation Factors for the Solid Waste Landfill	A-2-67
A.2-16	Source Characterization and Screening Summary for Constituents of Potential Concern for the Solid Waste Landfill	A-2-69
A.2-17	Perched Water Source Concentrations and Masses for the Vadose Zone Modeling, Solid Waste Landfill	A-2-72
A.2-18	Comparison of Great Miami Aquifer Water and Background for Constituents of Potential Concern in Groundwater	A-2-74
A.2-19	Summary of Constituents of Potential Concern and Source Pathways for the Solid Waste Landfill	A-2-75
A.2-20	Predicted Perched Water Concentrations and Screening Summary for Constituents of Potential Concern, Solid Waste Landfill	A-2-76

LIST OF TABLES
(Continued)

Table	Title	Page No.
A.2-21	Solid Waste Landfill Comparison of Perched Water and Background for Constituents of Potential Concern in Perched Water	A-2-80
A.2-22	List of Constituents of Potential Concern for Vadose Zone Modeling for the Lime Sludge Ponds	A-2-81
A.2-23	Retardation Factors for the Lime Sludge Ponds	A-2-82
A.2-24	Source Characterization and Screening Summary of Constituents of Potential Concern Lime Sludge Ponds	A-2-84
A.2-25	Perched Water Zone Concentrations and Masses for the Vadose Zone Modeling, Lime Sludge Ponds	A-2-86
A.2-26	Summary of Constituents of Potential Concern and Source Pathways for the Lime Sludge Ponds	A-2-88
A.2-27	Lime Sludge Ponds Comparison of Great Miami Aquifer Water and Background for Constituents of Potential Concern in Groundwater	A-2-89
A.2-28	Predicted Perched Water Concentrations and Screening Summary for Constituents of Potential Concern, Lime Sludge Ponds	A-2-90
A.2-29	Lime Sludge Ponds Comparison of Perched Water and Background for Potential Constituents of Concern in Perched Water	A-2-92
A.2-30	List of Constituents of Potential Concern for Vadose Zone Modeling for the Inactive Flyash Pile and South Field	A-2-93
A.2-31	Retardation Factors for the Inactive Flyash Pile and South Field	A-2-95
A.2-32	Source Characterization and Screening Summary for Constituents of Potential Concern for the Inactive Flyash Pile and South Field	A-2-97
A.2-33	Perched Water Concentrations and Masses for the Vadose Zone Modeling, Inactive Flyash Pile and South Field	A-2-102
A.2-34	Seep Water Source Concentrations and Masses for the Vadose Zone Modeling, Inactive Flyash Pile and South Field	A-2-103
A.2-35	Flow Rates for Seeps and Perched Water Subsurface Seeps Inactive Flyash Pile and South Field	A-2-104
A.2-36	Screening for Constituents of Potential Concern After Dilution in the Great Miami Aquifer for the Inactive Flyash Pile and South Field	A-2-105
A.2-37	Summary of Constituents of Potential Concern and Source Pathways for the Inactive Flyash Pile and South Field	A-2-106
A.2-38	Comparison of Great Miami Aquifer Water and Background for Constituents of Potential Concern in Groundwater South Field, Inactive Flyash Pile, and Active Flyash Pile	A-2-108

LIST OF TABLES
(Continued)

Table	Title	Page No.
A.2-39	List of Constituents of Potential Concern for Vadose Zone Modeling for the Active Flyash Pile	A-2-110
A.2-40	Retardation Factors for the Active Flyash Pile	A-2-111
A.2-41	Source Characterization and Screening Summary of Constituents of Potential Concern Active Flyash Pile	A-2-112
A.2-42	Perched Water Concentration and Masses for the Vadose Zone Modeling, Active Flyash Pile	A-2-114
A.2-43	Screening for Constituents of Potential Concern After Dilution in the Great Miami Aquifer for the Active Flyash Pile	A-2-115
A.2-44	Summary of Constituents of Potential Concern and Source Pathways for the Active Flyash Pile	A-2-116
A.2-45	Distribution Coeffiecients and Decay Factors Used in the SWIFT III Model	A-2-122
A.2-46	Parameters Used in the SWIFT III Model	A-2-123
A.2-47	Summary of Constituents of Potential Concern for Surface Water Runoff Loading to the Great Miami Aquifer From the Inactive Flyash Pile and the South Field	A-2-125
A.2-48	Summary of Constituents of Potential Concern for Surface Water Runoff Loading to the Great Miami Aquifer from the Active Flyash Pile	A-2-128
A.2-49	Summary of SWIFT Modeling Results for the Solid Waste Landfill	A-2-129
A.2-50	Summary of SWIFT Modeling Results for the Lime Sludge Ponds	A-2-132
A.2-51	Summary of SWIFT Modeling Results for the Inactive Flyash Pile and South Field	A-2-144
A.2-52	Summary of SWIFT Modeling Results at the Time and Location of the U-238 Maximum Concentration for the Inactive Flyash Pile and South Field	A-2-146
A.2-53	Summary of SWIFT Modeling Results for the Active Flyash Pile	A-2-162
A.2-54	Summary of SWIFT Modeling Results at the Time and Location of the U-238 Maximum Concentration for the Active Flyash Pile	A-2-187
A.2-54A	Summary of SWIFT Modeling Results at the Time and Location of the U-238 Maximum Concentration for all Operable Unit 2 Subunits	A-2-188
A.2-55	Summary of Vadose Zone Modeling Results if Waste and Perched Water Concentrations Were at Background Levels, Solid Waste Landfill	A-2-190

LIST OF TABLES
(Continued)

Table	Title	Page No.
A.2-56	Summary of Vadose Zone Modeling Results if Waste and Perched Water Concentrations Were at Background Levels, Lime Sludge Ponds	A-2-191
A.2-57	Summary of Vadose Zone Modeling Results if Waste and Perched Water Concentrations Were at Background Levels, Inactive Flyash Pile and South Field	A-2-192
A.2-57A	Summary of the Impact to the Great Miami Aquifer If Waste and Perched Water are at Background Concentrations, Inactive Flyash Pile and South Field	A-2-194
A.2-58	Summary of Vadose Zone Modeling Results if Waste and Perched Water Concentrations Were at Background Levels, Active Flyash Pile	A-2-195
A.2-58A	Summary of the Impact to the Great Miami Aquifer if the Active Flyash Pile is at Background Concentration	A-2-198
A.2-59	Sensitivity of Calculated Infiltration by HELP Model to the SCS Runoff Curve Number	A-2-203
A.2-60	Sensitivity of Calculated Infiltration by HELP Model to the Hydraulic Conductivity of the Glacial Till	A-2-204
A.2-61	Sensitivity of the Calculated Infiltration by HELP Model to the Hydraulic Conductivity of Waste/Fill	A-2-205
A.2-62	Sensitivity of the Calculated Infiltration by HELP Model to the Hydraulic Conductivity of the Great Miami Aquifer	A-2-211
A.3-1	Dispersion Options Used in ISCLT Modeling of Operable Unit 2	A-3-6
A.3-2	Mixing Heights in Meters Used Operable Unit 2 ISCLT, Air Transport Modeling	A-3-7
A.3-3	Ambient Air Temperature in Degrees Kelvin Used in ISCLT Modeling	A-3-8
A.3-4	Particle Size Distributions for Operable Unit 2 Subunits	A-3-21
A.3-5	Particulate Matter Emission Rates Used in ISCLT2 Modeling	A-3-27
A.3-6	RAECOM Model Input Parameters and RN-222 Emission Rates	A-3-30
A.3-7	Discrete Receptors and Distance From Origin	A-3-31
A.3-8	Maximum Annual Concentrations and Locations of On-Subunit, On-Property, and Off-Property Receptors for Operable Unit 2 Subunits, Current Scenario	A-3-34
A.3-9	Maximum Annual Deposition Rates and Locations of On-Subunit, On-Property, and Off-Property Receptors for Operable Unit 2 Subunits, Current Scenario	A-3-35

LIST OF TABLES
(Continued)

Table	Title	Page No.
A.3-10	Maximum Annual Concentrations and Locations of On-Subunit, On-Property, and Off-Property Receptors for Operable Unit 2 Subunits, Future Scenario	A-3-36
A.3-11	Maximum Annual Deposition Rates and Locations of On-Subunit, On-Property, and Off-Property Receptors for Operable Unit 2 Subunits, Future Scenario	A-3-37
A.3-12	Maximum Concentrations ($\mu g/m^3$) at Sensitive Receptors Current Scenario Operable Unit 2 Subunits	A-3-38
A.3-13	Maximum Deposition Rates (g/m^2) at Sensitive Receptors Current Scenario Operable Unit 2 Subunits	A-3-39
A.3-14	Maximum Concentrations ($\mu g/m^3$) at Sensitive Receptors Future Scenario Operable Unit 2 Subunits	A-3-40
A.3-15	Maximum Deposition Rates (g/m^2) at Sensitive Receptors Future Scenario Operable Unit 2 Subunits	A-3-41
A.3-16	Preliminary Exposure Point Concentrations for the Active Flyash Pile	A-3-42
A.3-17	Preliminary Annual Exposure Point Deposition Rates for the Active Flyash Pile	A-3-43
A.3-18	Preliminary Maximum Concentrations from Air Dispersion Modeling South Field - Current Scenario	A-3-44
A.3-19	Preliminary Annual Deposition Rates From Air Dispersion Modeling South Field - Current Scenarios	A-3-45
A.3-20	Preliminary Maximum Concentrations From Air Dispersion Modeling South Field - Future Scenario	A-3-46
A.3-21	Preliminary Annual Deposition Rates From Air Dispersion Modeling South Field - Future Scenario	A-3-47
A.3-22	Preliminary Maximum Concentrations From Air Dispersion Modeling Inactive Flyash Pile - Current and Future Scenarios	A-3-48
A.3-23	Preliminary Maximum Deposition Rates From Air Dispersion Modeling Inactive Flyash Pile - Current and Future Scenarios	A-3-49
A.3-24	Preliminary Maximum Concentrations From Air Dispersion Modeling Solid Waste Landfill - Current Scenario	A-3-50
A.3-25	Preliminary Maximum Annual Deposition Rate From Air Dispersion Modeling Solid Waste Landfill - Current Scenarios	A-3-51
A.3-26	Preliminary Maximum Concentrations From Air Dispersion Modeling Solid Waste Landfill - Future Scenarios	A-3-52

LIST OF TABLES
(Continued)

Table	Title	Page No.
A.3-27	Preliminary Maximum Annual Deposition Rates From Air Dispersion Modeling - Solid Waste Landfill - Future Scenarios	A-3-53
A.3-28	Preliminary Maximum Concentrations From Air Dispersion Modeling Lime Sludge Ponds - Current and Future Scenarios	A-3-54
A.3-29	Preliminary Maximum Annual Deposition Rates From Air Dispersion Modeling - Lime Sludge Ponds - Current and Future Scenarios	A-3-55

LIST OF FIGURES

Figure	Title	Page No.
A.1-1	Conceptual Model of Surface Water Runoff	A-1-2
A.1-2	Surface Water to Groundwater Pathway Transport Modeling Diagram	A-1-5
A.1-3	Topography and Drainage Scenario of Solid Waste Landfill	A-1-10
A.1-4	Topography and Drainage Scenario for Inactive Flyash Pile and South Field	A-1-11
A.1-5	Topography and Drainage Scenario for Active Flyash Pile	A-1-12
A.1-6A	Surface Water Runoff Infiltration to the Great Miami Aquifer from the Solid Waste Landfill	A-1-40
A.1-6B	Surface Water Runoff Infiltration to the Great Miami Aquifer from the South Field and Flyash Piles	A-1-41
A.2-1	Overall Fate and Transport Modeling Framework	A-2-3
A.2-2	Constituent Transport Modeling Diagram	A-2-5
A.2-3	Approach for Screening and Incorporation of Monitoring Data into the Modeling Process	A-2-8
A.2-4	Conceptual Model of Loading to the Great Miami Aquifer and Contaminant Transport by Groundwater	A-2-15
A.2-5	Conceptual Vadose Zone Model	A-2-16
A.2-6	Extent of Waste and Modeled Swift Grid Cells, Solid Waste Landfill	A-2-19
A.2-7	Extent of Waste and Modeled Swift Grid Cells, Lime Sludge Ponds	A-2-20
A.2-8	Extent of Waste and Modeled Swift Grid Cells, South Field and Inactive Flyash Pile	A-2-21
A.2-9	Conceptual Model for Lateral Drainage Infiltrating to the Unsaturated Great Miami Aquifer	A-2-22
A.2-10	Conceptual Model for Perched Water Subsurface Seeps	A-2-26
A.2-11	Extent of Waste and Modeled Swift Grid Cells, Active Flyash Pile	A-2-32
A.2-12	Procedure for Estimating Leachate Concentrations	A-2-37
A.2-13	Potential Constituents of Concern Screening Diagram	A-2-46
A.2-14	Swift III Local Area Model Grid	A-2-118
A.2-17	Technetium-99 Loading to the Great Miami Aquifer from the Lime Sludge Pond	A-2-127
A.2-18	Projected Increase in Technetium-99 Concentration in Great Miami Aquifer after 30 Years Due to Loading from the Lime Sludge Ponds	A-2-131

000030

LIST OF FIGURES
(Continued)

Figure	Title	Page No.
A.2-19A	Location Map With Calibration Target and Flow Direction, Inactive Flyash Pile	A-2-134
A.2-19B	Projected Increase in Uranium-238 Concentration in Great Miami Aquifer at 40 Years Due to Loading From the Inactive Flyash Pile and South Field	A-2-135
A.2-20	Uranium-238 Loading to the Great Miami Aquifer from the Inactive Flyash Pile and South Field	A-2-136
A.2-21	Projected Increase in Uranium-238 Concentration in Great Miami Aquifer at 160 Years Due to Loading From the Inactive Flyash Pile and South Field	A-2-138
A.2-22	Projected Increase in Uranium-238 Concentration in Great Miami Aquifer At 220 Years Due to Loading From the Inactive Flyash Pile and South Field	A-2-139
A.2-23	Projected Increase in Uranium-238 Concentration in Great Miami Aquifer At 1000 Years Due to Loading From the Inactive Flyash Pile and South Field	A-2-140
A.2-24	U-234 vs. U-238 in Soil Samples, South Field and Flyash Piles	A-2-141
A.2-25	U-235/236 vs. U-238 in Soil Samples, South Field and Flyash Piles	A-2-142
A.2-26	U-238 vs. U-Total in Soil Samples, South Field and Inactive Flyash Pile	A-2-143
A.2-27	Neptunium-237 Loading to the Great Miami Aquifer from the Inactive Flyash Pile and South Field	A-2-148
A.2-28	Projected Increase in Meptunium-237 Concentration in the Great Miami Aquifer At 160 Years Due to Loading From the Inactive Flyash Pile and South Field	A-2-149
A.2-29	Projected Increase in Neptunium-237 Concentration in the Great Miami Aquifer At 220 Years Due to Loading From the Inactive Flyash Pile and South Field	A-2-150
A.2-30	Projected Increase in Neptunium-237 Concentration in the Great Miami Aquifer At 360 Years Due to Loading From the Inactive Flyash and South Field	A-2-151
A.2-31	Projected Increase in Neptunium-237 Concentration in the Great Miami Aquifer At 540 Years Due to Loading From the Inactive Flyash Pile and South Field	A-2-152

LIST OF FIGURES
(Continued)

Figure	Title	Page No.
A.2-32	Projected Increase in Neptunium-237 Concentration in the Great Miami Aquifer at 1000 Years DUe to Loading from the Inactive Flyash Pile and South Field	A-2-153
A.2-33	Technetium-99 Loading to the Great Miami Aquifer from the Inactive Flyash Pile and South Field	A-2-154
A.2-34	Projected Increase in Technetium-99 Concentration in the Great Miami Aquifer At 40 Years Due to Loading From the Inactive Flyash Pile and South Field	A-2-155
A.2-35	Projected Increase in Technetium-99 Concentration in the Great Miami Aquifer at 160 Years Due to Loading From the Inactive Flyash Pile and South Field	A-2-156
A.2-36	Projected Increase in Technetium-99 Concentration in Great Miami Aquifer at 220 Years Due to Loading From the Inactive Flyash Pile and South Field	A-2-157
A.2-37	Projected Increase in Technetium-99 Concentration in Great Miami Aquifer at 1000 Years Due to Loading From the Inactive Flyash Pile and the South Field	A-2-158
A.2-38	Lead Loading to the Great Miami Aquifer from the Inactive Flyash Pile and the South Field Area	A-2-159
A.2-39	Projected Increase in Lead Concentration in Great Miami Aquifer at 1000 Years Due to Loading From the Inactive Flyash Pile and South Field Area Subunuts	A-2-160
A.2-43	U-238 vs. U-Total in Soil Samples, Active Flyash Pile	A-2-161
A.2-44	Uranium-238 Loading to the Great Miami Aquifer From the Active Flyash Pile	A-2-165
A.2-45	Projected Increase in Uranium-238 Concentration in Great Miami Aquifer at 40 Years Loading From the Active Flyash Pile	A-2-166
A.2-46	Projected Increase in Uranium-238 Concentration in the Great Miami Aquifer at 100 Years Due to Loading From the Active Flyash Pile	A-2-167
A.2-47	Projected Increase in Uranium-238 Concentration in the Great Miami Aquifer at 120 Years Due to Loading From the Active Flyash Pile	A-2-168
A.2-48	Projected Increase in Uranium-238 Concentration in the Great Miami Aquifer at 1000 Years Due to Loading From the Active Flyash Pile	A-2-169
A.2-49	Neptunium-237 Loading to the Great Miami Aquifer From the Active Flyash Pile	A-2-170

LIST OF FIGURES
(Continued)

Figure	Title	Page No.
A.2-50	Projected Increase in Neptunium-237 Concentration in the Great Miami Aquifer at 100 Years Due to Loading From the Active Flyash Pile	A-2-171
A.2-51	Projected Increase in Neptunium-237 Concentration in the Great Miami Aquifer at 160 Years Due to Loading From the Active Flyash Pile	A-2-172
A.2-52	Projected Increase in Neptunium-237 Concentration in the Great Miami Aquifer at 280 Years Due to Loading From the Active Flyash Pile	A-2-173
A.2-53	Projected Increase in Neptunium-237 Concentration in the Great Miami Aquifer at 1000 Years Due to Loading From the Active Flyash Pile	A-2-174
A.2-54	Strontium-90 Loading to the Great Miami Aquifer From the Active Flyash Pile	A-2-175
A.2-55	Projected Increase in Strontium-90 Concentration in the Great Miami Aquifer at 100 Years Due to Loading From the Active Flyash Pile	A-2-176
A.2-56	Projected Increase in Strontium-90 Concentration in the Great Miami Aquifer at 160 Years Due to Loading From the Active Flyash Pile	A-2-177
A.2-57	Arsenic Loading to the Great Miami Aquifer From the Active Flyash Pile	A-2-178
A.2-58	Projected Increase in Arsenic Concentration in the Great Miami Aquifer at 1000 Years Due to Loading From the Active Flyash Pile	A-2-179
A.2-59	Lead Loading to the Great Miami Aquifer From the Active Flyash Pile	A-2-180
A.2-60	Projected Increase in Lead Concentration in the Great Miami Aquifer at 1000 Years Due to Loading From the Active Flyash Pile	A-2-181
A.2-63	Projected Increase in Uranium-238 Concentration in the Great Miami Aquiferat 160 Years Due to Loading From All Area Subunits	A-2-183
A.2-64	Projected Increase in Neptunium-237 Concentration in the Great Miami Aquifer at 160 Years Due to Loading From All Area Subunits	A-2-184
A.2-65	Projected Increase in Technetium-99 Concentration in the Great Miami Aquifer at 40 Years Due to Loading From All Area Subunits	A-2-185
A.2-66	Projected Increase in Lead Concentration in the Great Miami Aquifer at 1000 Years Due to Loading From All Area Subunits	A-2-186
A.2-67	Sensitivity of ODAST Model Results to Dispersivity	A-2-202
A.2-68	Sensitivity of ODAST Model Results to the Great Miami Aquifer Distribution COefficient for U-238 Inactive Flyash Pile and South Field	A-2-207
A.2-69	Sensitivity of ODAST Model Results to Glacial Till Distribution Coefficient for Uranium-238, Active Flyash Pile	A-2-208

LIST OF FIGURES
(Continued)

Figure	Title	Page No.
A.2-70	Sensitivity of ODAST Model Results to Biodegradation Half-life for bis(2-Ethylhexyl) Phthalate Inactive Flyash Pile and South Field	A-2-209
A.2-72	Sensitivity of ODAST Model Results to Biodegradation Half-life for bis(2-Ethylehexyl) Phthalate, Lime Sludge Ponds	A-2-210
A.3-1	Wind Rose for the FEMP Site Year - 1987	A-3-10
A.3-2	Wind Rose for the FEMP Site Year - 1988	A-3-11
A.3-3	Wind Rose for the FEMP Site Year - 1989	A-3-12
A.3-4	Wind Rose for the FEMP Site Year - 1991	A-3-13
A.3-5	Wind Rose for the FEMP Site Year - 1992	A-3-14
A.3-6	Active Flyash Pile Sources	A-3-15
A.3-7	South Field Sources	A-3-16
A.3-8	Inactive Flyash Pile Source	A-3-17
A.3-9	Solid Waste Landfill Sources	A-3-18
A.3-10	Lime Sludge Ponds Sources	A-3-19
A.3-11	Operable Unit 2 Receptor Grid	A-3-29

LIST OF ACRONYMS AND ABBREVIATIONS

AEC	Atomic Energy Commission
ALARA	as low as reasonably acceptable
ARAR	applicable or relevant and appropriate requirement
ASI	Advanced Sciences, Inc.
ASL	Analytical Support Level
ASTM	American Society for Testing and Materials
BDN	bio-denitrification
BOB	bottom of boring
CAA	Clean Air Act
CERCLA	Comprehensive Environmental Response, Compensation, and Liability Act of 1980
CERCLIS	Comprehensive Environmental Response, Compensation, and Liability Information System
CFR	Code of Federal Regulations
CIS	Characterization Investigation Study
CLP	Contract Laboratory Program (EPA)
cm/s	centimeter/second
COA	Certificate of Analysis
COE	U.S. Army Corps of Engineers
COC	contaminant of concern
cpm	counts per minute
CPC	constituent of potential concern
CRARE	Comprehensive Response Action Risk Evaluation
CSM	conceptual site model
CT	central tendency
CWA	Clean Water Act
DCR	Document Change Request
DOE	U.S. Department of Energy
dpm	disintegrations per minute
DQO	data quality objective
EIS	environmental impact statement
EM	electromagnetic
EP	extraction procedure
EP Tox	EP toxicity
EPA	U.S. Environmental Protection Agency
ERDA	U.S. Energy Research and Development Administration
ERMC	Environmental Restoration Management Contractor
ESA	Endangered Species Act

°F	degrees Fahrenheit
FEMA	Federal Emergency Management Agency
FEMP	Fernald Environmental Management Project
FERMCO	Fernald Environmental Restoration Management Company
FFCA	Federal Facility Compliance Agreement
FID	flame ionization detector
FIDLER	field instrument for detecting low-energy radiation
FMPC	Feed Materials Production Center
FR	Federal Register
FS	feasibility study
ft^3/sec	cubic feet per second
ft^3	cubic feet
ft/yr	feet/year
g	gram
GC/MS	gas chromatograph/mass spectrometry
GFAA	Graphite Furnace Atomic Absorption
GIS	Geographic Information System
GPR	ground penetrating radar
HCI	hydrochloric acid
HELP	Hydrologic Evaluation of Landfill Performance
HI	hazard index
HQ	hazard quotient
HSL	Hazardous Substance List
HWMU	hazardous waste management unit (RCRA)
ICAP	Inductively Coupled Atomic Plasma
ID	inner-diameter
ILCR	incremental lifetime cancer risk
ISCLT	Industrial Source Complex Long Term
IT	IT Corporation
m	meter
μg/g	microgram/gram
μg/L	microgram/liter
μg/kg	microgram/kilogram
μm	micrometer
K_d	partition coefficient
MCL	maximum contaminant level
MCLG	maximum contaminant level goal
MEK	2-butanone (synonym: methyl ethyl ketone)

LIST OF ACRONYMS AND ABBREVIATIONS
(Continued)

mg/kg	milligram/kilogram
mg/L	milligram/liter
mL	milliliter
MSL	mean sea level
MUSLE	Modified Universal Soil Loss Equation
NaOH	sodium hydroxide
NAD	North American Datum
NCP	National Oil and Hazardous Substance Pollution Contingency Plan
NESHAP	National Emission Standards for Hazardous Air Pollutants
NEPA	National Environmental Policy Act
NLO	National Lead (Company) of Ohio
HNO_3	nitric acid
NOAA	National Oceanic and Atmospheric Administration
NPDES	National Pollutant Discharge Elimination System
NPL	National Priorities List
NRC	U.S. Nuclear Regulatory Commission
NRHP	National Register of Historic Places
NTS	Nevada Test Site
NWS	National Weather Service
O&M	operations and maintenance
OAC	Ohio Administrative Code
ODAST	one-dimensional analytical solute transport
ODH	Ohio Department of Health
OEPA	Ohio Environmental Protection Agency
ORAU	Oak Ridge Associated Universities
OVA	organic vapor analyzer
OVM	organic vapor measure
PAH	polynuclear aromatic hydrocarbon
PC	personal computer
PCB	polychlorinated biphenyls
pCi/g	picoCuries per gram
pCi/L	picoCuries per liter
PIC	products of incomplete combustion
PID	photoionization detector
PP	proposed plan
PPE	personal protective equipment

LIST OF ACRONYMS AND ABBREVIATIONS
(Continued)

ppm	parts per million
QA	quality assurance
QAPP	quality assurance project plan
QC	quality control
R	retardation factors
RA	risk assessment
RAGS	Risk Assessment Guidance for Superfund
RCRA	Resource Conservation and Recovery Act
RD	remedial design
RFA/CC	request for analysis/chain of custody
RfD	reference dose
RFI	RCRA Facility Investigation
RI	remedial investigation
RI/FS	Remedial Investigation/Feasibility Study
RM	river mile
RME	reasonable maximum exposure
RMI	Reactive Metals, Inc.
ROD	record of decision
RSE	Removal Site Evaluation
S	second
SAP	Sampling and Analysis Plan
SARA	Superfund Amendment and Reauthorization Act of 1986
SAR/CR	site-wide analysis request/custody record
SC/DM	Site Characterization/Data Management
SCQ	Site-Wide CERCLA Quality Assurance Project Plan
SCS	Soil Conservation Service
SDWA	Safe Drinking Water Act
SED	Site-wide Environmental Database
SHPO	State Historic Preservation Officer
SPA	scintillation detector
SR	State Route
STAR	stability array
SVOC	semivolatile organic compound
SWIFT III	Sandia Waste Isolation Flow and Transport (computer model)
SWMU	solid waste management unit (RCRA)
TAL	target analyte list

LIST OF ACRONYMS AND ABBREVIATIONS
(Continued)

TBC	to be considered
TCA	trichloroethane
TCLP	toxicity characteristic leaching procedure
TFV	threshold friction velocity
TLD	thermoluminescence dosimeters
TOC	total organic carbon
UCL	upper confidence limit
UF_4	uranium tetrafluoride (green salt)
UO_3	uranium trioxide (orange oxide)
USCS	Unified Soils Classification System
USDA	United States Department of Agriculture
USGS	U.S. Geological Survey
VOA	volatile organic analysis
VOC	volatile organic compound
WEMCO	Westinghouse Environmental Management Company of Ohio
WMCO	Westinghouse Materials Company of Ohio

A.1.0 SURFACE WATER MODELING

A.1.1 INTRODUCTION

The modeling approach used to estimate constituent concentrations in surface water and sediments resulting from transport by storm water runoff from Operable Unit 2 is described in this appendix. The transport of constituents in storm water is predicated by characterizing the constituent present in surface soil or waste and using runoff and partitioning models to quantify the migration of constituents into stream sediments and surface water.

Constituents in surface soil can be released and transported to surface water via storm water runoff. During a rainfall event, a portion of rainwater infiltrates the soil surface while the remainder runs off the surface as shown in Figure A.1-1. The amount of runoff increases with the increase in the clay content and moisture content of the soil, intensity and duration of rainfall, and ground slope steepness. Runoff decreases with increased vegetative cover or greater ground slope length.

Constituents from the surface soil can be transported in runoff either in the dissolved phase or adsorbed to soil particles. The less soluble a constituent is in water, the more likely it will be adsorbed to soil particles. Because the water solubility of constituents in Operable Unit 2 vary greatly, contaminant transport is modeled for both dissolved-phase and adsorbed-phase of the constituents.

This section also describes the use of the surface water modeling results to define source terms for the groundwater modeling. Paddys Run and the Storm Sewer Outfall Ditch are considered potential sources to groundwater because portions of their streambeds are in direct contact with the Great Miami Aquifer.

A.1.2 CONCEPTUAL MODEL

Storm water runoff from Operable Unit 2 that reaches Paddys Run was considered a significant potential pathway for constituent migration to surface water. Another pathway for constituent migration to surface water is storm runoff carrying contaminated seep water to surface water, before the seep water can infiltrate to the Great Miami Aquifer. Paddys Run is an intermittent stream that flow southward along the western edge of the Fernald Environmental Management Project (FEMP). Natural drainage from Operable Unit 2 subunits flows to Paddys Run or the Storm Sewer Outfall

5659

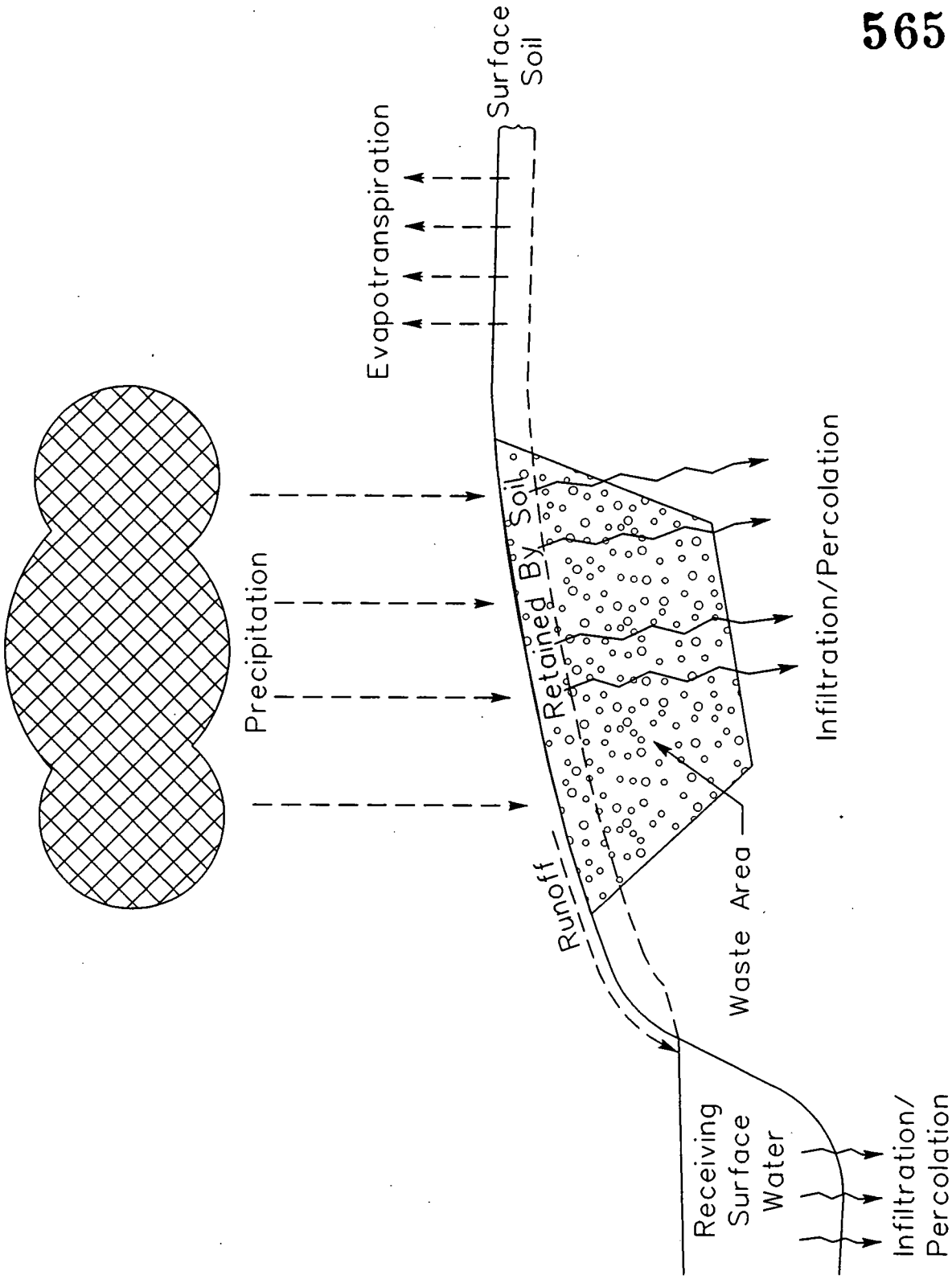

FIGURE A.1-1
CONCEPTUAL MODEL OF SURFACE WATER RUNOFF

figa0101.dgn

Ditch. The Storm Sewer Outfall Ditch flows into Paddys Run at the southwest corner of the site. Paddys Run flows into the Great Miami River 1.5 miles south of the FEMP.

NO. A-6 The predicted constituent loading to Paddys Run and subsequent predicted loading to the Great Miami Aquifer and the Great Miami River is only from the sources within the Operable Unit 2 battery limits. These predictions were made to evaluation the Operable Unit 2 impact to these media and is not meant to imply that Operable Unit 2 is the only source of constituents to these media.

Two sets of overlapping assumptions were made in the conceptual surface water and groundwater models to assure worst case levels for both surface water and groundwater pathways. These assumptions are:

- Forty-four percent of the water (CPC mass) reaching the Storm Sewer Outfall Ditch from the Active Flyash Pile was assumed to reach Paddys Run for the surface water conceptual model. At the same time, ~~while~~ all water (CPC mass) flowing to the Storm Sewer Outfall Ditch from Active Flyash Pile was considered to infiltrate the Great Miami Aquifer for the groundwater conceptual model. NO. A-1
- All of the flow in Paddys Run was assumed to discharge to the Great Miami River for the surface water conceptual model. At the same time, ~~while~~ 30 percent of the CPC mass loading in the runoff water ~~(water and sediment)~~ to Paddys Run was assumed to be a source to the Great Miami Aquifer in the groundwater conceptual model.

The estimates that 44 percent of the water reaching the Storm Sewer Outfall ditch and 30 percent of the total runoff in Paddys Run infiltrates to the Great Miami Aquifer are used based on predictions from VS2DT modeling (U.S.DOE 1993f).

These overlapping assumptions result in assigning more than 100 percent of CPC mass in the runoff water to surface and groundwater receptors. This additional mass accounts for further leaching of CPC from the sediments as sediments are transported to Paddys Run and the Great Miami River.

Storm water runoff from the South Field, Inactive Flyash Pile, and Solid Waste Landfill was considered to reach Paddys Run that in turn discharges to the Great Miami River or infiltrates to the Great Miami Aquifer. Surface water modeling for the Lime Sludge Ponds was not performed because the berms surrounding the ponds contain precipitation received during a storm event.

A.1.3 TECHNICAL APPROACH

The modeling approach used to estimate constituent concentrations in surface water and sediments resulting from transport by surface water runoff is described in this section.

A uniform concentration was assigned for surface soil constituents in each subunit. The constituent concentrations used in this assessment are the upper 95 percent confidence level on the means (UCL) of the surface soil concentrations from the remedial investigation. Section 6.0 and Appendix B describe the selection of constituents of potential concern and source concentration term for surface water modeling. Figure A.1-2 shows the overall approach for surface water modeling and screening of CPCs. While determining CPCs in Section 6.0 and Appendix B, nutrients, constituents at background levels, and constituents with soil concentrations below the EPA RAGs, Part B screening values are screened out. Source term concentrations are also calculated and shown in Appendix B. Consistent with the conceptual model, runoff concentrations are then developed and screened against the EPA RAGs, Part B screening concentrations. Concentrations in Paddys Run and the Great Miami River are then calculated for the remaining CPCs. Sediment concentrations in Paddys Run and the Great Miami River are not calculated because the baseline risk assessment uses more conservative (higher) on-subunit sediment concentrations.

NO. A-47

Two soil loss models described in the EPA "Superfund Exposure Assessment Manual" (EPA 1988b), the Universal Soil Loss Equation (USLE) and Modified Universal Soil Loss Equation (MUSLE), were considered for tools to quantify soil migration. The USLE model is similar to MUSLE, with the exception that the USLE uses an area-dependent method to determine runoff, while MUSLE employs event-specific runoff volume and flow rate variables. The MUSLE model was chosen over the USLE model to facilitate evaluation of an event-specific worst-case conservative scenario as opposed to a yearly average constituent transport scenario. The MUSLE model calculates the total mass of soil transported by surface water in a single rainfall event using the input of the event-specific runoff volume, storm duration, and flow rate parameters. The direction of surface water flow is determined by examining the topographic map of the Operable Unit 2 subunits. The volume of runoff is estimated and used to determine the amount that stream flow may be increased by a storm event and to estimate dissolved constituent loading.

Additional equations were used to approximate constituent partitioning between soil and water in the runoff flow. These partitioning equations provide estimates of the constituent concentration dissolved

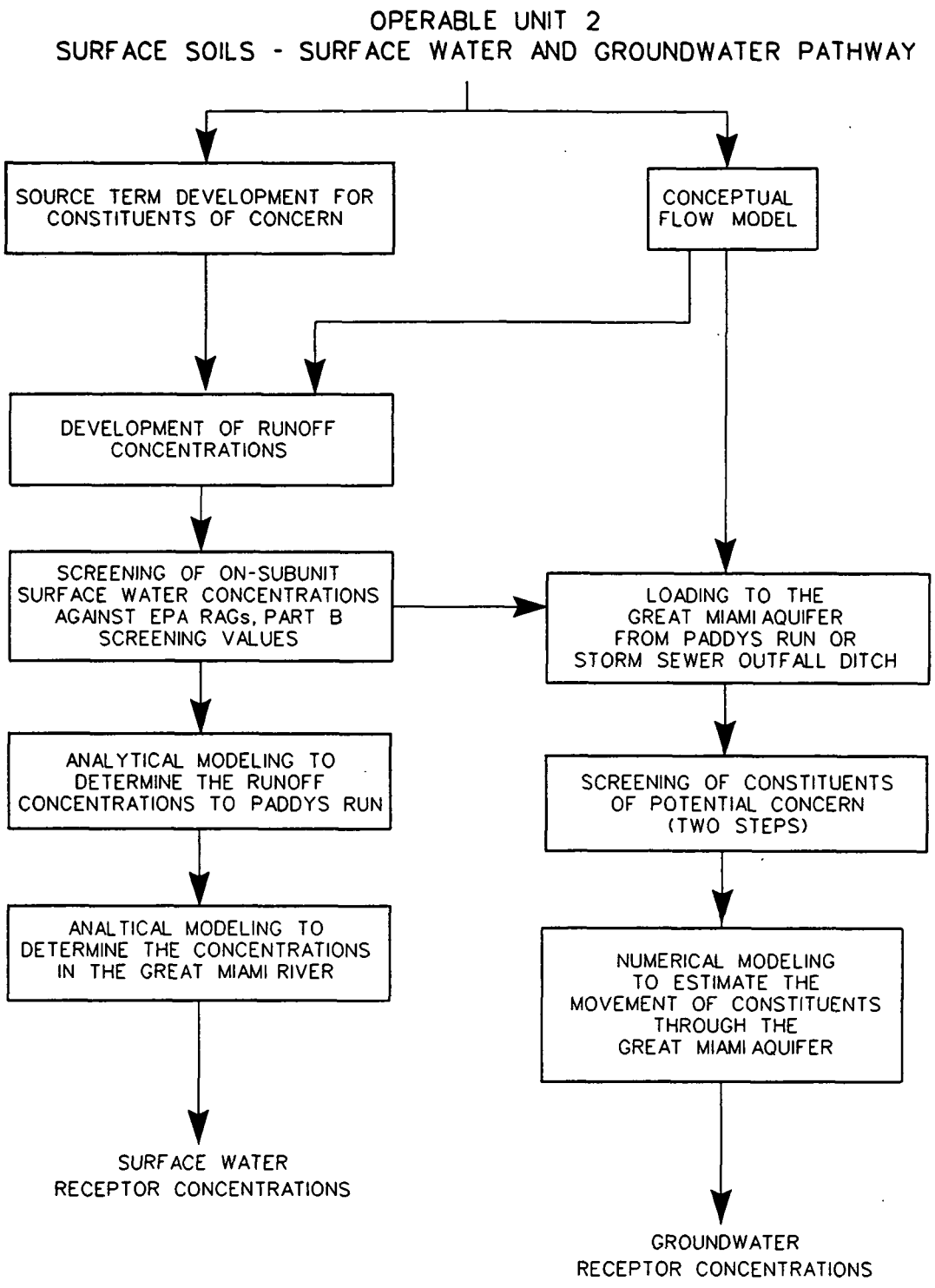

figa0102.dgn

FIGURE A.1-2
SURFACE WATER TRANSPORT MODELING DIAGRAM

in water runoff and that which is adsorbed to the soil carried in the runoff that deposits in the sediment of receiving stream (Haith 1980; Mills et al. 1982; Mockus 1972).

Local meteorological data was used to obtain estimates of the amount and duration of rainfall at the site. The volume of storm water runoff flowing to Paddys Run was estimated using the Soil Conservation Service (SCS) curve method. The storm runoff modeling was based on a single storm event (2.5 inches in 24 hours; Hershfield, 1961) resulting in a flow rate in Paddys Run of 4 ft^3/sec (Dames and Moore, 1985a). No flow from upgradient runoff was assumed for the Storm Sewer Outfall Ditch.

Information on the soil types identified in Operable Unit 2, using the U.S. Soil Conservation Service designation, is presented in detail in Section 3.0 of this RI report. The types and areal density of vegetation in Operable Unit 2 were provided by aerial photos, site reconnaissance, and interviews with personnel familiar with the Operable Unit 2 study area.

NO. A-47

The maximum detected concentrations in the seeps for the subsurface soil CPCs in the Inactive Flyash Pile and South Field, and the estimated seep flow rates, were also used to define on-subunit surface water concentrations during a storm event and the source term for ~~Paddys Run and~~ the Great Miami River and the Great Miami Aquifer. It was assumed that during the storm event, all seep water will reach Paddys Run. Estimated flow rates for seeps were 2 and 10 gallons per minute (gpm) for the Inactive Flyash Pile and South Field, respectively.

NO. A-49

Constituent concentrations in Paddys Run and the Great Miami River were calculated by ~~diluting~~ mixing the dissolved concentrations in storm water runoff or seeps with the flows in the receiving streams. The results from Paddys Run were compared to observed conditions and are presented in Section A.1.5. Constituent concentrations in the Storm Sewer Outfall Ditch were assumed to be the same as runoff concentrations to simulate a "no-flow" condition upstream of the Active Flyash Pile in the Storm Sewer Outfall Ditch.

An average flow rate of 3,300 ft^3/sec was used for the Great Miami River based on previous studies (DOE 1993a). To estimate the worst surface water conditions, it was assumed that all flow and all constituent mass in Paddys Run discharges to the Great Miami River.

Figure A.1-2 presents the technical approach used to define source term from the surface water pathway to the Great Miami Aquifer. After concentrations in the surface water are modeled, some of the constituent mass is assumed to infiltrate to the Great Miami Aquifer. To estimate the worst conditions in groundwater due to surface water as a source, it was assumed that 30 percent of constituent mass and flow in Paddys Run infiltrates to the Great Miami Aquifer. All constituent mass in the Storm Sewer Outfall Ditch was also assumed to infiltrate the Great Miami Aquifer. This accounts for loading due to infiltrating runoff water as well as leaching of sediments. On-site maximum Great Miami Aquifer concentrations were estimated using a 30-foot wide section of Paddys Run and a 10-foot wide section of the Storm Sewer Outfall Ditch. ~~Predicted Great Miami Aquifer concentrations were compared to conservative risk based screening criteria which were derived by EPA Region III and based on a carcinogenic risk of 1 x 10^{-7} and a non carcinogenic Hazard Index (HI) of 0.1. If predicted on site maximum Great Miami Aquifer concentrations were greater than the screening concentration, then full SWIFT III block (125 foot wide) dilution was calculated to see if predicted SWIFT III model concentrations will exceed the screening concentrations anywhere in the SWIFT model. If the full block dilution concentration exceeded the screening concentration, the source term for the constituent of potential concern (CPC) was assigned for groundwater modeling.~~ Runoff loading from four storm events (2.5 inch in 24 hours) was assumed to equal the annual loading to the stream. The predicted Great Miami Aquifer concentrations were compared to conservative risk-based screening values calculated using the EPA Risk Assessment Guidance (RAGs), Part B (EPA 1991d) short equations for water. If the predicted on-site maximum Great Miami Aquifer concentrations were greater than the screening concentration, then the full SWIFT III block (125 foot wide) mixing was calculated to see if the predicted SWIFT III model concentrations will exceed the screening concentrations anywhere in the SWIFT model. If the full block mixing concentration exceeded the screening concentration, the source term for the CPC was assigned for groundwater modeling.

NO. A-47

A.1.4 SURFACE WATER MODEL DESCRIPTION

The MUSLE model was used to calculate the total mass of soil transported by storm water in a single rainfall event using event-specific runoff volume, storm duration, and flow rate parameters. Additional equations were used to describe constituent partitioning between soil and water in the runoff flow. Model assumptions and equations are presented in this section.

A.1.4.1 Model Assumptions

Surface water models are based on the following major assumptions:

NO. A-2

- Constituents adsorbed to soils in runoff remain adsorbed in the stream sediments. However, it was assumed that once a contaminant has partitioned into the dissolved phase in the runoff water, and the adsorbed phase on the eroded soil particles at the subunit, further partitioning or dilution of contaminant adsorbed to eroded soil does not take place.

- Constituents dissolved in runoff water remain in the dissolved phase in the receiving stream prior to further dilution or infiltration to the Great Miami Aquifer.

A.1.4.2 Calculation of Soil Loss from Runoff

MUSLE is used to model the amount of contaminated soil migrating to Paddys Run or the Storm Sewer Outfall Ditch from erosion by storm water runoff. The MUSLE model is based on the following equation.

$$Y(s)_E = (CF)[(V_r)(q_p)]^{0.56})(K)(LS)(C)(P)$$

where

$Y(s)_E$	=	Soil loss in runoff (metric tons per event)
CF	=	Conversion factor (11.8 for metric units)
V_r	=	Volume of runoff (m^3)
q_p	=	Peak runoff flow rate (m^3/s)
K	=	Soil erodibility factor (metric tons/ha/unit erosion potential)
LS	=	Product of slope length factor and slope steepness factor (unitless)
C	=	Cover factor (unitless)
P	=	Erosion control practice factor (unitless)

The erosion control practice factor was set to 1.0 to simulate an uncontrolled hazardous waste site. This represents a worst-case (conservative) assumption (EPA, 1988). Intermediate parameters V_r and q_p are calculated by:

$$V_r = (100)(A)(Q_r)$$

$$Q_r = (R_t - 0.2S_w)^2/(R_t + 0.8S_w)$$

$$S_w = (2.54)[(1000/CN)-10]$$

$$q_p = [(0.028)(A)(R_t)(Q_r)]/[(T_r)(R_t - 0.2\ S_w)]$$

where

A	=	Contaminated surface area (ha)
Q_r	=	Depth of runoff (cm)
R_t	=	Depth of rainfall event (cm)
S_w	=	Soil water retention factor (cm)
CN	=	SCS runoff curve number (unitless)
T_r	=	Rainfall duration (hours)

Figures A.1-3 through A.1-5 shows the topography of the Operable Unit 2 subunits considered in surface water modeling. These figures also provide information on the slope of the ground surface in the Operable Unit 2 subunits, and the distance to Paddys Run or the Storm Sewer Outfall Ditch. Table A.1-1 lists the parameter values used in the Operable Unit 2 surface water runoff assessment and calculating loss of soil from runoff.

A.1.4.3 Calculation of Constituent Partitioning and Loading

The portion of constituent from the eroded soil that remains with the sediment or that is dissolved in the water is estimated using the following equations, respectively:

$$S_s = [1/(1+\theta_c/(K_d \bullet \rho))]\ (C_i)(\rho)(A')(CF)$$

and

$$M_s = [1/(1+(K_d \bullet \rho)/\theta_c)](C_i)(\rho)(A')(CF)$$

where

S_s	=	Available quantity of constituent absorbed to sediment (g)
M_s	=	Available quantity of constituent dissolved in water (g)
θ_c	=	Water capacity of surface soil (unitless)
K_d	=	Chemical-specific sorption partition coefficient (cm^3/g)
ρ	=	Bulk soil density (g/cm^3)
C_i	=	Concentration of constituent in soil (mg/kg)
~~A'~~	~~=~~	~~Contaminated volume (ha-cm)~~
NO A-3 A'	=	$A\ Q_r$ = Contaminated volume (ha-cm)
CF	=	Conversion factor (100 $kg/mg \bullet cm^2/ha$)

The mass of absorbed constituent in the source area is:

$$PX_i = [Y(s)_E/100(\rho)(A')](S_s)$$

5659

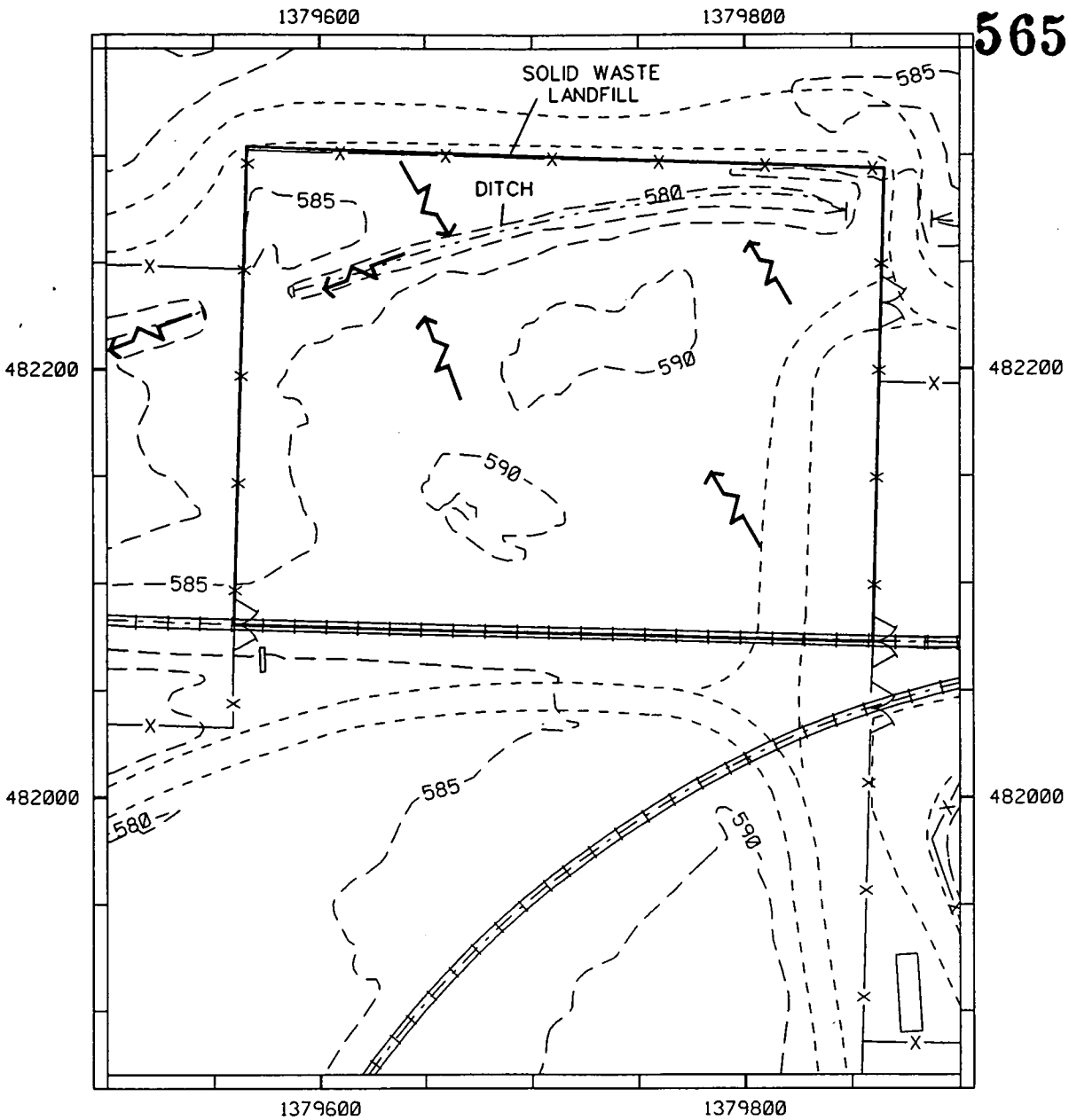

NOTE:
Coordinates are in State Planar NAD 1927.
Surface contours based on 1992 flyover.

SCALE (FT)
0 40 80 160

LEGEND

- ROADS
- STREAM
- FENCE
- RAILROAD
- TOPOGRAPHIC CONTOUR LINE
- SURFACE WATER DRAINAGE

FIGURE A.1-3
TOPOGRAPHY AND DRAINAGE SCENARIO FOR SOLID WASTE LANDFILL

figa0103.dgn

000049

5659

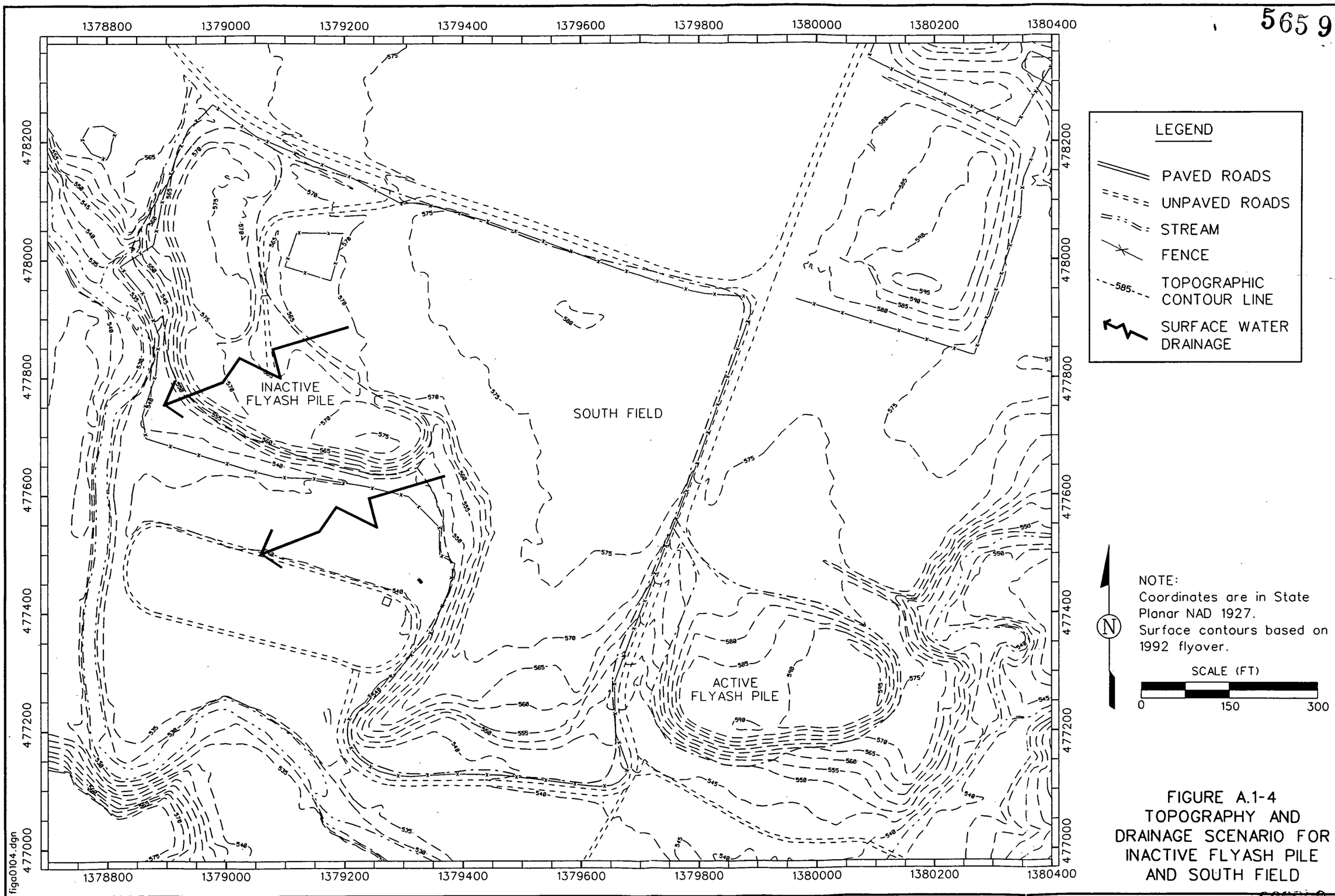

FIGURE A.1-4
TOPOGRAPHY AND DRAINAGE SCENARIO FOR INACTIVE FLYASH PILE AND SOUTH FIELD

5659

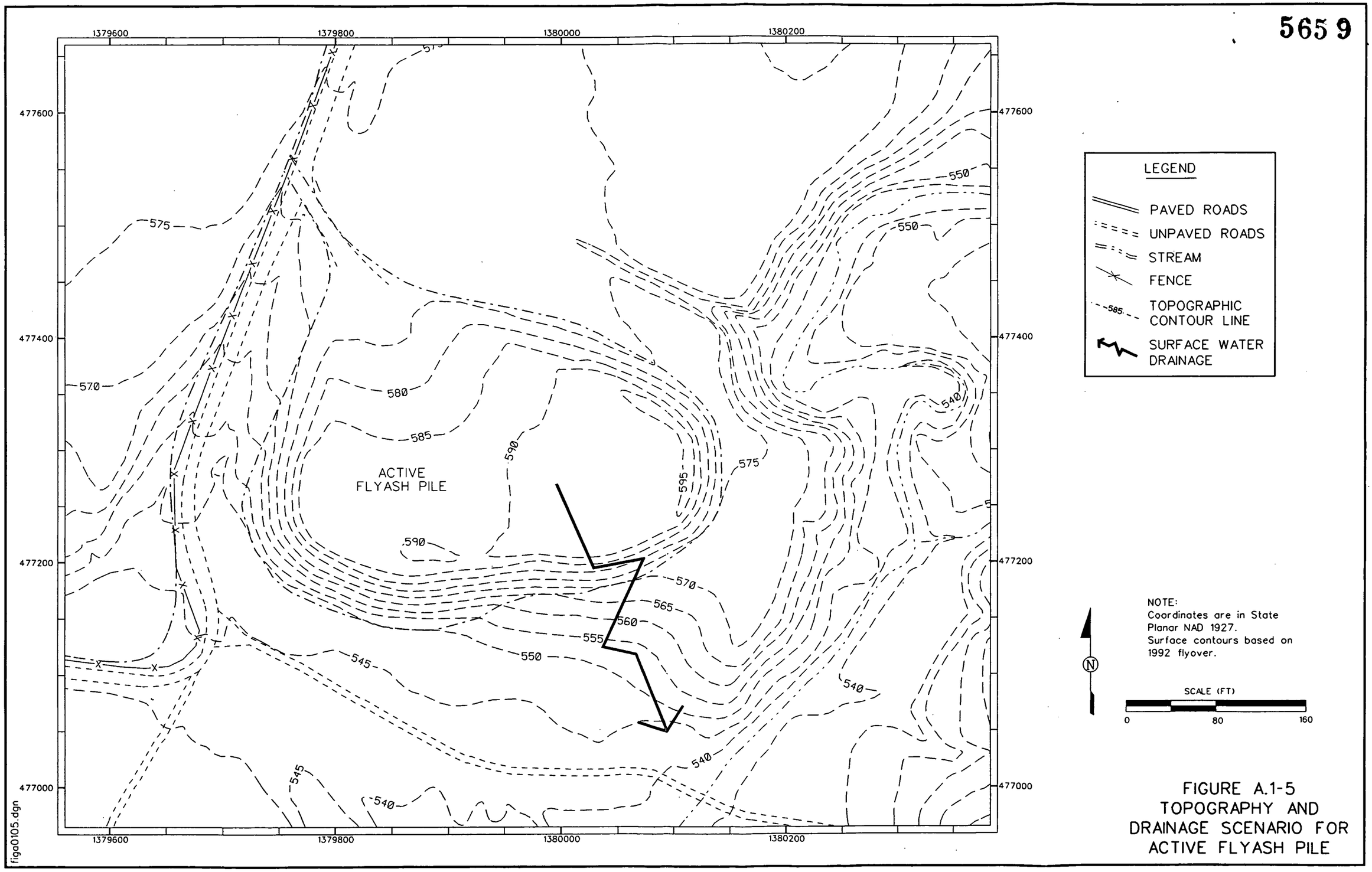

FIGURE A.1-5
TOPOGRAPHY AND DRAINAGE SCENARIO FOR ACTIVE FLYASH PILE

TABLE A.1-1

VARIABLES USED IN THE SURFACE WATER RUNOFF MODEL OPERABLE UNIT 2 REMEDIAL INVESTIGATION FERNALD ENVIRONMENTAL MANAGEMENT PROJECT

Variables	Units	Active Flyash Pile	Inactive Flyash Pile	South Field	Solid Waste Landfill
LS, slope length and steepness factor[a]	unitless	3.3	3.3	1.5	1.0
C, cover factor[b]	unitless	1.000	0.042	0.042	0.042
A, contaminated area[c]	ha	0.9040	1.3901	3.8706	0.6881
CN, SCS runoff curve No.[d]	unitless	86	55	61	58
Θ_c, available water capacity[c]	unitless	0.150	0.150	0.154	0.154
ρ, soil bulk density[c]	g/cm^3	0.861	0.861	1.702	1.830
Rr, rainfall and runoff factor[e]	unitless	1	1	1	1
K, soil erodibility factor[f]	ton/ha	0.26	0.26	0.26	0.29
R_t, total storm rainfall[g]	cm	6.35	6.35	6.35	6.35
T_r, storm duration[g]	hrs	24	24	24	24

[a]United States Environmental Protection Agency, 1988. "Superfund Exposure Assessment Manual." Office of Remedial Response, Washington, D.C., EPA/5401/1-88/001. EPA, 1988, Figure 2-6 and Site-Specific Information.

[b]Atlantic Environmental Services (AES), 1988. "Management of Manufactured Gas Plant Sites." Volume III, Risk Assessment, Gas Research Institute, Chicago, IL. GRI-87/0260.3. AES, 1988, Exhibit 7-5, 60% Grass Cover Assumed for Inactive Flyash Pile, South Field, and Solid Waste Landfill, 0% Grass Cover Assumed for Active Flyash Pile.

[c]Calculated from Site-Specific Information.

[d]United States Environmental Protection Agency, 1988. "Superfund Exposure Assessment Manual." Office of Remedial Response, Washington, D.C., EPA/5401/1-88/001. EPA, 1988, Figure 2-6 and Site-Specific Information.

[e]Atlantic Environmental Services, 1988. "Management of Manufactured Gas Plant Sites." Volume III, Risk Assessment, Gas Research Institute, Chicago, IL. GRI-87/0260.3; Mills, W.B., Dean, J.D., Porcella, D.B., Gherini, S.A., Hudson, R.J.M., Frick, W.E., Rupp, G.L., and Bowie, G.L., 1982, "Water Quality Assessment: A Screening Procedure for Toxic and Conventional Pollutants: Parts 1, 2, and 3," EPA-6001 6-82-004 a, b, c, EPA Environmental Research Laboratory, Office of Research and Development, Athens, GA. AES, 1988, Exhibit 7-11: Mills et al., 1982.

[f]Atlantic Environmental Services (AES), 1988. "Management of Manufactured Gas Plant Sites." Volume III, Risk Assessment, Gas Research Institute, Chicago, IL. GRI-87/0260.3. AES, 1988, Exhibit 7-2 and Site-Specific Information.

[g]Hershfield, D.M., 1961. "Rainfall Frequency Atlas of the United States: For Durations from 30 Minutes to 24 Hours and Retain Periods from 1 to 100 Years." U.S. Department of Commerce, Washington, D.C., Technical Paper No. 40. 1-year, 24-Hour Storm Event (HERSHFIELDS, 1961).

Other Comment No. A-47

The constituent concentration in sediment of the receiving water body is:

$$C_s = PX_i/Y(s)_E$$

where

C_s = Concentration of constituent in sediment (mg/kg)
PX_i = Absorbed quantity of constituent (g)

The mass of dissolved constituent from the source area is:

$$PQ_i = M_s(Q_r/R_t)$$

where

PQ_i = Dissolved constituent available per event (g)

The constituent concentration in the runoff effluent is:

$$C_e = PQ_i/V_r$$

where

PQ_i = Dissolved substance available per event (g)
C_e = Concentration of constituent in runoff (mg/ℓ)
V_r = Volume of runoff (m^3)

The dissolved constituent concentration in Paddys Run ~~or the Storm Sewer Outfall Ditch~~ downstream is:

NO. A-42

$$\cancel{C_w = (C_e)(Q_e)/(Q_t + Q_e)}$$

$$C_w = (C_e)(Q_e)/(Q_t)$$

where

C_w = Concentration of constituent in water downstream (mg/L)
Q_e = Average runoff effluent flow rate (V_r/T_r; m^3/hr)
Q_t = Flow rate of receiving water body (m^3/hr)

Note that Q_t includes the runoff water from the subunit.

The dissolved constituent concentration in the Great Miami River is estimated by:

$$\cancel{Cgmr = (C_w)(Q_i)/(Qgmr + Q_i)}$$

$$Cgmr = (C_w)(Q_i)/(Qgmr)$$

where

Cgmr = Concentration of constituent in the Great Miami River (mg/L)
Qgmr = Flow rate of the Great Miami River (m^3/hr)

Flow rate of the Great Miami Aquifer includes the flow contribution from the Paddys Run.

A.1.5 RESULTS OF SURFACE WATER RUNOFF MODELING

This section presents the results of surface water modeling for each subunit in Operable Unit 2.

A.1.5.1 Solid Waste Landfill

NO

~~Table A.1-2 presents the results of surface water modeling for the Solid Waste Landfill based on a single storm event using the MUSLE model. The model results show that the small mass of constituents from the Solid Waste Landfill that partition into the water, combined with a dilution in Paddys Run from a flow of 4 ft^3/sec results in low surface water concentrations. Radionuclide concentrations in Paddys Run range from a minimum of 2.8×10^{-6} pCi/L for plutonium 239/240 to a maximum of 0.06 pCi/L for uranium 238. Concentrations in the Great Miami River range from a minimum of 3.3×10^{-9} pCi/L for plutonium 239/240 to a maximum of 3.88×10^{-4} pCi/L for uranium 234. All inorganics and organics were predicted to remain below 5×10^{-3} μg/L in Paddys Run and 6×10^{-6} μg/L in the Great Miami River. These concentrations remain only through the duration of the storm.~~

Tables A.1-2a and A.1-2b present the results of surface water modeling for the Solid Waste Landfill based on a single storm event using the MUSLE model. Table A.1-2a also shows the screening of CPCs based on comparison of on-subunit runoff concentration against the EPA RAGs, Part B based screening concentrations for water. A total runoff of 23.2 m^3 was calculated during the 24-hour storm event. The model results show that the small mass of constituents from the Solid Waste Landfill that partition into the water, combined with dilution in the Great Miami River from a flow of 3300 ft^3/sec results in low surface water concentrations. The radionuclide concentrations in on-subunit runoff range from a minimum of 1.2×10^{-3} pCi/L for plutonium-239/240 to a maximum of

TABLE A.1-2A

RUNOFF EFFLUENT AND SEDIMENT LOADING FROM THE SOLID WASTE LANDFILL OPERABLE UNIT 2 REMEDIAL INVESTIGATION FERNALD ENVIRONMENTAL MANAGEMENT PROJECT

Constituent of Potential Concern After Initial Screening	Partition Coefficient K_d (mL/g)	Waste Area Surface Soil Concentration Ci (mg/kg)	Total Annual Loading to Stream Tl (g)	Sediment Concentration Cs (mg/kg)	On-Subunit Runoff Effluent Concentration Ce (pCi/L RAD) (µg/L non-RAD)	Screening Concentration (pCi/L RAD) (µg/L non-RAD)	Final CPC For On-Subunit Runoff Water (Y/N)
INORGANICS							
Arsenic	$2.00 \times 10^{+2}$	$6.67 \times 10^{+0}$	7.52×10^{-2}	$6.67 \times 10^{+0}$	8.09×10^{-1}	1.46×10^{-4}	Yes
Berylium	$1.30 \times 10^{+3}$	6.98×10^{-1}	1.22×10^{-3}	6.98×10^{-1}	1.30×10^{-2}	2.37×10^{-4}	Yes
Lead	$3.00 \times 10^{+3}$	$1.90 \times 10^{+1}$	1.43×10^{-2}	$1.90 \times 10^{+1}$	1.54×10^{-1}	NA[a]	NA
RADIONUCLIDES							
Neptunium-237	$5.50 \times 10^{+1}$	1.69×10^{-3}	6.92×10^{-3}	1.69×10^{-3}	5.25×10^{-1}	2.16×10^{-2}	Yes
Plutonium-238	$1.70 \times 10^{+3}$	4.51×10^{-8}	6.00×10^{-11}	4.51×10^{-8}	1.10×10^{-2}	2.16×10^{-2}	No
Plutonium-239/240	$1.70 \times 10^{+3}$	1.32×10^{-6}	1.76×10^{-9}	1.32×10^{-6}	1.17×10^{-3}	2.07×10^{-2}	No
Radium-226	$6.96 \times 10^{+2}$	1.41×10^{-6}	4.60×10^{-9}	1.41×10^{-6}	4.86×10^{-2}	1.76×10^{-4}	Yes
Radium-228	$6.96 \times 10^{+2}$	6.18×10^{-9}	2.01×10^{-11}	6.18×10^{-9}	5.85×10^{-2}	4.75×10^{-2}	Yes
Strontium-90	$1.00 \times 10^{+1}$	6.97×10^{-9}	1.56×10^{-9}	6.91×10^{-9}	$2.30 \times 10^{+0}$	1.32×10^{-1}	Yes
Thorium-228	$5.80 \times 10^{+3}$	1.98×10^{-9}	7.72×10^{-13}	1.98×10^{-9}	6.79×10^{-3}	8.64×10^{-2}	No
Thorium-230	$5.80 \times 10^{+3}$	3.14×10^{-4}	1.22×10^{-7}	3.14×10^{-4}	2.71×10^{-2}	3.65×10^{-1}	No
Thorium-232	$5.80 \times 10^{+3}$	$1.37 \times 10^{+1}$	5.36×10^{-3}	$1.37 \times 10^{+1}$	6.30×10^{-3}	2.79×10^{-2}	No
Uranium-234	$7.50 \times 10^{+1}$	6.77×10^{-3}	2.04×10^{-4}	6.76×10^{-3}	$1.36 \times 10^{+1}$	2.97×10^{-1}	Yes
Uranium-235/236	$7.50 \times 10^{+1}$	$1.31 \times 10^{+0}$	3.94×10^{-2}	$1.31 \times 10^{+0}$	9.14×10^{-1}	2.97×10^{-1}	Yes
Uranium-238	$7.50 \times 10^{+1}$	$2.30 \times 10^{+2}$	$6.92 \times 10^{+0}$	$2.30 \times 10^{+2}$	$2.50 \times 10^{+1}$	1.70×10^{-1}	Yes
Uranium-Total (non-RAD)	$7.50 \times 10^{+1}$	$2.25 \times 10^{+2}$	$6.76 \times 10^{+0}$	$2.25 \times 10^{+2}$	$7.27 \times 10^{+1}$	$1.09 \times 10^{+1}$	Yes

TABLE A.1-2A
(Continued)

Constituent of Potential Concern After Initial Screening	Partition Coefficient K_d (mL/g)	Waste Area Surface Soil Concentration Ci (mg/kg)	Total Annual Loading to Stream Tl (g)	Sediment Concentration Cs (mg/kg)	On-Subunit Runoff Effluent Concentration Ce (pCi/L RAD) (μg/L non-RAD)	Screening Concentration (pCi/L RAD) (μg/L non-RAD)	Final CPC For On-Subunit Runoff Water (Y/N)
ORGANICS							
Benzo(a)anthracene	$2.63 \times 10^{+3}$	3.66×10^{-1}	3.15×10^{-4}	3.66×10^{-1}	3.38×10^{-3}	2.82×10^{-3}	Yes
Benzo(a)pyrene	$6.28 \times 10^{+3}$	3.40×10^{-1}	1.22×10^{-4}	3.40×10^{-1}	1.31×10^{-3}	2.82×10^{-4}	Yes
Benzo(b)fluoranthene	$2.45 \times 10^{+4}$	7.10×10^{-1}	6.56×10^{-5}	7.10×10^{-1}	7.03×10^{-4}	2.82×10^{-3}	No
Benzo(g,h,i)perylene	$2.13 \times 10^{+4}$	5.00×10^{-1}	5.32×10^{-5}	5.00×10^{-1}	5.69×10^{-4}	NA	NA
Dibenzo(a,h)anthracene	$6.14 \times 10^{+3}$	2.00×10^{-1}	7.36×10^{-5}	2.00×10^{-1}	7.90×10^{-4}	2.82×10^{-4}	Yes
Indeno(1,2,3,cd)pyrene	$3.01 \times 10^{+5}$	4.80×10^{-1}	3.61×10^{-6}	4.80×10^{-1}	3.87×10^{-5}	2.82×10^{-3}	No
Phenanthrene	$9.54 \times 10^{+0}$	$5.31 \times 10^{+0}$	5.14×10^{-1}	5.30×10^{-1}	$5.52 \times 10^{+1}$	NA	NA

[a]NA = EPA RAGs, Part B Screening Value could not be calculated.

Other Comment No. A-47

000056

5659

TABLE A.1-2B

CONTAMINANT LOADING TO THE GREAT MIAMI RIVER FROM THE SOLID WASTE LANDFILL OPERABLE UNIT 2 REMEDIAL INVESTIGATION FERNALD ENVIRONMENTAL MANAGEMENT PROJECT

Constituent of Potential Concern for Surface Water Runoff	Runoff Effluent Concentration Ce (pCi/L RAD) (μg/L non-RAD)	Concentration in Surface Water (Paddy's Run) during Storm Event Cw (pCi/L RAD) (μg/L non-RAD)	Great Miami River Concentration Cgmr (pCi/L RAD) (μg/L non-RAD)
INORGANICS			
Arsenic	8.09×10^{-1}	1.91×10^{-3}	2.31×10^{-6}
Berylium	1.30×10^{-2}	3.08×10^{-5}	3.72×10^{-8}
Lead	1.54×10^{-1}	3.63×10^{-4}	4.38×10^{-7}
RADIONUCLIDES			
Neptunium-237	5.25×10^{-1}	1.24×10^{-3}	1.50×10^{-6}
Radium-226	4.86×10^{-2}	1.15×10^{-4}	1.39×10^{-7}
Radium-228	5.85×10^{-2}	1.38×10^{-4}	1.67×10^{-7}
Strontium-90	$2.30 \times 10^{+0}$	5.43×10^{-3}	6.55×10^{-6}
Uranium-234	$1.36 \times 10^{+1}$	3.22×10^{-2}	3.88×10^{-5}
Uranium-235/236	9.14×10^{-1}	2.16×10^{-3}	2.61×10^{-6}
Uranium-238	$2.50 \times 10^{+1}$	5.90×10^{-2}	7.12×10^{-5}
Uranium-Total (non-RAD)	$7.27 \times 10^{+1}$	1.72×10^{-1}	2.07×10^{-4}
ORGANICS			
Benzo(a)anthracene	3.38×10^{-3}	7.98×10^{-6}	9.63×10^{-9}
Benzo(a)pyrene	1.31×10^{-3}	3.10×10^{-6}	3.75×10^{-9}
Benzo(g,h,i)perylene	5.69×10^{-4}	1.35×10^{-6}	1.62×10^{-9}
Dibenzo(a,h)anthracene	7.90×10^{-4}	1.87×10^{-6}	2.25×10^{-9}
Phenanthrene	5.52×10^{-1}	1.30×10^{-3}	1.57×10^{-6}

Other Comment No. A-47

25 pCi/L for uranium-238. Note that the plutonium-239/240 runoff concentration is below the screening value. Concentrations in the Great Miami River range from a minimum of 1.4 x 10^{-7} pCi/L for radium-226 to a maximum of 7.1 x 10^{-5} pCi/L for uranium-238. Maximum inorganic concentrations were 0.8 μg/L in runoff and 2.3 x 10^{-6} μg/L in the Great Miami River for Arsenic. Except for phenanthrene, all organics in runoff were predicted to remain below 3.4 x 10^{-3} μg/L and below 9.6 x 10^{-9} μg/L in the Great Miami River. Phenanthrene, a CPC for which EPA RAGs, Part B screening concentration is not available, is predicted to be at a concentration of 55 μg/L in runoff and 1.6 x 10^{-4} μg/L in the Great Miami River. These concentrations remain only through the duration of the storm.

Modeled sediment concentrations resulting from a single runoff event are comparable to the source term soil concentrations for the Solid Waste Landfill ~~because sediment mixing and desorption in Paddys Run were not considered~~. For example, the modeled sediment concentration for uranium-238 was 229.7 mg/kg compared to 230 mg/kg in the soil source term. ~~Sediment concentrations would be expected to decrease following the rainfall event because of dispersion through sediment transport, gradual mixing with sediment from other sources, and leaching of constituents in Paddys Run.~~

A.1.5.2 Lime Sludge Ponds

The Lime Sludge Ponds are contained within soil berms that contain storm water and therefore were not considered a source of contaminants to the surface waters. No surface water pathway modeling was conducted.

A.1.5.3 Inactive Flyash Pile

NO A-47

~~Table A.1-3~~ Tables A.1-3A and A.1-3B presents the results of surface water modeling ~~of~~ for the Inactive Flyash Pile, based on a designated single storm event using the MUSLE model and loading from seeps in the Inactive Flyash Pile during the storm event. ~~Modeling results show low surface water concentrations in Paddys Run from the Inactive Flyash Pile, usually much less than parts per billion. For radionuclides, concentrations in the Paddys Run range from a minimum of a 2.4 x 10^{-5} pCi/L for cesium-137 to a maximum of 0.66 pCi/L for uranium-238.~~ Table A.1-3A also shows the screening of CPCs based on a comparison of on-subunit runoff concentration against the EPA RAGs, Part B based screening concentrations for water. A total runoff of 29.1 m^3 was calculated during the 24-hour storm event. For radionuclides, on-subunit surface water concentrations range from a minimum of a 8.1 x 10^{-3} pCi/L for cesium-137 (below the screening concentration for cesium-137) to

TABLE A.1-3A

RUNOFF EFFLUENT AND SEDIMENT LOADING FROM THE INACTIVE FLYASH PILE OPERABLE UNIT 2 REMEDIAL INVESTIGATION FERNALD ENVIRONMENTAL MANAGEMENT PROJECT

Constituent of Potential Concern After Initial Screening	Partition Coefficient K_d (mL/g)	Waste Area Surface Soil Concentration Ci (mg/kg)	Total Annual Loading to Stream Tl (g)	Seep Concentration (pCi/L RAD) (μg/L non-RAD)	Sediment Concentration Cs (mg/kg)	Runoff Effluent Concentration Ce (pCi/L RAD) (μg/L non-RAD)	On-Subunit Surface Water Concentration (pCi/L RAD) (μg/L non-RAD)	Screening Concentration (pCi/L RAD) (μg/L non-RAD)	Final CPC For On-Subunit Runoff Water (Y/N)
INORGANICS									
Arsenic	$2.00 \times 10^{+2}$	$3.32 \times 10^{+1}$	4.56×10^{-1}	$1.40 \times 10^{+0}$	$3.32 \times 10^{+1}$	$3.92 \times 10^{+0}$	$3.23 \times 10^{+0}$	1.46×10^{-3}	Yes
Beryllium	$2.50 \times 10^{+2}$	$2.27 \times 10^{+0}$	2.50×10^{-3}	ND[a]	$2.27 \times 10^{+0}$	2.14×10^{-1}	1.56×10^{-1}	2.37×10^{-4}	Yes
Lead	$3.80 \times 10^{+1}$	$2.39 \times 10^{+1}$	1.72×10^{-8}	$8.30 \times 10^{+0}$	$2.38 \times 10^{+1}$	$1.48 \times 10^{+1}$	1.30×10^{-11}	NA[b]	NA
ORGANICS									
2-Methylnaphthalene	$3.67 \times 10^{+1}$	1.6×10^{-1}	5.05×10^{-1}	ND	1.59×10^{-1}	4.34×10^{-10}	3.15×10^{-10}	NA	NA
Dibenzo(a,h)anthracene	$1.70 \times 10^{+3}$	$2.20 \times 10^{+0}$	3.56×10^{-3}	ND	$2.20 \times 10^{+0}$	3.06×10^{-2}	2.22×10^{-2}	2.82×10^{-4}	Yes
RADIONUCLIDES									
Cesium-137	$1.37 \times 10^{+3}$	7.41×10^{-9}	1.49×10^{-11}	ND	7.41×10^{-9}	1.11×10^{-2}	8.07×10^{-3}	1.07×10^{-1}	No
Neptunium-237	$5.00 \times 10^{+0}$	1.94×10^{-4}	1.03×10^{-4}	7.90×10^{-1}	1.87×10^{-4}	6.26×10^{-1}	6.71×10^{-1}	2.16×10^{-4}	Yes
Plutonium-238	$1.00 \times 10^{+2}$	4.74×10^{-9}	1.30×10^{-10}	$2.91 \times 10^{+0}$	4.73×10^{-9}	1.91×10^{-2}	8.08×10^{-1}	2.16×10^{-2}	Yes
Plutonium-239/240	$1.00 \times 10^{+2}$	3.38×10^{-7}	9.28×10^{-9}	2.00×10^{-1}	3.37×10^{-7}	4.95×10^{-3}	5.82×10^{-2}	2.07×10^{-4}	Yes
Radium-226	$1.06 \times 10^{+2}$	2.00×10^{-6}	5.20×10^{-8}	1.48×10^{-1}	2.00×10^{-6}	4.40×10^{-1}	3.60×10^{-1}	1.76×10^{-4}	Yes
Radium-228	$1.06 \times 10^{+2}$	8.24×10^{-9}	2.14×10^{-10}	ND	8.23×10^{-9}	4.99×10^{-1}	3.63×10^{-1}	4.75×10^{-2}	Yes
Strontium-90	$1.06 \times 10^{+2}$	6.35×10^{-9}	1.64×10^{-10}	ND	6.34×10^{-9}	1.94×10^{-1}	1.41×10^{-1}	1.32×10^{-1}	Yes
Thorium-228	$3.20 \times 10^{+3}$	3.30×10^{-9}	2.84×10^{-12}	ND	3.30×10^{-9}	2.00×10^{-2}	1.45×10^{-2}	8.64×10^{-2}	No
Thorium-230	$3.20 \times 10^{+3}$	1.34×10^{-4}	1.15×10^{-7}	6.53×10^{-1}	1.34×10^{-4}	2.04×10^{-2}	1.93×10^{-1}	3.65×10^{-1}	No
Thorium-232	$3.20 \times 10^{+3}$	$2.12 \times 10^{+1}$	1.82×10^{-2}	ND	$2.12 \times 10^{+1}$	1.72×10^{-2}	1.25×10^{-2}	2.79×10^{-3}	No

See footnotes at end of table

FER\CRU2RI\APP-A\TABA-1.3A\June 6, 1994 2:50pm

000059

5659

TABLE A.1-3A
(Continued)

Constituent of Potential Concern After Initial Screening	Partition Coefficient K_d (mL/g)	Waste Area Surface Soil Concentration Ci (mg/kg)	Total Annual Loading to Stream Tl (g)	Seep Concentration (pCi/L RAD) (μg/L non-RAD)	Sediment Concentration Cs (mg/kg)	Runoff Effluent Concentration Ce (pCi/L RAD) (μg/L non-RAD)	On-Subunit Surface Water Concentration (pCi/L RAD) (μg/L non-RAD)	Screening Concentration (pCi/L RAD) (μg/L non-RAD)	Final CPC For On-Subunit Runoff Water (Y/N)
RADIONUCLIDES (Continued)									
Uranium-234	$1.48 \times 10^{+0}$	1.39×10^{-3}	2.31×10^{-3}	$2.65 \times 10^{+2}$	1.24×10^{-3}	$1.24 \times 10^{+2}$	$1.63 \times 10^{+2}$	2.97×10^{-1}	Yes
Uranium-235/236	$1.48 \times 10^{+0}$	2.79×10^{-1}	4.64×10^{-1}	$1.40 \times 10^{+1}$	2.50×10^{-1}	$8.60 \times 10^{+0}$	$1.10 \times 10^{+1}$	2.97×10^{-1}	Yes
Uranium-238	$1.48 \times 10^{+0}$	$2.64 \times 10^{+1}$	$4.40 \times 10^{+1}$	$2.57 \times 10^{+2}$	$2.36 \times 10^{+1}$	$1.27 \times 10^{+2}$	$1.62 \times 10^{+2}$	1.70×10^{-1}	Yes
Uranium-Total (non-RAD)	$1.48 \times 10^{+0}$	$2.62 \times 10^{+1}$	$4.36 \times 10^{+1}$	$8.20 \times 10^{+2}$	$2.34 \times 10^{+1}$	$3.74 \times 10^{+2}$	$4.96 \times 10^{+2}$	$1.09 \times 10^{+1}$	Yes

[a]ND = Not detected
[b]NA = EPA RAGs, Part B screening value could not be calculated.

Other Comment No. A-47

5659

TABLE A.1-3B

CONTAINMENT LOADING TO THE GREAT MIAMI RIVER FROM THE INACTIVE FLYASH PILE
OPERABLE UNIT 2 REMEDIAL INVESTIGATION
FERNALD ENVIRONMENTAL MANAGEMENT PROJECT

Constituent of Potential Concern For On-Subunit Runoff	On-Subunit Surface Water Concentration (pCi/L RAD) (µg/L non-RAD)	Concentration in Paddys Run during Storm Event Cw (pCi/L RAD) (µg/L non-RAD)	Great Miami River Concentration Cgmr (pCi/L Rad) (µg/L Non-Rad)
INORGANICS			
Arsenic	$3.23 \times 10^{+0}$	1.31×10^{-2}	1.59×10^{-5}
Beryllium	1.56×10^{-1}	6.32×10^{-4}	7.64×10^{-7}
Lead	$1.30 \times 10^{+1}$	5.29×10^{-2}	6.40×10^{-5}
ORGANICS			
2 - Methylnaphthalene	$3.15 \times 10^{+0}$	1.28×10^{-2}	1.54×10^{-5}
Dibenzo(a,h)anthracene	2.22×10^{-2}	9.02×10^{-5}	1.09×10^{-7}
RADIONUCLIDES			
Neptunium-237	6.71×10^{-1}	2.73×10^{-3}	3.32×10^{-6}
Plutonium-238	8.08×10^{-1}	3.30×10^{-3}	3.99×10^{-6}
Plutonium-239/240	5.82×10^{-2}	2.37×10^{-4}	2.87×10^{-7}
Radium-226	3.60×10^{-1}	1.46×10^{-3}	1.77×10^{-6}
Radium-228	3.63×10^{-1}	1.47×10^{-3}	1.78×10^{-6}
Strontium-90	1.41×10^{-1}	5.71×10^{-4}	6.90×10^{-7}
Uranium-234	$1.63 \times 10^{+2}$	6.65×10^{-1}	8.06×10^{-4}
Uranium-235/236	$1.01 \times 10^{+1}$	4.10×10^{-2}	4.96×10^{-5}
Uranium-238	$1.62 \times 10^{+2}$	6.65×10^{-1}	8.06×10^{-4}
Uranium-Total (non-RAD)	$4.96 \times 10^{+2}$	$2.02 \times 10^{+0}$	2.44×10^{-3}

Other Comment No. A-47

a maximum of 163 pCi/L for uranium-234. For CPCs above screening concentrations, radionuclide concentrations ~~Concentrations of radionuclides~~ in the Great Miami River range from a low of ~~2.8 x 10^{-8}~~ 2.9 x 10^{-7} pCi/L for ~~cesium-137~~ plutonium-239/240 to a high of 8.0 x 10^{-4} pCi/L for uranium-~~238~~234. All inorganics and organics were predicted to remain below ~~0.37~~ 13 μg/L in ~~Paddys Run~~ on-subunit surface water and ~~4.5 x 10^{-4}~~ 6.4 x 10^{-5} in the Great Miami River. These concentrations remain only through the duration of the storm.

Modeled sediment concentrations resulting from a single runoff event are comparable to the source term soil concentrations for the Inactive Flyash Pile ~~because sediment mixing and desorption in Paddys Run were not considered~~. For example, the modeled uranium-238 sediment concentration was 23.6 mg/kg compared to 26.4 mg/kg in the surface soil source term. ~~Sediment concentrations would be expected to decrease following the rainfall event because of dispersion through sediment transport, gradual mixing with sediment from other sources, and leaching of constituents in Paddys Run.~~

A.1.5.4 South Field

NO. A-47

~~Table A.1-4 presents the results of surface water modeling from the South Field based on a designated single storm event using the MUSLE model. Modeling results showed low surface water concentrations in Paddys Run from the South Field, usually much less than parts per billion. For radionuclides, concentrations in Paddys Run range from a low of 1.7 x 10^{-4} pCi/L for cesium 137 to a high of 412 pCi/L for technetium 99. Concentrations of radionuclides in the Great Miami River ranged from 2.1 x 10^{-7} pCi/L for cesium 137 to 0.51 pCi/L for technetium 99. Modeled uranium 238 concentrations were 3.7 pCi/L and 4.5 x 10^{-3} pCi/L for Paddys Run and the Great Miami River, respectively. All inorganics were predicted to be below 2.4 μg/L in Paddys Run and below 2.9 x 10^{-3} μg/L in the Great Miami River. All organics were predicted to be below 0.56 μg/L and 6.9 x 10^{-4} μg/L, in Paddys Run and the Great Miami River, respectively. These concentrations remain only through the duration of the storm.~~

Tables A.1-4A and A.1-4B present the results of surface water modeling from the South Field based on a designated single storm event using the MUSLE model. Table A.1-4A also shows the screening of CPCs based on a comparison of on-subunit runoff concentrations against the EPA RAGs, Part B based screening concentrations for water. A total runoff of 192 m^3 was calculated during the 24-hour storm event. Modeling results showed that on-subunit surface water radionuclide concentrations range

TABLE A.1-4A

RUNOFF EFFLUENT AND SEDIMENT LOADING FROM THE SOUTH FIELD OPERABLE UNIT 2 REMEDIAL INVESTIGATION FERNALD ENVIRONMENTAL MANAGEMENT PROJECT

Constituent of Potential Concern After Initial Screening	Partition Coefficient K_d (mL/g)	Waste Area Surface Soil Concentration Ci (mg/kg)	Total Annual Loading to Stream Tl (g)	Seep Concentration (pCi/L RAD) (μg/L non-RAD)	Sediment Concentration Cs (mg/kg)	Runoff Effluent Concentration Ce (pCi/L RAD) (μg/L non-RAD)	On-Subunit Surface Water Concentration pCi/L Rad μg/L non-RAD	Screening Concentration (pCi/L RAD) (μg/L non-RAD)	Final CPC For On-Subunit Runoff Water (Y/N)
INORGANICS									
Arsenic	$2.00 \times 10^{+2}$	$7.27 \times 10^{+0}$	6.80×10^{-1}	ND[a]	$7.27 \times 10^{+0}$	8.81×10^{-1}	6.84×10^{-1}	1.46×10^{-4}	Yes
Beryllium	$2.50 \times 10^{+2}$	9.42×10^{-1}	7.04×10^{-2}	ND	9.42×10^{-1}	9.14×10^{-2}	7.09×10^{-2}	2.37×10^{-4}	Yes
Lead	$3.80 \times 10^{+1}$	$2.46 \times 10^{+1}$	$1.21 \times 10^{+1}$	ND	$2.45 \times 10^{+1}$	$1.57 \times 10^{+1}$	$1.22 \times 10^{+1}$	NA[b]	NA
ORGANICS									
Aroclor-1254	$1.95 \times 10^{+3}$	8.90×10^{-2}	8.52×10^{-4}	ND	8.90×10^{-2}	1.11×10^{-3}	8.62×10^{-4}	1.10×10^{-3}	No
Aroclor-1260	$2.35 \times 10^{+3}$	5.20×10^{-2}	4.12×10^{-4}	ND	5.20×10^{-2}	5.37×10^{-4}	4.17×10^{-4}	1.10×10^{-3}	No
Benzo(a)anthracene	$7.28 \times 10^{+2}$	$5.50 \times 10^{+0}$	1.41×10^{-1}	ND	$5.50 \times 10^{+0}$	1.83×10^{-1}	1.42×10^{-1}	2.82×10^{-3}	Yes
Benzo(a)pyrene	$1.74 \times 10^{+3}$	$9.40 \times 10^{+0}$	1.01×10^{-1}	ND	$9.40 \times 10^{+0}$	1.31×10^{-1}	1.02×10^{-1}	2.82×10^{-4}	Yes
Benzo(b)fluoranthene	$6.77 \times 10^{+3}$	$6.20 \times 10^{+0}$	1.71×10^{-2}	ND	$6.20 \times 10^{+0}$	2.22×10^{-2}	1.72×10^{-2}	2.82×10^{-3}	Yes
Benzo(k)fluoranthene	$1.26 \times 10^{+4}$	$7.30 \times 10^{+0}$	1.08×10^{-2}	ND	$7.30 \times 10^{+0}$	1.41×10^{-2}	1.09×10^{-2}	2.82×10^{-2}	No
Benzo(g,h,i)perylene	$9.88 \times 10^{+3}$	$6.2 \times 10^{+0}$	4.82×10^{-1}	ND	$6.20 \times 10^{+0}$	6.28×10^{-1}	4.87×10^{-1}	NA	NA
Dibenzo(a,h)anthracene	$1.70 \times 10^{+3}$	$1.90 \times 10^{+0}$	2.09×10^{-2}	ND	$1.90 \times 10^{+0}$	2.71×10^{-2}	2.10×10^{-2}	2.82×10^{-4}	Yes
Dieldrin	$5.75 \times 10^{+0}$	9.70×10^{-3}	3.10×10^{-2}	ND	9.55×10^{-3}	4.03×10^{-3}	3.13×10^{-2}	1.12×10^{-4}	Yes
Indeno(1,2,3-cd)pyrene	$8.32 \times 10^{+4}$	$6.00 \times 10^{+0}$	1.35×10^{-3}	ND	$6.00 \times 10^{+0}$	1.75×10^{-3}	1.36×10^{-3}	2.82×10^{-3}	No
Phenanthrene	$1.17 \times 10^{+1}$	$2.30 \times 10^{+0}$	$1.50 \times 10^{+1}$	ND	$2.30 \times 10^{+0}$	$1.95 \times 10^{+2}$	$1.51 \times 10^{+2}$	NA	NA

See footnote at end of table

FER\CRU2RI\APP-A\TABA-1.4A\June 6, 1994 2:50pm

000063

5659

TABLE A.1-4A
(Continued)

Constituent of Potential Concern After Initial Screening	Partition Coefficient K_d (mL/g)	Waste Area Surface Soil Concentration Ci (mg/kg)	Total Annual Loading to Stream Tl (g)	Seep Concentration (pCi/L RAD) (μg/L non-RAD)	Sediment Concentration Cs (mg/kg)	Runoff Effluent Concentration Ce (pCi/L RAD) (μg/L non-RAD)	On-Subunit Surface Water Concentration pCi/L Rad μg/L non-RAD	Screening Concentration (pCi/L RAD) (μg/L non-RAD)	Final CPC For On-Subunit Runoff Water (Y/N)
RADIONUCLIDES									
Cesium-137	$1.37 \times 10^{+3}$	5.77×10^{-9}	7.88×10^{-11}	ND	5.77×10^{-9}	8.84×10^{-3}	6.86×10^{-3}	1.70×10^{-1}	No
Neptunium-237	$5.00 \times 10^{+0}$	3.04×10^{-4}	1.11×10^{-3}	ND	2.98×10^{-4}	$1.03 \times 10^{+0}$	8.00×10^{-1}	2.16×10^{-2}	Yes
Plutonium-238	$1.00 \times 10^{+2}$	6.78×10^{-9}	1.27×10^{-9}	ND	6.77×10^{-9}	2.81×10^{-4}	2.18×10^{-2}	2.16×10^{-2}	Yes
Plutonium-239/240	$1.00 \times 10^{+2}$	1.22×10^{-6}	2.28×10^{-7}	ND	1.22×10^{-6}	1.84×10^{-2}	1.43×10^{-2}	2.07×10^{-2}	No
Radium-226	$1.06 \times 10^{+2}$	3.11×10^{-5}	5.48×10^{-6}	ND	3.11×10^{-5}	$7.03 \times 10^{+0}$	$5.46 \times 10^{+0}$	1.76×10^{-4}	Yes
Radium-228	$1.06 \times 10^{+2}$	1.43×10^{-8}	2.52×10^{-9}	ND	1.43×10^{-8}	8.89×10^{-1}	6.90×10^{-1}	4.75×10^{-4}	Yes
Strontium-90	$2.50 \times 10^{+0}$	1.17×10^{-9}	8.46×10^{-9}	ND	1.13×10^{-9}	$1.50 \times 10^{+0}$	$1.16 \times 10^{+0}$	1.32×10^{-1}	Yes
Technetium-99	7.00×10^{-2}	8.35×10^{-3}	9.72×10^{-1}	ND	3.64×10^{-3}	$2.15 \times 10^{+4}$	$1.67 \times 10^{+4}$	$3.65 \times 10^{+0}$	Yes
Thorium-228	$3.20 \times 10^{+3}$	5.38×10^{-9}	3.14×10^{-11}	ND	5.38×10^{-9}	3.34×10^{-2}	2.59×10^{-2}	8.64×10^{-2}	No
Thorium-230	$3.20 \times 10^{+3}$	6.70×10^{-4}	3.91×10^{-6}	ND	6.70×10^{-4}	1.05×10^{-1}	8.15×10^{-2}	3.65×10^{-1}	No
Thorium-232	$3.20 \times 10^{+3}$	$3.63 \times 10^{+1}$	2.12×10^{-4}	ND	$3.63 \times 10^{+1}$	3.03×10^{-2}	2.35×10^{-2}	2.79×10^{-2}	No
Uranium-234	$1.48 \times 10^{+0}$	1.39×10^{-3}	1.65×10^{-2}	$1.59 \times 10^{+2}$	1.31×10^{-3}	$1.34 \times 10^{+2}$	$1.40 \times 10^{+2}$	2.97×10^{-1}	Yes
Uranium-235/236	$1.48 \times 10^{+0}$	4.11×10^{-1}	$4.89 \times 10^{+0}$	$7.47 \times 10^{+0}$	3.88×10^{-1}	$1.37 \times 10^{+1}$	$1.23 \times 10^{+1}$	2.97×10^{-1}	Yes
Uranium-238	$1.48 \times 10^{+0}$	$2.77 \times 10^{+1}$	$3.30 \times 10^{+2}$	$1.74 \times 10^{+2}$	$2.61 \times 10^{+1}$	$1.44 \times 10^{+2}$	$1.51 \times 10^{+2}$	1.7×10^{-1}	Yes
Uranium-Total (non-RAD)	$1.48 \times 10^{+0}$	$2.96 \times 10^{+1}$	$3.52 \times 10^{+2}$	$4.87 \times 10^{+2}$	$2.79 \times 10^{+1}$	$4.57 \times 10^{+2}$	$4.64 \times 10^{+2}$	1.09×10^{-2}	Yes

[a]ND = Not detected
[b]NA = EPA RAGs, Part B screening values could not be calculated.
Other Comment No. A-47

See footnote at end of table

FER\CRU2RI\APP-A\TABA-1.4A\June 6, 1994 2:50pm

TABLE A.1-4B

CONTAMINANT LOADING TO THE GREAT MIAMI RIVER FROM THE SOUTH FIELD
OPERABLE UNIT 2 REMEDIAL INVESTIGATION
FERNALD ENVIRONMENTAL MANAGEMENT PROJECT

Constituent of Potential Concern for On-Subunit Runoff	On-Subunit Surface Water Concentration (pCi/g RAD) (μg/L non-RAD)	Concentration in Paddys Run during Storm Event Cw (pCi/L RAD) (μg/L non-RAD)	Great Miami River Concentration Cgmr (pCi/L RAD (μg/L non-RAD)
INORGANICS			
Arsenic	6.84×10^{-1}	1.69×10^{-2}	2.08×10^{-5}
Beryllium	7.09×10^{-2}	1.75×10^{-3}	2.15×10^{-6}
Lead	$1.22 \times 10^{+1}$	3.01×10^{-1}	3.69×10^{-4}
ORGANICS			
Benzo(a)anthracene	1.42×10^{-1}	3.52×10^{-3}	4.32×10^{-6}
Benzo(a)pyrene	1.02×10^{-1}	2.52×10^{-3}	3.09×10^{-6}
Benzo(b)fluoranthene	1.72×10^{-2}	4.26×10^{-4}	5.24×10^{-7}
Benzo(g,h,i)perylene	4.87×10^{-1}	1.21×10^{-2}	1.48×10^{-5}
Dibenzo(a,h)anthracene	2.10×10^{-2}	5.20×10^{-4}	6.39×10^{-7}
Dieldrin	3.13×10^{-2}	7.73×10^{-4}	9.50×10^{-7}
Phenantarene	$1.51 \times 10^{+2}$	$3.75 \times 10^{+0}$	4.61×10^{-3}
RADIONUCLIDES			
Neptunium-237	8.00×10^{-1}	1.96×10^{-2}	2.41×10^{-5}
Plutonium-238	2.18×10^{-2}	5.39×10^{-4}	6.63×10^{-7}
Radium-226	$5.46 \times 10^{+0}$	1.35×10^{-1}	1.66×10^{-4}
Radium-228	6.90×10^{-1}	1.71×10^{-2}	2.10×10^{-5}
Strontium-90	$1.16 \times 10^{+0}$	2.88×10^{-2}	3.54×10^{-3}
Technetium-99	$1.67 \times 10^{+4}$	$4.12 \times 10^{+2}$	5.06×10^{-1}

TABLE A.1-4B
(Continued)

Constituent of Potential Concern for On-Subunit Runoff	On-Subunit Surface Water Concentration (pCi/g RAD) (μg/L non-RAD)	Concentration in Paddys Run during Storm Event Cw (pCi/L RAD) (μg/L non-RAD)	Great Miami River Concentration Cgmr (pCi/L RAD (μg/L non-RAD)
RADIONUCLIDES (Continued)			
Uranium-234	$1.40 \times 10^{+2}$	$3.44 \times 10^{+0}$	4.17×10^{-3}
Uranium-235/236	$1.23 \times 10^{+1}$	3.03×10^{-1}	3.65×10^{-4}
Uranium-238	$1.51 \times 10^{+2}$	$3.72 \times 10^{+0}$	4.51×10^{-3}
Uranium-Total (non-RAD)	$4.64 \times 10^{+2}$	$1.15 \times 10^{+1}$	1.39×10^{-2}

Other Comment No. A-47

from a low of 6.9×10^{-3} pCi/L for cesium-137 to a high of $1.7 \times 10^{+4}$ pCi/L for technetium-99. For some radionuclides, like cesium-137, predicted on-subunit surface water concentrations are below the screening concentrations. For the remaining radionuclide CPCs, concentrations in the Great Miami River ranged from 6.6×10^{-7} pCi/L for plutonium-238 to 0.51 pCi/L for technetium-99. Modeled uranium-238 concentrations were 151 pCi/L and 4.5×10^{-3} pCi/L for on-subunit surface water and the Great Miami River, respectively. All inorganics were predicted to be below 12.2 μg/L in on-subunit surface water and below 3.7×10^{-4} μg/L in the Great Miami River. Phenanthrene was predicted to be at 151 μg/L in on-subunit surface water and 4.7×10^{-3} μg/L in the Great Miami River. Other organics were predicted to be below 0.49 μg/L and 1.5×10^{-5} μg/L, in on-subunit surface water and the Great Miami River, respectively. These concentrations remain only through the duration of the storm.

Modeled sediment concentrations resulting from a single runoff event are comparable to the source term soil concentrations for the South Field ~~because sediment mixing and desorption in Paddys Run were not considered~~. For example, the modeled uranium-238 sediment concentration was 26.1 mg/kg compared to 27.7 mg/kg in the soil source term. ~~Sediment concentrations would be expected to decrease following the rainfall event because of dispersion through sediment transport, gradual mixing with sediment from other sources, and leaching of constituents in Paddys Run.~~

A.1.5.5 Active Flyash Pile

NO. A-47

~~Table A.1-5~~ Tables A.1-5A and A.1-5B presents the results of surface water modeling from the Active Flyash Pile based on a single storm event using the MUSLE model. Table A.1-5A also shows the screening of CPCs based on a comparison of on-subunit runoff concentrations against the EPA RAGs, Part B based screening concentrations for water. A total runoff of 285.5 m^3 was calculated during the 24-hour storm event. No dilution of runoff concentrations was assumed in the Storm Sewer Outfall Ditch. Therefore, runoff concentration and the Storm Sewer Outfall Ditch concentrations are modeled to be equal. This is a very conservative assumption since during the storm event, it is likely that runoff from the east side of the Storm Sewer Outfall Ditch and upgradient of the Active Flyash Pile will also drain into the Storm Sewer Outfall Ditch. ~~The model shows that the mass of constituents that partition into the water would result in maximum surface water concentrations of 300 μg/L in the Storm Sewer Outfall Ditch (Table A.1-5). No dilution of runoff concentration was assumed in the Storm Sewer Outfall Ditch. This is a very conservative assumption since during the storm event, it is likely that runoff from the east side of the Storm Sewer~~

TABLE A.1-5A

RUNOFF EFFLUENT AND SEDIMENT LOADING FROM THE ACTIVE FLYASH PILE OPERABLE UNIT 2 REMEDIAL INVESTIGATION FERNALD ENVIRONMENTAL MANAGEMENT PROJECT

Constituent of Potential Concern After Initial Screening	Partition Coefficient K_d (mL/g)	Waste Area Surface Soil Concentration Ci (mg/kg)	Total Annual Loading to Stream Tl (g)	Runoff Sediment Concentration Cs (mg/kg)	On-Subunit Runoff Effluent or Storm Sewer Outfall Ditch Concentration Ce (pCi/L RAD) (μg/L non-RAD)	Screening Concentration (pCi/L RAD) (μg/L non-RAD)	Final CPC For On-Subunit Runoff Water (Y/N)
INORGANICS							
Arsenic	$2.00 \times 10^{+2}$	$8.98 \times 10^{+1}$	$1.21 \times 10^{+1}$	$8.97 \times 10^{+1}$	$1.06 \times 10^{+1}$	1.46×10^{-4}	Yes
Beryllium	$2.50 \times 10^{+2}$	$4.67 \times 10^{+0}$	5.04×10^{-1}	$4.67 \times 10^{+0}$	4.41×10^{-1}	2.37×10^{-4}	Yes
Lead	$3.80 \times 10^{+1}$	$5.54 \times 10^{+1}$	$3.89 \times 10^{+1}$	$5.48 \times 10^{+1}$	$3.40 \times 10^{+1}$	NA[a]	NA
Thallium	$1.50 \times 10^{+3}$	$2.66 \times 10^{+0}$	4.76×10^{-2}	$2.66 \times 10^{+0}$	4.19×10^{-2}	2.55×10^{-1}	No
RADIONUCLIDES							
Neptunium-237	$5.00 \times 10^{+0}$	7.77×10^{-3}	4.08×10^{-2}	7.51×10^{-3}	$2.51 \times 10^{+1}$	2.16×10^{-2}	Yes
Plutonium-238	$1.00 \times 10^{+2}$	4.22×10^{-8}	1.14×10^{-8}	4.21×10^{-8}	1.70×10^{-1}	2.16×10^{-2}	Yes
Plutonium-239/240	$1.00 \times 10^{+2}$	5.32×10^{-6}	1.43×10^{-6}	5.31×10^{-6}	7.79×10^{-2}	2.07×10^{-2}	Yes
Radium-226	$1.06 \times 10^{+2}$	4.66×10^{-6}	1.18×10^{-6}	4.65×10^{-6}	$1.02 \times 10^{+0}$	1.76×10^{-4}	Yes
Radium-228	$1.06 \times 10^{+2}$	1.17×10^{-8}	2.98×10^{-9}	1.17×10^{-8}	7.08×10^{-1}	4.75×10^{-2}	Yes
Strontium-90	$1.06 \times 10^{+2}$	3.26×10^{-8}	8.28×10^{-9}	3.26×10^{-8}	9.94×10^{-1}	1.32×10^{-1}	Yes
Thorium-228	$3.20 \times 10^{+3}$	4.65×10^{-9}	3.92×10^{-11}	4.65×10^{-9}	2.81×10^{-4}	8.64×10^{-2}	No
Thorium-230	$3.20 \times 10^{+3}$	1.78×10^{-4}	1.50×10^{-6}	1.78×10^{-4}	2.71×10^{-2}	3.65×10^{-1}	No
Thorium-232	$3.20 \times 10^{+3}$	$2.42 \times 10^{+1}$	2.04×10^{-1}	$2.42 \times 10^{+1}$	1.97×10^{-3}	2.79×10^{-2}	No
Uranium-234	$1.48 \times 10^{+0}$	5.79×10^{-4}	9.44×10^{-3}	5.18×10^{-4}	$5.14 \times 10^{+1}$	2.97×10^{-1}	Yes
Uranium-235/236	$1.48 \times 10^{+0}$	7.42×10^{-2}	$1.21 \times 10^{+0}$	6.64×10^{-2}	$2.29 \times 10^{+0}$	2.97×10^{-1}	Yes
Uranium-238	$1.48 \times 10^{+0}$	$1.07 \times 10^{+1}$	$1.74 \times 10^{+2}$	$9.57 \times 10^{+0}$	$5.13 \times 10^{+1}$	1.70×10^{-1}	Yes
Uranium-Total (non-RAD)	$1.48 \times 10^{+0}$	$1.26 \times 10^{+1}$	$2.05 \times 10^{+2}$	$1.13 \times 10^{+1}$	$1.80 \times 10^{+2}$	$1.09 \times 10^{+1}$	Yes

[a]NA = EPA RAGs, Part B Screening Value could not be calculated.

Other Comment No. A-47

FER\CRU2RI\TLC\APP-A\TABA-1.5a\June 6, 1994 2:51pm

TABLE A.1-5B

CONTAMINANT LOADING TO THE GREAT MIAMI RIVER FROM THE ACTIVE FLYASH PILE OPERABLE UNIT 2 REMEDIAL INVESTIGATION FERNALD ENVIRONMENTAL MANAGEMENT PROJECT

Constituent of Potential Concern for On-Subunit Runoff	On-Subunit Runoff Effluent or Storm Sewer Outfall Ditch Concentration Ce (pCi/L Rad) (ug/L non-Rad)	Paddys Run Concentration during Storm Event Cw (pCi/L RAD) (μg/L non-RAD)	Great Miami River Concentration Cgmr (pCi/L RAD) (μg/L non-RAD)
INORGANICS			
Arsenic	$1.06 \times 10^{+1}$	1.32×10^{-1}	1.60×10^{-4}
Beryllium	4.41×10^{-1}	5.40×10^{-3}	6.67×10^{-6}
Lead	$3.40 \times 10^{+1}$	4.25×10^{-1}	5.15×10^{-4}
RADIONUCLIDES			
Neptunium-237	$2.51 \times 10^{+1}$	3.13×10^{-1}	3.79×10^{-4}
Plutonium-238	1.70×10^{-1}	2.12×10^{-3}	2.57×10^{-6}
Plutonium-239/240	7.79×10^{-2}	9.74×10^{-4}	1.18×10^{-6}
Radium-226	$1.02 \times 10^{+0}$	1.28×10^{-2}	1.55×10^{-5}
Radium-228	7.08×10^{-1}	8.84×10^{-3}	1.07×10^{-5}
Strontium-90	9.94×10^{-1}	1.24×10^{-2}	1.50×10^{-5}
Uranium-234	$5.14 \times 10^{+1}$	6.43×10^{-1}	7.78×10^{-4}
Uranium-235/236	$2.29 \times 10^{+0}$	2.86×10^{-2}	3.46×10^{-5}
Uranium-238	$5.13 \times 10^{+1}$	6.41×10^{-1}	7.77×10^{-4}
Uranium-Total (non-RAD)	$1.80 \times 10^{+2}$	$2.25 \times 10^{+0}$	2.72×10^{-3}

Other Comment No. 47

FE[illegible]RU2RI\TLC\APP-A\TABA-1.5b\June8, 1994 9:31am

630000

5659

~~Outfall Ditch and upgradient of the Active Flyash Pile will also drain into the Storm Sewer Outfall Ditch.~~ The amount of runoff contribution to the Storm Sewer Outfall Ditch from the east side of the Storm Sewer Outfall Ditch is estimated to be the same order of magnitude as the runoff from the Active Flyash Pile. However, for modeling purposes, flow from a storm event from the east side of the Storm Sewer Outfall Ditch was assumed to be zero. Although most of the flow in the Storm Sewer Outfall Ditch infiltrates to the Great Miami Aquifer, it was assumed that 44 percent of the flow reaches Paddys Run.

The predicted concentrations of radionuclides from the Active Flyash Pile into the Storm Sewer Outfall Ditch ranged from 2.0 x 10^{-2} pCi/L for thorium-232 to 51.4 pCi/L for uranium-234. Radionuclide concentrations in the Great Miami River were predicted to range between 1.2 x 10^{-7} pCi/L for plutonium-239/240 to 7.8 x 10^{-4} pCi/L for uranium-234 and uranium-238. ~~The maximum organic concentration was for toluene was 2.2 μg/L.~~ For inorganic parameters, the predicted concentrations in runoff and the Storm Sewer Outfall Ditch ranged from ~~4.3~~ 4.2 x 10^{-2} μg/L for thallium to ~~297~~ 34 μg/L for ~~barium~~ lead. Inorganic concentrations in the Great Miami River were predicted to remain below 5.2 x 10^{-4} μg/L. There were no organic CPCs identified for the surface soils from the Active Flyash Pile. These concentrations remain only through the duration of the storm. When rainfall and runoff cease, no surface water is expected in the Storm Sewer Outfall Ditch.

~~The predicted concentrations of radionuclides in the Paddys Run range from 2.5 x 10^{-4} pCi/L for thorium 232 to 0.64 pCi/L for uranium 234 or uranium 238. Radionuclide concentrations in the Great Miami River were predicted to range between 3.0 x 10^{-7} pCi/L for thorium 232 to 7.8 x 10^{-4} pCi/L for uranium 234 or uranium 238. For inorganics and organics, predicted concentrations in the Paddys Run ranged from 5.3 x 10^{-4} μg/L for thallium to 3.7 μg/L for barium. Concentrations of all inorganics and organics in the Great Miami River were predicted to remain below 4.5 x 10^{-3} μg/L. These concentrations remain only through the duration of the storm. When rainfall and runoff cease, no surface water is expected in the Storm Sewer Outfall Ditch.~~

Modeled sediment concentrations resulting from a single runoff event are comparable to the source term soil concentrations for the Active Flyash Pile because sediment mixing was not considered. For example, the modeled uranium-238 sediment concentration was 9.57 mg/kg, compared to 10.7 mg/kg in the soil source term. Sediment concentrations would be expected to decrease downgradient and

following the rainfall event because of dispersion through sediment transport and gradual mixing with sediment from other sources.

Table A.1-6 compares predicted and observed concentrations in the Storm Sewer Outfall Ditch. The modeling results are comparable to analytical results from filtered samples. However, due to a small database for the filtered surface water samples, Table A.1-6 also presents analytical results from unfiltered samples and samples whose filtered/unfiltered status is unknown. Predicted and observed concentrations for the CPCs are on the same order of magnitude, with the exception of ~~barium,~~ lead~~,~~ and total uranium. The model predicts more than ~~an~~ one order of magnitude higher concentrations than the observed data for these two constituents. Comparison to within an order of magnitude is considered acceptable because there are additional FEMP sources to the Storm Sewer Outfall Ditch that were not modeled and surface water samples were not taken during a storm event corresponding to the modeled condition of 2.5 inches of rainfall in 24 hours. Data corresponding to the modeled storm conditions are difficult to obtain and are not available.

NO. A-41

A.1.5.6 Combined Modeling Results

Modeling results indicate that surface water runoff from the Solid Waste Landfill, Inactive Flyash Pile, South Field, and Active Flyash Pile reaches Paddys Run. Table A.1-7 shows the combined effect of all Operable Unit 2 subunits on Paddys Run and the Great Miami River. Combined sediment concentrations in the Paddys Run or the Great Miami Aquifer were not calculated because these combined sediment concentrations were not needed for the baseline risk assessment. For radionuclides, total concentrations in Paddys Run range from a low of ~~2.01×10^{-4}~~ 1.2×10^{-3} pCi/L for ~~cesium-137~~ plutonium-239/240 to a high of 412 pCi/L for technetium-99. Concentrations of radionuclides in the Great Miami River ranged from ~~2.44×10^{-7}~~ 1.5×10^{-6} pCi/L for ~~cesium-137~~ plutonium-239 to ~~4.99×10^{-1}~~ 0.5 pCi/L for technetium-99. All inorganics were predicted to be below ~~27.6~~ 0.8 ug/L in Paddys Run and below ~~3.34×10^{-2}~~ 9.4×10^{-4} ug/L in the Great Miami River. All organics, except phenanthrene, were predicted to be ~~below 5.57×10^{-1}~~ at 3.88 ug/L and ~~6.8×10^{-4}~~ 4.7×10^{-3}~~,~~ ug/L in Paddys run and the Great Miami River, respectively. Combined contaminant loading from all the subunits to Paddys Run and subsequently to the Great Miami Aquifer and the Great Miami River was calculated by adding the contaminant loading from each of the subunits. This was done because all subunit calculations use the same flow rate (includes all runoff flow) in Paddys Run and the Great Miami River.

NO. A-4

TABLE A.1-6

COMPARISON OF MODELED RESULTS TO MEASURED SURFACE WATER CONCENTRATIONS IN THE STORM SEWER OUTFALL DITCH OPERABLE UNIT 2 REMEDIAL INVESTIGATION FERNALD ENVIRONMENTAL MANAGEMENT PROJECT

Constituent of Potential Concern[a]	Units	Modeled Concentrations in SSOD[b,c]	Range of Measured Concentrations in SSOD[d]		
			Filtered	Unfiltered	Unknown
RADIONUCLIDES					
Uranium-234	pCi/L	51.4	15.9	-[e]	-
Uranium-238	pCi/L	51.3	15.9	-	-
Total Uranium	μg/L	180	14-44	14-24	-
INORGANICS					
Lead	μg/L	34.0	-	-	2.2

[a]CPC listed only if measured data were available for comparison

[b]Modeled from surface soil sources in the Active Flyash Pile only

[c]SSOD - Storm Sewer Outfall Ditch

[d]Concentrations in samples from locations ASIT-002, ASIT-006, and ASIT-007

[e]Data not available or all were nondetects

Other Comment No. A-47

565 9

TABLE A.1-7

IMPACT OF ALL OPERABLE UNIT 2 SUBUNITS ON PADDYS RUN AND THE GREAT MIAMI RIVER

Constituent of Potential Concern	Unit	Paddys Run Concentration From					Great Miami River Concentration
		Solid Waste Landfill	Inactive Flyash Pile	South Field	Active Flyash Pile	Total	
INORGANICS							
Arsenic	µg/L	1.91×10^{-3}	1.31×10^{-2}	1.69×10^{-2}	1.32×10^{-1}	1.64×10^{-1}	1.99×10^{-4}
Beryllium	µg/L	3.08×10^{-5}	6.32×10^{-4}	1.75×10^{-3}	5.40×10^{-3}	7.81×10^{-3}	9.46×10^{-6}
Lead	µg/L	3.63×10^{-4}	5.29×10^{-2}	3.01×10^{-1}	4.25×10^{-1}	7.79×10^{-1}	9.43×10^{-4}
ORGANICS							
Benzo(a)anthracene	µg/L	7.98×10^{-6}	–[a]	3.52×10^{-3}	–	3.52×10^{-3}	4.27×10^{-6}
Benzo(a)pyrene	µg/L	3.10×10^{-6}	–	2.52×10^{-3}	–	2.52×10^{-3}	3.05×10^{-6}
2-Methynapthalene	µg/L	–	1.28×10^{-2}	–	–	1.28×10^{-2}	1.55×10^{-5}
Benzo(b)fluoranthene	µg/L	–	–	4.26×10^{-4}	–	4.26×10^{-4}	5.16×10^{-7}
Benzo(g,h,i)peryle	µg/L	1.35×10^{-6}		1.21×10^{-2}		1.21×10^{-2}	1.46×10^{-5}
Dibenzo(a,h)anthracene	µg/L	1.87×10^{-6}	9.02×10^{-5}	5.20×10^{-4}	–	6.12×10^{-4}	7.41×10^{-7}
Dieldrin	µg/L	–	–	7.73×10^{-4}	–	7.73×10^{-4}	9.36×10^{-7}
Ideno(1,2,3-cd)pyrene	µg/L	9.14×10^{-8}	–	–	–	9.14×10^{-8}	1.11×10^{-10}
Phenanathrene	µg/L	1.30×10^{-1}	–	$3.75 \times 10^{+0}$	–	$3.88 \times 10^{+0}$	4.70×10^{-3}
RADIONUCLIDES							
Neptunium-237	pCi/L	1.24×10^{-3}	2.73×10^{-3}	1.96×10^{-2}	3.79×10^{-3}	2.39×10^{-2}	2.90×10^{-3}
Plutonium-238	pCi/L	–	3.30×10^{-3}	5.39×10^{-4}	2.12×10^{-3}	5.96×10^{-3}	7.21×10^{-6}
Plutonium-239/240	pCi/L	–	2.37×10^{-4}	–	9.74×10^{-4}	1.21×10^{-3}	1.47×10^{-6}
Radium-226	pCi/L	1.15×10^{-4}	1.46×10^{-3}	1.35×10^{-1}	1.28×10^{-2}	1.49×10^{-2}	1.81×10^{-4}
Radium-228	pCi/L	1.38×10^{-4}	1.47×10^{-3}	1.71×10^{-2}	8.84×10^{-3}	2.75×10^{-2}	3.33×10^{-5}
Strontium-90	pCi/L	5.43×10^{-3}	5.71×10^{-4}	2.88×10^{-1}	1.24×10^{-3}	3.06×10^{-1}	3.71×10^{-4}
Technetium-99	pCi/L	–	–	$4.12 \times 10^{+2}$	–	$4.12 \times 10^{+2}$	4.99×10^{-1}
Uranium-234	pCi/L	3.22×10^{-3}	6.65×10^{-1}	$3.44 \times 10^{+0}$	6.43×10^{-1}	$4.78 \times 10^{+0}$	5.78×10^{-3}
Uranium-235/236	pCi/L	2.16×10^{-3}	4.10×10^{-2}	3.03×10^{-1}	2.86×10^{-2}	3.75×10^{-1}	4.54×10^{-4}
Uranium-238	pCi/L	5.90×10^{-2}	6.65×10^{-1}	$3.72 \times 10^{+0}$	6.41×10^{-1}	$5.08 \times 10^{+0}$	6.15×10^{-3}
Total Uranium (non-RAD)	µg/L	1.30×10^{-1}	$2.02 \times 10^{+0}$	$1.15 \times 10^{+1}$	$2.25 \times 10^{+0}$	$1.59 \times 10^{+1}$	1.92×10^{-2}

[a]Dash = Not a constituent of potential concern for this subunit. Therefore, surface water concentrations were not calculated.

Other Comment No. A-47

Table A.1-8 compares model predicted and measured concentrations in Paddys Run. Modeled results represent constituent concentrations in the dissolved phase, therefore, the results should only be compared to analytical results from filtered samples. However, due to a small database for the filtered surface water samples, Table A.1-8 also presents analytical results from unfiltered samples and samples whose filtered/unfiltered status is unknown. Table A.1-8 shows that the model predictions are comparable to observed data for uranium isotopes and neptunium-237, and are one to ~~three~~ two orders of magnitude below the observed data for other constituents. ~~This is expected because other up gradient sources to Paddys Run were not included in the model predictions.~~ Comparison to within one to two order(s) of magnitude is considered acceptable because there are additional FEMP sources to the Paddys Run that were not modeled and surface water samples were not taken during a storm event corresponding to the modeled condition of 2.5 inches of rainfall in 24 hours. Data corresponding to the modeled storm conditions are difficult to obtain and are not available.

NO. A-41

A.1.6 UNCERTAINTIES IN THE SURFACE WATER MODEL

The surface water model (like any other model) is a mathematical tool which simplifies the actual situation. Uncertainties in the output from the model are introduced from four primary sources:

- Source Term Uncertainty: Source terms for the modeling were defined based on analytical results from the surface soil samples collected during the RI/FS field investigations. It was assumed that these concentrations are representative of CPC concentrations in the past. Although CPC concentrations in the past may have exceeded the present concentrations, use of the UCL concentration may counter the uncertainties introduced by using analytical results from the RI/FS field investigation. Use of uniform CPC concentration at UCL also introduces a potential for overestimation of contaminant mass.

- Input Parameter Uncertainty: The accuracy of the model prediction is highly dependent on the accuracy of the input parameters. Input parameters such as the SCS runoff curve number, rainfall and runoff factor, soil erodibility factor, slope length and steepness factor, cover factor, etc. are approximate numbers representing the physical characteristics of a given site. The chemical-specific distribution coefficient (Kd) values, used to calculate the fraction of contaminants sorbed to soil particles, are another source of uncertainty.

- Modeling Uncertainty: Any mathematical model representing a physical process tends to be simplified by making approximations and assumptions. The uncertainties in model predictions will increase with increased simplification of the model. Several portions of the surface water model equations consist of empirical equations, which are approximations of actual physical processes.

- Scenario Uncertainty: The assumption that each subunit of Operable Unit 2 acts as a point source contamination will introduce some uncertainty in the model predictions. Wherever

TABLE A.1-8

COMPARISON OF MODELED RESULTS TO MEASURED SURFACE WATER CONCENTRATIONS IN PADDYS RUN OPERABLE UNIT 2 REMEDIAL INVESTIGATION FERNALD ENVIRONMENTAL MANAGEMENT PROJECT

Constituent of Potential Concern[a]	Units	Modeled Concentrations in Paddys Run[b]	Range of Measured Concentrations in Paddys Run[c]		
			Filtered	Unfiltered	Unknown
RADIONUCLIDES					
Neptunium-237	pCi/L	0.02	ND[e]	0.435	ND
Plutonium-238	pCi/L	0.006	ND	0.17	ND
Plutonium-239/240	pCi/L	0.001	ND	0.25-0.266	ND
Strontium-90	pCi/L	0.31	ND	ND	24
Uranium-234	pCi/L	4.78	2.2-3.2	1.42-5.0	3.68-4.26
Uranium-238	pCi/L	5.08	2.8-6.2	1.74-6.8	3.5-3.66
Total Uranium	μg/L	15.9	9-15	4.57-9.0	-[d]
INORGANICS					
Arsenic	μg/L	0.16	38	ND	ND
Lead	μg/L	0.78	ND	ND	6-9

[a]CPC listed only if measured data were available for comparison

[b]Modeled from surface soil sources in the Solid Waste Landfill, South Field, and Inactive Flyash Pile

[c]Concentrations in samples from locations W-11, ASIT-003, IFP-SW-03, and IFP-SW-04

[d]Data not available

[e]ND = Data were all nondetects

Other Comment No. A-47

possible, conservative assumptions were made so that the model can predict worst-case conditions.

A.1.7 LOADING TO THE GREAT MIAMI AQUIFER

A contaminant migration pathway exists into the Great Miami Aquifer from Paddys Run and the Storm Sewer Outfall Ditch because portions of their streambeds contact with the Great Miami Aquifer. As discussed below, a screening procedure and method of deriving the constituent loading to the Great Miami Aquifer from Paddys Run and the Storm Sewer Outfall Ditch were developed to account for the surface water as a source to the groundwater (Section A.2).

A.1.7.1 Screening Procedure

Figure A.1-2 presented the surface water to groundwater transport modeling diagram. This diagram identifies screening steps used to identify the CPCs in the Great Miami Aquifer from surface water loading. Screening consists of comparing predicted constituent concentrations in the Great Miami Aquifer to screening levels. Screening levels have been determined for the Operable Unit 2 CPCs ~~constituents~~ based on ~~a 10^{-7} increased risk for carcinogens and a 0.1 HI for non carcinogens (see Appendix B for the development of screening concentration levels)~~ the EPA RAGs, Part B short equations for water.

NO. A-17

The screening procedure for the Great Miami Aquifer actually consists of two steps. These two steps compare conservative estimates of the Great Miami Aquifer concentrations to the screening levels. If a constituent is still of potential concern after the first two phases, more detailed modeling is performed.

The first step consists of estimating the maximum constituent concentration in the Great Miami Aquifer based on the surface water concentration and dilution in the Great Miami Aquifer resulting only within the width of the streambed (30 feet for Paddys Run and 10 feet for the Storm Sewer Outfall Ditch). Constituents were eliminated from further modeling if their values were below screening levels.

The second step consists of estimating the constituent concentration in the Great Miami Aquifer by the dilution of the surface water concentration in the SWIFT III model grid of 125 feet by 125 feet. If the predicted diluted groundwater concentrations were below screening levels, detailed modeling was

not performed. However, the predicted maximum groundwater concentration predicted in the first step (based on streambed width) was reported as the maximum on-site concentration in the Great Miami Aquifer for that constituent.

The Great Miami Aquifer dilution factor is determined by a mixing equation based on the direct infiltration of 30 percent of the runoff effluent mass in Paddys Run or 100 percent of runoff effluent mass in the Storm Sewer Outfall Ditch, prior to dilution in the stream, into the Great Miami Aquifer as described below.

The predicted theoretical diluted concentration in the Great Miami Aquifer based on mixing of runoff effluent mass with the volume of water in the Great Miami Aquifer flowing in Layer 1 in the cell is:

$$C_{GMA} = (C_e)(V_{rcell})/(V_{rcell} + V_{cell})$$

where

C_{GMA} = Predicted theoretical diluted concentration in the Great Miami Aquifer (mg/L)
V_{cell} = Volume of groundwater in Layer 1 of the Great Miami Aquifer in the average thickness SWIFT cell block along Paddys Run or Storm Sewer Outfall Ditch in close proximity to Operable Unit 2 subunits (ft^3)
V_{rcell} = Runoff volume per SWIFT cell (ft^3/cell)

The volume of water flowing through the SWIFT cell is calculated from:

$$V_{cell} = (W_{PR})(L_{cell})(T)(\phi_{GMA})$$

where

W_{PR} = Average width of dilution area from Paddys Run or the Storm Sewer Outfall Ditch.
L_{cell} = Length of SWIFT cell (125 feet)
T = Thickness of Layer 1 of the Great Miami Aquifer in SWIFT cell (23.8 ft)
ϕ_{GMA} = Effective porosity of the Great Miami Aquifer (25 percent)

For the first screening step, W_{PR} was set to average width of the Paddys Run (30 ft) or the Storm Sewer Outfall Ditch (10 ft). For the second screening step, W_{PR} was set to the width of the SWIFT III model cell (125 ft). The runoff effluent volume per SWIFT cell along Paddys Run or Storm Sewer Outfall Ditch is estimated from:

$$V_{rcell} = (V_r)(I)/(N)$$

where

V_r = Runoff volume from MUSLE based on 24-hour storm event (ft^3/day)
I = Percentage of runoff effluent volume assumed to infiltrate to the Great Miami Aquifer through Paddys Run (30 percent, DOE, 1993d) or Storm Sewer Outfall Ditch (100 percent)
N = Number of SWIFT cells along Paddys Run or Storm Sewer Outfall Ditch between Operable Unit 2 and the FEMP property boundary.

NO. A-6

~~Figure A.1-6 shows the linear extent of surface water infiltration to the Great Miami Aquifer from Paddys Run and the Storm Sewer Outfall Ditch.~~ Figure A.1-6A shows the linear extent of surface water infiltration to the Great Miami Aquifer from Paddys Run for runoff from the Solid Waste Landfill. Figure A.1-6B shows the linear extent of surface water infiltration to the Great Miami Aquifer from Paddys Run and the Storm Sewer Outfall Ditch from the South Field and flyash piles. The value of N were 47, 17, and 11 for the Solid Waste Landfill, Inactive Flyash Pile/South Field, and Active Flyash Pile, respectively.

A.1.7.2 Solid Waste Landfill

Table A.1-9 shows predicted maximum Great Miami Aquifer concentrations due to surface water runoff. Table A.1-9 also compares predicted maximum Great Miami Aquifer concentration with the risk-based screening concentrations (first screening step). ~~As shown in Table A.1-9, none of the constituents are above the screening level~~. As shown in Table A.1-9, only arsenic concentration in the Great Miami Aquifer was above the screening concentration. However, when mixing with the full SWIFT cell was considered, predicted arsenic concentration was 1.82×10^{-4} μg/L, which is only marginally above the screening concentration of 1.46×10^{-4} μg/L. Furthermore, the predicted arsenic concentration does not consider reduction in concentration due to adsorption. Therefore, no constituents were considered for further modeling in the Great Miami Aquifer using the SWIFT III Model from the surface water pathway.

No. A-47

A.1.7.3 Inactive Flyash Pile and South Field

Loading from surface runoff to the Great Miami Aquifer from Inactive Flyash Pile and the South Field was combined into one source term because of the close proximity of the Inactive Flyash to the South Field, resulting in surface runoff from both subunits to Paddys Run at approximately the same

5659

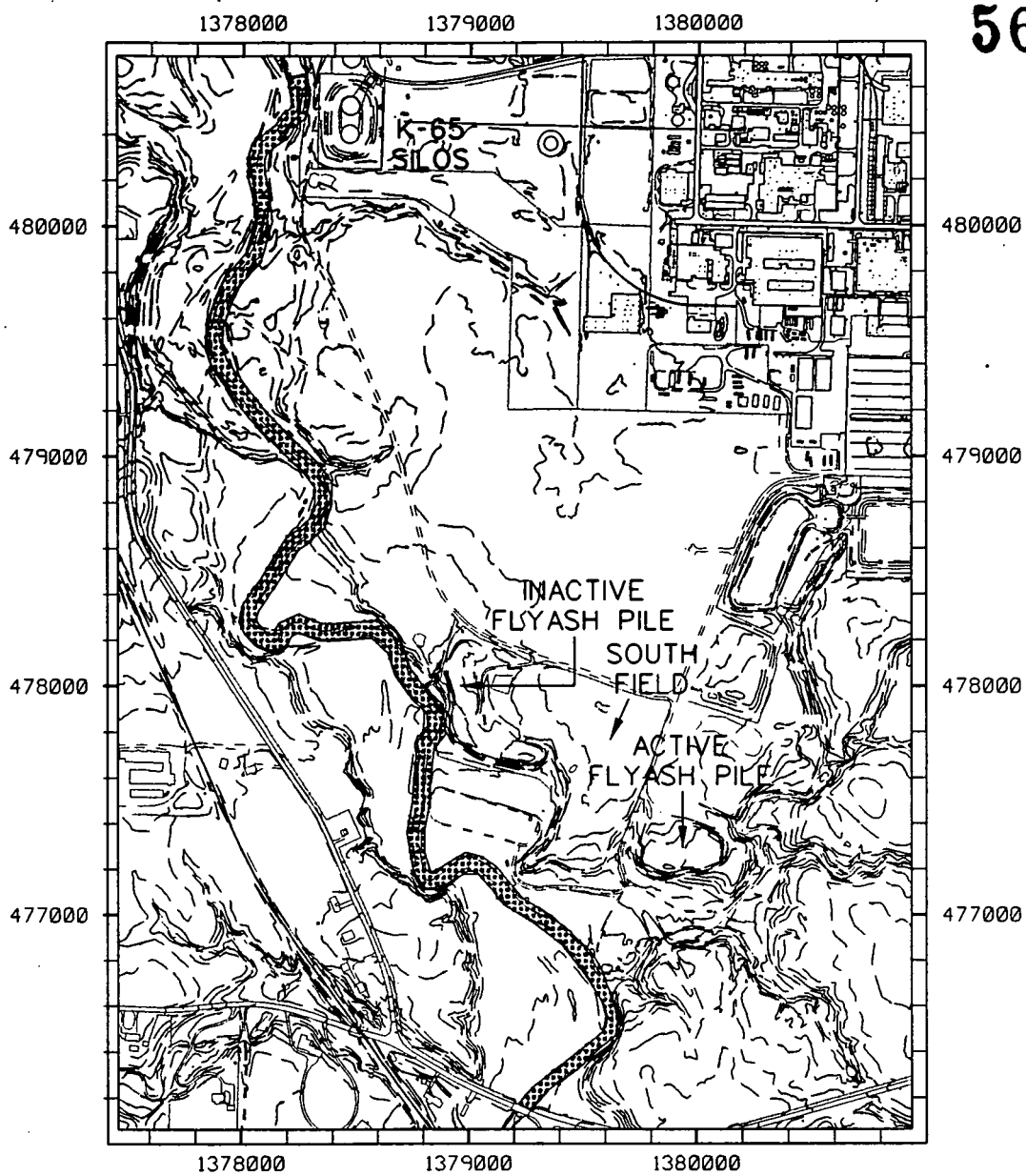

LEGEND

- PAVED ROADS
- UNPAVED ROADS
- STREAM
- FENCE
- 585 TOPOGRAPHIC CONTOUR LINE
- LINEAR EXTENT OF SURFACE WATER INFILTRATION TO THE GMA

NOTE:
Coordinates are in State Planar NAD 1927.
Surface contours based on 1992 flyover.

N

SCALE (FT)
0 400 800 1600

FIGURE A.1-6A
SURFACE WATER RUNOFF INFILTRATION TO THE GMA FROM SOLID WASTE LANDFILL

figa0107.dgn

000079

5659

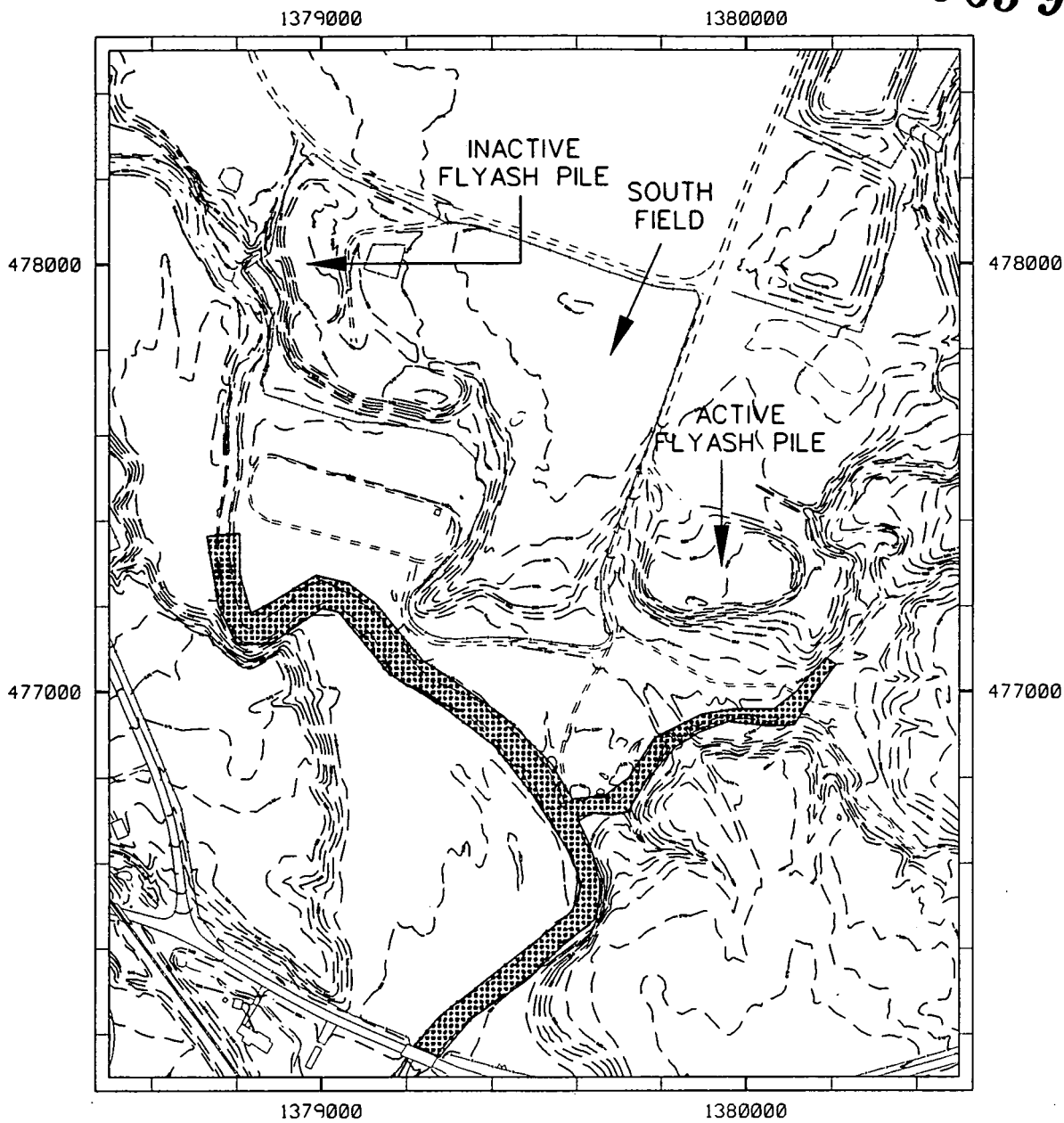

LEGEND

- PAVED ROADS
- UNPAVED ROADS
- STREAM
- FENCE
- 585 TOPOGRAPHIC CONTOUR LINE
- LINEAR EXTENT OF SURFACE WATER INFILTRATION TO THE GMA

NOTE:
Coordinates are in State Planar NAD 1927.
Surface contours based on 1992 flyover.

SCALE (FT)
0 200 400 800

FIGURE A.1-6B
SURFACE WATER RUNOFF INFILTRATION TO THE GMA FROM SOUTH FIELD AND FLYASH PILES

figa0106.dgn

000080

TABLE A.1-9

LOADING TO THE GREAT MIAMI AQUIFER FROM PADDYS RUN AND CPC SCREENING FOR GROUNDWATER MODELING, SOLID WASTE LANDFILL OPERABLE UNIT 2 REMEDIAL INVESTIGATION FERNALD ENVIRONMENTAL MANAGEMENT PROJECT

Constituents	Predicted Maximum Aquifer Concentration C_{GMA} (pCi/L RAD) (μg/L non-RAD)	Screening Concentrations (pCi/L RAD) (μg/L non-RAD)	Groundwater Modeling Required
INORGANICS			
Arsenic	7.58×10^{-4}	1.46×10^{-4}	Yes[a]
Berylium	1.22×10^{-3}	2.37×10^{-4}	No
Lead	1.44×10^{-4}	NA[b]	NA
ORGANICS			
Benzo(a)anthracene	3.17×10^{-6}	2.82×10^{-3}	No
Benzo(a)pyrene	1.23×10^{-6}	2.82×10^{-4}	No
Benzo(g,h,i)perylene	5.33×10^{-6}	NA	NA
Dibenzo(a,h)anthraene	7.40×10^{-7}	2.82×10^{-4}	No
Phenanthrene	5.17×10^{-2}	NA	NA
RADIONUCLIDES			
Neptunium-237	4.92×10^{-4}	2.16×10^{-2}	No
Radium-226	4.55×10^{-5}	1.76×10^{-4}	No
Radium-228	5.48×10^{-5}	4.75×10^{-2}	No
Strontium-90	2.15×10^{-3}	1.32×10^{-1}	No
Uranium-234	1.27×10^{-2}	2.97×10^{-1}	No
Uranium-235/236	8.56×10^{-4}	2.97×10^{-1}	No
Uranium-238	2.34×10^{-2}	1.70×10^{-1}	No
Uranium-Total (non-RAD)	6.81×10^{-2}	$1.09 \times 10^{+1}$	No

[a]After mixing in the full SWIFT cell, calculated arsenic concentration is 1.82×10^{-4} μg/L, which is marginally above the screening concentration. It is expected that losses due to adsorption to soils will reduce the concentration and therefore was not considered for further modeling.

[b]NA = EPA RAGs, Part B screening value could not be calculated.

Other Comment No. A-47

location. The loading to the Great Miami Aquifer consists of loading due to infiltration of surface water as well as leaching of sediments. This was assumed to equal 30 percent of the mass reaching Paddys Run. Because the seep pathway to groundwater was considered separately, the contribution to groundwater from seeps is not considered here.

Table A.1-10 shows the predicted maximum Great Miami Aquifer concentrations due to surface water runoff from Inactive Flyash Pile and South Field. Table A.1-10 also compares predicted maximum Great Miami Aquifer concentrations against the risk-based screening concentrations (first screening step). ~~As shown in Table A.1-10, only technetium-99 and uranium isotopes were above the screening level. The second screening step was not performed as technetium-99 and uranium isotopes were also above the screening levels for other pathways. Source term loading from the surface water runoff to the Great Miami Aquifer for technetium-99 and uranium isotopes were identified for further groundwater modeling.~~ As shown in Table A.1-10A, a number of CPCs may reach the Great Miami Aquifer above the screening concentrations. For those CPC having predicted maximum concentrations exceeding screening concentrations, the diluted Great Miami Aquifer concentrations in the full SWIFT cell were predicted and compared against the screening concentrations (Table A.1-10B). During this screening step, arsenic, beryllium, benzo(a)pyrene, dieldrin, radium-226, technetium-99, uranium-234, and uranium-238 were above the screening levels. However, beryllium, benzo(a)pyrene, dieldrin, and radium-226 concentrations only marginally exceed screening concentrations. Reduction in concentrations due to adsorption was not considered during this screening step, therefore, these CPCs were not considered for further modeling. Only arsenic, technetium-99, and uranium isotopes were identified for further groundwater modeling.

NO. A-47

A.1.7.4 Active Flyash Pile

Table A.1-11 shows the predicted maximum Great Miami Aquifer concentrations due to surface water runoff from Active Flyash Pile. Table A.1-11 also compares predicted maximum Great Miami Aquifer concentrations against the screening levels (first screening step). As shown in Table A.1-11, arsenic, beryllium, ~~lead,~~ neptunium-237, plutonium-238, plutonium 239/240, radium-226, radium-228, strontium-90, uranium-234, uranium 235/236, uranium-238, and total uranium were predicted to be above screening concentrations. For the constituents passing the first screening step, diluted Great Miami Aquifer concentration in full SWIFT cell were predicted and compared against the screening concentrations (Table A.1-12). During this screening step, predicted arsenic, beryllium, neptunium-237, uranium-234, and uranium-238 concentrations were above the screening levels~~, and therefore~~

NO. A-47

NO. A-47

TABLE A.1-10A

LOADING TO THE GREAT MIAMI AQUIFER FROM PADDYS RUN AND CPC SCREENING (FIRST STEP) FOR GROUNDWATER MODELING, INACTIVE FLYASH PILE/SOUTH FIELD OPERABLE UNIT 2 REMEDIAL INVESTIGATION FERNALD ENVIRONMENTAL MANAGEMENT PROJECT

Constituents	Predicted Maximum Aquifer Concentration C_{GMA} (pCi/L RAD) (μg/L non-RAD)	Concentrations (pCi/L RAD) (μg/L non-RAD)	Groundwater Modeling Required
INORGANICS			
Arsenic	3.09×10^{-3}	1.46×10^{-4}	Yes
Beryllium	2.60×10^{-3}	2.37×10^{-4}	Yes
Lead	3.77×10^{-1}	NA[a]	NA
ORGANICS			
2-Methylnaphthalene	1.37×10^{-2}	NA	NA
Benzo(a)anthracene	3.84×10^{-3}	2.82×10^{-3}	Yes
Benzo(a)pyrene	2.75×10^{-3}	2.82×10^{-4}	Yes
Benzo(b)fluoranthene	4.66×10^{-3}	2.82×10^{-3}	No
Benzo(g,h,i)perylene	1.32×10^{-2}	NA	NA
Dibenzo(a,h)anthracene	6.66×10^{-4}	2.82×10^{-4}	Yes
Dieldrin	8.47×10^{-4}	1.12×10^{-4}	Yes
Phenanthrene	$4.10 \times 10^{+0}$	NA	NA
RADIONUCLIDES			
Neptunium-237	2.36×10^{-2}	2.16×10^{-2}	Yes
Plutonium-238	6.51×10^{-4}	2.16×10^{-2}	No
Plutonium-239/240	4.02×10^{-4}	2.16×10^{-2}	No
Radium-226	1.49×10^{-1}	1.76×10^{-2}	Yes
Radium-228	2.03×10^{-2}	4.75×10^{-2}	No
Strontium-90	3.21×10^{-2}	1.32×10^{-1}	No
Technetium-99	$4.52 \times 10^{+2}$	$3.65 \times 10^{+0}$	Yes
Uranium-234	$3.21 \times 10^{+0}$	2.97×10^{-1}	Yes
Uranium-235/236	3.15×10^{-1}	2.97×10^{-1}	Yes
Uranium-238	$3.43 \times 10^{+0}$	1.70×10^{-1}	Yes
Uranium-Total (non-RAD)	$1.08 \times 10^{+1}$	$1.09 \times 10^{+1}$	Yes

[a]EPA RAGs Screening Value could not be calculated.

Other Comment No. A-47

TABLE A.1-10B

CPC SCREENING FOR GROUNDWATER MODELING USING FULL SWIFT CELL DILUTION
INACTIVE FLYASH PILE/SOUTH FIELD
OPERABLE UNIT 2 REMEDIAL INVESTIGATION
FERNALD ENVIRONMENTAL MANAGEMENT PROJECT

Constituent of Potential Concern	Units	Runoff Concentration		Predicted Diluted Great Miami Aquifer Concentration	Screening Concentration	Predicted Concentration Above Screening Concentration
		Inactive Flyash Pile	South Field			
INORGANICS						
Arsenic	μg/L	$3.92 \times 10^{+0}$	8.81×10^{-1}	7.56×10^{-3}	1.46×10^{-4}	Yes
Beryllium	μg/L	2.14×10^{-1}	9.14×10^{-2}	6.35×10^{-4}	2.37×10^{-4}	Yes[a]
Lead	μg/L	$1.48 \times 10^{+1}$	$1.57 \times 10^{+1}$	9.21×10^{-2}	NA[b]	NA
ORGANICS						
2-methylnapthalene	μg/L	$4.34 \times 10^{+0}$	-[c]	3.36×10^{-3}	NA	NA
Benzo(a)anthracene	μg/L	-	1.83×10^{-1}	9.40×10^{-4}	2.82×10^{-3}	No
Benzo(a)pyrene	μg/L	-	1.31×10^{-1}	6.73×10^{-4}	2.82×10^{-4}	Yes[a]
Benzo(g,h,i)perylene	μg/L	-	6.28×10^{-1}	3.23×10^{-3}	NA	NA
Dibenzo(a,h)anthracene	μg/L	3.06×10^{-2}	2.71×10^{-2}	1.63×10^{-4}	2.82×10^{-4}	No
Dieldrin	μg/L	-	4.03×10^{-2}	2.07×10^{-4}	1.12×10^{-4}	Yes[a]
Phenanthrene	μg/L	-	$1.95 \times 10^{+2}$	$1.00 \times 10^{+0}$	NA	NA
RADIONUCLIDES						
Neptunium-237	pCi/L	6.26×10^{-1}	$1.03 \times 10^{+0}$	5.78×10^{-3}	2.16×10^{-2}	No
Radium-226	pCi/L	4.40×10^{-1}	$7.03 \times 10^{+0}$	3.65×10^{-2}	1.76×10^{-2}	Yes[a]
Technetium-99	pCi/L	-	$2.15 \times 10^{+4}$	$1.10 \times 10^{+2}$	$3.65 \times 10^{+0}$	Yes
Uranium-234	pCi/L	$1.24 \times 10^{+2}$	$1.34 \times 10^{+2}$	7.84×10^{-1}	2.97×10^{-1}	Yes
Uranium-235/236	pCi/L	$8.06 \times 10^{+1}$	$1.37 \times 10^{+1}$	7.66×10^{-2}	2.97×10^{-1}	No

See footnote at end of table.

FER\CRU2RI\JLG\APP-A\TABA2-10b\June 6, 1994 2:55pm

TABLE A.1-10B
(Continued)

Constituent of Potential Concern	Units	Runoff Concentration: Inactive Flyash Pile	Runoff Concentration: South Field	Predicted Diluted Great Miami Aquifer Concentration	Screening Concentration	Predicted Concentration Above Screening Concentration
RADIONUCLIDES (Continued)						
Uranium-238	pCi/L	$1.27 \times 10^{+2}$	$1.44 \times 10^{+2}$	8.38×10^{-1}	1.70×10^{-1}	Yes
Uranium-Total (non-RAD)	μg/L	$3.74 \times 10^{+2}$	$4.57 \times 10^{+2}$	$2.64 \times 10^{+0}$	$1.09 \times 10^{+1}$	No

[a]Diluted Great Miami Aquifer concentration marginally exceeds screening concentration. However, it is expected that maximum concentration in the Great Miami Aquifer will be about an order of magnitude lower and, therefore, CPC's were not modeled further.

[b]NA = EPA RAGs, Part B screening value could not be calculated.

[c]Dash = not a constitutent of potential concern for this subunit for surface soils or subsurface soils. Therefore, surface water concentrations were not calculated.

Other Comment No. A-47

TABLE A.1-11

LOADING TO THE GREAT MIAMI AQUIFER FROM THE STORM SEWER OUTFALL DITCH AND CPC SCREENING (FIRST STEP) FOR GROUNDWATER MODELING, ACTIVE FLYASH PILE OPERABLE UNIT 2 REMEDIAL INVESTIGATION FERNALD ENVIRONMENTAL MANAGEMENT PROJECT

Constituents	Predicted Maximum Aquifer Concentration C_{GMA} (pCi/L RAD) (μg/L non-RAD)	Screening Concentrations (pCi/L RAD) (μg/L non-RAD)	Groundwater Modeling Required
INORGANICS			
Arsenic	$3.50 \times 10^{+0}$	1.46×10^{-4}	Yes
Beryllium	1.46×10^{-1}	2.37×10^{-4}	Yes
Lead	$1.12 \times 10^{+1}$	NA[a]	NA[a]
RADIONUCLIDES			
Neptunium-237	$8.29 \times 10^{+0}$	2.16×10^{-2}	Yes
Plutonium-238	5.61×10^{-2}	2.16×10^{-2}	Yes
Plutonium-239/240	2.57×10^{-2}	2.07×10^{-2}	Yes
Radium-226	3.37×10^{-1}	1.76×10^{-4}	Yes
Radium-228	2.34×10^{-1}	4.75×10^{-2}	Yes
Strontium-90	3.28×10^{-1}	1.32×10^{-1}	Yes
Uranium-234	$1.70 \times 10^{+1}$	$2.97 \times 10^{+0}$	Yes
Uranium-235/236	7.56×10^{-1}	2.97×10^{-1}	Yes
Uranium-238	$1.69 \times 10^{+1}$	1.70×10^{-1}	Yes
Uranium-Total (non-RAD)	$5.94 \times 10^{+1}$	$1.09 \times 10^{+1}$	Yes

[a]EPA RAGs, Part B screening value could not be calculated.

Other Comment No. A-47

TABLE A.1-12

CPC SCREENING FOR GROUNDWATER MODELING USING FULL SWIFT CELL DILUTION, ACTIVE FLYASH PILE OPERABLE UNIT 2 REMEDIAL INVESTIGATION FERNALD ENVIRONMENTAL MANAGEMENT PROJECT

Constituent of Potential Concern	Units	Surface Water Runoff Concentration	Predicted Diluted GMA Concentration	Screening Concentration	Predicted Concentration Above Screening Concentration
RADIONUCLIDES					
Neptunium-237	pCi/L	$2.51 \times 10^{+1}$	9.52×10^{-1}	2.16×10^{-2}	Yes
Plutonium-238	pCi/L	1.70×10^{-1}	6.45×10^{-3}	2.16×10^{-2}	No
Plutonium-239/240	pCi/L	7.79×10^{-2}	2.96×10^{-3}	2.07×10^{-2}	No
Radium-226	pCi/L	$1.02 \times 10^{+0}$	3.87×10^{-2}	1.76×10^{-4}	Yes
Radium-228	pCi/L	7.08×10^{-1}	2.69×10^{-2}	4.75×10^{-3}	No
Strontium-90	pCi/L	9.94×10^{-1}	3.77×10^{-2}	1.32×10^{-1}	No
Uranium-234	pCi/L	$5.14 \times 10^{+1}$	$1.95 \times 10^{+0}$	2.97×10^{-1}	Yes
Uranium-235/236	pCi/L	$2.29 \times 10^{+0}$	8.69×10^{-2}	2.97×10^{-1}	No
Uranium-238	pCi/L	$5.13 \times 10^{+1}$	$1.95 \times 10^{+0}$	1.70×10^{-1}	Yes
INORGANICS					
Arsenic	μg/L	$1.06 \times 10^{+1}$	4.02×10^{-1}	1.46×10^{-4}	Yes
Beryllium	μg/L	4.41×10^{-1}	1.67×10^{-2}	2.37×10^{-4}	Yes
Lead	μg/L	$3.40 \times 10^{+1}$	$1.29 \times 10^{+0}$	NA[a]	NA[a]
Uranium-Total	μg/L	$1.80 \times 10^{+2}$	$6.83 \times 10^{+0}$	$1.09 \times 10^{+1}$	No

[a]NA = EPA RAGs, Part B screening value could not be calculated.
Other Comment No. A-47

FE[illegible]U2RI\JLG\APP-A\TABA1-12.NEW\June 6, 1994 2:55pm

~~source term loading from the surface water runoff pathway to groundwater for these constituents was developed.~~ However, the radium-226 concentration calculated without considering adsorption effects is only marginally above the screening concentration, and therefore radium-226 was not considered for further modeling. Source term loadings from the surface water runoff pathway to groundwater were developed for arsenic, beryllium, neptunium-237, uranium-234, and uranium-238.

Table A.1-13 compares model predicted concentrations in the Great Miami Aquifer due to surface water pathway to concentrations observed in monitoring wells near the Storm Sewer Outfall Ditch. Observed concentration range and predicted concentrations are generally on the same order of magnitude, however, the range of concentrations for uranium isotopes is quite large. This may be reflective of up-gradient source contributions before installation of storm water retention basins.

A.1.7.5 Combined Loading

NO. A-47

Table A.1-14 lists all the CPCs for groundwater from the surface water pathway. No CPCs ~~were identified from the Solid Waste Landfill, and surface water modeling for the Lime Sludge Ponds was not performed. Only technetium 99 and uranium isotopes are CPCs from Inactive Flyash Pile and South Field. Active Flyash Pile results in three inorganics and six radionuclides as CPCs. However, only arsenic, beryllium, neptunium 237, and uranium isotopes CPCs after the second screening step, and were considered for detailed groundwater modeling (see Section A.1.7.4).~~ from the Solid Waste Landfill were considered for further modeling, and surface water modeling for the Lime Sludge Ponds was not performed. Although 17 CPCs were identified for the surface water pathway to the Great Miami Aquifer from the Inactive Flyash Pile and South Field, only arsenic, technetium-99 and uranium isotopes were considered for detailed modeling in the Great Miami Aquifer. The Active Flyash Pile results in three inorganic and nine radionuclides as CPCs. However, only arsenic, beryllium, neptunium-237, and uranium isotopes remained CPCs after the second screening step, and were considered for detailed groundwater modeling.

TABLE A.1-13

COMPARISON OF GREAT MIAMI AQUIFER AND MODELED RESULTS FROM SURFACE RUNOFF PATHWAY, ACTIVE FLYASH PILE OPERABLE UNIT 2 REMEDIAL INVESTIGATION FERNALD ENVIRONMENTAL MANAGEMENT PROJECT

Constituents of Potential Concern[a]	Units	GMA Wells 2014 and 2049[b]		Model Predicted GMA Concentration from SSOD Loading[c]
		Minimum	Maximum	
		RADIONUCLIDES (Unfiltered)[d]		
Neptunium-237	pCi/L	0.48	0.48	8.290
Radium-226	pCi/L	0.17	1.40	0.337
Uranium-234	pCi/L	1.00	83.20	17.000
Uranium-235/236	pCi/L	0.22	1.86	0.756
Uranium-238	pCi/L	2.10	89.90	17.000
		INORGANICS (Filtered)		
Lead	μg/L	6.00	6.00	11.2

[a]CPC listed only if measured data were available for comparison

[b]These two GMA wells are close to the SSOD

[c]Model predicted concentrations are considered equivalent to filtered samples

[d]Only unfiltered data were available for comparison for radionuclides

GMA - Great Miami Aquifer

SSOD - Storm Sewer Outfall Ditch

Other Comment No. A-47

TABLE A.1-14

SUMMARY OF CONSTITUENTS OF CONCERN FOR GROUNDWATER FROM SURFACE WATER PATHWAY OPERABLE UNIT 2 REMEDIAL INVESTIGATION FERNALD ENVIRONMENTAL MANAGEMENT PROJECT

Constituents of Potential Concern (CPC)[a]	Units	Model Predicted Maximum GMA[b] Concentration
SOLID WASTE LANDFILL		
Arsenic[c]	µg/L	2.51×10^{-3}
Benzo(g,h,i)perylene[d]	µg/L	1.77×10^{-6}
Phenanthrene[d]	µg/L	5.17×10^{-2}
LIME SLUDGE PONDS		
None		
SOUTH FIELD/INACTIVE FLYASH PILE		
Arsenic	µg/L	3.09×10^{-2}
Beryllium[c]	µg/L	2.60×10^{-3}
Lead[d]	µg/L	3.77×10^{-1}
2-Methylnaphthalene[d]	µg/L	1.37×10^{-2}
Benzo(a)anthracene[e]	µg/L	3.84×10^{-3}
Benzo(a)pyrene[c]	µg/L	2.75×10^{-3}
Benzo(g,h,i)perylene[d]	µg/L	1.32×10^{-3}
Dibenzo(a,h)anthracene[e]	µg/L	6.66×10^{-4}
Dieldrin[c]	µg/L	8.47×10^{-4}
Phenanthrene[d]	µg/L	$4.10 \times 10^{+0}$
Neptunium-237[e]	pCi/L	2.36×10^{-2}
Radium-226[c]	pCi/L	1.49×10^{-1}
Technetium-99	pCi/L	$4.52 \times 10^{+2}$
Uranium-234	pCi/L	$3.21 \times 10^{+0}$
Uranium-235/236	pCi/L	3.15×10^{-1}
Uranium-238	pCi/L	$3.43 \times 10^{+0}$
Uranium-Total (Non-Rad)[e]	µg/L	$1.08 \times 10^{+1}$
ACTIVE FLYASH PILE		
Arsenic	µg/L	3.50
Beryllium	µg/L	0.15
Lead[d]	µg/L	11.20
Neptunium-237	pCi/L	8.29
Plutonium-238[e]	pCi/L	0.06
Plutonium-238/240[e]	pCi/L	0.03
Radium-226[e]	pCi/L	0.34
Radium-228[e]	pCi/L	0.23

TABLE A.1-14
(Continued)

Constituents of Potential Concern (CPC)[a]	Units	Model Predicted Maximum GMA[b] Concentration
ACTIVE FLYASH PILE (Continued)		
Strontium-90[e]	pCi/L	0.33
Uranium-234	pCi/L	17.00
Uranium-235/236[e]	pCi/L	0.76
Uranium-238	pCi/L	16.90
Uranium-Total[e]	μg/L	59.4

[a]CPC listed only if above screening concentration.
[b]GMA - Great Miami Aquifer.
[c]These CPCs were not considered for detailed groundwater modeling because predicted diluted GMA concentration without adsorption effects is marginally above the screening concentration.
[d]Lead, 2-methylnaphthalene, benzo(g,h,i)perylene, and phenanthrene were not screened and further modeled because RAGs Part B screening concentrations could not be calculated.
[e]These CPCs were screened out in the second screening step which uses dilution in the full SWIFT cell.

Other Comment No. A-47

A.2.0 GROUNDWATER FATE AND TRANSPORT MODELING

A.2.1 INTRODUCTION

The objective of this section is to evaluate the fate and transport of constituents as they migrate from the Operable Unit 2 area through the vadose zone, Paddys Run streambed, or Storm Sewer Outfall Ditch streambed to the Great Miami Aquifer. This section provides a more detailed discussion of the modeling that is summarized in Section 5.0.

Groundwater fate and transport models are used to predict constituent movement from sources (waste areas) to receptor locations through the groundwater pathway. Used in conjunction with monitoring data, these models predict future constituent concentrations at potential exposure locations. The modeling provides future exposure predictions by extrapolating from known field data. Conservative assumptions are used in the modeling to provide a reasonable "worst case" with regard to risk. The modeled future concentrations are based on the unremediated baseline case for the Operable Unit 2 waste areas. The results of the groundwater fate and transport modeling are used in the Operable Unit 2 baseline risk assessment (Appendix B) to estimate potential risks to the environment and human health.

This Appendix presents a description of the technical approach and the methods used to quantitatively predict constituent concentrations for use in the Operable Unit 2 baseline risk assessment. Specifically, this appendix:

- Presents background information on the hydrogeologic setting
- Defines the conceptual groundwater flow model based upon a reasonable and conservative depiction of the hydrogeologic setting
- Outlines the screening processes to finalize the list of CPCs
- Presents a description and results of vadose zone modeling
- Presents a description and results of aquifer modeling
- Compares modeling results with field data
- Presents a description and results of vadose zone modeling if waste units and perched water were at background concentrations.

A.2.1.1 Technical Approach

The fate and transport evaluation included modeling of surface water, groundwater, and air releases. Figure A.2-1 shows the overall fate and transport modeling framework used to support the Operable Unit 2 baseline risk assessment. Five pathways are considered in the groundwater fate and transport analysis:

- Vadose Zone Pathway: Migration of CPCs from the waste unit laterally and vertically through the vadose zone to the aquifer was designated as the vadose zone pathway.
- Perched Water Infiltration: Vertical migration of perched water through the glacial till to the Great Miami Aquifer was designated as the perched water infiltration pathway.
- Perched Water Subsurface Seep Pathway: Lateral migration of CPCs occurs when perched water in sand and gravel layers within the glacial overburden come in contact with waste material. Perched water moves laterally in the sand layer until it is intercepted at the sand/gravel and waste interface. At that point, perched water moves along the slope of waste and till interface until it comes in contact with the unsaturated Great Miami Aquifer. This water containing CPCs then vertically infiltrates to the aquifer.
- Seep Pathway: Migration of CPCs from seeps to an area where glacial overburden is not present, and then through the unsaturated portion of the Great Miami Aquifer to the groundwater was designated as the seep pathway.
- Surface Water Pathway: Migration of CPCs from the surface soils due to storm event runoff to Paddys Run or the Storm Sewer Outfall Ditch, and then vertically to the aquifer as the surface water pathway.

This appendix considers all of the steps of the vadose zone, seep, perched water subsurface seep, and perched water infiltration pathways. For the surface water pathway, Appendix A.1.0 describes the definition of constituents, the conceptual model for the surface water pathway, the surface water modeling, the screening of constituents, and the predicted concentrations in Paddys Run, the Storm Sewer Outfall Ditch, and the Great Miami Aquifer. This section presents all of the Great Miami Aquifer modeling results including the impact to the aquifer from constituent concentrations in the surface water pathway determined in Appendix A.1.

Conservative assumptions were built into the modeling process in order to provide a reasonable worst-case scenario regarding the migration of constituents from the waste areas, and to account for uncertainties associated with the database and models. Screening of CPCs was performed at various stages during the fate and transport modeling to effectively focus on those compounds that could potentially pose a carcinogenic cancer risk greater than 1×10^{-7} or noncarcinogenic HI of 0.1.

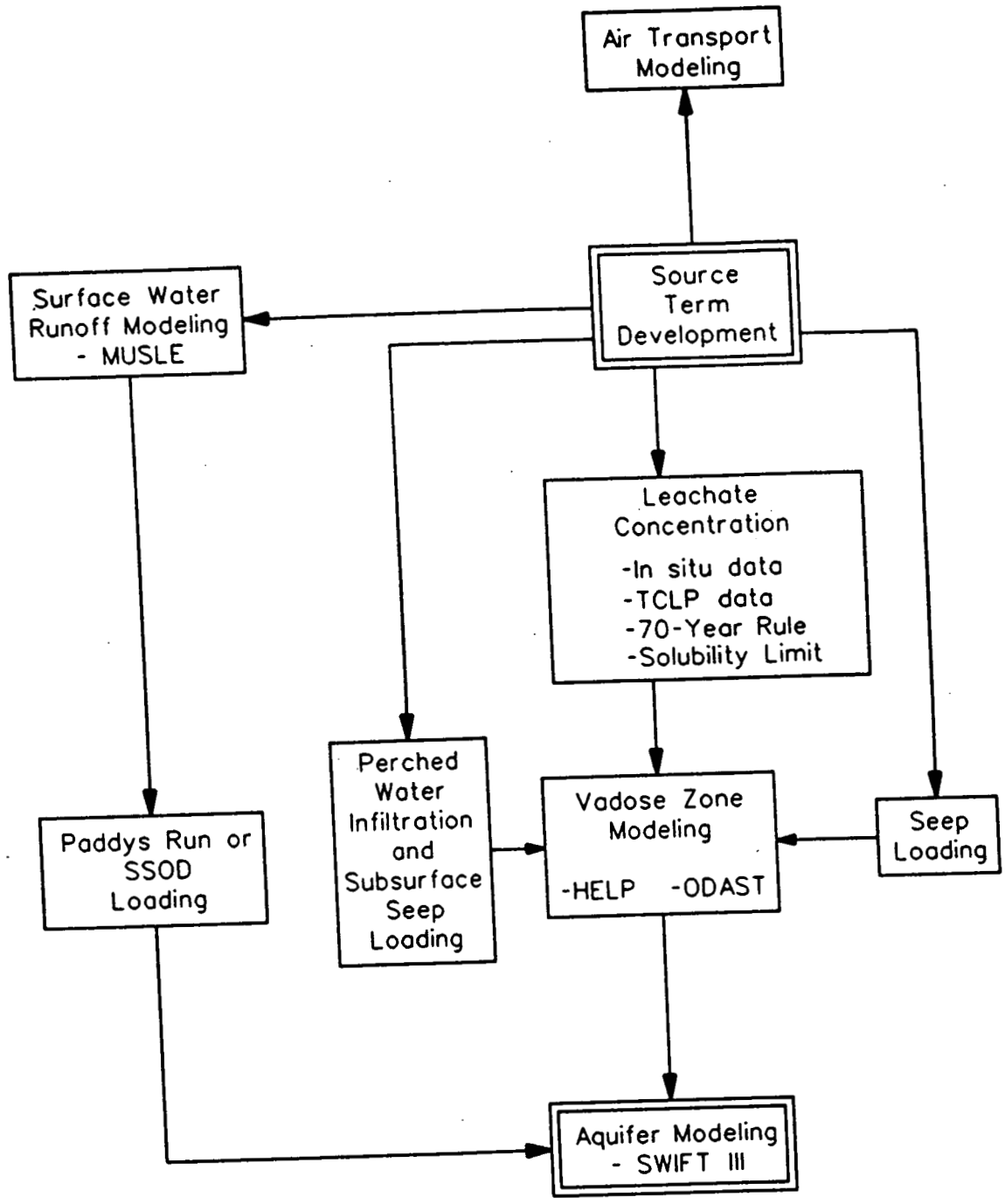

figa0201.dgn

FIGURE A.2-1
OVERALL FATE AND TRANSPORT MODELING FRAMEWORK

000094

The fate and transport analysis assumed that the waste areas would remain essentially in their current conditions, without any remedial actions taken. The groundwater fate and transport modeling results are summarized for the CPCs that are predicted to reach the Great Miami Aquifer from the Operable Unit 2 subunits within 1000 years. The simulation time period of 1000 years was selected based on the Risk Assessment Work Plan Addendum (DOE 1992a). Contributions to constituent concentrations from other FEMP sources and background concentrations are not included in the results presented in this appendix. The results presented here represent the increase in constituent concentrations in the Great Miami Aquifer due to the loading from Operable Unit 2 subunits only.

Figure A.2-2 shows the steps in model development and the method of deriving the source and leachate concentrations. The extent to which a constituent may migrate through the groundwater system depends both on site characteristics and the nature of the constituent. Because of the variety of constituents in the subunits, and the heterogeneity in the vadose zone beneath the subunits, a separate conceptual model is developed for each of the subunits within Operable Unit 2. The development of these models involves the following steps:

- Review of the available information on the specific subunit to establish the characteristics of the subunit
- Identification of CPCs by reviewing the production history and by analyzing site characterization data
- Identification of the hydrologic processes governing the fate and transport of the constituents within each hydrostratigraphic unit
- Development of a conceptual hydrogeologic model for each subunit based on information about the constituents present in that subunit and its location-specific geologic setting

Once the conceptual models were developed, existing computer codes that allow the creation of a proper mathematical representation of the conceptual models were selected. The mathematical representations used at the FEMP generally consider the rate at which the modeled processes occur, the interaction of different processes with each other, and the initial conditions of both the subunit and the surrounding geologic formations. Some of the major steps involved in constructing mathematical representations of the conceptual models used at the FEMP include:

- Quantification of the concentrations of constituents in the waste and the physical parameters defining the volume and mass of constituents in each subunit

5659

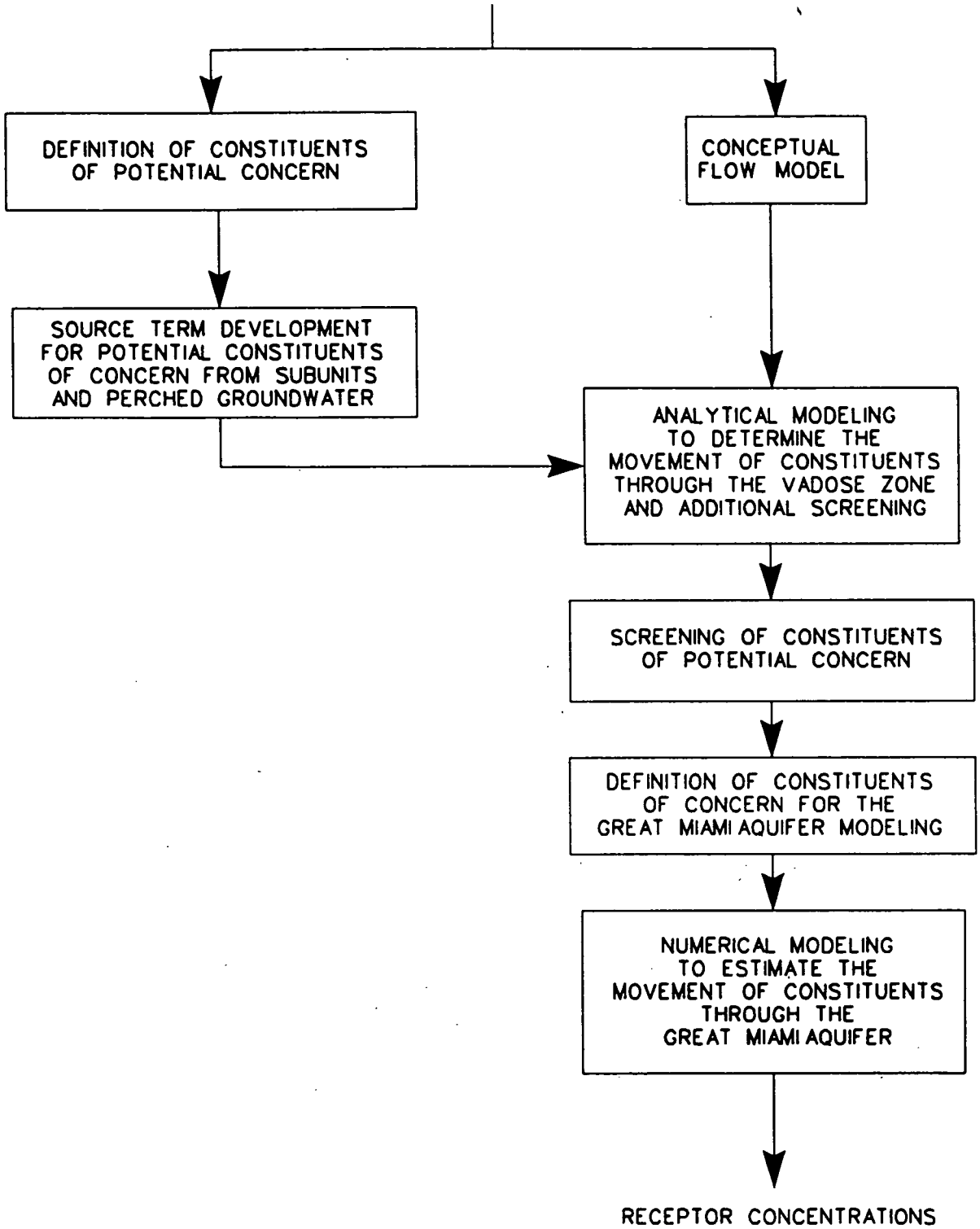

figa0202.dgn

FIGURE A.2-2
CONSTITUENT TRANSPORT MODELING DIAGRAM

000096

- Use of measured data to determine the chemical speciation projected to result from the reactions of infiltrating water with the waste materials

- Definition of physical parameters of the vadose zone system beneath each subunit

- Estimation of the rate constants describing the cationic retardation of the modeled CPCs (These rate constants are based on partitioning coefficients developed from site-specific measurements and from an extensive literature search.)

- Estimation of the rate constants describing constituent retardation attributable to interactions with organic carbon in the geological formation (These constants are based upon the grain-size distributions and organic carbon content of the waste, glacial overburden matrix, and the Great Miami Aquifer matrix.)

- Estimation of the rate constants describing the decay rates of the modeled constituents (These first-order rate constants are based upon radioactive half-lives and biodegradation half-lives in groundwater for radionuclides and organic chemicals, respectively.)

- Calibration of the model to field data (~~Selected~~ Analytic results for 1000 and 2000 series wells in the vicinity of the subunits were evaluated to determine constituents that have reached the perched water and the aquifer. Initial model results at 40-50 years were compared to these data and estimated parameters were adjusted to approximately reproduce these constituent values within the operating time frame of 40-50 years.)

NO. A-11

The CPCs from Operable Unit 2 subunits were defined based upon sampling data and prescreening and background/nutrient screening activities (Appendix B). Prior to Great Miami Aquifer fate and transport modeling, additional screening steps were undertaken to reject those that clearly would not pose a significant risk. By screening constituents, computational time was reduced. Screening steps consider travel time through the vadose zone, organic and radiologic decay, immediate dilution in the Great Miami Aquifer, and comparison with ~~toxicity levels~~ EPA RAGs, Part B screening concentrations.

NO. A-48

After existing computer codes and site-specific input parameters were selected, the codes were used to (1) calculate constituent loading rates to the aquifer beneath the waste areas; and (2) perform flow and solute transport modeling to determine the effects of dispersion, retardation, and constituent degradation or decay on the projected concentrations in the Great Miami Aquifer and perched water.

A.2.1.2 Approach to Screening and Modeling

The primary purpose of the fate and transport modeling is to provide predicted concentrations of key, risk-causing constituents so that overall risk may be determined. Because the modeling is resource

intensive, screening steps were undertaken to eliminate constituents that pose little or no risk using conservative assumptions. In addition, because modeling contains uncertainty by being a predictive tool based on many assumptions, actual monitoring data was reviewed to check certain model results and assumptions. For example, if a constituent was predicted to be attenuated in the vadose zone for many years, yet it is presently found in the aquifer, then the model assumptions were reviewed. Figure A.2-3 shows the approach that has been followed in screening out constituents, in defining risk from the remaining constituents, and in incorporating monitoring results in the modeling process. This figure represents the two major screening steps that remove CPCs from further consideration (see detailed discussion in Section A.2.6).

If a constituent was detected above the detection limits in the Great Miami Aquifer groundwater in the vicinity of the subunits, the following steps were undertaken. First, these detected concentrations were compared against background and predicted concentrations. If these concentrations were below these criteria, then no further action was taken. However, if a constituent was detected at concentrations that were higher than background and the predicted concentrations, then model assumptions and parameters were reviewed and revised as necessary. For example, if constituents were detected in the Great Miami Aquifer sooner than their theoretical arrival time (as determined by the conceptual model parameters and chemical specific factors), then the distribution coefficient was adjusted downward to match the measured concentrations in the aquifer.

A.2.2 HYDROGEOLOGIC SETTING

The first step in the pathway analysis was to develop a conceptual understanding of the depositional history of the site and the general hydrogeologic characteristics of the deposits. This section describes the general geology and hydrogeology of the FEMP. For a detailed discussion, refer to the Groundwater Report (DOE 1990), and Section 3.0 of this report.

A.2.2.1 Geologic Setting

The geology of the area is dominated by the glacial and glaciofluvial deposits formed during the most recent continental glaciation (approximately 70,000 years before present). Prior to the advancement of the glaciers, a large valley was eroded into the shale bedrock. This valley, which is approximately 200 feet below the existing land surface, was filled with well-sorted sand and gravel glacial outwash during the retreat of early glaciers. Beneath the site, this outwash is divided by a clay layer at a depth of approximately 120 feet below the current surface. Later glacial advances (Shelbyville)

5659

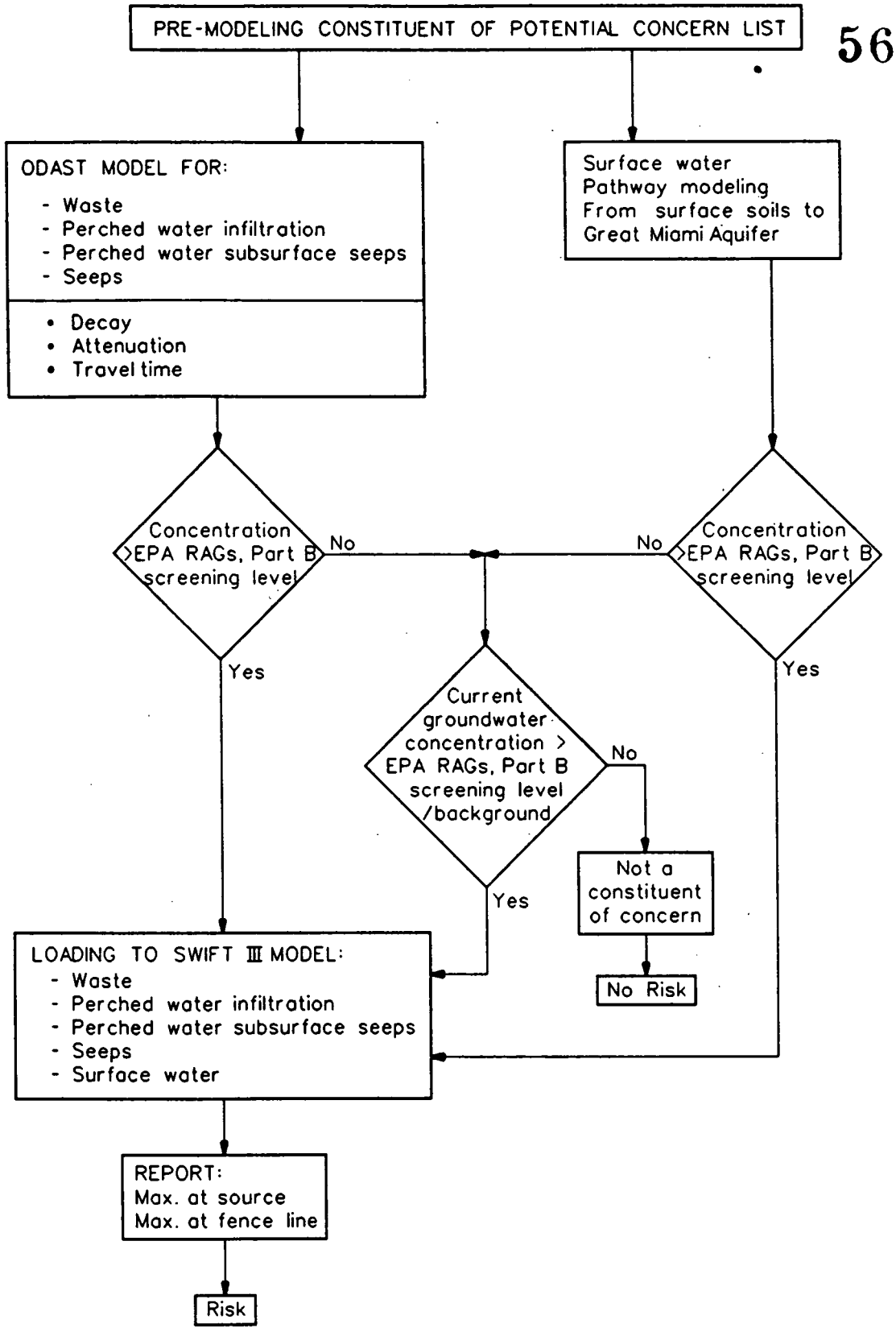

figa0203.dgn

FIGURE A.2-3
APPROACH FOR SCREENING AND INCORPORATION OF MONITORING DATA INTO THE MODELING PROCESS

000089

caused the displacement of the Dry Fork of the Whitewater River from its historic channel into its present channel. The Shelbyville ice deposited a moraine in the historic channel which formed a dam. The meltwater lake that formed behind the dam gave rise to the lacustrine deposits found in the area. This dam was breached at least two times, with the final breach draining the lake permanently. The lake basin is now occupied by Paddys Run.

In the Paddys Run floodway, recent deposits of silt (loess, fluvial, and lacustrine) form a terrace above the current stream elevation. Paddys Run has cut through this recent terrace and the glacial drift. The bed of Paddys Run is located on the well-sorted outwash material which fills the buried valley, on preglacial Whitewater River deposits. Since the last retreat of the continental glaciers, the streams in the area have removed much of the till and lacustrine mantle left by the ice sheets. In the Great Miami River valley, the stream has eroded through the till and is now in direct contact with the glaciofluvial outwash deposits that contain the buried valley aquifer.

The term glacial overburden has been selected to describe the deposits located stratigraphically above the glaciofluvial material of the Great Miami Aquifer. The glacial overburden includes the following types of materials:

- Loess - Considered ubiquitous in the Fernald area, it generally forms the uppermost layer of the glacial overburden. Loess is generally a homogeneous fine-grained blanket deposit, buff to light yellow or yellowish-brown in color. The deposit originated from windblown dust of Pleistocene age carried from the unconsolidated glacial and glaciofluvial deposits uncovered by glacial recession, but prior to the invasion of a vegetative cover.

- Lacustrine - Lacustrine deposits originated from the glacial lake consisting of well-sorted, stratified fine sands and clays formed in the Paddys Run valley. These varved clays can be interbedded with well-sorted beach deposits along the margins of the former lake basin.

- Till - Undifferentiated glacial till makes up the majority of the glacial overburden at the FEMP site. Because of its location at the ice margin, the till is likely to have been deposited by several modes including moraine deposits, ablation till, and subglacial till sheets arising from differing ice lobes. The primary feature of tills is that they are deposited directly by a glacier without fluvial sorting. The till at the site is a heterogeneous mixture of clays, silts, and pebbles.

- Glaciofluvial - Interbedded with the till are glaciofluvial beds that originated from meltwater streams that occurred along the margins of the ice sheets. These deposits of varying extent consist of well-sorted sands and fine gravels.

A.2.2.2 Vadose Zone

The unsaturated or vadose zone exists above the groundwater table or phreatic surface of the aquifer. In this zone, the interstices are occupied partially by water and partially by air. The partially filled soil water in the unsaturated zone is known as vadose water. Overlying the Great Miami Aquifer at the FEMP are approximately 15 to 35 feet of unsaturated sand and gravel outwash deposits. These deposits are assumed to have the same hydraulic characteristics as the underlying saturated material since their depositional histories are the same.

Dense, fine-grained glacial overburden overlies the unsaturated sand and gravel outwash deposits. These types of deposits have intergranular hydraulic conductivities that are very low, with values in the range of 10^{-7} to 10^{-5} feet/day (10^{-11} to 10^{-9} cm/s) (Heath 1983). Extensive deposits of clayey till can cause isolation from zones of near-surface groundwater flow.

In the Great Plains region and in parts of the Midwest, deposits of clayey or silty clay and glaciolacustrine clay have networks of predominantly vertical joints or fractures. This jointing pattern in the Wisconsin tills has also been noted in the area surrounding the FEMP (Brockman 1988). In the FEMP area, the joints which are commonly near vertical have a polygonal expression and are typically 18 to 25 inches (0.46 to 0.63 m) across. The joints are generally oxidized approximately two inches on either side of the joint. Within the FEMP, fractures have been noted in the till during the RI/FS drilling program and field reconnaissance. These fractures can impart an enhanced bulk hydraulic conductivity of up to 1000 times greater than that of an unweathered till (Hendry 1988). As a result of increased lateral stresses caused by overburden loading, the hydraulic conductivity of fractured till and clay decreases with depth.

Recent investigations in similar geologic settings indicate that till deposits can be divided from a hydrogeologic standpoint into a brown weathered zone and a gray unweathered zone (Barari and Hedges 1985; Hendry 1988; Cravens and Ruedisili 1987). These studies indicate that infiltration is primarily limited to the weathered till. While precipitation enters this upper zone, it does not act as a significant source of recharge to deeper aquifer zones and the majority of the water lost from till deposits is from evapotranspiration. In addition to the losses due to evapotranspiration, some water may be discharged to small seeps or drainage.

Although the degree of fracturing within the brown tills at the FEMP has not been documented, sufficient observations have been made at the site and in the literature to indicate their presence is a characteristic physical property of these tills. Since fractures have been noted as a dominant feature in most brown tills, it is necessary to consider the effect that these fractures have on water and contaminant transport within the tills. As stated earlier, fractures have been reported to enhance the bulk hydraulic conductivity of till as much as 1000 times with an expected increase of one to three times. It is reasonable to expect that constituents will be transported by seepage more quickly through fractured till than unfractured till. At the FEMP, the gray till, with its appreciable silt and clay content, was regarded as providing the Great Miami Aquifer with protection from activities at the site (Dove and Norris 1951). This line of reasoning has justification because the low hydraulic conductivity produces very low velocities even if the hydraulic gradients are large. In addition, most constituents being transported by seepage through the till matrix undergo attenuation and retardation.

If the till is fractured, these generalizations are not applicable because the velocities of water in the fractures are relatively large compared to the intergranular pore velocities in the unfractured matrix. It should be noted that although the velocities are relatively large, the constituent flux may be relatively small because the flow rate through the fractures is small.

Fractures not only control velocity but they generally impart a lower capability for attenuation and retardation by adsorption of contaminants. The adsorption processes are capable of removing more constituent mass from solution if the water is in contact with larger surface areas in the matrix. The exact nature of attenuation in fractured till is highly site specific and not well quantified. For example, if till fractures are coated with iron oxides, they may impart significant retardation on ionic solutions (Grisak et al. 1976).

Within the till deposits, there are many water-bearing zones that have limited interconnection. The majority of these zones are of glaciofluvial origin and consist of small beds of highly-sorted sands and gavels. These beds are probably the result of small meltwater streams that occurred along the ice margin and within the glacier itself. These intertill perched zones have the following general characteristics:

- High variability in areal extent, thickness, and volume
- Based on hydrograph analysis, the interconnection between the intertill significantly saturated zones is limited

- Hydraulic conductivities are highly variable with an expected range of 2.8 x 10^{-5} to 280 feet/day (10^{-8} to 0.1 cm/s) (Freeze and Cherry 1979)
- Porosities range from 22.1 to 36.7, with a mean of 31 percent (Morris and Johnson 1967)

Generally these glaciofluvial interbeds are considered to be water-bearing units within the glacial overburden. However, movement of water and constituents within these units will be limited due to limited areal and vertical extent and lack of interconnection of these units. ~~The perched water zones (saturated lenses of higher permeability sands) present beneath Operable Unit 2 subunits are not modeled separately, and the thickness and the hydraulic properties of the sand lenses are excluded in the vadose zone modeling.~~ These sand and gravel units within the glacial overburden were not included in the vadose zone pathway modeling because this layer has much higher hydraulic conductivity and low adsorption properties. In addition, the computer model selected to evaluate flow in the vadose zone is limited to two layers. By neglecting the sand and gravel units, the model underpredicts travel time, and is therefore conservative. At the FEMP, a series of slug tests on these perched water zones found hydraulic conductivities ranging from 0.016 to 12.5 feet/day (5.5 x 10^{-6} to 4.4 x 10^{-3} cm/s) in Wells 1950 and 1042, respectively.

NO A-12

A.2.2.3 Great Miami Aquifer

The hydrogeology of the FEMP and the surrounding area is a textbook example of a glaciofluvial buried valley aquifer (Walton 1970; Fetter 1989; Freeze and Cherry 1979). The primary aquifer in the region is the Great Miami Aquifer, a well-sorted sand and gravel water table system consisting of sand and gravel glacial outwash deposits. Groundwater in the aquifer enters the FEMP area via buried channels on the west, north, and east. Under natural conditions, the primary flow would be across the site to the south. However, large pumping wells east of the FEMP in the Big Bend area of the Great Miami River have created a pronounced cone of depression causing flow at the FEMP to have easterly, southeasterly, and southerly components.

The aquifer is divided by a clay aquitard 1 to 20 feet thick at a depth of approximately 120 feet. Flow direction and magnitude of the Great Miami Aquifer were simulated using Sandia Waste Isolation Fate and Transport (SWIFT) III, a numerical groundwater flow and solute transport model.

A.2.2.4 General Contaminant Hydrogeology at the FEMP

The depositional characteristics and the hydrostratigraphic units present at the FEMP impart general constituent transport characteristics on solutes migrating from the individual subunits to receptor locations. These characteristics include:

- Solute migration potential: Solutes have a high migration potential through the upper weathered tills due to the fractured nature of the layer. Solute migration can also occur through the unweathered till, however, at a much slower rate. Once the solute reaches the glacial outwash, the solute migration potential is high, based on the high hydraulic conductivity and low adsorption capacity of the matrix.

- Hydraulic intercommunication: The intercommunication between perched water-bearing zones is limited in the glacial environment. Communication between the upper water-bearing zones within the till and the Great Miami Aquifer is also limited but may occur over an extended period of time.

- Adsorption/attenuation characteristics: The layers found within the glacial overburden generally have sufficient organic carbon content to cause retardation of organic constituents. The clay mineralogy would result in significant cation retardation for inorganic constituents. Given the till matrix, it is also unlikely that all of the available sites for adsorption would be used by solutes. Therefore, it is unlikely that adsorption/attenuation breakthrough would occur. Adsorption/attenuation will occur at lower rates in the regional aquifer due to the lower organic carbon and clay content in the outwash.

Based on the general hydrogeologic and transport characteristics, there is a potential pathway from the waste areas through the vadose zone to the regional aquifer. Given the high permeability of the glacial outwash, the pathway would extend from the aquifer-vadose interface to downgradient receptors.

A.2.3 CONCEPTUAL MODEL

The Operable Unit 2 subunits exhibit considerable diversity in their contents and in the physical and chemical characteristics of the vadose zone beneath them. Because of this diversity, the modeling of the constituent migration through the vadose zone is considered imperative for the estimation of constituent loading rates to the regional aquifer model. To model the transport of these constituents, it is necessary to adapt the generic conceptual model presented in the Risk Assessment Work Plan Addendum (DOE 1992) to a series of specific conceptual models for each distinct waste area. These conceptual models consider the following:

- Contents of the waste area
- Presence of standing water in the waste area
- Presence/absence of perched water under the waste area

- Concentration of constituents in perched groundwater
- Identifiable geologic strata beneath the waste area
- Presence/absence of sand lenses under the waste area
- Thickness of each layer in the vadose zone
- Vertical permeability of the layers
- Interstitial fluid velocity through each layer based on saturation
- Dispersion coefficients of each layer
- Partition coefficient for each constituent in each layer

Figure A.2-4 shows a generalized picture of contaminant migration at the FEMP. Two primary pathways shown are: 1) vadose zone pathway and 2) surface water pathway. These and other pathways are discussed in Section A.2.1.1. For risk assessment purposes, maximum concentrations are determined in the Great Miami Aquifer within the FEMP property boundary and outside the FEMP property boundary.

Flow and constituent transport in the subsurface is conceptualized from the hydrogeology of the site. As discussed previously, the geology of the FEMP site is dominated by glacial sediments. Well-sorted sand and gravel glacial outwash forms the regional Great Miami Aquifer. Beneath the site, this aquifer is divided by a 1- to 20-foot-thick clay interbed at an approximate depth of 120 feet. The receptor pathway considered for this analysis is the upper part of the Great Miami Aquifer above the clay interbed. Constituent transport in the vadose zone includes the bulk migration of water and dissolved materials from waste (source) areas at the FEMP to the Great Miami Aquifer. This occurs as rain water infiltrates from the surface and percolates through the source of contamination, and its surrounding soil, into the saturated zone. Downward movement of water, driven by the forces resulting from gravitational potential, capillary pressure, and other components of total fluid potential, mobilize the constituents and carry them through the vadose zone. Vertical transport down through the vadose zone to the aquifer and the horizontal transport through the aquifer to the well of a potential human receptor is illustrated in Figure A.2-4.

Figure A.2-5 presents a generalized conceptual model of the vadose zone pathway. The vadose zone pathway is applicable for all subunits. As water moves through the waste units, it picks up constituents (in dissolved phase), forming an aqueous solution (leachate). This solution continues to percolate through the soil/waste matrix in the vadose zone as it moves toward the aquifer. The leachate often reacts with the soil/waste matrix through which it flows. These interactions determine what chemical species are present in the percolating water, and how fast they will move in the

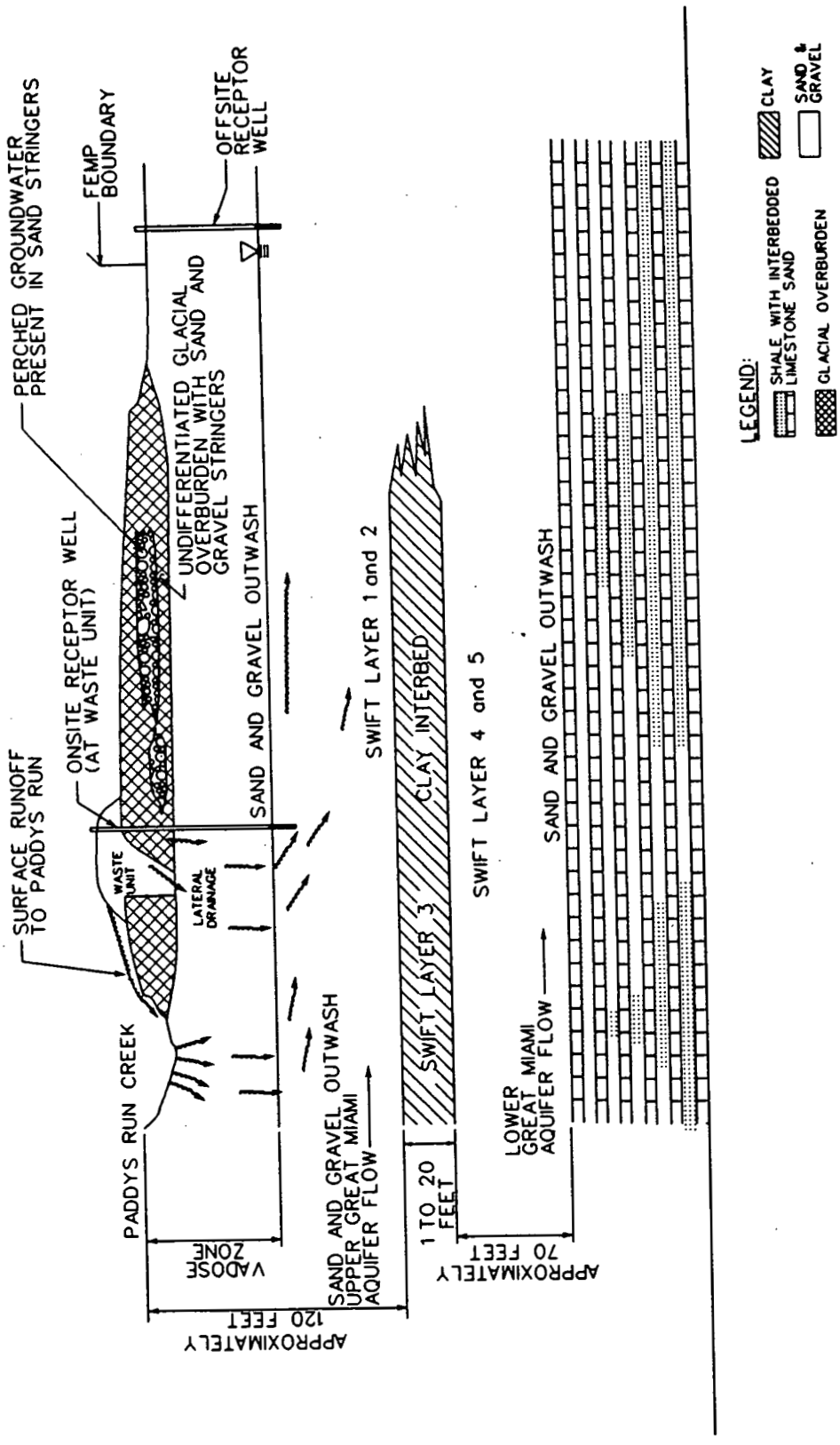

FIGURE A.2-4
CONCEPTUAL MODEL OF LOADING TO THE GREAT MIAMI AQUIFER AND CONTAMINANT TRANSPORT BY GROUNDWATER

figa0204.dgn

000106

5659

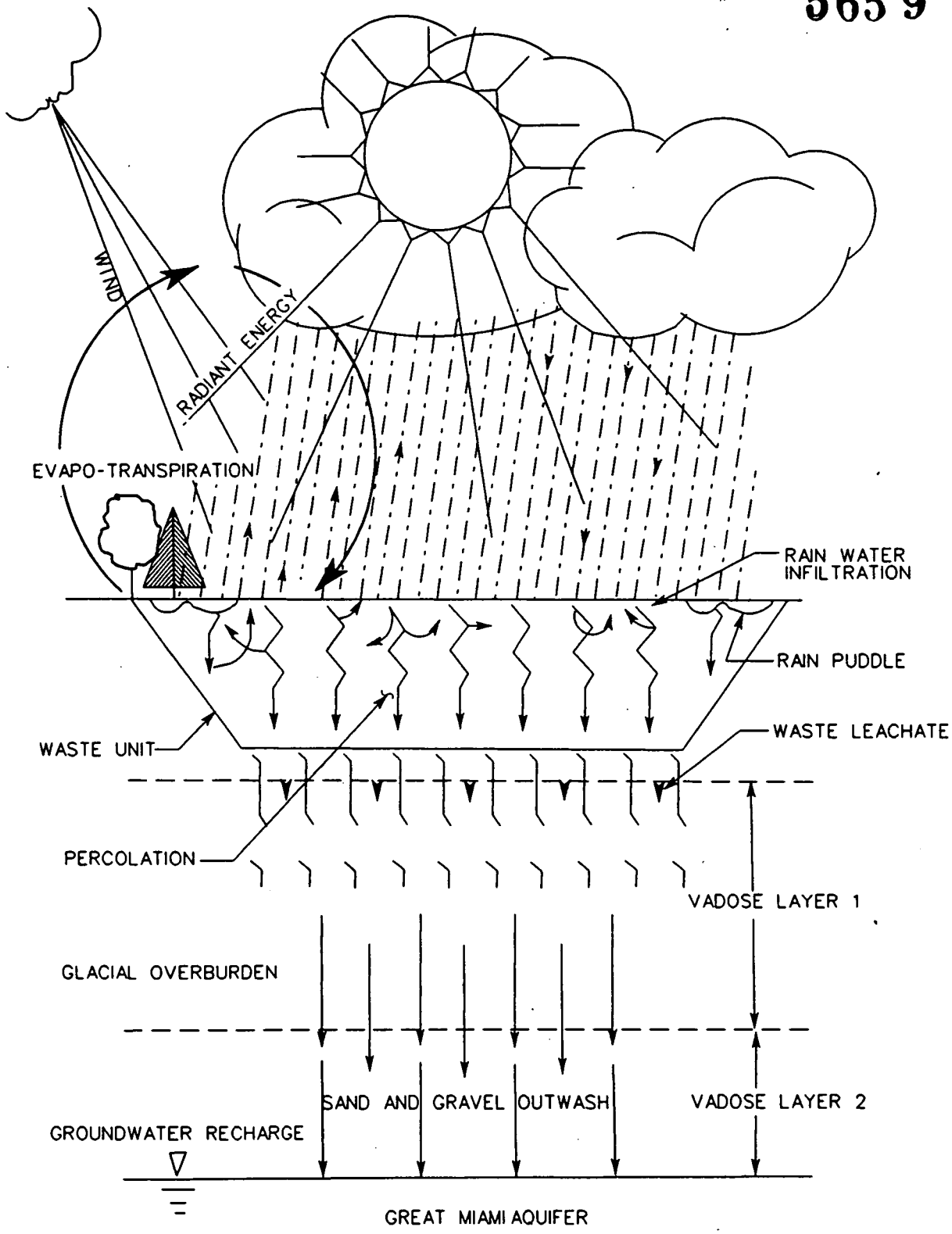

figa0205.dgn

FIGURE A.2-5
CONCEPTUAL VADOSE ZONE MODEL

000107

unsaturated zone. In this analysis, the composition of the leachate and the speed at which individual constituents migrate are treated individually.

The vadose zone was modeled as two layers, the glacial overburden underlying the subunits (Layer 1) and the unsaturated portion of the underlying Great Miami Aquifer (Layer 2). Layer 1 soils consist of till deposits in the glacial overburden. A sequence of fine-grained till deposits interbedded with sand and gravel glaciofluvial stringers forms the glacial overburden at the site. The sand and gravel unit within the glacial overburden was not included in the vadose zone modeling because this layer has much higher permeability and less adsorption potential as compared to clays and silts in glacial overburden. The thickness of till ranges between 0 and 38 feet for the subunits. Beneath the till is the unsaturated sand and gravel outwash layer (Layer 2), which is present beneath all the subunits. The thickness of Layer 2 ranges from 16 to 33 feet.

The perched water infiltration pathway is also applicable to all subunits. The conceptual model for the perched water infiltration pathway is similar to that of the vadose zone pathway. This pathway was also modeled with two layers. Layer 1 soils consist of till below the perched water zone and Layer 2 soils consist of the unsaturated portion of the Great Miami Aquifer. The thickness of Layer 1 ranged from 2 to 22 feet and the thickness of Layer 2 ranged from 17 to 33 feet. Constituent mass in the perched water, as well as adsorbed to sand layer, was considered in the source term for perched water infiltration. The perched water was simulated as additional source of constituent loading based on the concentration of constituents detected in the 1000 series wells located within the Operable Unit 2 subunits.

Based on the characteristics of the material underlying each Operable Unit 2 subunits, a detailed conceptual model is developed for the pathways applicable for each subunit. These more detailed models are developed to account for the variable stratigraphies of the soils of the subunits of Operable Unit 2. The areas overlying each SWIFT III grid block in all subunits were modeled separately with individual stratigraphy, constituent type and concentration, and infiltration parameters. Each constituent was simulated using retardation and decay factors taken from literature studies or site-specific data. The waste areas contained in Operable Unit 2 are assumed to remain in their existing locations for the purposes of the baseline fate and transport modeling. The detailed conceptual models are described below.

A.2.3.1 Solid Waste Landfill

Constituent migration pathways applicable to the Solid Waste Landfill were the vadose zone, surface water, and perched water infiltration pathways. Figure A.2-6 shows the SWIFT III grid cells directly beneath the waste at the Solid Waste Landfill and Table A.2.1 provides the physical parameters of various layers for each of the cells modeled. The average thickness of the waste was 8.5 feet. The conceptual model depicting flow in the subsurface soils at the Solid Waste Landfill considers two layers. Layer 1 soils consist of tills 31 to 38 feet thick. Within the till is interbedded sand and gravel stringers with thicknesses of 0.5 to 6 feet containing perched water. These stringers were not considered as a part of Layer 1 of the vadose zone pathway. The sand layers are underlain by 9 to 17 feet of glacial till. Beneath Layer 1 at the Solid Waste Landfill is the 19 to 25 feet thick unsaturated sand and gravel layer (Layer 2).

A.2.3.2 Lime Sludge Ponds

Only the vadose zone and perched water infiltration pathways are applicable to the Lime Sludge Ponds. As discussed in Section A.1.2, surface water pathway was not applicable to the Lime Sludge Ponds. ~~As Lime Sludge Ponds are underlain by the till everywhere, perched water subsurface seep and seep pathways were also not applicable to the Lime Sludge Ponds.~~ Borings 1956 through 1963 are located in the Lime Sludge Ponds (see Figure 2-7a). The glacial till/lime sludge interface was encountered in these bore holes at depth ranging from 3.5 to 11.5 feet. Also, glacial till was encountered in all peripheral borings/wells (2042, 1042, 1934, 1210, 2935, 2936, 1039, 2939, 1937, and 1940). This confirms that the Lime Sludge Ponds are located on glacial till. Consequently, perched water surface seep and seep pathways were also not applicable to the Lime Sludge Ponds. Figure A.2-7 shows the SWIFT III grid blocks directly under the waste at the Lime Sludge Ponds. The hydrostratigraphic units beneath the Lime Sludge Ponds consists of 24 to 35 feet of till (excluding 3 to 6 feet of sand and gravel beds) forming model Layer 1 for the vadose zone pathway, and 16 to 21 feet of buried valley glaciofluvial material forming vadose model Layer 2 (Table A.2.2). The base of the ponds is assumed to be located in the unweathered gray tills. Perched water has been observed in the sand and gravel layers under the Lime Sludge Ponds. Thickness of the till below the sand and gravel ranges from 11 to 22 feet (Layer 1 of the perched water vertical infiltration pathway). Only the vadose zone and perched water infiltration pathways are applicable to the Lime Sludge Ponds.

NO. A-14

000109

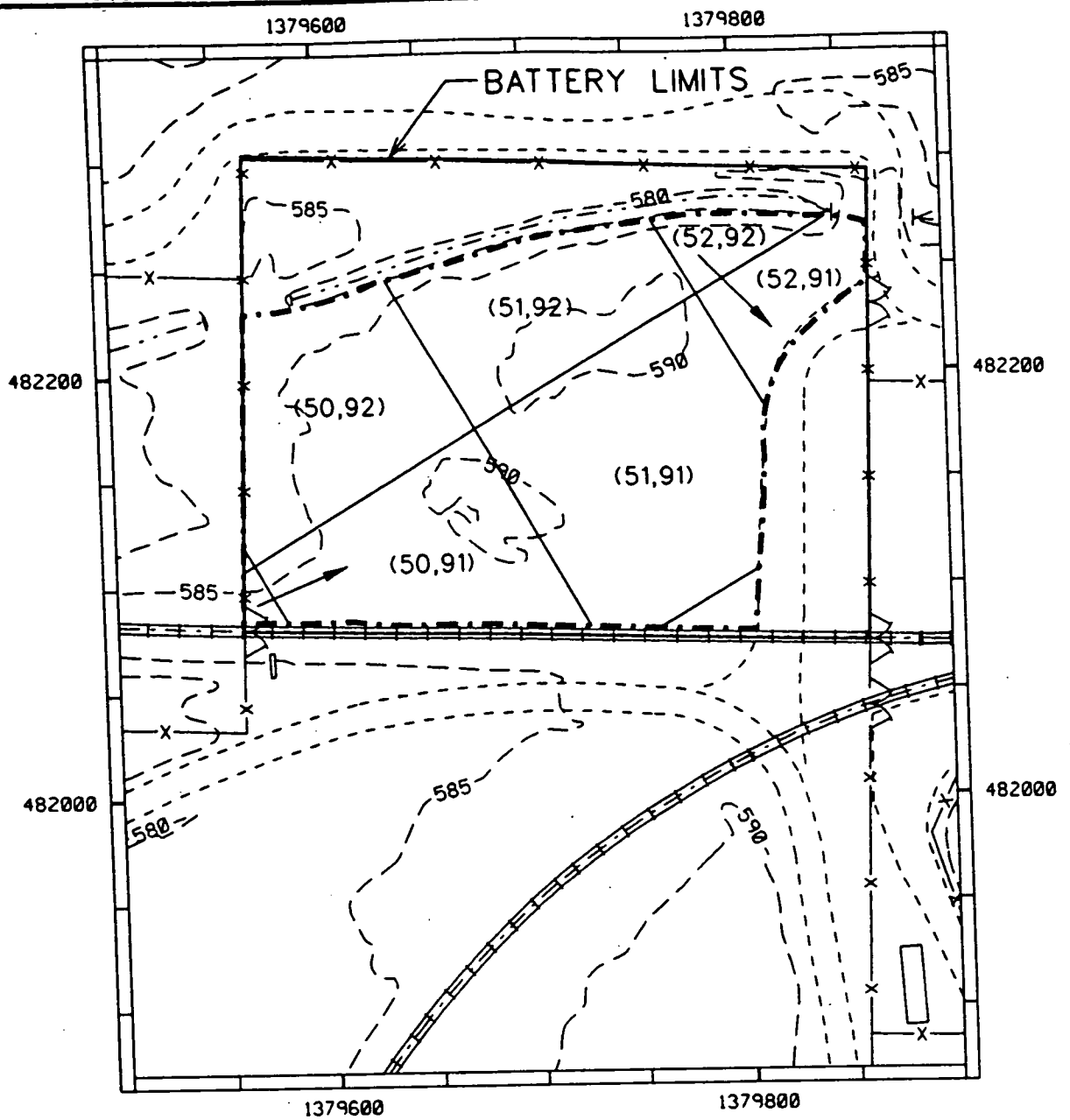

LEGEND

- 575 ELEVATION CONTOURS
- ROADS
- DRAINAGE
- FENCE
- RAILROAD
- EXTENT OF WASTE
- WASTE FROM CELL IS INCLUDED IN OTHER CELL
- (51,90) SWIFT MODEL CELL (COLUMN, ROW)

NOTE:
Coordinates are in State Planar NAD 1927.
Surface contours based on 1992 flyover.

SCALE (FT)
0 40 80 160

FIGURE A.2-6
EXTENT OF WASTE AND MODELED SWIFT GRID CELLS, SOLID WASTE LANDFILL

figo0206.dgn

000110

5659

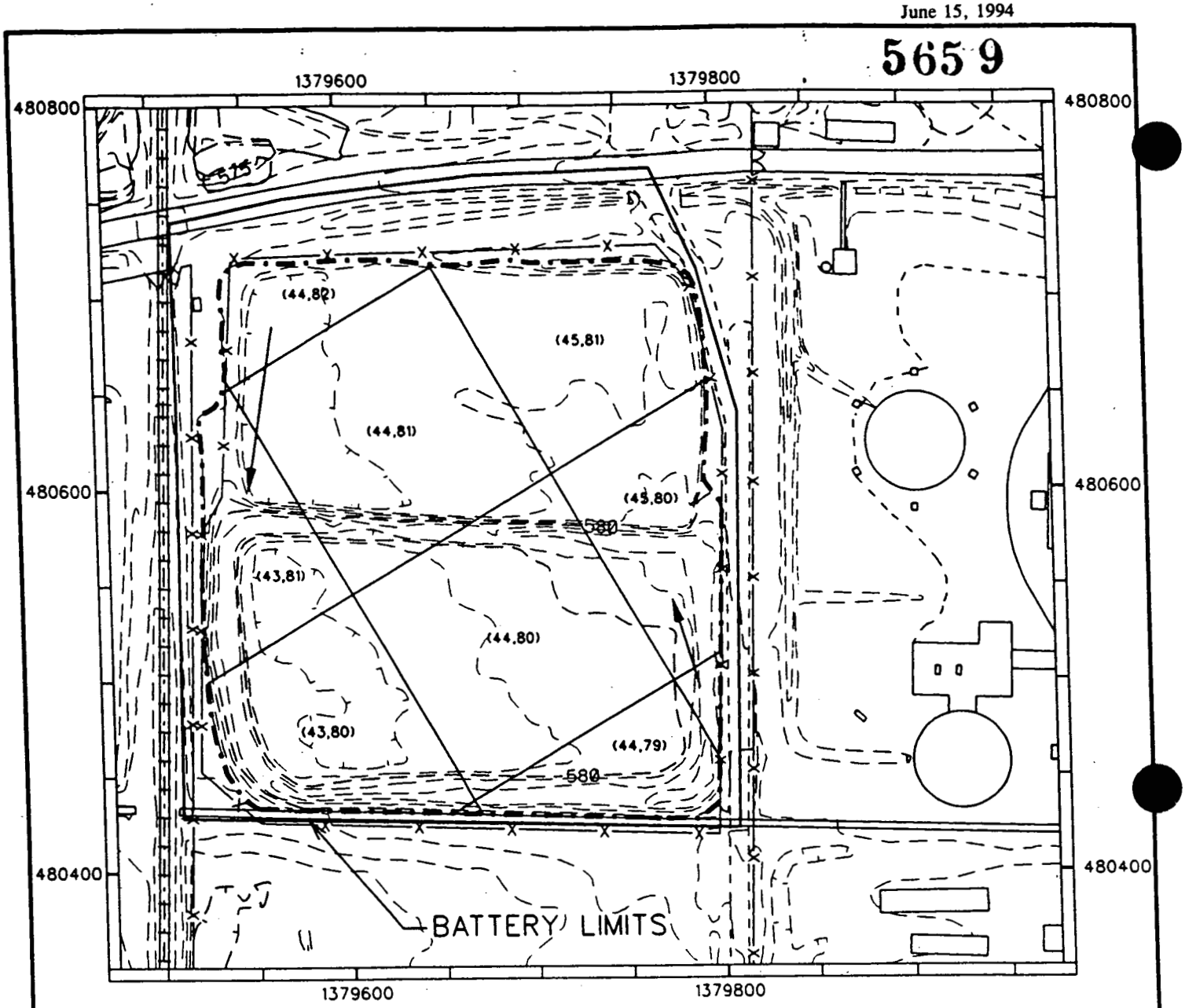

LEGEND

- ELEVATION CONTOURS
- ROADS
- DRAINAGE
- FENCE
- RAILROAD
- WASTE FROM CELL IS INCLUDED IN OTHER CELL
- EXTENT OF WASTE
- SWIFT MODEL CELL (COLUMN, ROW)

NOTE:
Coordinates are in State Planar NAD 1927.
Surface contours based on 1992 flyover.

SCALE (FT)
0 50 100

figa0214.dgn

000111

FIGURE A.2-7
EXTENT OF WASTE AND MODELED SWIFT GRID CELLS, LIME SLUDGE PONDS

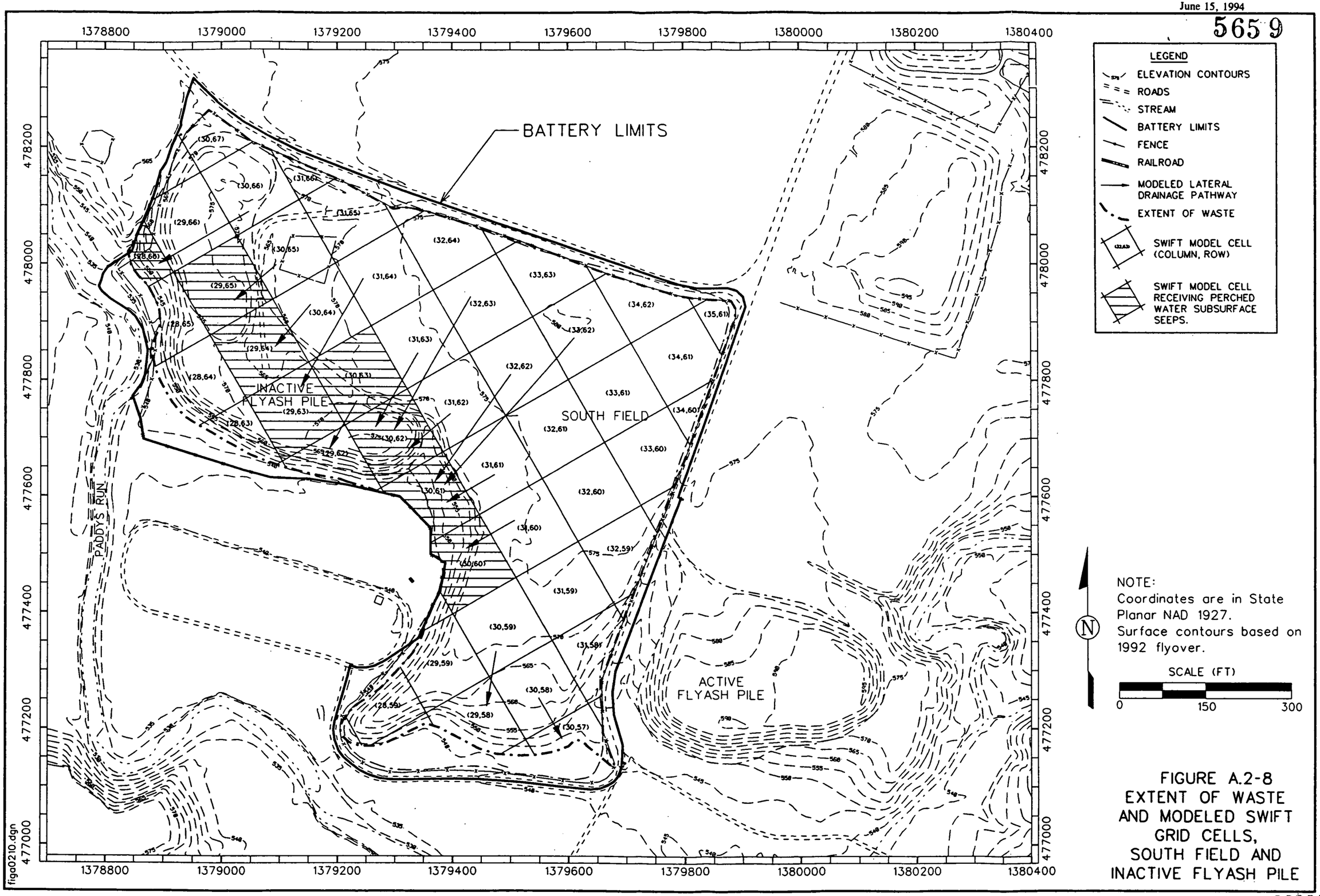

FIGURE A.2-8
EXTENT OF WASTE
AND MODELED SWIFT
GRID CELLS,
SOUTH FIELD AND
INACTIVE FLYASH PILE

5659

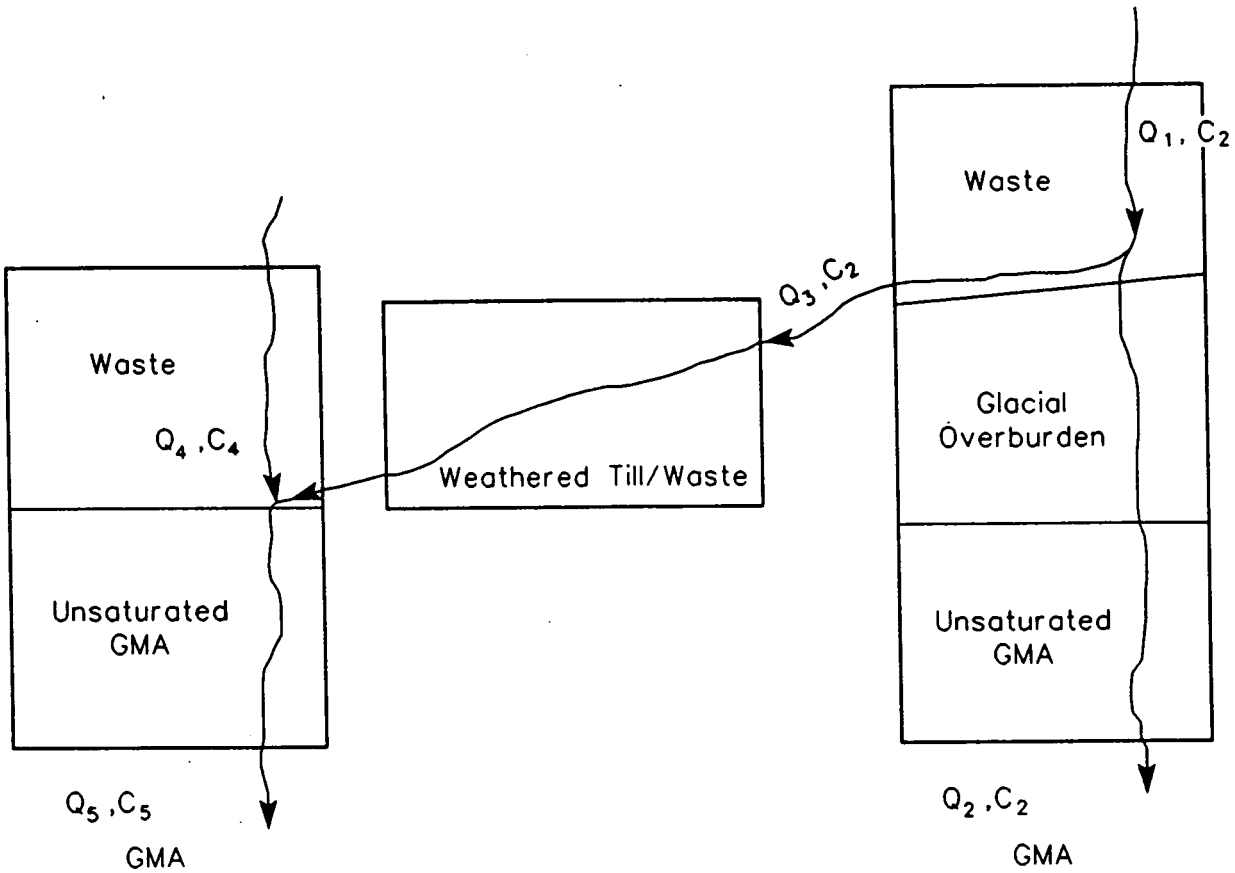

$$Q_1 = Q_2 + Q_3$$

$$Q_5 = Q_3 + Q_4$$

$$C_5 = \frac{Q_3 C_2 + Q_4 C_4}{Q_3 + Q_4}$$

NOTE:
C_i - CONSTITUENT CONCENTRATION
Q_i - FLOW RATE

figa0209.dgn

FIGURE A.2-9
CONCEPTUAL MODEL FOR LATERAL DRAINAGE INFILTRATING TO THE UNSATURATED GREAT MIAMI AQUIFER

000113

TABLE A.2-1

PHYSICAL PARAMETERS FOR THE SWIFT III CELLS IMPACTED BY THE SOLID WASTE LANDFILL OPERABLE UNIT 2 REMEDIAL INVESTIGATION FERNALD ENVIRONMENTAL MANAGEMENT PROJECT

Row	Column	Fill or Waste Area (ft^2)	Fill or Waste Volume (ft^3)	Fill or Waste Thickness (ft)	Unsaturated GMA Thickness (ft)	Glacial Overburden Thickness (ft)	Thickness of Till Above the Sand/Gravel (ft)	Thickness of Sand/Gravel In Till (ft)	Thickness of Till Below the Sand/Gravel (ft)	Total Till Thickness (ft)
ZONE 1 - LESS THAN 2 FEET SAND										
52	91	3404	27600	8.8	23.3	35.8	21.2	0.6	14.1	35.3
51	90	652	4375	7.0	25.7	35.5	25.1	1.0	9.4	34.5
52	92	1577	11388	9.1	22.2	36.1	19.2	1.6	15.4	34.5
Zone 1 Average		1878	14454	8.3	23.7	35.8	21.8	1.1	12.9	34.8
ZONE 2 - 2-3 FEET OF SAND										
51	91	14062	121906	8.5	23.5	36.3	19.4	2.6	14.4	33.8
51	92	7906	66213	8.2	20.6	38.6	17.9	3.4	17.3	35.2
Zone 2 Average		10984	94059	8.3	22.1	37.5	18.7	3.0	15.8	34.5
ZONE 3 - MORE THAN 4 FEET OF SAND, SIGNIFICANT TILL										
50	91	8697	85163	9.7	21.7	35.9	14.8	4.8	16.3	31.1
50	92	9313	73088	7.8	19.4	38.0	16.3	5.0	16.6	32.9
Zone 3 Average		9005	79125	8.8	20.6	36.9	15.5	4.9	16.5	32.0

NOTE: GMA = Great Miami Aquifer

TABLE A.2-2

PHYSICAL PARAMETERS FOR THE SWIFT III GRID CELLS IMPACTED BY THE LIME SLUDGE PONDS OPERABLE UNIT 2 REMEDIAL INVESTIGATION FERNALD ENVIRONMENTAL MANAGEMENT PROJECT

Row	Column	Fill or Waste Area (ft^2)	Fill or Waste Volume (ft^3)	Fill or Waste Thickness (ft)	Unsaturated GMA Thickness (ft)	Glacial Overburden Thickness (ft)	Thickness of Till Above the Sand/Gravel (ft)	Thickness of Sand/Gravel In Till (ft)	Thickness of Till Below the Sand/Gravel (ft)	Total Till Thickness (ft)
ZONE 1 - 2 TO FOUR FEET OF FILL										
44	79	5427	15019	2.7	17.7	38.4	15.9	3.6	18.9	34.8
45	80	9163	31863	3.6	19.0	36.3	17.3	5.5	13.5	30.8
43	81	10313	36381	3.9	18.3	35.9	10.3	5.9	19.7	30.0
Zone 1 Average		8288	27754	3.4	18.3	36.8	14.5	5.0	17.4	31.8
ZONE 2 - 6.5 TO 8.5 FEET OF FILL										
44	81	15625	100156	6.4	19.7	31.7	11.3	3.8	16.6	27.9
43	80	10322	69238	6.9	16.7	34.9	7.5	5.4	22.0	29.4
45	81	11414	89781	8.5	20.5	29.6	11.9	6.1	11.6	23.6
Zone 2 Average		12454	94969	7.4	20.1	30.7	11.6	5.0	14.1	25.7
ZONE 3 - 9.4 FEET OF FILL										
44	80	15625	146931	9.4	18.2	31.3	9.1	3.6	18.6	27.6

NOTE: GMA = Great Miami Aquifer

000125

565 9

A.2.3.3 Inactive Flyash Pile and South Field

All five constituent migration pathways are applicable to the Inactive Flyash Pile and South Field. The Inactive Flyash Pile and South Field contain the most surface area of any of the Operable Unit 2 subunits (Figure A.2-8). The lithology of this area is variable with the southwestern portion containing virtually no tills, while the till thicknesses increases to 22 feet towards the northeastern portion of the South Field. The thickness of the unsaturated zone in the Great Miami Aquifer (Layer 2) ranges from 17 to 33 feet (Table A.2.3). When leachate from waste arrives at the interface of waste and till, a portion of the leachate infiltrates through the glacial overburden (till and sand/gravel stringers) and the rest is laterally drained to areas where till does not exist. Figure A.2-9 shows the conceptual model for lateral drainage. The area receiving lateral drainage has increased flow. Horizontal travel time is simulated by travel through an equivalent Layer 1 using permeability of waste material. One vadose zone modeling run is used to simulate vertical infiltration. A separate vadose zone modeling run is used for simulating contribution from lateral drainage and was added to the Great Miami Aquifer before screening. Lateral drainage and infiltration through waste were added to calculate total vertical percolation rate and interstitial fluid velocity for the areas receiving lateral drainage from upgradient waste areas.

NO. A-13

Perched water has been observed in 0 to 3-feet thick sand and gravel layers in the glacial overburden.

NO. A-56

It is recognized that the glacial till is saturated. However, only the perched water in the sand and gravel layer represents a source for the Great Miami Aquifer. These sand and gravel layers are underlain by 2 to 11-feet thick till layer. Perched water not only represents a source for vertical infiltration, but it also serves as a source for perched water subsurface seeps. Figure A.2.10 shows the conceptual model for the perched water subsurface seeps. Sand and gravel layer within the glacial overburden (containing perched water) comes in contact with the waste in sections of the Inactive Flyash Pile and South Field. Perched water moves laterally in the sand layer until it is intercepted at the sand/gravel and waste interface. At that point, perched water moves along the slope of waste and till interface until it comes in contact with the unsaturated Great Miami Aquifer. The subsurface seep water then vertically infiltrates to the aquifer. Figure A.2-8 identifies eight blocks which receive subsurface seep water.

Furthermore, two seeps have been observed adjacent to or in areas of these subunits. One seep exists on the western boundary of the Inactive Flyash Pile, while the other was observed on the eastern side

5659

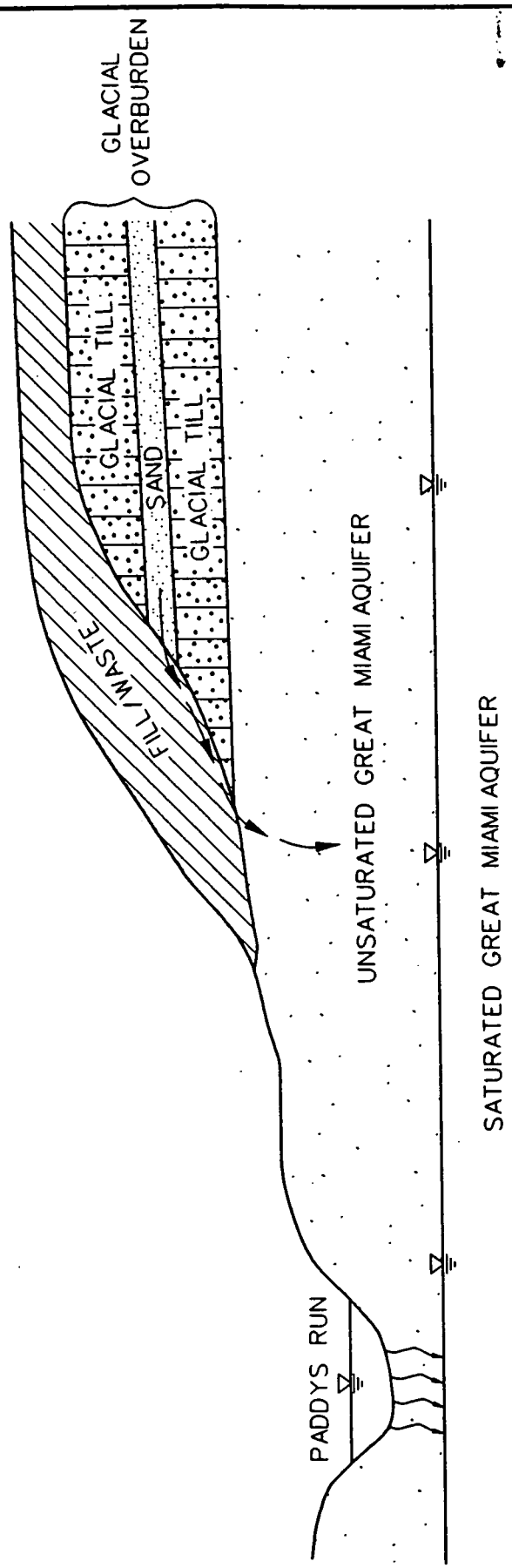

FIGURE A.2-10
CONCEPTUAL MODEL FOR PERCHED WATER SUBSURFACE SEEPS

figa0247.dgn

000127

TABLE A.2-3

PHYSICAL PARAMETERS FOR THE SWIFT III GRID CELLS IMPACTED BY THE INACTIVE FLYASH PILE AND SOUTH FIELD OPERABLE UNIT 2 REMEDIAL INVESTIGATION FERNALD ENVIRONMENTAL MANAGEMENT PROJECT

Row	Column	Fill or Waste Area (ft)	Fill or Waste Volume (ft^3)	Fill or Waste Thickness (ft)	Unsaturated GMA Thickness (ft)	Glacial Overburden Thickness (ft)	Thickness of Till Above the Sand/Gravel (ft)	Thickness of Sand/Gravel In Till (ft)	Thickness of Till Below the Sand/Gravel (ft)	Total Till Thickness (ft)	Slope at the Base of Fill/Waste (%)
ZONE 1 - NO SAND, NO TILL, MEDIUM FILL/WASTE											
28	59	11720	155938	15.6	16.7	0.0	0.0	0.0	0.0	0.0	
28	63	7029	104463	15.2	18.9	0.0	0.0	0.0	0.0	0.0	
28	65	8907	133369	15.2	19.6	0.0	0.0	0.0	0.0	0.0	
29	62	8869	151588	16.2	18.5	0.0	0.0	0.0	0.0	0.0	
29	64	15625	285594	18.3	25.5	0.0	0.0	0.0	0.0	0.0	
30	62	15625	292094	18.7	24.1	0.0	0.0	0.0	0.0	0.0	
Zone 1 Average		11296	187174	16.5	20.6	0.0	0.0	0.0	0.0	0.0	0.0
ZONE 2 - NO SAND, NO TILL, MAXIMUM FILL/WASTE											
28	64	13618	292531	21.3	19.7	0.0	0.0	0.0	0.0	0.0	
29	63	15625	382981	24.5	20.8	0.0	0.0	0.0	0.0	0.0	
Zone 2 Average		14622	337756	22.9	20.2	0.0	0.0	0.0	0.0	0.0	0.0
ZONE 3 - NO SAND, LESS THAN 2 FEET FILL/WASTE											
29	60	1392	1706	1.4	25.4	0.0	0.0	0.0	0.0	0.0	
30	57	8444	1006	0.1	21.3	0.0	0.0	0.0	0.0	0.0	
30	61	12342	21281	1.6	24.8	0.0	0.0	0.0	0.0	0.0	
Zone 3 Average		7393	7998	1.0	23.8	0.0	0.0	0.0	0.0	0.0	0.0

See note at end of table

FER\CRU2RI\JLG\APP-A\TABA2-3\June 7, 1994 12:56pm

5659

TABLE A.2-3
(Continued)

Row	Column	Fill or Waste Area (ft)	Fill or Waste Volume (ft^3)	Fill or Waste Thickness (ft)	Unsaturated GMA Thickness (ft)	Glacial Overburden Thickness (ft)	Thickness of Till Above the Sand/Gravel (ft)	Thickness of Sand/Gravel In Till (ft)	Thickness of Till Below the Sand/Gravel (ft)	Total Till Thickness (ft)	Slope at the Base of Fill/Waste (%)
ZONE 4 - NO SAND, LESS THAN 10 FEET FILL/WASTE											
28	66	4480	15288	3.5	21.3	6.0	0.0	0.0	6.0	6.0	
30	60	13981	87850	6.4	29.0	7.0	0.3	0.0	6.7	7.0	
31	58	11040	56950	5.7	29.6	6.0	0.0	0.0	5.9	6.0	
31	59	15625	131675	8.4	31.4	11.8	3.2	0.1	8.6	11.8	
Zone 4 Average		11282	72941	6.0	27.8	7.7	0.0	0.0	7.7	7.7	1.5
ZONE 5 - NO SAND, LESS THAN 2 FEET TILL, MORE THAN 10 FEET FILL/WASTE											
29	58	12171	137888	11.0	18.2	0.0	0.0	0.0	0.0	0.0	
29	59	14263	297838	20.7	20.2	0.0	0.0	0.0	0.0	0.0	
29	65	15625	398850	25.5	24.8	0.0	0.0	0.0	0.0	0.0	
Zone 5 Average		14020	278192	19.1	21.1	0.0	0.0	0.0	0.0	0.0	8.5
ZONE 6 - NO SAND, MORE THAN 2 FEET SAND, MORE THAN 10 FEET FILL/WASTE											
30	58	15625	164338	10.5	21.7	7.4	0.0	0.0	7.4	7.4	
30	59	15625	231375	14.8	28.2	6.5	0.0	0.0	6.5	6.5	
30	63	15625	294731	18.9	24.8	3.3	0.0	0.0	3.3	3.3	
30	64	15625	245375	15.7	26.4	4.4	0.0	0.0	4.4	4.4	
Zone 6 Average		15625	233955	15.0	25.3	5.4	0.0	0.0	5.4	5.4	5
ZONE 7 - NORTHERN PART OF INACTIVE FLYASH PILE											
29	67	3837	13519	3.6	32.5	8.5	3.3	3.0	2.2	5.4	
30	67	6665	55444	8.9	29.7	8.4	1.7	2.7	3.9	5.7	
Zone 7 Average		5251	34481	6	31	8	2	3	3.1	5.5	0.0

See note at end of table

FER\CRU2RI\JLG\APP-A\TABA2-3\June 7, 1994 12:56pm

000119
5659

TABLE A.2-3
(Continued)

Row	Column	Fill or Waste Area (ft)	Fill or Waste Volume (ft^3)	Fill or Waste Thickness (ft)	Unsaturated GMA Thickness (ft)	Glacial Overburden Thickness (ft)	Thickness of Till Above the Sand/Gravel (ft)	Thickness of Sand/Gravel In Till (ft)	Thickness of Till Below the Sand/Gravel (ft)	Total Till Thickness (ft)	Slope at the Base of Fill/Waste (%)
ZONE 8											
29	66	15241	227906	15.2	32.0	4.0	0.3	1.4	2.3	2.6	0.0
ZONE 9											
30	65	15625	117675	7.5	27.3	10.1	0.4	0.4	9.2	9.7	4
ZONE 10 - LESS THAN 3 FEET OF TILL ABOVE SAND											
30	66	15429	154863	9.9	28.6	10.3	1.6	1.6	7.1	8.7	
31	61	15625	149431	9.6	30.8	10.8	2.1	1.3	7.4	9.5	
31	62	15625	134256	8.6	30.1	11.5	2.3	0.8	8.4	10.7	
31	63	15625	162263	10.4	29.5	12.2	1.8	0.7	9.7	11.5	
Zone 10 Average		15576	150203	9.6	29.8	11.2	1.9	1.1	8.2	10.1	4
ZONE 11 - LESS THAN 1 FEET OF FILL, MORE THAN 5 FEET OF TILL ABOVE SAND											
31	66	3615	4919	0.9	28.7	18.5	8.3	0.8	9.4	17.7	
34	60	3509	1269	0.3	32.7	22.7	12.8	2.1	7.8	20.6	
35	61	4123	788	0.2	32.2	23.9	12.8	2.0	9.1	21.9	
Zone 11 Average			2325	0.5	31.2	21.7	11.3	1.6	8.8	20.1	0
ZONE 12 - 2-3 FEET OF FILL, GOOD TILL LAYER ABOVE SAND											
31	65	13612	31419	2.3	28.6	18.0	5.8	1.5	10.7	16.5	
32	64	14238	41544	3.0	29.6	22.0	10.6	1.8	9.6	20.2	
33	59	1860	3688	2.0	33.0	18.3	9.8	1.3	7.2	17.0	
33	60	14234	26344	1.8	32.7	20.4	10.7	2.0	7.7	18.4	
33	61	15625	39369	2.5	31.8	21.7	10.7	1.8	9.2	20.0	
33	63	12928	29019	2.4	30.6	23.5	12.1	1.7	9.6	21.7	

See note at end of table

TABLE A.2-3
(Continued)

Row	Column	Fill or Waste Area (ft)	Fill or Waste Volume (ft^3)	Fill or Waste Thickness (ft)	Unsaturated GMA Thickness (ft)	Glacial Overburden Thickness (ft)	Thickness of Till Above the Sand/Gravel (ft)	Thickness of Sand/Gravel In Till (ft)	Thickness of Till Below the Sand/Gravel (ft)	Total Till Thickness (ft)	Slope at the Base of Fill/Waste (%)
ZONE 12 - 2-3 FEET OF FILL, GOOD TILL LAYER ABOVE SAND (Continued)											
34	61	15140	39388	2.6	32.1	22.2	11.0	2.0	9.1	20.1	
34	62	10365	26269	2.8	31.5	22.6	11.2	1.7	9.7	20.9	
Zone 12 Average		12250	29630	2.4	31.2	21.1	10.3	1.7	9.1	19.3	0
ZONE 13 - MORE THAN 4 FEET OF FILL WITH LATERAL DRAINAGE											
31	60	15625	121769	7.8	31.6	14.0	4.1	1.4	8.6	12.7	
31	64	15625	104775	6.7	29.1	15.9	4.5	0.8	10.6	15.1	
32	62	15625	96975	6.2	30.7	18.8	7.3	2.5	9.0	16.3	
32	63	15625	96025	6.2	30.1	19.7	8.4	2.1	9.3	17.6	
33	62	15625	63881	4.1	31.1	21.7	10.3	1.7	9.8	20.1	
Zone 13 Average		15625	96685	6.2	30.5	18.0	6.9	1.7	9.5	16.4	0.9
ZONE 14 - MORE THAN 4 FEET OF FILL, NO LATERAL DRAINAGE											
32	59	12620	60931	4.9	32.5	14.8	6.3	0.7	7.9	14.1	
32	60	15625	70544	4.5	32.3	17.6	7.6	2.5	7.5	15.1	
32	61	15625	66731	4.3	31.4	18.6	7.7	2.3	8.6	16.3	
Zone 14 Average		14623	66069	4.6	32.1	17.0	7.2	1.8	8.0	15.2	0

NOTE: GMA = Great Miami Aquifer

000121

5659

of the South Field. Seep water travels on the top of the glacial overburden until it flows into the unsaturated sand and gravels of the Great Miami Aquifer. These seeps were included as source terms for the Great Miami Aquifer.

5659

A.2.3.4 Active Flyash Pile

The constituent migration pathways applicable to the Active Flyash Pile were the vadose zone, perched water infiltration, and the surface water pathways. Figure A.2-11 shows the SWIFT III grid blocks directly under the flyash at the Active Flyash Pile. The Active Flyash Pile overlies a variable, 0 to 22 feet thick layer of till (Layer 1) for vadose zone pathway followed immediately by 22 to 33 feet of sand and gravel layer (Layer 2) (Table A.2-4). For the purposes of modeling, colluvial material was assumed to have the same properties as the sands of the Great Miami Aquifer. Lateral drainage of infiltrated leachate was simulated as shown in Figure A.2-9. Although no sand/gravel layers were identified under the Active Flyash Pile during field activities, perched water has been observed in monitoring wells installed just north of the Active Flyash Pile. Therefore, a 3-foot perched water layer in the middle of the glacial overburden was used for perched water infiltration pathway simulation.

A.2.4 APPROACH FOR SOURCE TERM DEVELOPMENT

In the geochemical assessment of leachate formation, the events leading to the failure of the waste areas and exposure of the waste to precipitation are not considered. The conceptual scenario used to model the release of contaminants from Operable Unit 2 subunits is illustrated in Figure A.2-5. Rainwater infiltrates the waste and reacts with waste solids to form a waste leachate. This leachate concentration is assumed to be unchanged by reaction with the glacial overburden materials. Waste leachate is used to constrain the initial constituent concentrations for the groundwater fate and transport model (vadose zone model). Constituent concentrations in the waste were assumed to be uniform in each subunit except for uranium-238. For uranium-238, block by block concentrations were estimated using geostatistical modeling.

A.2.4.1 Site-Specific Data

Analytical data used for deriving leachate concentrations from the waste areas were available from several sources:

- RI/FS Phase I Field Investigation Leachate Samples - Chemical and Radiological Analysis

5659

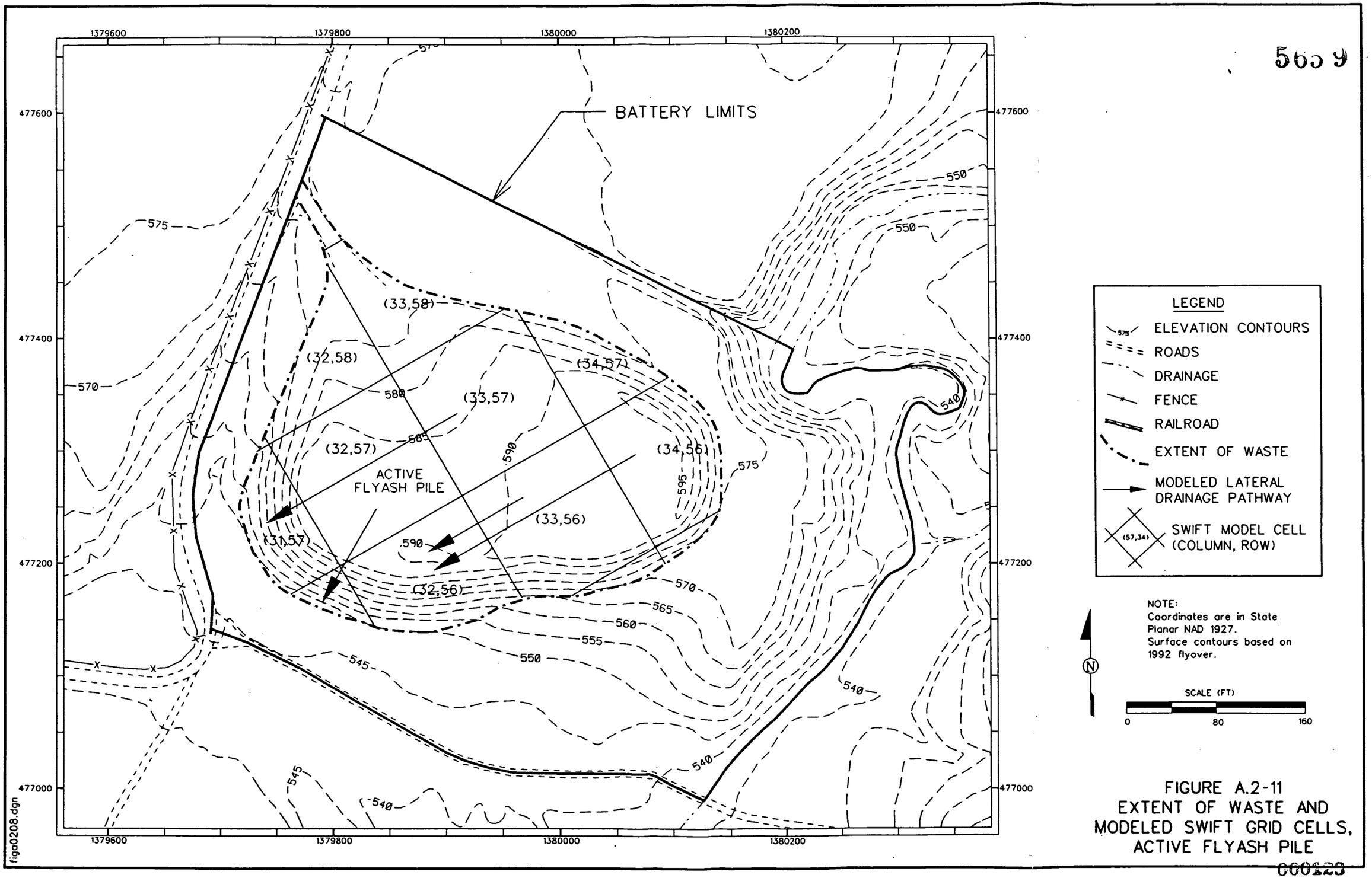

FIGURE A.2-11
EXTENT OF WASTE AND MODELED SWIFT GRID CELLS, ACTIVE FLYASH PILE

000123

TABLE A.2-4

PHYSICAL PARAMETERS FOR THE SWIFT III GRID CELLS IMPACTED BY THE ACTIVE FLYASH PILE OPERABLE UNIT 2 REMEDIAL INVESTIGATION FERNALD ENVIRONMENTAL MANAGEMENT PROJECT

Row	Column	Fill or Waste Area (ft)	Fill or Waste Volume (ft^3)	Fill or Waste Thickness (ft)	Unsaturated GMA Thickness (ft)	Glacial Overburden Thickness (ft)	Slope at the Base of Fill/Waste (%)
ZONE 1 - CENTRAL PORTION OF THE ACTIVE FLYASH PILE							
32	57	15625	449800	28.8	30.1	5.7	
33	56	15240	319700	21.2	30.8	15.8	
33	57	15595	276300	17.7	31.6	14.9	
34	56	11205	188350	15.9	31.2	22.2	
Zone 1 Average		14416	308538	20.9	30.9	14.7	5
ZONE 2 - NORTHERN SLOPING SURFACE							
32	58	7095	55100	8.0	31.7	12.7	
33	58	7350	42250	5.6	32.6	16.6	
34	57	5885	68700	12.2	32.1	20.0	
Zone 2 Average		6777	55350	8.6	32.1	16.4	0
ZONE 3 - FLYASH DIRECTLY ON THE GREAT MIAMI AQUIFER							
31	56	1625	16100	8.6	22.1	0.0	
31	57	6240	90550	16.1	25.8	0.0	
32	56	11570	246250	20.7	28.3	0.0	
Zone 3 Average		6478	117633	15.1	25.4	0.0	0

NOTE: GMA = Great Miami Aquifer

- RI/FS Phase I and II Soil Samples - Chemical and Radiological Analysis
- RI/FS Phase I and II Field Investigation Toxicity Characteristic Leaching Procedure (TCLP) Samples - Chemical and Radiological Analysis

These data sets are contained in Appendices C through G. Analytical data for the leachate data sets are most complete for the Solid Waste Landfill. TCLP extracts were analyzed for metals and the some radionuclides. Limitations associated with the available data are outlined when model results are discussed in this section. Only validated analytical results were used for developing source terms.

A.2.4.2 Source Term Development

Waste constituent concentrations (except uranium-238) used in the groundwater modeling are the upper 95 percent confidence level on the means (UCL) of the waste concentrations reported in individual samples for RI/FS subsurface soil data for each subunit. Constituent inventory in the waste/fill was calculated by multiplying waste concentration, waste volume, and bulk density of the waste. Waste volumes were calculated on a block-by-block basis from the difference between surface elevations and elevations of the base of waste/fill. The surface elevations are based on 1992 fly-over data and elevations of the base of waste/fill were derived from soil borings, Hydropunch data, preconstruction (1952) surface contours, and aerial photographs from 1951 (preconstruction) to 1992. Elevations were interpolated on a 25-by-25 foot grid. Tables A.2-1 through A.2-4 provide waste volumes on a 125-by-125 foot block. Average waste bulk densities were obtained from the geotechnical analysis of ~~soil~~ waste/fill samples collected during field investigations. Table A.2-5 provides a summary of physical parameters of the waste used in the vadose zone modeling.

NO. A-15

For uranium-238, the concentration in each block was estimated using kridging. This approach was selected for uranium, as uranium controls the risk from groundwater pathways and to simulate known hot spots identified during field investigations.

All validated uranium-238 data from RI/FS Phase I and Phase II field investigations for each subunit were segregated by waste/fill, glacial overburden, and sand/gravel of the Great Miami Aquifer. Furthermore, a relationship between uranium-238 and total-uranium concentration was developed from all samples analyzed for uranium-238 and total-uranium. For soil samples analyzed for total uranium but not for uranium-238, uranium-238 concentration was estimated from the subunit-specific

TABLE A.2-5

SUMMARY OF SOURCE AREAS AND PHYSICAL PARAMETERS FOR OPERABLE UNIT 2 AQUIFER MODEL
OPERABLE UNIT 2 REMEDIAL INVESTIGATION
FERNALD ENVIRONMENTAL MANAGEMENT PROJECT

Location	Area of Waste (m^2)	Area of Waste (ft^2)	Volume of Waste Material (m^3)	Volume of Waste Material (ft^3)	Dry Density (kg/m^3)	Number of Swift III Cells Modeled
Solid Waste Landfill	4,237	45,611	11,036	389,692	1,830	6
Lime Sludge Ponds	7,236	77,889	13,857	489,305	760	7
Inactive Flyash Pile/South Field	55,431	596,673	162,437	5,735,763	1,701.18	49
Active Flyash Pile	9,040	97,304	49,687	1,754,498	860.2	10

000123
5659

uranium-238 and total uranium relationship. Uranium-238 concentrations in each 25 x 25 x 2.5 foot block were then estimated using three-dimensional kridging for each media type. Kridging for each medium used analytical results from soil samples from that medium only. Average waste concentrations in 125 x 125 foot SWIFT III grid cells were then calculated from 25 x 25 x 2.5 foot thick blocks. These concentrations are reported later in Section A.2.7.2.2.

Source terms for seep and perched water (infiltration and subsurface seep) pathways were estimated using the following equation:

$$\text{Mass} = (\phi\, C_w + \rho_b K_d C_w)\, Ab$$

where

- A = Area of cell (125 x 125 ft^2)
- b = Average perched water zone thickness
- C_w = Upper 95 percent confidence level on the means (UCL) of the perched water concentrations
- K_d = Distribution coefficient
- ϕ = Porosity
- ρ_b = Bulk (dry) density

A.2.4.3 ESTIMATION OF LEACHATE CONCENTRATIONS

All constituent concentrations used as input data in the fate and transport model are constrained by (in order of preference): in situ leachate analyses, TCLP data, or the EPA 70-year rule (EPA 1988a). Figure A.2-12 summarizes the approach for estimating leachate concentrations. Geochemical modeling was not used due to large uncertainty associated with leachate concentrations derived from geochemical modeling.

As shown in Figure A.2-12, the preferred data for estimating constituent concentrations in waste leachate are analyses of in situ leachate. When these data were unavailable, the next best available data, TCLP data, was used. When a constituent was detected in TCLP data or in situ leachate, the maximum detected concentration was used as leachate concentration. If in situ leachate or TCLP analyses indicated that the compound was not detected, then the leachate concentration of a particular CPC was conservatively estimated as the maximum detection limit value. For CPCs that lack in situ or TCLP data, the EPA 70-year rule calculation was used to estimate their leachate concentration. If

5659

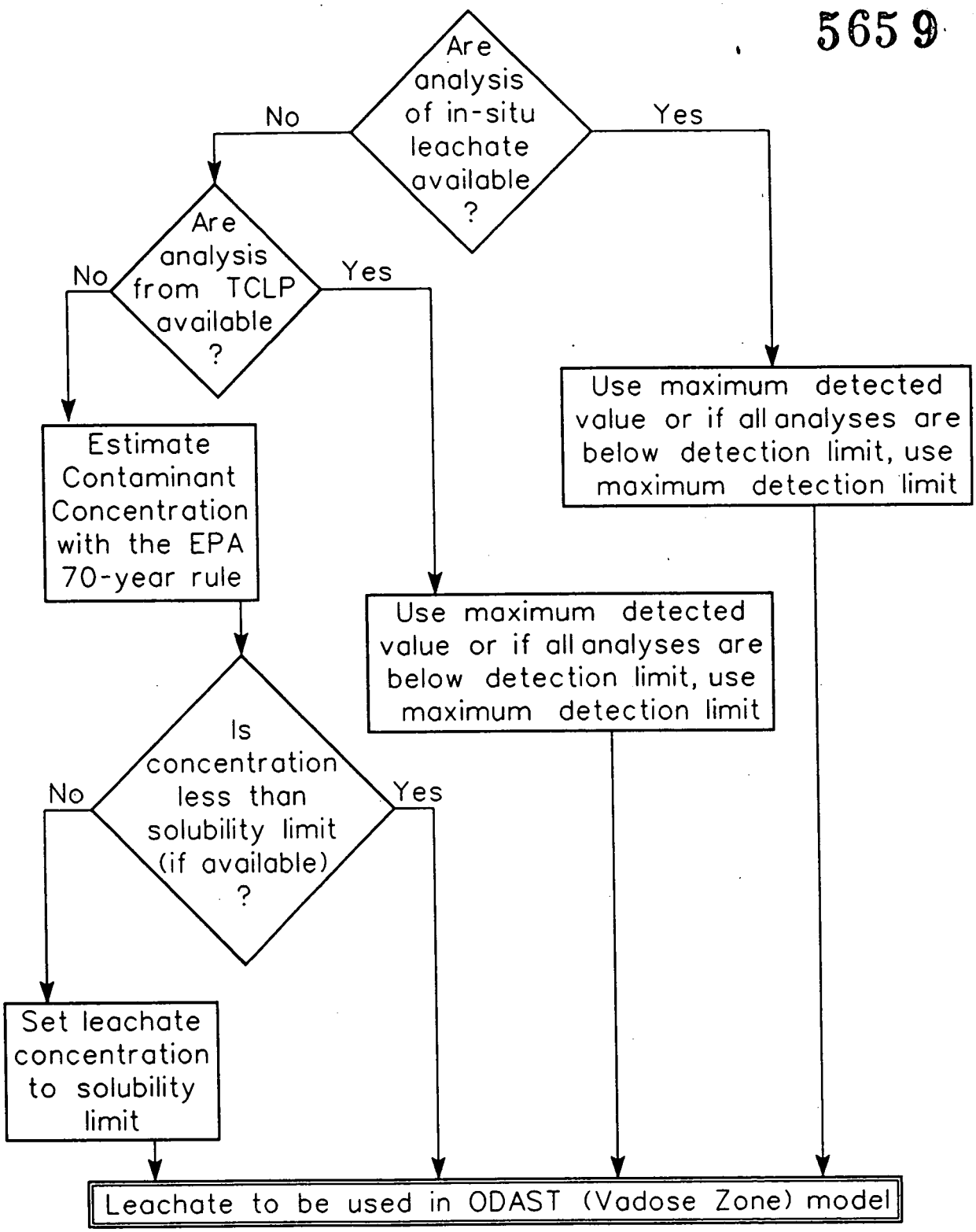

figa0211.dgn

FIGURE A.2-12
PROCEDURE FOR ESTIMATING LEACHATE CONCENTRATION

000128

the leachate concentration estimated from the EPA 70-year rule exceeded the solubility limit, then the leachate concentration was set to the solubility limit.

In Situ Leachate

In situ leachate reflects the complex interactions that take place between the waste solids and contact solution at the waste environment. Duplicating these conditions in laboratory tests is difficult and time consuming. The method describing the sampling and testing procedure can be found in the sampling and analysis plan (DOE 1992a).

Toxicity Characteristic Leaching Procedure

When in situ leachate data are unavailable, available TCLP data are used to constrain the CPC concentrations in waste leachate. TCLP data are derived by leaching the waste with acetic acid. The use of acetic acid as the leachate (rather than rainwater which acts as the leachant for in situ leachate) results in estimates of CPC concentrations that may be too high. That is, a conservative uncertainty is likely to be introduced into the estimation of leachate compositions. This occurs because acetic acid degrades into the acetate ion, which is very effective at complexing heavy metals in solution and maintaining their concentrations above expected solubility levels.

EPA 70-Year Rule

When in situ and TCLP data are lacking, the EPA 70-year rule is the suggested guidance for estimating leachate compositions (EPA 1988). The 70-year method is based on the assumption that the constituent inventory will be depleted within this time period, which is assumed to equal the average lifetime of a human being.

A.2.4.4 Uncertainty in Estimating Leachate Compositions

As waste composition in Operable Unit 2 subunits is generally heterogeneous, it is possible that in situ leachate concentration may not be a representative value of leachate concentration in each block. Uncertainty is also introduced into the estimation of leachate composition whenever in situ leachate analyses are not available. The logic behind using the decision hierarchy shown in Figure A.2-12 is to apply the best available site-specific data to the estimation of leachate compositions. Each successively lower step on this hierarchy represents a more conservative method for estimating constituent concentrations in leachate. For example, the use of TCLP data to estimate leachate composition will probably result in constituent concentrations that are greater than values expected for

in situ leachate. The acetic acid leaching used in the TCLP procedure results in greater concentrations for many metals because acetic acid is a more aggressive leaching agent than rain water. Calculations carried out to estimate constituent concentrations using the EPA 70-year rule will introduce a large conservative uncertainty for all but the most soluble constituents (e.g., bromide and cesium). The possibility exists to underestimate the constituent concentration when the EPA 70-year rule is applied to very soluble constituents. However, the baseline risk assessment uses the maximum predicted concentration for the full 70-year average life span of humans.

A.2.5 PARAMETERS

The parameters used to perform the fate and transport modeling can be divided into flow parameters and transport parameters. Flow parameters affect the velocity of groundwater movement. Transport parameters affect the rate of migration and the fate of constituents. Wherever possible, site-specific values are used for the analyses. Certain parameters, however, were not available for all of the subunits, and were estimated based on pertinent scientific literature search, geochemical investigations, and were checked for consistency between model results and historical data. Conservative estimates were used when a range of values are indicated or parameter values were not available. The formulations employed for the estimation of the parameters are described in the Risk Assessment Work Plan Addendum (DOE 1992). Uncertainty in the selection of model parameter values was addressed by performing sensitivity analyses. Sensitivity analyses were performed by varying parameters within reasonable ranges. Additional information regarding the sensitivity analysis is presented in Section A.2.10.

The conceptual model depicting flow in the vadose zone considers two layers. Layer 1 soils consist of tills in glacial overburden. Beneath the till is the unsaturated Great Miami Aquifer layer (Layer 2). The physical parameters of the media for Operable Unit 2 subunits are presented in Tables A.2-6 and A.2-7. Average values for bulk density and fines passing 200 mesh are reported in Table A.2-6. Field measurements are reported in Appendices C through G. For organic carbon content, minimum measured values in each subunit were selected for fate and transport modeling. This represents a conservative assumption. Porosity, specific yield, and field capacity were estimated from soil descriptions and values reported for similar soils in the Hydrologic Evaluation of Landfill Performance (HELP) model documentation.

TABLE A.2-6

MEDIA PARAMETERS FOR VADOSE ZONE MODEL
OPERABLE UNIT 2 REMEDIAL INVESTIGATION
FERNALD ENVIRONMENTAL MANAGEMENT PROJECT

Parameter	Vadose Zone	
	Layer 1[a]	Layer 2[b]
SOLID WASTE LANDFILL		
Porosity (%)	41	39
Specific yield (%)	6	25
Bulk density (g/cc)	1.89	1.60
Field capacity (%)	37.1	4.5
Organic content (%)	1.43	0.87
Fines passing less than 200 mesh (%)	70.1	16.5
LIME SLUDGE PONDS		
Porosity (%)	41	39
Specific yield (%)	6	25
Bulk density (g/cc)	1.73	1.60
Field capacity (%)	28	14
Organic content (%)	1.65	0.87
Fines passing less than 200 mesh (%)	70.1	16.5
INACTIVE FLYASH PILE		
Porosity (%)	41	39
Specific yield (%)	6	25
Bulk density (g/cc)	1.85	1.60
Field capacity (%)	37.1	4.5
Organic content (%)	1.69	0.87
Fines passing less than 200 mesh (%)	70.9	16.5

See footnotes at end of table

TABLE A.2-6
(Continued)

Parameter	Vadose Zone Layer 1[a]	Vadose Zone Layer 2[b]
SOUTH FIELD		
Porosity (%)	41	39
Specific yield (%)	6	25
Bulk density (g/cc)	1.85	1.60
Field capacity (%)	37.1	4.5
Organic content (%)	1.69	0.87
Fines passing less than 200 mesh (%)	70.9	16.5
ACTIVE FLYASH PILE		
Porosity (%)	41	39
Specific yield (%)	6	25
Bulk density (g/cc)	1.850	1.600
Field capacity (%)	37.1	4.5
Organic content (%)	1.69	0.87
Fines passing less than 200 mesh (%)	70.9	16.5

[a]Layer 1 consists of a clay-rich glacial till interbedded with glaciofluvial sand and gravel stringers. However, Layer 1 consists of only glacial till.

[b]Layer 2 consists of unsaturated well-sorted sand and gravel outwash deposits existing above the Great Miami Aquifer.

Other Comment No. A-48

TABLE A.2-7

VADOSE ZONE MODEL INPUT PARAMETERS
OPERABLE UNIT 2 REMEDIAL INVESTIGATION
FERNALD ENVIRONMENTAL MANAGEMENT PROJECT

Waste Subunit	Layer[a]	Thickness Range (ft)	K_v (ft/day)	q Range (ft/day)
Lime Sludge Ponds	1	23.6 - 34.0	5.386×10^{-3}	3.33×10^{-3}
	2	16.7 - 20.5	45	3.33×10^{-3}
Solid Waste Landfill	1	31.1 - 35.3	5.386×10^{-3}	2.1×10^{-3}
	2	19.4 - 25.7	45	2.1×10^{-3}
Active Flyash Pile	1	0 - 22.2	3.969×10^{-4}	5.18×10^{-4} to 6.48×10^{-3}
	2	16 - 32	45	5.18×10^{-4} to 6.48×10^{-3}
Inactive Flyash Pile/South Field	1	0 - 21.9	3.969×10^{-4}	2.83×10^{-4} to 3.58×10^{-3}
	2	0 - 21.9	45	2.83×10^{-4} to 3.58×10^{-3}

K_v = vertical hydraulic conductivity
q = vertical flow rate

[a]Layer 1 is glacial till
Layer 2 is unsaturated Great Miami Aquifer

000133

The vertical hydraulic conductivity values for Layer 1 (see Table A.2-7) were obtained from geometric average horizontal hydraulic conductivities of 1000-series wells completed in dark gray clay or clayey silt or from maximum permeability measurements conducted on core samples. The vertical hydraulic conductivity for Layer 2 was obtained by dividing the horizontal hydraulic conductivity of the Great Miami Aquifer by 10. The factor of 10 represents a typical horizontal to vertical hydraulic conductivity ratio. The vertical hydraulic conductivity was estimated to be 1.9×10^{-6} to 1.4×10^{-7} centimeter per second (cm/sec) for Layer 1. The vertical hydraulic conductivity of Layer 2 was 1.6×10^{-2} cm/sec for all of the Operable Unit 2 subunits.

Table A.2-7 also shows the vertical flow rates (q) simulated with the HELP model. The estimates of the vertical seepage velocities ~~(Vx)~~ (V) used in the vadose zone transport model were based on the methods presented in the Risk Assessment Work Plan Addendum (DOE 1992). These methods calculate seepage velocity as a function of flow rate (q), porosity, and empirically derived soil factors. The longitudinal dispersion coefficients (D_x), a function of dispersivity, interstitial seepage, velocity and molecular diffusion coefficient were estimated by the methods presented by Biggar and Nielsen (1976), and Mills et al. (1982).

NO. A-16

- The seepage velocity is calculated using the following equation (USEPA, 1988):

NO. A-16

$$V = q^{\left(1-\frac{1}{2b+3}\right)} \left[\frac{K_s^{\left(\frac{1}{2b+3}\right)}}{\theta_s} \right]$$

where

q	=	percolation rate (length/time)
$\frac{1}{2b+3}$	=	empirical soil-dependent parameter
K_s	=	saturated hydraulic conductivity(length/time)
Θ_s	=	saturated moisture content (volume/volume)

Empirical soil-dependent parameter was assumed to be 0.039 and 0.09 for glacial till and unsaturated Great Miami Aquifer, respectively (USEPA, 1988).

NO. A-43

$$D = 0.6 + 2.93\ v^{1.11}$$

where

D = Dispersion coefficient in cm^2/sec, and
v = seepage velocity in cm/sec.

Flow and solute transport through the porous media are not only determined by the parameters considered in the conceptual model description above, they are also affected by retardation factors (R) and decay rates. The retardation factor was used to account for those reversible reactions that slow the arrival of a contaminant front, but do not act as a sink. The retardation factor can be expressed as the ratio between the rate of groundwater movement and the rate of contaminant movement. These parameters are both chemical- and media-specific. The retardation factors were calculated from (Walton, 1984; Mills et al., 1982):

$$R = 1 + \frac{\rho_b K_d}{\Theta}$$

where

K_d = Distribution coefficient
R = Retardation factor
ρ_b = Bulk dry density
Θ = Soil moisture content

NO. A-50

~~The distribution coefficient for radionuclides and inorganics is constituent specific.~~ For organic constituents, the distribution coefficient depends on the constituent itself as well as matrix parameters. The following equations were used to calculate distribution coefficients for organic CPCs:

$$K_{oc} = 0.63\ K_{ow}$$

$$K_d = 0.2\ K_{oc}\ f_{oc}\ (1 + 4\ F)$$

where

K_{ow} = Octonal water partitioning coefficient
f_{oc} = Total organic carbon content, fraction
F = Fines passing 200 mesh, fraction

000135

NO. A-50

The distribution coefficient for radionuclides and inorganics is constituent specific. The Risk Assessment Work Plan Addendum was used as the source of all distribution coefficient values for radionuclides and inorganics except uranium. Distribution coefficients (K_d) for uranium-238 were obtained from a site-specific study (Uranium Partition Coefficient Evaluation Study for Operable Unit 2, 1993). For each media, the minimum reported value of K_d was selected for fate and transport modeling. For all Operable Unit 2 subunits, a distribution coefficient of 200 ml/g for Layer 1 was used. Minimum value of K_d for the Great Miami Aquifer soils (Layer 2) was 8.4 ml/g. Fate and Transport calculations for Operable Unit 2 subunits were first run with a K_d of 8.4 ml/g for uranium in the Great Miami Aquifer. However, predicted results and observed results could not be reasonably matched using a Layer 2 K_d of 8.4 ml/g. During the model calibration process, the K_d for uranium-238 was estimated to be 1.48 ml/g for the Great Miami Aquifer. This value was used in previous studies and is consistent with experimental data available (DOE 1993a) which indicates these values are conservatively low. Distribution coefficients for other uranium isotopes were assumed to be same as for uranium-238.

The radioactive decay constants and biodegradation coefficients are estimated based on the degradation rates (Howard et al. 1991) using the formulation presented in the Risk Assessment Work Plan Addendum (DOE 1992).

Table A.2-8 shows the distribution coefficients and/or K_{ow} for all the CPCs for Operable Unit 2 subunits. This table also presents the radioactive decay half lives for radionuclides and the biodegradation decay half lives for the organic constituents. These distribution coefficients, K_{ow} and decay half lives are used in analytical modeling of transport in the vadose zone and numeric modeling of transport in the aquifer.

A.2.6 CONSTITUENT SCREENING AND REVIEW - VADOSE ZONE PATHWAY

The list of CPCs was screened from further analysis in several ways to eliminate constituents that pose insignificant risk. In addition, groundwater monitoring data was reviewed to determine constituents that were found in the aquifer so that these constituents can be evaluated in the computation of total risk. These screening steps were performed because vadose zone and aquifer modeling require long computational times and to allow the analysis to focus on the constituents that cause the high percentage of the risk. Figure A.2-13 shows the different screening steps for the vadose zone pathway. (Figure A.2-3 shows approach for screening from all pathways and

A-48

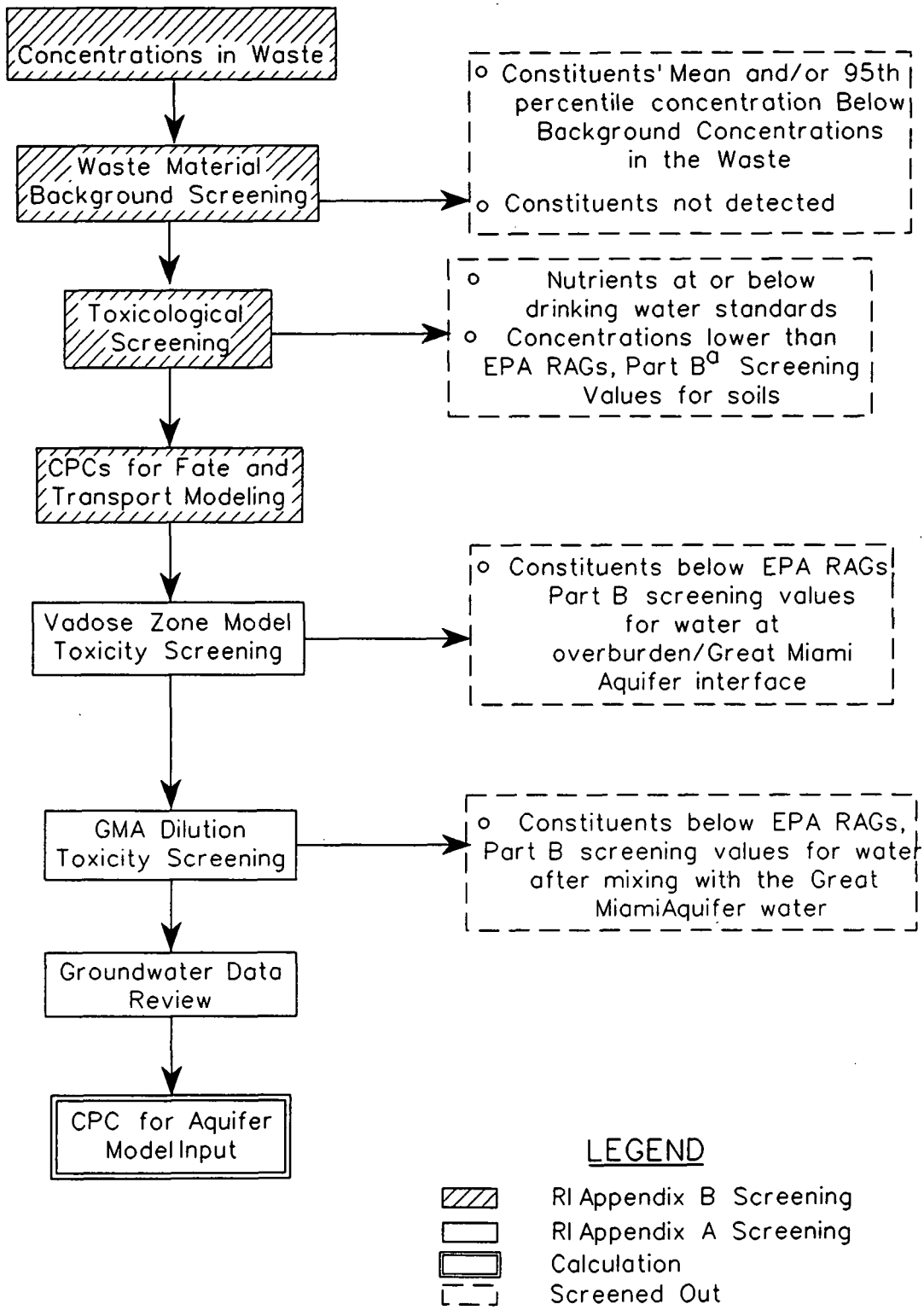

[a] EPA Risk Assessment Guidence, Part B (EPA, 1991).

FIGURE A.2-13
POTENTIAL CONSTITUENT OF CONCERN SCREENING DIAGRAM

figa0212.dgn

000137

TABLE A.2-8

DISTRIBUTION COEFFICIENTS, K_{ow}, AND DECAY HALF LIVES FOR CONSTITUENTS OF POTENTIAL CONCERN OPERABLE UNIT 2 REMEDIAL INVESTIGATION FERNALD ENVIRONMENTAL MANAGEMENT PROJECT

Constituent of Potential Concern	Distribution Coefficient (mL/g)		K_{ow} (mL/g)	Decay Half-Life (days)
	Glacial Overburden	Great Miami Aquifer		
RADIONUCLIDES				
Cesium-137	$1.81 \times 10^{+3}$	$1.37 \times 10^{+3}$	NA	$1.10 \times 10^{+4}$
Lead-210	$3.00 \times 10^{+3}$	$3.80 \times 10^{+1}$	NA	$8.13 \times 10^{+3}$
Neptunium-237	$5.50 \times 10^{+1}$	$5.00 \times 10^{+0}$	NA	$7.81 \times 10^{+8}$
Plutonium-238	$1.70 \times 10^{+3}$	$1.00 \times 10^{+2}$	NA	$3.20 \times 10^{+4}$
Plutonium-239/240	$1.70 \times 10^{+3}$	$1.00 \times 10^{+2}$	NA	$8.81 \times 10^{+6}$
Radium-224	$6.96 \times 10^{+2}$	$1.06 \times 10^{+2}$	NA	$3.62 \times 10^{+0}$
Radium-226	$6.96 \times 10^{+2}$	$1.06 \times 10^{+2}$	NA	$5.84 \times 10^{+5}$
Radium-228	$6.96 \times 10^{+2}$	$1.06 \times 10^{+2}$	NA	$2.10 \times 10^{+3}$
Ruthenium-106	$8.00 \times 10^{+2}$	$5.50 \times 10^{+1}$	NA	3.67×10^{-4}
Strontium-90	$1.00 \times 10^{+1}$	$2.50 \times 10^{+0}$	NA	$1.04 \times 10^{+4}$
Technetium-99	1.18×10^{-1}	7.00×10^{-2}	NA	$7.77 \times 10^{+7}$
Thorium-228	$5.80 \times 10^{+3}$	$3.20 \times 10^{+3}$	NA	$6.98 \times 10^{+2}$
Thorium-230	$5.80 \times 10^{+3}$	$3.20 \times 10^{+3}$	NA	$2.81 \times 10^{+7}$
Thorium-232	$5.80 \times 10^{+3}$	$3.20 \times 10^{+3}$	NA	$5.10 \times 10^{+12}$
Uranium-234	$2.00 \times 10^{+2}$	$1.48 \times 10^{+0}$	NA	$8.92 \times 10^{+7}$
Uranium-235/236	$2.00 \times 10^{+2}$	$1.48 \times 10^{+0}$	NA	$2.57 \times 10^{+11}$
Uranium-238	$2.00 \times 10^{+2}$	$1.48 \times 10^{+0}$	NA	$1.63 \times 10^{+12}$
Uranium-Total	$2.00 \times 10^{+2}$	$1.48 \times 10^{+0}$	NA	$1.63 \times 10^{+12}$
ORGANICS				
1,2-Diethylbenzene	Variable	$5.37 \times 10^{+1}$	$2.95 \times 10^{+4}$	ND
1,4-Dioxane	Variable	6.91×10^{-4}	3.80×10^{-1}	6.60×10^{-1}
1,1,2 Trichlorotrifluoroethane	Variable	1.82×10^{-1}	$1.00 \times 10^{+2}$	$1.47 \times 10^{+3}$
2-Methylnaphthalene	Variable	$1.32 \times 10^{+1}$	$7.24 \times 10^{+3}$	ND
Acrylonitrle	Variable	3.09×10^{-3}	$1.70 \times 10^{+0}$	$4.59 \times 10^{+1}$
Aroclor-1254	Variable	$1.95 \times 10^{+3}$	$1.07 \times 10^{+6}$	none
Aroclor-1260	Variable	$2.35 \times 10^{+3}$	$1.29 \times 10^{+6}$	none
Benzo(a)anthracene	Variable	$7.28 \times 10^{+2}$	$4.00 \times 10^{+5}$	$2.77 \times 10^{+3}$
Benzo(a)pyrene	Variable	$1.74 \times 10^{+3}$	$9.55 \times 10^{+5}$	$2.77 \times 10^{+3}$

See notes at end of table

5659

TABLE A.2-8
(Continued)

Constituent of Potential Concern	Distribution Coefficient (mL/g)		K_{ow} (mL/g)	Decay Half-Life (days)
	Glacial Overburden	Great Miami Aquifer		
ORGANICS (Continued)				
Benzo(b)fluoranthene	Variable	$6.77 \times 10^{+3}$	$3.72 \times 10^{+6}$	$2.48 \times 10^{+3}$
Benzo(g,h,i)perylene	Variable	$5.90 \times 10^{+3}$	$3.24 \times 10^{+6}$	$1.30 \times 10^{+3}$
bis(2-Ethylhexyl)phthalate	Variable	$1.73 \times 10^{+0}$	$9.50 \times 10^{+2}$	$3.89 \times 10^{+2}$
Carbazole	Variable	$3.55 \times 10^{+0}$	$1.95 \times 10^{+3}$	ND
Dibenzo(a,h)anthracene	Variable	$1.70 \times 10^{+3}$	$9.33 \times 10^{+5}$	$3.85 \times 10^{+3}$
Dieldrin	Variable	$5.75 \times 10^{+0}$	$3.16 \times 10^{+3}$	$2.55 \times 10^{+3}$
Endosulfan Sulfate	Variable	$8.32 \times 10^{+0}$	$4.57 \times 10^{+3}$	ND
Heptachlorodibenzo-p-dioxin	Variable	$1.91 \times 10^{+4}$	$1.05 \times 10^{+7}$	none
Heptachlorodibenzofuran	Variable	$1.91 \times 10^{+4}$	$1.05 \times 10^{+7}$	$1.12 \times 10^{+2}$
Ideno(1,2,3-cd)pyrene	Variable	$8.32 \times 10^{+4}$	$4.57 \times 10^{+7}$	$2.89 \times 10^{+3}$
Octachlorodibenzo-p-dioxin	Variable	$2.88 \times 10^{+5}$	$1.58 \times 10^{+8}$	none
Phenanthrene	Variable	$2.64 \times 10^{+1}$	$1.45 \times 10^{+4}$	$4.00 \times 10^{+2}$
Tetrachlorodibenzofuran	Variable	$1.20 \times 10^{+3}$	$6.61 \times 10^{+5}$	none
Tributyl Phosphate	Variable	$1.82 \times 10^{+1}$	$1.00 \times 10^{+4}$	ND
INORGANICS				
Antimony	$2.50 \times 10^{+2}$	$4.50 \times 10^{+1}$	NA	none
Arsenic	$2.00 \times 10^{+2}$	$2.00 \times 10^{+2}$	NA	none
Beryllium	$1.30 \times 10^{+3}$	$2.50 \times 10^{+2}$	NA	none
Lead	$3.00 \times 10^{+3}$	$3.80 \times 10^{+1}$	NA	none
Thallium	$1.50 \times 10^{+3}$	$1.50 \times 10^{+3}$	NA	none

NA - Not Applicable
ND - No data available
none - Constituent does not decay
Variable - Distribution coefficient for Glacial Overburden varies from subunit to subunit

Comment No. A-48

000139

NO. A-48

incorporation of monitoring data into the modeling process). These steps include ~~pre-screening and background~~ background and initial soil toxicologic screening (performed and presented in Section 6.0 and Appendix B), vadose zone output concentration screening and Great Miami Aquifer dilution screening~~, and the review of groundwater monitoring data~~. Each subunit was treated separately in these screening analyses. These screening steps are described in the following subsections.

~~A.2.6.1 Prescreening~~

~~Prescreening was performed on the validated sampling and analysis data sets. Each constituent on the data set was evaluated based on the criteria defined in the Risk Assessment Work Plan Addendum (DOE 1992). At this stage in the process, two types of decisions were made:~~

- ~~Nutrients at or below drinking water standards were screened out~~
- ~~Constituents that were not detected in waste area materials were screened out~~

~~The results of this prescreening are presented in Appendix B.~~

A.2.6.1 Background Screening

The first screening step was conducted to remove constituents that were below background concentrations and constituents that were not detected. Each constituent that was detected was compared to background concentrations following the process defined in Appendix B. This process included mean of subunit-specific data with the mean of the background data and comparison of 95th percentile of the subunit-specific data with the 95th percentile of the background data. Constituents with concentrations determined to be below background concentrations were screened out. The results of this background screening are presented in Appendix B.

NO. A-48

~~A.2.6.2 Background Screening~~

~~A second preliminary screening step was conducted to remove constituents that were below background concentrations. Each constituent that passes prescreening was compared to background concentrations following the process defined in Appendix B. Constituents with concentrations determined to be below background concentrations were screened out. The results of this background screening are presented in Appendix B.~~

~~The constituents that "passed" the prescreening and background screening were designated "constituents of potential concern (CPCs)" for fate and transport modeling purposes.~~

NO. A-48

A.2.6.2 Toxicologic Screening

Toxicological screening, a second preliminary screening step, was performed on each constituent passing background screening to exclude constituents that are unlikely to have a human health risk at levels detected. The following criteria were used to eliminate constituents in this screening step:

- Constituents which were detected only once in one medium and not in any other media were removed.
- Nutrients that are nontoxic (e.g., sodium, potassium, iron) were screened out.
- Constituents that ubiquitous (e.g., aluminum, silica) in nature were screened out.
- Nonspecific class of compounds (e.g, TOC, TPH, PAH) were screened out.
- Constituents with concentrations lower than the screening values calculated based on EPA RAGs, Part B guidelines, were screened out.

The results of this prescreening are presented in Appendix B.

The constituents that "passed" the background and toxicological screening were designated "constituents of potential concern (CPCs)" for fate and transport modeling purposes.

NO. A-48

~~A.2.6.3 Review of Monitoring Data~~

~~Water samples have been taken from the Great Miami Aquifer and analyzed periodically. The results for the 1000 series wells indicate the degree of contamination from the FEMP operation in the perched water. If a constituent was detected above the 10^{-7} risk or 0.1 HI levels in perched water and was detected in the waste, then it was included as a CPC, and was included in the vadose zone modeling and screening.~~

NO. A-48

A.2.6.3 Vadose Zone Model Toxicity Screening

Prior to performing aquifer modeling, the output from the vadose zone model was screened against the ~~10^{-7} cancer risk or 0.1 HI concentration~~ EPA RAGs, Part B screening concentrations. Since concentrations can only be further diluted when leachate mixes with the aquifer waters, this screening step removes constituents that will clearly be below the ~~10^{-7} risk or 0.1 HI based standard~~ EPA RAGs, Part B screening concentrations in the aquifer. To perform this screening, the maximum output from the vadose zone model for a particular constituent was compared with the ~~10^{-7} risk or 0.1 HI based concentrations~~ EPA RAGs, Part B screening concentrations. If this maximum value (from

000141

all grid blocks) was below the screening concentration, then the constituent was screened out and was not modeled further.

A.2.6.4 Great Miami Aquifer Dilution Screening

CPCs passing the vadose zone model toxicity screening were further screened by predicting dilution in the Great Miami Aquifer. Predicted Great Miami Aquifer concentration was calculated using:

$$C_{GMA} = \frac{C_v \, q \, A}{Q_{GMA}}$$

where

A	=	Area of cell (125 x 125 ft^2)
C_{GMA}	=	Predicted maximum Great Miami Aquifer concentration
C_v	=	Maximum output concentration from the vadose zone model
Q_{GMA}	=	Groundwater flow rate through the upper layer of the SWIFT III model in the cell with maximum vadose zone concentration
q	=	Infiltration rate in the cell with maximum vadose zone concentration

Predicted maximum concentration, C_{GMA}, is typically an order of magnitude lower than from the detailed calculations using the SWIFT III model. The above dilution calculation is conservative because waste storage in the cell is not considered. The C_{GMA} for a particular constituent is compared with the ~~10^{-7} risk level for carcinogens or the 0.1 HI level for noncarcinogens~~ EPA RAGs, Part B screening concentrations. If C_{GMA} was below the screening concentration, then the constituent was screened out and was not modeled further.

NO. A-48

A.2.7 VADOSE ZONE MODELING

Vadose zone modeling was performed to estimate CPC loading rates to the Great Miami Aquifer from a given source as a function of time. The overburden may have great capacity for immobilization and retardation of CPCs due to adsorption, precipitation, biodegradation, and radioactive decay. This capacity to prevent or slow the movement of CPCs to the aquifer is evaluated with respect to future risk.

The following criteria were used in selecting specific analytical models:

- Capability of treating adsorption, radioactive and organic decay, and longitudinal dispersion
- Capability of calculating concentrations over long time periods
- Availability of code
- Degree of code documentation
- Degree of code verification

The primary model selected was the One-Dimensional Analytical Solute Transport (ODAST) model (Javendel et al, 1984). To estimate time for source depletion and to calculate seepage velocity (required ODAST input parameters), leachate infiltration rates were calculated using the HELP model. These models are discussed below.

A.2.7.1 Estimating Infiltration Rates

A.2.7.1.1 Description of HELP Model

The HELP model was used to determine the infiltration rates through the waste. The HELP model (EPA 1984) is a quasi-two-dimensional hydrologic model of water movement across, into, through, and out of a waste unit. The model accepts climatologic, soil, and design data and simulates a number of hydraulic processes including surface storage, runoff, infiltration, percolation, evapotranspiration, soil moisture storage, and lateral drainage. The systems that can be modeled by HELP include various combinations of vegetation, cover soils, waste cells, drainage layers, and relatively impermeable barrier soils.

The HELP model is designed to perform water budget calculations for a system having as many as 12 layers by modeling each of the hydrologic processes that occur. Each layer must be identified as either a vertical percolation, lateral drainage, or barrier soil layer. The identification of each layer used in the model is critical because the program models water flow through the various types of layers in different ways. Runoff is computed using the Soil Conservation Service (SCS) runoff curve number method by considering daily precipitation totals. ~~Percolation and vertical water routing are modeled using Darcy's Law for saturated flow with modifications for unsaturated conditions.~~ Percolation and vertical water flow is modeled using Darcy's Law with hydraulic conductivity as a function of saturation, i.e, relative permeability effects. Evapotranspiration is estimated by a modified Penman method adjusted for limiting soil moisture conditions.

NO. A-17

000143

The HELP model output consists of input data echo, simulation results, and a summary. The input data echo includes all the information used for input including the values chosen from the model's built-in data base and any manually input data. Following the input data echo, the program produces a table of the daily results, monthly totals, and annual totals for each year if the options for detailed output are used. Following these outputs, the summary output is given. The summary includes average monthly totals, average annual totals, and peak daily values for the simulation variables. The average monthly totals report precipitation, runoff, evapotranspiration, percolation through the base of each layer, and lateral drainage through each layer for a particular month for all the years of a simulation. The average annual total reports values on an annual basis. The summary of peak daily values represents the maximum values that occurred on any day during the simulation period.

A.2.7.1.2 Infiltration Rate Results

HELP modeling for Operable Unit 2 included separate runs for each subunits. Within each subunit, various zones of similar thickness for waste, till, and unsaturated Great Miami Aquifer were grouped together (zones). Properties for various layers (except for thickness) remained the same for all zones within each subunit. These properties are shown in Table A.2-9. The soil physical parameters used in the simulations were varied for each subunit to reflect the varying conditions at each subunit. These values were defined based upon RI sampling activities (Table A.2-9). Permeabilities were defined based upon field and laboratory tests. In each simulation, the climatologic data of precipitation and mean monthly temperature were assumed to be same as for Cincinnati, Ohio from 1974 to 1978. Average rainfall in this period was 40.64 inches/year.

Layer thickness for each zone within a subunit was further varied. In general, layers were defined for waste area material, waste drainage layer (bottom one foot of waste if lateral drainage applies), glacial till, and upper unsaturated Great Miami Aquifer sands.

The HELP model was run to "steady state," that is, until successive simulations showed no appreciable change in soil moisture content in any of the layers. Summary of HELP results (infiltration and lateral drainage rates) are presented in Tables A.2-10 through A.2-13. Vertical infiltration rates varied from 1.24 inches/year for the Zone 11 (with more than 20 feet of till) in the Inactive Flyash Pile/South Field to 14.57 inches/year for the Lime Sludge Ponds.

TABLE A.2-9

MEDIA PARAMETERS FOR HELP MODEL
OPERABLE UNIT 2 REMEDIAL INVESTIGATION
FERNALD ENVIRONMENTAL MANAGEMENT PROJECT

Parameter	Unit	Solid Waste Landfill	Lime Sludge Pond	Inactive Flyash Pile	South Field	Active Flyash Pile
Hydraulic Conductivity	cm/sec					
Waste/Fill		1.10×10^{-4}	1.00×10^{-3}	1.80×10^{-4}	2.00×10^{-4}	1.80×10^{-4}
Glacial Till		1.90×10^{-6}	1.90×10^{-6}	1.40×10^{-7}	1.40×10^{-7}	1.40×10^{-7}
Unsaturated GMA		1.59×10^{-2}	1.59×10^{-2}	1.59×10^{-2}	1.59×10^{-2}	1.59×10^{-2}
Porosity	%					
Waste/Fill		52	55	44	52	44
Glacial Till		41	41	41	41	41
Unsaturated GMA		39	39	39	39	39
Field Capacity	%					
Waste/Fill		29.4	37.8	28.4	29.4	28.4
Glacial Till		37.1	37.1	37.1	37.1	37.1
Unsaturated GMA		4.5	4.5	4.5	4.5	4.5
Wilting Point	%					
Waste/Fill		14.0	26.5	13.5	14.0	13.5
Glacial Till		25.1	25.1	25.1	25.1	25.1
Unsaturated GMA		2.0	2.0	2.0	2.0	2.0
Vegetative Cover		poor	bare ground	good	good	bare ground
Maximum Leaf Area Index	0-5 scale	1	0	3.3	2-3.3	0
Evaporation Zone Depth	inches	15	9	38	21-38	9
SCS Runoff Curve Number	0-100 scale	58	86	55	61	86

SCS - Soil Conservation Service

TABLE A.2-10

HELP MODEL RESULTS FOR THE SOLID WASTE LANDFILL OPERABLE UNIT 2 REMEDIAL INVESTIGATION FERNALD ENVIRONMENTAL MANAGEMENT PROJECT

Zone No.	SWIFT III Grid Block	Infiltration Rate (inches/year)	Seepage Velocity in Glacial Till (inches/year)	Seepage Velocity in the UGMA (inches/year)	Average Waste Thickness (ft)	Average Glacial Till Thickness (ft)	Average Unsaturated Great Miami Aquifer Thickness (ft)
1	52,91 51,90	9.03	22.7	56.9	8.3	34.8	23.7
2	51,91 51,92	9.03	22.7	56.9	8.3	34.5	22.1
3	50,91 50,92	9.03	22.7	56.9	8.8	32.0	20.6

UGMA = Unsaturated Great Miami Aquifer

USEPA Comment No. A-16

000146
5659

TABLE A.2-11

HELP MODEL RESULTS FOR THE LIME SLUDGE PONDS
OPERABLE UNIT 2 REMEDIAL INVESTIGATION
FERNALD ENVIRONMENTAL MANAGEMENT PROJECT

Zone No.	SWIFT III Grid Block	Infiltration Rate (inches/year)	Seepage Velocity in Glacial till (inches/year)	Seepage Velocity in the UGMA (inches/year)	Average Waste Thickness (ft)	Average Glacial Till Thickness (ft)	Average Unsaturated Great Miami Aquifer Thickness (ft)
1	44,79 45,80 43,81	14.57	36.2	88.0	3.4	31.8	18.3
2	44,81 43,80 45,81	14.57	36.2	88.0	7.4	25.7	20.1
3	44,80	14.57	36.2	88.0	9.4	27.6	18.2

UGMA = Unsaturated Great Miami Aquifer

USEPA Comment No. A-16

TABLE A.2-12

HELP MODEL RESULTS FOR THE INACTIVE FLYASH PILE AND SOUTH FIELD
OPERABLE UNIT 2 REMEDIAL INVESTIGATION
FERNALD ENVIRONMENTAL MANAGEMENT PROJECT

Zone No.	SWIFT III Grid Block	Vertical Infiltration Rate through the Waste (inches/year)	Lateral Drainage from Grid Blocks (inches/year)	Combined Vertical and Lateral Infiltration to GMA* (inches/year)	Seepage Velocity in Glacial Till (inches/year)	Seepage Velocity in the UGMA (inches/year)	Average Waste Thickness (ft)	Average Glacial Till Thickness (ft)	Average Unsaturated GMA Thickness (ft)
1	28,59 28,63 28,65 29,62[a] 29,64[b] 30,62[c]	7.01	0	7.01 7.01 7.01 11.09 11.09 15.72	NA NA NA NA NA NA	45.2 45.2 45.2 68.6 68.6 94.3	16.5	0	20.6
2	28,64 29,63[d]	7.00	0	7.00 8.37	NA NA	45.1 53.1	22.9	0	20.2
3	29,60 30,57[e] 30,61[f]	9.28	0	9.28 13.36 15.69	NA NA NA	58.3 81.3 94.1	1.0	0	23.8
4	28,66[g] 30,60[h] 31,58 31,59	2.44	0	6.11 3.81 2.44 2.44	14.2 9.0 5.9 5.9	39.9 26.0 17.3 17.3	6.0	7.7	27.8
5	29,58[i] 29,59 29,65[j]	5.80	0	9.88 5.80 8.54	NA NA NA	61.8 38.0 54.1	19.1	0	21.1
6	30,58 30,59 30,63 30,64	8.26	4.08	4.18 4.18 4.18 4.18	9.9 9.9 9.9 9.9	28.2 28.2 28.2 28.2	15.0	5.4	25.3
7	29,67 30,67	2.9	0	2.90 2.90	6.9 6.9	20.2 20.2	6.0	5.0	31.0

565 9
000148

5659

TABLE A.2-12
(Continued)

Zone No.	SWIFT III Grid Block	Vertical Infiltration Rate through the Waste (inches/year)	Lateral Drainage from Grid Blocks (inches/year)	Combined Vertical and Lateral Infiltration to GMA* (inches/year)	Seepage Velocity in Glacial Till (inches/year)	Seepage Velocity in the UGMA (inches/year)	Average Waste Thickness (ft)	Average Glacial Till Thickness (ft)	Average Unsaturated GMA Thickness (ft)
8	29,66	7.01	0	7.01	16.2	45.2	15.2	2.6	32.0
9	30,65	5.53	2.74	2.79	6.7	19.6	7.5	9.6	27.3
10	30,66 31,61 31,62 31,63	6.67	3.67	3.00 3.00 3.00 3.00	7.2 7.2 7.2 7.2	20.9 20.9 20.9 20.9	9.6	10.1	29.8
11	31,66 34,60 35,61	1.24	0	1.24 1.24 1.24	3.1 3.1 3.1	9.3 9.3 9.3	0.5	20.1	31.2
12	31,65 32,64 33,59 33,60 33,61 33,63 34,61 34,62	1.86	0	1.86 1.86 1.86 1.86 1.86 1.86 1.86 1.86	4.5 4.5 4.5 4.5 4.5 4.5 4.5 4.5	13.5 13.5 13.5 13.5 13.5 13.5 13.5 13.5	2.4	19.4	31.2
13	31,60 31,64 32,62 32,63 33,62	3.58	1.37	2.21 2.21 2.21 2.21 2.21	5.3 5.3 5.3 5.3 5.3	15.8 15.8 15.8 15.8 15.8	6.2	14.6	30.5

TABLE A.2-12
(Continued)

Zone No.	SWIFT III Grid Block	Vertical Infiltration Rate through the Waste (inches/year)	Lateral Drainage from Grid Blocks (inches/year)	Combined Vertical and Lateral Infiltration to GMA* (inches/year)	Seepage Velocity in Glacial Till (inches/year)	Seepage Velocity in the UGMA (inches/year)	Average Waste Thickness (ft)	Average Glacial Till Thickness (ft)	Average Unsaturated GMA Thickness (ft)
14	32,59 32,60 32,61	2.23	0	2.23 2.23 2.23	5.4 5.4 5.4	15.9 15.9 15.9	4.6	15.2	32.1

[a]Grid Block (29,62) receives lateral drainage from Grid Block (30,63)
[b]Grid Block (29,64) receives lateral drainage from Grid Block (30,64)
[c]Grid Block (30,62) receives lateral drainage from Grid Blocks (31,62), (31,63), and (32,63)
[d]Grid Block (29,63) receives lateral drainage from Grid Block (31,64)
[e]Grid Block (30,57) receives lateral drainage from Grid Block (30,58)
[f]Grid Block (30,61) receives lateral drainage from Grid Blocks (31,61), (32,62), and (33,62)
[g]Grid Block (28,66) receives lateral drainage from Grid Block (30,66)
[h]Grid Block (30,60) receives lateral drainage from Grid Block (31,60)
[i]Grid Block (29,58) receives lateral drainage from Grid Block (30,59)
[j]Grid Block (29,65) receives lateral drainage from Grid Block (30,65)

*GMA - Great Miami Aquifer
UGMA - Unsaturated Great Miami Aquifer
NA - Not applicable

USEPA Comment No. A-16

000154

TABLE A.2-13

HELP MODEL RESULTS FOR THE ACTIVE FLYASH PILE OPERABLE UNIT 2 REMEDIAL INVESTIGATION FERNALD ENVIRONMENTAL MANAGEMENT PROJECT

Zone No.	SWIFT III Grid Block	Vertical Infiltration Rate through the Waste (inches/year)	Lateral Drainage from Grid Blocks (inches/year)	Combined Vertical and Lateral Infiltration to GMA* (inches/year)	Seepage Velocity in Glacial Till (inches/year)	Seepage Velocity in the UGMA (inches/year)	Representative Waste Thickness (ft)	Representative Glacial Till Thickness (ft)	Representative Unsaturated GMA Thickness (ft)
1	32,57 33,56 33,57 34,56	11.57	8.41	3.16 3.16 3.16 3.16	7.5 7.5 7.5 7.5	21.9 21.9 21.9 21.9	22.0	16.0	32.0
2	32,58 33,58 34,57	2.27	0	2.27 2.27 2.27	11.7 11.7 11.7	16.2 16.2 16.2	5.0	15.0	32.0
3	31,56[a] 31,57[b] 32,56[c]	11.56	0	19.97 19.97 28.38	NA NA NA	117.2 117.2 161.3	38.0	0	32.0

[a]Grid Block (31,56) receives lateral drainage from Grid Block (32,57)
[b]Grid Block (31,57) receives lateral drainage from Grid Block (33,57)
[c]Grid Block (32,56) receives lateral drainage from Grid Blocks (33,56) and (34,56)

*GMA - Great Miami Aquifer

UGMA - Unsaturated Great Miami Aquifer
NA - Not Applicable

USEPA Comment No. A-16

A.2.7.2 ODAST Description

The model selected to evaluate flow in the vadose zone is ODAST (Javendel et al. 1984). ODAST is used for determining fate and transport of the constituents not previously screened out. This computer code is based on the solution originally developed by Ogata and Banks (1961) and calculates the normalized concentrations of a given constituent in a uniform flow field from a source having a constant or varying concentration in the initial layer. ODAST evaluates the basic one-dimensional analytical solute transport equation as a function of seepage velocity, dispersion coefficient, source decay, retardation factor, depletion time, and source rate. ODAST has been extensively verified against STRIP1B (Batu 1989).

The ODAST model implements an analytical solution to the partial differential equation

$$D\frac{\partial^2 C}{\partial x^2} - V\frac{\partial C}{\partial x} - \lambda RC = R\frac{\partial C}{\partial t}$$

where

C = solute concentration and with the constant coefficients
D = dispersion coefficient
V = seepage velocity
R = retardation factor
λ = solute decay factor
t = time

The solution must satisfy the initial and boundary conditions

$$C(x,0) = 0$$

$$-D\frac{\partial C}{\partial x} + VC\,|_{x=0} = \begin{cases} VC_o\, e^{-\alpha t} & 0 \le t \le \tau_o \\ 0, & t > \tau_o \end{cases}$$

$$\frac{\partial C}{\partial x}\Big|_{x\to\infty} = 0$$

$$\alpha = \frac{\ln_2}{T_{1/2}} = \frac{0.693}{T_{1/2}}$$

where the constants

C_o = initial source (waste leachate) concentration
α = source depletion factor
τ_o = source depletion time
$T_{1/2}$ = decay half life

The solution is obtained using a Laplace transform technique and involves products of exponential and complementary error functions (Javandel et al. 1984). The solution for C is divided by C_0 to yield normalized concentrations.

Because the coefficients in the governing equation are constant and the solution must satisfy a zero concentration gradient condition as x approaches infinity, ODAST is only strictly applicable to one-dimensional transport in homogeneous, semi-infinite media. However, the present application of ODAST is intended only to provide conservative estimates of aquifer mass loading histories.

A superposition technique is used to combine calculations for the two homogeneous layers comprising the vadose zone conceptual model. The ODAST solution at the bottom of Layer 1 is divided into 1000 small time steps and a Layer 2 run is performed for each of these steps. Each of these Layer 2 runs assumes no source decay, a recharge period 1/1000 of the total modeling time, and a source concentration equal to the averaged Layer 1 solution for that time period. The solution at the bottom of Layer 2 is obtained by summing the results of the 1000 Layer 2 runs at specified time steps. For RI/FS modeling, concentrations are calculated up to 1,000 years, typically in steps of 20 years. Constituents that migrate quickly, such as organics, require smaller time steps for accurate representation of loading curves.

ODAST requires a formatted ASCII file containing the input parameters for a particular problem. This is the only input required. Likewise, output is contained in a single formatted ASCII file. The unit conventions for the input file parameters are: 1) specified calculation times and source depletion time expressed in years, all other parameters use days, 2) and any consistent length scale may be used.

The first parameters appearing in the input file are specifications of the values of the independent variables for which the calculations are desired. These include the number of positions where concentrations are desired, number of times, and the actual positions where concentrations are desired

(measured positive downward from the top of the layer) and times. Because concentrations are required at the bottom of the layer, only one position, representing layer thickness, is used. Layer thicknesses vary among and within the subunits and were obtained from interpolated measurements at the FEMP. As previously stated, times up to 1,000 years in 20 year increments were normally used. The number of times may be greater and increments smaller if the constituent migrates rapidly.

The final line of the input file contains the zone area, solute, and medium dependent parameters. In order of appearance in the file, they are the dispersion coefficient, seepage velocity, retardation factor, source depletion time, solute decay factor, and source depletion factor.

Seepage velocity and the dispersion coefficient depend upon the characteristics of the waste area and the vadose zone medium. Seepage velocity was calculated as an empirical function of the percolation rate obtained from the HELP model, saturated hydraulic conductivity, and porosity (US EPA 1988). Grid blocks receiving lateral drainage (see Figures A.2-8 and A.2-11) included percolation from waste as well as lateral drainage (Figure A.2-9). The dispersion coefficient was obtained as an empirical function of seepage velocity (Biggar and Nielsen 1976).

NO. A-43

$$D = 0.6 + 2.93\, v^{1.11}$$

where

D = Dispersion coefficient in cm^2/sec, and

v = seepage velocity in cm/sec.

NO. A-45

The source depletion time and depletion factor are calculated based on the procedure used for calculating the leachate concentration. When the 70-year rule was used to calculate the leachate concentration, the depletion time was 70 years and source leachate concentration remains constant for the 70 years. When the leachate concentration from in-situ leachate or TCLP analysis was available, an exponentially declining source leachate concentration term was used:

$$C = C_o\, Exp(-\alpha t)$$

where

$$\alpha = \frac{qAC_o}{M}$$

A = area of the grid cell (125 ft x 125 ft),

C_o = initial leachate concentration determined from the in-situ leachate or TCLP analysis,

M = mass of contaminant in the grid cell, and

q = infiltration rate.

The depletion factor (α) is inversely proportional to the depletion half life.

The retardation factor accounts for transport delays due to reversible reactions between the chemical constituent and the vadose zone solid matrix. It is thus dependent on both solute and media characteristics, and was calculated as a function of the constituent's partitioning coefficient and the vadose zone bulk density and moisture content (Walton 1984 and Mills et al. 1985). (See Section A.2.5).

The solute decay factor is constituent dependent. This parameter accounts for biodegradation in organics and radioactive decay in radionuclides, and is zero for stable inorganics (ASI/IT 1992b).

Source depletion time and factor control the mass flux history of the constituent at the top of the modeled layer. As can be seen from the upstream boundary condition, source mass flux decays exponentially. To calculate depletion time and factor for the waste at the top of layer 1, the time dependent expression for mass flow from the source was integrated from zero to the source depletion time. This integral was equated to the depleted mass of the constituent to provide a single equation in two unknowns. A second equation was obtained by arbitrarily specifying a mass depletion fraction. This is the level (very close to, but less than one) at which the source is declared depleted; technically, the source is depleted only as time approaches infinity. As stated previously, depletion factor was zero and depletion time was 1/1000 of the total modeling time for the layer 2 runs.

For the 1,000-year scenario, the projected concentration of the leachate entering the Great Miami Aquifer beneath the waste area was calculated by multiplying the normalized concentration at the base

of the lowest layer by the source term (initial waste leachate concentration). The loading rates were calculated by multiplying the projected concentration beneath the SWIFT grid block by the volumetric recharge rate for the grid block. The plots of loading rates versus time were then produced for the constituents which were projected to reach the aquifer within 1,000 years.

A.2.7.3 ODAST Modeling Results and Screening of CPCs

Loading rates to the Great Miami Aquifer were estimated for each CPC for the Operable Unit 2 subunits using ODAST. Loading rates of a constituent from ODAST to the aquifer from a given source vary over time. Typically, loading rates experience a mild increase representing the dispersion front followed by a sharp increase representing the principle breakthrough of the constituent. They can then stabilize or decrease depending upon the depletion time of the source. For a long depletion time the source remains active for a longer period during the simulation. The depletion rate is low for long depletion times, this ensures a mild change in the source term with time and helps to approach a steady-state condition within the simulation time of 1,000 years. For short depletion time, the source term vanishes earlier during the simulation period. For high depletion rates, the source term decreases faster during the simulation period. These factors cause an unsteady variation along with a sharp decline in the loading rates.

Solid Waste Landfill

Figure A.2-6 shows the areal extent of the waste in the Solid Waste Landfill and the SWIFT III grid block impacted by the direct loading from the Solid Waste Landfill. Waste overlying the SWIFT III grid block (49,91) was included with SWIFT III waste overlying grid block (50,91). Similarly constituent loadings for SWIFT III grid blocks (52,92) were combined and loaded from the grid block (52,91). Table A.2-14 lists the CPCs considered for the fate and transport modeling and Table A.2-15 lists the calculated retardation factors for the Solid Waste Landfill. Table A.2-16 shows CPC concentrations in the waste, inventory in waste, predicted maximum leachate concentration, predicted maximum concentration from vadose zone layer 2, and screening concentrations for the Solid Waste Landfill. Two other pathways, besides the vadose zone pathway, were considered for the Solid Waste Landfill fate and transport modeling. One of these pathways was surface water pathway. However, no CPCs were identified from this pathway (see Appendix A-1). The second pathway was the perched water infiltration pathway. Table A.2-17 lists the perched water source concentrations and masses for the vadose zone modeling. Results of the perched water infiltration pathway are included in Table A.2-16. A summary of screening for CPCs from the Solid Waste Landfill is also included in

TABLE A.2-14

LIST OF CONSTITUENTS OF POTENTIAL CONCERN FOR VADOSE ZONE MODELING FOR THE SOLID WASTE LANDFILL OPERABLE UNIT 2 REMEDIAL INVESTIGATION FERNALD ENVIRONMENTAL MANAGEMENT PROJECT

Constituents of Potential Concern		
Radionuclides	Organics	Inorganics
Cesium-137	1,4-Dioxane	Antimony
Lead-210	2-Methylnaphthalene	Arsenic
Neptunium-237	Aroclor-1254	Beryllium
Plutonium-238	Aroclor-1260	Lead
Plutonium-239/240	Benzo(a)anthracene	
Radium-224	Benzo(a)pyrene	
Radium-226	Benzo(b)fluoranthene	
Radium-228	Benzo(g,h,i)perylene	
Strontium-90	Carbazole	
Technetium-99	Dibenzo(a,h)anthracene	
Thorium-228	Endosulfan Sulfate	
Thorium-230	Heptachlorodibenzo-p-dioxin	
Thorium-232	Heptachlorodibenzofuran	
Uranium-234	Indeno(1,2,3-cd)pyrene	
Uranium-235/236	Octachlorodibenzo-p-dioxin	
Uranium-238	Phenanthrene	
Uranium Total		

Other Comment No. A-48

000157

TABLE A.2-15

RETARDATION FACTORS FOR THE SOLID WASTE LANDFILL OPERABLE UNIT REMEDIAL INVESTIGATION FERNALD ENVIRONMENTAL MANAGEMENT PROJECT

Constituent of Potential Concern	Retardation Factor for Glacial Overburden	Retardation Factor for Unsaturated Great Miami Aquifer
RADIONUCLIDES		
Cesium-137	$8.35 \times 10^{+3}$	$1.67 \times 10^{+4}$
Lead-210	$1.38 \times 10^{+4}$	$4.65 \times 10^{+2}$
Neptunium-237	$2.55 \times 10^{+2}$	$6.21 \times 10^{+1}$
Plutonium-238	$7.84 \times 10^{+3}$	$1.22 \times 10^{+3}$
Plutonium-239/240	$7.84 \times 10^{+3}$	$1.22 \times 10^{+3}$
Radium-224	$3.21 \times 10^{+3}$	$1.30 \times 10^{+3}$
Radium-226	$3.21 \times 10^{+3}$	$1.30 \times 10^{+3}$
Radium-228	$3.21 \times 10^{+3}$	$1.30 \times 10^{+3}$
Strontium-90	$4.71 \times 10^{+1}$	$3.15 \times 10^{+1}$
Technetium-99	$1.54 \times 10^{+0}$	$1.86 \times 10^{+0}$
Thorium-228	$2.67 \times 10^{+4}$	$3.91 \times 10^{+4}$
Thorium-230	$2.67 \times 10^{+4}$	$3.91 \times 10^{+4}$
Thorium-232	$2.67 \times 10^{+4}$	$3.91 \times 10^{+4}$
Uranium-234	$9.23 \times 10^{+2}$	$1.91 \times 10^{+1}$
Uranium-235/236	$9.23 \times 10^{+2}$	$1.91 \times 10^{+1}$
Uranium-238	$9.23 \times 10^{+2}$	$1.91 \times 10^{+1}$
Uranium Total	$9.23 \times 10^{+2}$	$1.91 \times 10^{+1}$
ORGANICS		
1,4 Dioxane	$1.01 \times 10^{+0}$	$1.01 \times 10^{+0}$
2-Methylnaphthalene	$2.25 \times 10^{+2}$	$1.62 \times 10^{+2}$
Aroclor-1254	$3.38 \times 10^{+4}$	$2.38 \times 10^{+4}$
Aroclor-1260	$4.08 \times 10^{+4}$	$2.87 \times 10^{+4}$
Benzo(a)anthracene	$1.26 \times 10^{+4}$	$8.89 \times 10^{+3}$
Benzo(a)pyrene	$3.02 \times 10^{+4}$	$2.12 \times 10^{+4}$
Benzo(b)fluoranthene	$1.18 \times 10^{+5}$	$8.27 \times 10^{+4}$
Benzo(g,h,i)perylene	$1.00 \times 10^{+5}$	$7.21 \times 10^{+4}$
Carbazole	$6.26 \times 10^{+1}$	$4.43 \times 10^{+1}$
Dibenzo(a,h)anthracene	$2.95 \times 10^{+4}$	$2.07 \times 10^{+4}$
Endosulfan Sulfate	$1.42 \times 10^{+2}$	$1.03 \times 10^{+2}$
Heptachlorodibenzo-p-dioxin	$3.31 \times 10^{+5}$	$2.33 \times 10^{+5}$
Heptachlorodibenzofuran	$3.31 \times 10^{+5}$	$2.33 \times 10^{+5}$
Indeno(1,2,3-cd)pyrene	$1.44 \times 10^{+6}$	$1.02 \times 10^{+6}$
Octachlorodibenzo-p-dioxin	$4.99 \times 10^{+6}$	$3.51 \times 10^{+6}$
Phenanthrene	$4.50 \times 10^{+2}$	$3.23 \times 10^{+2}$

TABLE A.2-15
(Continued)

Constituent of Potential Concern	Retardation Factor for Glacial Overburden	Retardation Factor for Unsaturated Great Miami Aquifer
	INORGANICS	
Antimony	$1.15 \times 10^{+3}$	$5.51 \times 10^{+2}$
Arsenic	$9.23 \times 10^{+2}$	$2.44 \times 10^{+3}$
Beryllium	$5.99 \times 10^{+3}$	$3.05 \times 10^{+3}$
Lead	$1.38 \times 10^{+4}$	$4.65 \times 10^{+2}$

Other Comment No. A-48

TABLE A.2-16

SOURCE CHARACTERIZATION AND SCREENING SUMMARY FOR CONSTITUENTS OF POTENTIAL CONCERN, SOLID WASTE LANDFILL OPERABLE UNIT 2 REMEDIAL INVESTIGATION FERNALD ENVIRONMENTAL MANAGEMENT PROJECT

Constituent of Potential Concern	Upper 95% C.I. on Mean Concentration (mg/kg)	Constituent Inventory in the Waste (mg)	Initial Maximum Leachate Concentration (pCi/L RAD) (μg/L non-RAD)	Constraint[a]	Maximum Loading Concentration from ODAST (Vadose Layer 2) (pCi/L RAD) (μg/L non-RAD)	EPA RAGs, Part B Screening Concentration (pCi/L RAD) (μg/L non-RAD)	CPC ≥ Screening Concentration and Requires SWIFT Modeling
RADIONUCLIDES							
Cesium-137	2.89×10^{-9}	5.84×10^{-2}	$2.00 \times 10^{+1}$	ISL	0.0[b]	1.70×10^{-1}	No
Lead-210	1.35×10^{-8}	2.72×10^{-1}	$2.79 \times 10^{+2}$	70-Year	0.0	7.20×10^{-3}	No
Neptunium-237	4.98×10^{-4}	$1.01 \times 10^{+4}$	$1.00 \times 10^{+0}$	ISL	0.0	2.16×10^{-2}	No
Plutonium-238	1.92×10^{-8}	3.87×10^{-1}	$1.00 \times 10^{+0}$	ISL	0.0	2.16×10^{-2}	No
Plutonium-239/240	1.10×10^{-5}	$2.21 \times 10^{+2}$	$1.00 \times 10^{+0}$	ISL	0.0	2.07×10^{-2}	No
Radium-224	1.35×10^{-11}	2.72×10^{-4}	$7.28 \times 10^{+2}$	70-Year	0.0	1.25×10^{-1}	No
Radium-226	1.57×10^{-6}	$3.17 \times 10^{+1}$	$1.00 \times 10^{+0}$	ISL	0.0	1.76×10^{-4}	No
Radium-228	9.41×10^{-9}	1.90×10^{-1}	$3.00 \times 10^{+0}$	ISL	0.0	4.75×10^{-2}	No
Strontium-90	1.15×10^{-8}	2.33×10^{-1}	$5.00 \times 10^{+0}$	ISL	0.0	1.32×10^{-1}	No
Technetium-99	4.44×10^{-3}	$8.96 \times 10^{+2}$	$3.00 \times 10^{+1}$	ISL	$2.85 \times 10^{+1}$	$3.65 \times 10^{+0}$	Yes
Thorium-228	4.13×10^{-9}	8.35×10^{-2}	$1.00 \times 10^{+0}$	ISL	0.0	8.64×10^{-2}	No
Thorium-230	5.97×10^{-4}	$1.21 \times 10^{+4}$	$1.00 \times 10^{+0}$	ISL	0.0	3.65×10^{-1}	No
Thorium-232	$3.26 \times 10^{+1}$	$6.59 \times 10^{+8}$	$1.00 \times 10^{+0}$	ISL	0.0	2.79×10^{-3}	No
Uranium-234	1.56×10^{-2}	$3.15 \times 10^{+5}$	$9.42 \times 10^{+2}$	ISL	0.0	2.97×10^{-1}	No
Uranium-235/236	$3.72 \times 10^{+0}$	$7.52 \times 10^{+7}$	$1.05 \times 10^{+2}$	ISL	0.0	2.97×10^{-1}	No
Uranium-238		$3.39 \times 10^{+9}$	$8.68 \times 10^{+2}$	ISL	0.0	1.70×10^{-1}	No
Grid # 52,91	$6.01 \times 10^{+1}$	$1.21 \times 10^{+8}$	$8.68 \times 10^{+2}$	ISL			
Grid # 51,90	$1.21 \times 10^{+2}$	$2.73 \times 10^{+7}$	$8.68 \times 10^{+2}$	ISL			
Grid # 51,91	$2.00 \times 10^{+2}$	$1.26 \times 10^{+9}$	$8.68 \times 10^{+2}$	ISL			
Grid # 51,92	$5.36 \times 10^{+1}$	$1.84 \times 10^{+8}$	$8.68 \times 10^{+2}$	ISL			

See footnote at end of table

FER\CRU2RI\ULG\APP-A\TABA2-16\June7, 1994 1:37pm

TABLE A.2-16
(Continued)

Constituent of Potential Concern	Upper 95% C.I. on Mean Concentration (mg/kg)	Constituent Inventory in the Waste (mg)	Initial Maximum Leachate Concentration (pCi/L RAD) (μg/L non-RAD)	Constraint[a]	Maximum Loading Concentration from ODAST (Vadose Layer 2) (pCi/L RAD) (μg/L non-RAD)	EPA RAGs, Part B Screening Concentration (pCi/L RAD) (μg/L non-RAD)	CPC ≥ Screening Concentration and Requires SWIFT Modeling
RADIONUCLIDES (Continued)							
Grid # 50,91	$3.19 \times 10^{+2}$	$1.41 \times 10^{+9}$	$8.68 \times 10^{+2}$	ISL			
Grid # 50,92	$1.02 \times 10^{+2}$	$3.86 \times 10^{+8}$	$8.68 \times 10^{+2}$	ISL			
Uranium - Total (non-RAD)	$1.77 \times 10^{+3}$	$3.58 \times 10^{+10}$	$1.61 \times 10^{+3}$	mdl-ISL	0.0	1.09×10^{-2}	No
ORGANICS							
1,4 Dioxane	$1.29 \times 10^{+1}$	$2.61 \times 10^{+8}$	$4.70 \times 10^{+1}$	mdl-ISL	0.0	NA[c]	No
2-Methylnaphthalene	1.0×10^{-1}	$2.02 \times 10^{+6}$	$7.00 \times 10^{+1}$	mdl-ISL	0.0	NA	No
Aroclor-1254	4.80×10^{-2}	$1.01 \times 10^{+6}$	2.00×10^{-0}	mdl-ISL	0.0	1.10×10^{-3}	No
Aroclor-1260	7.70×10^{-2}	$1.62 \times 10^{+6}$	2.00×10^{-0}	mdl-ISL	0.0	1.10×10^{-3}	No
Benzo(a)anthracene	$7.50 \times 10^{+0}$	$1.52 \times 10^{+8}$	$1.00 \times 10^{+1}$	mdl-ISL	0.0	2.82×10^{-3}	No
Benzo(a)pyrene	$8.20 \times 10^{+0}$	$1.66 \times 10^{+8}$	$1.00 \times 10^{+1}$	mdl-ISL	0.0	2.82×10^{-4}	No
Benzo(b)fluoranthene	$1.50 \times 10^{+0}$	$3.03 \times 10^{+7}$	$1.00 \times 10^{+1}$	mdl-ISL	0.0	2.82×10^{-3}	No
Benzo(g,h,i)perylene	4.90×10^{-1}	$9.90 \times 10^{+6}$	$1.00 \times 10^{+1}$	mdl-ISL	0.0	NA	No
Carbazole	$4.20 \times 10^{+0}$	$8.48 \times 10^{+7}$	$1.00 \times 10^{+1}$	mdl-ISL	1.45×10^{-3}	4.25×10^{-1}	No
Dibenzo(ah)anthracene	2.50×10^{-1}	$5.05 \times 10^{+6}$	$1.00 \times 10^{+1}$	mdl-ISL	0.0	2.82×10^{-4}	No
Endosulfan Sulfate	6.20×10^{-3}	$1.25 \times 10^{+5}$	2.0×10^{-1}	mdl-ISL	0.0	NA	No
Heptachlorodibenzo-p-dioxin	9.00×10^{-4}	$1.82 \times 10^{+4}$	2.40×10^{-3}	SOL	0.0	1.19×10^{-6}	No
Heptachlorodibenzofuran	2.50×10^{-4}	$5.05 \times 10^{+3}$	8.51×10^{-2}	70-Year	0.0	1.19×10^{-6}	No
Indeno(1,2,3-cd)pyrene	$5.50 \times 10^{+0}$	$1.11 \times 10^{+8}$	$1.00 \times 10^{+1}$	mdl-ISL	0.0	2.82×10^{-3}	No
Octachlorodibenzo-p-dioxin	1.37×10^{-2}	$2.63 \times 10^{+5}$	4.00×10^{-4}	SOL	0.0	1.19×10^{-5}	No
Phenanthrene	$4.80 \times 10^{+0}$	$9.70 \times 10^{+7}$	$8.9 \times 10^{+1}$	mdl-ISL	0.0	NA	No

See footnote at end of table

TABLE A.2-16
(Continued)

Constituent of Potential Concern	Upper 95% C.I. on Mean Concentration (mg/kg)	Constituent Inventory in the Waste (mg)	Initial Maximum Leachate Concentration (pCi/L RAD) (μg/L non-RAD)	Constraint[a]	Maximum Loading Concentration from ODAST (Vadose Layer 2) (pCi/L RAD) (μg/L non-RAD)	EPA RAGs, Part B Screening Concentration (pCi/L RAD) (μg/L non-RAD)	CPC ≥ Screening Concentration and Requires SWIFT Modeling
INORGANICS							
Antimony	$2.20 \times 10^{+1}$	$4.44 \times 10^{+8}$	$3.00 \times 10^{+1}$	mdl-ISL	0.0	$1.46 \times 10^{+0}$	No
Arsenic	$1.38 \times 10^{+1}$	$2.79 \times 10^{+8}$	$1.81 \times 10^{+1}$	mdl-ISL	0.0	1.46×10^{-4}	No
Beryllium	$1.08 \times 10^{+0}$	$2.17 \times 10^{+7}$	2.00×10^{-0}	mdl-ISL	0.0	2.37×10^{-3}	No
Lead	$2.83 \times 10^{+1}$	$5.72 \times 10^{+8}$	$1.95 \times 10^{+1}$	mdl-ISL	0.0	NA	No

[a]Constraint on reported concentration is by In Situ Leachate (ISL), Toxicity Characteristic Leaching Procedure (TCLP), maximum detection limit (MDL), by US EPA 70-year rule (70-Year), or by the Solubility Limit (SOL).

[b]Zero indicates that predicted concentration is at least three orders of magnitude below the screening concentrations.

[c]NA = no data available to calculate EPA RAGs, Part B screening value.

Other Comment No. A-48

TABLE A.2-17

PERCHED WATER SOURCE CONCENTRATIONS AND MASSES FOR THE VADOSE ZONE MODELING, SOLID WASTE LANDFILL OPERABLE UNIT 2 REMEDIAL INVESTIGATION FERNALD ENVIRONMENTAL MANAGEMENT PROJECT

Constituents of Potential Concern	Initial Perched Water Concentration (pCi/L RAD) (μg/L non-RAD)	Total Mass (mg)	EPA RAGs, Part B Screening Concentration (pCi/L RAD) (μg/L non-RAD)
RADIONUCLIDES			
Neptunium-237	1.94×10^{0}	$8.86 \times 10^{+1}$	2.16×10^{-2}
Plutonium-238	6.70×10^{-1}	2.42×10^{-2}	2.16×10^{-2}
Radium-226	5.11×10^{0}	$3.39 \times 10^{+0}$	1.76×10^{-4}
Radium-228	3.72×10^{0}	8.96×10^{-3}	4.75×10^{-2}
Strontium-90	1.35×10^{0}	1.65×10^{-4}	1.32×10^{-1}
Thorium-228	$1.40 \times 10^{+1}$	3.37×10^{-1}	8.64×10^{-2}
Thorium-230	$1.38 \times 10^{+1}$	$1.32 \times 10^{+4}$	3.65×10^{-1}
Thorium-232	$1.15 \times 10^{+1}$	$2.06 \times 10^{+9}$	2.79×10^{-2}
Uranium-234	6.10×10^{0}	$1.03 \times 10^{+1}$	2.97×10^{-1}
Uranium-235/236	4.30×10^{-1}	$2.09 \times 10^{+3}$	2.97×10^{-1}
Uranium-238	$1.52 \times 10^{+1}$	$4.74 \times 10^{+5}$	1.70×10^{-1}
Uranium-Total (non-RAD)	$1.72 \times 10^{+1}$	$1.80 \times 10^{+5}$	$1.09 \times 10^{+1}$
INORGANICS			
Arsenic	4.40×10^{0}	$5.44 \times 10^{+6}$	1.46×10^{-4}
Beryllium	2.20×10^{0}	$3.40 \times 10^{+6}$	2.37×10^{-4}
Lead	$3.14 \times 10^{+1}$	$7.40 \times 10^{+6}$	NA[a]

[a]No data available to calculate EPA RAGs, Part B screening values.

Other Comment No. A-48

000163

NO. A-48

Table A.2-16. Only technetium-99 was found to reach the Great Miami Aquifer above the ~~10^{-7} lifetime cancer risk level or 0.1 Hazard Index level~~ EPA RAGs, Part B screening concentration. Great Miami Aquifer dilution screening for technetium-99 was not performed since the ODAST output concentration was ~~two~~ one orders of magnitude higher than the screening concentration.

An increase in CPC concentrations in the Great Miami Aquifer due to source term loading from Solid Waste Landfill was not predicted to occur at the concentration levels observed in 2000-series wells close to the Solid Waste Landfill. Table A.2-18 compares the background concentration and the field measured concentrations in the Great Miami Aquifer from 2000-series wells in the Solid Waste Landfill. ~~Except for bis(2-Ethylhexyl) phthalate, all other constituents were detected at concentrations within the range of background concentrations in the Great Miami Aquifer. If the source for bis(2-Ethylhexyl) phthalate is the Solid Waste Landfill, then it should have been detected in the perched water as well. However, bis(2-Ethylhexyl) phthalate was not detected in perched water beneath or in the vicinity of the Solid Waste Landfill.~~ For all the CPCs, observed concentrations are comparable with the background concentration, which is consistent with the model prediction that the impact of the Solid Waste Landfill on the Great Miami is negligible.

NO. A-48

As only technetium-99 reached the Great Miami Aquifer above the 10^{-7} risk level or 0.1 Hazard Index level, it was selected for modeling in the Great Miami Aquifer. Table A.2-19 lists the constituent that survived the various screening processes and was simulated using the SWIFT III model.

In addition to predicting constituent loading to the Great Miami Aquifer, future perched water concentration increases were also predicted using the ODAST. Only one layer was considered. This layer consisted of till above the perched water zone (sand/gravel in the glacial overburden). Thickness of this layer for various blocks are shown in Table A.2-1. CPC waste inventory, CPC concentration in the waste, leachate concentration (all shown in Table A.2-16), and retardation factors (Table A.2-15) are the same as those for the vadose zone modeling to the Great Miami Aquifer.

Table A.2-20 shows the predicted perched water concentrations beneath the Solid Waste Landfill and the screening summary. Only technetium-99 and carbazole are predicted to reach the perched water zone above the ~~10^{-7} lifetime cancer risk level or 0.1 Hazard Index level~~ EPA RAGs, Part B screening concentrations. ~~An~~ The predicted increase in CPC concentration in the perched water due to source term loading from Solid Waste Landfill was not predicted to occur at the concentration levels

NO. 8 & 1

TABLE A.2-18

COMPARISON OF GREAT MIAMI AQUIFER WATER AND BACKGROUND FOR CONSTITUENTS OF POTENTIAL CONCERN IN GROUNDWATER SOLID WASTE LANDFILL OPERABLE UNIT 2 REMEDIAL INVESTIGATION FERNALD ENVIRONMENTAL MANAGEMENT PROJECT

Constituent Potential of Concern	Units	Detects in 2000-Series Well Water Samples					Background		2000-Series Comparable to Background?
		Samples	Hits	Minimum	Maximum	Mean[a]	Minimum	Maximum	
RADIONUCLIDES									
NP-237	pCi/L	16	1	0.32	0.32	0.41	NA	1.10[c]	Yes
PU-238	pCi/L	19	3	0.05	0.28	0.33	NA	1.00[c]	Yes
RA-226	pCi/L	17	10	0.22	1.6	0.67	1.10	8.50	Yes
RA-228	pCi/L	17	1	4.30	4.3	1.43	3.10	5.50	Yes
SR-90	pCi/L	19	6	0.75	2.38	2.01	NA	5.00[c]	Yes
TH-228	pCi/L	19	1	0.03	0.03	0.34	1.20	2.90	Yes
TH-230	pCi/L	19	3	0.31	0.71	0.44	1.20	3.44	Yes
U-234	pCi/L	18	11	0.17	4.74	1.23	1.20	4.20	Yes
U-235/236	pCi/L	19	3	0.05	0.28	0.34	NA	1.30[c]	Yes
U-238	pCi/L	18	11	0.16	3.69	1.12	0.90	4.40	Yes
INORGANICS									
Arsenic	μg/L	7	2	2.5	2.5	1.1	2.0	550.0	Yes
Lead	μg/L	7	3	2.8	4.5	2.0	2.6	140.0	Yes

[a]Mean calculated by using half of the detection limit for non-detects.
[b]Not detected in background samples. Value reported is minimum detection limit.
[c]Not detected in background samples. Value reported is maximum detection limit.

NA - Not Available.

Other Comment No. A-48

TABLE A.2-19

SUMMARY OF CONSTITUENTS OF POTENTIAL CONCERN AND SOURCE PATHWAYS FOR THE SOLID WASTE LANDFILL OPERABLE UNIT 2 REMEDIAL INVESTIGATION FERNALD ENVIRONMENTAL MANAGEMENT PROJECT

	Source Pathways[a]		
Constituent of Potential Concern	Solid Waste Landfill Wastes	Perched Groundwater	Paddy's Run Loading from Surface Water Runoff
RADIONUCLIDES			
Technetium-99	Yes	NA[b]	NA

[a]Yes - Indicates concentrations were above screening concentrations from this source pathway
[b]NA - Not Applicable, not present in the perched groundwater or surface water

TABLE A.2-20

PREDICTED PERCHED WATER CONCENTRATIONS AND SCREENING SUMMARY FOR CONSTITUENTS OF POTENTIAL CONCERN, SOLID WASTE LANDFILL OPERABLE UNIT 2 REMEDIAL INVESTIGATION FERNALD ENVIRONMENTAL MANAGEMENT PROJECT

Constituent	Units	Maximum Leachate Concentration	Predicted Maximum Perched Water Concentration	Screening Concentration	Predicted Concentration Above Screening Concentration
RADIONUCLIDES					
Cesium-137	pCi/L	$2.00 \times 10^{+1}$	0.00[a]	1.70×10^{-1}	No
Lead-210	pCi/L	$2.79 \times 10^{+2}$	0.00	7.20×10^{-3}	No
Neptunium-237	pCi/L	$1.00 \times 10^{+0}$	1.11×10^{-5}	2.16×10^{-2}	No
Plutonium-238	pCi/L	$1.00 \times 10^{+0}$	0.00	2.16×10^{-2}	No
Plutonium-239/240	pCi/L	$1.00 \times 10^{+0}$	0.00	2.07×10^{-2}	No
Radium-224	pCi/L	$7.28 \times 10^{+2}$	0.00	1.25×10^{-1}	No
Radium-226	pCi/L	$1.00 \times 10^{+0}$	0.00	1.76×10^{-4}	No
Radium-228	pCi/L	$3.00 \times 10^{+0}$	0.00	4.75×10^{-2}	No
Strontium-90	pCi/L	$5.00 \times 10^{+0}$	1.43×10^{-3}	1.32×10^{-1}	No
Technetium-99	pCi/L	$3.00 \times 10^{+1}$	$2.89 \times 10^{+1}$	$3.65 \times 10^{+0}$	Yes
Thorium-228	pCi/L	$1.00 \times 10^{+0}$	0.00	8.64×10^{-2}	No
Thorium-230	pCi/L	$1.00 \times 10^{+0}$	0.00	3.65×10^{-1}	No
Thorium-232	pCi/L	$1.00 \times 10^{+0}$	0.00	2.79×10^{-2}	No
Uranium-234	pCi/L	$9.42 \times 10^{+2}$	0.00	2.97×10^{-1}	No
Uranium-235/236	pCi/L	$1.05 \times 10^{+2}$	0.00	2.97×10^{-1}	No
Uranium-238	pCi/L	$8.68 \times 10^{+2}$	0.00	1.70×10^{-1}	No
Uranium-Total (non-RAD)	μg/L	$1.61 \times 10^{+3}$	0.00	$1.09 \times 10^{+1}$	No

See footnotes at end of table

FER\CRU2RI\JLG\APP-A\TABA2-20\June7, 1994 1:48pm

TABLE A.2-20
(Continued)

Constituent	Units	Maximum Leachate Concentration	Predicted Maximum Perched Water Concentration	Screening Concentration	Predicted Concentration Above Screening Concentration
ORGANICS					
1,4-Dioxane	µg/L	$4.70 \times 10^{+1}$	0.00	NA[b]	No
2-Methylnaphthalene	µg/L	$7.00 \times 10^{+1}$	$7.00 \times 10^{+4}$ [c]	NA	NA
Aroclor-1254	µg/L	$2.00 \times 10^{+0}$	0.00	1.10×10^{-3}	No
Aroclor-1260	µg/L	$2.00 \times 10^{+0}$	0.00	1.10×10^{-3}	No
Benzo(a)anthracene	µg/L	$1.00 \times 10^{+1}$	0.00	2.82×10^{-3}	No
Benzo(a)pyrene	µg/L	$1.00 \times 10^{+1}$	0.00	2.82×10^{-4}	No
Benzo(b)fluoranthene	µg/L	$1.00 \times 10^{+1}$	0.00	2.82×10^{-3}	No
Benzo(g,h,i)perylene	µg/L	$1.00 \times 10^{+1}$	0.0	NA	No
Carbazole	µg/L	$1.00 \times 10^{+1}$	$9.61 \times 10^{+0}$	4.25×10^{-1}	Yes
Dibenzo(a,h)anthracene	µg/L	$1.00 \times 10^{+1}$	0.00	2.82×10^{-4}	No
Endosulfan Sulfate	µg/L	2.0×10^{-1}	2.00×10^{-1} [c]	NA	No
Heptachlorodibenzo-p-dioxin	µg/L	2.40×10^{-3}	0.00	1.19×10^{-6}	No
Heptachlorodibenzofuran	µg/L	8.51×10^{-2}	0.00	1.19×10^{-6}	No
Ideno(1,2,3-cd)pyrene	µg/L	$1.00 \times 10^{+1}$	0.00	2.82×10^{-3}	No
Octachlorodibenzo-p-dioxin	µg/L	4.00×10^{-4}	0.00	1.19×10^{-5}	No
Phenanthrene	µg/L	$8.9 \times 10^{+1}$	0.0	NA	No
INORGANICS					
Antimony	µg/L	$3.00 \times 10^{+1}$	0.00	$1.46 \times 10^{+0}$	No
Arsenic	µg/L	$1.81 \times 10^{+1}$	0.00	1.46×10^{-4}	No

See footnotes at end of table

FER\CRU2RI\JLG\APP-A\TABA2-20\June7, 1994 1:48pm

TABLE A.2-20
(Continued)

Constituent	Units	Maximum Leachate Concentration	Predicted Maximum Perched Water Concentration	Screening Concentration	Predicted Concentration Above Screening Concentration
INORGANICS (Continued)					
Beryllium	μg/L	$2.00 \times 10^{+0}$	0.00	2.37×10^{-4}	No
Lead	μg/L	$1.95 \times 10^{+1}$	0.00	NA	No

[a]Zero indicates that predicted concentration is at least three orders of magnitude below the screening concentration.

[b]NA = No data available to calculate EPA RAGs, Part B screening value.

[c]Assumed to be the same as the initial leachate due to lack of data on biodegradation. These will require modeling if toxicity data becomes available at a later time.

Other Comment #A-48

See footnotes at end of table

observed. Table A.2-21 compares the background concentrations and the field measured concentrations in the perched water. Thorium-232, uranium-234, uranium-238, ~~uranium total, and manganese~~ and uranium total were observed above background levels. All other CPC's were detected at concentrations within the rane of background concentrations. These detected CPCs occur in Well 1952, located southeast of the Solid Waste Landfill and south of the railroad track, which may be impacted by sources other than the Solid Waste Landfill. Detected total uranium concentration in the upgradient well for perched water (Well 1035) ranged from 2 to 17 ug/L with an average value of 6 ug/L. Total uranium in Well 1950 was detected at 11 ug/L, comparable to the upgradient well. Similarly, detected total uranium concentration at Well 1038 ranged from 4 to 5 ug/L, again comparable to the upgradient well. Only one downgradient well, Well 1952, detected total uranium at concentration of 55.8 μg/L, which is higher than upgradient well (see Figure 4-5, page 4-73). Although uranium is leachable (leachate concentration of 1610 ug/L was used in modeling as shown in Table 5-20), it is believed that the Solid Waste Landfill is not responsible for the high hits for CPCs occur in Well 1952, located southeast of the Solid Waste Landfill and south of railroad.

NO. A-51 & A-48

NO. A-51

Lime Sludge Ponds

Figure A.2-7 shows the areal extent of the waste in the Lime Sludge Ponds and the SWIFT III grid cells impacted by the direct loading from the Lime Sludge Ponds. Waste overlying the SWIFT III grid block (44,82) was included with the waste overlying the SWIFT III grid block (43,81). Similarly constituent loadings from SWIFT III grid blocks (45,79) and (45,80) were combined and loaded from the grid block (45,80). Table A.2-22 lists the CPCs considered for the fate and transport modeling and Table A.2-23 lists the calculated retardation factors for the Lime Sludge Ponds modeling. Pathways considered or the Lime Sludge Ponds modeling were the vadose zone and the perched water infiltration pathways. Table A.2-24 shows CPC concentration in the waste, constituent inventory in the waste, predicted maximum leachate concentration, predicted maximum concentration from vadose zone layer 2 from both pathways, and screening concentrations for the Lime Sludge Ponds.

Table A.2-25 provides the perched water source concentrations and masses for the vadose zone modeling. A summary of screening for CPCs for the Lime Sludge Ponds is also included in Table A.2-24. Only technetium-99 was found to reach the Great Miami Aquifer from the Lime Sludge Ponds above the ~~10^{-7} lifetime cancer risk level or 0.1 Hazard Index level~~ EPA RAGs, Part B

A-48

TABLE A.2-21

COMPARISON OF PERCHED WATER AND BACKGROUND FOR CONSTITUENTS OF POTENTIAL CONCERN IN PERCHED WATER FOR THE SOLID WASTE LANDFILL OPERABLE UNIT 2 REMEDIAL INVESTIGATION FERNALD ENVIRONMENTAL MANAGEMENT PROJECT

Constituent of Potential Concern	Units	Detects in Perched Water (1000-Series Wells)					Background		Perched Water Comparable to Background?
		Samples	Hits	Minimum	Maximum	Mean[a]	Minimum	Maximum	
RADIONUCLIDES									
NP-237	pCi/L	11	2	0.3	1.94	0.54	0.50[b]	0.60[c]	Yes
PU-238	pCi/L	13	3	0.14	0.67	0.32	0.50[b]	0.50[c]	Yes
RA-226	pCi/L	13	3	0.19	5.11	0.73	1.00	1.00	Yes
RA-228	pCi/L	13	1	3.72	3.72	1.37	4.50	5.20	Yes
SR-90	pCi/L	12	2	0.90	1.35	1.41	2.50[b]	2.50[c]	Yes
TH-228	pCi/L	13	2	0.57	14	1.41	1.04	1.60	Yes
TH-230	pCi/L	13	4	0.26	13.8	1.45	2.00	2.00	Yes
TH-232	pCi/L	13	2	0.65	11.5	1.21	0.50[b]	0.60[c]	No
U-234	pCi/L	13	11	1.1	12	3.03	1.06	1.90	No
U-235/236	pCi/L	13	3	0.21	0.43	0.34	0.50[b]	0.50[c]	Yes
U-238	pCi/L	13	12	0.67	15.2	3.08	1.07	1.50	No
U-TOTAL	μg/L	13	13	2	55.8	8.37	0.8	5.3	No
INORGANICS									
Arsenic	μg/L	6	4	1.1	4.4	1.885	15.0	122.0	Yes
Beryllium	μg/L	6	1	2.2	2.2	0.84	1.0	1.8	Yes
Lead	μg/L	6	2	1	31.4	6.08	2.0	50.0	Yes

[a]Mean calculated by using half of the detection limit for non-detects.
[b]Not detected in background samples. Value reported is minimum detection limit.
[c]Not detected in background samples. Value reported is maximum detection limit.

Other Comment No. A-48

TABLE A.2-22

LIST OF CONSTITUENTS OF POTENTIAL CONCERN FOR VADOSE ZONE MODELING FOR THE LIME SLUDGE PONDS OPERABLE UNIT 2 REMEDIAL INVESTIGATION FERNALD ENVIRONMENTAL MANAGEMENT PROJECT

Constituents of Potential Concern		
Radionuclides	Organics	Inorganics
Cesium-137	1,1,2-Trichlorotrifluoroethane	Arsenic
Neptunium-237	1,2-Diethylbenzene	Beryllium
Plutonium-238	Acrylonitrile	Lead
Plutonium-239/240	Aroclor-1254	
Radium-226	Benzo(g,h,i)perylene	
Radium-228	bis(2-Ethylhexyl) phthalate	
Strontium-90	Dibenzo(a,h)anthracene	
Technetium-99	Indeno(1,2,3-cd)pyrene	
Thorium-228	Phenanthrene	
Thorium-230		
Thorium-232		
Uranium-234		
Uranium-235/236		
Uranium-238		
Uranium Total		

Other Comment No. A-48

TABLE A.2-23

RETARDATION FACTORS FOR THE LIME SLUDGE PONDS OPERABLE UNIT 2 REMEDIAL INVESTIGATION FERNALD ENVIRONMENTAL MANAGEMENT PROJECT

Constituent of Potential Concern	Retardation Factor for Glacial Overburden	Retardation Factor for Unsaturated Great Miami Aquifer
RADIONUCLIDES		
Cesium-137	$7.64 \times 10^{+3}$	$1.67 \times 10^{+4}$
Neptunium-237	$2.33 \times 10^{+2}$	$6.21 \times 10^{+1}$
Plutonium-238	$7.17 \times 10^{+3}$	$1.22 \times 10^{+3}$
Plutonium-239/240	$7.17 \times 10^{+3}$	$1.22 \times 10^{+3}$
Radium-226	$2.94 \times 10^{+3}$	$1.30 \times 10^{+3}$
Radium-228	$2.94 \times 10^{+3}$	$1.30 \times 10^{+3}$
Strontium-90	$4.32 \times 10^{+1}$	$3.15 \times 10^{+1}$
Technetium-99	$1.50 \times 10^{+0}$	$1.86 \times 10^{+0}$
Thorium-228	$2.45 \times 10^{+4}$	$3.91 \times 10^{+4}$
Thorium-230	$2.45 \times 10^{+4}$	$3.91 \times 10^{+4}$
Thorium-232	$2.45 \times 10^{+4}$	$3.91 \times 10^{+4}$
Uranium-234	$8.45 \times 10^{+2}$	$1.91 \times 10^{+1}$
Uranium-235/236	$8.45 \times 10^{+2}$	$1.91 \times 10^{+1}$
Uranium-238	$8.45 \times 10^{+2}$	$1.91 \times 10^{+1}$
Uranium-Total	$8.45 \times 10^{+2}$	$1.91 \times 10^{+1}$
ORGANICS		
1,1,2-Trichlorotrifluoroethane	$4.34 \times 10^{+0}$	$3.22 \times 10^{+0}$
1,2-Diethylbenzene	$1.06 \times 10^{+3}$	$6.57 \times 10^{+2}$
Acrylonitrile	$1.06 \times 10^{+0}$	$1.04 \times 10^{+0}$
Aroclor-1254	$3.57 \times 10^{+4}$	$2.38 \times 10^{+4}$
Benzo(g,h,i)perylene	$1.16 \times 10^{+5}$	$7.21 \times 10^{+4}$
bis(2-Ethylhexyl) phthalate	$3.27 \times 10^{+1}$	$2.21 \times 10^{+1}$
Dibenzo(a,h)anthracene	$3.11 \times 10^{+4}$	$2.07 \times 10^{+4}$
Indeno(1,2,3-cd)pyrene	$1.53 \times 10^{+6}$	$1.02 \times 10^{+6}$
Phenanthrene	$5.20 \times 10^{+2}$	$3.23 \times 10^{+2}$

000173

TABLE A.2-23
(Continued)

Constituent of Potential Concern	Retardation Factor for Glacial Overburden	Retardation Factor for Unsaturated Great Miami Aquifer
	INORGANICS	
Arsenic	$8.45 \times 10^{+2}$	$2.44 \times 10^{+3}$
Beryllium	$5.49 \times 10^{+3}$	$3.05 \times 10^{+3}$
Lead	$1.50 \times 10^{+4}$	$4.65 \times 10^{+2}$

Other Comment No. A-48

TABLE A.2-24

SOURCE CHARACTERIZATION AND SCREENING SUMMARY OF CONSTITUENTS OF POTENTIAL CONCERN
LIME SLUDGE PONDS
OPERABLE UNIT 2 REMEDIAL INVESTIGATION
FERNALD ENVIRONMENTAL MANAGEMENT PROJECT

Constituent of Potential Concern	Upper 95% C.I. on Mean Concentration (mg/kg)	Constituent Inventory in the Waste (mg)	Initial Maximum Leachate Concentration (pCi/L RAD) (μg/L non-RAD)	Constraint[a]	Maximum Loading Concentration from ODAST (Vadose Layer 2) (pCi/L RAD) (μg/L non-RAD)	EPA RAGs, Part B Screening Concentration (pCi/L RAD) (μg/L non-RAD)	CPC ≥Screening Concentration and Requires SWIFT Modeling?
RADIONUCLIDES							
Cesium-137	1.95×10^{-9}	2.05×10^{-3}	$1.42 \times 10^{+1}$	70-Year	0.0[b]	1.70×10^{-1}	No
Neptunium-237	4.58×10^{-4}	$4.65 \times 10^{+3}$	$2.62 \times 10^{+1}$	70-Year	1.10×10^{-3}	2.16×10^{-2}	No
Plutonium-238	1.46×10^{-8}	1.23×10^{-1}	$1.67 \times 10^{+1}$	70-Year	0.0	2.16×10^{-2}	No
Plutonium-239/240	1.71×10^{-6}	$1.80 \times 10^{+1}$	$8.91 \times 10^{+0}$	70-Year	0.0	2.07×10^{-2}	No
Radium-226	1.58×10^{-6}	$1.66 \times 10^{+1}$	$1.31 \times 10^{+2}$	70-Year	0.0	1.76×10^{-4}	No
Radium-228	6.62×10^{-9}	6.97×10^{-2}	$1.51 \times 10^{+2}$	70-Year	0.0	4.75×10^{-2}	No
Strontium-90	6.14×10^{-9}	6.47×10^{-2}	$7.07 \times 10^{+1}$	70-Year	0.0	1.32×10^{-3}	No
Technetium-99	6.18×10^{-4}	$6.50 \times 10^{+3}$	$8.82 \times 10^{+1}$	70-Year	$7.64 \times 10^{+1}$	$3.65 \times 10^{+0}$	Yes
Thorium-228	1.88×10^{-9}	1.98×10^{-2}	$1.29 \times 10^{+2}$	70-Year	0.0	8.64×10^{-2}	No
Thorium-230	4.07×10^{-4}	$4.28 \times 10^{+3}$	$7.05 \times 10^{+2}$	70-Year	0.0	3.65×10^{-3}	No
Thorium-232	$9.73 \times 10^{+0}$	$1.02 \times 10^{+8}$	$9.00 \times 10^{+1}$	70-Year	0.0	2.79×10^{-2}	No
Uranium-234	9.94×10^{-4}	$1.05 \times 10^{+4}$	$5.20 \times 10^{+2}$	70-Year	0.0	2.97×10^{-3}	No
Uranium-235/236	2.01×10^{-1}	$2.12 \times 10^{+6}$	$3.66 \times 10^{+1}$	70-Year	0.0	2.97×10^{-3}	No
Uranium-238		$8.30 \times 10^{+7}$		70-Year	0.0	1.70×10^{-1}	No
Grid #44,79	$2.16 \times 10^{+1}$	$6.25 \times 10^{+6}$	$1.85 \times 10^{+2}$	70-Year			
Grid #45,80	$7.63 \times 10^{+0}$	$4.81 \times 10^{+6}$	$2.32 \times 10^{+2}$	70-Year			
Grid #43,81	$2.07 \times 10^{+1}$	$8.57 \times 10^{+6}$	$2.35 \times 10^{+2}$	70-Year			
Grid #44,81	$2.33 \times 10^{+0}$	$4.72 \times 10^{+6}$	$4.28 \times 10^{+2}$	70-Year			
Grid #43,80	$1.59 \times 10^{+1}$	$2.22 \times 10^{+7}$	$4.48 \times 10^{+2}$	70-Year			
Grid #45,81	$5.39 \times 10^{+0}$	$9.53 \times 10^{+6}$	$5.25 \times 10^{+2}$	70-Year			
Grid #44,80	$8.45 \times 10^{+0}$	$6.27 \times 10^{+7}$	$2.40 \times 10^{+2}$	70-Year			

See footnote at end of table

FER\CRU2RI\ULG\TABA2-20\June7, 1994 1:58pm

TABLE A.2-24
(Continued)

Constituent of Potential Concern	Upper 95% C.I. on Mean Concentration (mg/kg)	Constituent Inventory in the Waste (mg)	Initial Maximum Leachate Concentration (pCi/L RAD) (μg/L non-RAD)	Constraint[a]	Maximum Loading Concentration from ODAST (Vadose Layer 2) (pCi/L RAD) (μg/L non-RAD)	EPA RAGs, Part B Screening Concentration (pCi/L RAD) (μg/L non-RAD)	CPC ≥Screening Concentration and Requires SWIFT Modeling?
RADIONUCLIDES (Continued)							
Uranium - Total (non-RAD)	$2.22 \times 10^{+1}$	$2.34 \times 10^{+8}$	$1.87 \times 10^{+3}$	70-Year	0.0	$1.09 \times 10^{+1}$	No
ORGANICS							
1,1,2-Trichlorotrifluoroethane	2.00×10^{-2}	$2.11 \times 10^{+5}$	1.68×10^{0}	70-Year	0.0	NA[c]	No
1,2-Diethylbenzene	4.10×10^{-2}	$4.34 \times 10^{+5}$	$3.45 \times 10^{+0}$	70-Year	0.0	NA	No
Acrylonitrile	2.00×10^{-1}	$2.11 \times 10^{+6}$	$1.68 \times 10^{+1}$	70-Year	0.0	5.93×10^{-3}	No
Aroclor-1254	4.30×10^{-2}	$4.53 \times 10^{+5}$	3.62×10^{0}	70-Year	0.0	1.10×10^{-3}	No
Benzo(g,h,i)perylene	1.70×10^{-1}	$1.80 \times 10^{+6}$	$1.43 \times 10^{+1}$	70-Year	0.0	NA	No
bis(2-Ethylhexyl) phthalate	$1.70 \times 10^{+0}$	$1.79 \times 10^{+7}$	$1.43 \times 10^{+2}$	70-Year	0.0	6.07×10^{-4}	No
Dibenzo(a,h)anthracene	1.10×10^{-1}	$1.16 \times 10^{+6}$	9.25×10^{0}	70-Year	0.0	2.82×10^{-4}	No
Indeno(1,2,3-cd)pyrene	2.10×10^{-1}	$2.21 \times 10^{+6}$	$1.77 \times 10^{+1}$	70-Year	0.0	2.82×10^{-4}	No
Phenanthrene	8.20×10^{-2}	$8.67 \times 10^{+5}$	$6.90 \times 10^{+0}$	70-Year	0.0	NA	No
INORGANICS							
Arsenic	$6.78 \times 10^{+0}$	$7.15 \times 10^{+7}$	$4.99 \times 10^{+2}$	TCLP	0.0	1.46×10^{-4}	No
Beryllium	$1.27 \times 10^{+0}$	$1.33 \times 10^{+7}$	$1.07 \times 10^{+2}$	70-Year	0.0	2.37×10^{-4}	No
Lead	$2.40 \times 10^{+2}$	$2.54 \times 10^{+9}$	$2.02 \times 10^{+4}$	70-Year	0.0	NA	No

[a]Constraint on reported concentration is by In Situ Leachate (ISL), Toxicity Characteristic Leaching Procedure (TCLP), maximum detection limit (MDL), or by US EPA 70-year rule (70-Year).
[b]Zero indicates that predicted concentration is at least three orders of magnitude below the screening concentrations.
[c]NA - No data available to calculate EPA RAGs, Part B screening value.

Other Comment No. A-48

FER\CRU2RI\JLG\TABA2-20\June7, 1994 1:58pm

5659
000176

TABLE A.2-25

PERCHED WATER SOURCE CONCENTRATIONS AND MASSES FOR THE VADOSE ZONE MODELING, LIME SLUDGE PONDS OPERABLE UNIT 2 REMEDIAL INVESTIGATION FERNALD ENVIRONMENTAL MANAGEMENT PROJECT

Constituent	Initial Perched Groundwater Concentration (μg/L non-RAD) (pCi/L RAD)	Total Mass (mg)	EPA RAGs, Part B Screening Concentration (μg/L non-RAD) (pCi/L RAD)
RADIONUCLIDES			
Neptunium-237	8.39×10^{-1}	$4.11 \times 10^{+1}$	2.16×10^{-2}
Radium-226	1.40×10^{0}	9.91×10^{-1}	1.76×10^{-4}
Radium-228	3.80×10^{0}	9.78×10^{-3}	4.75×10^{-2}
Strontium-90	3.45×10^{0}	4.54×10^{-4}	1.32×10^{-1}
Thorium-228	2.87×10^{0}	7.39×10^{-2}	8.64×10^{-2}
Thorium-230	2.51×10^{-1}	$2.57 \times 10^{+2}$	3.65×10^{-1}
Thorium-232	2.60×10^{0}	$4.99 \times 10^{+8}$	2.79×10^{-2}
Uranium-234	2.45×10^{0}	$4.46 \times 10^{+0}$	2.97×10^{-1}
Uranium-235/236	1.80×10^{-1}	$9.43 \times 10^{+2}$	2.97×10^{-1}
Uranium-238	2.12×10^{0}	$9.16 \times 10^{+4}$	1.70×10^{-1}
Uranium-Total (non-RAD)	6.30×10^{0}	$7.13 \times 10^{+4}$	$1.09 \times 10^{+1}$
ORGANICS			
bis(2-Ethylhexyl)phthalate	2.00×10^{0}	$2.59 \times 10^{+4}$	6.07×10^{-1}
INORGANICS			
Arsenic	$1.40 \times 10^{+1}$	$1.85 \times 10^{+7}$	1.46×10^{-4}

Other Comment No. A-48

000177

screening concentrations. Table A.2-26 lists the constituents that passed through the various screening processes and were simulated using the SWIFT III model.

An increase in CPC concentrations in the Great Miami Aquifer, due to the source term loading from Lime Sludge Ponds, was not predicted to occur at the concentration levels observed. Table A.2-27 compares the background concentration and the field measured concentrations in the Great Miami Aquifer. All constituents were detected at concentrations within the range of background concentrations in the Great Miami Aquifer.

In addition to predicting constituent loading to the Great Miami Aquifer, future perched water concentration increases were also predicted using ODAST. Only one layer consisting of till above the perched water zone was considered. Thickness of this layer for various blocks are shown in Table A.2-2. CPC waste inventory, CPC concentration in the waste, leachate concentration (all shown in Table A.2-24), and retardation factors (Table A.2-23) are the same as those for the vadose zone modeling to the Great Miami Aquifer.

Table A.2-28 shows the predicted perched water concentrations beneath the Lime Sludge Ponds and the screening summary. Neptunium-237, strontium-90, technetium-99, arsenic, and manganese are predicted to reach perched water above the ~~10^{-7} lifetime cancer risk or 0.1 Hazard Index concentration levels~~ EPA RAGs, Part B screening concentrations.

NO. A-48

An increase in CPC concentration in the perched water, due to source term loading, from the Lime Sludge Ponds was not predicted to occur at the concentration levels observed. Table A.2-29 compares the background concentrations and the field measured concentrations in the perched water beneath or in the vicinity of the Lime Sludge Ponds. Thorium-232, uranium-234, uranium-238, total-uranium, beryllium, manganese, ~~vanadium,~~ and bis(2-Ethylhexyl)phthalate were detected above the background concentrations. Perched water under the Lime Sludge Ponds may be affected by other FEMP sources.

NO. A-52

Inactive Flyash Pile/South Field

Figure A.2-8 shows the areal extent of the waste in the Inactive Flyash Pile/South Field and the SWIFT III grid cells impacted by the direct loading from these subunits. Many SWIFT III grid blocks received lateral drainage. These grid blocks are identified in Figure A.2-8. Table A.2-30

TABLE A.2-26

SUMMARY OF CONSTITUENTS OF POTENTIAL CONCERN AND SOURCE PATHWAYS FOR THE LIME SLUDGE PONDS OPERABLE UNIT 2 REMEDIAL INVESTIGATION FERNALD ENVIRONMENTAL MANAGEMENT PROJECT

Constituents of Potential Concern	Source Pathways[a]	
	Lime Sludge Pond Wastes	Perched Groundwater
RADIONUCLIDES		
Technetium-99	Yes	NA[b]

[a]Yes - Indicates concentrations were above screening concentrations from this source pathway
[b]NA - Not applicable, not present in the perched groundwater

TABLE A.2-27

COMPARISON OF GREAT MIAMI AQUIFER WATER AND BACKGROUND FOR CONSTITUENTS OF POTENTIAL CONCERN IN GROUNDWATER FOR THE LIME SLUDGE PONDS OPERABLE UNIT 2 REMEDIAL INVESTIGATION FERNALD ENVIRONMENTAL MANAGEMENT PROJECT

Constituent of Potential Concern	Units	Detects in 2000-Series Well Water Samples					Background		2000-Series Comparable to Background?
		Samples	Hits	Minimum	Maximum	Mean[a]	Minimum	Maximum	
RADIONUCLIDES									
Neptunium-237	pCi/L	8	3	0.20	0.41	0.37	NA	1.10[b]	Yes
Plutonium-238	pCi/L	8	3	0.05	0.12	0.23	NA	1.00[b]	Yes
Radium-226	pCi/L	9	4	0.16	0.79	0.41	1.10	8.50	Yes
Radium-228	pCi/L	9	1	1.54	1.74	1.36	3.10	5.50	Yes
Thorium-228	pCi/L	9	2	0.10	1.60	0.40	1.20	2.90	Yes
Thorium-230	pCi/L	9	4	0.13	1.00	0.40	1.20	3.44	Yes
Uranium-234	pCi/L	8	6	1.10	1.50	1.08	1.20	4.20	Yes
Uranium-235/236	pCi/L	9	4	0.08	0.13	0.27	NA	1.30[b]	Yes
Uranium-238	pCi/L	9	6	0.58	1.62	1.01	0.90	4.40	Yes
INORGANICS									
Arsenic	μg/L	6	2	1.1	1.2	0.7	2.0	550.0	Yes

[a]Means calculated by using half of the detection limit for non-detects.

[b]Not detected in background samples. Value reported is maximum detection limit.

NA = Not Available

Comment No. A-48

FER\CRU2RI\TDO\APP-A\TABA2-27\June1, 1994 2:18pm

TABLE A.2-28

PREDICTED PERCHED WATER CONCENTRATIONS AND SCREENING SUMMARY FOR CONSTITUENTS OF POTENTIAL CONCERN, LIME SLUDGE PONDS OPERABLE UNIT 2 REMEDIAL INVESTIGATION FERNALD ENVIRONMENTAL MANAGEMENT PROJECT

Constituent	Units	Maximum Leachate Concentration	Predicted Maximum Perched Water Concentration	Screening Concentration	Predicted Concentration Above Screening Concentration
RADIONUCLIDES					
Cesium-137	pCi/L	$1.42 \times 10^{+1}$	0.0[a]	1.70×10^{-1}	No
Neptunium-237	pCi/L	$2.62 \times 10^{+1}$	$5.06 \times 10^{+0}$	2.16×10^{-2}	Yes
Plutonium-238	pCi/L	$1.67 \times 10^{+1}$	0.0	2.16×10^{-2}	No
Plutonium-239/240	pCi/L	$8.91 \times 10^{+0}$	0.0	2.07×10^{-2}	No
Radium-226	pCi/L	$1.31 \times 10^{+2}$	0.0	1.76×10^{-4}	No
Radium-228	pCi/L	$1.51 \times 10^{+2}$	0.0	4.75×10^{-2}	No
Strontium-90	pCi/L	$7.07 \times 10^{+1}$	$1.91 \times 10^{+0}$	1.32×10^{-1}	Yes
Technetium-99	pCi/L	$8.82 \times 10^{+1}$	$8.23 \times 10^{+1}$	$3.65 \times 10^{+0}$	Yes
Thorium-228	pCi/L	$1.29 \times 10^{+2}$	0.0	8.64×10^{-2}	No
Thorium-230	pCi/L	$7.05 \times 10^{+2}$	0.0	3.65×10^{-1}	No
Thorium-232	pCi/L	$9.00 \times 10^{+1}$	0.0	2.79×10^{-2}	No
Uranium-234	pCi/L	$5.20 \times 10^{+2}$	2.01×10^{-2}	2.97×10^{-1}	No
Uranium-235/236	pCi/L	$3.66 \times 10^{+1}$	1.42×10^{-3}	2.97×10^{-1}	No
Uranium-238	pCi/L	$6.27 \times 10^{+2}$	1.64×10^{-2}	1.70×10^{-1}	No
Uranium-Total (non-RAD)	μg/L	$1.87 \times 10^{+3}$	7.24×10^{-2}	$1.09 \times 10^{+1}$	No

TABLE A.2-28
(Continued)

Constituent	Units	Maximum Leachate Concentration	Predicted Maximum Perched Water Concentration	Screening Concentration	Predicted Concentration Above Screening Concentration
ORGANICS					
1,1,2-Trichlorotrifluoroethane	μg/L	$1.68 \times 10^{+0}$	1.66×10^{-1}	NA[b]	NA
1,1-Diethylbenzene	μg/L	$3.45 \times 10^{+0}$	1.00×10^{-4}	NA	NA
Acrylonitrile	μg/L	$1.68 \times 10^{+1}$	4.12×10^{-5}	2.82×10^{-3}	No
Aroclor-1254	μg/L	$3.62 \times 10^{+0}$	0.0	1.00×10^{-3}	No
Benzo(g,h,i) Perylene	μg/L	$1.43 \times 10^{+1}$	0.0	NA	No
bis(2-Ethylhexyl)phthalate	μg/L	$1.43 \times 10^{+2}$	0.0	6.07×10^{-1}	No
Dibenzo(a,h)anthracene	μg/L	$9.25 \times 10^{+0}$	0.0	2.82×10^{-4}	No
Ideno(1,2,3-cd)pyrene	μg/L	$1.77 \times 10^{+1}$	0.0	2.82×10^{-3}	No
Phenanthrene	μg/L	$6.90 \times 10^{+0}$	0.0	NA	No
INORGANICS					
Arsenic	μg/L	$4.99 \times 10^{+2}$	1.45×10^{-2}	1.46×10^{-4}	Yes
Beryllium	μg/L	$1.07 \times 10^{+2}$	0.0	2.37×10^{-4}	No
Lead	μg/L	$2.02 \times 10^{+4}$	0.0	NA	No

[a]Zero indicates that predicted concentraiton is at least three order of magnitued below the screening concentrations.
[b]NA = No data available to calculate EPA RAGs, Part B screening value.
Other Comment No. A-48

000182

TABLE A.2-29

COMPARISON OF PERCHED WATER AND BACKGROUND FOR POTENTIAL CONSTITUENTS OF CONCERN IN PERCHED WATER FOR THE LIME SLUDGE PONDS OPERABLE UNIT 2 REMEDIAL INVESTIGATION FERNALD ENVIRONMENTAL MANAGEMENT PROJECT

Constituent of Potential Concern	Units	Detects in Perched Water (1000-Series Well)					Background		Perched Water Comparable to Background?
		Samples	Hits	Minimum	Maximum	Mean[a]	Minimum	Maximum	
RADIONUCLIDES									
Neptunium-237	pCi/L	9	3	0.15	0.08	0.4	0.50[a]	0.60[b]	Yes
Radium-226	pCi/L	12	6	0.21	1.4	0.6	1.00	1.00	Yes
Radium-228	pCi/L	12	2	3.68	3.8	3.7	4.50	5.20	Yes
Strontium-90	pCi/L	12	1	3.45	3.5	3.5	2.50[a]	2.50[b]	Yes
Thorium-228	pCi/L	14	6	0.78	2.9	1.6	1.04	1.60	Yes
Thorium-230	pCi/L	14	8	0.25	6.7	2.3	2.00	2.00	Yes
Thorium-232	pCi/L	12	4	0.74	2.6	1.5	0.50[a]	0.60[b]	No
Uranium-234	pCi/L	16	15	0.39	11.0	3.1	1.06	1.90	No
Uranium-235/236	pCi/L	11	8	0.08	0.7	0.2	0.50[a]	0.50[b]	Yes
Uranium-238	pCi/L	18	17	0.30	11.8	3.5	1.07	1.50	No
Total Uranium	µg/L	22	20	1	58	12.8	0.8	5.3	No
INORGANICS									
Arsenic	µg/L	10	5	2.2	14	5.9	15.0	122.0	Yes
Beryllium	µg/L	8	2	1.9	6.8	4.4	1.0	1.8	No
Lead	µg/L	12	7	2	51.4	14.8	2.0	50.0	Yes
ORGANICS									
bis(2-Ethylhexyl)phthlate	µg/L	3	2	1	2	1.5	0.0	0.0	No

[a]Not detected in background samples. Value reported is minimum detection limit.

[b]Not detected in background samples. Value reported is maximum detection limit.

Comment No. A-48

TABLE A.2-30

LIST OF CONSTITUENTS OF POTENTIAL CONCERN FOR VADOSE ZONE MODELING FOR THE INACTIVE FLYASH PILE AND SOUTH FIELD OPERABLE UNIT 2 REMEDIAL INVESTIGATION FERNALD ENVIRONMENTAL MANAGEMENT PROJECT

Potential Constituents of Potential Concern		
Radionuclides	Organics	Inorganics
Cesium-137	2-Methylnaphthalene	Arsenic
Lead-210	Aroclor-1254	Beryllium
Neptunium-237	Aroclor-1260	Lead
Plutonium-238	Benzo(a)anthracene	
Plutonium-239/240	Benzo(a)pyrene	
Radium-224	Benzo(b)fluoranthene	
Radium-226	bis(2-Ethylhexyl) phthalate	
Radium-228	Dieldrin	
Ruthenium-106	Octachlorodibenzo-p-dioxin	
Strontium-90	Phenanthrene	
Technetium-99	Tetrachlorodibenzofuran	
Thorium-228	Tributyl Phosphate	
Thorium-230		
Thorium-232		
Uranium-234		
Uranium-235/236		
Uranium-238		
Uranium Total		

Comment No. A-48

shows the list of CPCs for vadose zone modeling for the Inactive Flyash Pile and South Field. Table A.2-31 lists the retardation factors used for vadose zone modeling for the Inactive Flyash Pile and South Field. All five pathways discussed in Section A.2.1 were applicable for these two subunits. For the vadose zone pathway, Table A.2-32 shows the CPC concentration in the waste, constituent inventory in the waste, and predicted maximum leachate concentration. Tables A.2-33 and A.2-34 shows concentrations and masses for the perched water (both vertical infiltration and subsurface pathways) and seep pathways. Table A.2-35 shows the flow rates for the seeps and perched water subsurface seeps. While seep flow rates are based on field observations, subsurface seep flow rates were estimated from the perched water hydraulic gradients and hydraulic conductivity of the perched water zone. Concentration and mass loading due to the surface water pathway are discussed in Appendix A-1.

CPCs from these two units were screened together because of close proximity of subunits. A summary of screening for CPCs from the vadose zone pathway, perched water infiltration pathway, perched water subsurface seep pathway, and seep pathway is included in Table A.2-32. CPCs passing the screening in Table A.2-32 were further screened using predicted dilution in the Great Miami Aquifer. Table A.2-36 shows the results of the Great Miami Aquifer dilution screening. Table A.2-37 lists the constituents that survived the various screening processes and were simulated using the SWIFT III model for the Inactive Flyash Pile and South Field.

NO. A-53 & A-27

Table A.2-38 compares the background concentrations and the field measured concentrations in the Great Miami Aquifer. Uranium, ~~bis(2-Ethylhexyl) phthalate, carbon disulfide, and trichloroethane~~ and bis(2-ethylhexyl) phthalate were detected above background levels. Uranium was simulated using the SWIFT III model. Results of uranium calibration are presented in Section A.2.8. ~~Vadose zone modeling predicted low concentrations for bis(2-Ethylhexyl) phthalate, carbon disulfide, and trichloroethane. Furthermore, frequency of detection in Great Miami Aquifer for these contaminants was low. Therefore, further calibration for these chemicals was not considered and were not included for SWIFT III modeling.~~ Vadose zone modeling predicted no increase in bis(2-Ethylhexyl) phthalate concentration. However, the frequency of detection of bis(2-Ethylhexyl) phthalate in the Great Miami Aquifer was low and it is also a common laboratory contaminant. Therefore, further calibration for bis(2-Ethylhexyl) phthalate was not considered and was not included for SWIFT III modeling.

TABLE A.2-31

RETARDATION FACTORS FOR THE INACTIVE FLYASH PILE AND SOUTH FIELD OPERABLE UNIT 2 REMEDIAL INVESTIGATION FERNALD ENVIRONMENTAL MANAGEMENT PROJECT

Constituent	Retardation Factor for Glacial Overburden	Retardation Factor for Unsaturated Great Miami Aquifer
RADIONUCLIDES		
Cesium-137	$9.05 \times 10^{+3}$	$1.67 \times 10^{+4}$
Lead-210	$1.50 \times 10^{+4}$	$4.65 \times 10^{+2}$
Neptunium-237	$2.76 \times 10^{+2}$	$6.21 \times 10^{+1}$
Plutonium-238	$8.50 \times 10^{+3}$	$1.22 \times 10^{+3}$
Plutonium-239/240	$8.50 \times 10^{+3}$	$1.22 \times 10^{+3}$
Radium-224	$3.48 \times 10^{+3}$	$1.30 \times 10^{+3}$
Radium-226	$3.48 \times 10^{+3}$	$1.30 \times 10^{+3}$
Radium-228	$3.48 \times 10^{+3}$	$1.30 \times 10^{+3}$
Ruthenium-106	$4.00 \times 10^{+3}$	$6.73 \times 10^{+2}$
Strontium-90	$5.10 \times 10^{+1}$	$3.15 \times 10^{+1}$
Technetium-99	$1.59 \times 10^{+0}$	$1.86 \times 10^{+0}$
Thorium-228	$2.90 \times 10^{+4}$	$3.91 \times 10^{+4}$
Thorium-230	$2.90 \times 10^{+4}$	$3.91 \times 10^{+4}$
Thorium-232	$2.90 \times 10^{+4}$	$3.91 \times 10^{+4}$
Uranium-234	$1.00 \times 10^{+3}$	$1.91 \times 10^{+1}$
Uranium-235/236	$1.00 \times 10^{+3}$	$1.91 \times 10^{+1}$
Uranium-238	$1.00 \times 10^{+3}$	$1.91 \times 10^{+1}$
Uranium Total	$1.00 \times 10^{+3}$	$1.91 \times 10^{+1}$
ORGANICS		
2-Methylnaphthalene	$2.68 \times 10^{+2}$	$1.62 \times 10^{+2}$
Aroclor-1254	$4.37 \times 10^{+4}$	$2.38 \times 10^{+4}$
Aroclor-1260	$5.27 \times 10^{+4}$	$2.87 \times 10^{+4}$
Benzo(a)anthracene	$1.63 \times 10^{+4}$	$8.89 \times 10^{+3}$
Benzo(a)pyrene	$3.90 \times 10^{+4}$	$2.12 \times 10^{+4}$
Benzo(b)fluoranthene	$1.52 \times 10^{+5}$	$8.27 \times 10^{+4}$
bis(2-Ethylhexyl) phthalate	$3.98 \times 10^{+1}$	$2.21 \times 10^{+1}$
Dieldrin	$1.30 \times 10^{+2}$	$7.12 \times 10^{+1}$
Octachlorodibenzo-p-dioxin	$6.45 \times 10^{+6}$	$3.51 \times 10^{+6}$
Phenanthrene	$5.33 \times 10^{+2}$	$3.23 \times 10^{+2}$
Tetrachlorodibenzofuran	$2.70 \times 10^{+4}$	$1.47 \times 10^{+4}$
Tributyle Phosphate	$3.68 \times 10^{+2}$	$2.23 \times 10^{+2}$

TABLE A.2-31
(Continued)

Constituent	Retardation Factor for Glacial Overburden	Retardation Factor for Unsaturated Great Miami Aquifer
	INORGANICS	
Arsenic	$1.00 \times 10^{+3}$	$2.44 \times 10^{+3}$
Beryllium	$6.50 \times 10^{+3}$	$3.05 \times 10^{+3}$
Lead	$1.50 \times 10^{+4}$	$4.65 \times 10^{+2}$

Comment No. A-48

TABLE A.2-32

SOURCE CHARACTERIZATION AND SCREENING SUMMARY FOR CONSTITUENTS OF POTENTIAL CONCERN FOR THE INACTIVE FLYASH PILE AND SOUTH FIELD

Constituents of Potential Concern	Upper 95% C.I. on Mean Concentration (mg/kg)	Constituents Inventory in the Waste (mg)	Initial Maximum Leachate Concentration (pCi/L RAD) (μg/L non-RAD)	Constraint[a]	Maximum Loading Concentration from ODAST (Vadose Layer 2) (pCi/L RAD) (μg/L non-RAD)	EPA RAGs, Part B Screening Concentration (pCi/L RAD) (μg/L non-RAD)	CPC ≥ Screening Concentration and Requires SWIFT Modeling?
RADIONUCLIDES							
Cesium-137	2.74×10^{-9}	6.06×10^{-1}	$2.49 \times 10^{+2}$	70-Year	0.0[b]	1.70×10^{-1}	No
Lead-210	7.87×10^{-8}	$1.74 \times 10^{+1}$	$6.31 \times 10^{+3}$	70-Year	0.0	7.20×10^{-3}	No
Neptunium-237	4.26×10^{-4}	$9.39 \times 10^{+4}$	$3.15 \times 10^{+2}$	70-Year	$1.06 \times 10^{+2}$	2.16×10^{-2}	Yes
Plutonium-238	2.34×10^{-9}	$5.17 \times 10^{+1}$	$4.21 \times 10^{+1}$	70-Year	8.53×10^{-3}	2.16×10^{-2}	No
Plutonium-239/240	3.37×10^{-7}	$7.45 \times 10^{+1}$	$2.19 \times 10^{+1}$	70-Year	0.0	2.07×10^{-2}	No
Radium-224	1.97×10^{-11}	4.35×10^{-3}	$3.29 \times 10^{+3}$	70-Year	0.0	1.25×10^{-1}	No
Radium-226	2.95×10^{-6}	$6.52 \times 10^{+2}$	$3.06 \times 10^{+3}$	70-Year	1.58×10^{-1}	1.76×10^{-4}	Yes
Radium-228	6.09×10^{-9}	$1.35 \times 10^{+0}$	$1.74 \times 10^{+3}$	70-Year	0.0	4.75×10^{-2}	No
Ruthenium-106	3.87×10^{-10}	8.55×10^{-2}	$1.36 \times 10^{+3}$	70-Year	0.0	5.00×10^{-1}	No
Strontium-90	9.93×10^{-9}	$2.19 \times 10^{+0}$	$1.43 \times 10^{+3}$	70-Year	$1.53 \times 10^{+1}$	1.32×10^{-2}	Yes
Technetium-99	5.29×10^{-5}	$1.17 \times 10^{+4}$	$9.45 \times 10^{+2}$	70-Year	$7.72 \times 10^{+2}$	3.65×10^{0}	Yes
Thorium-228	2.08×10^{-9}	4.59×10^{-1}	$1.78 \times 10^{+3}$	70-Year	0.0	8.64×10^{-2}	No
Thorium-230	2.07×10^{-4}	$4.57 \times 10^{+4}$	$4.48 \times 10^{+3}$	70-Year	0.0	3.65×10^{-1}	No
Thorium-232	$1.39 \times 10^{+1}$	$3.07 \times 10^{+9}$	$1.61 \times 10^{+3}$	70-Year	0.0	2.79×10^{-2}	No
Uranium-234	4.85×10^{-3}	$1.07 \times 10^{+6}$	$3.17 \times 10^{+4}$	70-Year	$1.10 \times 10^{+4}$	2.97×10^{-1}	Yes
Uranium-235/236	$2.67 \times 10^{+0}$	$5.89 \times 10^{+8}$	$6.06 \times 10^{+3}$	70-Year	$2.11 \times 10^{+3}$	2.97×10^{-1}	Yes
Uranium-238		$1.82 \times 10^{+10}$			$5.44 \times 10^{+5}$	1.70×10^{-1}	Yes
Grid#28,59	$1.88 \times 10^{+1}$	$1.41 \times 10^{+8}$	$4.24 \times 10^{+3}$	70-Year			
Grid#28,63	$1.62 \times 10^{+2}$	$4.13 \times 10^{+8}$	$1.72 \times 10^{+4}$	70-Year			

See footnote at end of table

FER\CRU2RI\JLG\APP-A\TABA2-32\June7, 1994 2:29pm

TABLE A.2-32
(Continued)

Constituents of Potential Concern	Upper 95% C.I. on Mean Concentration (mg/kg)	Constituents Inventory in the Waste (mg)	Initial Maximum Leachate Concentration (pCi/L RAD) (μg/L non-RAD)	Constraint[a]	Maximum Loading Concentration from ODAST (Vadose Layer 2) (pCi/L RAD) (μg/L non-RAD)	EPA RAGs, Part B Screening Concentration (pCi/L RAD) (μg/L non-RAD)	CPC ≥Screening Concentration and Requires SWIFT Modeling?
			RADIONUCLIDES				
Uranium-238 (Continued)							
Grid#28,65	$1.28 \times 10^{+2}$	$4.17 \times 10^{+8}$	$1.36 \times 10^{+4}$	70-Year			
Grid#29,62	$3.04 \times 10^{+1}$	$1.12 \times 10^{+8}$	$3.69 \times 10^{+3}$	70-Year			
Grid#29,64	$7.66 \times 10^{+1}$	$5.33 \times 10^{+8}$	$9.89 \times 10^{+3}$	70-Year			
Grid#30,62	$2.18 \times 10^{+1}$	$1.55 \times 10^{+8}$	$2.88 \times 10^{+3}$	70-Year			
Grid#28,64	$3.04 \times 10^{+1}$	$2.17 \times 10^{+8}$	$4.62 \times 10^{+3}$	70-Year			
Grid#29,63	$4.16 \times 10^{+1}$	$3.88 \times 10^{+8}$	$7.21 \times 10^{+3}$	70-Year			
Grid#29,60	$7.85 \times 10^{+0}$	$6.45 \times 10^{+5}$	$6.37 \times 10^{+2}$	70-Year			
Grid#30,57	$1.59 \times 10^{+1}$	$7.69 \times 10^{+5}$	$1.51 \times 10^{+2}$	70-Year			
Grid#30,61	$1.81 \times 10^{+1}$	$1.85 \times 10^{+7}$	$2.06 \times 10^{+3}$	70-Year			
Grid#28,66	$5.34 \times 10^{+2}$	$1.99 \times 10^{+8}$	$3.70 \times 10^{+4}$	70-Year			
Grid#30,60	$1.18 \times 10^{+1}$	$4.99 \times 10^{+7}$	$2.98 \times 10^{+3}$	70-Year			
Grid#31,58	$1.38 \times 10^{+1}$	$3.80 \times 10^{+7}$	$3.03 \times 10^{+3}$	70-Year			
Grid#31,59	$1.38 \times 10^{+1}$	$8.73 \times 10^{+7}$	$4.66 \times 10^{+3}$	70-Year			
Grid#29,58	$1.42 \times 10^{+1}$	$9.45 \times 10^{+7}$	$2.72 \times 10^{+3}$	70-Year			
Grid#29,59	$9.89 \times 10^{+0}$	$1.42 \times 10^{+8}$	$3.49 \times 10^{+3}$	70-Year			
Grid#29,65	$7.30 \times 10^{+2}$	$7.09 \times 10^{+9}$	$1.59 \times 10^{+5}$	70-Year			
Grid#30,58	$1.77 \times 10^{+1}$	$1.40 \times 10^{+8}$	$2.20 \times 10^{+3}$	70-Year			
Grid#30,59	$1.69 \times 10^{+1}$	$1.88 \times 10^{+8}$	$2.96 \times 10^{+3}$	70-Year			
Grid#30,63	$1.45 \times 10^{+1}$	$2.06 \times 10^{+8}$	$3.25 \times 10^{+3}$	70-Year			

See footnote at end of table

TABLE A.2-32
(Continued)

Constituents of Potential Concern	Upper 95% C.I. on Mean Concentration (mg/kg)	Constituents Inventory in the Waste (mg)	Initial Maximum Leachate Concentration (pCi/L RAD) (μg/L non-RAD)	Constraint[a]	Maximum Loading Concentration from ODAST (Vadose Layer 2) (pCi/L RAD) (μg/L non-RAD)	EPA RAGs, Part B Screening Concentration (pCi/L RAD) (μg/L non-RAD)	CPC ≥Screening Concentration and Requires SWIFT Modeling?
RADIONUCLIDES							
Uranium-238 (Continued)							
Grid#30,64	$4.30 \times 10^{+1}$	$5.08 \times 10^{+8}$	$8.00 \times 10^{+3}$	70-Year			
Grid#29,67	$2.10 \times 10^{+1}$	$6.92 \times 10^{+6}$	$1.27 \times 10^{+3}$	70-Year			
Grid#30,67	$1.46 \times 10^{+1}$	$1.97 \times 10^{+7}$	$2.08 \times 10^{+3}$	70-Year			
Grid#29,66	$3.29 \times 10^{+2}$	$1.83 \times 10^{+9}$	$3.48 \times 10^{+4}$	70-Year			
Grid#30,65	$4.77 \times 10^{+2}$	$2.71 \times 10^{+9}$	$6.37 \times 10^{+4}$	70-Year			
Grid#30,66	$8.25 \times 10^{+1}$	$3.11 \times 10^{+8}$	$6.16 \times 10^{+3}$	70-Year			
Grid#31,61	$2.12 \times 10^{+1}$	$1.53 \times 10^{+8}$	$2.98 \times 10^{+3}$	70-Year			
Grid#31,62	$2.07 \times 10^{+1}$	$1.34 \times 10^{+8}$	$2.62 \times 10^{+3}$	70-Year			
Grid#31,63	$2.11 \times 10^{+1}$	$1.65 \times 10^{+8}$	$3.22 \times 10^{+3}$	70-Year			
Grid#31,66	$2.61 \times 10^{+1}$	$6.19 \times 10^{+6}$	$2.81 \times 10^{+3}$	70-Year			
Grid#34,60	$6.29 \times 10^{+1}$	$3.84 \times 10^{+6}$	$1.80 \times 10^{+3}$	70-Year			
Grid#35,61	$6.29 \times 10^{+1}$	$2.39 \times 10^{+6}$	$1.01 \times 10^{+3}$	70-Year			
Grid#31,65	$2.17 \times 10^{+1}$	$3.28 \times 10^{+7}$	$2.63 \times 10^{+3}$	70-Year			
Grid#32,64	$2.34 \times 10^{+1}$	$4.67 \times 10^{+7}$	$3.92 \times 10^{+3}$	70-Year			
Grid#33,59	$1.61 \times 10^{+1}$	$2.86 \times 10^{+6}$	$1.68 \times 10^{+3}$	70-Year			
Grid#33,60	$8.10 \times 10^{+0}$	$1.03 \times 10^{+7}$	$7.90 \times 10^{+2}$	70-Year			
Grid#33,61	$3.41 \times 10^{+1}$	$6.47 \times 10^{+7}$	$4.53 \times 10^{+3}$	70-Year			
Grid#33,63	$1.01 \times 10^{+2}$	$1.41 \times 10^{+8}$	$1.31 \times 10^{+4}$	70-Year			
Grid#34,61	$6.29 \times 10^{+1}$	$1.19 \times 10^{+8}$	$8.62 \times 10^{+3}$	70-Year			

See footnote at end of table

FER\CRU2RI\JLG\APP-A\TABA2-32\June7, 1994 2:29pm

000150

565 9

TABLE A.2-32
(Continued)

Constituents of Potential Concern	Upper 95% C.I. on Mean Concentration (mg/kg)	Constituents Inventory in the Waste (mg)	Initial Maximum Leachate Concentration (pCi/L RAD) (μg/L non-RAD)	Constraint[a]	Maximum Loading Concentration from ODAST (Vadose Layer 2) (pCi/L RAD) (μg/L non-RAD)	EPA RAGs, Part B Screening Concentration (pCi/L RAD) (μg/L non-RAD)	CPC ≥ Screening Concentration and Requires SWIFT Modeling?
RADIONUCLIDES							
Uranium-238 (Continued)							
Grid#34,62	$2.12 \times 10^{+2}$	$2.68 \times 10^{+8}$	$2.92 \times 10^{+4}$	70-Year			
Grid#31,60	$1.32 \times 10^{+1}$	$7.75 \times 10^{+7}$	$2.82 \times 10^{+3}$	70-Year			
Grid#31,64	$2.46 \times 10^{+1}$	$1.24 \times 10^{+8}$	$4.51 \times 10^{+3}$	70-Year			
Grid#32,60	$1.30 \times 10^{+1}$	$4.40 \times 10^{+7}$	$1.60 \times 10^{+3}$	70-Year			
Grid#32,61	$1.07 \times 10^{+1}$	$3.42 \times 10^{+7}$	$1.24 \times 10^{+3}$	70-Year			
Grid#32,62	$2.66 \times 10^{+1}$	$1.24 \times 10^{+8}$	$4.52 \times 10^{+3}$	70-Year			
Grid#32,63	$2.92 \times 10^{+1}$	$1.35 \times 10^{+8}$	$4.90 \times 10^{+3}$	70-Year			
Grid#33,62	$1.60 \times 10^{+2}$	$4.93 \times 10^{+8}$	$1.79 \times 10^{+4}$	70-Year			
Grid#32,59	$1.00 \times 10^{+1}$	$2.95 \times 10^{+7}$	$2.15 \times 10^{+3}$	70-Year			
Uranium Total (non-RAD)	$1.04 \times 10^{+2}$	$2.29 \times 10^{+10}$	$1.09 \times 10^{+5}$	70-Year	$3.79 \times 10^{+4}$	$1.09 \times 10^{+1}$	Yes
ORGANICS							
2-methylnapthalene	5.60×10^{-2}	$1.24 \times 10^{+7}$	$5.89 \times 10^{+1}$	70-Year	$1.98 \times 10^{+1}$	NA[c]	NA
Aroclor-1254	4.30×10^{-1}	$9.50 \times 10^{+7}$	$4.52 \times 10^{+2}$	70-Year	0.0	1.10×10^{-3}	No
Aroclor-1260	8.90×10^{-2}	$1.97 \times 10^{+7}$	$9.35 \times 10^{+1}$	70-Year	0.0	1.10×10^{-3}	No
Benzo(a)anthracene	1.30×10^{-1}	$2.87 \times 10^{+7}$	$1.37 \times 10^{+2}$	70-Year	0.0	2.82×10^{-3}	No
Benzo(a)pyrene	1.10×10^{-1}	$2.43 \times 10^{+7}$	$1.16 \times 10^{+2}$	70-Year	0.0	2.82×10^{-4}	No
Benzo(b)fluoranthene	1.40×10^{-1}	$3.09 \times 10^{+7}$	$1.47 \times 10^{+2}$	70-Year	0.0	2.82×10^{-3}	No
bis(2-Ethylhexyl) phthalate	8.60×10^{-1}	$1.90 \times 10^{+8}$	$9.03 \times 10^{+2}$	70-Year	0.0	6.07×10^{-1}	No
Dieldrin	1.60×10^{-2}	$3.53 \times 10^{+6}$	$1.68 \times 10^{+1}$	70-Year	0.0	1.12×10^{-4}	No

See footnote at end of table

TABLE A.2-32
(Continued)

Constituents of Potential Concern	Upper 95% C.I. on Mean Concentration (mg/kg)	Constituents Inventory in the Waste (mg)	Initial Maximum Leachate Concentration (pCi/L RAD) (μg/L non-RAD)	Constraint[a]	Maximum Loading Concentration from ODAST (Vadose Layer 2) (pCi/L RAD) (μg/L non-RAD)	EPA RAGs, Part B Screening Concentration (pCi/L RAD) (μg/L non-RAD)	CPC ≥Screening Concentration and Requires SWIFT Modeling?
ORGANICS (Continued)							
Octachlorodibenzo-p-dioxin	3.60×10^{-3}	$7.96 \times 10^{+5}$	$3.78 \times 10^{+0}$	70-Year	0.0	1.19×10^{-5}	No
Phenanthrene	2.10×10^{-1}	$4.64 \times 10^{+7}$	$2.21 \times 10^{+2}$	70-Year	0.0	NA	No
Tetrachlorodibenzofuran	1.80×10^{-5}	$3.98 \times 10^{+3}$	1.89×10^{-2}	70-Year	0.0	1.19×10^{-7}	No
Tributyl Phosphate	2.00×10^{-1}	$4.42 \times 10^{+7}$	$2.10 \times 10^{+2}$	70-Year	$3.95 \times 10^{+1}$	NA	NA
INORGANICS							
Arsenic	$1.21 \times 10^{+1}$	$2.66 \times 10^{+9}$	$4.00 \times 10^{+2}$	TCLP	1.29×10^{-5}	1.46×10^{-4}	No
Beryllium	$1.44 \times 10^{+0}$	$3.18 \times 10^{+8}$	$1.51 \times 10^{+3}$	70-Year	0.0	2.37×10^{-4}	No
Lead	$2.81 \times 10^{+1}$	$6.20 \times 10^{+9}$	$2.00 \times 10^{+2}$	TCLP	$5.61 \times 10^{+1}$	NA	NA

[a]Constraint on reported concentration is by In Situ Leachate (ISL), Toxicity Characteristic Leaching Procedure (TCLP), maximum detection limit (MDL), or by US EPA 70-year rule (70-Year).
[b]Zero indicates that the predicted concentration is at least three orders of magnitude below the screening concentration.
[c]NA = No data available to calculate EPA RAGs, Part B screening value.

Other Comment No. A-48

000192

TABLE A.2-33

PERCHED WATER CONCENTRATIONS AND MASSES FOR THE VADOSE ZONE MODELING, INACTIVE FLYASH PILE AND SOUTH FIELD

Constituents of Potential Concern	Initial Perched Water Concentration (pCi/L RAD) (μg/L non-RAD)	Total Mass (mg)	EPA RAGs, Part B Screening Concentration (pCi/L RAD) (μg/L non-RAD)
RADIONUCLIDES			
Neptunium-237	4.90×10^{-1}	$6.59 \times 10^{+1}$	2.16×10^{-2}
Plutonium-238	2.90×10^{-1}	3.08×10^{-2}	2.16×10^{-2}
Radium-226	2.50×10^{-1}	4.86×10^{-1}	1.76×10^{-4}
Thorium-228	4.80×10^{-2}	3.40×10^{-3}	8.64×10^{-2}
Thorium-230	3.15×10^{-1}	$8.88 \times 10^{+2}$	3.65×10^{-1}
Uranium-234	$2.79 \times 10^{+1}$	$1.38 \times 10^{+2}$	2.97×10^{-1}
Uranium-235/236	$1.72 \times 10^{+0}$	$2.46 \times 10^{+4}$	2.97×10^{-1}
Uranium-238	$2.57 \times 10^{+2}$ ($1.88 \times 10^{+3}$)[a]	$2.36 \times 10^{+7}$	1.70×10^{-1}
Uranium - Total (non-RAD)	$6.45 \times 10^{+1}$	$1.99 \times 10^{+6}$	$1.09 \times 10^{+1}$
INORGANICS			
Arsenic	$3.00 \times 10^{+0}$	$1.09 \times 10^{+7}$	1.46×10^{-4}
Lead	$6.00 \times 10^{+1}$	$4.16 \times 10^{+7}$	NA[b]

[a]In grid blocks (28,66) and (29,65) perched water concentration for uranium-238 was set to 1882 pCi/L.

[b]No data available to calculate EPA RAGs, Part B screening value.

Other Comment No. A-48

TABLE A.2-34

SEEP WATER SOURCE CONCENTRATIONS AND MASSES FOR THE VADOSE ZONE MODELING, INACTIVE FLYASH PILE AND SOUTH FIELD OPERABLE UNIT 2 REMEDIAL INVESTIGATION FERNALD ENVIRONMENTAL MANAGEMENT PROJECT

Constituents of Potential Concern	Seep Loading Concentration (pCi/L RAD) (μg/L non-RAD)	Total Mass (mg)	EPA RAGs, Part B Screening Concentration (pCi/L RAD) (μg/L non-RAD)
INACTIVE FLYASH PILE SEEP			
Neptunium-237	7.90×10^{-1}	$5.46 \times 10^{+1}$	2.16×10^{-2}
Plutonium-238	$2.91 \times 10^{+0}$	8.29×10^{-3}	2.16×10^{-2}
Plutonium-239/240	2.00×10^{-1}	1.57×10^{-1}	2.07×10^{-2}
Radium-226	1.48×10^{-1}	7.29×10^{-3}	1.76×10^{-4}
Thorium-230	6.53×10^{-1}	$1.54 \times 10^{+0}$	3.65×10^{-1}
Uranium-234	$2.34 \times 10^{+2}$	-[a]	2.97×10^{-1}
Uranium-235/236	$1.24 \times 10^{+1}$	-[a]	2.97×10^{-1}
Uranium-238	$2.57 \times 10^{+2}$	$4.52 \times 10^{+8}$	1.70×10^{-1}
Uranium - Total (non-RAD)	$9.15 \times 10^{+2}$	-[a]	$1.09 \times 10^{+1}$
Arsenic	$1.40 \times 10^{+0}$	$8.28 \times 10^{+5}$	1.46×10^{-4}
Bis(2-Ethylhexyl) phthalate	$1.00 \times 10^{+0}$	$4.87 \times 10^{+4}$	6.07×10^{-1}
Lead	$8.30 \times 10^{+0}$	$4.04 \times 10^{+5}$	NA[b]
SOUTH FIELD SEEP			
Uranium-234	$1.58 \times 10^{+2}$	-[a]	2.97×10^{-1}
Uranium-235/236	$8.40 \times 10^{+0}$	-[a]	2.97×10^{-1}
Uranium-238	$1.74 \times 10^{+2}$	$3.35 \times 10^{+8}$	1.70×10^{-1}
Uranium - Total (non-RAD)	$6.19 \times 10^{+2}$	-[a]	$1.09 \times 10^{+1}$

[a]Total mass was not computed because total uranium and uranium isotopes are modeled by applying ratios to uranium-238 results.
[b]No data available to calculate EPA RAGs, Part B screening value.
Other Comment No. A-48

5659

TABLE A.2-35

FLOW RATES FOR SEEPS AND PERCHED WATER SUBSURFACE SEEPS INACTIVE FLYASH PILE AND SOUTH FIELD OPERABLE UNIT 2 REMEDIAL INVESTIGATION FERNALD ENVIRONMENTAL MANAGEMENT PROJECT

	Flow Rate	
Grid Cell	Gallons/minute	Inch/year
INACTIVE FLYASH PILE SEEP		
(28,66)	0.35	18.9
SOUTH FIELD SEEP		
(30,57)	0.26	14.0
PERCHED WATER SUBSURFACE SEEP		
(28,66)	0.44	23.6
(29,62)	0.15	8.1
(29,63)	0.45	24.4
(29,64)	0.77	41.8
(29,65)	1.73	93.6
(30,60)	0.20	10.9
(30,61)	0.40	21.7
(30,62)	0.40	21.7

000195

TABLE A.2-36

SCREENING FOR CONSTITUENTS OF POTENTIAL CONCERN AFTER DILUTION IN THE GREAT MIAMI AQUIFER FOR THE INACTIVE FLYASH PILE AND SOUTH FIELD OPERABLE UNIT 2 REMEDIAL INVESTIGATION FERNALD ENVIRONMENTAL MANAGEMENT PROJECT

Constituent	Units	Concentration at the Groundwater Table	Diluted Great Miami Aquifer Concentration	Screening Concentration	Diluted Concentration Exceeds Screening Concentration
RADIONUCLIDES					
Neptunium-237	pCi/L	$1.06 \times 10^{+2}$	$3.84 \times 10^{+0}$	2.16×10^{-2}	Yes
Radium-226	pCi/L	1.58×10^{-1}	9.14×10^{-2}	1.76×10^{-4}	Yes
Strontium-90	pCi/L	$1.53 \times 10^{+1}$	$1.52 \times 10^{+0}$	1.32×10^{-1}	Yes
Technetium-99	pCi/L	$7.72 \times 10^{+2}$	$2.79 \times 10^{+1}$	$3.65 \times 10^{+0}$	Yes
Uranium-234	pCi/L	$1.10 \times 10^{+4}$	$3.98 \times 10^{+2}$	2.97×10^{-1}	Yes
Uranium-235/236	pCi/L	$2.11 \times 10^{+3}$	$1.21 \times 10^{+2}$	2.97×10^{-1}	Yes
Uranium-238	pCi/L	$5.44 \times 10^{+5}$	$2.89 \times 10^{+3}$	1.70×10^{-1}	Yes
Uranium-Total	μg/L	$3.79 \times 10^{+4}$	$1.37 \times 10^{+0}$	$1.09 \times 10^{+1}$	Yes
ORGANICS					
2-methylnapthalene	μg/L	$1.98 \times 10^{+1}$	7.17×10^{-1}	NA[a]	NA
Tributyl phosphate	μg/L	$3.95 \times 10^{+1}$	$1.43 \times 10^{+0}$	NA	NA
INORGANICS					
Lead	μg/L	$5.61 \times 10^{+1}$	$3.25 \times 10^{+1}$	NA	NA

[a]NA = No data available to calculate EPA RAGs, Part B screening value.
[b]Diluted Great Miami Aquifer concentration marginally exceeds screening concentration. However, it is expected that maximum concentration in the Great Miami Aquifer will be about an order of magnitude lower and, therefore, silver was not modeled further.
Other Comment No. A-48

000136
5659

TABLE A.2-37

SUMMARY OF CONSTITUENTS OF POTENTIAL CONCERN AND SOURCE PATHWAYS FOR THE INACTIVE FLYASH PILE AND SOUTH FIELD OPERABLE UNIT 2 REMEDIAL INVESTIGATION FERNALD ENVIRONMENTAL MANAGEMENT PROJECT

Contaminants of Potential Concern	Source Pathways[a]				
	Inactive Flyash Pile/South Field Waste[b]	Inactive Flyash Pile Seep	South Field Seep	Perched Groundwater Subsurface Seeps in Inactive Flyash Pile/South Field	Paddy's Run Loading from Inactive Flyash Pile/ South Field Runoff
RADIONUCLIDES					
Neptunium-237	Yes	Yes	No	Yes	No
Radium-226	Yes	Yes	No	Yes	Yes
Strontium-90	Yes	No	No	No	No
Technetium-99	Yes	No	No	No	Yes
Uranium-234	Yes	Yes	Yes	Yes	Yes
Uranium-235/236	Yes	Yes	Yes	Yes	No
Uranium-238	Yes	Yes	Yes	Yes	Yes
Uranium - Total (non-RAD)	Yes	Yes	Yes	Yes	No
ORGANICS					
2-methylnaphthalene[c]	NA[c]	No	No	No	NA
Benzo(a)pyrene[d]	No	No	No	No	Yes[d]
Benzo(g,h,i)perylene[c]	No	No	No	No	NA
Dieldrin[d]	No	No	No	No	Yes[d]
Phenanthrene[c]	No	No	No	No	NA
Tributyl phosphate[c]	NA	No	No	No	No
INORGANICS					
Arsenic	No	Yes	No	No	Yes
Beryllium[d]	No	No	No	No	Yes[d]

See footnotes at end of table

FER\CRU2RI\NMG\APP-A\TABA2-37\June7, 1994 2:44pm

000157

5659

TABLE A.2-37
(Continued)

Contaminants of Potential Concern	Source Pathways[a]				
	Inactive Flyash Pile/South Field Waste[b]	Inactive Flyash Pile Seep	South Field Seep	Perched Groundwater Subsurface Seeps in Inactive Flyash Pile/South Field	Paddy's Run Loading from Inactive Flyash Pile/ South Field Runoff
INORGANICS (Continued)					
Lead[c]	NA[c]	NA	No	NA	NA

[a]"Yes" indicates that predicted CPC concentration was above screening concentration; "No" indicates that the predicted CPC concentration was below screening concentration.

[b]Includes loading from perched groundwater source leakage through till and unsaturated GMA, if applicable.

[c]NA = no data available to calculate EPA RAGs, Part B screening values for 2-Methylnaphthalene, benzo(g,h,i)perylene, phenanthrene and lead. These CPCs were not considered for further modeling using SWIFT.

[d]Not modeled using SWIFT because diluted GMA concentration without absorption effects is marginaly above the screening concentration. Typical concentration reduction in the GMA is approximately by a factor of 20.

Other Comment No. A-48

TABLE A.2-38

COMPARISON OF GREAT MIAMI AQUIFER WATER AND BACKGROUND FOR CONSTITUENTS OF POTENTIAL CONCERN IN GROUNDWATER SOUTH FIELD, INACTIVE FLYASH PILE, AND ACTIVE FLYASH PILE OPERABLE UNIT 2 REMEDIAL INVESTIGATION FERNALD ENVIRONMENTAL MANAGEMENT PROJECT

Constituents Potential of Concern	Units	Detects in 2000-Series Well Groundwater Samples				Background		2000-Series Comparable to Background?
		Samples	Hits	Minimum	Maximum	Minimum	Maximum	
RADIONUCLIDES								
NP-237	pCi/L	57	8	0.15	0.962	NA	1.10[a]	Yes
PU-238	pCi/L	59	7	0.07	0.637	NA	1.00[a]	Yes
PU-239/240	pCi/L	59	1	0.06	0.06	NA	1.00[a]	Yes
RA-226	pCi/L	52	14	0.13	1.4	1.10	8.50	Yes
TH-228	pCi/L	60	4	1.10	1.4	1.20	2.90	Yes
TH-230	pCi/L	59	18	0.21	2.06	1.20	3.44	Yes
TH-232	pCi/L	59	5	0.04	1.49	1.20	2.90	Yes
U-234	pCi/L	61	57	0.68	662	1.20	4.20	No
U-235/236	pCi/L	60	28	0.15	31.70	NA	1.30[a]	No
U-238	pCi/L	60	54	0.338	384	0.90	4.40	No
U-Total	µg/L	60	56	2.0	2070.0	NA	NA	No[b]
INORGANICS								
Arsenic	µg/L	16	6	1.2	3.9	2.0	550.0	Yes
Lead	µg/L	16	7	1.3	16.0	2.6	140.0	Yes
ORGANICS								
bis(2-Ethylhexyl) phthalate	µg/L	22	3	2.0	6.0	NA	NA	No

[a]Not detected in background samples. Value reported is maximum detection limit.
[b]Perched water concentration is lower then the Great Miami Aquifer concentration.

NA - Not available.

Other Comment No. A-48

000159
5659

Active Flyash Pile

Figure A.2-11 shows the aerial extent of the waste in the Active Flyash Pile and the SWIFT III grid cells impacted by direct loading from this subunit. Three SWIFT III grid cells were modeled to receive lateral drainage from adjacent grid cells' waste (Figure A.2-11). Table A.2-39 shows the list of CPCs and Table A.2-40 shows the retardation factors used for vadose zone modeling for the Active Flyash Pile. Three pathways of CPC migration to the Great Miami Aquifer were modeled from the Active Flyash Pile. These pathways were the vadose zone pathway, perched water infiltration pathway, and surface water pathway. For the vadose zone pathway, Table A.2-41 shows CPC concentrations in the waste, constituent inventory in the waste, and the maximum predicted leachate concentration. Table A.2-42 shows concentration and mass for the perched water infiltration pathway concentration and mass loading due to surface water pathway are discussed in Appendix A-1.

A summary of screening for CPC for the vadose zone pathway and perched water infiltration pathway is included in Table A.2-39. CPCs passing the screening in Table A.2-39 were further screened using predicted dilution in the Great Miami Aquifer. Table A.2-43 shows the results of the Great Miami Aquifer dilution. Table A.2-44 lists the constituents that survived the various screening processes and were simulated using the SWIFT III model for the Active Flyash Pile. The predicted CPC concentrations were not compared to the field analytical results because this subunit is in close proximity and downgradient of the Inactive Flyash Pile and South Field.

A.2.8 AQUIFER MODELING

Aquifer modeling was performed on CPCs passing through screening and are defined from all applicable five pathways for each subunit. The derivation of the CPCs for the surface water pathway and the surface water modeling is presented in Section A.1.

A.2.8.1 Background, Description, and Development of Model

Groundwater modeling for the Operable Unit 2 baseline risk assessment was performed using the calibrated groundwater flow model for the FEMP. This model utilizes the SWIFT III code and was previously calibrated using groundwater elevations obtained during the April 1986 monitoring period. A brief summary of the calibration and the results of the calibration are presented in this section. The groundwater modeling program was initiated to define groundwater transport in and around the FEMP. The groundwater model used in support of the risk analysis is a finite-difference computer model of groundwater flow and solute transport. The computer program used was SWIFT/386

5659

TABLE A.2-39

LIST OF CONSTITUENTS OF POTENTIAL CONCERN FOR VADOSE ZONE MODELING FOR THE ACTIVE FLYASH PILE OPERABLE UNIT 2 REMEDIAL INVESTIGATION FERNALD ENVIRONMENTAL MANAGEMENT PROJECT

Constituents of Potential Concern		
Radionuclides	Inorganics	Organics
Lead-210	Arsenic	2-Methylnaphthalene
Neptunium-237	Beryllium	Phenanthrene
Plutonium-238	Lead	
Plutonium-239/240	Thallium	
Radium-224		
Radium-226		
Radium-228		
Strontium-90		
Thorium-228		
Thorium-230		
Thorium-232		
Uranium-234		
Uranium-235/236		
Uranium-238		

Other Comment No. A-48

000201

5659

TABLE A.2-40

RETARDATION FACTORS FOR THE ACTIVE FLYASH PILE OPERABLE UNIT 2 REMEDIAL INVESTIGATION FERNALD ENVIRONMENTAL MANAGEMENT PROJECT

Constituent	Retardation Factor for Glacial Overburden	Retardation Factor for Unsaturated Great Miami Aquifer
RADIONUCLIDES		
Lead-210	$1.35 \times 10^{+4}$	$4.65 \times 10^{+2}$
Neptunium-237	$2.49 \times 10^{+2}$	$6.21 \times 10^{+1}$
Plutonium-238	$7.67 \times 10^{+3}$	$1.22 \times 10^{+3}$
Plutonium-239/240	$7.67 \times 10^{+3}$	$1.22 \times 10^{+3}$
Radium-224	$3.14 \times 10^{+3}$	$1.30 \times 10^{+3}$
Radium-226	$3.14 \times 10^{+3}$	$1.30 \times 10^{+3}$
Radium-228	$3.14 \times 10^{+3}$	$1.30 \times 10^{+3}$
Strontium-90	$4.61 \times 10^{+1}$	$3.15 \times 10^{+1}$
Thorium-228	$2.62 \times 10^{+4}$	$3.91 \times 10^{+4}$
Thorium-230	$2.62 \times 10^{+4}$	$3.91 \times 10^{+4}$
Thorium-232	$2.62 \times 10^{+4}$	$3.91 \times 10^{+4}$
Uranium-234	$9.03 \times 10^{+2}$	$1.91 \times 10^{+1}$
Uranium-235/236	$9.03 \times 10^{+2}$	$1.91 \times 10^{+1}$
Uranium-238	$9.03 \times 10^{+2}$	$1.91 \times 10^{+1}$
Total Uranium	$9.03 \times 10^{+2}$	$1.91 \times 10^{+1}$
ORGANICS		
2-Methylnaphthalene	$2.68 \times 10^{+2}$	$1.62 \times 10^{+2}$
Phenanthrene	$5.33 \times 10^{+2}$	$3.23 \times 10^{+2}$
INORGANICS		
Arsenic	$9.03 \times 10^{+2}$	$2.44 \times 10^{+3}$
Beryllium	$5.87 \times 10^{+3}$	$3.05 \times 10^{+3}$
Lead	$1.35 \times 10^{+4}$	$4.65 \times 10^{+2}$
Thallium	$6.77 \times 10^{+3}$	$1.83 \times 10^{+4}$

Other Comment No. A-48

TABLE A.2-41

SOURCE CHARACTERIZATION AND SCREENING SUMMARY OF CONSTITUENTS OF POTENTIAL CONCERN
ACTIVE FLYASH PILE
OPERABLE UNIT 2 REMEDIAL INVESTIGATION
FERNALD ENVIRONMENTAL MANAGEMENT PROJECT

Constituents of Potential Concern	Upper 95% C.I. on Mean Concentration (mg/kg)	Constituent Inventory in the Waste (mg)	Initial Maximum Leachate Concentration (pCi/L RAD) (μg/L non-RAD)	Constraint[a]	Maximum Loading Concentration from ODAST (Vadose Layer 2) (pCi/L RAD) (μg/L non-RAD)	EPA RAGs, Part B Screening Concentration (pCi/L RAD) (μg/L non-RAD)	CPC ≥Screening Concentration and Requires SWIFT Modeling?
RADIONUCLIDES							
Lead-210	2.13×10^{-8}	9.12×10^{-1}	$1.25 \times 10^{+3}$	70-Year	0.0[b]	7.20×10^{-3}	No
Neptunium-237	6.38×10^{-4}	$2.73 \times 10^{+4}$	$3.45 \times 10^{+2}$	70-Year	$3.28 \times 10^{+1}$	2.16×10^{-2}	Yes
Plutonium-238	7.19×10^{-9}	3.07×10^{-1}	$9.43 \times 10^{+1}$	70-Year	0.0	2.16×10^{-2}	No
Plutonium-239/240	1.77×10^{-6}	$7.57 \times 10^{+1}$	$8.43 \times 10^{+1}$	70-Year	0.0	2.07×10^{-2}	No
Radium-224	2.35×10^{-11}	1.01×10^{-3}	$2.87 \times 10^{+3}$	70-Year	0.0	1.25×10^{-1}	No
Radium-226	5.30×10^{-6}	$2.27 \times 10^{+2}$	$4.02 \times 10^{+3}$	70-Year	0.0	1.76×10^{-4}	No
Radium-228	1.59×10^{-8}	6.81×10^{-1}	$3.32 \times 10^{+3}$	70-Year	0.0	4.75×10^{-2}	No
Strontium-90	7.04×10^{-9}	3.01×10^{-1}	$7.39 \times 10^{+2}$	70-Year	$1.79 \times 10^{+1}$	1.32×10^{-1}	Yes
Thorium-228	7.06×10^{-9}	3.02×10^{-1}	$4.44 \times 10^{+3}$	70-Year	0.0	8.64×10^{-2}	No
Thorium-230	2.78×10^{-4}	$1.19 \times 10^{+4}$	$4.38 \times 10^{+3}$	70-Year	0.0	3.65×10^{-1}	No
Thorium-232	$3.51 \times 10^{+1}$	$1.50 \times 10^{+9}$	$2.96 \times 10^{+3}$	70-Year	0.0	2.79×10^{-2}	No
Uranium-234	1.43×10^{-3}	$6.12 \times 10^{+4}$	$6.82 \times 10^{+3}$	70-Year	$8.54 \times 10^{+2}$	2.97×10^{-1}	Yes
Uranium-235/236	$1.91 \times 10^{+0}$	$8.15 \times 10^{+7}$	$3.16 \times 10^{+3}$	70-Year	$3.95 \times 10^{+2}$	2.97×10^{-1}	Yes
Uranium-238		$6.45 \times 10^{+8}$			$4.87 \times 10^{+2}$	1.70×10^{-1}	Yes
Grid #31,56	$1.51 \times 10^{+1}$	$6.32 \times 10^{+6}$	$6.78 \times 10^{+2}$	70-Year			
Grid #31,57	$1.51 \times 10^{+1}$	$3.33 \times 10^{+7}$	$9.39 \times 10^{+2}$	70-Year			
Grid #32,56	$1.51 \times 10^{+1}$	$9.13 \times 10^{+7}$	$1.39 \times 10^{+3}$	70-Year			
Grid #32,57	$1.51 \times 10^{+1}$	$1.64 \times 10^{+8}$	$1.84 \times 10^{+3}$	70-Year			
Grid #32,58	$1.51 \times 10^{+1}$	$1.95 \times 10^{+7}$	$2.50 \times 10^{+3}$	70-Year			

See footnote at end of table

TABLE A.2-41
(Continued)

Constituents of Potential Concern	Upper 95% C.I. on Mean Concentration (mg/kg)	Constituent Inventory in the Waste (mg)	Initial Maximum Leachate Concentration (pCi/L RAD) (μg/L non-RAD)	Constraint[a]	Maximum Loading Concentration from ODAST (Vadose Layer 2) (pCi/L RAD) (μg/L non-RAD)	EPA RAGs, Part B Screening Concentration (pCi/L RAD) (μg/L non-RAD)	CPC ≥ Screening Concentration and Requires SWIFT Modeling?
RADIONUCLIDES (Continued)							
Uranium-238 (Continued)							
Grid #33,56	$1.51 \times 10^{+1}$	$1.18 \times 10^{+8}$	$1.37 \times 10^{+3}$	70-Year			
Grid #33,57	$1.51 \times 10^{+1}$	$1.03 \times 10^{+8}$	$1.77 \times 10^{+3}$	70-Year			
Grid #33,58	$1.51 \times 10^{+1}$	$1.61 \times 10^{+7}$	$1.97 \times 10^{+3}$	70-Year			
Grid #34,56	$1.51 \times 10^{+1}$	$6.78 \times 10^{+7}$	$1.06 \times 10^{+3}$	70-Year			
Grid #34,57	$1.51 \times 10^{+1}$	$2.53 \times 10^{+7}$	$3.89 \times 10^{+3}$	70-Year			
Uranium Total (non RAD)	$3.00 \times 10^{+1}$	$1.28 \times 10^{+9}$	$2.30 \times 10^{+4}$	70-Year	$2.88 \times 10^{+3}$	$1.09 \times 10^{+1}$	Yes
ORGANICS							
2-Methylnaphthalene	$1.60 \times 10^{+1}$	$6.85 \times 10^{+6}$	$1.23 \times 10^{+2}$	70-Year	$9.18 \times 10^{+0}$	NA[c]	NA
Phenanthrene	7.20×10^{-2}	$3.08 \times 10^{+6}$	$5.54 \times 10^{+1}$	70-Year	0.0	NA	No
INORGANICS							
Arsenic	$6.43 \times 10^{+1}$	$2.75 \times 10^{+9}$	$9.80 \times 10^{+1}$	TCLP	0.0	1.46×10^{-4}	No
Beryllium	$3.38 \times 10^{+0}$	$1.44 \times 10^{+8}$	$2.59 \times 10^{+3}$	70-Year	0.0	2.37×10^{-4}	No
Lead	$4.54 \times 10^{+1}$	$1.94 \times 10^{+9}$	$6.04 \times 10^{+1}$	TCLP	$2.87 \times 10^{+1}$	NA	NA
Thallium	$2.08 \times 10^{+0}$	$8.91 \times 10^{+7}$	$1.60 \times 10^{+3}$	70-Year	0.0	2.55×10^{-1}	No

[a]Constraint on reported concentration is by In Situ Leachate (ISL), Toxicity Characteristic Leaching Procedure (TCLP), maximum detection limit (mdl), or by US EPA 70-year rule (70-Year).
[b]Zero indicates that predicted concentration is at least three orders of magnitude below the screening concentration.
[c]NA = no data available to calculate EPA RAGs, Part B screening value.
Other Comment #A-48

000204

TABLE A.2-42

PERCHED WATER CONCENTRATIONS AND MASSES FOR THE VADOSE ZONE MODELING, ACTIVE FLYASH PILE OPERABLE UNIT 2 REMEDIAL INVESTIGATION FERNALD ENVIRONMENTAL MANAGEMENT PROJECT

Constituents of Potential Concern	Initial Perched Groundwater Concentration (pCi/L RAD) (μg/L non-RAD)	Total Mass (mg)	EPA RAGs, Part B Screening Concentration (pCi/L RAD) (μg/L non-RAD)
RADIONUCLIDES			
Neptunium-237	$1.00 \times 10^{+0}$	$5.52 \times 10^{+2}$	2.16×10^{-2}
Plutonium-238	$1.00 \times 10^{+0}$	7.01×10^{-1}	2.16×10^{-2}
Plutonium-239/240	$1.00 \times 10^{+0}$	$1.93 \times 10^{+2}$	2.07×10^{-2}
Radium-226	$1.00 \times 10^{+0}$	$4.96 \times 10^{+0}$	1.76×10^{-4}
Radium-228	$3.00 \times 10^{+0}$	5.41×10^{-2}	4.75×10^{-2}
Strontium-90	$1.19 \times 10^{+0}$	6.26×10^{-4}	1.32×10^{-1}
Thorium-228	$2.93 \times 10^{+0}$	1.46×10^{-1}	8.64×10^{-2}
Thorium-230	$1.13 \times 10^{+0}$	$2.24 \times 10^{+3}$	3.65×10^{-1}
Thorium-232	$1.00 \times 10^{+0}$	$3.72 \times 10^{+8}$	2.79×10^{-2}
Uranium-234	$6.60 \times 10^{+0}$	$1.50 \times 10^{+3}$	2.97×10^{-1}
Uranium-235/236	$1.00 \times 10^{+0}$	$6.53 \times 10^{+5}$	2.97×10^{-1}
Uranium-238	$6.90 \times 10^{+0}$	$2.90 \times 10^{+7}$	1.70×10^{-1}
Uranium - Total	$3.13 \times 10^{+1}$	$4.42 \times 10^{+7}$	$1.09 \times 10^{+1}$
INORGANICS			
Arsenic	$3.40 \times 10^{+0}$	$4.80 \times 10^{+6}$	1.46×10^{-4}
Lead	$6.00 \times 10^{+1}$	$1.27 \times 10^{+9}$	NA[a]

[a]NA = No data available to calculate EPA RAGs, Part B screening value.

Other Comment No. A-48

TABLE A.2-43

SCREENING FOR CONSTITUENTS OF POTENTIAL CONCERN AFTER DILUTION IN THE GREAT MIAMI AQUIFER FOR THE ACTIVE FLYASH PILE OPERABLE UNIT 2 REMEDIAL INVESTIGATION FERNALD ENVIRONMENTAL MANAGEMENT PROJECT

Constituent	Units	Concentration in Vadose Zone at the Groundwater Table	Diluted Great Miami Aquifer Concentration	Screening Concentration	Diluted Concentration Exceeds Screening Concentration
RADIONUCLIDES					
Neptunium-237	pCi/L	$3.28 \times 10^{+1}$	$6.98 \times 10^{+0}$	2.16×10^{-2}	Yes
Strontium-90	pCi/L	$1.79 \times 10^{+1}$	$3.80 \times 10^{+0}$	1.32×10^{-1}	Yes
Uranium-234	pCi/L	$8.54 \times 10^{+2}$	$1.28 \times 10^{+2}$	2.97×10^{-1}	Yes
Uranium-235/236	pCi/L	$3.95 \times 10^{+2}$	$5.92 \times 10^{+1}$	2.97×10^{-1}	Yes
Uranium-238	pCi/L	$4.87 \times 10^{+2}$	$7.28 \times 10^{+1}$	1.70×10^{-1}	Yes
Uranium-total(Non-RAD)	pCi/L	$2.88 \times 10^{+3}$	$4.31 \times 10^{+2}$	$1.09 \times 10^{+1}$	Yes
ORGANICS					
2-Methylnaphthalene	μg/L	$9.18 \times 10^{+0}$	$1.95 \times 10^{+0}$	NA[a]	NA
INORGANICS					
Lead	μg/L	$2.87 \times 10^{+1}$	$6.11 \times 10^{+0}$	NA	NA

[a]NA = no data available to calculate EPA, RAGs, Part B screening volume.

Other Comment No. A-48

FER\CRU2RI\ULG\APP-A\TABA2-43\June7, 1994 2:55pm

TABLE A.2-44

SUMMARY OF CONSTITUENTS OF POTENTIAL CONCERN AND SOURCE PATHWAYS FOR THE ACTIVE FLYASH PILE OPERABLE UNIT 2 REMEDIAL INVESTIGATION FERNALD ENVIRONMENTAL MANAGEMENT PROJECT

Contaminants of Potential Concern	Source Pathways[a]	
	Infiltration through Active Flyash Pile[b]	SSOD Loading from Active Flyash Pile Runoff
RADIONUCLIDES		
Neptunium-237	Yes	Yes
Strontium-90	Yes	No
Uranium-234	Yes	Yes
Uranium-235/236	Yes	No
Uranium-238	Yes	Yes
Uranium Total	Yes	No
ORGANICS		
2-Methylnaphthalene	NA[d]	No
INORGANICS		
Arsenic	No	Yes
Beryllium	No	Yes
Lead	NA	NA

[a]"Yes" indicates predicted CPC concentration was above screening concentration; "No" indicates that the predicted CPC concentration was below screening concentration.
[b]Includes loading from perched groundwater source leakage through till and unsaturated GMA, if applicable.
[c]Not modeled based on diluted GMA concentration less than EPA RAGs, Part B screening concentration.
[d]NA = no data available to calculate EPA, RAGs, Part B screening value.
Other Comment No. A-48

Version 2.51. A comprehensive verification study of the SWIFT III code has been completed (IT 1990). A detailed presentation of the model, its development, and the baseline input data was issued as a part of the overall modeling report prepared under the RI/FS (DOE 1990) and revised and issued as a separate report (DOE 1993). Only the most pertinent information for the Operable Unit 2 Remedial Investigation is presented here.

The steps in the development of the model for application to the FEMP included:

- Construction and calibration of a regional, two-dimensional, steady-state groundwater flow model
- Construction and calibration of a regional, three-dimensional, steady-state groundwater flow model
- Application of a local, two-dimensional, analytical solute transport model to help strategize the numerical solute transport model
- Construction of a local, two-dimensional, transient solute transport model
- Construction and calibration of a local, three-dimensional, transient solute transport model with uranium concentration data from the monitoring wells

The regional model covers an area of 28.7 square miles, including the FEMP, the Southern Ohio Water Company (SOWC) collector wells, and a portion of the Great Miami River. The regional model's grid spacing varies between 250 feet and 2,000 feet, and has the closest grid spacing in the area of the SOWC collector wells. It was calibrated against field data using a steady-state flow condition and calibration results were incorporated into the local area model.

The local model covers a smaller area than the regional model and uses a tighter grid spacing, with grid cells 125 feet on each side. The smaller grid was established to include the area of the existing uranium plume, and extends from the northern part of the FEMP to approximately 1,500 feet north of the Great Miami River (Figure A.2-14). The grid size was selected based on the need to simulate a uranium dispersivity of 100 feet longitudinally, which was the preferred value based on literature review (IT 1990). Using this dispersivity value, the grid size was selected to accommodate dispersivity values as low as 62.5 feet, or half the distance of the local grid area of 125 feet. The relationship between the local and regional models was established by imposing the steady-state flow field predicted by the regional model onto the local solute transport model.

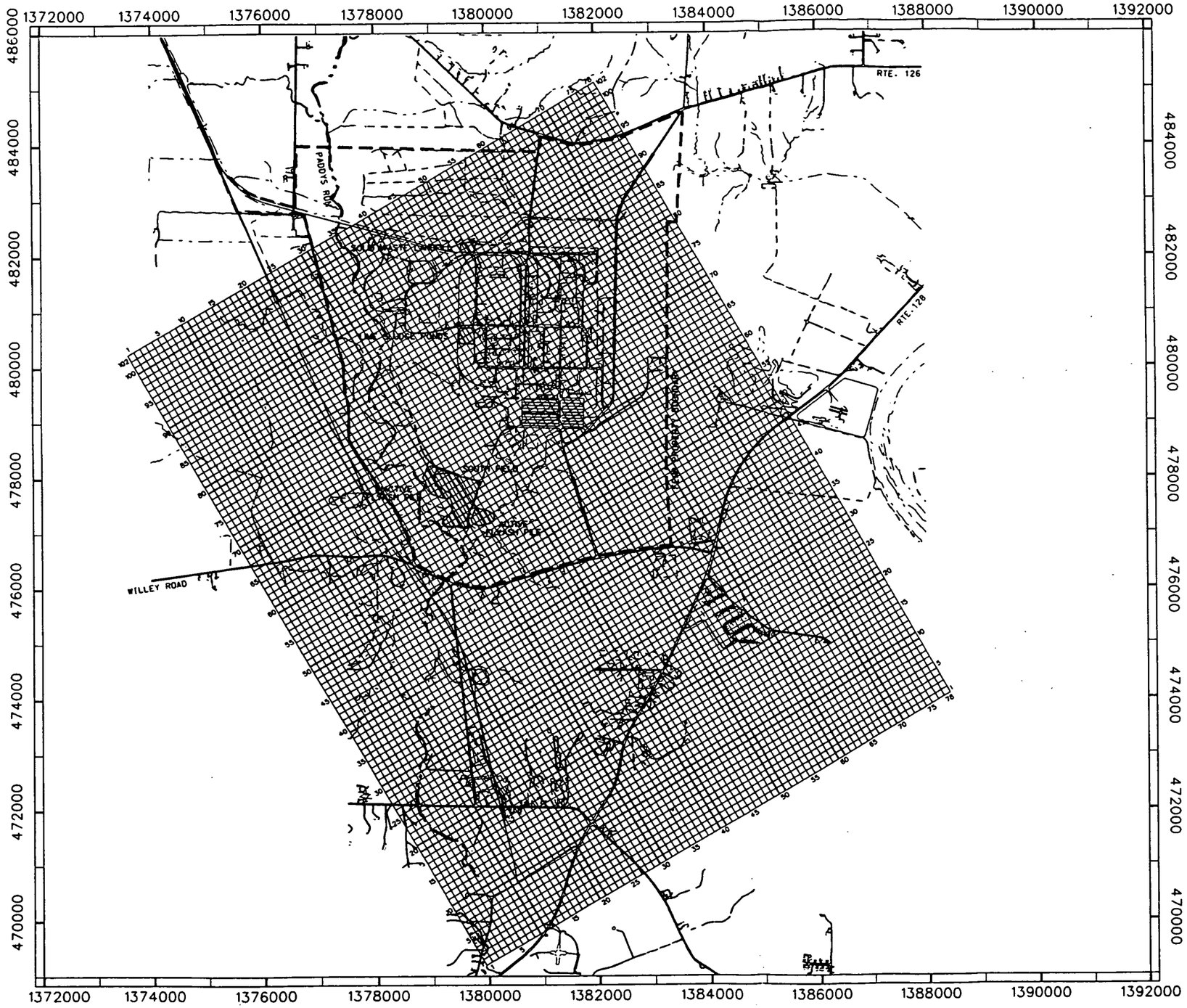

LEGEND

- ROADS
- STREAM
- WASTE AREA
- RAILROAD
- FEMP PROPERTY BOUNDARY

NOTE:
Coordinates are in State Planar NAD 1927.
Surface contours based on 1992 flyover.
Other source loadings and background concentrations not included.

N

SCALE (FT)

0 2000 4000

000209

figa0214.dgn

FIGURE A.2-14
SWIFT III LOCAL AREA MODEL GRID

The regional and local models each contain five layers. These layers are conceptually shown in Figure A.2-4. The uppermost two layers represent the upper and lower parts of the upper Great Miami Aquifer that underlies the area. The middle layer represents a clay interbed that is present in the immediate vicinity of the FEMP site, and the lowermost two layers represent the upper and lower parts of the lower Great Miami Aquifer. In regions where the clay interbed is not present, the middle layer has the same characteristics as the upper two layers. The layers extend laterally into bedrock to the edges of the buried valley that contains the aquifer. The number of aquifer cells in each layer was decreased with depth in the aquifer to simulate the narrowing bedrock valley. This was done using bedrock topography maps of the region and simulated the U-shaped buried valley which contains the Great Miami Aquifer.

Pumping wells are located in the area spanned by both the regional and local models. These include a FEMP production well (there are four total, but only one pumps significant quantities of water) and three industrial wells located south of the FEMP site in both models. Pumping from each of these wells was assigned to the proper cell and layer in the model. In addition, the regional model also simulates the presence of two large capacity collector wells owned by the SOWC located by the Great Miami River. Although they are not directly included in the local model, they do influence its results by way of the boundary conditions brought in from the regional model.

The calibration of the groundwater flow model was performed by comparing hydraulic heads calculated by the model against heads measured in numerous monitoring wells throughout the FEMP and surrounding areas. This calibration was performed using the regional flow model. Reasonable estimates of hydraulic conductivity and recharge were initially input into the model and then varied within an acceptable range to adjust model-computed heads into agreement with observed monitoring well heads.

The model used varying hydraulic conductivity values for the five layers based on the results of the calibration. The uppermost and middle layers were assigned hydraulic conductivity values of 450 feet/day (0.16 cm/sec), and the lowermost layers used 600 ft/day (0.21 cm/sec). In addition, a portion of the middle layer which underlies the FEMP was assigned 0.0003 ft/day (1×10^{-7} cm/sec) as a hydraulic conductivity value to represent the clay interbed (as shown by geologic borings). This simulated the presence of a low permeability clay and created a semi-confining layer underneath part of the FEMP and its surrounding area. Vertical to horizontal hydraulic conductivity ratios were set

for all layers at 0.1. Results of the recent South Plume pump test calculated aquifer values for vertical to horizontal hydraulic conductivity ratios from 0.07 to 0.17 (i.e., over a range which includes this value) (Parsons 1993). Further details concerning determination of hydraulic conductivity values can be found in "Groundwater Modeling Report - Summary of Model Development" (DOE 1993a).

NO. A-21

Recharge rates set as a result of the regional model calibration were assigned to several different zones. In areas where the sand and gravel aquifer is overlain by glacial overburden, a recharge of 6 inches per year (in/yr) (15 cm/yr) was used. Regions where the Great Miami Aquifer is exposed at the surface use 14 in/yr (36 cm/yr), and Paddys Run channel was assigned a value of 32 in/yr (0.81 cm/yr) in the local model to simulate its increased infiltration. An additional region, the area covered by the FEMP former Production Area, was also created as a consequence of the sensitivity analysis. This region was assigned a value of 2 in/yr (5 cm/yr) ~~to simulate the developed nature of the site and the effects of storm water drainage into the storm sewer system~~ because a large portion of the area is covered or underlain by the drainage system. Further rationale for the reduced infiltration rate in the former Production Area is provided in the "Groundwater Modeling Report - Summary of Model Development" (DOE 1993a).

NO. A-19

Groundwater flow conditions simulated by the model were successful and reproduced the observed flow conditions throughout the study area. Based on water levels from 55 wells, the arithmetic mean residual (observed head minus calculated head at the monitoring well) for the calibrated flow model was 0.33 feet. The excellent match portrayed by this residual value is realized when compared to a total change in hydraulic head of approximately 20 feet over the modeling area. The mean of the absolute values of the residuals was 1.08 feet, with a standard deviation of 1.36 feet. Water balances performed using the model showed total inflow and total outflow from the model to agree within 0.2 percent. Further details on the SWIFT model calibration are provided in a separate report (DOE 1993a).

NO. A-20

To maintain hydraulic similarity between the regional and local flow models, a computer program was used to check, cell by cell, the correspondence of heads in the local model with heads in the regional model. The program verified that the regional flow model calibration was preserved in the local model which was used for solute transport; thus, no new flow calibration was necessary. The local model used hydraulic parameters identical to those used in the calibrated regional model.

Boundary conditions for the local model were set from corresponding cells in the regional model to maintain the hydraulic similarity.

A.2.8.2 SWIFT III Modeling

The calibrated groundwater flow model for the FEMP was used to simulate the transport of constituents in the Great Miami Aquifer. A series of constant loading periods were defined for ODAST output for each constituent for the SWIFT III modeling based upon source decay, retardation, and constituent decay factors. Typically, a 10 year loading interval was used for CPCs with low retardation factors (e.g., technetium-99) while a 20 year period was defined for CPCs with high retardation factors (e.g., manganese and uranium-238). Loading rates for each period were calculated by averaging the results of the vadose zone modeling over the length of each period. In this way, total mass inflow into the aquifer was maintained. A simulation time of 1000 years was used for CPCs in the Great Miami Aquifer.

Loading rates were calculated, using ODAST, for each of the SWIFT III grid blocks under potential source areas in the model to account for the varying surface area and thickness of the waste within each subunit. The loading rate for each compound in each grid block was calculated from the volume of the waste overlying it, the constituent concentration, and other physical parameters (see Section A.2.7).

Initial background concentrations of each compound in the aquifer were set to zero. The model simulations for the Operable Unit 2 CPCs used a longitudinal dispersivity value of 100 feet and transverse dispersivity of 10 feet. These values were determined during the solute transport calibration for uranium and are based on values taken from literature review (DOE 1990 and Walton 1985). Distribution coefficients, retardation factors, and decay factors for simulated compounds were also taken from various sources (see Section A.2.4) and are shown in Table A.2-45. Other key parameters used by the SWIFT III model are listed in Table A.2-46.

Model simulations were performed using SWIFT/386 on a Powerbox PC microcomputer or Silicon Graphics workstation. Simulation execution times varied between 18 and 37 hours on Powerbox PC and 8 to 15 hours on Silicon Graphics workstation and required extensive computing capacity. Output was written to a single file from which relevant data was extracted using data manipulation programs written for that purpose. Contour plots were made for selected constituents at different

TABLE A.2-45

DISTRIBUTION COEFFICIENTS AND DECAY FACTORS USED IN THE SWIFT III MODEL OPERABLE UNIT 2 REMEDIAL INVESTIGATION FERNALD ENVIRONMENTAL MANAGEMENT PROJECT

Parameters	Distribution Coefficient K_d (mL/g)	Decay Half Life (days)
RADIONUCLIDES		
Neptunium-237	$5.00 \times 10^{+0}$	$7.81 \times 10^{+8}$
Radium-226	$1.06 \times 10^{+2}$	$5.84 \times 10^{+5}$
Strontium-90	$2.50 \times 10^{+0}$	$1.04 \times 10^{+4}$
Technetium-99	7.00×10^{-2}	$7.77 \times 10^{+7}$
Uranium-234	$1.48 \times 10^{+0}$	$8.92 \times 10^{+7}$
Uranium-235/236	$1.48 \times 10^{+0}$	$2.57 \times 10^{+11}$
Uranium-238	$1.48 \times 10^{+0}$	$1.63 \times 10^{+12}$
Uranium - Total	$1.48 \times 10^{+0}$	$1.63 \times 10^{+12}$[a]
INORGANICS		
Arsenic	$2.00 \times 10^{+2}$	none
Beryllium	$2.50 \times 10^{+2}$	none
Lead	$3.80 \times 10^{+1}$	none

none - constituent does not decay

[a]Decay half-life for Uranium - Total was assumed to be the same as that of Uranium-238

Comment No. A-48

TABLE A.2-46

PARAMETERS USED IN THE SWIFT III MODEL

Parameter	Value
Hydraulic Conductivity	
Layer 1	K_H = 450 ft/day; K_v = 45 ft/day
Layer 2	K_H = 450 ft/day; K_v = 45 ft/day
Layer 3	K_H = 1.00 x 10^{-3} ft/day; K_v = 1.00 x 10^{-4} ft/day
Layer 4	K_H = 600 ft/day; K_v = 60 ft/day
Layer 5	K_H = 600 ft/day; K_v = 60 ft/day
Effective Porosity	0.25
Longitudinal Dispersity	100 ft
Transversal Dispersity	10 ft
Soil Bulk Density (dry)	1.60 g/cm^3

Comment No. A-48

simulation times for CPCs exceeding screening concentration to represent CPC plumes and plume changes over time. Contour plots are presented at the time of maximum concentration on-site and at the FEMP property boundary, at the time of uranium maximum concentration on-site and at the FEMP property boundary, and at 1000 years.

A.2.8.2.1 Source Loading to the Great Miami Aquifer

Constituent loading to the Great Miami Aquifer came from:

- The leaching of CPCs from the soil matrix into the dissolved phase and then migrating to the Great Miami Aquifer through the vadose zone
- The infiltration of contaminated surface water from Operable Unit 2 subunits to the Storm Sewer Outfall Ditch and Paddys Run and then to the Great Miami Aquifer
- Percolation of perched water beneath the subunits through the vadose zone to the underlying Great Miami Aquifer
- Lateral migration of perched water beneath the subunits and then infiltrating through an area where glacial overburden is not present (subsurface seeps).
- Infiltration of contaminated seep water to the Great Miami Aquifer

Loading from perched water, waste leachate, and seeps to the Great Miami Aquifer was modeled using ODAST and results are presented in Section A.2.7. Appendix A.1 describes modeling of CPCs through the surface water pathway. CPCs that follow the surface water pathway to the Great Miami Aquifer were first screened to remove constituents that pose insignificant risk. If theoretical Great Miami Aquifer concentrations were below the screening concentrations then the constituent was screened out and was not modeled in the aquifer. All CPCs were screened out from the surface water pathway for the Solid Waste Landfill and the surface water pathway is not applicable for the Lime Sludge Ponds. Table A.2-47 provides a summary of surface water runoff loading to the Great Miami Aquifer from the Inactive Flyash Pile, and South Field, while Table A.2-48 provides a summary of surface water runoff loading to the Great Miami Aquifer from the Active Flyash Pile. One-hundred percent of the constituent mass in the runoff effluent reaching the Storm Sewer Outfall Ditch and 30 percent of the constituent mass in the runoff effluent reaching Paddys Run was assumed to infiltrate to the Great Miami Aquifer (IT, 1993) during storm events. This loading consists of CPC mass in runoff water in dissolved phase as well as leaching of sediments. Note that 43.4% of runoff water from the Storm Water Outfall Ditch was also assumed to reach Paddys Run and eventually to the Great Miami River. Similarly, one hundred percent of CPC mass reaching Paddys Run was assumed

TABLE A.2-47

SUMMARY OF CONSTITUENTS OF POTENTIAL CONCERN FOR SURFACE WATER RUNOFF LOADING TO THE GREAT MIAMI AQUIFER FROM THE INACTIVE FLYASH PILE AND THE SOUTH FIELD OPERABLE UNIT 2 REMEDIAL INVESTIGATION FERNALD ENVIRONMENTAL MANAGEMENT PROJECT

Constituents of Potential Concern	Maximum Loading Concentration to the Aquifer from the Inactive Flyash Pile (pCi/L RAD) (μg/L non-RAD)	Maximum Loading Concentration to the Aquifer from the South Field (pCi/L RAD) (μg/L non-RAD)	Annual Loading Mass (g) (μg/L non-RAD)	EPA RAGs, Part B Screening Concentration (pCi/L RAD) (μg/L non-RAD)
Arsenic	$3.92 \times 10^{+0}$	8.81×10^{-1}	$1.14 \times 10^{+0}$	1.46×10^{-3}
Technetium-99	0.0	$2.15 \times 10^{+4}$	9.72×10^{-1}	$3.65 \times 10^{+0}$
Uranium-238[a]	$1.27 \times 10^{+2}$	$1.44 \times 10^{+2}$	$3.74 \times 10^{+2}$	1.70×10^{-1}

[a]The Great Miami Aquifer concentrations for other uranium isotopes and total uranium were scaled from the results for uranium-238.

Other Comment No. A-48 and EPA Comment No. A-22

NO. A-22 to reach the Great Miami River. Uranium-238 was modeled using SWIFT III. The other uranium isotopes and total uranium results were scaled from the uranium-238 results.

A.2.8.3 Results of SWIFT III Modeling

A.2.8.3.1 Solid Waste Landfill

The groundwater fate and transport modeling results are summarized in Table A.2-49 for technetium-99, the only CPC that will reach the Great Miami Aquifer within 1000 years from the Solid Waste Landfill above the screening concentrations. This table also presents the arrival time for the constituents to reach the aquifer, the maximum loading concentration, the maximum concentrations of the CPC that would be expected in the aquifer within 1000 years and the time required for the constituents to reach the maximum value. It also presents the predicted maximum concentration at the FEMP boundary due to loading from the Solid Waste Landfill. Screening levels have been developed based on a ~~10^{-7} lifetime risk of cancer~~ EPA RAGs, Part B guidelines, presented NO. A-48 in Appendix B, and provide a basis for understanding the risk to human health from the ingestion of water from the Great Miami Aquifer at the hypothetical receptor location.

~~Figure A.2-15 shows cumulative mass loading and ODAST output concentration in the grid cell with maximum concentration as a function of time to the Great Miami Aquifer from the Solid Waste Landfill. Contour plots for projected increase in the concentrations of technetium-99 at the time of maximum concentrations in the Great Miami Aquifer (70 60 years) are shown in Figure A.2-16. At~~ NO. A-24 ~~1000 years, concentrations of technetium-99 were predicted to be significantly below the screening concentration. Figure A.2-16 shows that technetium-99 migration is toward the east.~~

NO. A-48 Maximum predicted technetium-99 concentration in the Great Miami Aquifer was 0.61 pCi/L, which is more than an order of magnitude below the screening concentration. Due to low concentrations, no contour map of technetium-99 concentration was produced.

A.2.8.3.2 Lime Sludge Ponds

The groundwater fate and transport modeling results are summarized in Table A.2-50 for technetium-99, the only CPC that will reach the Great Miami Aquifer within 1000 years from the Lime Sludge Ponds. The table also presents the arrival time for the constituents in the aquifer, the maximum loading concentration, the maximum concentrations of technetium-99 that would be expected in the

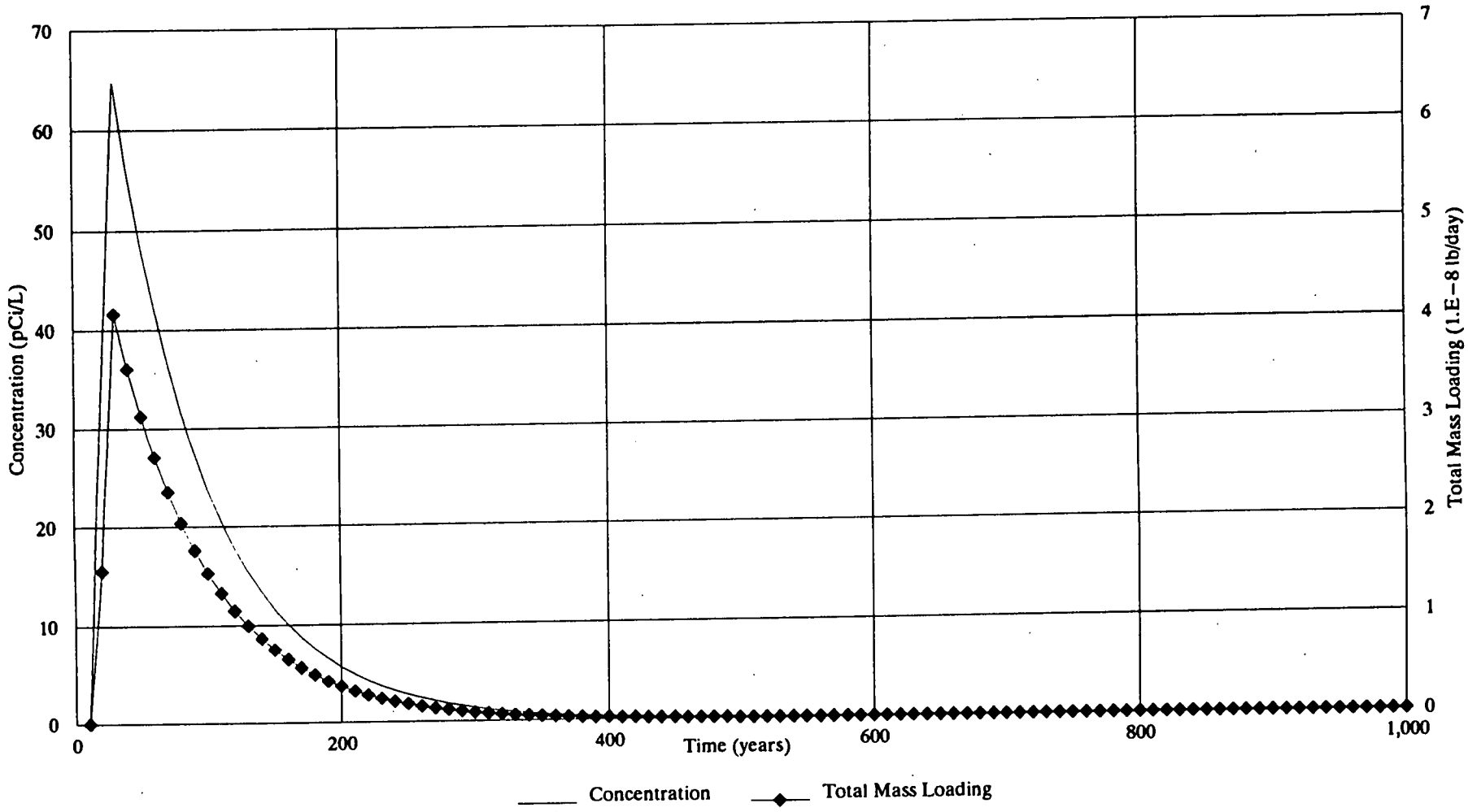

Maximum concentration (64.8 pCi/L) occurs in grid block (44,80).

Concentrations are plotted for grid block (44,80).

FIGURE A.2–17. TECHNETIUM–99 LOADING TO THE GREAT MIAMI AQUIFER FROM THE LIME SLUDGE POND

000218

TABLE A.2-48

SUMMARY OF CONSTITUENTS OF POTENTIAL CONCERN FOR SURFACE WATER RUNOFF LOADING TO THE GREAT MIAMI AQUIFER FROM THE ACTIVE FLYASH PILE OPERABLE UNIT 2 REMEDIAL INVESTIGATION FERNALD ENVIRONMENTAL MANAGEMENT PROJECT

Constituents of Potential Concern	Maximum Loading Concentration to the Aquifer (pCi/L RAD) (μg/L non-RAD)	Loading Mass (g)	EPA RAGs, Part B Screening Concentration (pCi/L RAD) (μg/L non-RAD)
Arsenic	$1.06 \times 10^{+1}$	$1.21 \times 10^{+1}$	1.46×10^{-4}
Beryllium	4.44×10^{-1}	5.04×10^{-1}	2.37×10^{-4}
Neptunium-237	$2.51 \times 10^{+1}$	4.08×10^{-2}	2.16×10^{-2}
Uranium-238[a]	$5.13 \times 10^{+1}$	$1.74 \times 10^{+2}$	1.70×10^{-1}

[a]The Great Miami Aquifier concentrations for other uranium isotopes and total uranium were selected from the results for uranium-238.

Comment No. A-48 and Comment No. A-25

000219

TABLE A.2-49

SUMMARY OF SWIFT MODELING RESULTS FOR THE SOLID WASTE LANDFILL OPERABLE UNIT 2 REMEDIAL INVESTIGATION FERNALD ENVIRONMENTAL MANAGEMENT PROJECT

Constituents of Potential Concern	Maximum Loading Concentration from ODAST (pCi/L)	Minimum Time of Arrival to the Aquifer (years)	Time of Maximum On-Site Concentration (years)	Maximum On-Site Concentration in the Aquifer (pCi/L)	Time of Maximum Concentration at the FEMP Boundary (years)	Maximum Concentration at the FEMP Boundary (pCi/L)	EPA RAGs, Part B Screening Concentration (pCi/L)
RADIONUCLIDES							
Technetium-99	28.5	10-20	60	0.61	70	0.054	3.65

Comment No. A-48

FER\CRU2RI\NMG\APP-A\TABA2-49\June7, 1994 3:30pm

aquifer within 1000 years and the time required for the constituents to reach the maximum value. It also shows that the predicted maximum concentration at the FEMP boundary due to loading from the Lime Sludge Ponds is below the screening level, i.e., off-site impact of Lime Sludge Ponds is negligible. Screening levels have been developed based on a ~~10^{-7} lifetime risk of cancer~~ EPA RAGs, Part B guidelines, presented in Appendix B, and provide a basis for understanding the risk to human health from the ingestion of water from the Great Miami Aquifer at the hypothetical receptor location. ~~Figure A.2-17 shows the loading of technetium-99 that increases sharply initially and then follows an exponentially declining curve.~~

NO. A-48

NO. A-26

Figure A.2-17 shows the Great Miami Aquifer loading curve for technetium-99 loading from the Lime Sludge Ponds. Figure A.2-17 shows that the breakthrough occurs at 10 years and the peak loading to the Great Miami Aquifer occurs at 30 years. During these two time steps, concentration of technetium-99 in the Great Miami Aquifer increases from zero and also moved away from the Lime Sludge Ponds. As more technetium-99 is added at later time, it mixes with the technetium-99 already present in the Great Miami Aquifer under the Lime Sludge Ponds and maximum on-site technetium-99 concentration occurs at 40 years due to cumulative effects. Meanwhile, technetium-99 loaded to the Great Miami Aquifer before 40 years has moved off-site. Due to exponentially declining loading, low retardation, and flow dynamics including effects of dispersion, off-site maximum technetium-99 concentration also occurs at 40 years (Table A.2-50). It must be noted that off-site maximum concentration is less than on-site maximum concentration.Figure A.2-18 shows the contour plots for projected increase in the concentrations of technetium-99 at the time of maximum concentrations (40 years).

Figure A.2-18 shows that plume migration from the Lime Sludge Ponds is in an east-southeasterly direction. At 1,000 years, concentrations of technetium-99 were predicted to be significantly below the screening level.

A.2.8.3.3 Inactive Flyash Pile/South Field

The Operable Unit 2 SWIFT III model and parameters were calibrated for uranium-238. Uranium-238 was selected for calibration because of its high detection frequency, very sensitive analytic procedure, because it was expected to be the main parameter of concern for risk assessment, and because hot spots for it were identified and modeled. Use of uranium at the site began in the 1950's. Current uranium-238 concentrations in the Great Miami Aquifer in the vicinity of the South Field area

5659

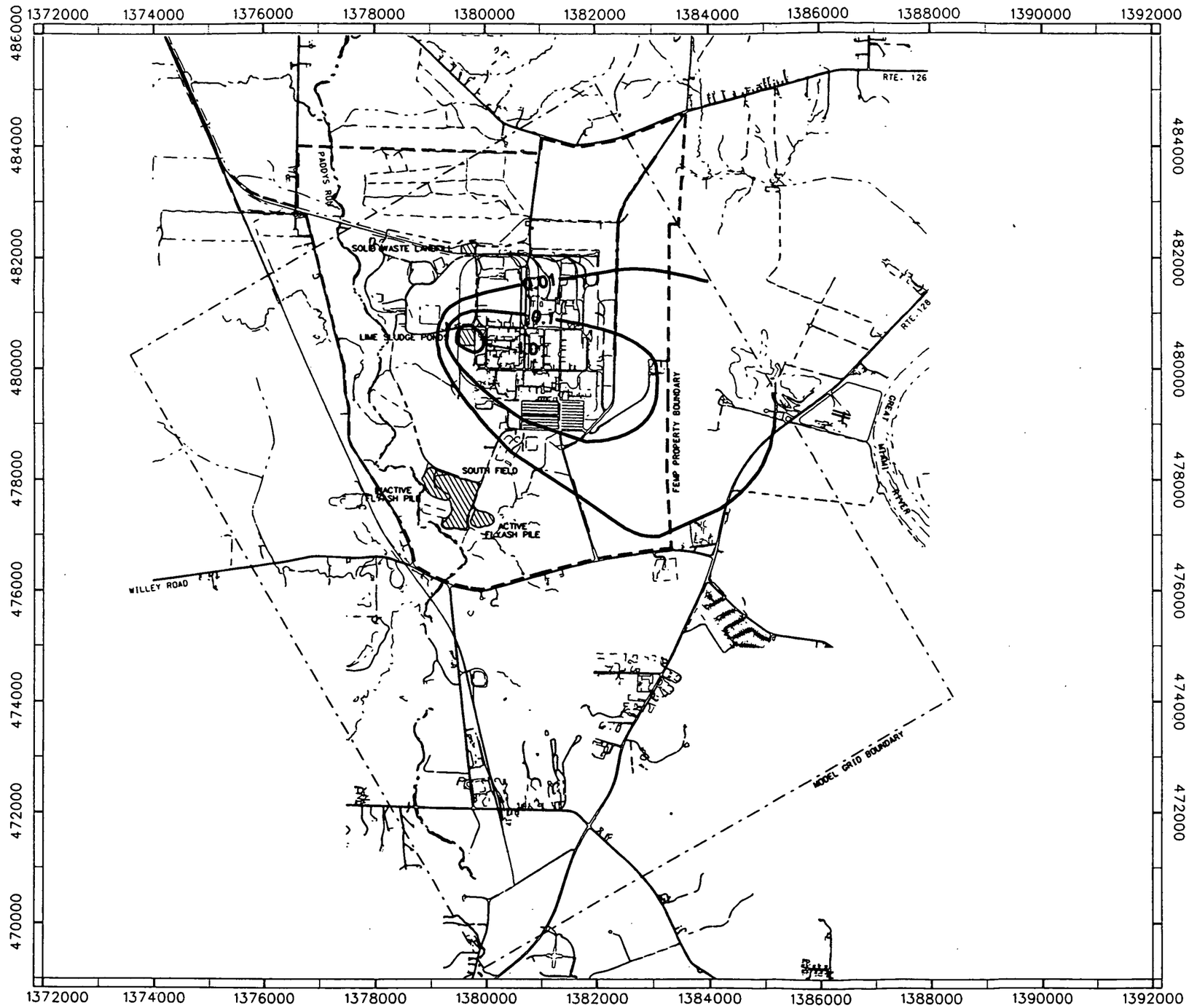

MAXIMUM INCREASE IN CONCENTRATION = 2.51 pCi/L

figa0219.dgn

LEGEND

- ROADS
- STREAM
- WASTE AREA
- RAILROAD
- FEMP PROPERTY BOUNDARY
- MODEL GRID BOUNDARY
- BEDROCK BOUNDARY
- 10 — TECHNETIUM-99 CONCENTRATION CONTOUR (pCi/L)

NOTE:
Coordinates are in State Planar NAD 1927.
Surface contours based on 1992 flyover.
Other source loadings and background concentrations not included.

N

SCALE (FT)
0 2000 4000

FIGURE A.2-18
PROJECTED INCREASE IN TECHNETIUM-99 CONCENTRATION IN GREAT MIAMI AQUIFER AT 40 YEARS DUE TO LOADING FROM THE LIME SLUDGE PONDS

000222

TABLE A.2-50

SUMMARY OF SWIFT MODELING RESULTS FOR THE LIME SLUDGE PONDS OPERABLE UNIT 2 REMEDIAL INVESTIGATION FERNALD ENVIRONMENTAL MANAGEMENT PROJECT

Constituents of Potential Concern	Maximum Loading Concentration from ODAST (pCi/L)	Minimum Time of Arrival to the Aquifer (years)	Time of Maximum On-Site Concentration (years)	Maximum On-Site Concentration in the Aquifer (pCi/L)	Time of Maximum Concentration at the FEMP Boundary (years)	Maximum Concentration at the FEMP Boundary (pCi/L)	EPA RAGs, Part B Screening Levels (pCi/L)
RADIONUCLIDES							
Technetium-99	76.4	20-30	40	2.96	40	0.17	3.65

Other Comment #A-48

was detected as high as 384 pCi/L at well 2945 in the validated filtered samples and on-site (non-validated) analysis indicated that the total uranium concentration is as high as 2100 μg/L (equivalent to 587 pCi/L of uranium-238). Figure A.2-19A shows present day concentrations at calibration targets and flow direction for the fate and transport model calibration.

NO. A-9

SWIFT III was first run using a K_d of 8.4 ml/g for uranium (Uranium Partition Coefficient Evaluation Study for Operable Unit 2, 1993) in the Great Miami Aquifer. SWIFT III model results indicated that it will take more than 200 years to reach current concentrations levels in the Great Miami Aquifer. Since uranium break through for k_d of 8.4 ml/g does not occur until after 16 years, calibration cannot be done by increasing waste concentration alone. Through calibration process, the K_d value in the Great Miami Aquifer (and ODAST) was reduced to 1.48 ml/g. At 40 years from placement of waste in the South Field area subunits (approximately current conditions), model predicted uranium-238 concentrations in the Great Miami Aquifer to be 134 pCi/L (Figure A.2-19B) in the grid cell containing the Well 2945. This is considered a good calibration of the model given the limitations that source areas smaller than 125-by-125 feet cannot be assigned. The uranium break through close to the Well 2945 is due to subsurface seeps. Although subsurface seeps do not travel laterally, 125 feet on the unsaturated Great Miami Aquifer, model limitations required that subsurface seep mass be loaded uniformally over the full 125-by-125 foot cell. If subsurface seeps infiltrate through a 20 to 50-foot wide area, this can easily result in underestimation of concentrations near subsurface seeps at 40 years by a factor of 3 to 6. Since the overall maximum loading is due to vadose zone pathway (Figure A.2-20), which is uniformly distributed over the full grid cell, the maximum predicted uranium-238 concentrations for the baseline risk assessment are not very sensitive to the above mentioned limitations of the model. Note that predicted uranium-238 shape (Figure A.2-19B) is consistent with the field observations.

NO. A-9

NO. A-9

Figure A.2-20 shows the loading of uranium-238 to Great Miami Aquifer from the Inactive Flyash Pile and the South Field. Figure A.2-20 shows that uranium-238 reaches the Great Miami Aquifer very early and loading increases very slowly up to 100 years (main contribution from perched water subsurface seeps), and then rises sharply and reaches a peak at 160 years (due to breakthrough from the vadose zone pathway). Uranium-238 loading then decreases exponentially. Figure A.2-20 shows uranium-238 concentration at the interface of vadose zone layer 2 (unsaturated Great Miami Aquifer) and saturated Great Miami Aquifer from the vadose zone pathway in grid block (29, 65). It does not

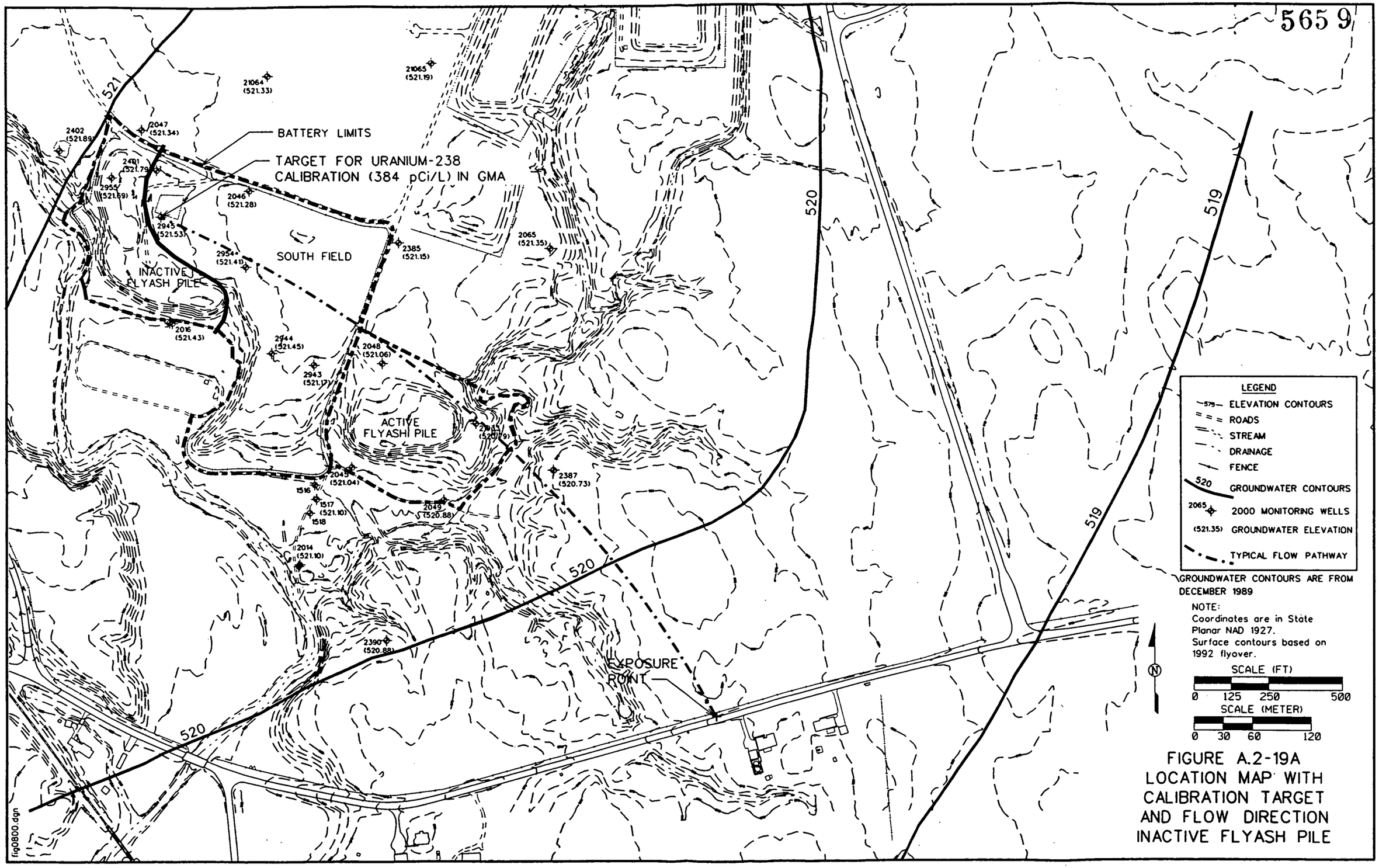

FIGURE A.2-19A
LOCATION MAP WITH CALIBRATION TARGET AND FLOW DIRECTION INACTIVE FLYASH PILE

5659

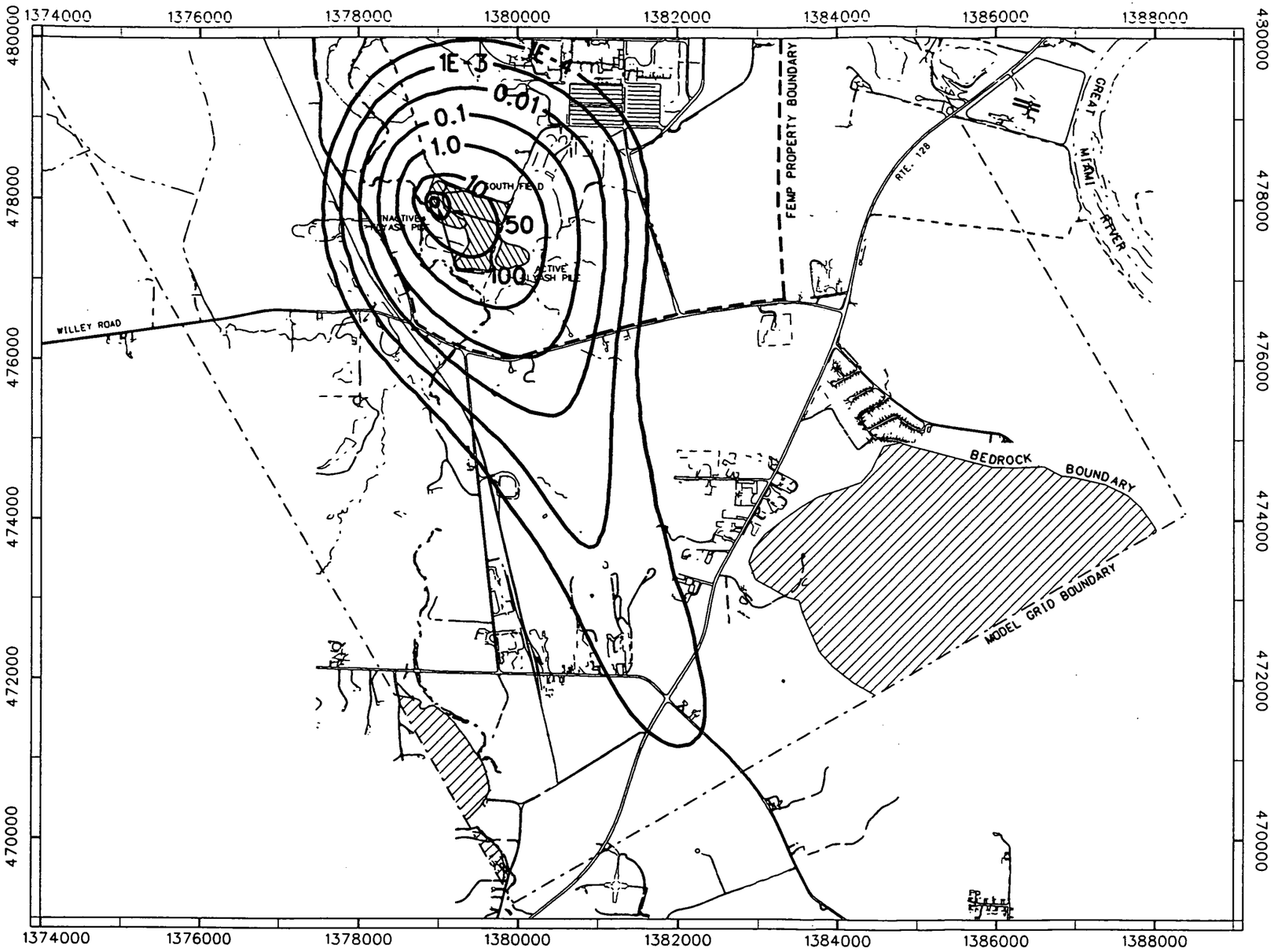

LEGEND

- ROADS
- STREAM
- WASTE AREA
- RAILROAD
- FEMP PROPERTY BOUNDARY
- MODEL GRID BOUNDARY
- BEDROCK BOUNDARY
- URANIUM-238 CONCENTRATION CONTOUR (pCi/L)

NOTE:
Coordinates are in State Planar NAD 1927.
Surface contours based on 1992 flyover.
Other source loadings and background concentration not included.

N

SCALE (FT)
0 1500 3000

MAXIMUM INCREASE IN CONCENTRATION = 134 pCi/L

figa0221.dgn

FIGURE A.2-19B
PROJECTED INCREASE IN URANIUM-238 CONCENTRATION IN GREAT MIAMI AQUIFER AT 40 YEARS DUE TO LOADING FROM THE INACTIVE FLYASH PILE AND SOUTH FIELD

000226

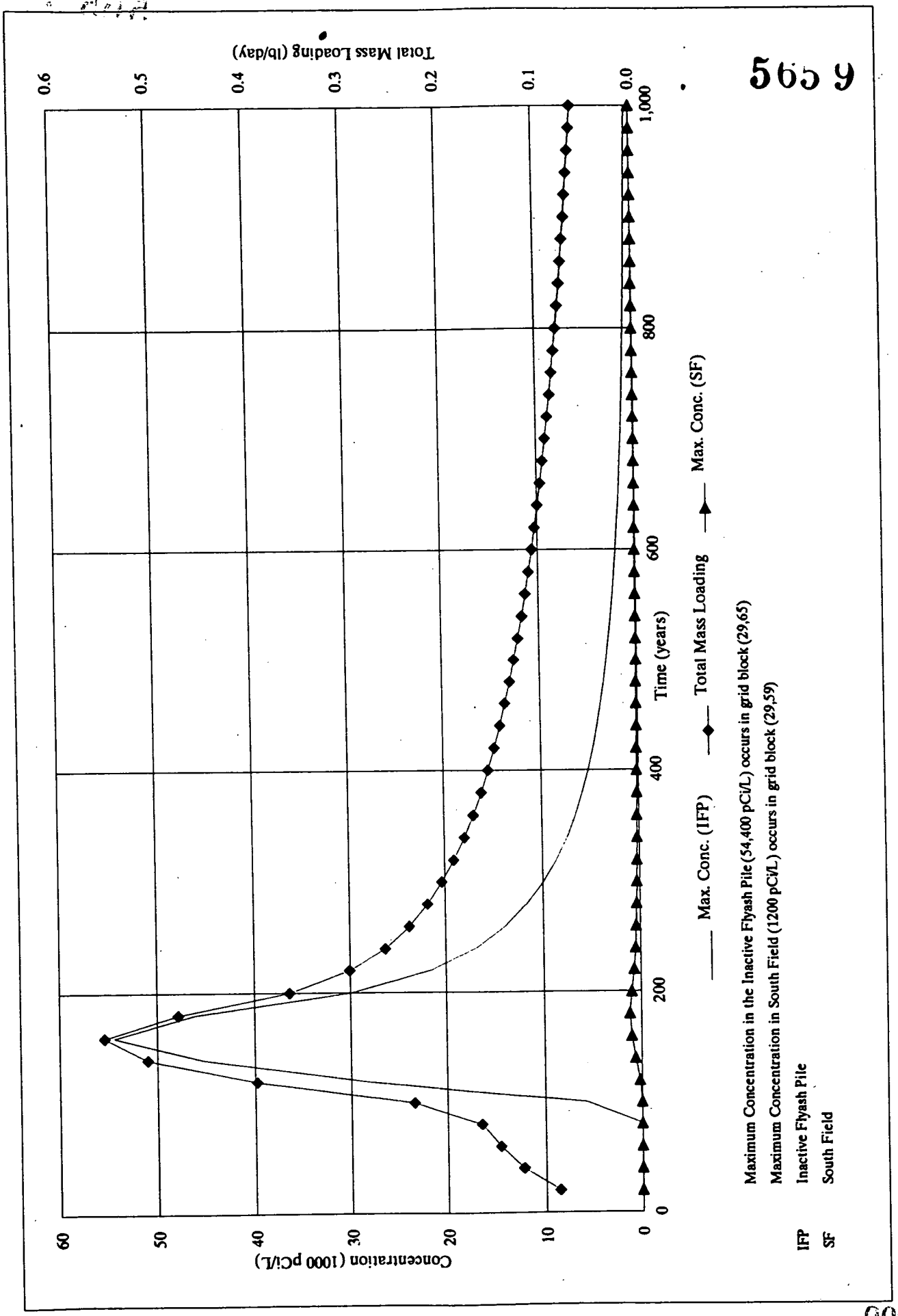

FIGURE A.2-20. URANIUM-238 LOADING TO THE GREAT MIAMI AQUIFER FROM THE INACTIVE FLYASH PILE AND SOUTH FIELD

show the concentration vs. time history of perched water subsurface seep in the same grid block, which has early arrival time but lower peak concentration value.

Figures A.2-21, A.2-22, and A.2-23 show the projected increase in uranium-238 concentrations due to the Inactive Flyash Pile and South Field at 160, 220, and 1,000 years, respectively. The maximum on-site uranium-238 concentration was predicted to occur at 160 years, while maximum off-site concentration was predicted to occur at 220 years.

The groundwater fate and transport modeling results are summarized in Table A.2-51 for the CPCs that will reach the Great Miami Aquifer within 1000 years from the South Field and Inactive Flyash Pile subunits. The table also presents the arrival time for the constituents to reach the aquifer, the maximum loading concentration, the maximum concentrations of the CPC that would be expected in the aquifer within 1000 years and the time required for the constituents to reach the maximum value. It also presents the predicted maximum concentration at the FEMP boundary due to loading from the Inactive Flyash Pile and the South Field. Screening levels are also presented to provide a basis for understanding the risk to human health from the ingestion of water from the Great Miami Aquifer. The uranium-238 concentration is most elevated compared to the screening concentration and may control the overall risk from groundwater pathway (see Section 6 and Appendix B). Table A.2-52 presents the on-site and off-site concentrations of other CPCs at uranium-238 maximum concentration location and time.

As noted earlier, total uranium, uranium-234, and uranium-235/236 concentrations were estimated from the results of uranium-238 modeling. Figures A.2-24 through A.2-26 show the site-specific relationship between uranium-234 and uranium-238 activity at the Inactive Flyash Pile/South Field/Active Flyash Pile, uranium-235/236 and uranium-238 activity at the Inactive Flyash Pile/South Field/Active Flyash Pile, and uranium-238 and total uranium mass at the Inactive Flyash Pile/South Field, respectively. The following relationships were observed between various uranium forms:

Uranium-234 = 0.91 (Uranium-238)	activity ratio
Uranium-235/236 = 0.048 (Uranium-238)	activity ratio
Uranium-238 = 0.832 (Uranium-total)	mass ratio at Inactive Flyash Pile/South Field only

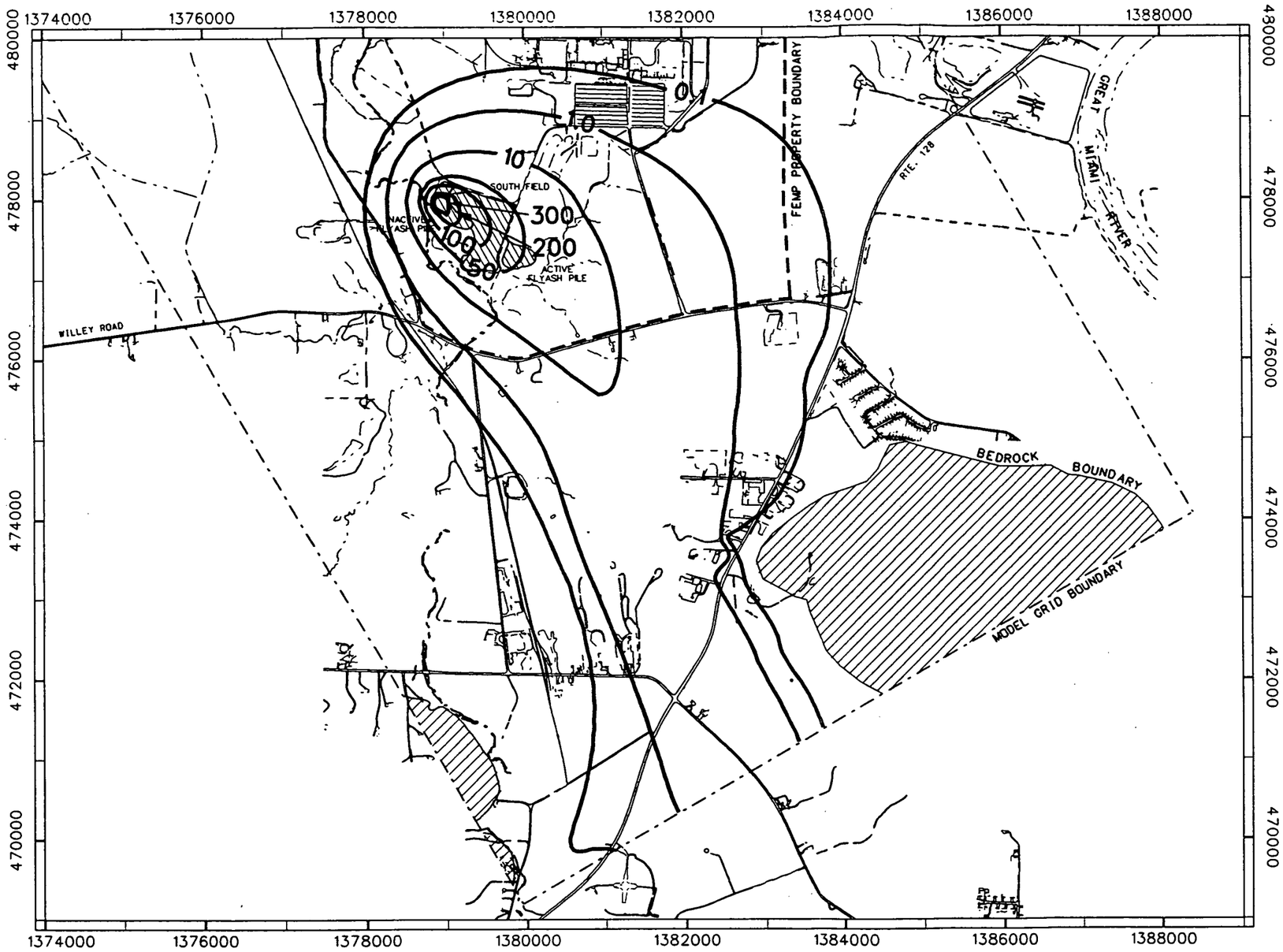

LEGEND

- ROADS
- STREAM
- WASTE AREA
- RAILROAD
- FEMP PROPERTY BOUNDARY
- MODEL GRID BOUNDARY
- BEDROCK BOUNDARY
- URANIUM-238 CONCENTRATION CONTOUR (pCi/L)

NOTE:
Coordinates are in State Planar NAD 1927.
Surface contours based on 1992 flyover.
Other source loadings and background concentration not included.

N

SCALE (FT)
0 1500 3000

MAXIMUM INCREASE IN CONCENTRATION = 517 pCi/L

FIGURE A.2-21
PROJECTED INCREASE IN URANIUM-238 CONCENTRATION IN GREAT MIAMI AQUIFER AT 160 YEARS DUE TO LOADING FROM THE INACTIVE FLYASH PILE AND SOUTH FIELD

figa0223.dgn

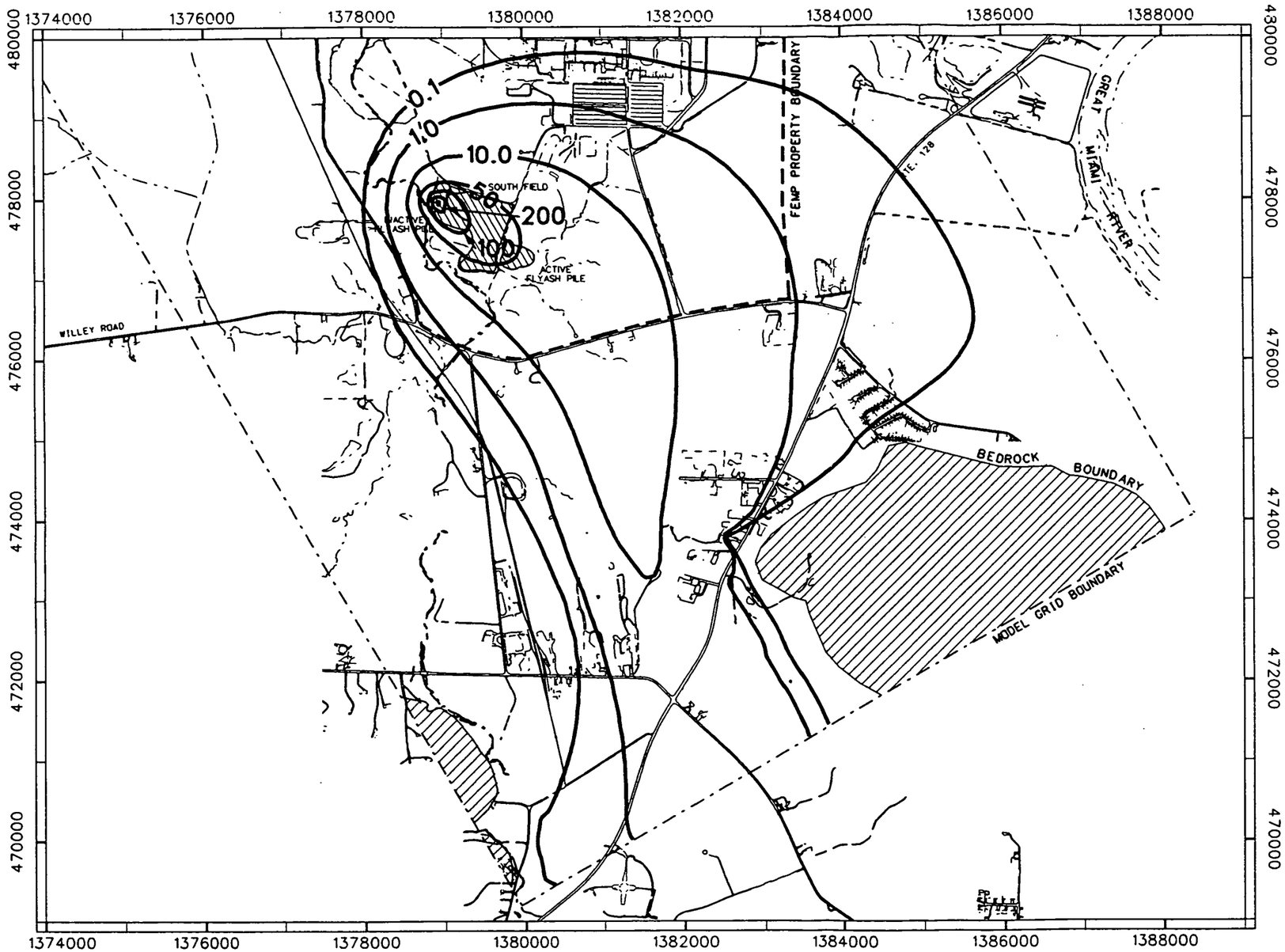

LEGEND

- ROADS
- STREAM
- WASTE AREA
- RAILROAD
- FEMP PROPERTY BOUNDARY
- MODEL GRID BOUNDARY
- BEDROCK BOUNDARY
- 10 URANIUM-238 CONCENTRATION CONTOUR (pCi/L)

NOTE:
Coordinates are in State Planar NAD 1927.
Surface contours based on 1992 flyover.
Other source loadings and background concentration not included.

N

SCALE (FT)
0 1500 3000

MAXIMUM INCREASE IN CONCENTRATION = 326 pCi/L

FIGURE A.2-22
PROJECTED INCREASE IN URANIUM-238 CONCENTRATION IN GREAT MIAMI AQUIFER AT 220 YEARS DUE TO LOADING FROM THE INACTIVE FLYASH PILE AND SOUTH FIELD

figa0224.dgn

565 9

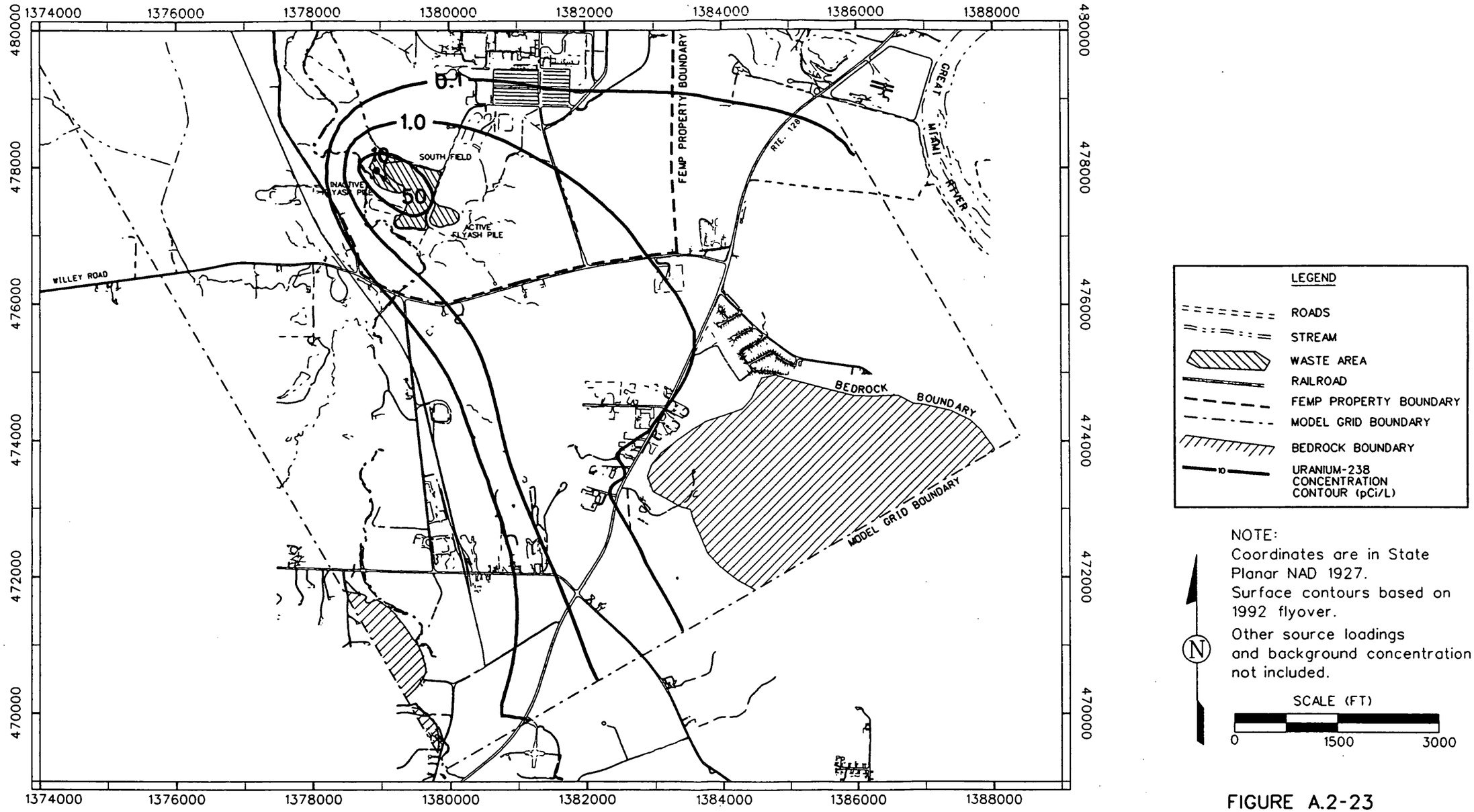

MAXIMUM INCREASE IN CONCENTRATION = 57.4 pCi/L

FIGURE A.2-23
PROJECTED INCREASE IN URANIUM-238 CONCENTRATION IN GREAT MIAMI AQUIFER AT 1000 YEARS DUE TO LOADING FROM THE INACTIVE FLYASH PILE AND SOUTH FIELD

figa0225.dgn

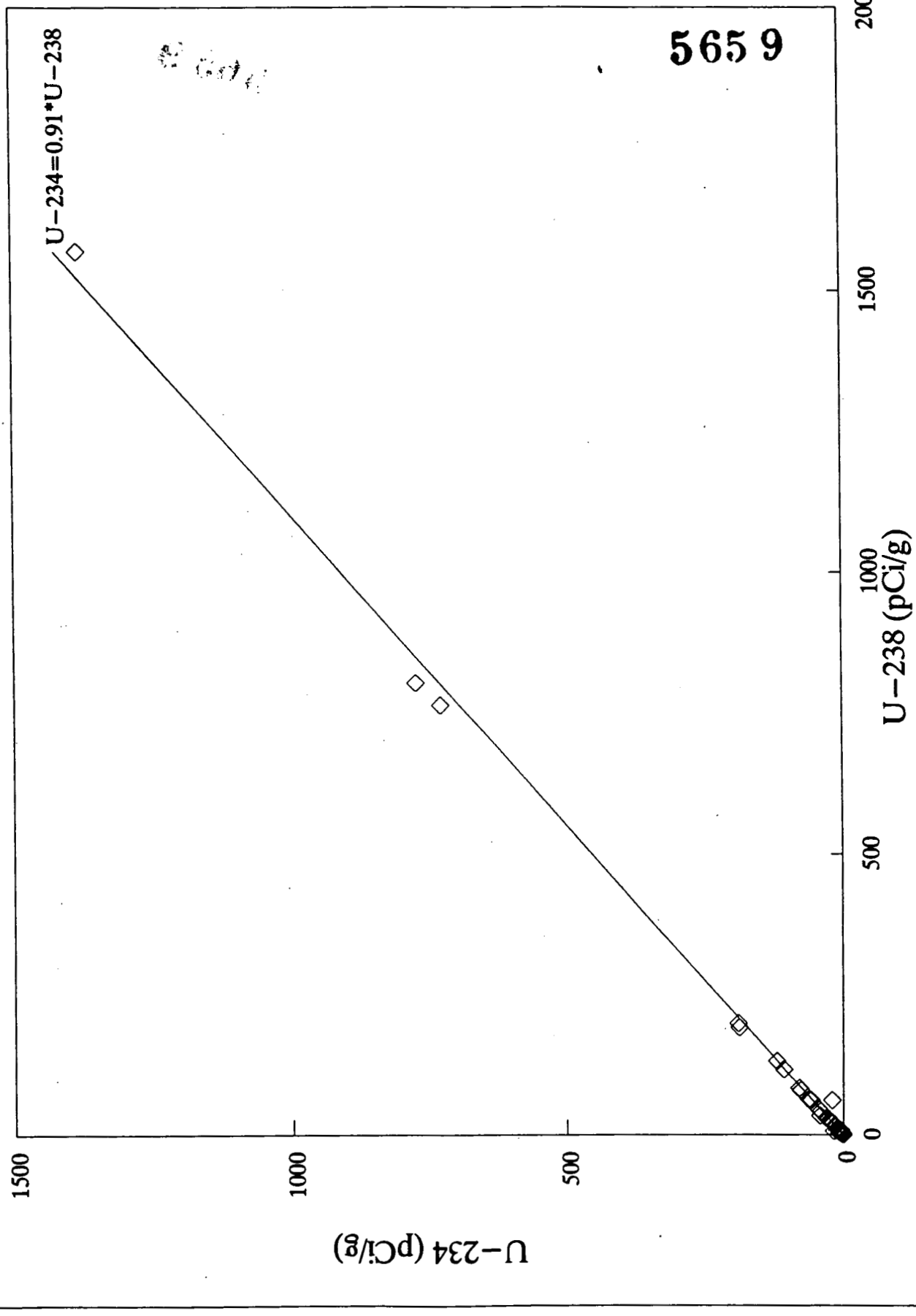

FIGURE A.2-24 : U-234 vs. U-238 IN SOIL SAMPLES, SOUTH FIELD & FLYASH PILES

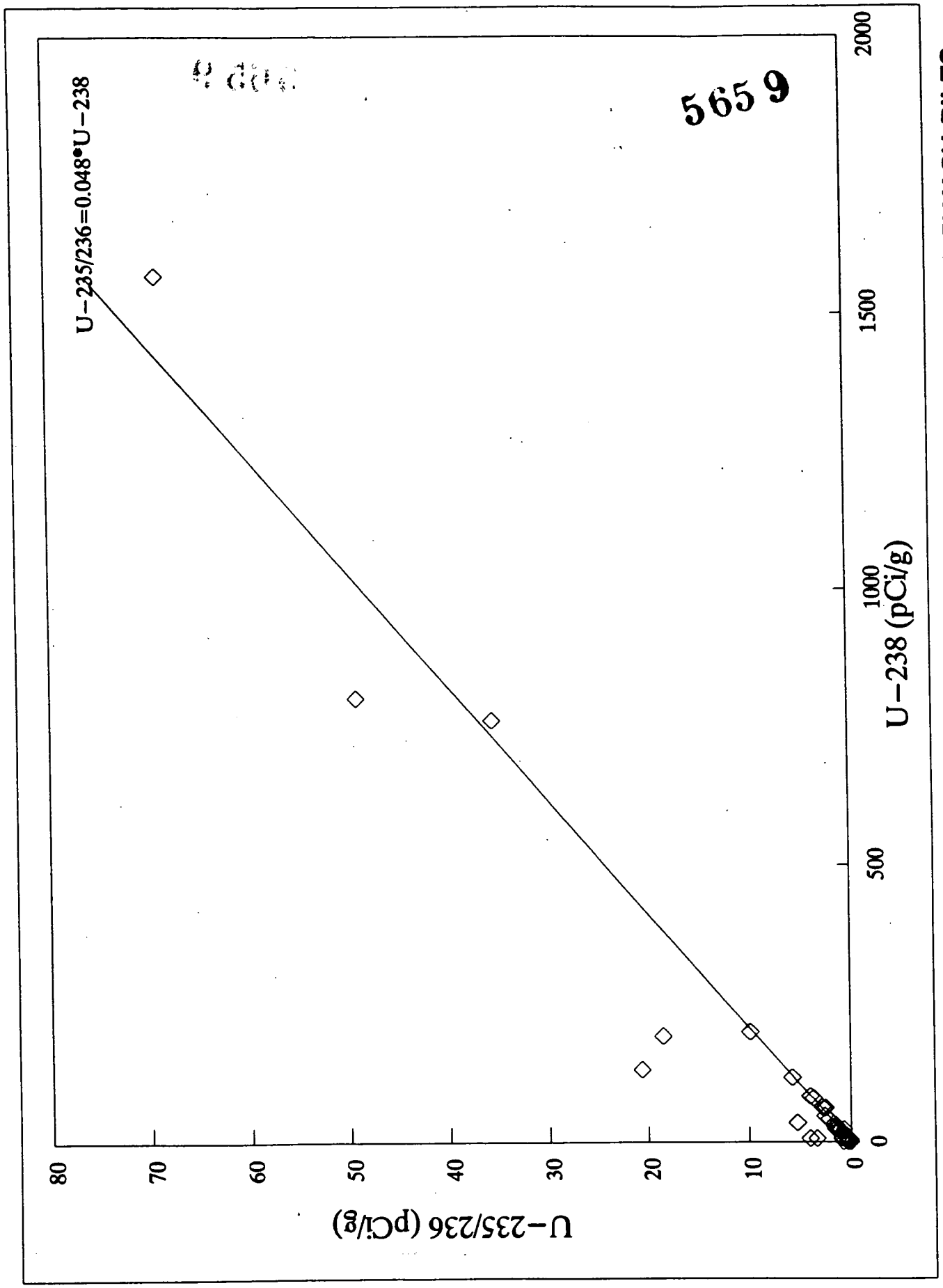

FIGURE A.2-25 : U-235/236 vs. U-238 IN SOIL SAMPLES, SOUTH FIELD & FLYASH PILES

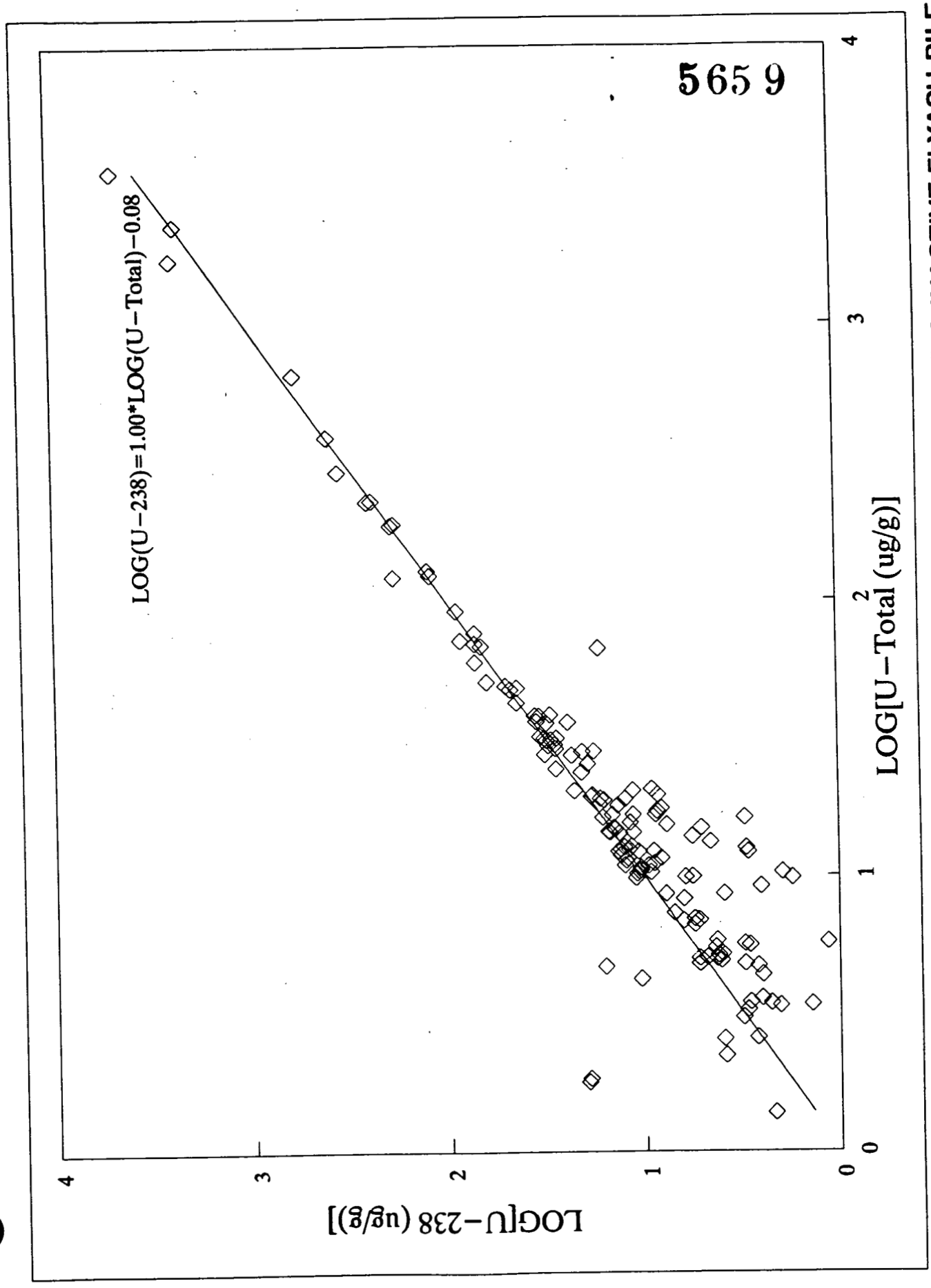

FIGURE A.2−26: U−238 vs. U−TOTAL IN SOIL SAMPLES, SOUTH FIELD & INACTIVE FLYASH PILE

TABLE A.2-51

SUMMARY OF SWIFT MODELING RESULTS FOR THE INACTIVE FLYASH PILE AND SOUTH FIELD OPERABLE UNIT 2 REMEDIAL INVESTIGATION FERNALD ENVIRONMENTAL MANAGEMENT PROJECT

Constituents of Potential Concern	Maximum Loading Concentration from ODAST (pCi/L RAD) (μg/L non-RAD)	Minimum Time of Arrival to the Aquifer (years)	Time of Maximum On-Site Concentration (years)	Maximum On-Site Concentration in the Aquifer (pCi/L RAD) (μg/L non-RAD)	Time of Maximum Concentration at the FEMP Boundary (years)	Maximum Concentration at the FEMP Boundary (pCi/L RAD) (μg/L non-RAD)	EPA RAGs, Part B Screening Levels (pCi/L RAD) (μg/L non-RAD)
RADIONUCLIDES							
Neptunium-237	$1.06 \times 10^{+2}$	40	360	9.33×10^{-1}	540	8.59×10^{-2}	2.16×10^{-2}
Radium-226	1.58×10^{-1}	760	1,000	8.90×10^{-3}	1,000	1.13×10^{-9}	1.76×10^{-4}
Strontium-90	$1.53 \times 10^{+4}$	60	140	2.07×10^{-1}	200	4.48×10^{-3}	1.32×10^{-1}
Technetium-99	$7.72 \times 10^{+2}$	0	40	$1.03 \times 10^{+1}$	40	2.86×10^{0}	$3.65 \times 10^{+0}$
Uranium-234[a]	-[a, b]	0	160	$4.69 \times 10^{+2}$	220	$2.40 \times 10^{+1}$	2.97×10^{-1}
Uranium-235/236[a]	-[a, b]	0	160	$2.50 \times 10^{+1}$	220	1.28×10^{0}	2.97×10^{-1}
Uranium-238	$5.44 \times 10^{+5}$	0	160	$5.17 \times 10^{+2}$	220	$2.65 \times 10^{+1}$	1.70×10^{-1}
Uranium Total - (non-RAD)[a]	-[a, b]	0	160	$1.84 \times 10^{+3}$	220	$9.45 \times 10^{+1}$	$1.09 \times 10^{+1}$
ORGANICS							
2-Methylnaphthalene[c]	$1.98 \times 10^{+4}$	40	360	1.74×10^{-1}	540	1.61×10^{-2}	NA[d]
Benzo(a)anthracene	-[e]	0	1000	3.84×10^{-3}	-[e]	-[e]	2.82×10^{-3}
Benzo(a)pyrene	-[f]	0	1000	2.75×10^{-3}	-[f]	-[f]	2.82×10^{-4}
Benzo(g,h,i)perylene	-[g]	0	1000	1.32×10^{-2}	-[g]	-[g]	NA
Dibenzo(a,h)anthracene	-[e]	0	1000	6.66×10^{-4}	-[e]	-[e]	2.82×10^{-4}
Dieldrin	-[f]	0	1000	8.47×10^{-4}	-[f]	-[f]	1.12×10^{-4}
Phenanthrene	-[g]	0	1000	$4.10 \times 10^{+0}$	-[g]	-[g]	NA
Tributyl phosphate[b]	$3.95 \times 10^{+4}$	60	660	4.01×10^{-1}	1000	3.72×10^{-2}	NA

TABLE A.2-51
(Continued)

Constituents of Potential Concern	Maximum Loading Concentration from ODAST (pCi/L RAD) (μg/L non-RAD)	Minimum Time of Arrival to the Aquifer (years)	Time of Maximum On-Site Concentration (years)	Maximum On-Site Concentration in the Aquifer (pCi/L RAD) (μg/L non-RAD)	Time of Maximum Concentration at the FEMP Boundary (years)	Maximum Concentration at the FEMP Boundary (pCi/L RAD) (μg/L non-RAD)	EPA RAGs, Part B Screening Levels (pCi/L RAD) (μg/L non-RAD)
				INORGANICS			
Arsenic[j]	1.29×10^{-5} [i]	0	1000	3.35×10^{-4}	1,000	8.56×10^{-5}	1.46×10^{-4}
Lead	$5.61 \times 10^{+1}$	200	1,000	4.86×10^{0}	1,000	5.94×10^{-3}	NA[d]
Beryllium[j]	-[i]	0	1000	2.61×10^{-5}	1000	6.73×10^{-6}	2.37×10^{-4}

[a]Results for uranium-234, uranium-235/236, and total uranium were established by using appropriate scaling ratios to uranium-238 results.
[b]ODAST results were not used for SWIFT III modeling and therefore not shown in this table.
[c]Results for 2-Methylnaphathalene were estimated based on the results for Neptunium-237.
[d]NA=No data available to calculate EPA RAGs, Part B screening value.
[e]Benzo(a)anthracene and dibenzo(a,h)anthracene were not modeled using SWIFT III because the concentrations in the Great Miami Aquifer fall below the EPA RAGs, Part B screening concentrations after mixing in the SWIFT III grid cell. The maximum predicted concentration based on 30-ft. wide Paddys Run are reported as the maximum on-site concentration.
[f]The predicted maximum concentration after mixing in the full SWIFT III grid cell is marginally above the EPA RAGs, Part B screening concentration. Therefore, SWIFT III modeling was not performed and the maximum predicted concentration based on 30 feet wide Paddys Run is reported as the maximum on-site concentration.
[g]Benzo(g,h,i)perylene and phenanthrene were not modeled using SWIFT III because EPA RAGs, Part B screening concentrations could not be calculated. Maximum predicted concentration based on 30 feet wide Paddys Run are reported as the maximum on-site concentration.
[h]Results for tributyl phosphate are estimated based on results for CPCs with similar adsorption properties.
[i]The main contribution to the Great Miami Aquifer is from the surface water runoff pathway.
[j]The results are scaled from the SWIFT III modeling results for the Active Flyash Pile because of no impact on overall risk, and the main pathway to the Great Miami Aquifer is the surface water runoff pathway.

Comment No. A-48

5659

TABLE A.2-52

SUMMARY OF SWIFT MODELING RESULTS AT THE TIME AND LOCATION OF THE U-238 MAXIMUM CONCENTRATION FOR THE INACTIVE FLYASH PILE AND SOUTH FIELD OPERABLE UNIT 2 REMEDIAL INVESTIGATION FERNALD ENVIRONMENTAL MANAGEMENT PROJECT

Constituents of Potential Concern	On-Site Concentration at 160 Years (pCi/L RAD) (μg/L non-RAD)	Concentration at the FEMP Boundary at 220 Years (pCi/L RAD) (μg/L non-RAD)	EPA RAGs, Part B Screening Levels (pCi/L RAD) (μg/L non-RAD)
RADIONUCLIDES			
Neptunium-237	1.90×10^{-2}	2.81×10^{-4}	2.16×10^{-2}
Radium-226	0.0	0.0	1.76×10^{-4}
Strontium-90	2.72×10^{-2}	2.26×10^{-3}	1.32×10^{-1}
Technetium-99	1.82×10^{0}	9.81×10^{-1}	$3.65 \times 10^{+0}$
Uranium-234[a]	$4.69 \times 10^{+2}$	$2.40 \times 10^{+1}$	2.97×10^{-1}
Uranium-235/236[a]	$2.50 \times 10^{+1}$	1.28×10^{0}	2.97×10^{-1}
Uranium-238	$5.17 \times 10^{+2}$	$2.65 \times 10^{+1}$	1.70×10^{-1}
Uranium - Total (non-RAD)[a]	$1.84 \times 10^{+3}$	$9.45 \times 10^{+1}$	$1.09 \times 10^{+1}$
ORGANICS			
2-Methylnaphthalene	3.55×10^{-3}	5.25×10^{-5}	NA[b]
Benzo(g,h,i)perylene	0.0	0.0	NA
Phenanthrene	0.0	0.0	NA
Tributyl phosphate	1.67×10^{-1}	3.11×10^{-6}	NA
INORGANICS			
Arsenic	0.0	0.0	1.46×10^{-4}
Lead	$1.43 \times 10^{+0}$	2.05×10^{-14}	NA

[a]Uranium-234, uranium-235/236, and total uranium were modeled by applying ratios to uranium-238 results.
[b]NA = Note data available to calculate EPA RAGs, Part B screening value.
Comment No. A-48

NO. A-48

The uranium-238 vs. total uranium relationship was used a limited number of times when total uranium analysis was available for a soil but uranium-238 analysis was not available. The total uranium analysis is not as accurate as the isotope analysis. Therefore, while converting modeled uranium-238 results to total uranium results, total uranium concentration was calculated by adding all uranium isotope concentrations. This is equivalent to assuming 99.25 percent of total uranium consists of uranium-238. This is consistent with naturally occurring uranium distribution. Although these relationships were developed from soil samples, these relationships should apply to uranium concentrations in the groundwater because all uranium isotopes have very long half-lives (greater than 10,000 years) and have similar adsorption properties. These relationships can be used to estimate uranium-234, uranium-235/256, and total uranium concentrations.

The constituents projected to be above the screening levels when they reach the Great Miami Aquifer directly beneath the Inactive Flyash Pile and South Field area were the uranium isotopes (uranium-234, uranium-235/236 and uranium-238), total uranium, neptunium-237, radium-226, strontium-90, technetium-99, antimony, cadmium, lead, manganese, and molybdenum. Only uranium isotopes (uranium-234, uranium-235/236 and uranium-238), total uranium, neptunium-237, technetium-99, lead, and manganese were predicted to exceed screening levels in the Great Miami Aquifer. Of these CPCs, only uranium isotopes, total uranium, neptunium-237, and technetium-99 are projected to be above the screening level at the FEMP boundary. Loading and contour plots were made for these CPCs at different time periods and are presented in Figures A.2-27 through ~~A.2-42~~ A.2-39. As an example, Figure A.2-30 depicts a plume of neptunium-237 in groundwater moving towards the southeastern boundary of the FEMP. Contour plots show the projected increase in the concentrations of contaminants. Figure A.2-32 shows two contours for 6.1 x 10^{-3} pCi/L Neptunium-237 concentration. This is due to early breakthrough time from some SWIFT cells and late breakthrough time from other SWIFT cells (see Figure A.2-27). The downgradient 6.1 x 10^{-3} pCi/L contour is related to early breakthrough while 6.1 x 10^{-3} pCi/L contour in the South Field vicinity is due to late breakthrough.

NO. A-48

NO. A-54

A.2.8.3.4 Active Flyash Pile

The groundwater fate and transport modeling results are summarized in Table A.2-53 for CPCs that will reach the Great Miami Aquifer from the Active Flyash Pile above the ~~10^{-7} risk or 0.1 Hazard Index screening level~~ EPA RAGs, Part B screening concentrations in 1,000 years. The table also presents the arrival time for CPCs in the aquifer, the maximum loading concentration, the maximum

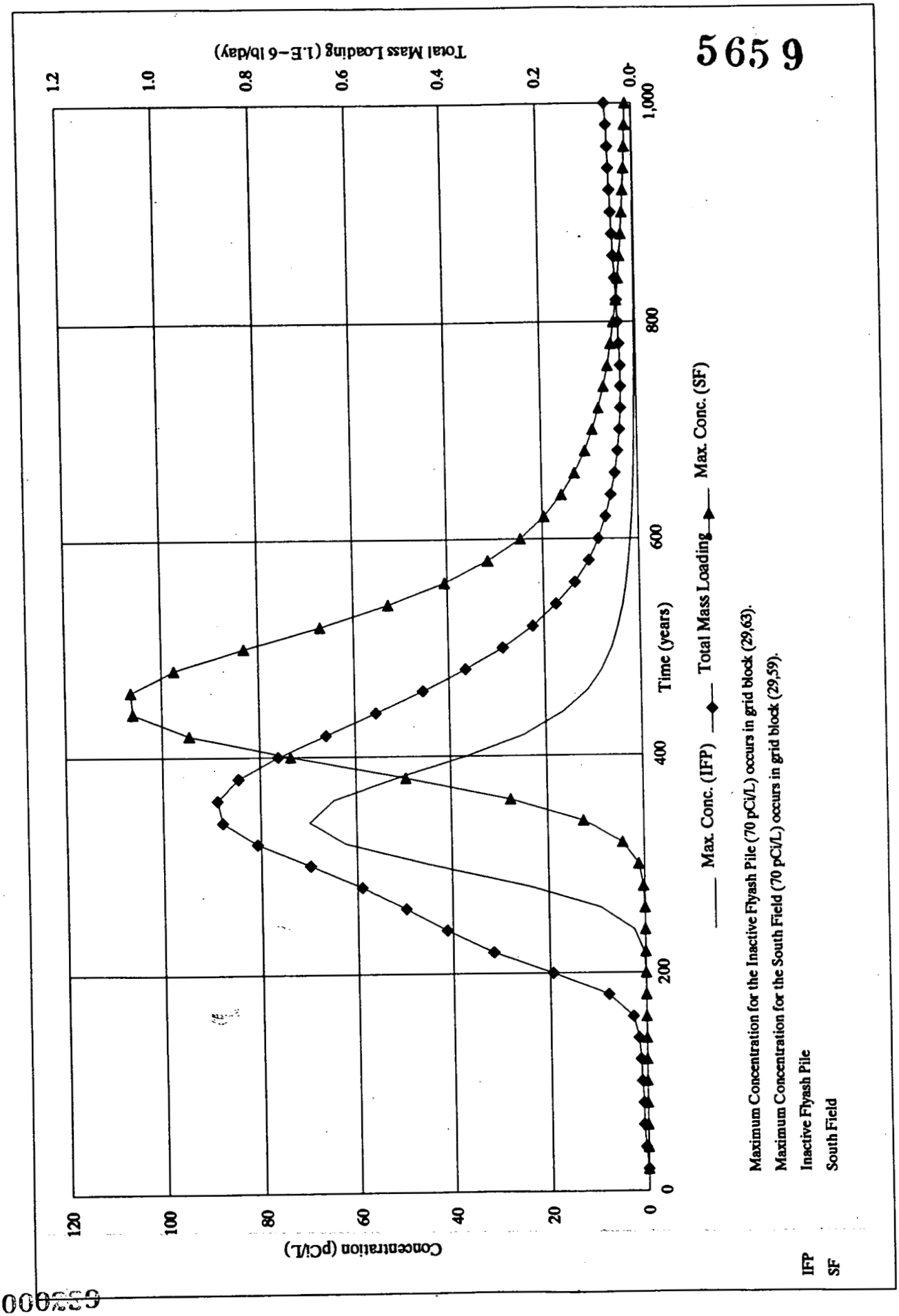

FIGURE A.2-27. NEPTUNIUM-237 LOADING TO THE GREAT MIAMI AQUIFER FOR THE INACTIVE FLYASH PILE AND SOUTH FIELD

5659

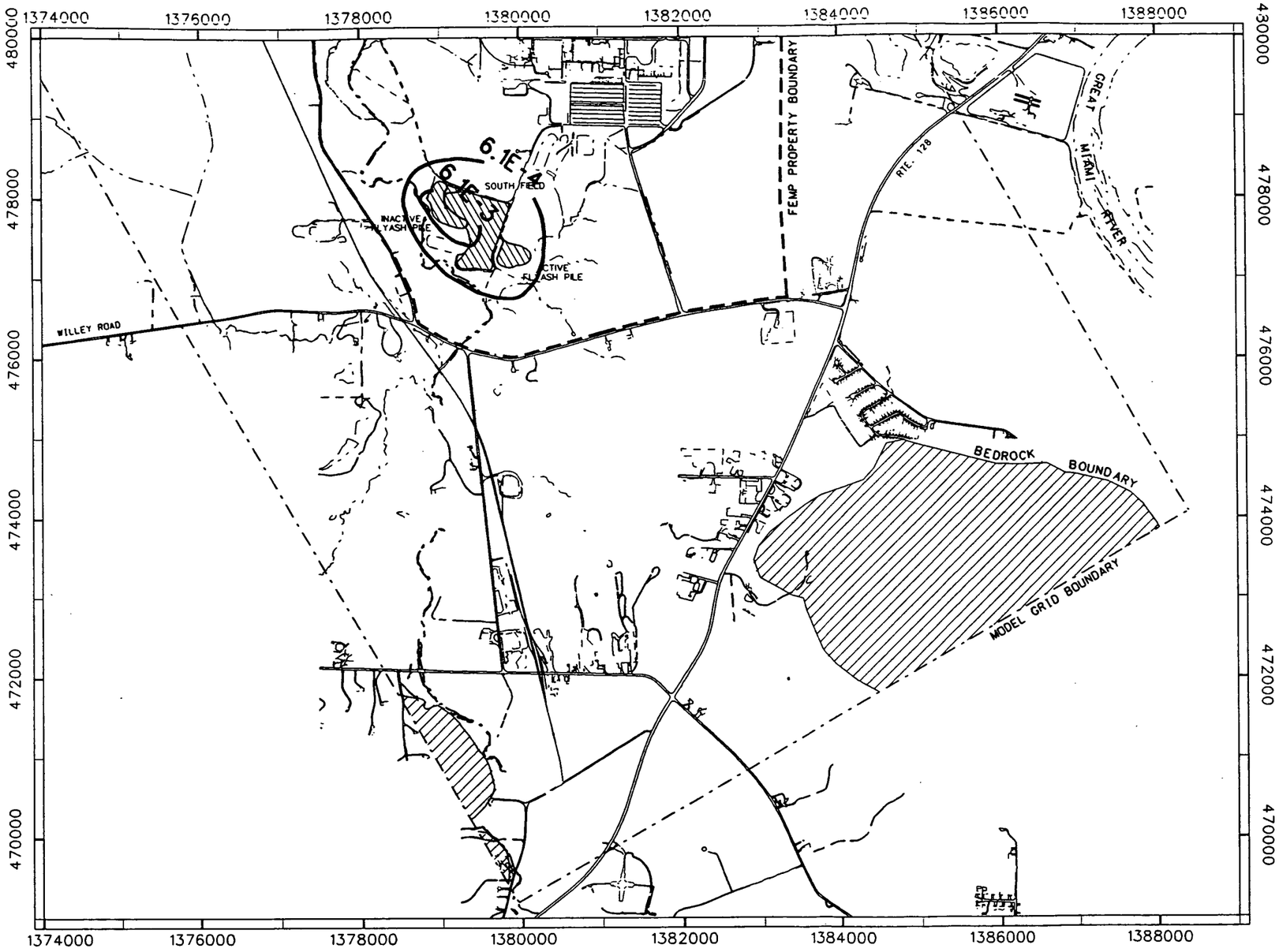

LEGEND

- ROADS
- STREAM
- WASTE AREA
- RAILROAD
- FEMP PROPERTY BOUNDARY
- MODEL GRID BOUNDARY
- BEDROCK BOUNDARY
- 10 — NEPTUNIUM-237 CONCENTRATION CONTOUR (pCi/L)

NOTE:
Coordinates are in State Planar NAD 1927.
Surface contours based on 1992 flyover.
Other source loadings and background concentration not included.

N

SCALE (FT)
0 1500 3000

MAXIMUM INCREASE IN CONCENTRATION = 0.019 pCi/L

FIGURE A.2-28
PROJECTED INCREASE IN NEPTUNIUM-237 CONCENTRATION IN GREAT MIAMI AQUIFER AT 160 YEARS DUE TO LOADING FROM THE INACTIVE FLYASH PILE AND SOUTH FIELD

figa0227.dgn

5659

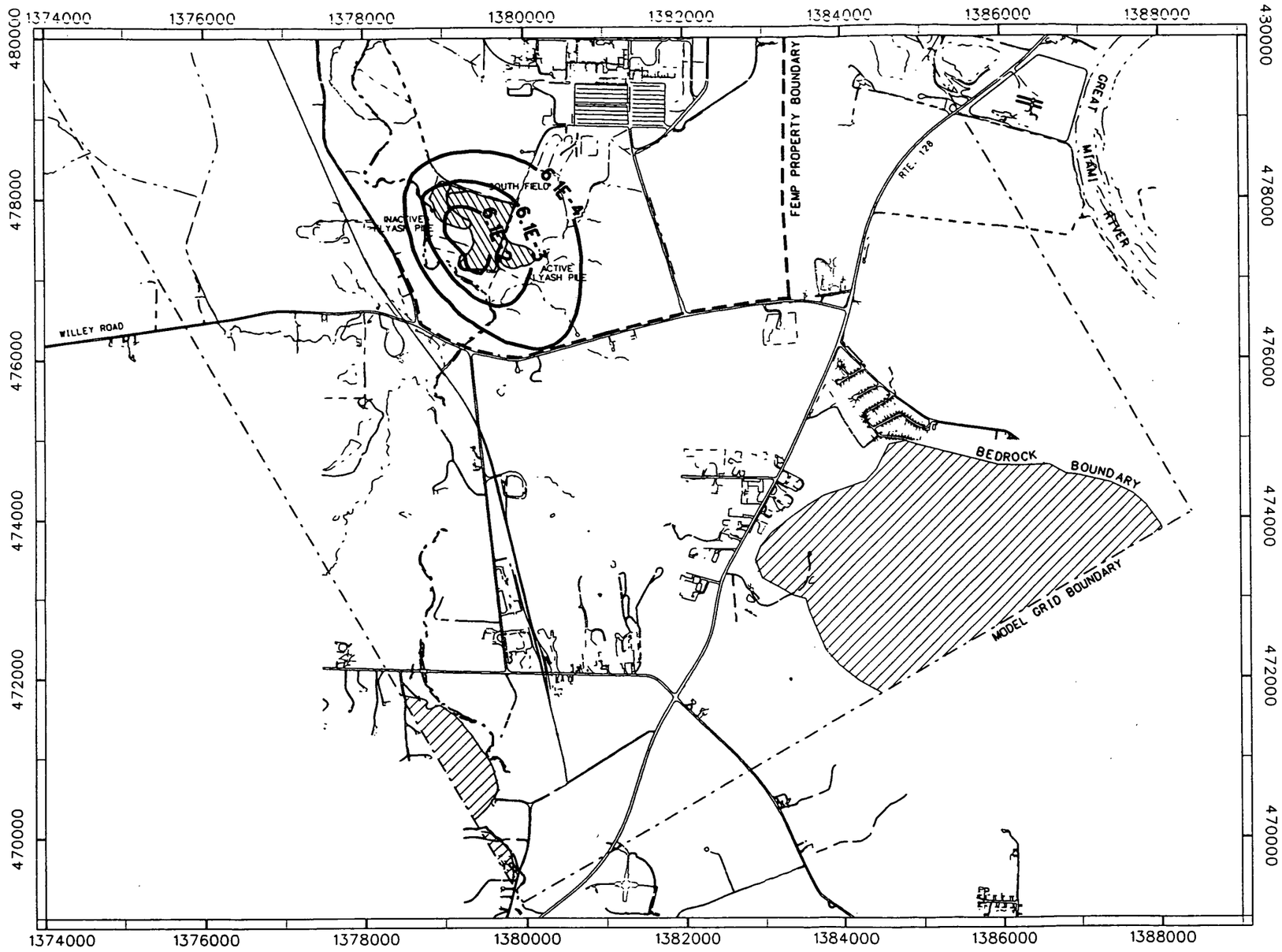

LEGEND

- ROADS
- STREAM
- WASTE AREA
- RAILROAD
- FEMP PROPERTY BOUNDARY
- MODEL GRID BOUNDARY
- BEDROCK BOUNDARY
- NEPTUNIUM-237 CONCENTRATION CONTOUR (pCi/L)

NOTE:
Coordinates are in State Planar NAD 1927.
Surface contours based on 1992 flyover.
Other source loadings and background concentration not included.

N

SCALE (FT)
0 1500 3000

MAXIMUM INCREASE IN CONCENTRATION = 0.36 pCi/L

FIGURE A.2-29
PROJECTED INCREASE IN NEPTUNIUM-237 CONCENTRATION IN GREAT MIAMI AQUIFER AT 220 YEARS DUE TO LOADING FROM THE INACTIVE FLYASH PILE AND SOUTH FIELD

figa0228.dgn

000241

5009

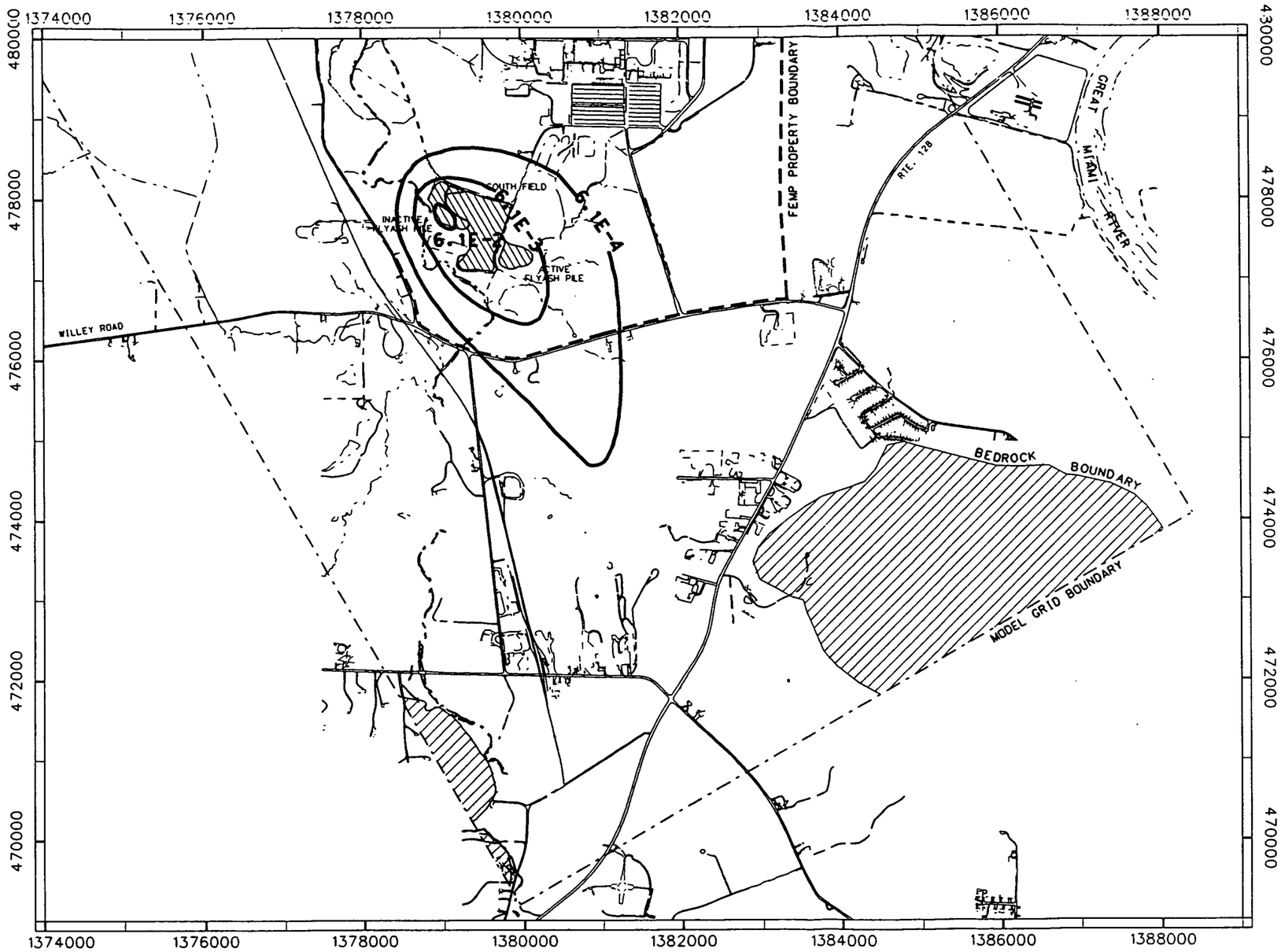

LEGEND

- ROADS
- STREAM
- WASTE AREA
- RAILROAD
- FEMP PROPERTY BOUNDARY
- MODEL GRID BOUNDARY
- BEDROCK BOUNDARY
- 10 — NEPTUNIUM-237 CONCENTRATION CONTOUR (pCi/L)

NOTE:
Coordinates are in State Planar NAD 1927.
Surface contours based on 1992 flyover.
Other source loadings and background concentration not included.

N

SCALE (FT)
0 1500 3000

MAXIMUM INCREASE IN CONCENTRATION = 0.92 pCi/L

figa0229.dgn

FIGURE A.2-30
PROJECTED INCREASE IN NEPTUNIUM-237 CONCENTRATION IN GREAT MIAMI AQUIFER AT 360 YEARS DUE TO LOADING FROM THE INACTIVE FLYASH PILE AND SOUTH FIELD

5659

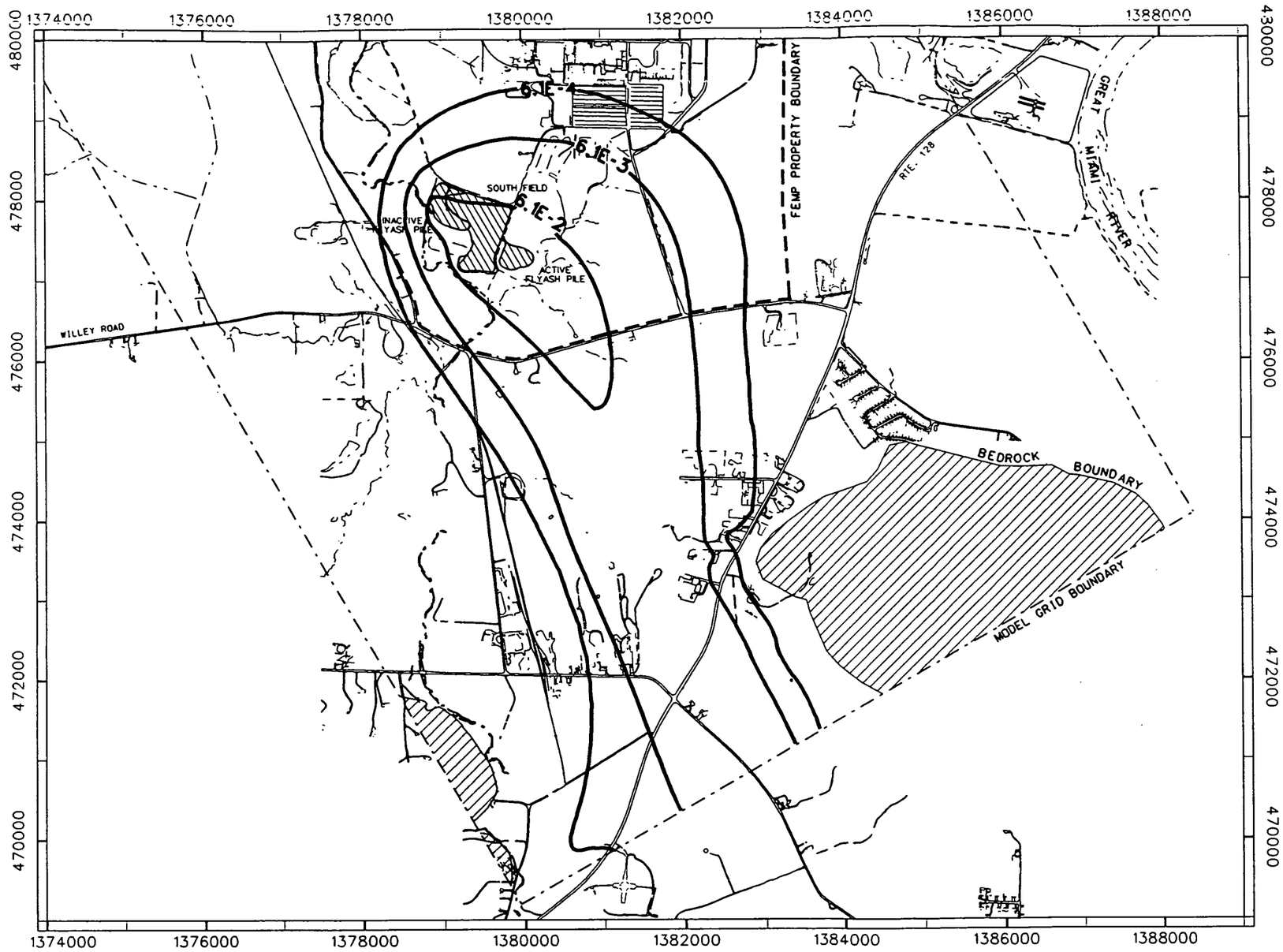

LEGEND

- ROADS
- STREAM
- WASTE AREA
- RAILROAD
- FEMP PROPERTY BOUNDARY
- MODEL GRID BOUNDARY
- BEDROCK BOUNDARY
- 10 — NEPTUNIUM-237 CONCENTRATION CONTOUR (pCi/L)

NOTE:
Coordinates are in State Planar NAD 1927.
Surface contours based on 1992 flyover.
Other source loadings and background concentration not included.

N

SCALE (FT)
0 1500 3000

MAXIMUM INCREASE IN CONCENTRATION = 0.35 pCi/L

FIGURE A.2-31
PROJECTED INCREASE IN NEPTUNIUM-237 CONCENTRATION IN GREAT MIAMI AQUIFER AT 540 YEARS DUE TO LOADING FROM THE INACTIVE FLYASH PILE AND SOUTH FIELD

figa0230.dgn

000243

5659

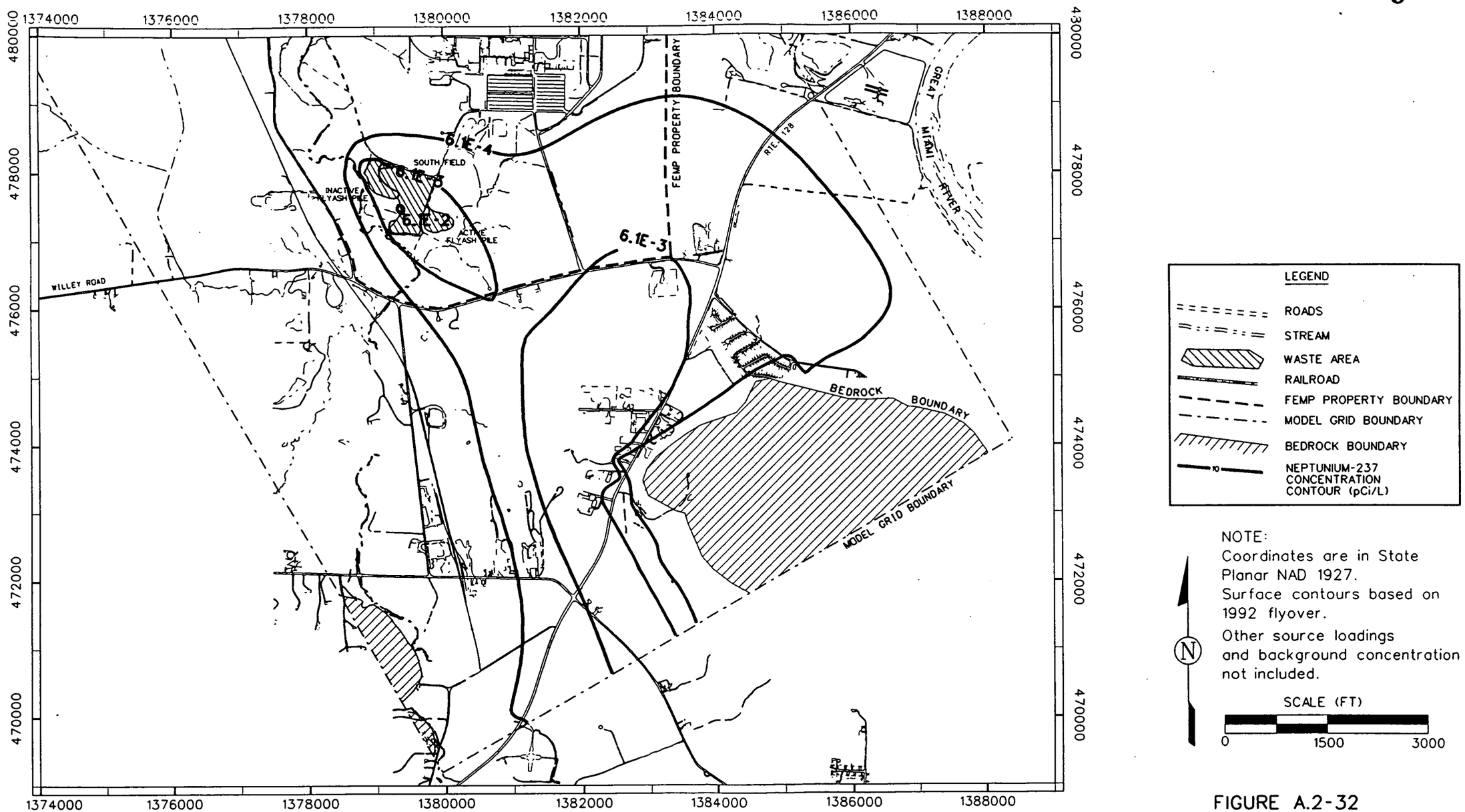

MAXIMUM INCREASE IN CONCENTRATION = 0.079 pCi/L

FIGURE A.2-32
PROJECTED INCREASE IN NEPTUNIUM-237 CONCENTRATION IN GREAT MIAMI AQUIFER AT 1000 YEARS DUE TO LOADING FROM THE INACTIVE FLYASH PILE AND SOUTH FIELD

figa0231.dgn

000244

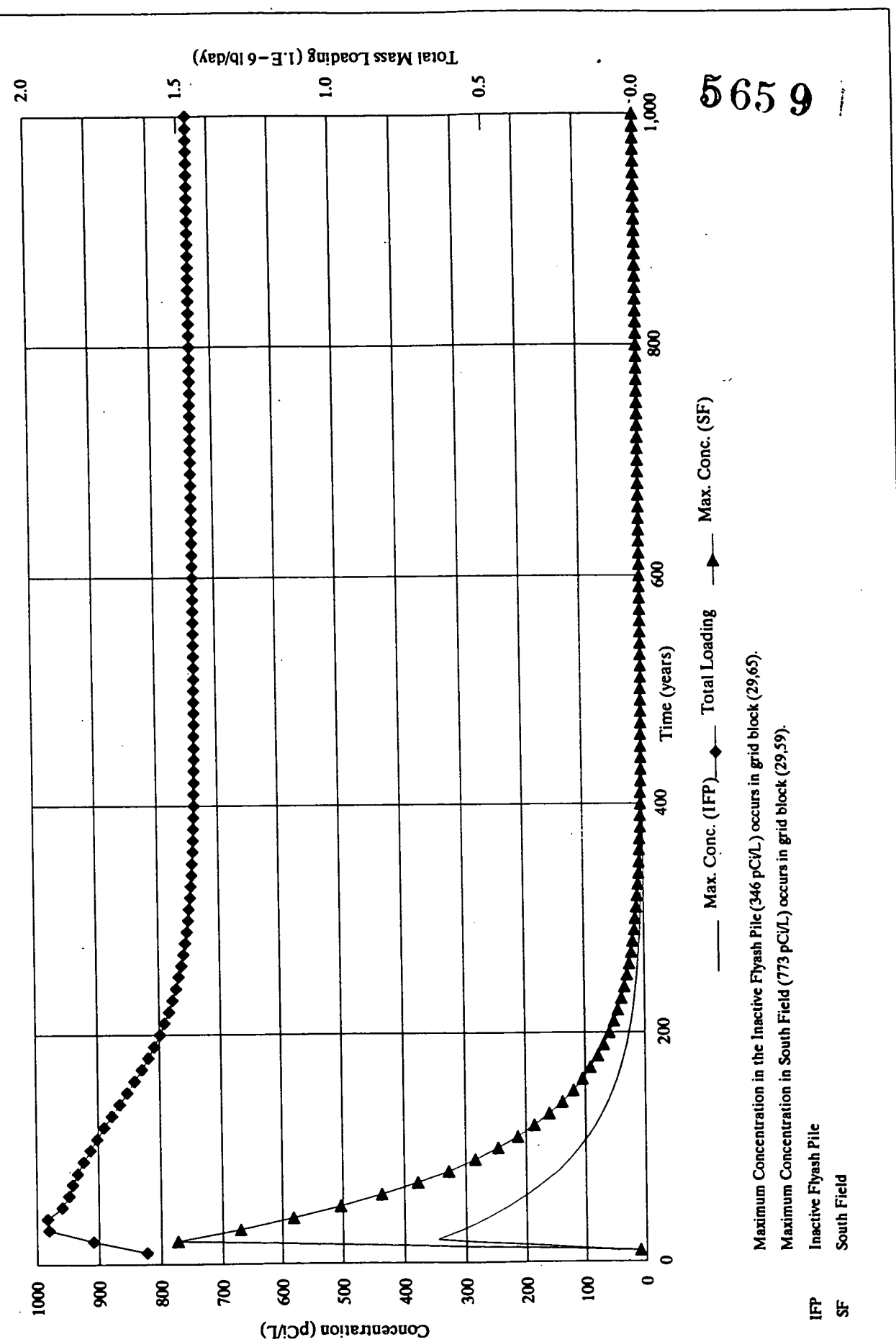

5659

Figure A.2-33. TECHNETIUM-99 LOADING TO THE GREAT MIAMI AQUIFER FOR THE INACTIVE FLYASH PILE AND SOUTH FIELI

000245

5659

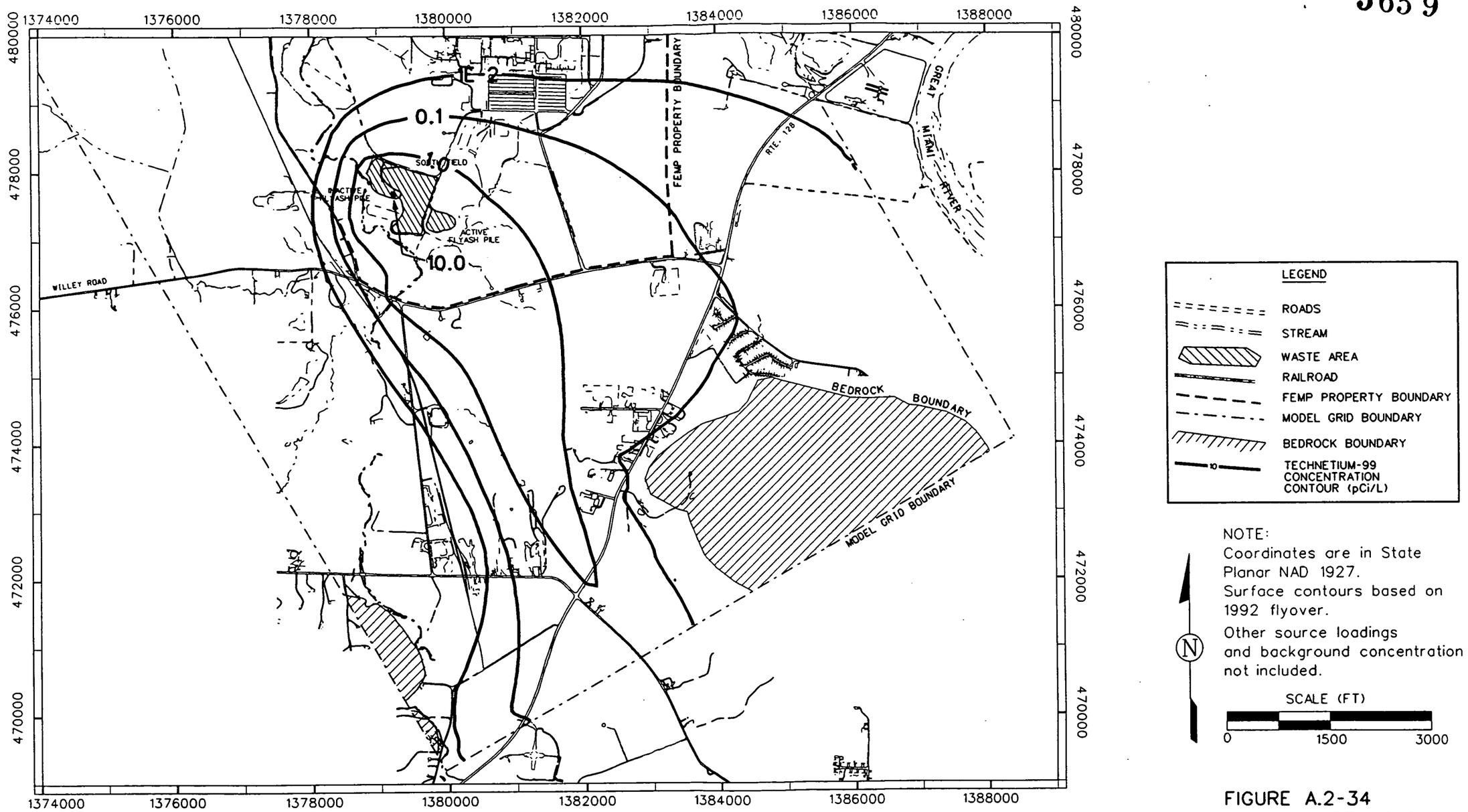

MAXIMUM INCREASE IN CONCENTRATION = 10.3 pCi/L

FIGURE A.2-34
PROJECTED INCREASE IN TECHNETIUM-99 CONCENTRATION IN GREAT MIAMI AQUIFER AT 40 YEARS DUE TO LOADING FROM THE INACTIVE FLYASH PILE AND SOUTH FIELD

figa0233.dgn

000246

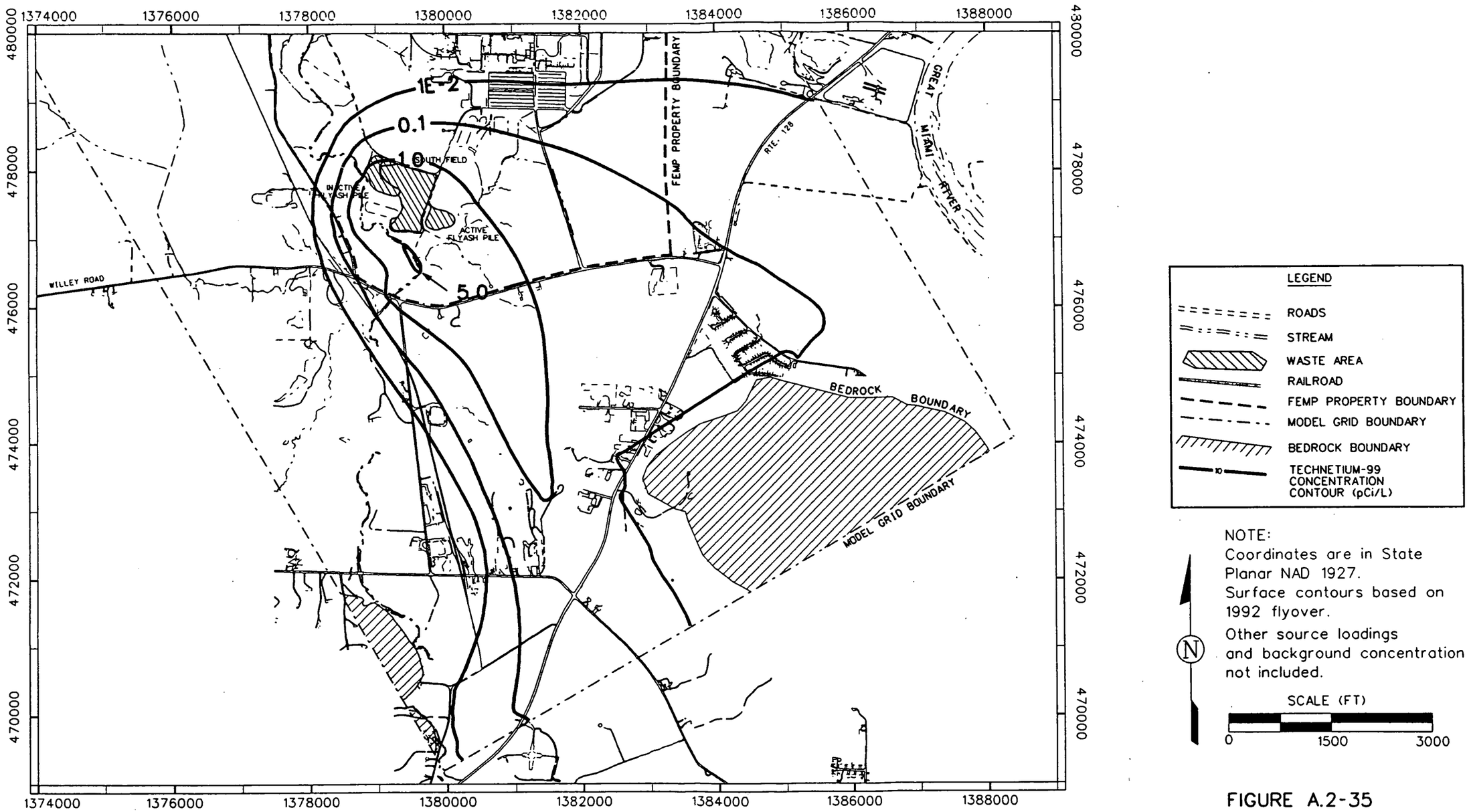

MAXIMUM INCREASE IN CONCENTRATION = 5.8 pCi/L

FIGURE A.2-35
PROJECTED INCREASE IN TECHNETIUM-99 CONCENTRATION IN GREAT MIAMI AQUIFER AT 160 YEARS DUE TO LOADING FROM THE INACTIVE FLYASH PILE AND SOUTH FIELD

figa0234.dgn

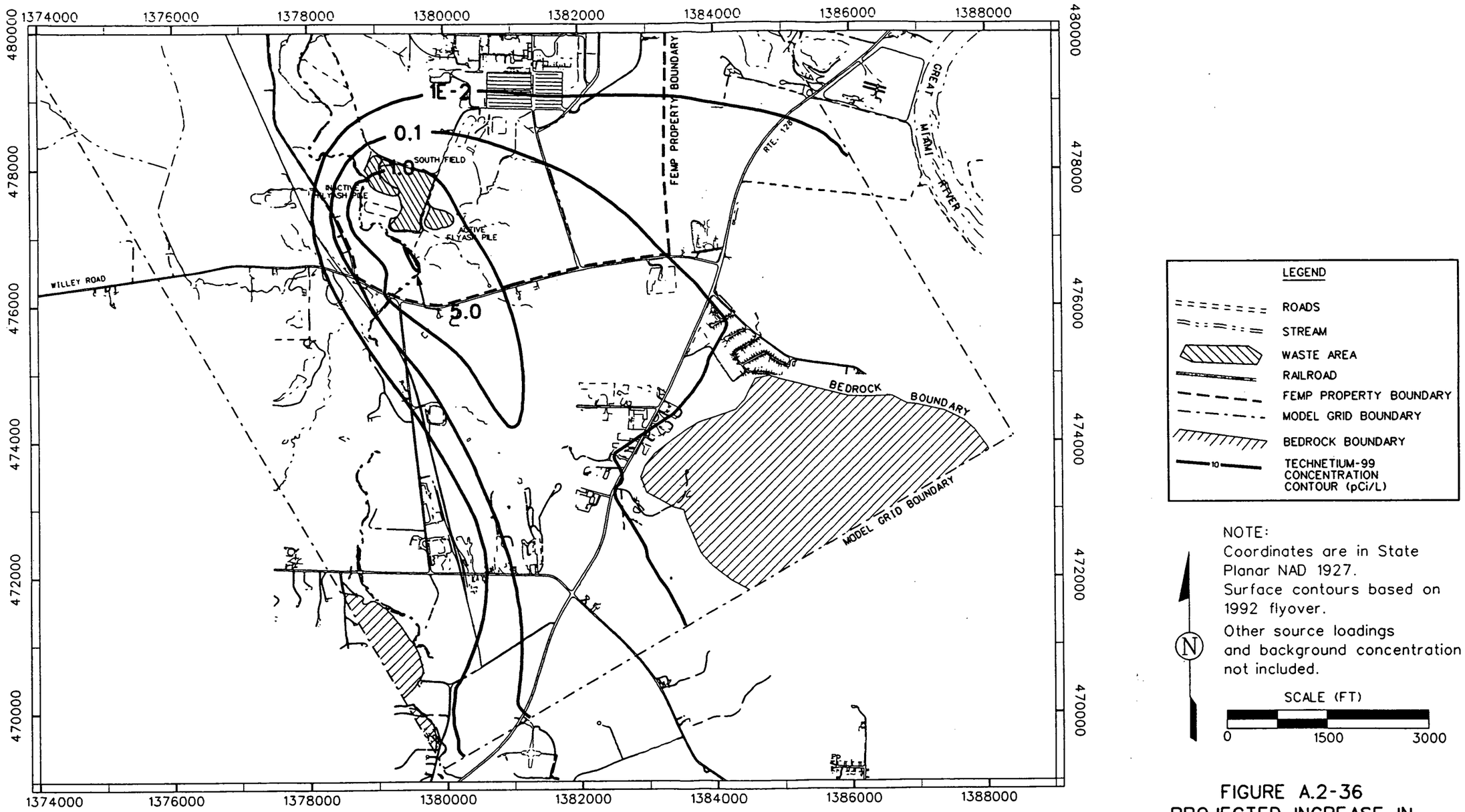

MAXIMUM INCREASE IN CONCENTRATION = 5.6 pCi/L

FIGURE A.2-36
PROJECTED INCREASE IN TECHNETIUM-99 CONCENTRATION IN GREAT MIAMI AQUIFER AT 220 YEARS DUE TO LOADING FROM THE INACTIVE FLYASH PILE AND SOUTH FIELD

figa0235.dgn

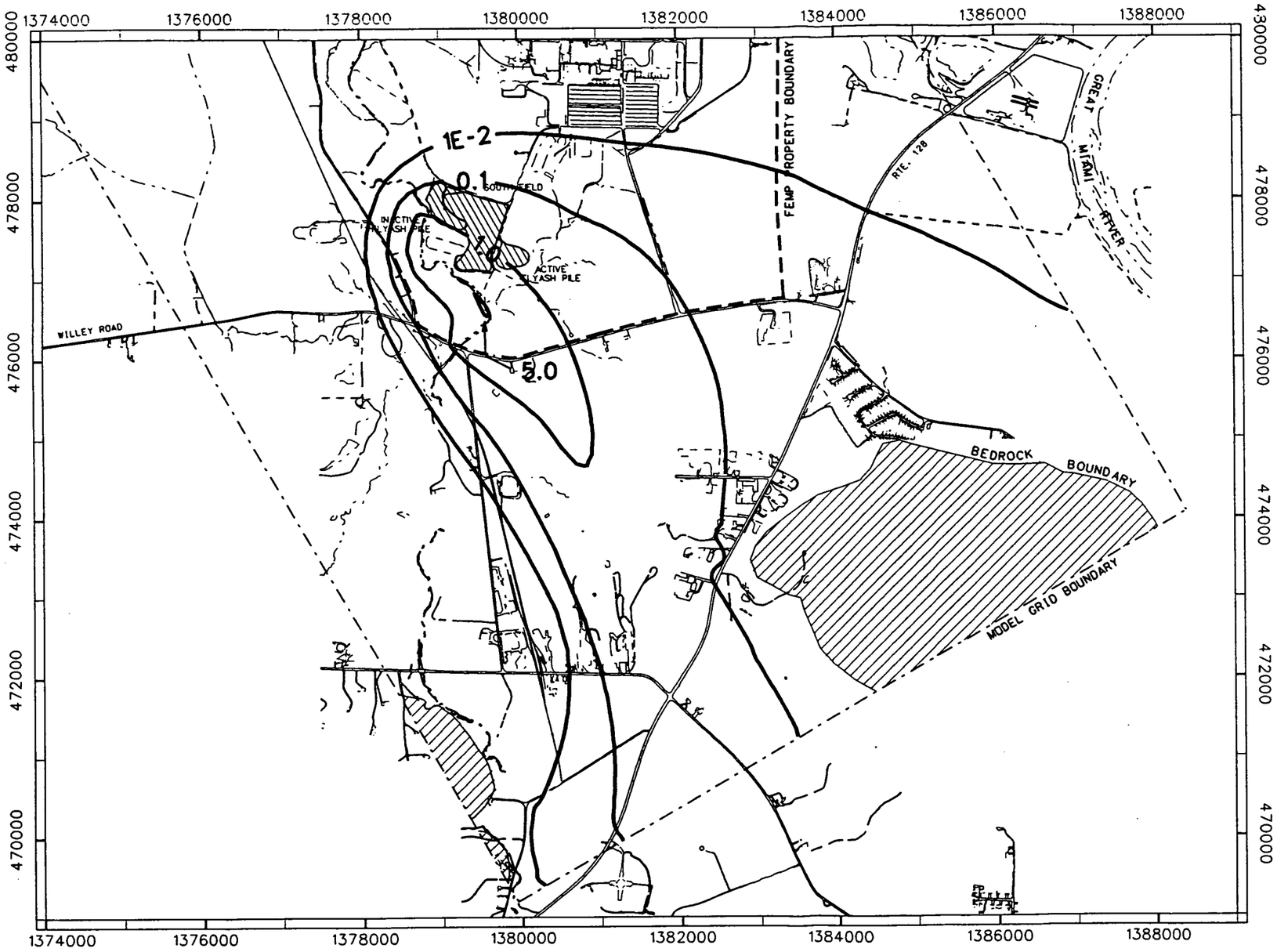

LEGEND

- ROADS
- STREAM
- WASTE AREA
- RAILROAD
- FEMP PROPERTY BOUNDARY
- MODEL GRID BOUNDARY
- BEDROCK BOUNDARY
- TECHNETIUM-99 CONCENTRATION CONTOUR (pCi/L)

NOTE:
Coordinates are in State Planar NAD 1927.
Surface contours based on 1992 flyover.
Other source loadings and background concentration not included.

N

SCALE (FT)
0 1500 3000

MAXIMUM INCREASE IN CONCENTRATION = 5.4 pCi/L

FIGURE A.2-37
PROJECTED INCREASE IN TECHNETIUM-99 CONCENTRATION IN GREAT MIAMI AQUIFER AT 1000 YEARS DUE TO LOADING FROM THE INACTIVE FLYASH PILE AND SOUTH FIELD

figa0236.dgn

5659

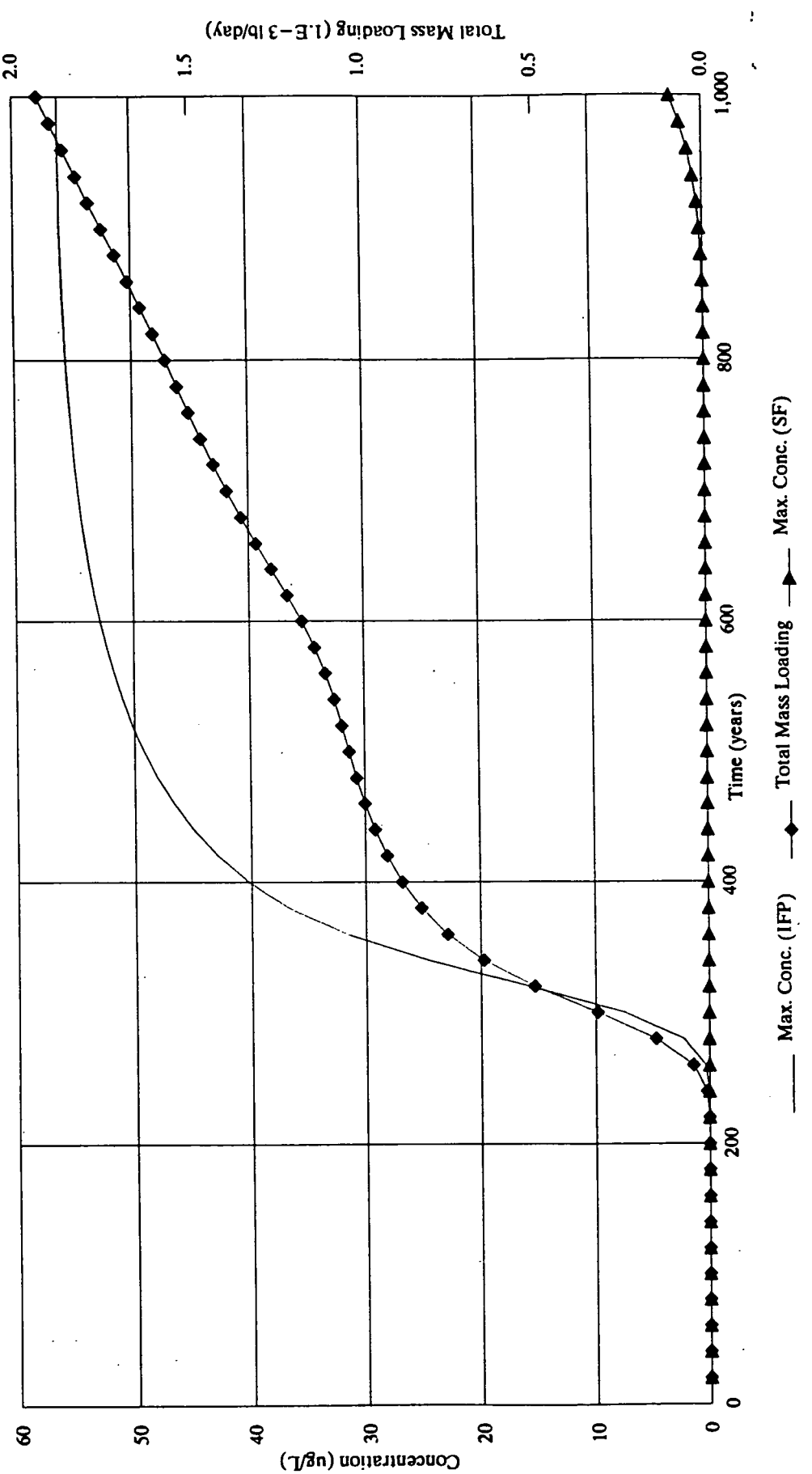

Maximum Concentration in the Inactive Flyash Pile (56.1 ug/L) occurs in grid block (29,65).
Maximum Concentration in South Field (2.8 ug/L) occurs in grid block (30,61).

IFP Inactive Flyash Pile
SF South Field

FIGURE A.2-38. LEAD LOADING TO THE GREAT MIAMI AQUIFER FROM THE INACTIVE FLYASH PILE AND SOUTH FIELD

000250

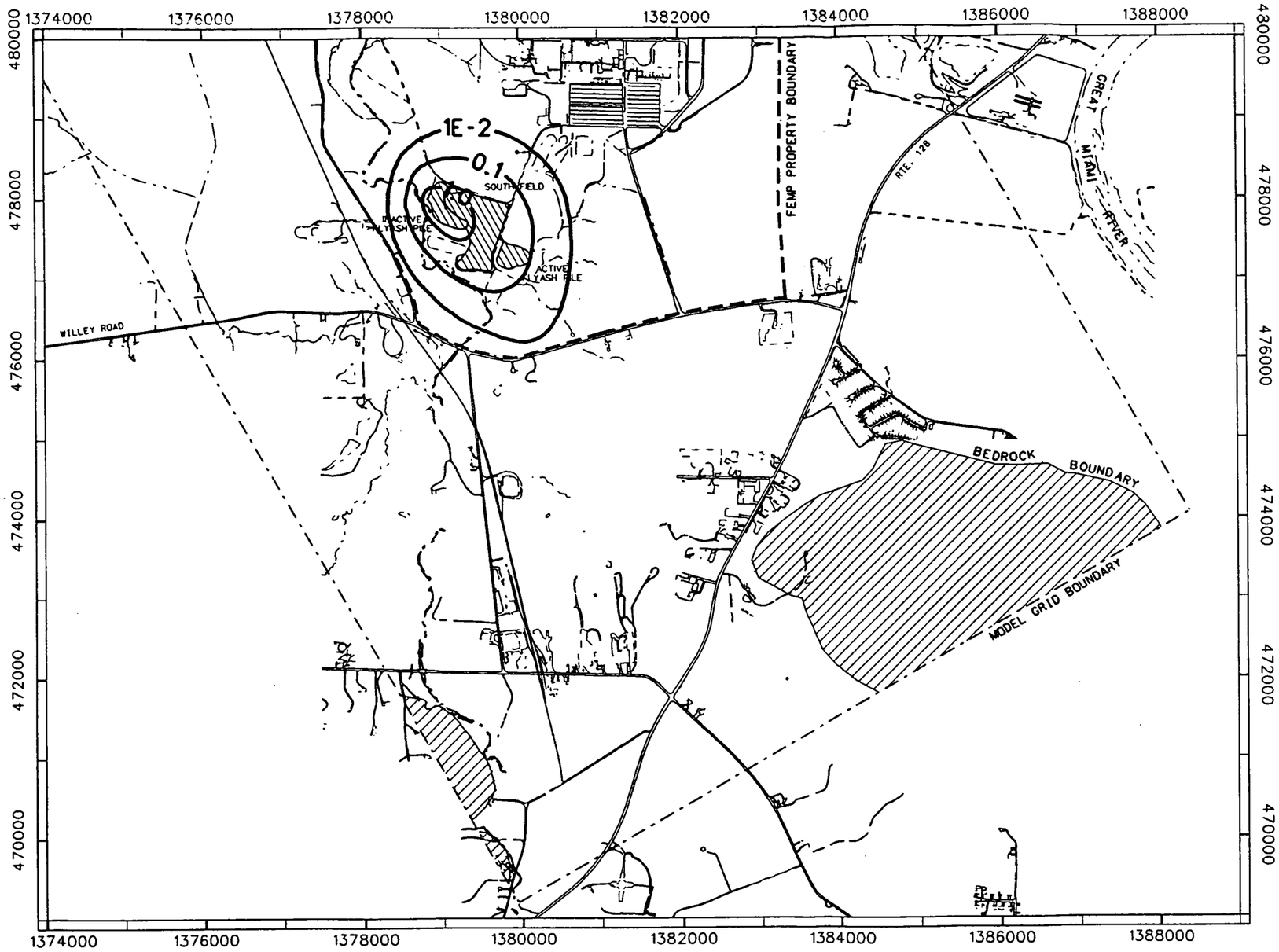

LEGEND

- ROADS
- STREAM
- WASTE AREA
- RAILROAD
- FEMP PROPERTY BOUNDARY
- MODEL GRID BOUNDARY
- BEDROCK BOUNDARY
- 10 LEAD CONCENTRATION CONTOUR (ug/L)

NOTE:
Coordinates are in State Planar NAD 1927.
Surface contours based on 1992 flyover.
Other source loadings and background concentration not included.

N

SCALE (FT)
0 1500 3000

MAXIMUM INCREASE IN CONCENTRATION = 4.86 ug/L

FIGURE A.2-39
PROJECTED INCREASE IN LEAD CONCENTRATION IN GREAT MIAMI AQUIFER AT 1000 YEARS DUE TO LOADING FROM THE INACTIVE FLYASH PILE AND SOUTH FIELD

figa0238.dgn

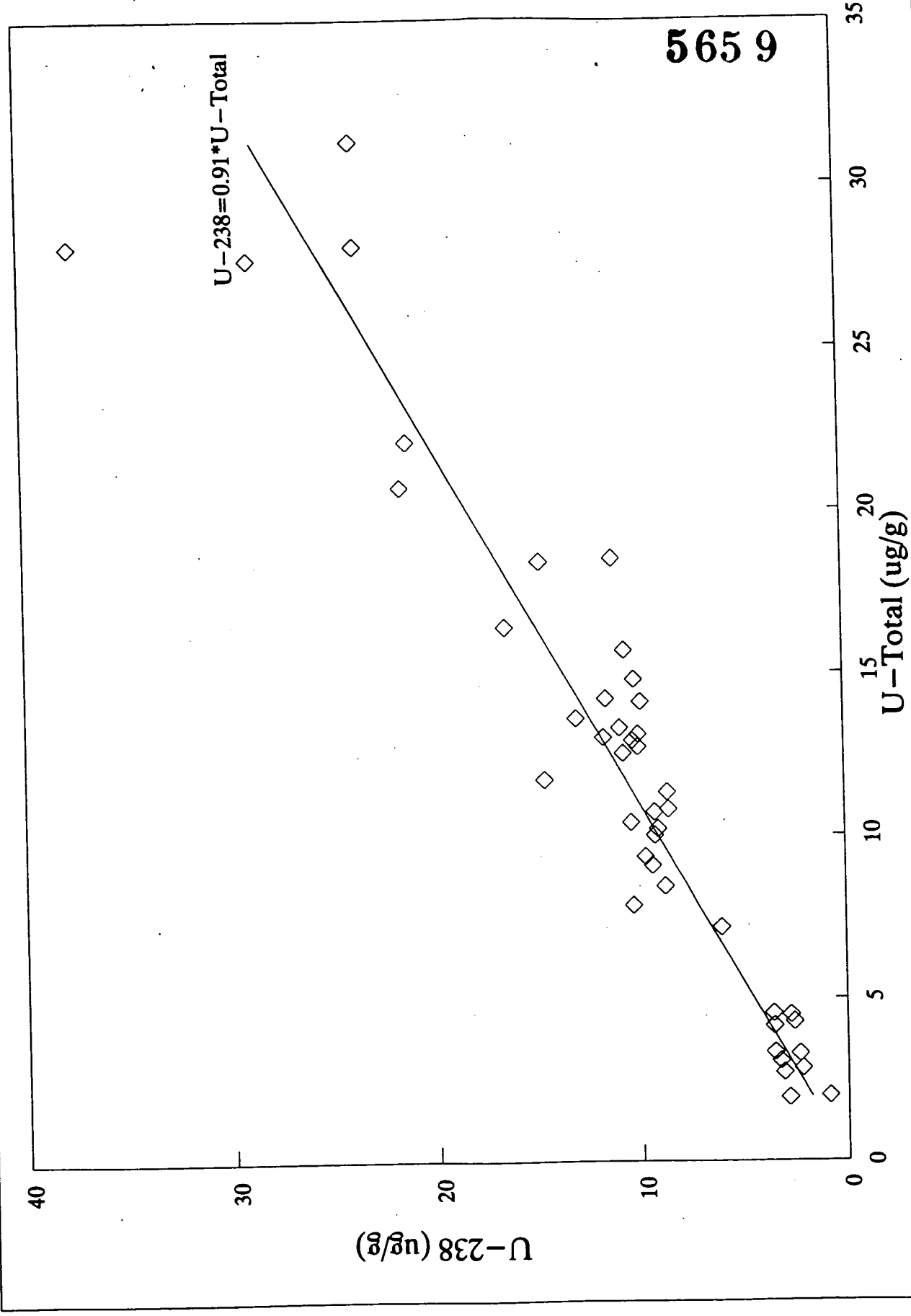

5659

FIGURE A.2-43 : U-238 vs. U-TOTAL IN SOIL SAMPLES, ACTIVE FLYASH PILE

000252

TABLE A.2-53

SUMMARY OF SWIFT MODELING RESULTS FOR THE ACTIVE FLYASH PILE OPERABLE UNIT 2 REMEDIAL INVESTIGATION FERNALD ENVIRONMENTAL MANAGEMENT PROJECT

Constituents of Potential Concern	Maximum Loading Concentration from ODAST (pCi/L RAD) (μg/L non-RAD)	Minimum Time of Arrival to the Aquifer (years)	Time of Maximum On-Site Concentration (years)	Maximum On-Site Concentration in the Aquifer (pCi/L RAD) (μg/L non-RAD)	Time of Maximum Concentration at the FEMP Boundary (years)	Maximum Concentration at the FEMP Boundary (pCi/L RAD) (μg/L non-RAD)	EPA RAGs, Part B Hazard Index Screening Levels (pCi/L RAD) (μg/L non-RAD)
RADIONUCLIDES							
Neptunium-237	$3.28 \times 10^{+1}$	0	160	$1.52 \times 10^{+1}$	280	1.63×10^{-1}	2.16×10^{-2}
Plutonium-238	-[c]	0	1000	5.61×10^{-2}	-[c]	-[c]	2.16×10^{-2}
Plutonium-239/240	-[c]	0	1000	2.57×10^{-3}	-[c]	-[c]	2.07×10^{-3}
Radium-226[c]	-[c]	0	1000	3.37×10^{-3}	-[c]	-[c]	1.76×10^{-4}
Radium-228[c]	-[c]	0	1000	2.34×10^{-4}	-[c]	-[c]	4.75×10^{-2}
Strontium-90	$1.79 \times 10^{+1}$	60	100	1.02×10^{0}	160	8.92×10^{-2}	1.32×10^{-1}
Uranium-234[a]	-[a, b]	0	100	$1.98 \times 10^{+1}$	120	2.58×10^{0}	2.97×10^{-1}
Uranium-235/236[a]	-[a, b]	0	100	1.05×10^{0}	120	1.38×10^{-1}	2.97×10^{-1}
Uranium-238	$4.87 \times 10^{+2}$	0	100	$2.18 \times 10^{+1}$	120	2.85×10^{0}	1.70×10^{-1}
Uranium - Total (non-RAD)[a]	-[a, b]	0	100	$7.76 \times 10^{+1}$	120	$1.02 \times 10^{+1}$	$1.09 \times 10^{+1}$
ORGANICS							
2-Methylnapthalene[e]	-[e]	-[e]	-[e]	$1.95 \times 10^{+0}$	-[e]	$1.95 \times 10^{+0}$	NA[d]

See footnotes at end of table

TABLE A.2-53
(Continued)

Constituents of Potential Concern	Maximum Loading Concentration from ODAST (pCi/L RAD) (μg/L non-RAD)	Minimum Time of Arrival to the Aquifer (years)	Time of Maximum On-Site Concentration (years)	Maximum On-Site Concentration in the Aquifer (pCi/L RAD) (μg/L non-RAD)	Time of Maximum Concentration at the FEMP Boundary (years)	Maximum Concentration at the FEMP Boundary (pCi/L RAD) (μg/L non-RAD)	EPA RAGs, Part B Hazard Index Screening Levels (pCi/L RAD) (μg/L non-RAD)
INORGANICS							
Arsenic	N/A[f]	0	1,000	7.12×10^{-2}	1,000	1.82×10^{-2}	1.46×10^{-4}
Beryllium	N/A	0	1,000	2.75×10^{-3}	1,000	7.08×10^{-4}	2.37×10^{-4}
Lead	$2.87 \times 10^{+1}$	0	1,000	1.64×10^{0}	1,000	3.47×10^{-2}	NA[d]

[a]Uranium-234, uranium-235/236, and total uranium were modeled by applying ratios to uranium-238 results.
[b]ODAST results were not used for SWIFT III modeling and therefore not shown in this table.
[c]Plutonium-238, plutonium-239/240, radium-226, and radium-228, were not modeled using SWIFT III because concentrations in the Great Miami Aquifer falls below the EPA RAGs, Part B screening concentration after mixing in SWIFT III grid cell. The maximum predicted concentration based on the Storm Sewer Outfall Ditch width of 10 feet is reported as the maximum on-site concentration.
[d]NA - No data available to calculate EPA RAGs, Part B screening value for lead and 2-methylnaphthalene
[e]2-Methylnaphthalene was not modeled using ODAST/SWIFT because EPA RAGs, Part B screening value cannot be calculated. Reported concentrations are same as predicted leachate values. If concentrations are needed for risk assessment in future, ODAST/SWIFT model or equivalent should be used to calculate the concentration in the Great Miami Aquifer.
[f]N/A = Not applicable because arsenic and beryllium did not have loading from the vadose zone pathway. The only loading for arsenic and beryllium was from the surface runoff pathway.

Comment No. A-48

concentration of CPCs that could be expected in the aquifer within 1000 years and the time required for the CPC to reach the maximum value. CPCs projected to be above screening levels as they reach the Great Miami Aquifer directly beneath the Active Flyash Pile were uranium isotopes (uranium-238, uranium-234, uranium-235/236), total uranium, neptunium-237, strontium-90, ~~arsenic, beryllium, cadmium, lead, and molybdenum~~ plutonium-238, plutonium-239/240, arsenic, and beryllium. ~~Out of these CPCs, uranium isotopes, neptunium 237, strontium 90, arsenic, lead, and molybdenum were predicted to be above screening levels in the Great Miami Aquifer. Only neptunium 237, uranium isotopes, and total uranium are expected to be above 10^{-7} cancer risk or 0.1 Hazard Index levels at the FEMP boundary.~~ Although all CPCs are above screening concentrations, only neptunium-237, uranium isotopes, arsenic, and beryllium are expected to be above screening concentrations at the FEMP boundary.

NO. A-48

As noted earlier, total uranium, uranium-234, and uranium-235/236 concentrations were estimated from the results of uranium-238 modeling. Figure A.2-43 shows site specific relationship between uranium-238 and total uranium at the Active Flyash Pile. Figure A.2-43 shows that 91% of total uranium mass consists of uranium-238. The uranium-238 vs. total uranium relationship was used a limited number of times when total uranium analysis was available for a soil but uranium-238 analysis was not available. Relationships of uranium-238 with uranium-234 and uranium-235/236 was shown in Figures A.2-24 and A.2-25. These relationships were used to estimate uranium-234, uranium-235/236, and total uranium concentrations.

NO. A-25 & A-48

~~Uranium 238 and neptunium 237~~ Uranium isotopes, neptunium-237, arsenic, and beryllium concentrations are significantly elevated compared to the screening concentrations and may pose a significant risk via the groundwater pathway. Table A.2-54 presents on-site and off-site concentrations of CPCs at uranium-238 maximum concentration location and time. Loading curves and contour plots for CPCs at different time periods are presented in Figure A.2-44 through ~~A.2-62~~ A.2-60.

NOs. A-29 & A-48

NO. A-48

Except for arsenic, all CPC loading curves show a typical sharp rise to a peak value and then exponential decline. Arsenic shows a constant loading curve, as arsenic loading was controlled from the surface water pathway where each storm event was assumed to provide the same loading to the Great Miami Aquifer. All concentration contours show a southerly migration from the Active Flyash

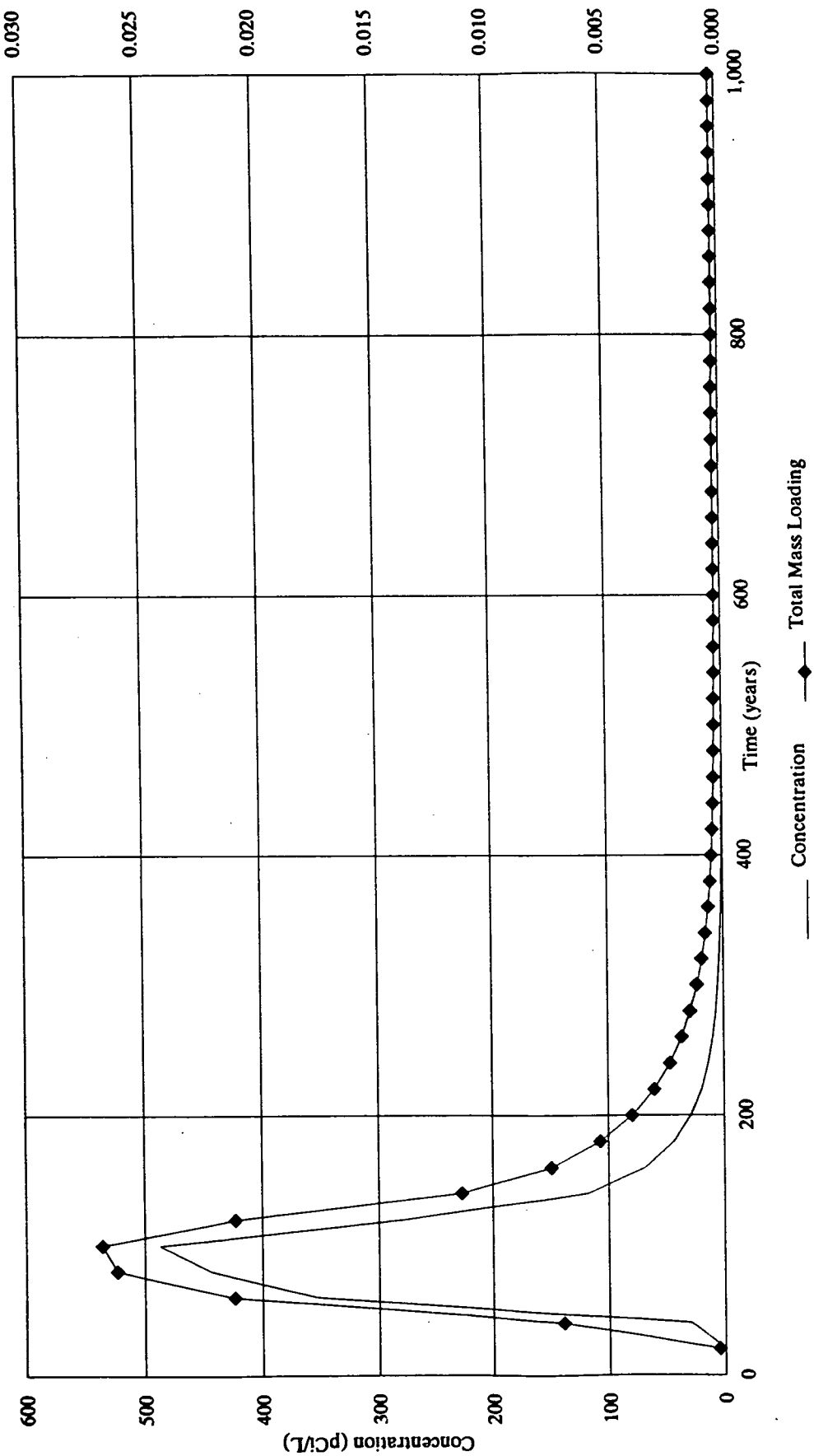

Maximum concentration (487 pCi/L) occurs in grid block (31,56).
Concentrations are plotted for grid block (31,56).

FIGURE A.2-44. URANIUM-238 LOADING TO THE GREAT MIAMI AQUIFER FROM THE ACTIVE FLYASH PILE

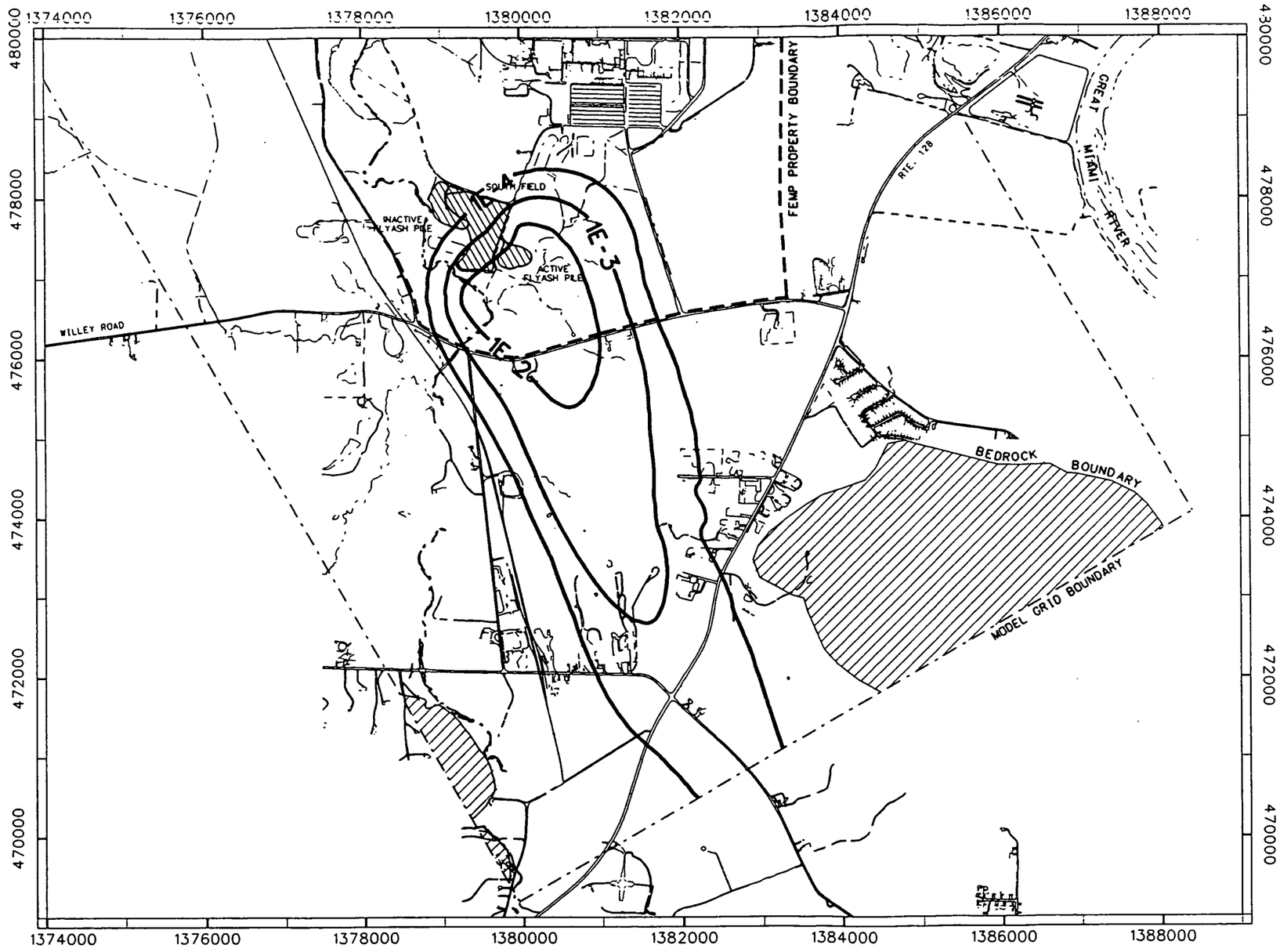

LEGEND

- ROADS
- STREAM
- WASTE AREA
- RAILROAD
- FEMP PROPERTY BOUNDARY
- MODEL GRID BOUNDARY
- BEDROCK BOUNDARY
- URANIUM-238 CONCENTRATION CONTOUR (pCi/L)

NOTE:
Coordinates are in State Planar NAD 1927.
Surface contours based on 1992 flyover.
Other source loadings and background concentration not included.

N

SCALE (FT)
0 1500 3000

MAXIMUM INCREASE IN CONCENTRATION = 0.11 pCi/L

FIGURE A.2-45
PROJECTED INCREASE IN URANIUM-238 CONCENTRATION IN GREAT MIAMI AQUIFER AT 40 YEARS DUE TO LOADING FROM THE ACTIVE FLYASH PILE

figa0251.dgn

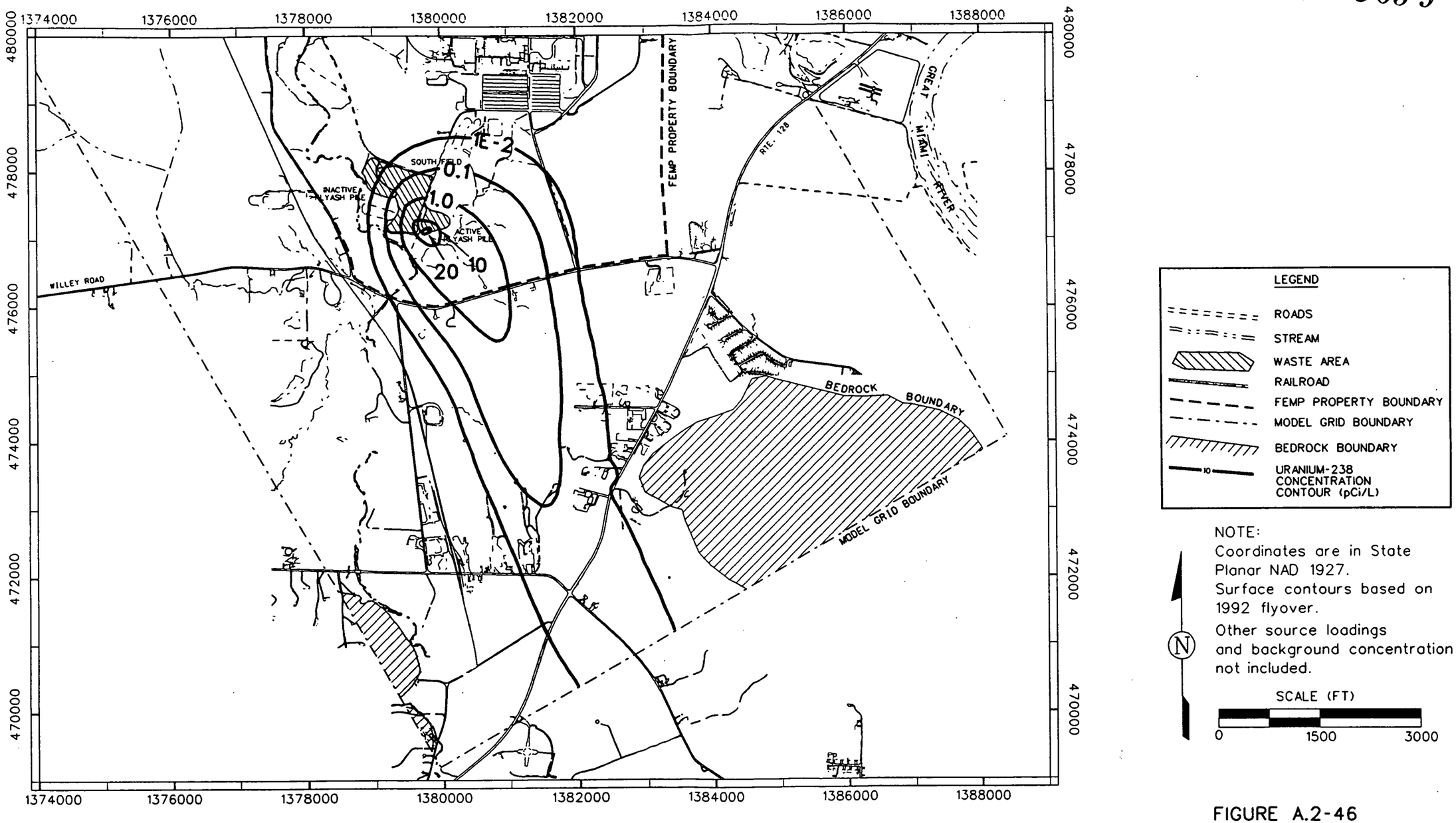

MAXIMUM INCREASE IN CONCENTRATION = 21.8 pCi/L

FIGURE A.2-46
PROJECTED INCREASE IN URANIUM-238 CONCENTRATION IN GREAT MIAMI AQUIFER AT 100 YEARS DUE TO LOADING FROM THE ACTIVE FLYASH PILE

figa0252.dgn

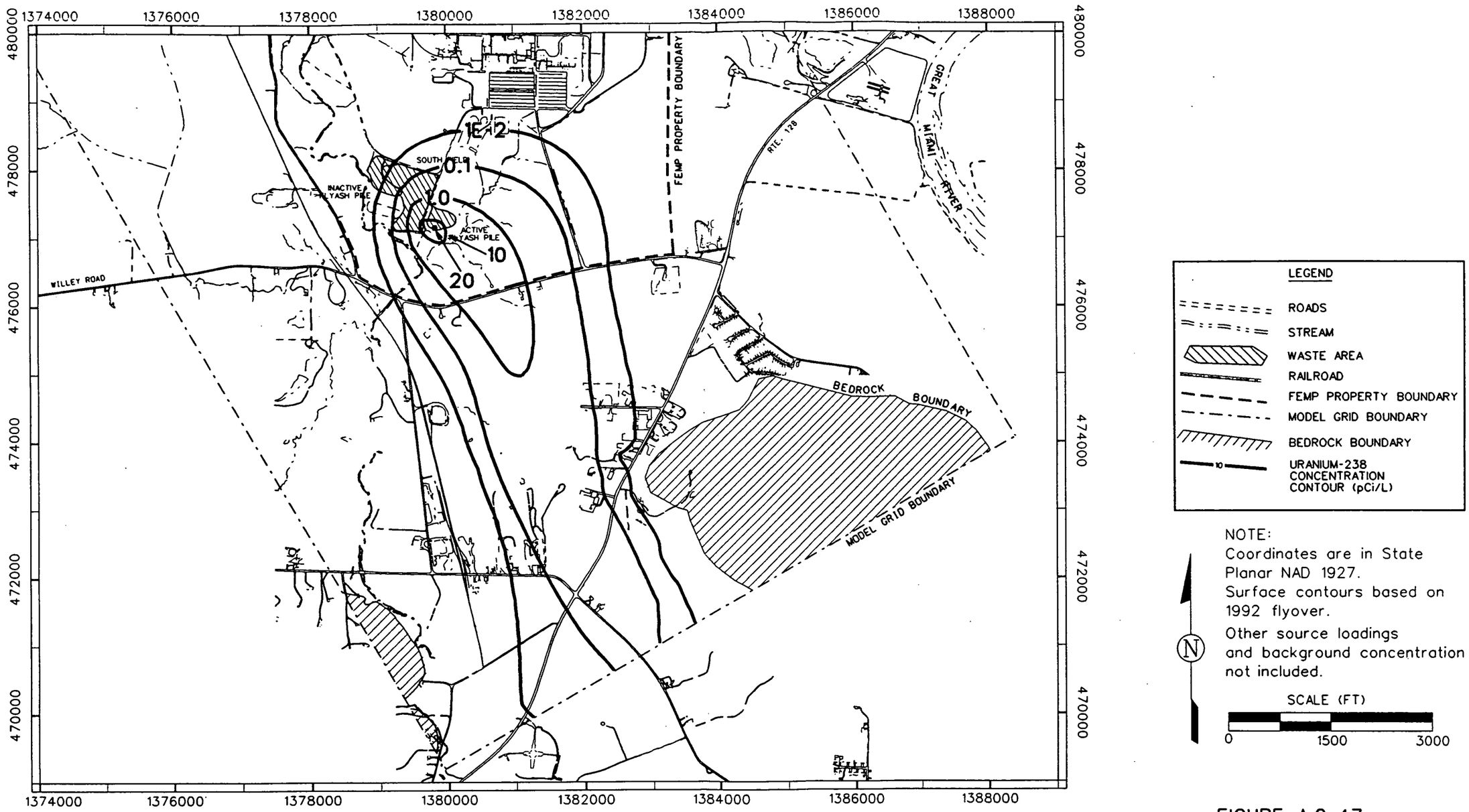

MAXIMUM INCREASE IN CONCENTRATION = 21.4 pCi/L

FIGURE A.2-47
PROJECTED INCREASE IN URANIUM-238 CONCENTRATION IN GREAT MIAMI AQUIFER AT 120 YEARS DUE TO LOADING FROM THE ACTIVE FLYASH PILE

figa0253.dgn

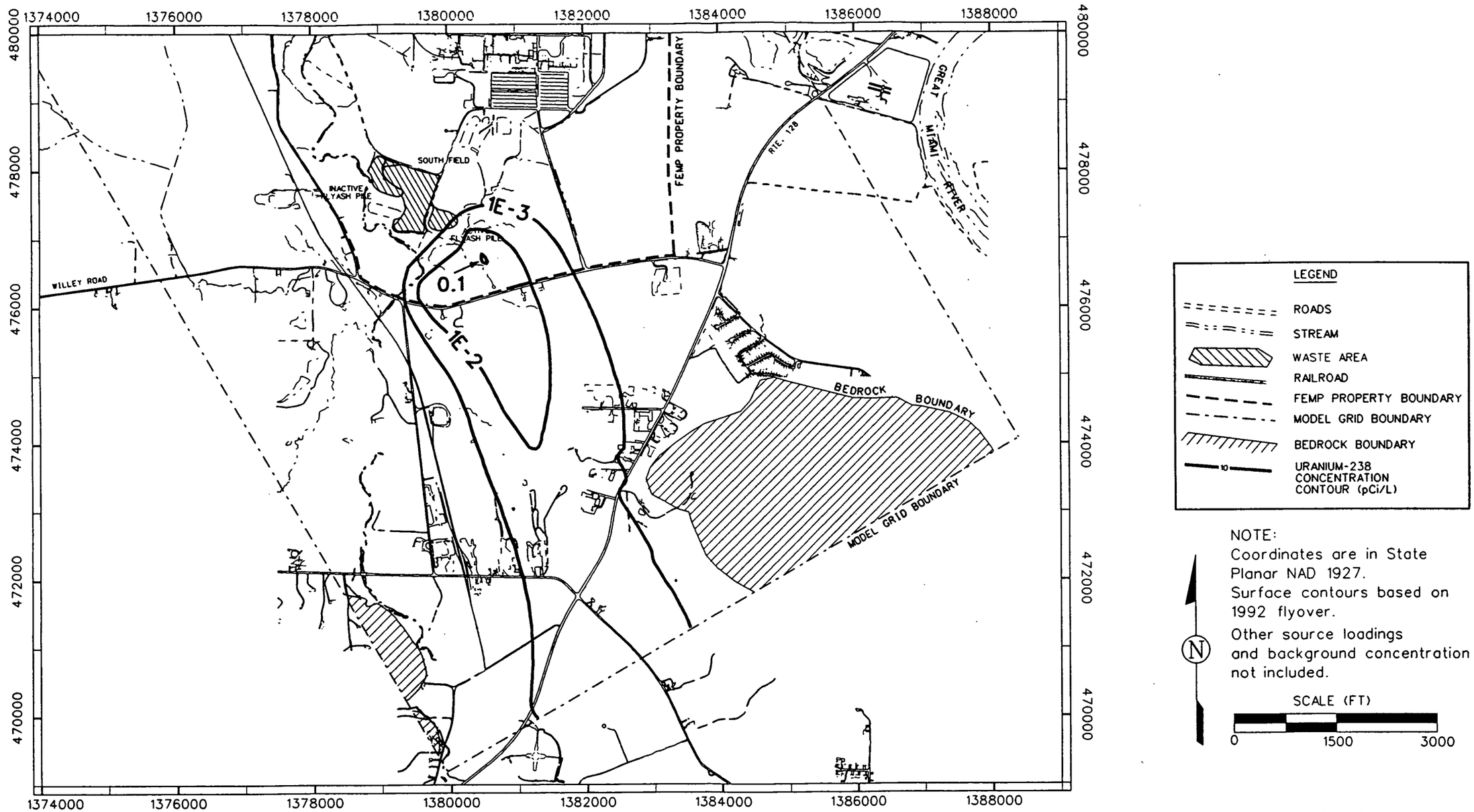

MAXIMUM INCREASE IN CONCENTRATION = 0.11 pCi/L

FIGURE A.2-48
PROJECTED INCREASE IN URANIUM-238 CONCENTRATION IN GREAT MIAMI AQUIFER AT 1000 YEARS DUE TO LOADING FROM THE ACTIVE FLYASH PILE

figa0254.dgn

5659

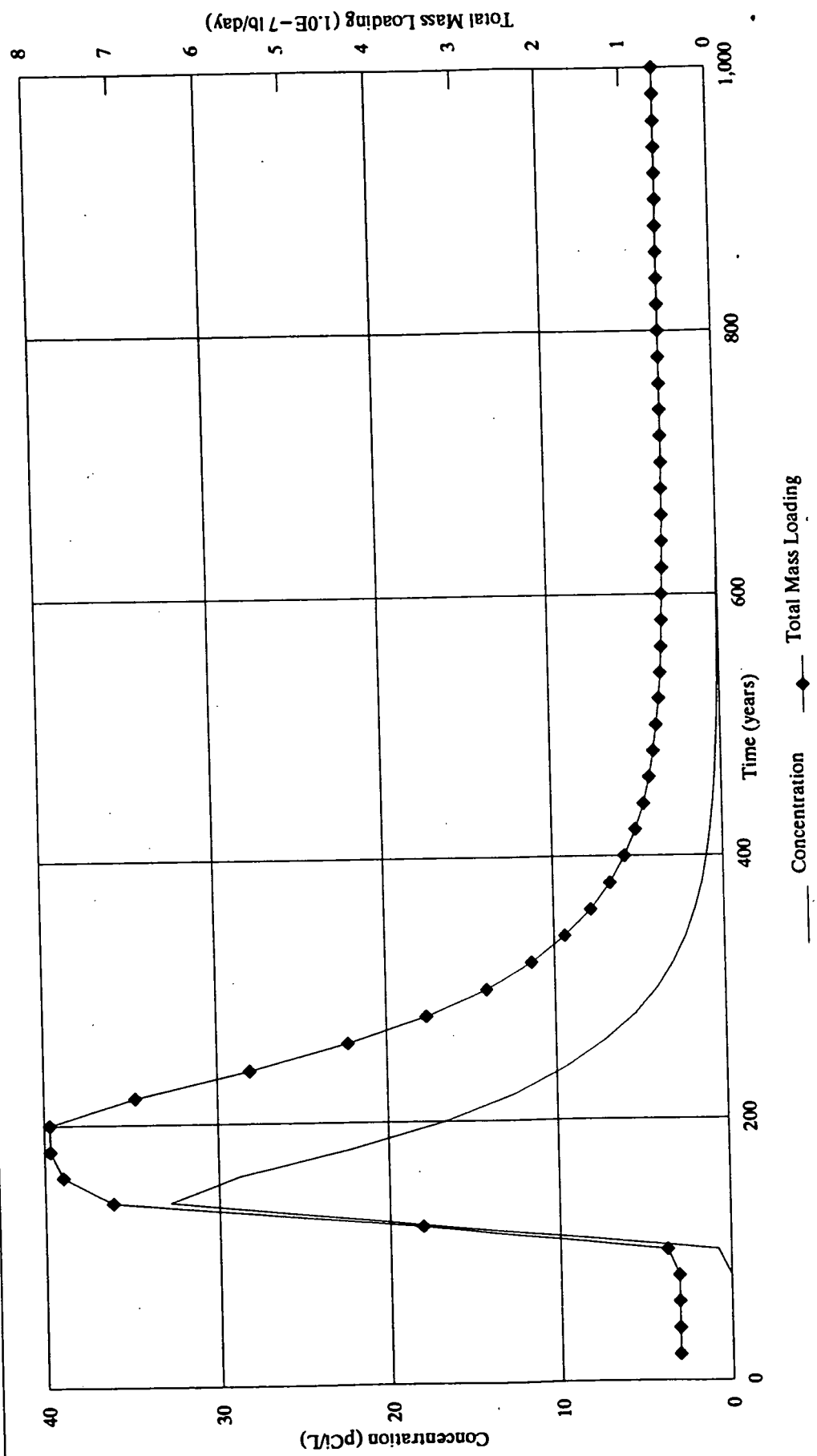

FIGURE A.2–49. NEPTUNIUM–237 LOADING TO THE GREAT MAIMI AQUIFER FROM THE ACTIVE FLYASH PILE

5659

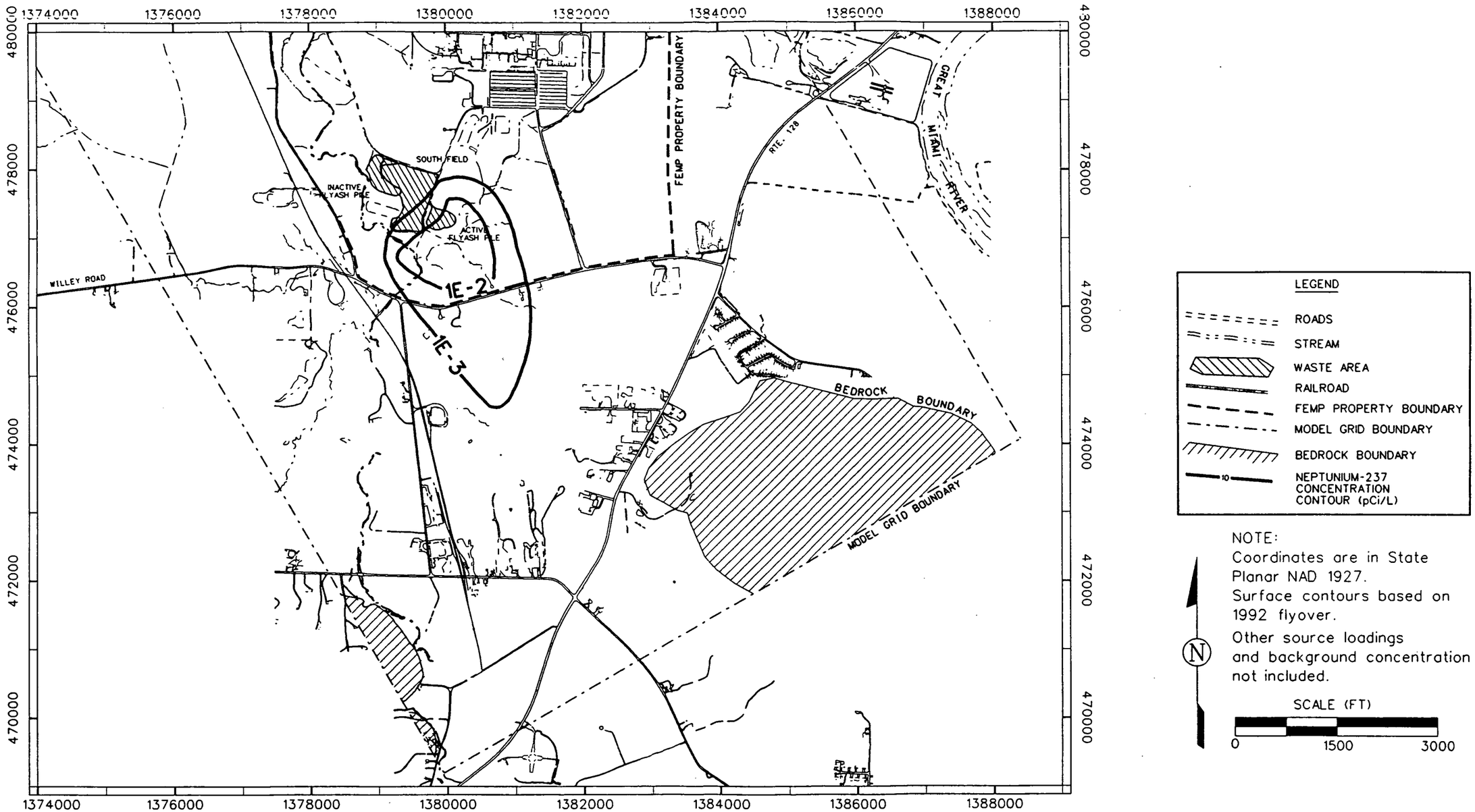

MAXIMUM INCREASE IN CONCENTRATION = 0.053 pCi/L

FIGURE A.2-50
PROJECTED INCREASE IN NEPTUNIUM-237 CONCENTRATION IN GREAT MIAMI AQUIFER AT 100 YEARS DUE TO LOADING FROM THE ACTIVE FLYASH PILE

figa0256.dgn

000262

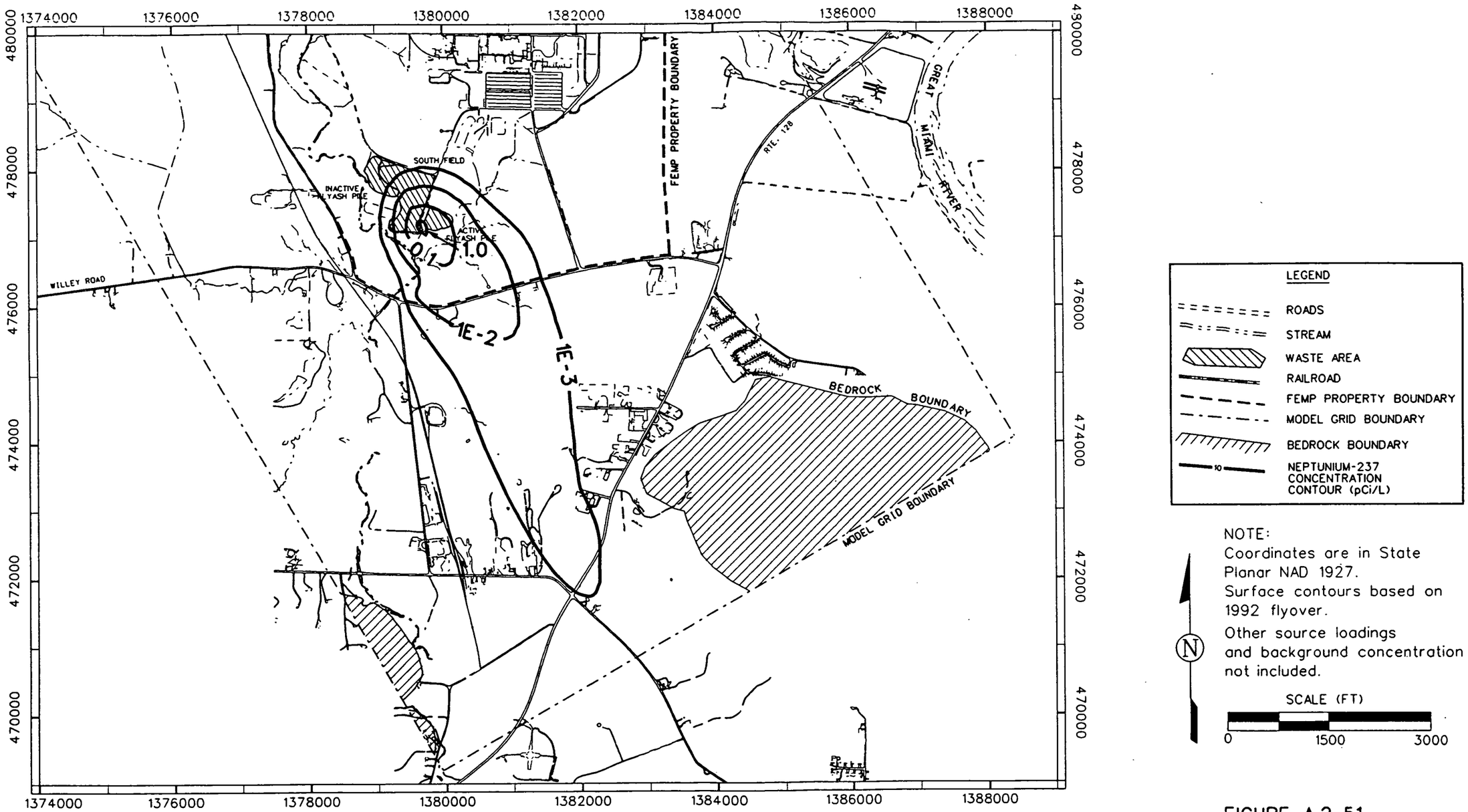

MAXIMUM INCREASE IN CONCENTRATION = 1.52 pCi/L

FIGURE A.2-51
PROJECTED INCREASE IN NEPTUNIUM-237 CONCENTRATION IN GREAT MIAMI AQUIFER AT 160 YEARS DUE TO LOADING FROM THE ACTIVE FLYASH PILE

figa0257.dgn

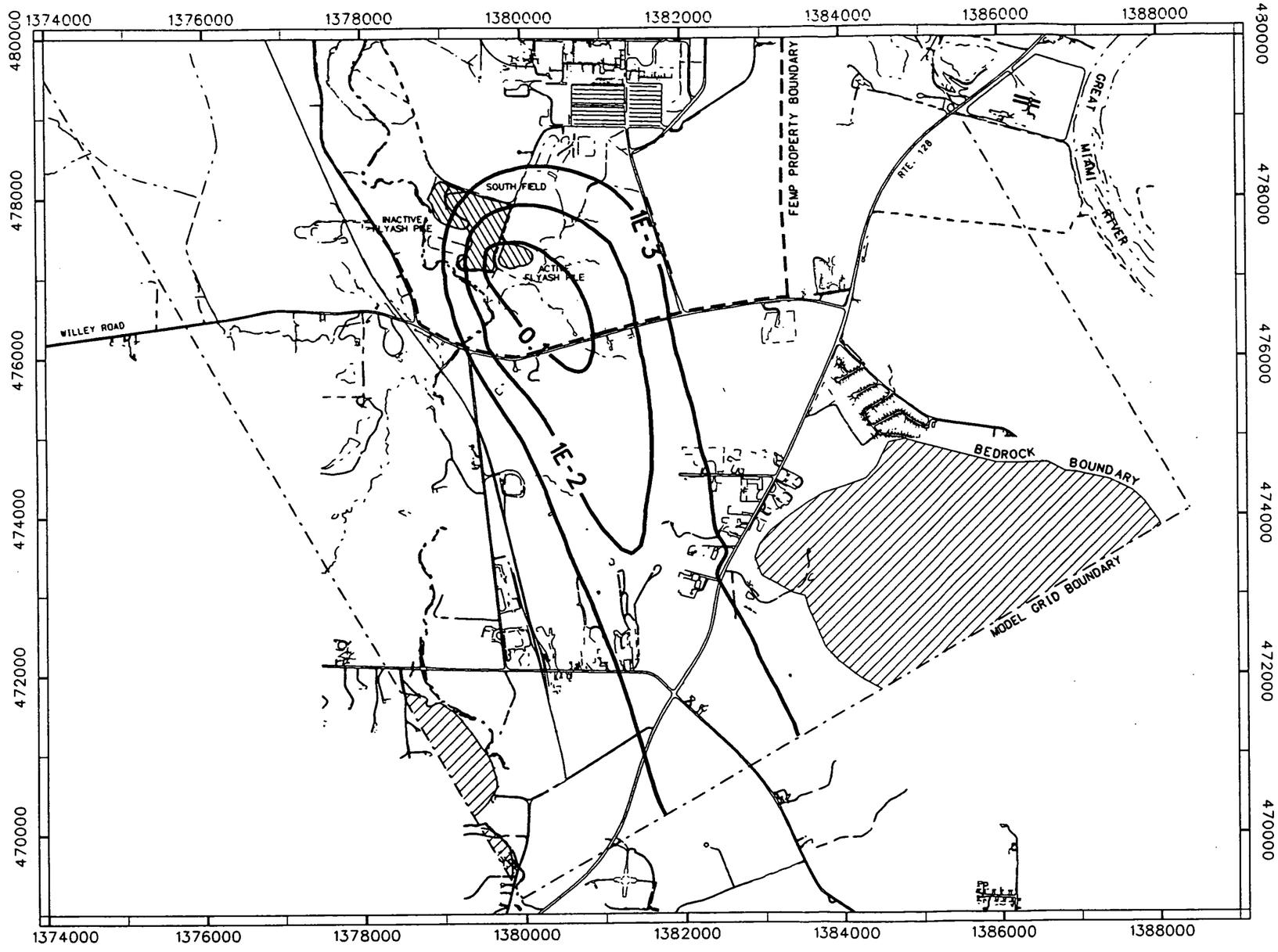

LEGEND

- ROADS
- STREAM
- WASTE AREA
- RAILROAD
- FEMP PROPERTY BOUNDARY
- MODEL GRID BOUNDARY
- BEDROCK BOUNDARY
- 10 — NEPTUNIUM-237 CONCENTRATION CONTOUR (pCi/L)

NOTE:
Coordinates are in State Planar NAD 1927.
Surface contours based on 1992 flyover.
Other source loadings and background concentration not included.

N

SCALE (FT)
0 1500 3000

MAXIMUM INCREASE IN CONCENTRATION = 0.75 pCi/L

FIGURE A.2-52
PROJECTED INCREASE IN NEPTUNIUM-237 CONCENTRATION IN GREAT MIAMI AQUIFER AT 280 YEARS DUE TO LOADING FROM THE ACTIVE FLYASH PILE

figa0258.dgn

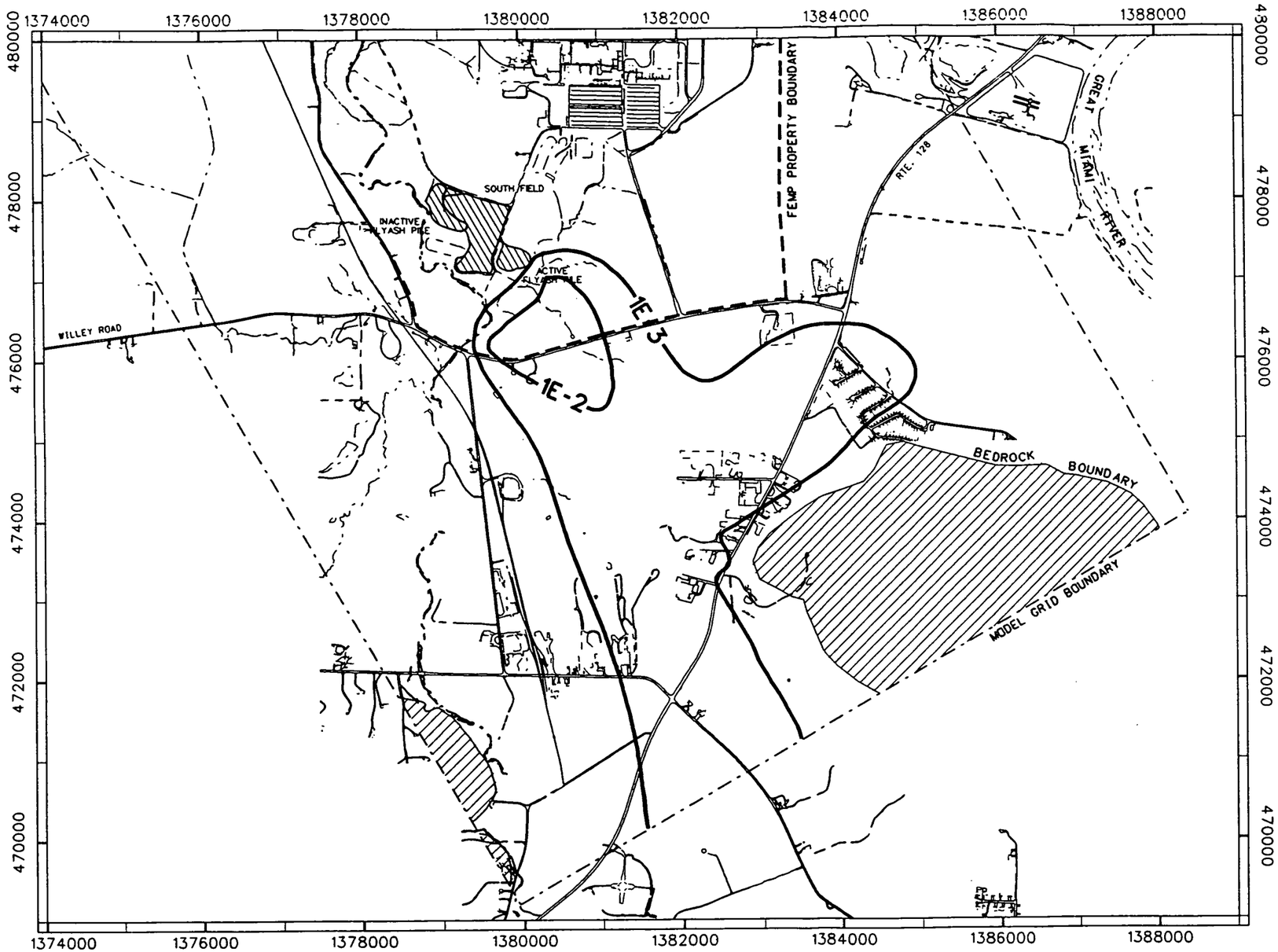

LEGEND

- ROADS
- STREAM
- WASTE AREA
- RAILROAD
- FEMP PROPERTY BOUNDARY
- MODEL GRID BOUNDARY
- BEDROCK BOUNDARY
- 10 — NEPTUNIUM-237 CONCENTRATION CONTOUR (pCi/L)

NOTE:
Coordinates are in State Planar NAD 1927.
Surface contours based on 1992 flyover.
Other source loadings and background concentration not included.

N

SCALE (FT)
0 1500 3000

MAXIMUM INCREASE IN CONCENTRATION = 0.054 pCi/L

FIGURE A.2-53
PROJECTED INCREASE IN NEPTUNIUM-237 CONCENTRATION IN GREAT MIAMI AQUIFER AT 1000 YEARS DUE TO LOADING FROM THE ACTIVE FLYASH PILE

figa0259.dgn

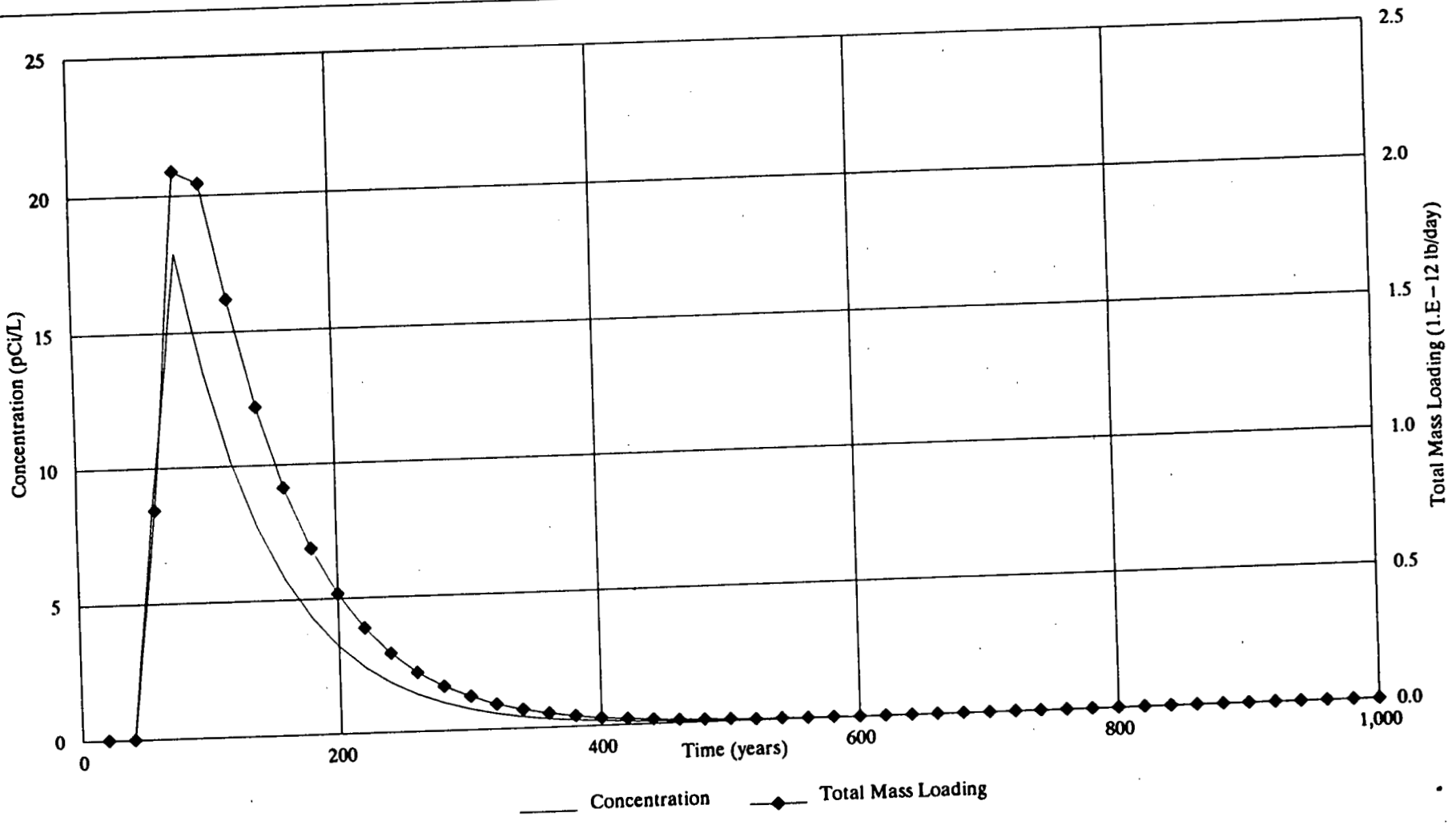

Maximum concentration (17.9 pCi/L) occurs in grid block (31,57).

Concentrations are plotted for grid block (31,57).

FIGURE A.2–54. STRONTIUM–90 LOADING TO THE GREAT MAIMI AQUIFER FROM THE ACTIVE FLYASH PILE

000200

5659

5659

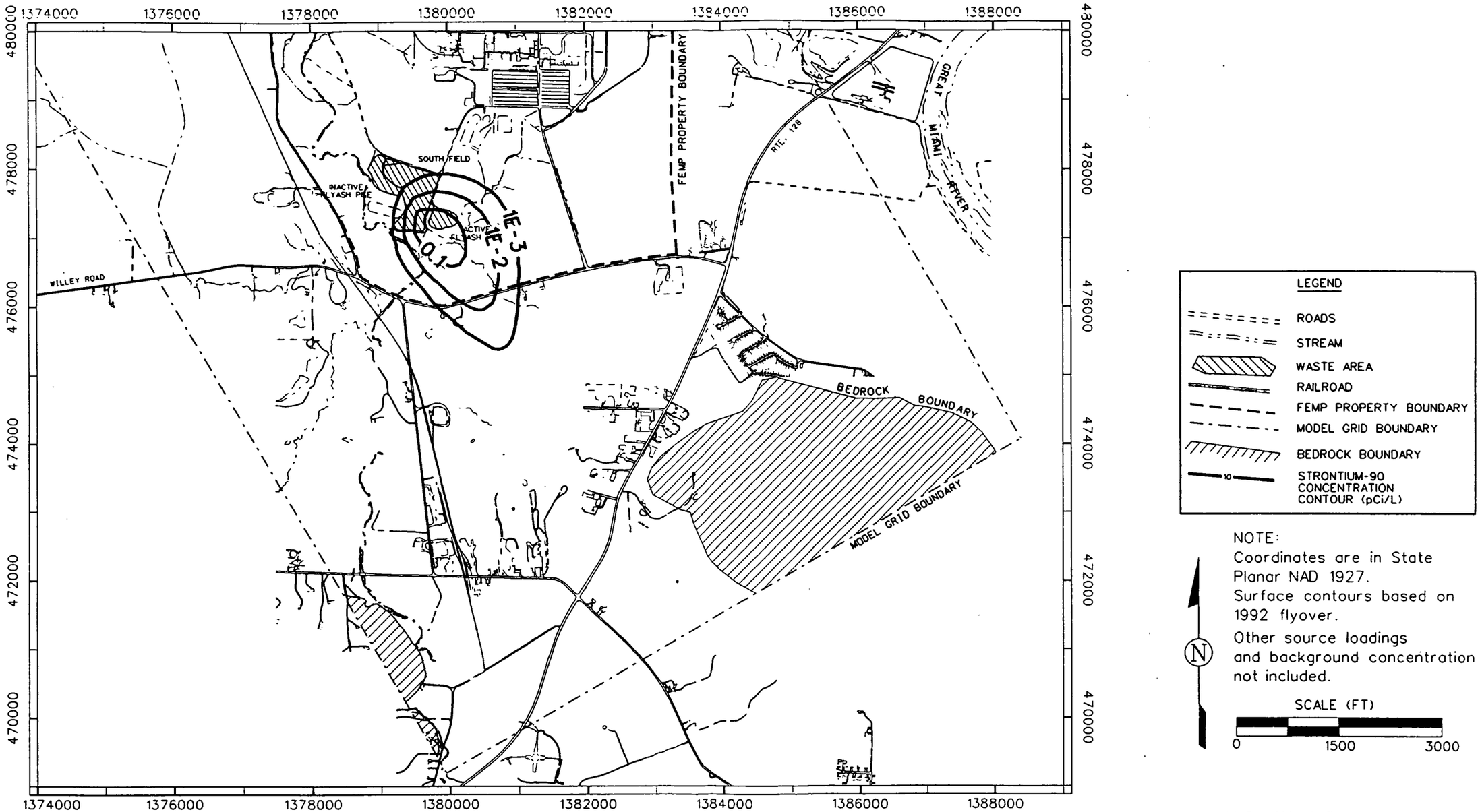

MAXIMUM INCREASE IN CONCENTRATION = 1.0 pCi/L

FIGURE A.2-55
PROJECTED INCREASE IN STRONTIUM-90 CONCENTRATION IN GREAT MIAMI AQUIFER AT 100 YEARS DUE TO LOADING FROM THE ACTIVE FLYASH PILE

figa0261.dgn

5659

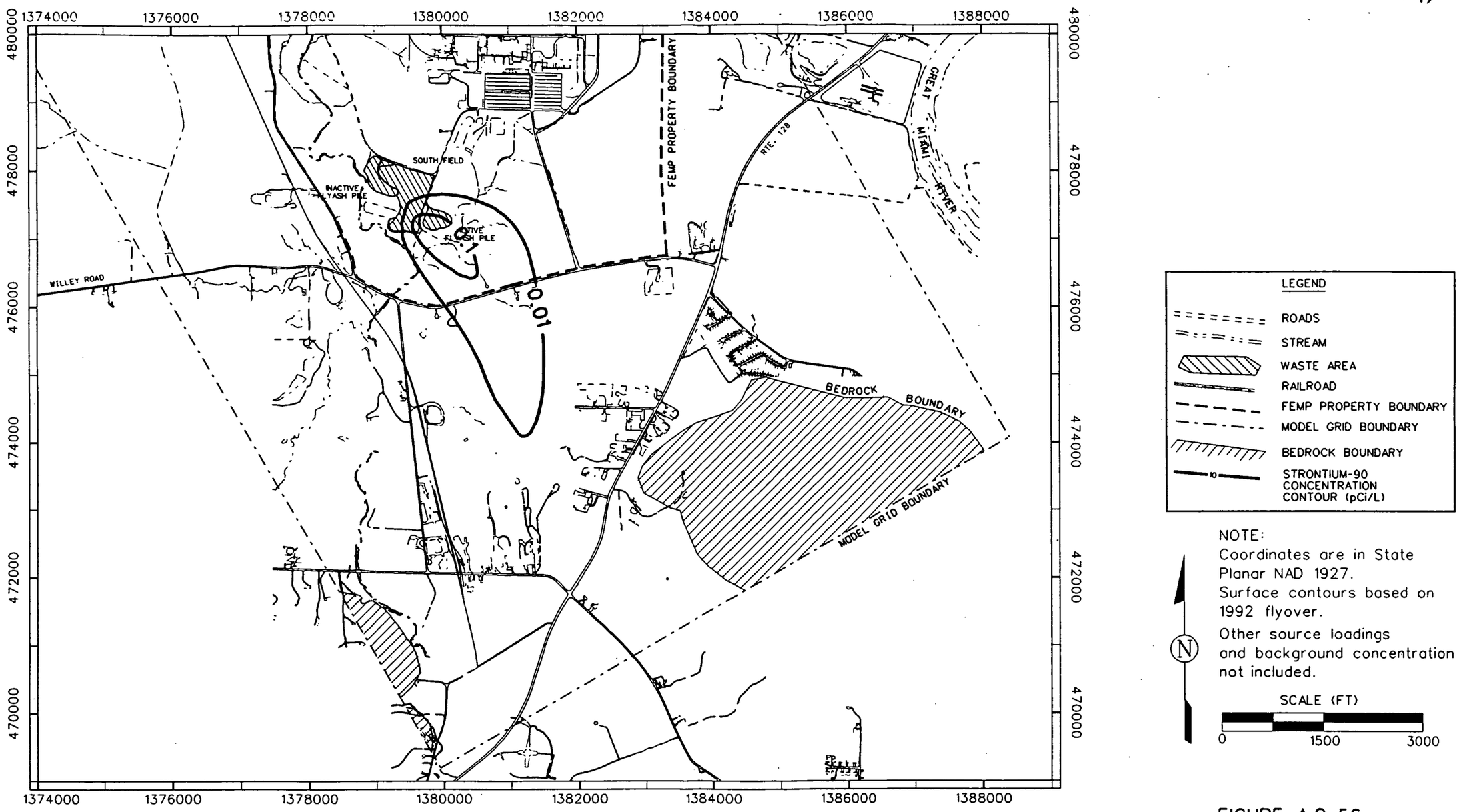

MAXIMUM INCREASE IN CONCENTRATION = 0.45 pCi/L

figa0262.dgn

FIGURE A.2-56
PROJECTED INCREASE IN STRONTIUM-90 CONCENTRATION IN GREAT MIAMI AQUIFER AT 160 YEARS DUE TO LOADING FROM THE ACTIVE FLYASH PILE

000268

5659

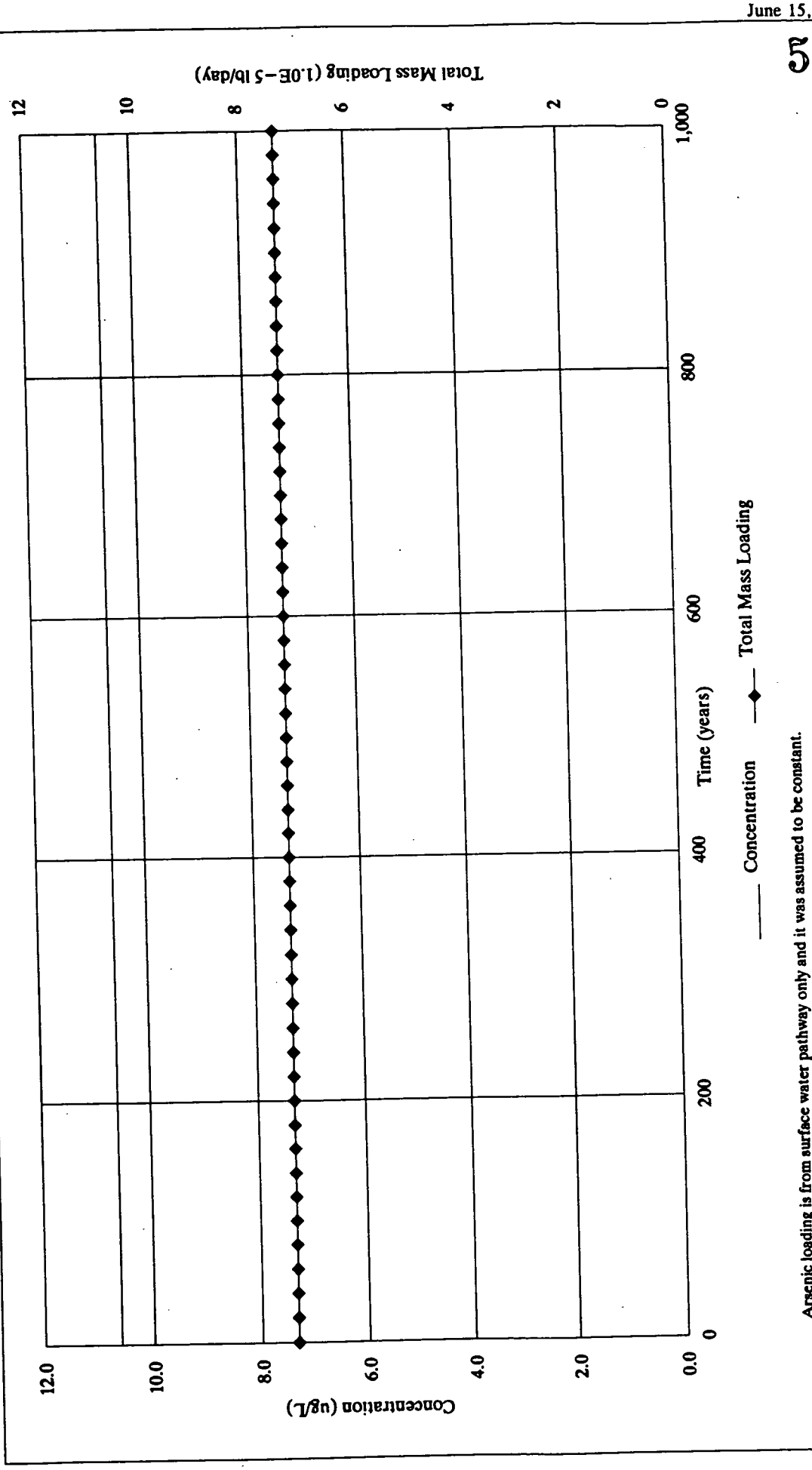

Arsenic loading is from surface water pathway only and it was assumed to be constant.

FIGURE A.2-57. ARSENIC LOADING TO THE GREAT MIAMI AQUIFER FROM THE ACTIVE FLYASH PILE

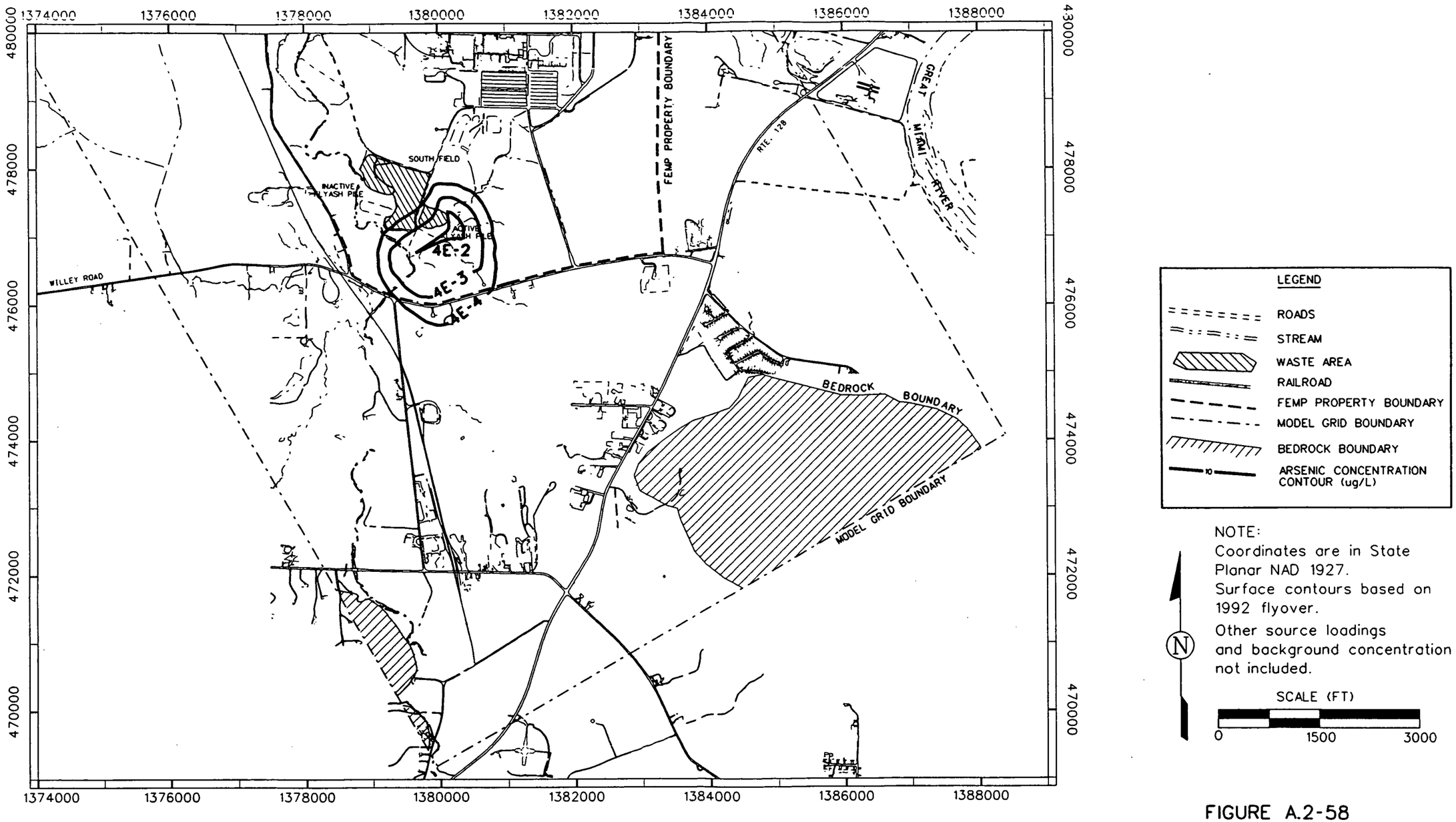

MAXIMUM INCREASE IN CONCENTRATION = 0.072 ug/L

FIGURE A.2-58
PROJECTED INCREASE IN ARSENIC CONCENTRATION IN GREAT MIAMI AQUIFER AT 1000 YEARS DUE TO LOADING FROM THE ACTIVE FLYASH PILE

figa0264.dgn

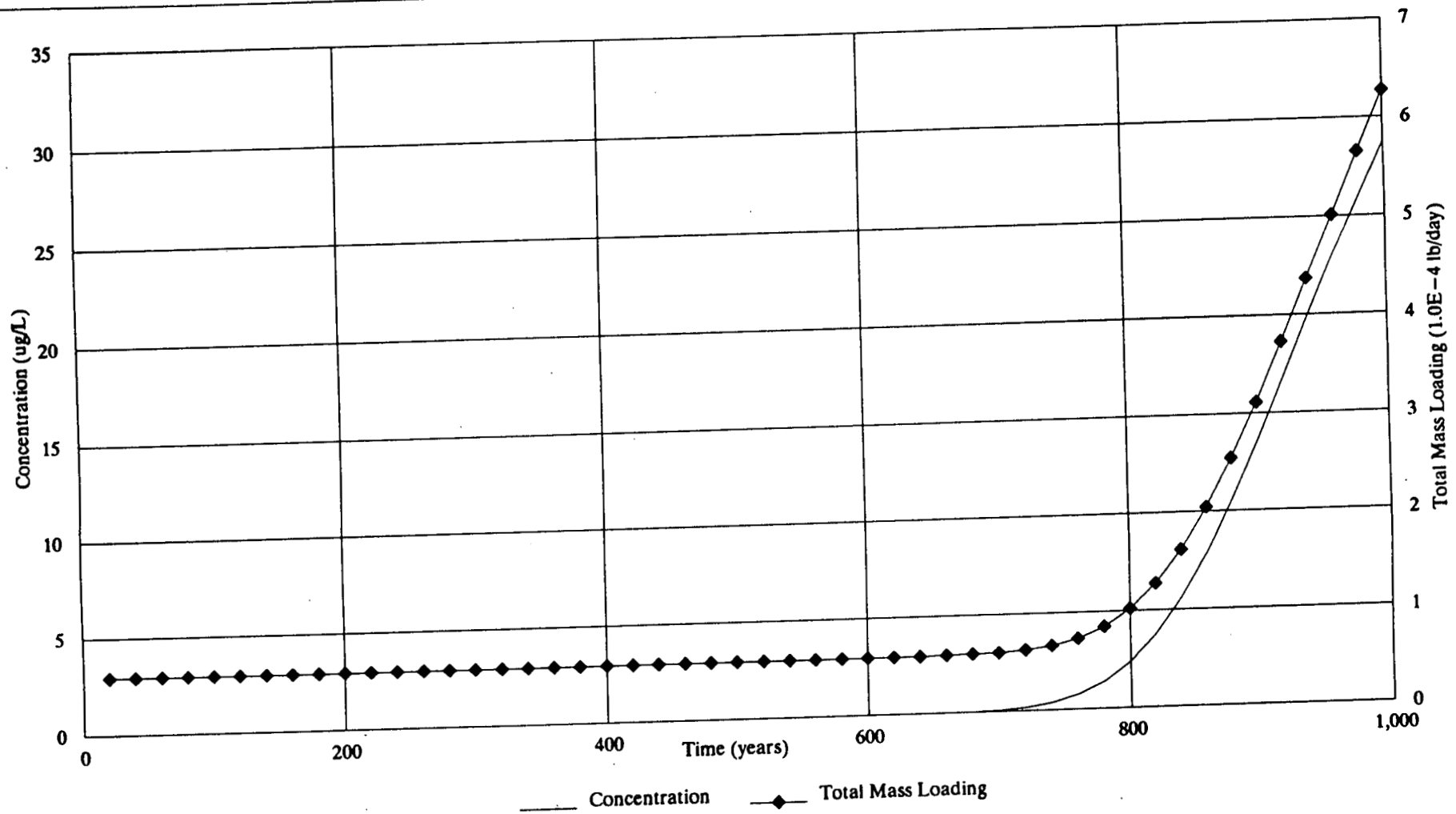

Maximum concentration (28.7 ug/L) occurs in grid block (31,57).

Concentrations are plotted for grid block (31,57).

FIGURE A.2–59. LEAD LOADING TO THE GREAT MIAMI AQUIFER FROM THE ACTIVE FLYASH PILE

5659

000271

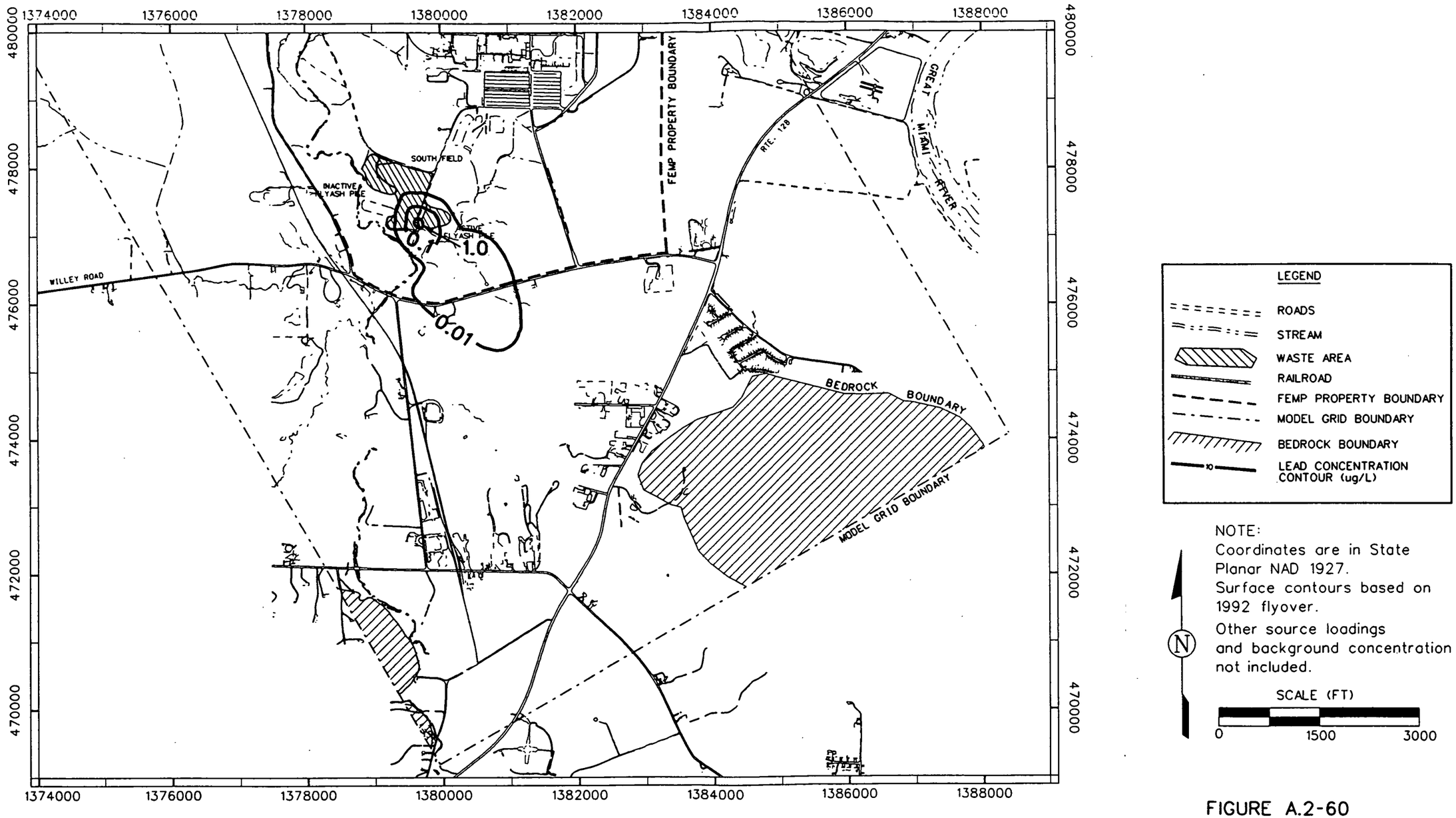

MAXIMUM INCREASE IN CONCENTRATION = 1.6 ug/L

FIGURE A.2-60
PROJECTED INCREASE IN LEAD CONCENTRATION IN GREAT MIAMI AQUIFER AT 1000 YEARS DUE TO LOADING FROM THE ACTIVE FLYASH PILE

figa0266.dgn

A-30

Pile. For uranium-238 and neptunium-237, the peak and most of the contaminant loading occurs before 400 years. Therefore, the center of the plume, as shown in Figures A.2-48 and A.2-53, has moved off the Active Flyash Pile at 1000 years. ~~Concentrations of strontium-90 and molybdenum at 1000 years are predicted to be below the 10^{-7} risk or 0.1 Hazard Index level. Therefore, no contours plots were produced for these two CPCs at 1000 years.~~

A.2.8.3.5 Combined Impact of All Operable Unit 2 Subunits

Subunits

Uranium isotopes, neptunium-237, technetium-99, and lead were the only constituents that were CPCs for groundwater from more than one subunit. Figures A.2-63 through A.2-66 show projected increase in concentrations of these CPCs at the time of maximum concentration in the Great Miami

NO. A-33

Aquifer. These figures present the overall impact of all ~~Operable Unit 2 subunits~~ applicable pathways for each Operable Unit 2 subunit. These figures were generated by adding the concentration contributions from individual subunits at the selected time.. These figures were generated at the time of maximum concentration on-site due to all Operable Unit 2 subunits. SWIFT results for each subunit were added at the selected time and then concentration contours were generated. For other constituents, which were CPCs from only one subunit, results are presented in Sections A.2.8.3.3 and A.2.8.3.4. Table A.2-54A provides the concentrations of all Operable Unit 2 CPCs for the Great Miami Aquifer at the location and time of uranium-238 maximums. Uranium-238 maximum time and location was selected because it has maximum influence on the baseline risk assessment.

A.2.9 MODELING RESULTS OF WASTE AT BACKGROUND CONCENTRATIONS

Modeling results presented so far are based on analytical results from soil samples and perched water samples in Operable Unit 2. This section presents results of vadose zone modeling if the waste and

NO. A-32

perched water were at background concentrations. Modeling using background concentrations was performed to test the level of conservativeness of the modeling methodology and check reasonableness of the assumptions. For example, if the 70-year rule was applied to the background soil concentrations, what Great Miami Aquifer concentrations would be predicted. Selected block(s) in each Operable Unit 2 subunits were modeled using ODAST to predict loading to the Great Miami Aquifer. Except for waste and perched water concentrations, the technical approach and parameters used in the modeling are same as presented in Sections A.2.1 through A.2.7. Leachate concentrations were estimated using the EPA 70-year rule. Only CPCs present in individual subunits and with non-zero background concentrations were modeled. No background concentrations were available for

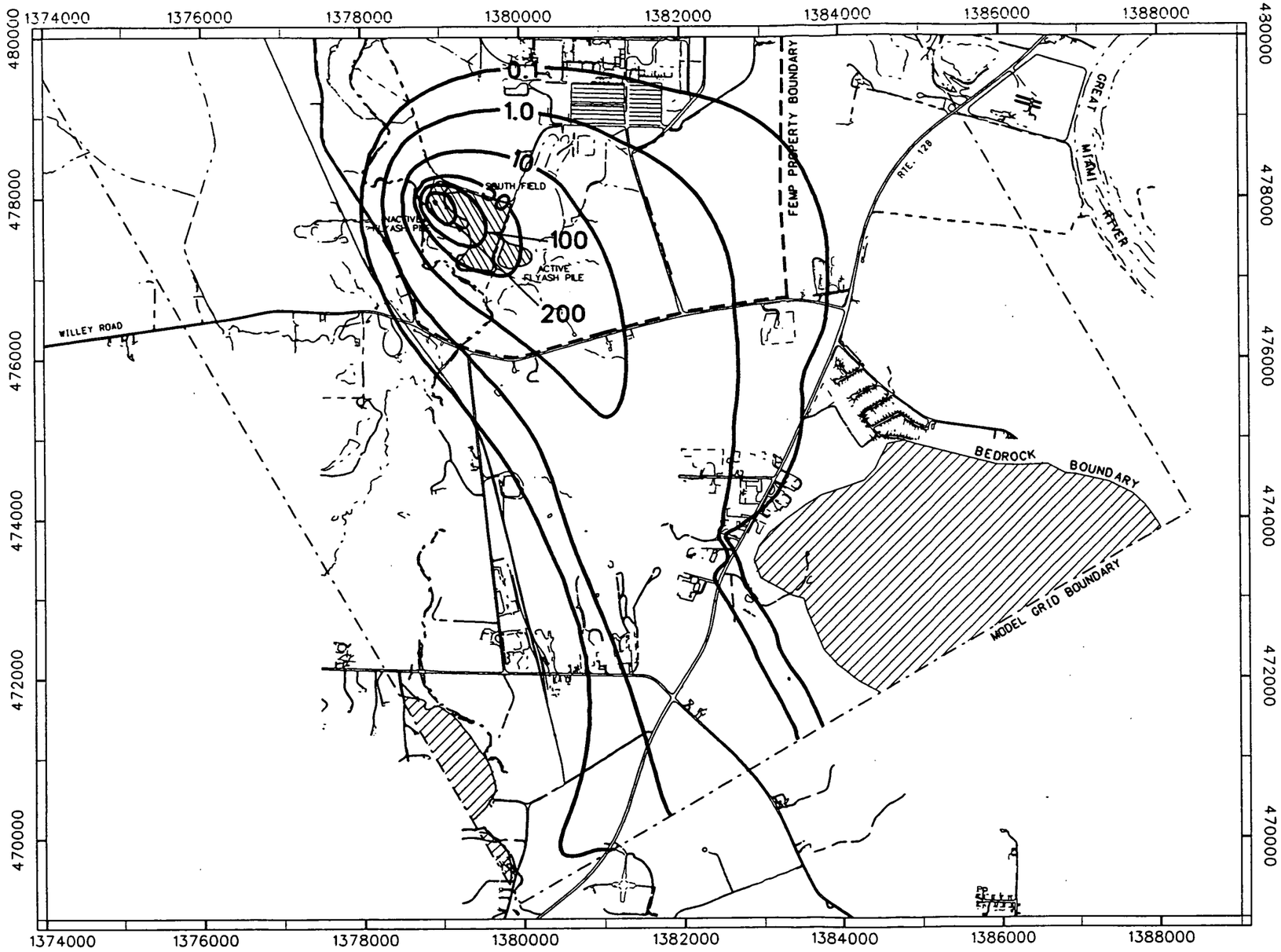

LEGEND

- ROADS
- STREAM
- WASTE AREA
- RAILROAD
- FEMP PROPERTY BOUNDARY
- MODEL GRID BOUNDARY
- BEDROCK BOUNDARY
- 10 URANIUM 238 CONCENTRATION CONTOUR (pCi/L)

NOTE:
Coordinates are in State Planar NAD 1927.
Surface contours based on 1992 flyover.
Other source loadings and background concentration not included.

N

SCALE (FT)
0 1500 3000

MAXIMUM INCREASE IN CONCENTRATION = 517 pCi/L

FIGURE A.2-63
PROJECTED INCREASE IN URANIUM-238 CONCENTRATION IN GREAT MIAMI AQUIFER AT 160 YEARS DUE TO LOADING FROM ALL AREA SUBUNITS

fig0a263.dgn

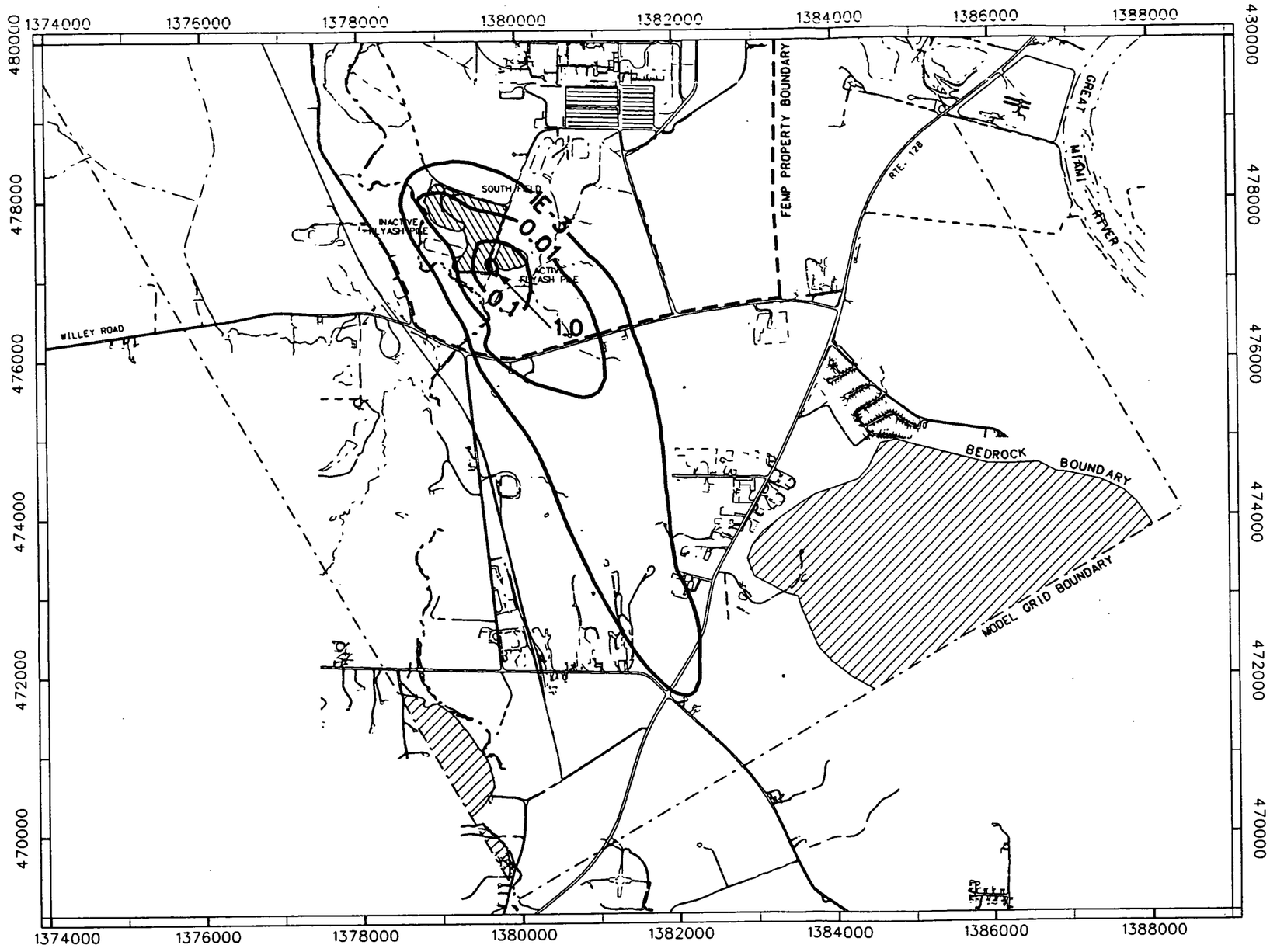

LEGEND

- ROADS
- STREAM
- WASTE AREA
- RAILROAD
- FEMP PROPERTY BOUNDARY
- MODEL GRID BOUNDARY
- BEDROCK BOUNDARY
- 10 NEPTUNIUM 237 CONCENTRATION CONTOUR (pCi/L)

NOTE:
Coordinates are in State Planar NAD 1927.
Surface contours based on 1992 flyover.
Other source loadings and background concentration not included.

N

SCALE (FT)
0 1500 3000

MAXIMUM INCREASE IN CONCENTRATION = 1.5 pCi/L

FIGURE A.2-64
PROJECTED INCREASE IN NEPTUNIUM-237 CONCENTRATION IN GREAT MIAMI AQUIFER AT 160 YEARS DUE TO LOADING FROM ALL AREA SUBUNITS

figa0270.dgn

LEGEND

- ROADS
- STREAM
- WASTE AREA
- RAILROAD
- FEMP PROPERTY BOUNDARY
- MODEL GRID BOUNDARY
- BEDROCK BOUNDARY
- 10 — TECHNETIUM-99 CONCENTRATION CONTOUR (pCi/L)

NOTE:
Coordinates are in State Planar NAD 1927.
Surface contours based on 1992 flyover.
Other source loadings and background concentrations not included.

N

SCALE (FT)
0 2000 4000

FIGURE A.2-65
PROJECTED INCREASE IN TECHNETIUM-99 CONCENTRATION IN GREAT MIAMI AQUIFER AT 40 YEARS DUE TO LOADING FROM ALL AREA SUBUNITS

figa0265.dgn

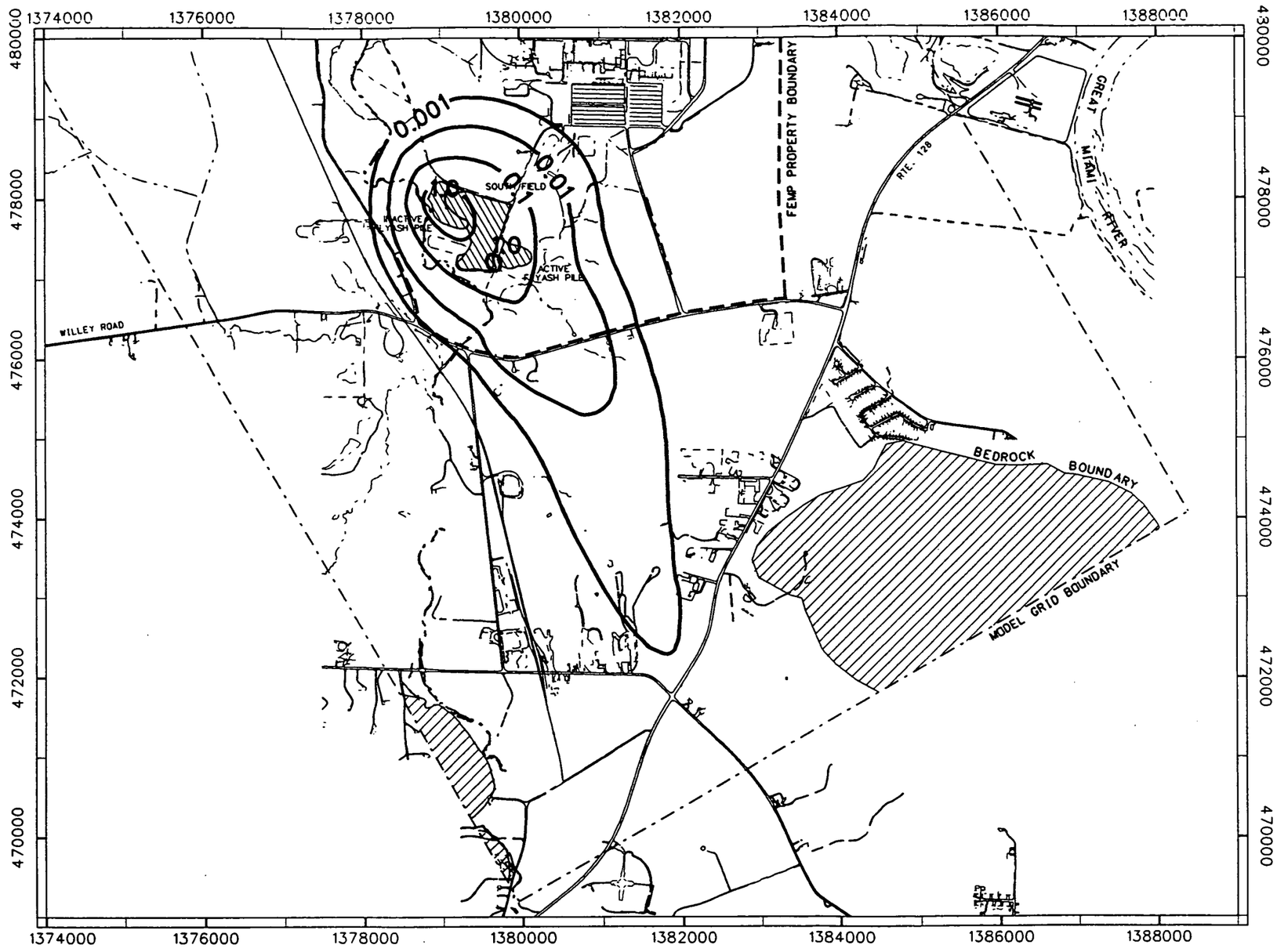

LEGEND

- ROADS
- STREAM
- WASTE AREA
- RAILROAD
- FEMP PROPERTY BOUNDARY
- MODEL GRID BOUNDARY
- BEDROCK BOUNDARY
- 10 LEAD CONCENTRATION CONTOUR (ug/L)

NOTE:
Coordinates are in State Planar NAD 1927.
Surface contours based on 1992 flyover.
Other source loadings and background concentration not included.

N

SCALE (FT)
0 1500 3000

MAXIMUM INCREASE IN CONCENTRATION = 4.9 ug/L

FIGURE A.2-66
PROJECTED INCREASE IN LEAD CONCENTRATION IN GREAT MIAMI AQUIFER AT 1000 YEARS DUE TO LOADING FROM ALL AREA SUBUNITS

figa0266.dgn

TABLE A.2-54

SUMMARY OF SWIFT MODELING RESULTS AT THE TIME AND LOCATION OF THE U-238 MAXIMUM CONCENTRATION FOR THE ACTIVE FLYASH PILE OPERABLE UNIT 2 REMEDIAL INVESTIGATION REPORT FERNALD ENVIRONMENTAL MANAGEMENT PROJECT

Constituents of Potential Concern	On-Site Concentration at 100 Years (pCi/L RAD) (μg/L non-RAD)	Concentration at the FEMP Boundary at 120 Years (pCi/L RAD) (μg/L non-RAD)	EPA RAGs, Part B Screening Levels (pCi/L RAD) (μg/L non-RAD)
RADIONUCLIDES			
Neptunium-237	3.14×10^{-4}	2.52×10^{-2}	2.16×10^{-2}
Strontium-90	5.47×10^{-1}	5.19×10^{-2}	1.32×10^{-1}
Uranium-234[a]	$1.98 \times 10^{+1}$	2.58×10^{0}	2.97×10^{-1}
Uranium-235/236[a]	1.05×10^{0}	1.38×10^{-1}	2.97×10^{-1}
Uranium-238	$2.18 \times 10^{+1}$	2.85×10^{0}	1.70×10^{-1}
Uranium - Total (non-RAD)[a]	$7.76 \times 10^{+1}$	$1.02 \times 10^{+1}$	$1.09 \times 10^{+1}$
ORGANICS			
2-Methylnaphthalene[b]	$1.95 \times 10^{+0}$	$1.95 \times 10^{+0}$	NA[c]
INORGANICS			
Arsenic	1.84×10^{-10}	7.46×10^{-5}	1.46×10^{-4}
Beryllium	1.82×10^{-12}	1.46×10^{-6}	2.37×10^{-4}
Lead	2.06×10^{-6}	5.82×10^{-3}	NA

[a]Uranium-234, uranium-235/236, and total uranium were modeled by applying ratios to uranium-238 results

[b]2-Methylnaphthalene was not modeled using SWIFT because EPA RAGs, Part B screening values cannot be calculated. Reported concentrations are predicted leachate values. If concentrations are needed for risk assessment in future, ODAST/SWIFT model or equivalent should be used to calculate the concentrations in the Great Miami Aquifer.
[c]NA = No data available to calculate EPA RAGs, Part B screening values.
Other Comment No. A-48

565 9

TABLE A.2-54A

SUMMARY OF SWIFT MODELING RESULTS AT THE TIME AND LOCATION OF THE U-238 MAXIMUM CONCENTRATION FOR ALL OPERABLE UNIT 2 SUBUNITS OPERABLE UNIT 2 REMEDIAL INVESTIGATION REPORT FERNALD ENVIRONMENTAL MANAGEMENT PROJECT

Constituent of Potential Concern	Units	On-Site Concentration at 160 Years	Concentration at the FEMP Boundary	EPA RAGs, Part B Screening Concentration
		RADIONUCLIDES		
Neptunium-237	pCi/L	1.90×10^{-2}	2.00×10^{-2}	2.16×10^{-2}
Radium-226	pCi/L	0.0	0.0	1.76×10^{-4}
Strontium-90	pCi/L	2.72×10^{-2}	5.00×10^{-2}	1.32×10^{-1}
Technetium-99	pCi/L	$1.80 \times 10^{+0}$	9.81×10^{-1}	$3.65 \times 10^{+0}$
Uranium-234	pCi/L	$4.69 \times 10^{+2}$	$2.54 \times 10^{+1}$	2.97×10^{-1}
Uranium-235/236	pCi/L	$2.50 \times 10^{+1}$	$1.35 \times 10^{+0}$	2.97×10^{-1}
Uranium-238	pCi/L	$5.17 \times 10^{+2}$	$2.80 \times 10^{+1}$	1.70×10^{-1}
Total Uranium (non-RAD)	μg/L	$1.84 \times 10^{+3}$	$9.98 \times 10^{+1}$	$1.09 \times 10^{+1}$
		ORGANICS		
2-Methylnaphthalene	μg/L	3.55×10^{-3}	5.25×10^{-5}	NA[a]
Benzo(g,h,i)perylene	μg/L	0.0	0.0	NA
Phenanthrene	μg/L	0.0	0.0	NA
Tributyl phosphate	μg/L	1.67×10^{-1}	3.11×10^{-6}	NA
		INORGANICS		
Arsenic	μg/L	0.0	1.00×10^{-4}	1.46×10^{-4}
Beryllium	μg/L	0.0	1.00×10^{-5}	2.37×10^{-4}
Lead	μg/L	$1.43 \times 10^{+0}$	2.00×10^{-2}	NA

[a]NA = No data available to calculate EPA RAGs, Part B screening concentrations

Comment No. A-33

organic CPCs and these were not expected to be present in the background soils and perched water. Therefore, no organic CPCs were modeled. Physical parameters including waste size and infiltration rates were assumed to remain at current conditions.

A.2.9.1 Solid Waste Landfill

Grid cell (51,91), the grid cell with the highest waste volume (Table A.2-1), was selected for background modeling in the Solid Waste Landfill. Table A.2-55 shows the summary of vadose zone modeling results if waste and perched water concentrations were at background levels. Table A.2-55 shows that the impact of the Solid Waste Landfill waste at background levels is negligible on the Great Miami Aquifer within 1000 years. ~~Only cyanide was predicted to reach the Great Miami Aquifer at 1.1 x 10^{-3} μg/L concentration, which is approximately 4 orders of magnitude lower than the 10^{-7} risk or 0.1 Hazard Index concentration (Table A.2-55).~~

NO. A-48

A.2.9.2 Lime Sludge Ponds

Grid cell (44,89), the grid cell with highest waste volume (Table A.2-2), was selected for background modeling in the Lime Sludge Ponds. Table A.2-56 shows the summary of vadose zone modeling results if waste and perched water concentrations were at background levels. Table A.2-56 shows that the impact of the Lime Sludge Ponds waste at background levels is negligible on the Great Miami Aquifer within 1000 years. Only strontium-90~~, mercury, and cyanide were~~ was predicted to reach the Great Miami Aquifer within 1000 years~~ at non-zero concentrations. However, all are below the 10^{-7} risk or 0.1 Hazard Index concentration (Table A.2-56).~~ However, strontium-90 concentration is more than three orders of magnitude below the screening concentration.

NO. A-48

A.2.9.3 Inactive Flyash Pile and South Field

Three grid cells were selected for background modeling in the Inactive Flyash Pile and South Field. Grid cell (31,60) represents a typical South Field grid cell where waste is underlain by the glacial overburden. Only the vadose zone and perched water vertical infiltration pathways are applicable to this grid cell. Grid cell (30,61) does not have glacial overburden beneath the waste. The vadose zone pathway including lateral drainage from other grid cells was simulated for the background modeling. Grid cell (29,65) receives the maximum flow of perched water subsurface seeps. This cell also receives lateral drainage. The vadose zone pathway (including lateral drainage) and perched water subsurface seep pathways were modeled for grid cell (29,65). Perched water subsurface seeps were modeled at background perched water concentrations. Table A.2-57 shows the summary of

TABLE A.2-55

SUMMARY OF VADOSE ZONE MODELING RESULTS IF WASTE AND PERCHED WATER CONCENTRATIONS WERE AT BACKGROUND LEVELS, SOLID WASTE LANDFILL OPERABLE UNIT 2 REMEDIAL INVESTIGATION REPORT FERNALD ENVIRONMENTAL MANAGEMENT PROJECT

Constituent	Units for Groundwater Concentration	Screening Concentration	Subsurface Soils Background Concentration (mg/kg non-RAD) (pCi/g RAD)	Perched Water Background Concentration	Predicted Maximum GMA Concentration	Critical CPC
RADIONUCLIDES						
Lead-210	pCi/L	7.20×10^{-3}	5.64×10^{-1}	0.00	0.00	NO
Radium-224	pCi/L	1.25×10^{-1}	6.62×10^{-1}	0.00	0.00	NO
Radium-226	pCi/L	1.76×10^{-4}	7.80×10^{-1}	$1.00 \times 10^{+0}$	0.00	NO
Radium-228	pCi/L	4.75×10^{-3}	8.52×10^{-1}	$4.50 \times 10^{+0}$	0.00	NO
Thorium-228	pCi/L	8.64×10^{-4}	8.82×10^{-1}	$1.04 \times 10^{+0}$	0.00	NO
Thorium-230	pCi/L	3.65×10^{-1}	$1.24 \times 10^{+0}$	$2.00 \times 10^{+0}$	0.00	NO
Thorium-232	pCi/L	2.79×10^{-4}	8.05×10^{-1}	0.00	0.00	NO
Uranium-234	pCi/L	2.97×10^{-1}	8.44×10^{-1}	$1.06 \times 10^{+0}$	0.00	NO
Uranium-235/236	pCi/L	2.97×10^{-1}	7.60×10^{-2}	0.00	0.00	NO
Uranium-238	pCi/L	1.70×10^{-1}	8.44×10^{-1}	$1.07 \times 10^{+0}$	0.00	NO
Total Uranium	μg/L	$1.09 \times 10^{+3}$	$2.54 \times 10^{+0}$	$3.22 \times 10^{+0}$	0.00	NO
INORGANICS						
Arsenic	μg/L	1.46×10^{-4}	$5.64 \times 10^{+0}$	$1.50 \times 10^{+1}$	0.00	NO
Beryllium	μg/L	2.37×10^{-4}	4.80×10^{-1}	$1.80 \times 10^{+0}$	0.00	NO
Lead	μg/L	NA[a]	$9.52 \times 10^{+0}$	$2.70 \times 10^{+0}$	0.00	NO

[a]No data available to calculate EPA RAGs, Part B screening value for lead.

Comment No. A-48

TABLE A.2-56

SUMMARY OF VADOSE ZONE MODELING RESULTS IF WASTE AND PERCHED WATER CONCENTRATIONS WERE AT BACKGROUND LEVELS, LIME SLUDGE PONDS OPERABLE UNIT 2 REMEDIAL INVESTIGATION REPORT FERNALD ENVIRONMENTAL MANAGEMENT PROJECT

Constituent	Units for Groundwater Concentration	Screening Concentration	Subsurface Soils Background Concentration (mg/kg non-RAD) pCi/g RAD)	Perched Water Background Concentration	Predicted Maximum GMA Concentration	Critical CPC
RADIONUCLIDES						
Radium-226	pCi/L	1.76×10^{-4}	7.80×10^{-1}	$1.00 \times 10^{+0}$	0.00	No
Radium-228	pCi/L	4.75×10^{-2}	8.52×10^{-1}	$4.50 \times 10^{+0}$	0.00	No
Strontium-90	pCi/L	1.32×10^{-1}	5.60×10^{-1}	0.00	4.92×10^{-5}	No
Thorium-228	pCi/L	8.64×10^{-2}	8.82×10^{-1}	$1.04 \times 10^{+0}$	0.00	No
Thorium-230	pCi/L	3.65×10^{-1}	$1.24 \times 10^{+0}$	$2.00 \times 10^{+0}$	0.00	No
Thorium-232	pCi/L	2.79×10^{-2}	8.05×10^{-1}	0.00	0.00	No
Uranium-234	pCi/L	2.97×10^{-1}	8.44×10^{-1}	$1.06 \times 10^{+0}$	0.00	No
Uranium-235/236	pCi/L	2.97×10^{-1}	7.60×10^{-2}	0.00	0.00	No
Uranium-238	pCi/L	1.70×10^{-1}	8.44×10^{-1}	$1.07 \times 10^{+0}$	0.00	No
Total Uranium	µg/L	$1.09 \times 10^{+1}$	$2.54 \times 10^{+0}$	$3.22 \times 10^{+0}$	0.00	No
INORGANICS						
Arsenic	µg/L	1.46×10^{-4}	$5.64 \times 10^{+0}$	$1.50 \times 10^{+1}$	0.00	No
Beryllium	µg/L	2.37×10^{-4}	4.80×10^{-1}	$1.80 \times 10^{+0}$	0.00	No
Lead	µg/L	NA[a]	$9.52 \times 10^{+0}$	$2.70 \times 10^{+0}$	0.00	No

[a]No data available to calculate EPA RAGs, Part B screening value for lead.

Comment No. A-48

FER\CRU2RI\JLG\APP-A\TABA2-56\June7, 1994 7:16pm

TABLE A.2-57

SUMMARY OF VADOSE ZONE MODELING RESULTS IF WASTE AND PERCHED WATER CONCENTRATIONS WERE AT BACKGROUND LEVELS, INACTIVE FLYASH PILE AND SOUTH FIELD OPERABLE UNIT 2 REMEDIAL INVESTIGATION REPORT FERNALD ENVIRONMENTAL MANAGEMENT PROJECT

					Waste Underlain by Till		Vertical and Lateral Drainage Loading		Vertical and Lateral Drainage and Perched Water Subsurface Seep Loading			
Constituent	Units for Groundwater Concentration	Screening Concentration	Subsurface Soils Background Concentration (mg/kg non-RAD) (pCi/g RAD)	Perched Water Background Concentration	Predicted Maximum GMA Concentration	Critical CPC	Predicted Maximum GMA Concentration	Critical CPC	Vadose Zone Pathway Concentration	Critical CPC	Perched Water Subsurface Seep Pathway Concentration	Critical CPC
RADIONUCLIDES												
Lead-210	pCi/L	7.20×10^{-2}	5.64×10^{-1}	0.0	0.0	NO	0.0	NO	0.0	NO	0.0	NO
Radium-224	pCi/L	1.25×10^{-1}	6.62×10^{-1}	0.0	0.0	NO	0.0	NO	0.0	NO	0.0	NO
Radium-226	pCi/L	1.76×10^{-2}	7.80×10^{-1}	$1.00 \times 10^{+0}$	0.0	NO	0.0	NO	0.0	NO	6.32×10^{-1}	YES
Radium-228	pCi/L	4.75×10^{-2}	8.52×10^{-1}	$4.50 \times 10^{+0}$	0.0	NO	0.0	NO	0.0	NO	0.0	NO
Strontium-90	pCi/L	1.32×10^{-1}	5.60×10^{-1}	0.0	0.0	NO	8.65×10^{-1}	YES	$2.07 \times 10^{+0}$	YES	0.0	NO
Thorium-228	pCi/L	8.64×10^{-2}	8.82×10^{-1}	$1.04 \times 10^{+0}$	0.0	NO	0.0	NO	0.0	NO	0.0	NO
Thorium-230	pCi/L	3.65×10^{-1}	$1.24 \times 10^{+0}$	$2.00 \times 10^{+0}$	0.0	NO	0.0	NO	0.0	NO	0.0	NO
Thorium-232	pCi/L	2.79×10^{-2}	8.05×10^{-1}	0.0	0.0	NO	0.0	NO	0.0	NO	0.0	NO
Uranium-234	pCi/L	2.97×10^{-1}	8.44×10^{-1}	$1.06 \times 10^{+0}$	0.0	NO	$1.52 \times 10^{+1}$	YES	$1.87 \times 10^{+2}$	YES	9.89×10^{-1}	YES
Uranium-235/236	pCi/L	2.97×10^{-1}	7.60×10^{-2}	0.0	0.0	NO	$1.37 \times 10^{+0}$	YES	$1.69 \times 10^{+1}$	YES	0.0	NO
Uranium-238	pCi/L	1.70×10^{-1}	8.44×10^{-1}	$1.07 \times 10^{+0}$	0.0	NO	$1.52 \times 10^{+1}$	YES	$1.87 \times 10^{+2}$	YES	$1.00 \times 10^{+0}$	YES
Total Uranium	ug/L	$1.09 \times 10^{+1}$	$2.54 \times 10^{+0}$	$3.22 \times 10^{+0}$	0.0	NO	$4.57 \times 10^{+1}$	YES	$5.64 \times 10^{+2}$	YES	$3.01 \times 10^{+0}$	NO
INORGANICS												
Arsenic	ug/L	1.46×10^{-2}	$5.64 \times 10^{+0}$	$1.50 \times 10^{+1}$	0.0	NO	0.0	NO	0.0	NO	6.44×10^{-5}	NO
Beryllium	ug/L	2.37×10^{-2}	4.80×10^{-1}	$1.80 \times 10^{+0}$	0.0	NO	0.0	NO	0.0	NO	0.0	NO
Lead	ug/L	NA[a]	$9.52 \times 10^{+0}$	$2.70 \times 10^{+0}$	0.0	NO	8.98×10^{-4}	NA	0.0	NO	$2.52 \times 10^{+0}$	NA

[a]NA = No data available to calculate EPA RAGs, Part B screening value for lead.

Comment No. A-34

vadose zone modeling results if waste and perched water concentrations were at background levels. Table A.2-57 shows that the impact of the waste at background levels is negligible on the Great Miami Aquifer within 1000 years if waste is underlain by glacial till. However, when waste at background concentrations is left in-place where glacial till is not present, concentrations of certain CPCs exceed screening concentrations ~~based on 10^{-7} risk or 0.1 Hazard Index~~ (Table A.2-57). In grid cell (30,61), where lateral drainage was simulated, uranium isotopes, total uranium, ~~strontium-90, barium, and cadmium~~ and strontium-90 concentrations exceed screening concentrations. In grid cell (29,65), which receives perched water subsurface seep water, uranium isotopes, total uranium, radium-226, ~~strontium-90, cadmium, chromium, lead, manganese, and molybdenum~~ and strontium-90 concentrations exceed screening concentrations.

NO. A-48

NO. A-48

Table A.2-57A shows the concentrations in the Great Miami Aquifer of the CPCs above screening concentrations in Table A.2-47. Concentrations are reported at the uranium-238 maximum (on-site and FEMP boundary) locations and time. These concentrations were estimated from the results reported in Tables A.2-51 and A.2-52 by applying a scaling factor equal to the ratio of ODAST output for background modeling to the ODAST output for the waste at current conditions. Table A.2-57A shows that except uranium-238, all CPCs are below the screening concentrations. Predicted maximum uranium-238 concentration in the Great Miami Aquifer was 0.18 pCi/L compared to a screening concentration of 0.17 pCi/L for uranium-238.

NO. A-47

A.2.9.4 Active Flyash Pile

Two grid cells were selected for background modeling in the Active Flyash Pile. Grid cell (32,57) represents a typical active Flyash Pile grid cell where flyash is underlain by the glacial till. Only the vadose zone and perched water vertical infiltration pathways are applicable to this grid cell. Grid cell (32,56) does not have glacial overburden beneath the flyash. The vadose zone pathway including lateral drainage from other grid cells was simulated for the background modeling. Table A.2-58 shows the summary of vadose zone modeling results if flyash and perched water concentrations are at background levels. Table A.2-58 shows that the impact of the flyash at background level is negligible on the Great Miami Aquifer within 1000 years if flyash is underlain by glacial till. However, when flyash at background concentrations is left in-place where glacial overburden is not present, concentrations of ~~certain CPCs exceed screening concentrations 10^{-7} risk or 0.1 Hazard Index (Table A.2-58). In grid cell (32, 56), where lateral drainage was simulated, uranium isotopes, total uranium, strontium-90, barium, and cadmium concentrations exceed screening concentrations~~ uranium isotopes,

NO. A-48

5659

TABLE A.2-57A

SUMMARY OF THE IMPACT TO THE GREAT MIAMI AQUIFER IF WASTE AND PERCHED WATER WERE AT BACKGROUND CONCENTRATIONS, INACTIVE FLYASH PILE AND SOUTH FIELD OPERABLE UNIT 2 REMEDIAL INVESTIGATION REPORT FERNALD ENVIRONMENTAL MANAGEMENT PROJECT

Constituent of Potential Concern	Units	On-Site Maximum Concentration at Uranium-238 Maximum Location and at 160 Years	FEMP Boundary Maximum Concentration at Uranium-238 Maximum Location and at 220 Years	EPA RAGs, Part B Screening Concentration
		RADIONUCLIDES		
Radium-226	pCi/L	0.0	0.0	1.76×10^{-4}
Strontium-90	pCi/L	3.67×10^{-3}	3.04×10^{-4}	1.32×10^{-1}
Uranium-234	pCi/L	1.78×10^{-1}	9.11×10^{-3}	2.97×10^{-1}
Uranium-235/236	pCi/L	1.61×10^{-2}	8.23×10^{-4}	2.97×10^{-1}
Uranium-238	pCi/L	1.78×10^{-1}	9.11×10^{-3}	1.70×10^{-1}
Total Uranium (non-RAD)	ug/L	5.36×10^{-1}	2.75×10^{-2}	$1.09 \times 10^{+1}$
		INORGANICS		
Arsenic	ug/L	6.42×10^{-2}	9.21×10^{-16}	NA

NA = No data available to calculate EPA RAGs, Part B screening concentration

Other Comment No. A-48

TABLE A.2-58

SUMMARY OF VADOSE ZONE MODELING RESULTS IF WASTE AND PERCHED WATER CONCENTRATIONS WERE AT BACKGROUND LEVELS, ACTIVE FLYASH PILE OPERABLE UNIT 2 REMEDIAL INVESTIGATION REPORT FERNALD ENVIRONMENTAL MANAGEMENT PROJECT

					Flyash Directly on Unsaturated GMA		Flyash Underlain by Till			
Constituent	Units for Groundwater Concentrations	Screening Concentration	Subsurface Soils Background Concentration (mg/kg non-RAD) (pCi/g RAD)	Perched Water Background Concentration	Predicted GMA Concentration	Critical CPC	Vadose Pathway Predicted GMA Concentration	Critical CPC	Perched Water Pathway Predicted GMA Concentration	Critical CPC
RADIONUCLIDES										
Lead-210	pCi/L	7.20×10^{-3}	5.64×10^{-1}	0.0	0.0	NO	0.0	NO	0.0	NO
Radium-224	pCi/L	1.25×10^{-1}	6.62×10^{-1}	0.0	0.0	NO	0.0	NO	0.0	NO
Radium-226	pCi/L	1.76×10^{-4}	7.80×10^{-1}	$1.00 \times 10^{+0}$	0.00	NO	0.0	NO	0.0	NO
Radium-228	pCi/L	4.75×10^{-2}	8.52×10^{-1}	$4.50 \times 10^{+0}$	0.0	NO	0.0	NO	0.0	NO
Strontium-90	pCi/L	1.32×10^{-1}	5.60×10^{-1}	0.0	$4.91 \times 10^{+0}$	YES	1.43×10^{-6}	NO	0.0	NO
Thorium-228	pCi/L	8.64×10^{-2}	8.82×10^{-1}	$1.04 \times 10^{+0}$	0.0	NO	0.0	NO	0.0	NO
Thorium-230	pCi/L	5.65×10^{-1}	$1.24 \times 10^{+0}$	$2.00 \times 10^{+0}$	0.0	NO	0.0	NO	0.0	NO
Thorium-232	pCi/L	2.79×10^{-3}	8.05×10^{-1}	0.0	0.0	NO	0.0	NO	0.0	NO
Uranium-234	pCi/L	2.97×10^{-1}	8.44×10^{-1}	$1.06 \times 10^{+0}$	$7.90 \times 10^{+1}$	YES	0.0	NO	2.37×10^{-4}	NO
Uranium-235/236	pCi/L	2.97×10^{-1}	7.60×10^{-2}	0.0	$7.13 \times 10^{+0}$	YES	0.0	NO	3.60×10^{-5}	NO
Uranium-238	pCi/L	1.70×10^{-1}	8.44×10^{-1}	$1.07 \times 10^{+0}$	$7.93 \times 10^{+1}$	YES	0.0	NO	2.48×10^{-4}	NO
Total Uranium	ug/L	$1.09 \times 10^{+1}$	$2.54 \times 10^{+0}$	3.22×10^{-3}	$2.38 \times 10^{+2}$	YES	0.0	NO	1.13×10^{-3}	NO
INORGANICS										
Arsenic	ug/L	1.46×10^{-4}	$5.64 \times 10^{+0}$	$1.50 \times 10^{+1}$	0.0	NO	0.0	NO	0.0	NO
Beryllium	ug/L	2.37×10^{-4}	4.80×10^{-1}	$1.80 \times 10^{+0}$	0.0	NO	0.0	NO	0.0	NO

FER\CRU2RI\ULG\APP-A\TABA2-58\June7, 1994 7:12pm

000286

TABLE A.2-58
(Continued)

Constituent	Units for Groundwater Concentrations	Screening Concentration	Subsurface Soils Background Concentration (mg/kg non-RAD) (pCi/g RAD)	Perched Water Background Concentration	Flyash Directly on Unsaturated GMA: Predicted GMA Concentration	Flyash Directly on Unsaturated GMA: Critical CPC	Flyash Underlain by Till: Vadose Pathway Predicted GMA Concentration	Flyash Underlain by Till: Vadose Pathway Critical CPC	Flyash Underlain by Till: Perched Water Pathway Predicted GMA Concentration	Flyash Underlain by Till: Perched Water Pathway Critical CPC
INORGANICS (Continued)										
Lead	ug/L	NA[a]	$9.52 \times 10^{+0}$	$2.70 \times 10^{+0}$	6.79×10^{-3}	NA	0.0	NO	0.0	NO
Thallium	ug/L	2.55×10^{-1}	4.90×10^{-1}	N/A[b]	0.0	NO	0.0	NO	0.0	NO

[a]NA - No data available to calculate EPA RAGs, Part B screening value for lead.

[b]N/A - Not analyzed, assumed to be zero.

Comment No. A-48

~~strontium-90, barium, and cadmium concentrations exceed screening concentrations~~ uranium isotopes, total uranium, and strontium-90 exceed EPA RAGs, Part B screening concentrations.

NO. A-47

Table A.2-58A shows the concentrations in the Great Miami Aquifer of the CPCs above screening concentrations in Table A.2-48. Concentrations are reported at the uranium-238 maximum (on-site and FEMP boundary) locations and time. These concentrations were estimated from the results reported in Tables A.2-53 and A.2-54 by applying a scaling factor equal to the ratio of ODAST output for background modeling to the ODAST output for the waste at current conditions. Table A.2-58A shows that maximum concentrations of uranium isotopes and strontium-90 can exceed screening concentrations.

A.2.10 UNCERTAINTY IN MODELING RESULTS

The groundwater fate and transport modeling performed for Operable Unit 2 is subject to uncertainty and variability due to factors such as the limited compound-specific characterization data, the inability of the models to simulate natural systems with 100 percent accuracy, and the assumptions for future site conditions for the waste units. Of these factors, the assumptions made for the future conditions of the waste units have the most impact on the modeling results. The waste units are all assumed to release contaminants to the environment without future maintenance. This is a worst-case scenario and thus yields higher contamination levels than would be considered if a vegetative cover or cap was constructed. However, this type of assumption is the primary premise in performing a baseline assessment and the most conservative for the purpose of evaluating the risk from the groundwater pathway.

The inherent assumptions built into the models and the assumptions made to develop input parameters for the models also have an impact on the final results. Some general uncertainties associated with modeling can be attributed to the following sources:

- Source terms for the modeling were defined based on analytical results from the soil and water samples collected during the RI/FS field investigations. It was assumed that these concentrations are representative of CPC concentrations in the past. Although CPC concentrations in the past may have exceeded the present concentrations or some hot spots may not have been identified, use of the UCL concentration may counter the uncertainties introduced by using analytical results from the RI/FS field investigation.

- Except for uranium-238, the total mass of each constituent is estimated by multiplying the UCL by the volume of the entire waste area, thus assuming the UCL concentration is

TABLE A.2-58A

SUMMARY OF THE IMPACT TO THE GREAT MIAMI AQUIFER IF THE ACTIVE FLYASH PILE WAS AT BACKGROUND CONCENTRATIONS OPERABLE UNIT 2 REMEDIAL INVESTIGATION REPORT FERNALD ENVIRONMENTAL MANAGEMENT PROJECT

Constituent of Potential Concern	Units	On-Site Maximum Concentration at Uranium-238 Maximum Location and at 100 Years	FEMP Boundary Maximum Concentration at Uranium-238 Maximum Location and at 120 Years	EPA RAGs, Part B Screening Concentration
		RADIONUCLIDES		
Strontium-90	pCi/L	1.50×10^{-1}	1.42×10^{-2}	1.32×10^{-1}
Uranium-234	pCi/L	$3.54 \times 10^{+0}$	4.62×10^{-1}	2.97×10^{-1}
Uranium-235/236	pCi/L	3.19×10^{-1}	4.17×10^{-2}	2.97×10^{-1}
Uranium-238	pCi/L	$3.55 \times 10^{+0}$	4.64×10^{-1}	1.70×10^{-1}
Total Uranium (non-RAD)	ug/L	$1.07 \times 10^{+1}$	$1.39 \times 10^{+0}$	$1.09 \times 10^{+1}$
		INORGANICS		
Lead	ug/L	4.87×10^{-10}	1.38×10^{-6}	NA

NA = No data available to calculate EPA RAGs, Part B screening concentration

Other Comment No. A-48

000589

5659

uniformly distributed through the entire source area. This methodology introduces an obvious potential for overestimation of CPC mass.

- The total mass of uranium-238 was estimated from average concentrations in each 125 ft by 125-foot model grid block and the associated volume.

- Uncertainty is introduced into the estimation of leachate compositions even when in situ leachate analysis are available. In situ leachate samples may have missed the highest leachate concentration in the subunit. Greater uncertainty is introduced when in situ leachate analysis are lacking. The use of TCLP data to estimate leachate composition will probably result in constituent concentrations that are greater than values expected for in situ leachate. As mentioned previously, this occurs due to the enhanced leaching by acetic acid versus rainwater. The possibility of underestimating leachate concentrations from TCLP data also exist if soil sample used for TCLP analysis does not contain representative concentrations of CPCs. Calculations carried out to estimate contaminant concentrations using the EPA 70-year rule will introduce a large conservative uncertainty for all but the most soluble contaminants (e.g., cesium). The possibility exists to underestimate the constituents concentration when the EPA 70-year rule is applied to very soluble constituents. Even if leaching time is underestimated by a factor of two to three, peak concentration in the Great Miami Aquifer will occur very early, while concentration of other (less soluble) contaminants is low. Therefore, if soluble constituent was screened out (all were), risk from the CPCs will still remain below a carcinogenic risk of 10^{-6} and a Hazard Index of 1 when peak concentration of risk controlling CPC is predicted in the Great Miami Aquifer.

- The selection of parameters related to the attenuation and retardation of constituents is a major uncertainty in the groundwater fate and transport analysis. The attenuation and retardation factors of every constituent except uranium were determined after an extensive literature search. It should be noted that the actual retardation factors at the FEMP may not follow the assumed literature values, particularly over the long term. Site-specific attenuation and retardation factors were used when available. The use of site-specific values are assumed to result in lower uncertainty than using literature values.

- The organic decay rates at the FEMP were determined after an extensive literature search. The actual decay rates may or may not follow the literature values because of site-specific conditions. The use of site data to determine organic decay rates would result in lower uncertainty than that resulting from the use of literature values.

NO. A-35

- Transport through the vadose zone was approximated by using a one-dimensional model and assuming each of the two ~~zones~~ layers, glacial till and the unsaturated Great Miami Aquifer, is homogeneous. The unsaturated seepage flow rate is a function of several parameters, such as porosity, residual saturation, and pore size distribution index. Due to the heterogeneous nature of the till, these parameters actually change from location to location and from depth to depth.

- Average properties and uniform loading in a 125 ft by 125 ft model grid block was used even when mass loading may occur through a much smaller area within the grid block. Although this may result in underestimating concentrations in the immediate vicinity of the

source covering partial grid cell, it does not affect concentrations significantly down gradient of that source area.

- The transport models individually made assumptions regarding the fate of individual constituents within source media. However, these models were not combined or linked to consider assumptions made regarding depletion of chemicals from one model and the effect of that assumption on another model (i.e., the leaching models did not consider source depletion from surface water runoff, volatilization, or fugitive emissions and the surface water runoff models did not consider losses via leaching). Furthermore, the direct exposure pathways to a particular source (i.e., incidental ingestion of surface soil) did not consider source depletion by leaching, surface water transport, or air emissions. Consequently, this assumption is considered very conservative.

These uncertainties for modeling collectively are assumed to moderately overestimate the concentrations expected in groundwater.

The following sections discuss uncertainty associated with the different models used in the fate and transport modeling.

A.2.10.1 HELP Model

The HELP model is mainly sensitive to the hydraulic conductivities of the glacial till and waste and moderately sensitive to parameters used to define evapotranspiration and runoff. The majority of water exiting the system is lost through evapotranspiration and runoff and the remaining water becomes the seepage passing through the waste unit. Evapotranspiration is controlled by the plant cover type used, which was assumed to be bare ground for the Active Flyash Pile and Lime Sludge Ponds, poor grass for the Solid Waste Landfill, and good cover for the Inactive Flyash Pile and South Field. The better the vegetative cover, the more evapotranspiration takes place, and less infiltration occurs. Conservative assumptions were used to underestimate evapotranspiration and overestimate infiltration. For example, vegetative cover at the Inactive Flyash Pile is excellent, but it was specified as good.

Runoff in the HELP model is controlled by the Soil Conservation Study (SCS) runoff curve number used, which in turn is derived from the ground type, vegetation type, and land use. Present conditions were used to define these factors. If future conditions change, available water for seepage could change and thus loading to the aquifer would change. For example, if vegetative cover is removed, runoff will increase, and evapotranspiration will decrease. SCS runoff curve number varies

A-36

~~number when the SCS runoff curve number is changed by 10.~~ Increasing the SCS runoff curve number increases the runoff. Table A.2-59 shows that reducing the SCS curve number by 10 (reducing runoff) from base case has very little impact on the infiltration. However, increasing runoff (SCS curve number) at the Active Flyash Pile, for example due to no vegetation and steep slopes, does reduce infiltration significantly. For other subunits, increasing SCS curve number by 10 from base case does not have any impact on the infiltration.

The unsaturated seepage flow rate is a function of the unsaturated hydraulic conductivity which depends on parameters such as porosity, residual saturation, and pore size distribution index. All of these parameters vary in a physical formation matrix and thus cannot be fully defined for use in a numerical model. A typical HELP run for the Operable Unit 2 subunits had three layers: (1) waste/fill, (2) till, and (3) unsaturated Great Miami Aquifer. Thicknesses as measured during field investigations were used. A further refinement of these layers is possible. However, zone by zone infiltration calculations (Tables A.2-10 through A.2-13) indicate that further refinement of layers is unwarranted.

The lowest hydraulic conductivity was that of the glacial till layer and it may control the overall infiltration rate. An increase in glacial till hydraulic conductivity by two orders of magnitude causes only a negligible increase in infiltration rate for the Solid Waste Landfill and the Lime Sludge Ponds (Table A.2-60). However, for the Active Flyash Pile and the Inactive Flyash Pile and South Field, increase in infiltration rate is significant when the glacial till hydraulic conductivity is increased by two orders of magnitude. Although not shown in Table A.2-60, this is accompanied by a reduction in lateral drainage. Lateral drainage was assumed to infiltrate in other waste areas where waste is directly underlain by the Great Miami Aquifer. Therefore, the overall impact of the increase in glacial till hydraulic conductivity is minimized. However, a decrease in hydraulic conductivity of till by an order of magnitude causes significant reduction in infiltration (Table A.2-60).

Table A.2-61 shows the effect of an order of magnitude change in waste hydraulic conductivity. The higher the waste hydraulic conductivity, the more infiltrates and less is available for evapotranspiration and runoff and visa versa.

Table A.2-62 shows the effect of an order of magnitude variation in the Great Miami Aquifer hydraulic conductivity. Whenever the Great Miami Aquifer is overlain by glacial till, infiltration is

5659

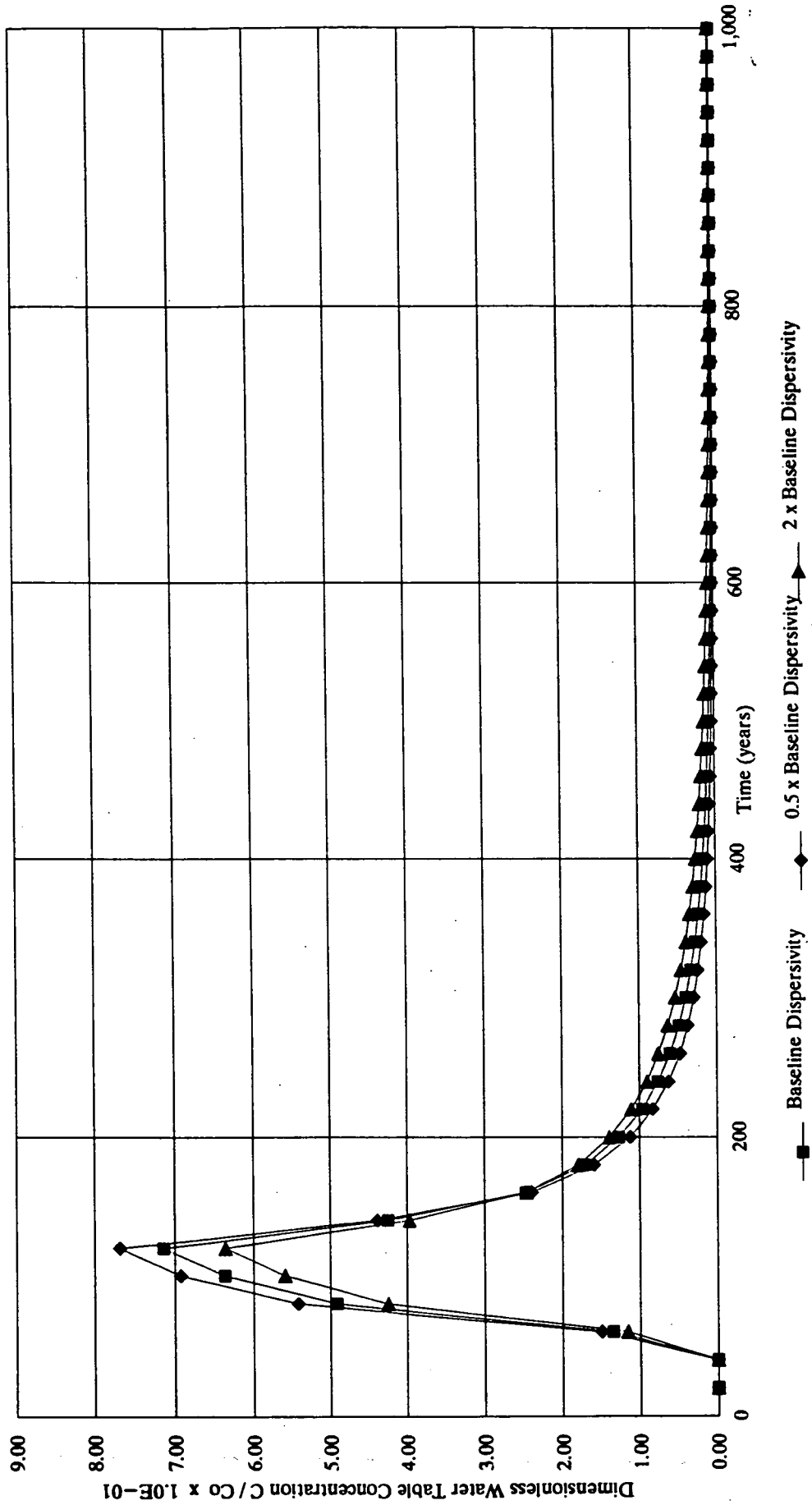

Figure A.2–67 – Sensitivity of ODAST Model Results to Dispersivity

TABLE A.2-59

SENSITIVITY OF CALCULATED INFILTRATION BY HELP MODEL TO THE SCS RUNOFF CURVE NUMBER OPERABLE UNIT 2 REMEDIAL INVESTIGATION FERNALD ENVIRONMENTAL MANAGEMENT PROJECT

			Infiltration in Inch/Year		
Subunit	Zone	Base Value of SCS* Runoff Curve Number	(Base -10) SCS Runoff Curve Number	Base SCS Runoff Curve Number	(Base +10) SCS Runoff Curve Number
Solid Waste Landfill	2	58	9.04	9.03	9.00
Lime Sludge Ponds	2	86	14.57	14.57	14.57
Inactive Flyash Pile and South Field	3	61	9.29	9.28	9.27
	5	61	5.81	5.81	5.76
	13	61	2.21	2.21	2.21
Active Flyash Pile	1	86	3.27	3.16	2.46
	3	86	12.84	11.56	5.48

*SCS - Soil Conservation Service

000284

5659

TABLE A.2-60

SENSITIVITY OF CALCULATED INFILTRATION BY HELP MODEL TO THE HYDRAULIC CONDUCTIVITY OF THE GLACIAL TILL OPERABLE UNIT 2 REMEDIAL INVESTIGATION FERNALD ENVIRONMENTAL MANAGEMENT PROJECT

			Infiltration in Inch/Year			
Subunit	Zone	Base Value of the Glacial Till Hydraulic Conductivity (cm/sec)	Base/10 Hydraulic Conductivity	Base Hydraulic Conductivity	Base x 10 Hydraulic Conductivity	Base X 100 Hydraulic Conductivity
Solid Waste Landfill	2	1.9×10^{-6}	2.88	9.03	9.03	9.03
Lime Sludge Ponds	2	1.9×10^{-6}	3.02	14.57	14.58	14.58
Inactive Flyash Pile and South Field	13	1.4×10^{-7}	0.23	2.21	8.22	8.27
Active Flyash Pile	1	1.4×10^{-7}	0.35	3.16	11.54	11.57

TABLE A.2-61

SENSITIVITY OF CALCULATED INFILTRATION BY HELP MODEL TO THE HYDRAULIC CONDUCTIVITY OF WASTE/FILL OPERABLE UNIT 2 REMEDIAL INVESTIGATION FERNALD ENVIRONMENTAL MANAGEMENT PROJECT

			Infiltration in Inch/Year		
Subunit	Zone	Base Value of Waste/Fill Hydraulic Conductivity (cm/sec)	Base/10 Hydraulic Conductivity	Base Hydraulic Conductivity	Base x 10 Hydraulic Conductivity
Solid Waste Landfill	2	1.1×10^{-4}	2.30	9.03	10.08
Lime Sludge Ponds	2	1.0×10^{-3}	12.01	14.57	15.98
Inactive Flyash Pile and South Field	3	2.0×10^{-4}	6.20	9.28	9.63
	5	2.0×10^{-4}	1.85	5.81	7.43
	13	2.0×10^{-4}	2.15	2.21	2.03
Active Flyash Pile	1	1.8×10^{-4}	3.69	3.16	2.13
	3	1.8×10^{-4}	5.11	11.56	16.05

000286

5659

not at all sensitive to the hydraulic conductivity of the Great Miami aquifer. However, when Great Miami Aquifer is directly overlain by the waste, infiltration is moderately sensitive to the hydraulic conductivity of the Great Miami Aquifer, particularly when the waste thickness is less than 2 feet (zone 3 of Inactive Flyash Pile/South Field in Table A.2-62). Otherwise infiltration is not sensitive to the hydraulic conductivity of the Great Miami Aquifer.

NO. A-37 At first glance, Table A.2-60 indicates that hydraulic conductivity of the glacial till at the Inactive Flyash Pile/South Field/Active Flyash Pile is an exception. However, increased infiltration is accompanied by a reduction in the lateral drainage at the interface of the glacial till and the waste/fill. Lateral drainage was assumed to infiltrate in other areas where waste/fill is directly underlain by the unsaturated Great Miami Aquifer. Therefore, the overall impact of increase in the till hydraulic conductivity on the subunit wide infiltration is minimal.

Selection of parameters used in HELP model runs for vadose zone modeling (base case) were such ~~that worst case~~ high infiltrations were predicted. Tables A.2-59 through A.2-62 indicates that either infiltration is not sensitive to estimated parameters or a change in estimated parameters will not significantly increase the infiltration, although a significant decrease in infiltration is possible.

A.2.10.2 ODAST Model

The selection of the longitudinal dispersivity and parameters for biodegradation and retardation of constituents is a major source of uncertainty in the ODAST model. These parameters were mostly estimated from an extensive literature search. These parameters mainly influence the concentration and time required for the maximum loading to reach the aquifer. Longitudinal dispersivity has a negligible impact on the time for maximum loading to reach the aquifer, and the vadose models are not sensitive to its value (Figure A.2-67). The maximum loading is moderately sensitive to dispersivity. As dispersivity increases, maximum loading decreases. However, concentration at the leading edge and trailing edge of the plume is sensitive to the value of longitudinal dispersivity.

The parameters for retardation influence the time required for the maximum loading to reach the aquifer, and the maximum concentration. As retardation factors increase, maximum concentration decreases and the time required for the maximum loading to reach aquifer increases (Figures A.2-68 and A.2-69). Figure A.2-68 shows that the sensitivity of the Great Miami Aquifer loading to the distribution coefficient for the Great Miami Aquifer, while Figure A.2-69 shows that the sensitivity of

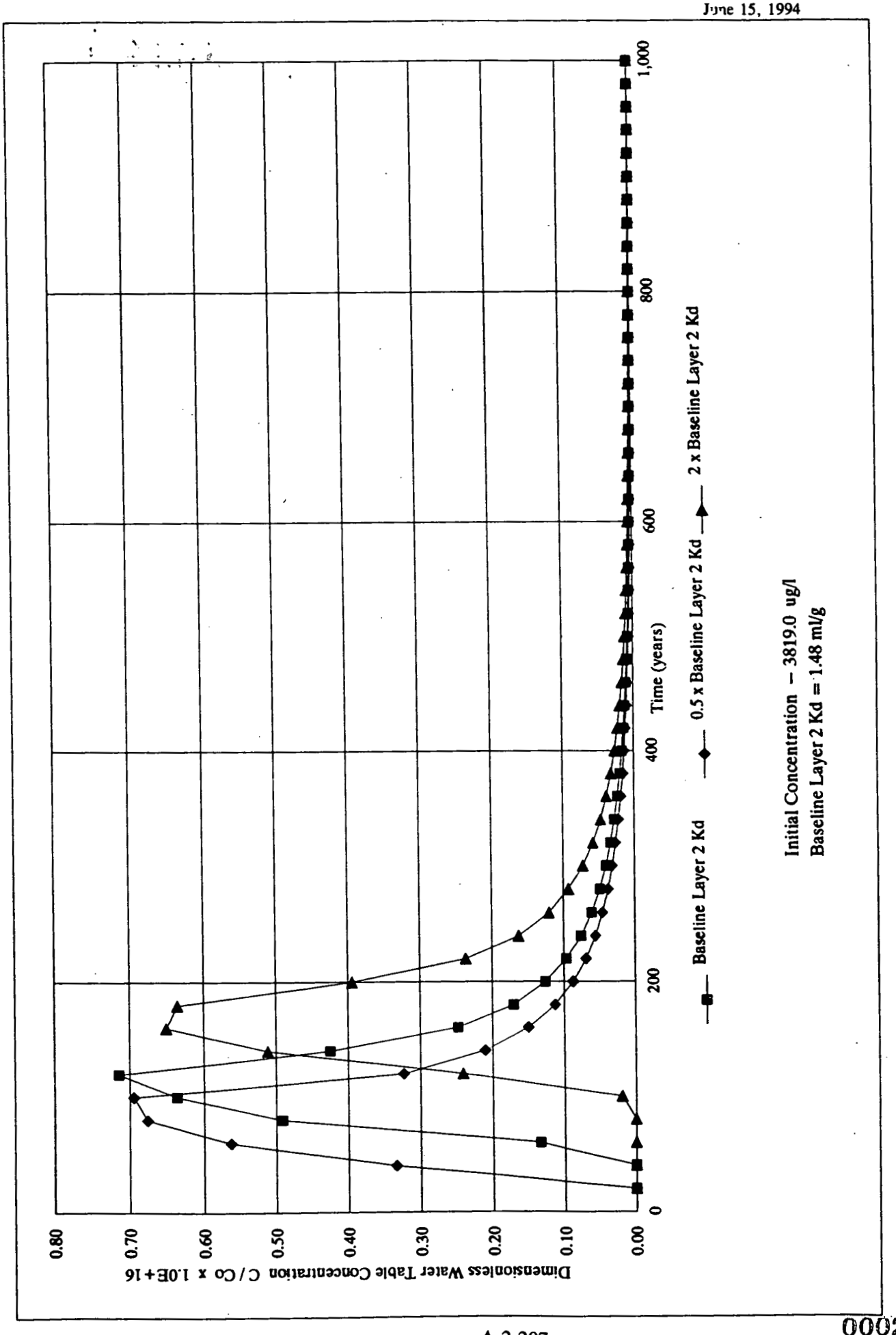

Figure A.2–68 – Sensitivity of ODAST Model Results to the Great Miami Aquifer Distribution Coefficient for U–238
Inactive Flyash Pile and South Field

5659

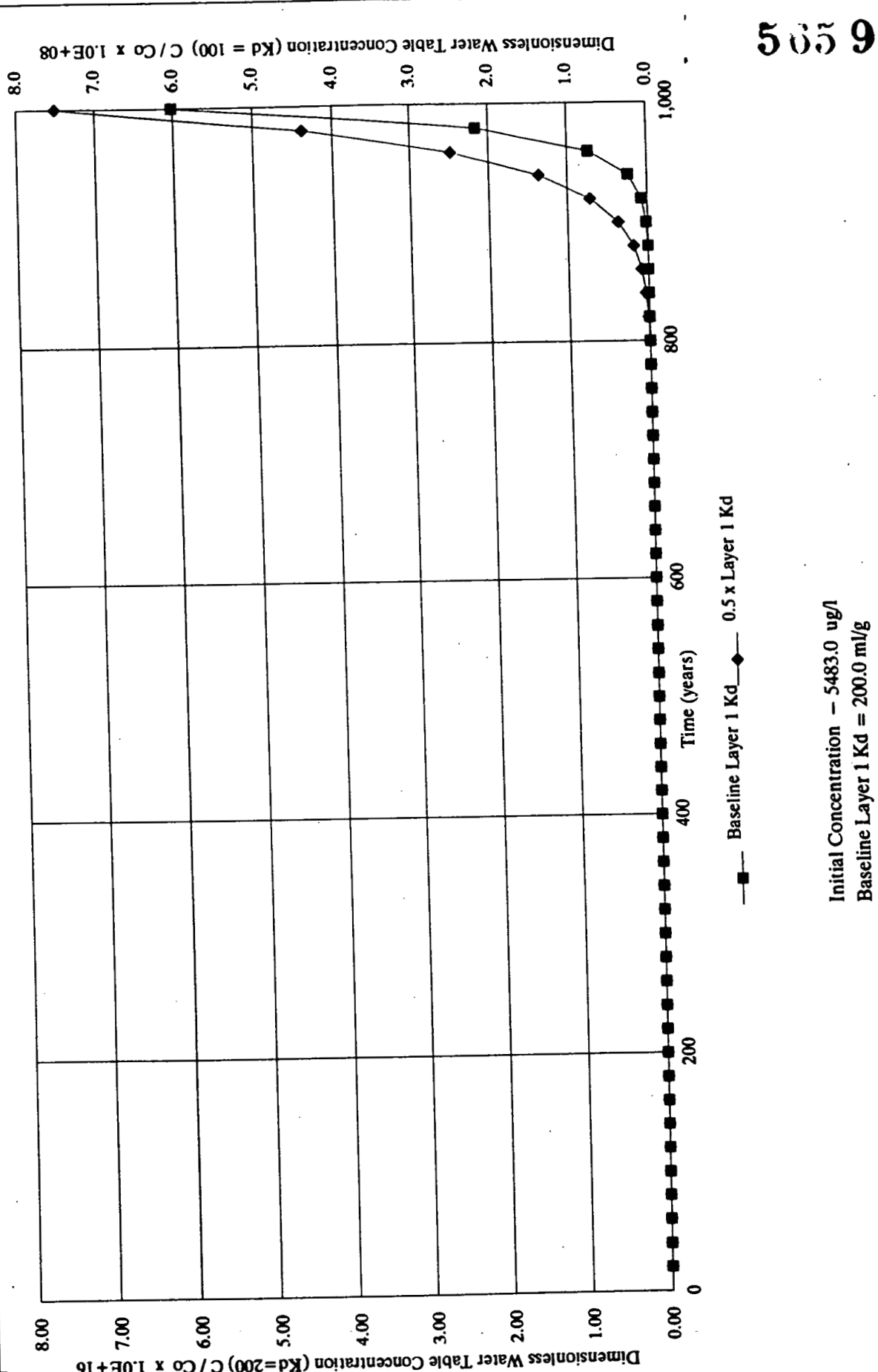

Figure A.2–69 – Sensitivity of ODAST Model Results to Glacial Till Distribution Coefficient for Uranium–238, Active Flyash Pile

65200

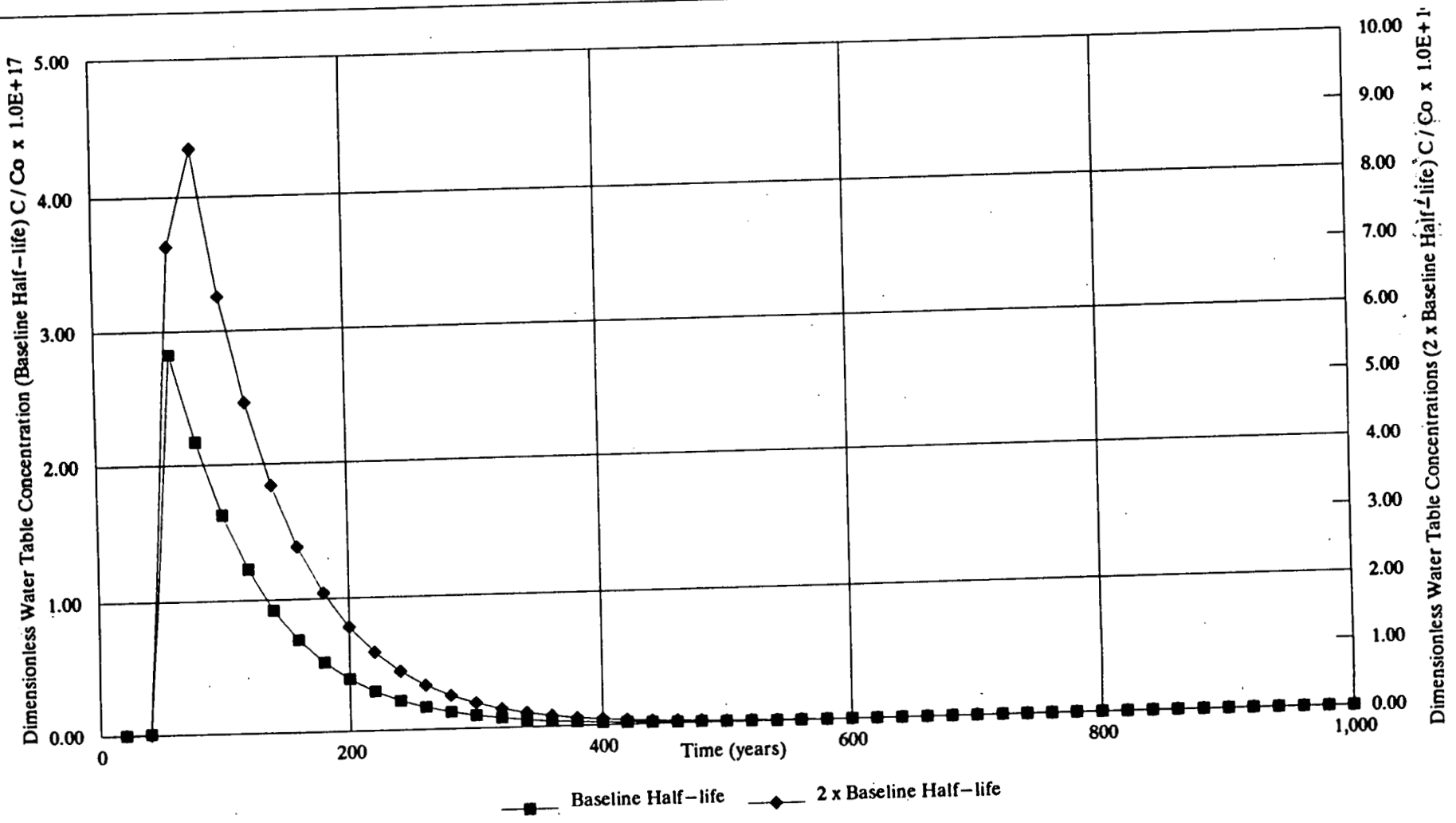

Baseline Half-life – 1.1 years
Initial Concentration – 150.8 ug/l

Figure A.2-70 – Sensitivity of ODAST Model Results to Biodegradation Half-life for bis(2-Ethylhexyl) Phthalate
Inactive Flyash Pile and South Field

5059

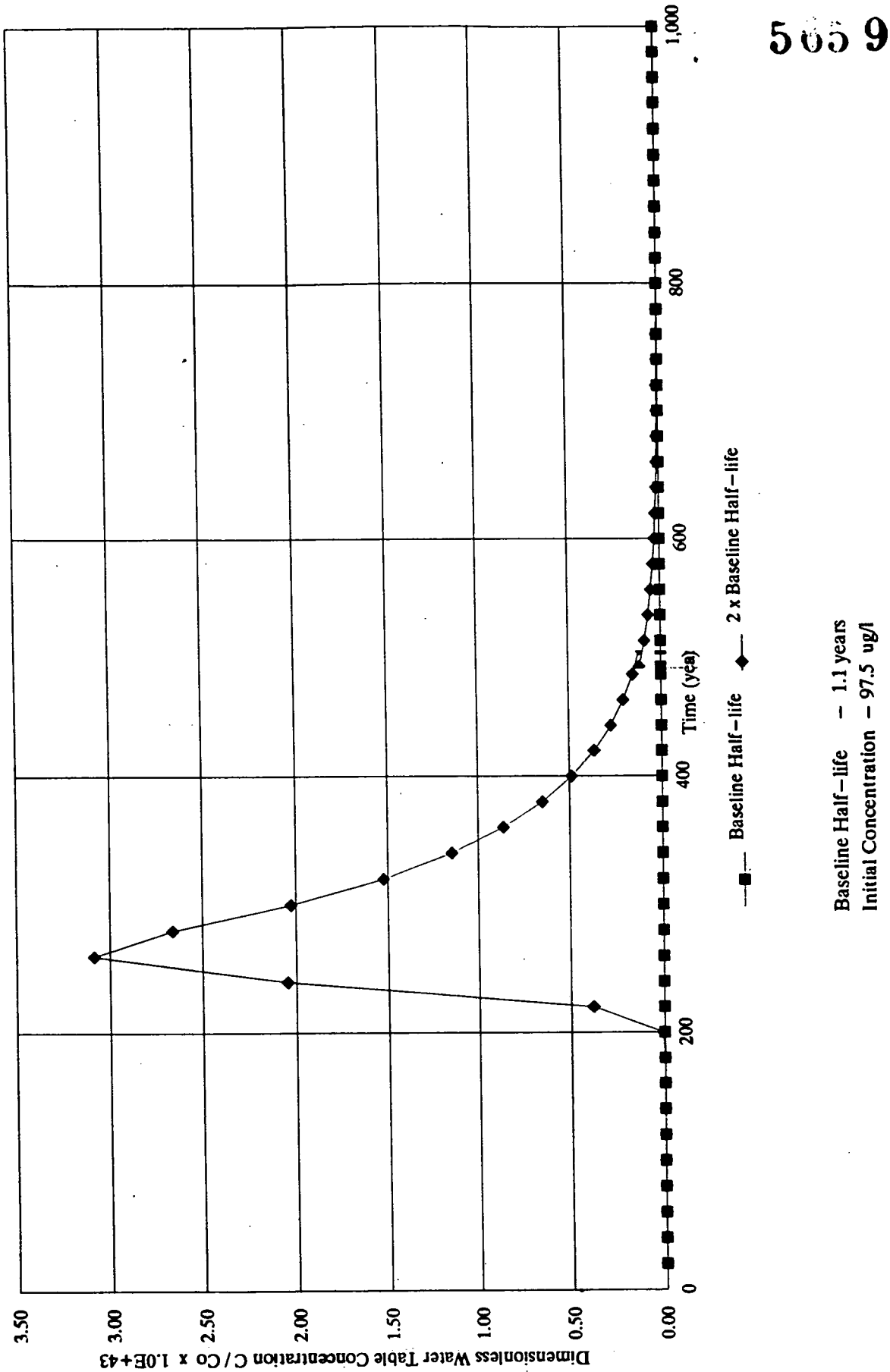

Figure A.2-72 - Sensitivity of ODAST Model Results to Biodegradation Half-life for bis(2-Ethylhexyl) Phthalate, Lime Sludge Ponds

000301

TABLE A.2-62

SENSITIVITY OF CALCULATED INFILTRATION BY HELP MODEL TO THE HYDRAULIC CONDUCTIVITY OF THE GREAT MIAMI AQUIFER OPERABLE UNIT 2 REMEDIAL INVESTIGATION FERNALD ENVIRONMENTAL MANAGEMENT PROJECT

			Infiltration in Inch/Year		
Subunit	Zone	Base Value of the GMA* Hydraulic Conductivity (cm/sec)	Base/10 Hydraulic Conductivity	Base Hydraulic Conductivity	Base x 10 Hydraulic Conductivity
Solid Waste Landfill	2	1.59×10^{-2}	9.03	9.03	9.03
Lime Sludge Ponds	2	1.59×10^{-2}	14.57	14.57	14.57
Inactive Flyash Pile and South Field	3	1.59×10^{-2}	8.59	9.28	10.05
	5	1.59×10^{-2}	5.81	5.81	5.81
	13	1.59×10^{-2}	2.21	2.21	2.21
Active Flyash Pile	1	1.59×10^{-2}	3.16	3.16	3.16
	3	1.59×10^{-2}	11.56	11.56	11.56

*GMA - Great Miami Aquifer

5659

000302

NO. A-57 the Great Miami Aquifer loading to the distribution coefficient for glacial overburden. Figure A.2-69 shows that decreasing uranium-238 K_d for glacial till from 200 to 100 mL/g results in approximately 25 percent increase in maximum loading concentration (ODAST output). The range for measured uranium desorption K_d for the glacial till was 200 to 9350 mL/g. Modeling used minimum desorption K_d of 200 mL/g. The adsorption K_d measured for the glacial till during OU2 Uranium Partition Coefficient Evaluation Study was 81 mL/g. Breakthrough time evaluations indicate that results for uranium in 1000 years at the Solid Waste Landfill and Lime Sludge Ponds does not change when K_d is lowered to 81 mL/g (no breakthrough in 1000 years). Conclusions for the Inactive Flyash Pile and South Field also do not change when glacial till K_d is lowered to 81 mL/g because early breakthrough at these subunits occurs from waste directly underlain by the Great Miami Aquifer which is independent of glacial till parameters.

Decay rates significantly influence maximum concentrations. As decay rates increase (half-life decrease), the maximum concentrations decrease. Radioactive decay rates are well defined in literature and are applicable to the FEMP. However, bidegration rates are site-specific. The movement of organic constituents to the Great Miami Aquifer is greatly impeded by high biodegradation rates (low half-lives). ~~Figures A.2-70 and A.2-71 show~~ Figure A.2-70 shows the effect of doubling biodegradation half-life on loading to the Great Miami Aquifer when Great Miami Aquifer is directly overlain by the waste. These figures show that effect of doubling half-life can result in a ~~1 to~~ 7 order of magnitude increase in maximum concentration depending on the half-life itself and other parameters controlling travel time. However, one should note that concentrations are still very small (for example less than 10^{-7} μg/L in Figure A.2-70).

NO. A-47

NO. A-47

When decay is combined with high retardation due to adsorption, the constituent concentration at the Great Miami Aquifer is significantly reduced. This is evident in a case when glacial till is present. Figure A.2-72 shows that concentration for bis (2-ethylhexyl) phthalate remains below 10^{-41} μgL even when decay is increased by a factor of 2.

Retardation parameters for all CPCs but uranium and the organic decay rates may or may not follow the literature values because of site-specific conditions. To be conservative, the lowest decay rates and retardation parameters were used in the fate and transport modeling.

The impact of the Darcy velocity and layer thickness on the models is somewhat limited due to the derivation of the parameters themselves. Layer thicknesses were derived from Operable Unit 2 boring data which should not vary over a large range within the operable unit. Darcy velocity is a function of the seepage rate (calculated by the HELP model), and the formation porosity, which is fairly well defined for the media simulated by the models. Sensitivity of seepage rates and the HELP model is discussed in Section A.2.10.1.

A.2.10.3 SWIFT Model

Like the vadose zone models, SWIFT is mostly influenced by the solute transport parameters it uses to simulate contaminant movement through the aquifer. Of these, retardation is the least well defined and has the most impact on the fate of contaminants in the groundwater. Calibration of the SWIFT model for uranium was performed as part of the RI/FS process. The SWIFT flow model was calibrated by comparing hydraulic heads calculated by the model against heads measured in numerous monitoring wells throughout the FEMP and surrounding areas. The flow calibration is described in Section 2.8. The SWIFT solute transport model was calibrated by simulation of uranium transport in the Great Miami Aquifer (IT 1990a) over the period of operation at the FEMP. A portion of this calibration involved testing uranium retardation values to determine which value fits historical loading data and present day groundwater concentration data most accurately. Uranium retardation factors below 4 were found to transport uranium too quickly through the system and thus did not match historical data. Retardation factors above 15 were found to not match present day uranium distributions without large aquifer dispersion values, which were felt to be unrealistic. Consequently, a retardation factor of 12 (K_d of 1.48 ml/g) was found to give the best match for uranium during the modeling process. A K_d value of 1.48 ml/g for uranium was also found to match the observed data for Operable Unit 2 and was used in uranium fate and transport modeling.

The major parameter affecting solute transport is retardation. Higher retardation factors delay the appearance of a concentration peak at a receptor almost proportionately. Experimental determination of retardation factors for CPCs, which have relatively large source terms and are relatively toxic is an important factor in reducing uncertainty in solute transport.

A.3.0 AIR TRANSPORT ANALYSIS

A.3.1 AIR DISPERSION MODELING OF OPERABLE UNIT 2

As part of the Baseline Risk Assessment (BRA) for Operable Unit 2 of the Fernald Environmental Management Project (FEMP), an analysis of the transport of contaminants through the air pathway was conducted to estimate its impact on the environment. This section describes the methodology used and the results of the analysis.

The objective of the air pathway analysis was to determine maximum annual concentrations and deposition rates at receptors located within the boundary of the individual subunits (on-subunit), between the subunit boundary and the FEMP boundary (on-property), and at or beyond the FEMP boundary (off-property).

The analysis was conducted in accordance with EPA guidance (EPA 1989). Two emission models and an air dispersion model were used to estimate air emissions from each source and to calculate annual average concentrations and deposition rates at the receptor locations. One emission model predicted the quantity of exposed soil that would be resuspended by the wind, and the other emission model estimated the flux of Rn-222 gas from soil and waste containing Ra-226. The air dispersion model accounted for dispersion and dilution of the contaminants under defined meteorological conditions, such as wind speed and direction, atmospheric stability, and mixing height. The primary meteorological parameters used were collected from an on-property meteorological station.

A.3.2 SITE DESCRIPTION OF OPERABLE UNIT 2

Operable Unit 2 consists of five separate subunits. These subunits are identified as: the Active Flyash Pile, the South Field, the Inactive Flyash Pile, the Solid Waste Landfill and the North and South Lime Sludge Ponds.

Active Flyash Pile

The Active Flyash Pile is located in the southern portion the FEMP. A recent site survey showed the flyash material to be void of vegetation and crusted due to weathering and the application of a dust suppressant agent. A plastic fence has been erected atop the flyash pile to act as a wind erosion control device. ~~However, to maintain conservative estimations the effects this control device were neglected.~~ The Active Flyash Pile could arguably have no erosion potential based on this

A-40

information. However, to develop a conservative baseline assessment, a limited erosion potential was assumed for this source.

South Field

The South Field is located approximately 50 meters west of the Active Flyash Pile and has the largest areal coverage, of the Operable Unit 2 subunits, approximately 10 acres. This particular subunit is heavily covered with vegetation is currently covered with thick vegetation in the form of grass, tall brush and trees.

Inactive Flyash Pile

The Inactive Flyash Pile is located adjacent to the northwest corner of the South Field. Similar to the South Field, the Inactive Flyash Pile is covered with thick vegetation.

Solid Waste Landfill

The Solid Waste Landfill is located in the northern portion of the FEMP, between the Production Area and the Operable Unit 1 Waste Pits. The Solid Waste Landfill is a small subunit only covering approximately 48,000 square feet. A recent site survey showed the landfill to be 85 percent covered with grass, weeds and small trees. The landfill is no longer used for disposal of waste material, therefore the vegetative cover should remain intact.

Lime Sludge Ponds

The Lime Sludge Ponds are located just west of the Production Area, almost in the center of the FEMP. The Lime Sludge Ponds consists of two separate ponds, the North Lime Sludge Pond and the South Lime Sludge Pond. Both of these ponds are of the same dimensions, covering approximately 32,000 square feet each.

Both ponds are approximately 1 to 2 feet below grade to enhance storm water and snow melt collection. Water covers approximately 10 percent of the North Lime Sludge Pond on an annual basis. Based on information collected during a site survey, the remaining 90 percent of the North Lime Sludge Pond has only 5 percent vegetative cover. The remaining soil is susceptible to wind erosion. Despite a relatively large area of non-vegetative soil, much of the exposed soil has crusted,

thus limiting the soil erosion potential. The ease with which the crust could be crumbled was not determined. Therefore, it was assumed that the crust could be easily broken and that particulate emissions could be determined using the limited erosion potential model.

Conversely, the South Lime Sludge Pond is 85 percent covered with vegetation thus limiting the wind erosion potential.

A.3.3 CONCEPTUAL AIR MODEL SOURCE SCENARIOS

Air emission source terms were adopted that best described current and projected land use conditions for each subunit. Air dispersion modeling was performed to determine amount of contamination to humans and animals due to inhalation and ingestion, via air pathway, for the following current scenario receptors:

NO. A-38

- A trespassing ~~child~~ youth on a given subunit
- An on-property groundskeeper
- An off-property resident ~~and~~ farmer and child with grazing livestock

For the current source term, the Operable Unit 2 subunits areas are assumed to have the following conditions:

- The Solid Waste Landfill is assumed to be 85 percent covered by vegetation.
- The North Lime Sludge Pond is assumed to have 10 percent of the surface area covered with water and only 5 percent covered by vegetation. The remaining area of the North Lime Sludge Pond is assumed to be non-vegetated and susceptible to wind erosion, however, much of the surface soil is crusted and thus has limited erosion potential.
- The South Lime Sludge Pond, the Inactive Flyash Pile and the South Field are assumed to be 85 percent covered by vegetation.
- The Active Flyash Pile is assumed to have no vegetative cover, however has limited erosion potential because of dust suppressant is used to control wind erosion and most of the material is composed of large agglomerations of flyash material.

In the future scenario, the only changes that occur to the subunit emission involved the Solid Waste Landfill and the South Field. Both of these subunits are assumed to be used for the farming of crops for human and animal consumption. On an annual basis these subunits area assumed to have crops for 6 months of the year to simulate the growing season, while during the remaining six months of

A-40

the year both subunits are assumed to have no vegetation. This scenario results in the assumption of a 50 percent vegetation cover factor. This assumption of the crop growing scenario is consistent with local agricultural practices. The emissions for all other Operable Unit 2 subunits remain the same as described above in the current scenario.

Future land use receptors exposed to air pathway contaminants include:

- An off-property farmer with grazing livestock
- A recreational user with free access on-site and on-subunit
- An on-property resident and farmer with grazing livestock

Not all future scenario conditions were applicable to all Operable Unit 2 subunits. The on-property farmer scenario was not considered for the Active Flyash Pile because it was impracticable to remove tons of flyash for farming purposes on such a small subunit. However, both South Field and the Solid Waste Landfill was cultivated for agricultural use by the on-property farmer. Consequently, this required removal of all vegetation which significantly increased the emission potential. Due to the small size of the Inactive Flyash Pile, no future scenarios involving farming activities were considered in the air dispersion analysis.

A.3.4 AIR DISPERSION MODEL

The annual average contaminant concentrations were determined using the Industrial Source Complex - Long Term (ISCLT2) air dispersion model. This model is recommended by EPA for air pathway analysis of Superfund sites (EPA 1989) and is identified as the model of choice in the Risk Assessment Work Plan Addendum (DOE 1992) for the site.

The ISCLT2 model was designed by the EPA for assessing the air quality impact of emissions at user-selected receptors from a variety of sources. It incorporates a steady-state Gaussian plume equation that is applicable for flat or gently rolling terrain. The ISCLT2 model calculates annual average concentrations due to airborne emissions at user-selected receptors, based on sector averaged statistical wind summaries known as STatistical ARrays (STAR). The user is required to select from; single or multiple point, area or volume sources as input to the model. Input data also included emission rates from the sources; location and configuration of sources; statistical summaries of wind

speed, wind direction and atmospheric stability; and locations of receptors of interest. The model options in the Operable Unit 2 air transport analysis are listed in Table A.3-1.

A.3.5 INPUT PARAMETERS

A.3.5.1 Meteorological Data

Five meteorological parameters: wind speed, wind direction, ambient air temperature, atmospheric stability and vertical mixing heights were used as input for the ISCLT2 modeling of Operable Unit 2. All parameters, with the exception of vertical mixing heights, were measured directly from FEMP's on-site meteorological tower. The on-site meteorological data used in this remedial investigation included five years of meteorological statistics. Each year was analyzed separately and the highest annual concentration or deposition rate from the five annual periods was reported. Vertical mixing heights were calculated from atmospheric sounding data compiled twice daily, from the National Weather Service (NWS) in Dayton, Ohio (See Table A.3-2). The NWS office in Dayton was selected because it was the closest source of atmospheric sounding data to the FEMP. It was assumed that atmospheric conditions recorded at the NWS Dayton office would best represent the conditions at the FEMP.

NO. A-55

Wind speed, wind direction and ambient air temperature data are measured at the FEMP meteorological tower at a height of 10 meters. The atmospheric stability category is derived from direct measurements of the standard deviation of the horizontal wind direction (sigma-theta) during the daytime and the low-level temperature difference (delta-T) at night. These procedures are in accordance with EPA methodology for estimating Pasquill stability categories in terms of the standard deviation of the horizontal wind direction and low level temperature differences, (EPA 1987b). The temperature difference is calculated from air temperature recorded at the 60 meter and 10 meter levels.

The ambient air temperatures measured at the FEMP meteorological tower and the temperatures used in the ISCLT2 model as a function of atmospheric stability categories A through F are given in Table A.3-3. Assignments of temperatures to stability categories were made as per U.S. EPA recommendations (EPA 1992a).

TABLE A.3-1

**DISPERSION OPTIONS USED IN ISCLT MODELING OF OPERABLE UNIT 2
OPERABLE UNIT 2 REMEDIAL INVESTIGATION
FERNALD ENVIRONMENTAL MANAGEMENT PROJECT**

Source Type	Area and Volume
Dispersion Mode	Rural
Calculation Mode	Concentration and deposition
Building Downwash	None
Flagpole Receptors	1.5 meters for concentration 0.0 meters for deposition
Discrete Receptors	Yes
Gravitational Settling	Yes For deposition only
Variable Emissions	None
Receptor Grid Type	Cartesian
Discrete Receptor Grid Type	Cartesian
Meteorology Input	Annual STAR Summaries*
Terrain Type	Flat
Averaging Period	Annual

*Individual annual on-property data for years 1987-1989, 1991 and 1992

TABLE A.3-2

MIXING HEIGHTS* IN METERS USED OPERABLE UNIT 2 ISCLT AIR TRANSPORT MODELING OPERABLE UNIT 2 REMEDIAL INVESTIGATION FERNALD ENVIRONMENTAL MANAGEMENT PROJECT

Year	Stability Class	Wind Speed Class					
		1	2	3	4	5	6
1987	A	2105	1961	1803	1802	1526	2349
	B	1403	1307	1202	1201	1017	1566
	C	1403	1307	1202	1201	1017	1566
	D	1403	1307	1202	1201	1017	1566
	E	5000	5000	5000	5000	5000	5000
	F	5000	5000	5000	5000	5000	5000
1988	A	2133	2351	2030	1812	1665	3255
	B	1422	1567	1353	1208	1110	2170
	C	1422	1567	1353	1208	1110	2170
	D	1422	1567	1353	1208	1110	2170
	E	5000	5000	5000	5000	5000	5000
	F	5000	5000	5000	5000	5000	5000
1989	A	1854	1995	1698	1524	1730	2313
	B	1236	1330	1132	1016	1153	1542
	C	1236	1330	1132	1016	1153	1542
	D	1236	1330	1132	1016	1153	1542
	E	5000	5000	5000	5000	5000	5000
	F	5000	5000	5000	5000	5000	5000
1991	A	1823	1991	1791	1695	1629	2313
	B	1215	1327	1194	1130	1086	1542
	C	1215	1327	1194	1130	1086	1542
	D	1215	1327	1194	1130	1086	1542
	E	5000	5000	5000	5000	5000	5000
	F	5000	5000	5000	5000	5000	5000
1992	A	1823	1991	1791	1695	1629	2313
	B	1215	1327	1194	1130	1086	1542
	C	1215	1327	1194	1130	1086	1542
	D	1215	1327	1194	1130	1086	1542
	E	5000	5000	5000	5000	5000	5000
	F	5000	5000	5000	5000	5000	5000

*Obtained from the National Weather Service (NWS) in Dayton, Ohio.

TABLE A.3-3

AMBIENT AIR TEMPERATURE IN DEGREES KELVIN USED IN ISCLT MODELING OPERABLE UNIT 2 REMEDIAL INVESTIGATION FERNALD ENVIRONMENTAL MANAGEMENT PROJECT

Year	Stability Class					
	A	B	C	D	E	F
1987	290	290	290	284	278	278
1988	291	291	291	284	279	279
1989	290	290	290	284	280	280
1991	292	292	292	286	281	281
1992	290	290	290	284	279	279

These recommendations suggest that the annual average maximum daily temperatures be assigned to the A, B, and C stability categories; annual average temperature be assigned to the D stability category; and annual average minimum daily temperature be assigned to the E and F categories. The format of the meteorological data required by the ISCLT2 model is in the form of the STAR program output. The STAR program output is a statistical meteorological data summary which gives the joint frequency distribution of six wind speed classes by sixteen wind sectors (i.e. north, north-northeast, northeast etc.) by six atmospheric stability categories (A through F). STAR data for the five years, 1987 through 1989 and 1991 through 1992, are listed in Attachment A.3.I of this Appendix.

The six wind speed classes are defined as 1 to 3 miles per hour (mph); 4 to 7 mph; 8 to 12 mph; 13 to 18 mph; 19 to 24 mph; and greater than 24 mph. Calm winds are wind speeds less than 1 mph with a variable wind direction. To account for the calm winds measured at the FEMP meteorological tower, the frequency of occurrence of calm winds were equally divided among the sixteen wind direction sectors and added to the 1 to 3 mph wind speed class.

According to meteorological wind data measured and recorded at FEMP facility, the prevailing wind direction blows from the west-southwest. Figures A.3-1 through A.3-5 graphically illustrate the meteorological wind profile for each year.

A.3.5.2 Source data

The ISCLT2 model defines sources as any point, area or volume that has the potential to emit emissions. Due to the ground level configuration of the Operable Unit 2 subunits and the large area of potential emissions each subunit was defined as an "area source". However, due to the three-dimensional storage pile configuration of the Active Flyash Pile it was modeled as a volume source.

One limitation of the ISCLT2 model is its inability to calculate annual concentrations or deposition rates from irregularly shaped sources. Therefore, the user is required to breakdown each irregularly shaped source into a series of squares that would best approximate the square area of that source (EPA 1992a). Figures A.3-6 through A.3-10 illustrate the breakdown of individual subunits into source squares according to EPA methodology.

FIGURE A.3-1

WIND ROSE FOR THE FEMP SITE YEAR - 1987
FERNALD ENVIRONMENTAL MANAGEMENT PROJECT

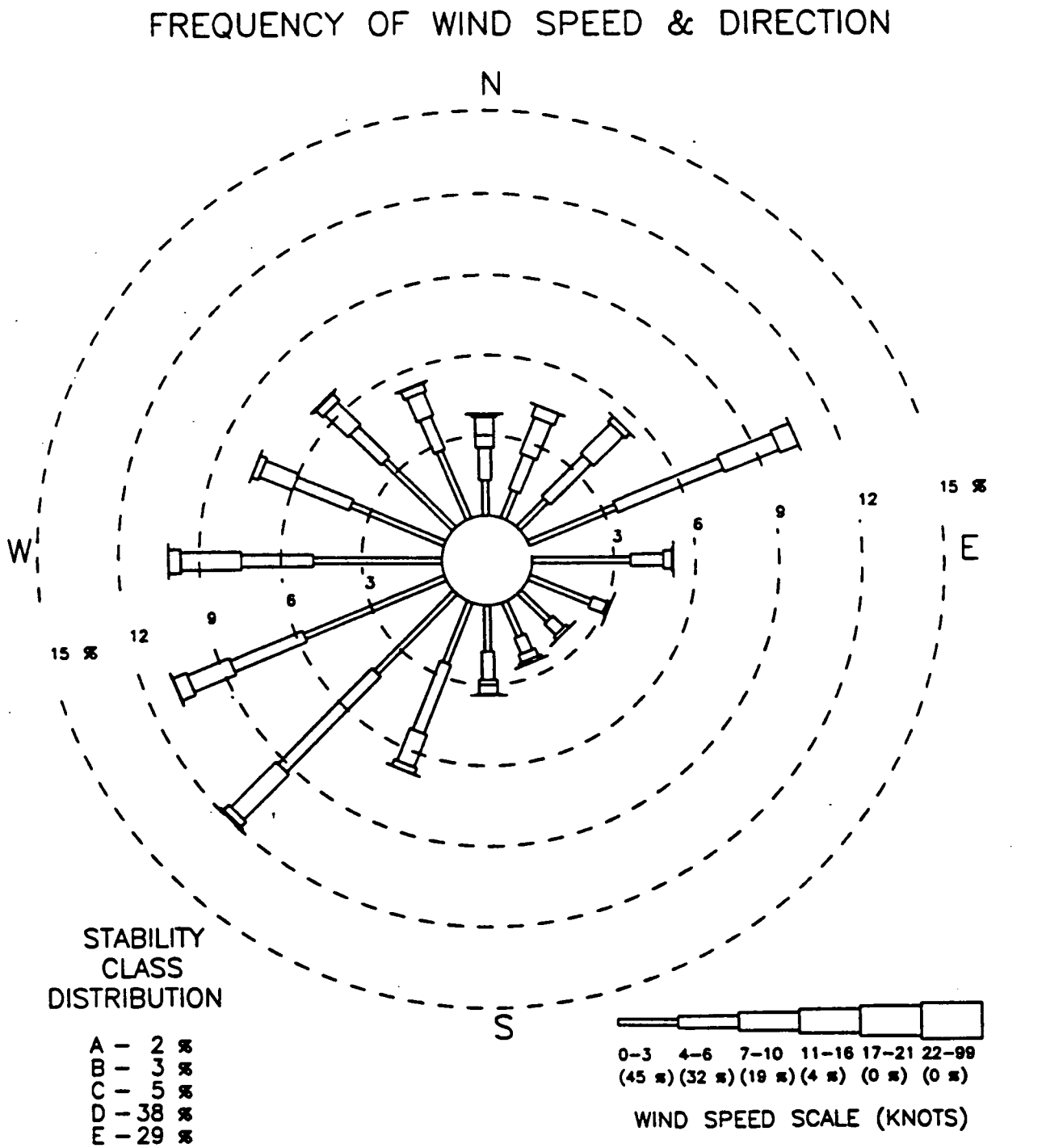

000314

FIGURE A.3-2

WIND ROSE FOR THE FEMP SITE YEAR - 1988
FERNALD ENVIRONMENTAL MANAGEMENT PROJECT

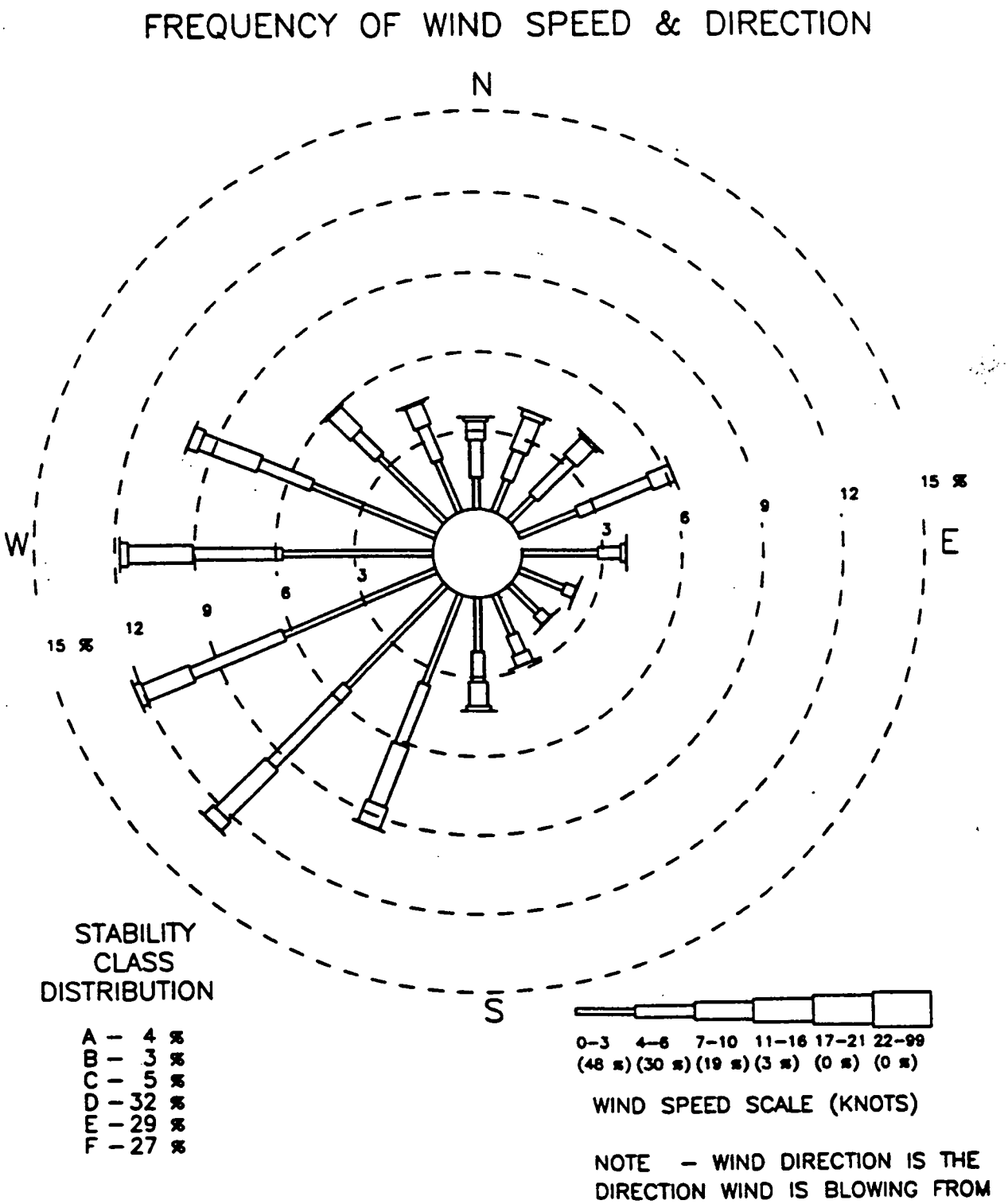

FIGURE A.3-3

WIND ROSE FOR THE FEMP SITE YEAR - 1989
FERNALD ENVIRONMENTAL MANAGEMENT PROJECT

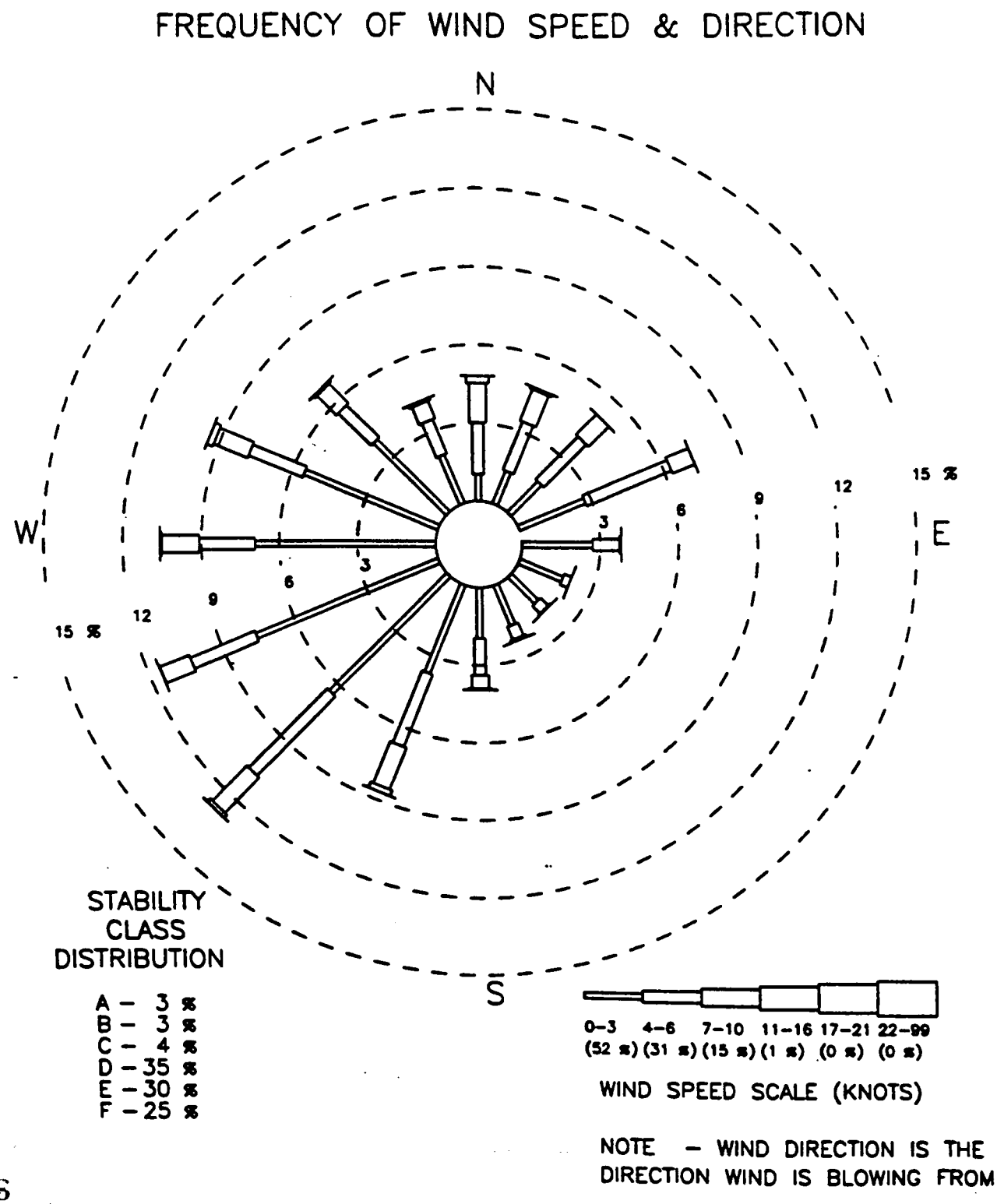

000316

FIGURE A.3-4

WIND ROSE FOR THE FEMP SITE YEAR - 1991
FERNALD ENVIRONMENTAL MANAGEMENT PROJECT

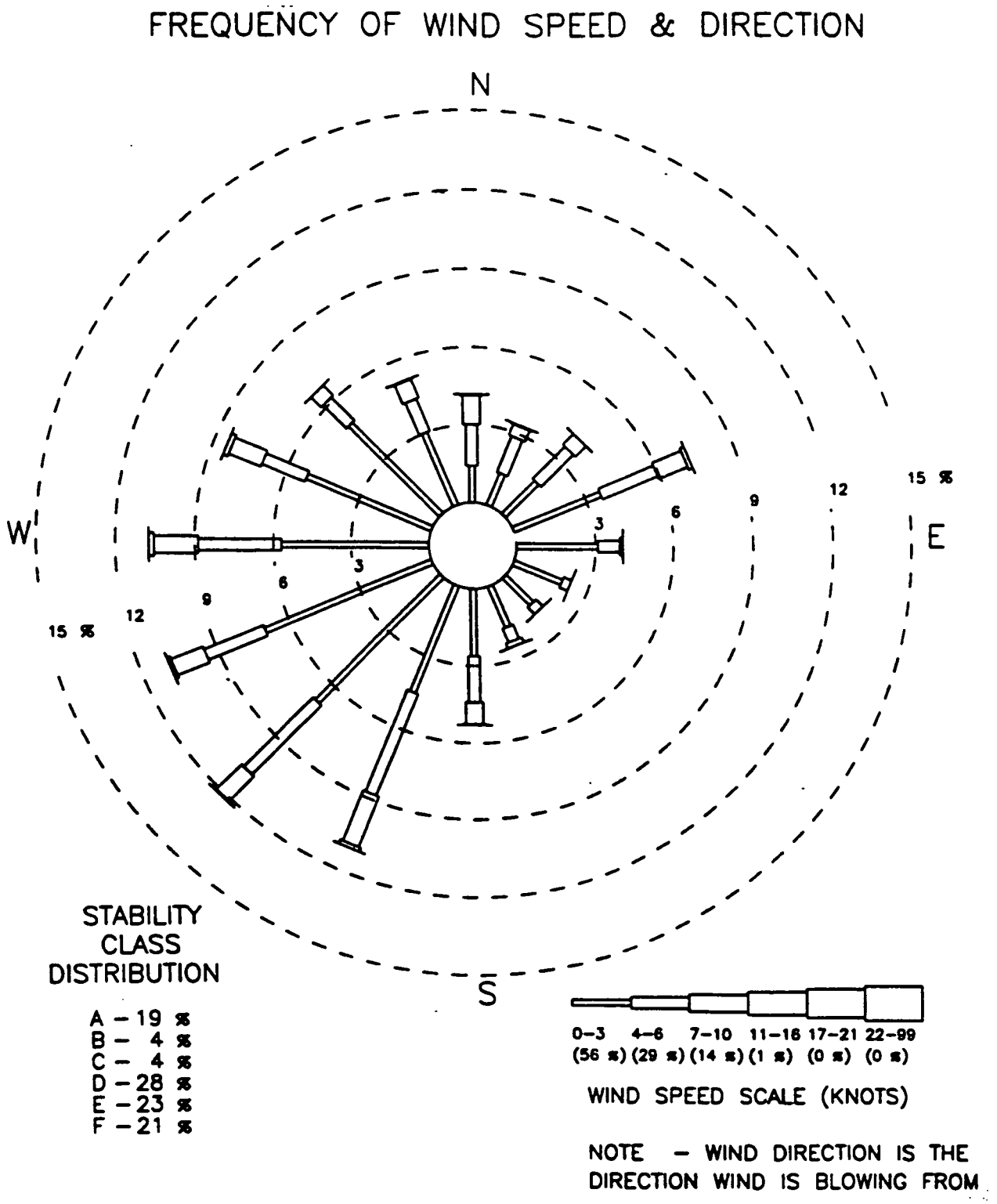

FIGURE A.3-5

WIND ROSE FOR THE FEMP SITE YEAR - 1992
FERNALD ENVIRONMENTAL MANAGEMENT PROJECT

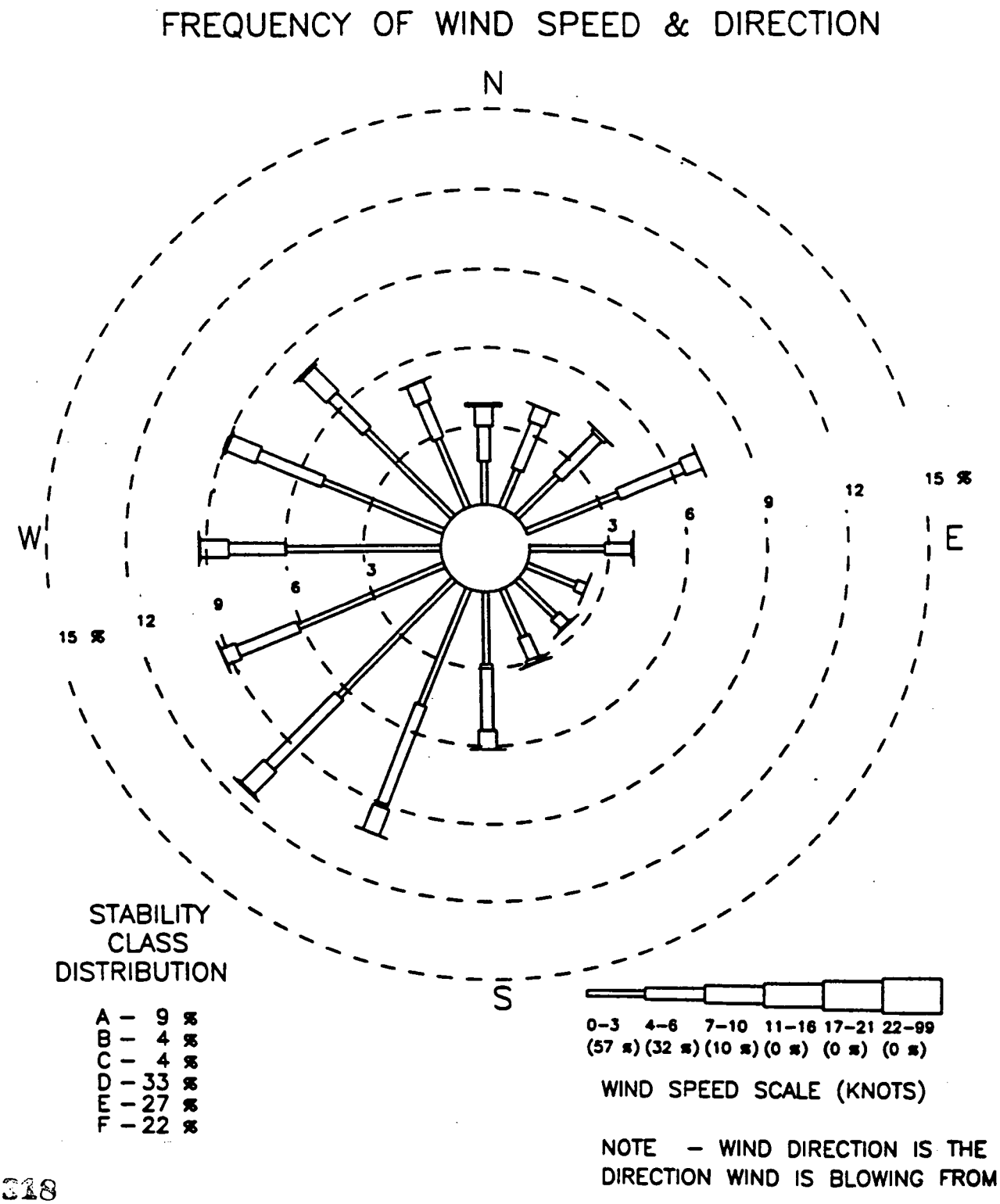

000318

FIGURE A.3-6
ACTIVE FLYASH PILE SOURCES

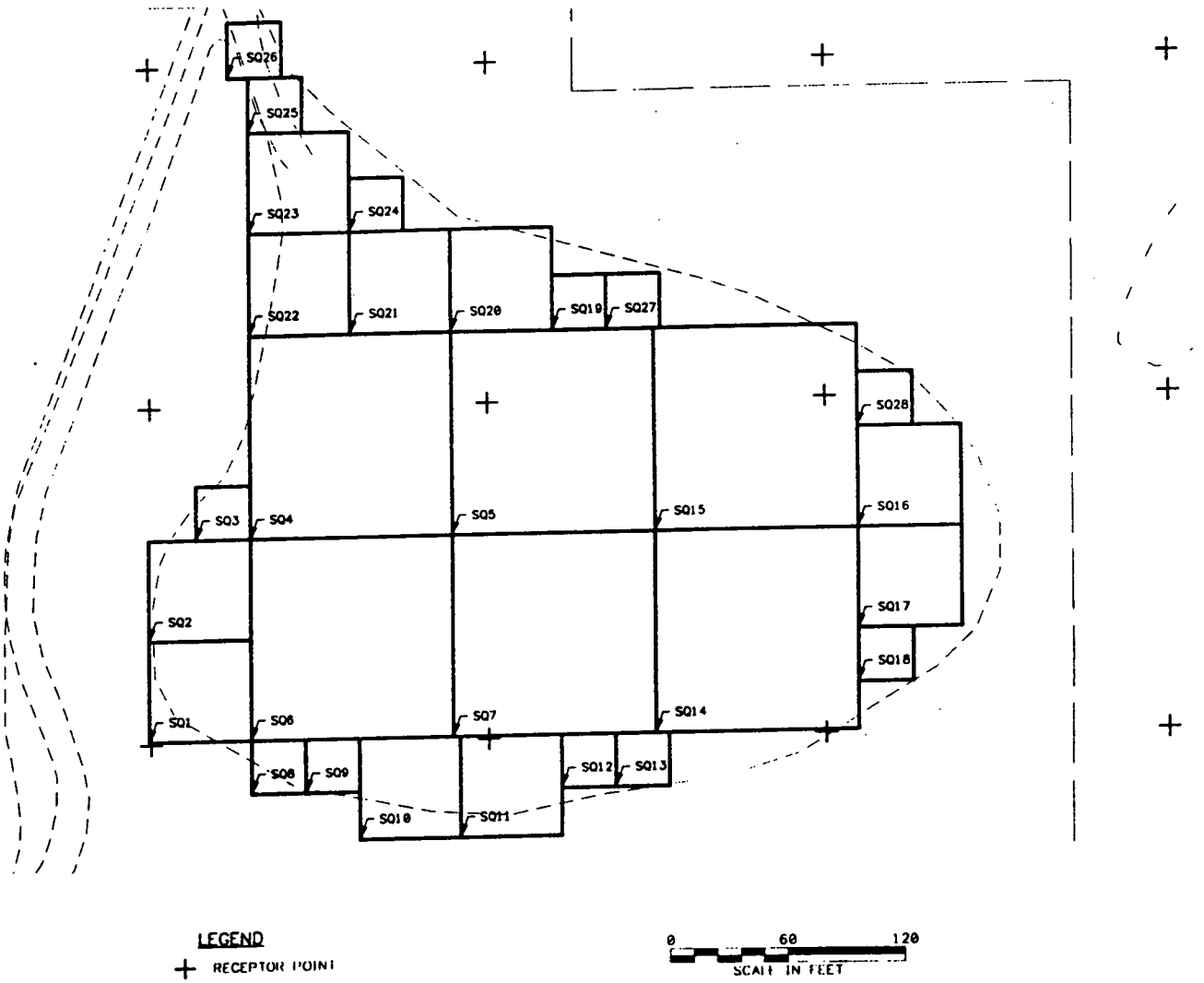

FIGURE A.3-7

SOUTH FIELD SOURCES

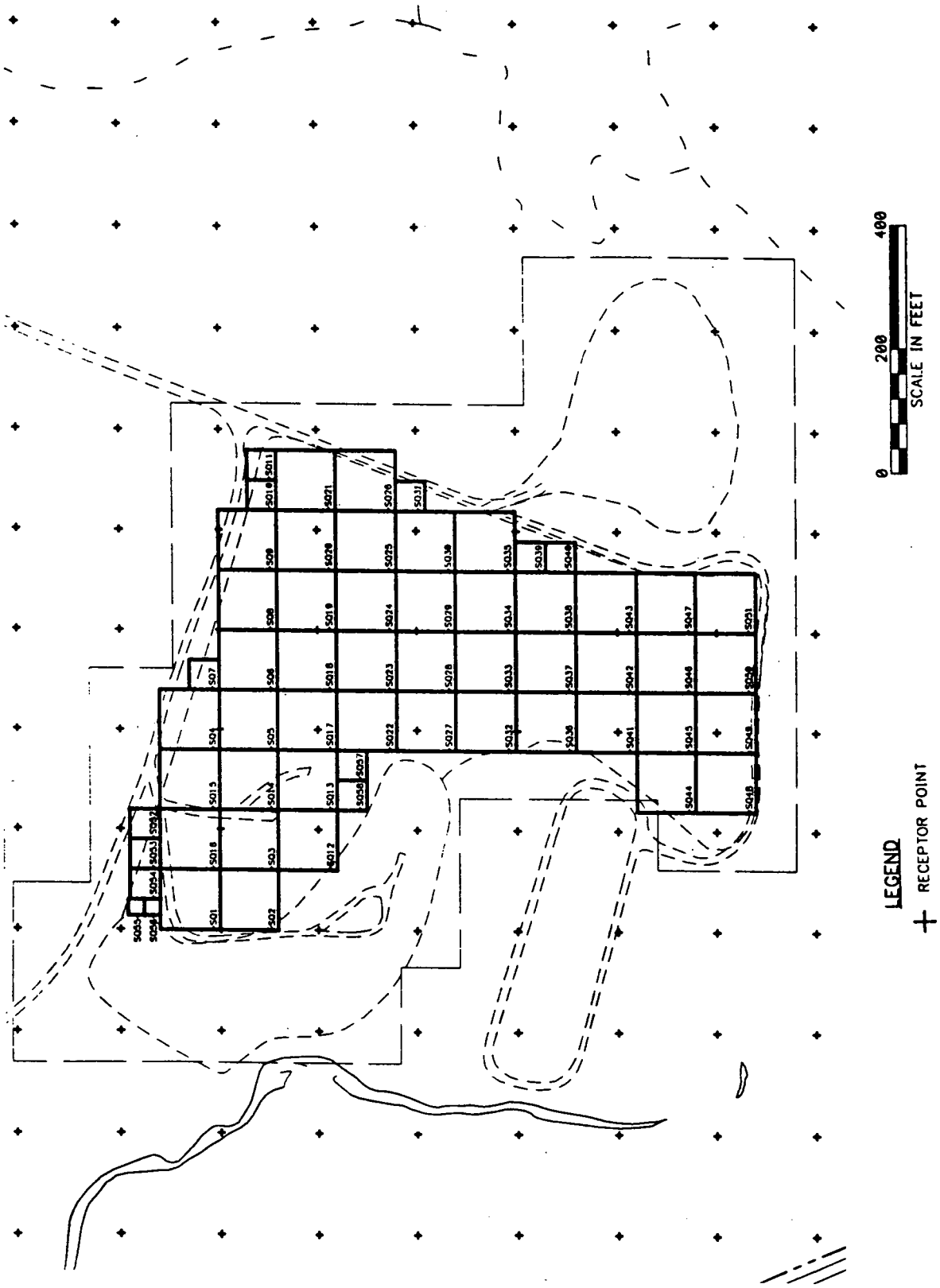

000320

FIGURE A.3-8

INACTIVE FLYASH PILE SOURCES

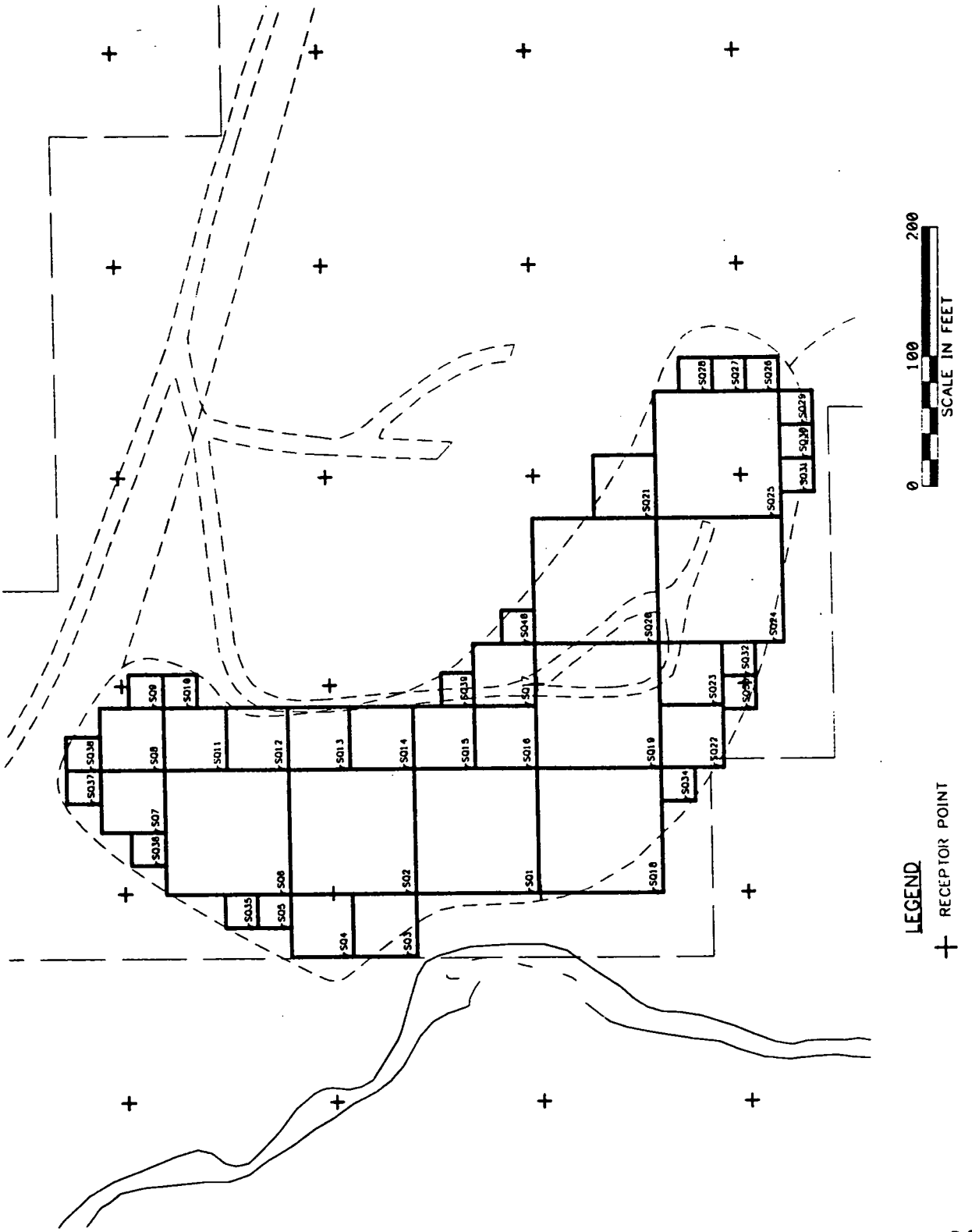

FIGURE A.3-9

SOLID WASTE LANDFILL SOURCES

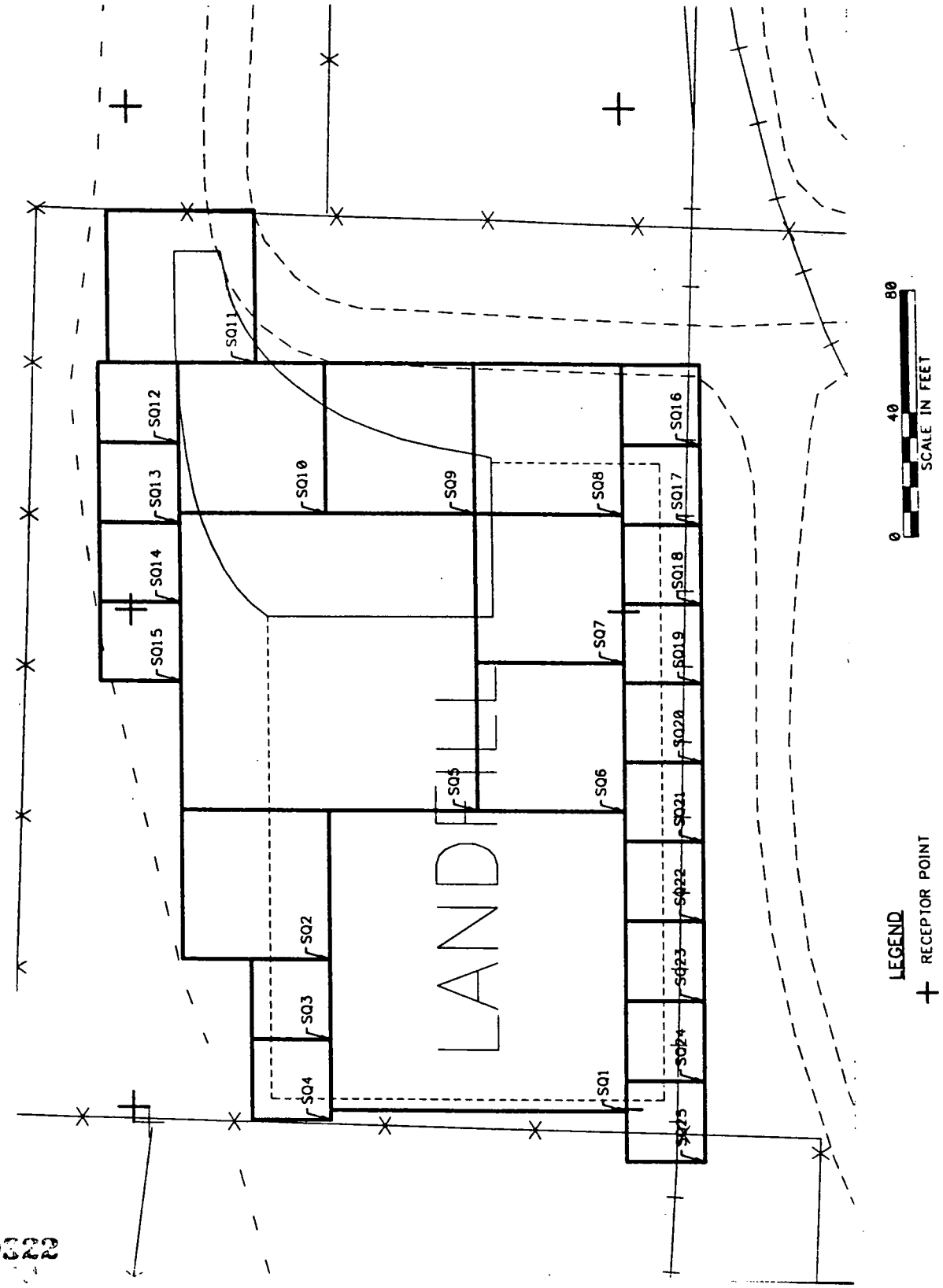

FIGURE A.3-10

LIME SLUDGE PONDS SOURCES

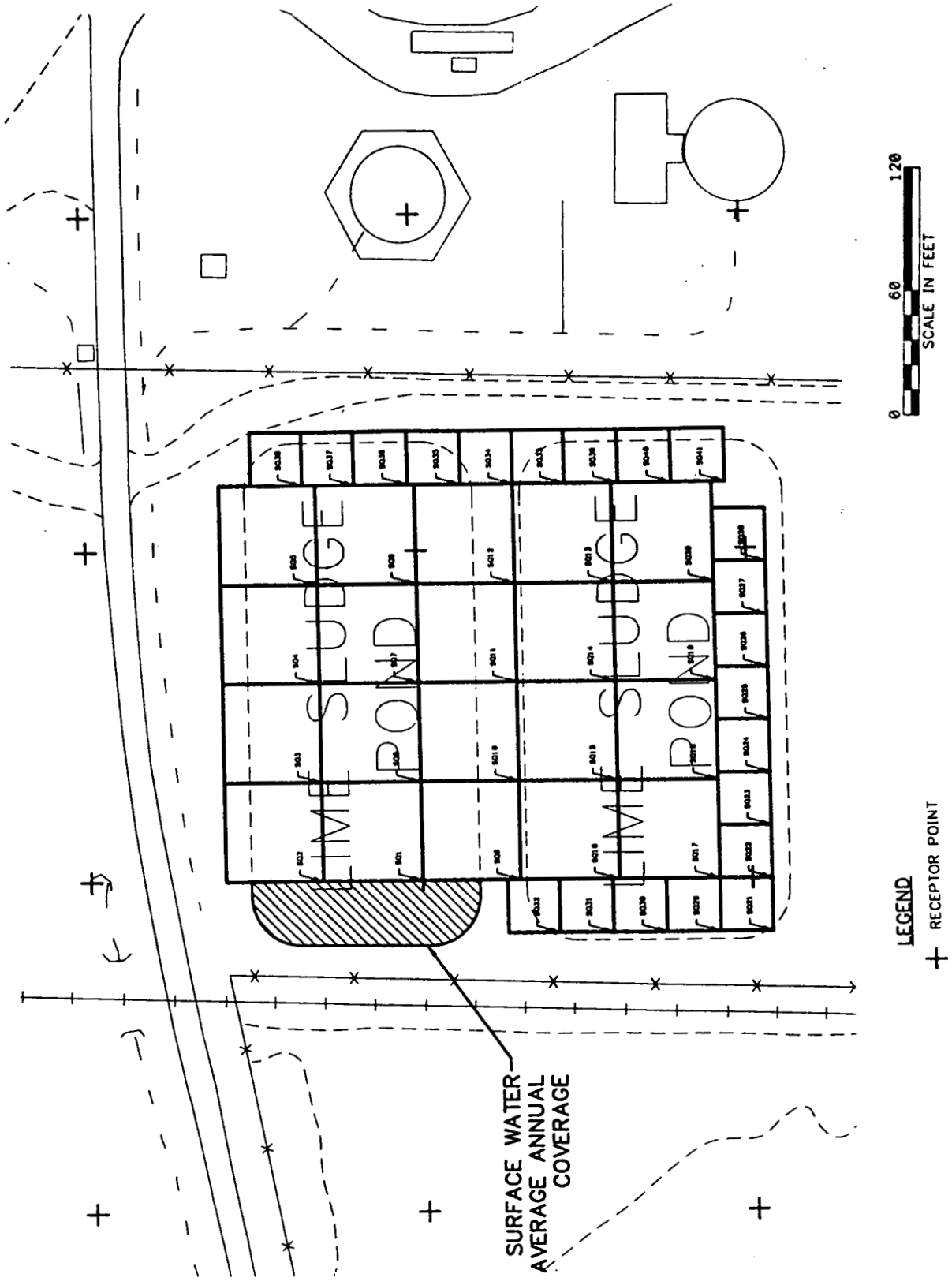

ISCLT2 requires the user to input coordinates of the southwest corner of individual squares along with the length of one side, assuming a box with four equal sides (EPA 1992a).

A.3.5.3 Emission rates

Emissions to the atmosphere from Operable Unit 2 include wind-blown particulate matter and radon gas emissions. The particulate matter contains radionuclides, inorganic and organic compounds. Radon gas is emitted from the radioactive decay of radium in the soils and materials. All organic compounds are assumed to be bound with the particulate matter. The vapor-phase emission rates for semivolatile and nonvolatile organic CPCs identified in Operable Unit 2 are several orders-of-magnitude below the particulate-phase emission rates. The volatile organic CPCs will typically degrade/volatilize from the site within the first year. Therefore, assuming that these compounds are emitted continuously with the particulate for many years provides a conservative assessment of chronic exposure to these compounds.

Particulate Matter Emissions

The method used to estimate inhalable particulate matter (PM_{10} - particle diameters $\leq$ 10 μm) and total suspended particulate (TSP - particle diameters $\leq$ 75 μm) emission rates for the FEMP is based on EPA guidance for estimating wind erosion rates from flat soil surfaces at hazardous waste sites (EPA 1985b). For risk assessment purposes, the PM_{10} emission rates were used to calculate air concentrations while the TSP emission rate was used to calculate total deposition rates. The EPA methodology assumes that a minimum wind speed is required for the suspension of respirable dust, and the emission rate is a nonlinear function of the "Threshold Friction Velocity" and the erosion potential of the site.

The erosion potential of each subunit depends on the particle size distribution of the surface soil, the crustiness of the surface and the relative quantity of vegetative cover. Essentially, sources that have continuous vegetative growth or where the surface soil has formed a hard crust are classified as having "limited" erosion potential. Conversely, sources with surface soil that are loose, fine or sandy are classified as having "unlimited" erosion potential which is dependent on the surface soil modal diameter. The particle size distributions for each subunit surface soil are presented in Table A.3-4.

NO A-39

Operable Unit 2 subunits were determined to have a limited erosion potential for almost all land use scenarios and receptors. This determination was made by a site survey in September 1993, which

TABLE A.3-4

PARTICLE SIZE DISTRIBUTIONS FOR OPERABLE UNIT 2 SUBUNITS OPERABLE UNIT 2 REMEDIAL INVESTIGATION FERNALD ENVIRONMENTAL MANAGEMENT PROJECT

Active Flyash Pile		Solid Waste Landfill		Lime Sludge Ponds		South Field		Inactive Flyash Pile	
Diameter (mm)	Percent Finer by Weight	Diameter (mm)	Percent Finer by Weight	Diameter (mm)	Percent Finer by Weight	Diameter (mm)	Percent Finer by Weight	Diameter (mm)	Percent Finer by Weight
75.	100.0	75.	100.0	75.	100.0	75.	100.0	75.	100.0
37.5	100.0	37.5	100.0	37.5	100.0	37.5	100.0	37.5	100.0
19.	100.0	19.	98.8	19.	100.0	19.	100.0	19.	100.0
9.5	100.0	9.5	97.3	9.5	100.0	9.5	97.6	9.5	94.8
4.75	97.8	4.75	96.5	4.75	100.0	4.75	93.2	4.75	90.4
2.	91.1	2.	93.8	2.	100.0	2.	89.8	2.	83.8
0.85	72.1	0.85	88.9	0.85	100.0	0.85	86.0	0.85	75.1
0.425	58.8	0.425	84.7	0.425	99.8	0.425	82.6	0.425	67.0
0.25	50.1	0.25	80.9	0.25	99.5	0.25	79.8	0.25	59.7
0.149	41.5	0.149	77.3	0.149	99.0	0.149	76.6	0.149	53.2
0.106	36.5	0.106	75.5	0.106	98.8	0.106	73.9	0.106	49.8
0.075	32.4	0.075	74.2	0.075	98.6	0.075	71.3	0.075	47.2
0.04747	26.8	0.05782	73.4	0.0546	95.2	0.0554	68.4	0.06493	38.4
0.03422	21.8	0.04198	67.6	0.03956	89.8	0.04017	63.5	0.04831	36.8
0.02205	16.7	0.03014	64.7	0.02928	79.1	0.02894	60.2	0.03302	34.3
0.01291	10.9	0.02108	38.6	0.02141	39.6	0.01924	50.3	0.02189	25.3
0.00932	6.7	0.01288	21.2	0.01351	8.6	0.014035	30.5	0.01264	18.8

See note at end of table

FER\CRU2RI\JLG\APP-A\TABA.3-4\June6, 1994 12:47pm

TABLE A.3-4
(Continued)

Active Flyash Pile		Solid Waste Landfill		Lime Sludge Ponds		South Field		Inactive Flyash Pile	
Diameter (mm)	Percent Finer by Weight	Diameter (mm)	Percent Finer by Weight	Diameter (mm)	Percent Finer by Weight	Diameter (mm)	Percent Finer by Weight	Diameter (mm)	Percent Finer by Weight
0.00666	3.3	0.00921	17.4	0.00956	3.2	0.00883	22.2	0.00921	14.7
0.00469	0.8	0.0065	13.5	0.0088	1.1	0.00627	18.1	0.00646	12.3
0.00322	0.0	0.00463	11.6	0.00481	0.0	0.00447	15.7	0.00453	8.8
0.00136	0.0	0.00326	10.6	0.00333	0.0	0.00316	13.2	0.00327	7.4
--	--	0.00140	7.7	0.00137	0.0	0.00137	9.9	0.0014	6.5

Source: IT Corporation, Particle Size Analysis (ASTM D 422), May-July 1993.

000526

indicated that the current conditions on all subunits included extensive vegetative cover, the presence of nonerodible elements and/or the presence of a crust. Therefore, the limited erosion model (EPA 1985b) was used for all current land use receptors and all future land use receptors that did not include the on-property farmer. The limited erosion model emission rate is determined by (EPA 1985b):

$$E_{10} = 0.83\ f\ P(u^{+})\ (1-V)\ /\ (PE/50)^2$$

where:

E_{10} = annual average PM_{10} emission rate per unit area of contaminated surface ($mg/hr/m^2$),

f = frequency of disturbance per month,

u^{+} = observed (or probable) fastest mile of wind (at the meteorological station anemometer height) for the period between disturbances (m/s),

$P(u^{+})$ = erosion potential, i.e., quantity of erodible particles present on the surface prior to the onset of wind erosion (g/m^2),

V = fraction of soil covered by vegetation, and

PE = Thornthwaite's Precipitation Evaporation Index used as a measure of average soil moisture content.

Estimates of the fastest mile and the evaporation index are presented in tables developed by the EPA (EPA 1985b). These tables have been reproduced in Attachment A.3.II of this Appendix. The fastest mile is approximately 24 m/s for the region. The PE Index is 103 for the southwest corner of Ohio. The erosion potential depends on the fastest mile as follows (EPA 1985b):

$$P(u^{+}) = 6.7\ [u^{+} - u_t(z)], \quad \text{for } u^{+} \geq u_t, \text{ and}$$
$$P(u^{+}) = 0, \quad \text{for } u^{+} < u_t,$$

and

$$u_t(z) = (u_* / 0.4)\ \ln\ (z/z_0)$$

where

$u_t(z)$ = erosion threshold wind speed at the meteorological station anemometer height (m/s),

u_* = threshold friction velocity at the surface roughness height (m/s),

z = meteorological station anemometer height (m), and

z_o = surface roughness height (m).

An estimate of the threshold friction velocity is necessary to determine ~~if a given subunit has a limited or unlimited erosion potential~~ the erosion potential. The threshold friction velocity can be determined from the EPA guidance document (EPA 1985b, Figure 3-4, presented in Attachment A.3.II) and the modal diameter of the surface soil in each subunit. The relationship between the modal diameter and the threshold friction velocity can be represented by the equation:

$$\log u_* = 1.812 + 0.4161 \log (d_p)$$

where

u_* = threshold friction velocity (cm/s), and
d_p = modal diameter of soil sample (mm).

The calculated threshold friction velocity should be corrected for the presence of nonerodible elements and surface crust. Nonerodible elements increase the threshold friction velocity for a given surface and crusted surfaces are regarded as having a limited reservoir of erodible material (EPA 1985b). ~~Based on a site survey in September 1993, the current surface conditions in the Operable Unit 2 subunits meet the criteria for limited erosion potential.~~ No correction was applied to the threshold friction velocity, thus producing a conservative baseline emission rate for the Operable Unit 2 subunits.

~~The equation used to predict PM_{10} emissions for soils with limited erosion potential is (EPA 1985):~~

NO. A-39

$$\cancel{E_{10} = 0.83\, f\, P(u^{+})\, (1-V) / (PE/50)^2}$$

~~where:~~

~~E_{10} = annual average PM_{10} emission rate per unit area of contaminated surface (mg/hr/m^2),~~

~~f = frequency of disturbance per month,~~

~~u^{+} = observed (or probable) fastest mile of wind (at the meteorological station anemometer height) for the period between disturbances (m/s),~~

~~$P(u^{+})$ = erosion potential, i.e., quantity of erodible particles present on the surface prior to the onset of wind erosion (g/m^2),~~

~~V = fraction of soil covered by vegetation, and~~

~~PE = Thornthwaite's Precipitation Evaporation Index used as a measure of average soil moisture content.~~

~~Estimates of the fastest mile and the evaporation index are presented in tables developed by the EPA (EPA 1985). These tables have been reproduced in Attachment A.3.II of this Appendix. The fastest mile is approximately 24 m/s for the region. The PE Index is 103 for the southwest corner of Ohio. The erosion potential depends on the fastest mile as follows (EPA 1985b):~~

$$\cancel{P(u^{+}) = 6.7\,[u^{+} - u_t(z)], \quad \text{for } u^{+} \geq u_t, \text{ and}}$$
$$\cancel{P(u^{+}) = 0, \quad \text{for } u^{+} < u_t,}$$

~~and~~

$$\cancel{u_t(z) = (u_* / 0.4) \ln (z/z_0)}$$

~~where~~

~~$u_t(z)$ = erosion threshold wind speed at the meteorological station anemometer height (m/s),~~

~~u_* = threshold friction velocity at the surface roughness height (m/s),~~

~~z = meteorological station anemometer height (m), and~~

~~z_0 = surface roughness height (m).~~

As ~~previously~~ discussed in Section A.3.3, the future source term for the Solid Waste Landfill and South Field must consider the impact that an on-subunit farmer would have on the erosion potential for these subunits. Since the surface of these subunits would be plowed on a regular basis, no correction to the calculated threshold friction velocity is considered. The calculated threshold friction velocity on these subunits is less than 75 cm/s (EPA 1985b); therefore, the unlimited erosion model is applied to the on-property farmer exposure scenario. The ~~resulting~~ unlimited erosion potential can be calculated by (EPA 1985b):

$$E_{10} = 0.036 \times (1-V) \times [(u/u_t)^3] \times F(y)$$

where

E_{10}	=	annual average PM_{10} emission rate per unit area of contaminated surface ($g/hr/m^2$),
V	=	fraction of soil covered by vegetation,
u	=	mean annual wind speed (m/s),
u_t	=	erosion threshold wind speed (m/s),
y	=	$0.886 \times u_t / u$,
F(y)	=	1.91 for $y < 0.5$,
F(y)	=	$0.18 \times (y^3 + 12y) \times EXP(-y^2)$ for $y > 2$, and
F(y)	=	See Figure 4-3, Attachment A.3.II (EPA 1985b), for $0.5 < y < 2$.

The equations presented above for limited and unlimited erosion potential calculate the PM_{10} emission rate used to determined airborne concentrations of particle-bound contaminants associated with each subunit. The TSP emission rate was calculated by multiplying the PM_{10} rate by the ratio of TSP-to-PM_{10} percentages from the subunit surface soil particle size distribution. The TSP emission rates were used to determine the total deposition rate of each contaminant from each subunit.

The approximate modal diameter and modeled PM_{10} emission rate, TSP emission rate, particle settling velocity, and particle reflection coefficient are presented in Table A.3-5. The settling velocity and reflection coefficient were based on each subunit particle modal diameter, calculated from the methods presented in the ISCLT2 User's Manual (EPA 1992b). An example calculation is presented in Attachment A.3.II.

Radon 222 Emission Rates

Total emissions of Rn-222 were calculated for surface and subsurface soil in each subunit. Rn-222 emissions were determined from the Ra-226 concentrations in the contaminated soil or waste using the RAECOM model algorithms developed for the NRC (NRC 1984). The model accounts for the half-lives of radon and radium as well as the density, porosity, moisture content, and depth of contaminated layers and cover layers in estimating Rn-222 emission rates. The model converts Ra-226 soil concentrations

TABLE A.3-5

PARTICULATE MATTER EMISSION RATES USED IN ISCLT2 MODELING OPERABLE UNIT 2 REMEDIAL INVESTIGATION FERNALD ENVIRONMENTAL MANAGEMENT PROJECT

Subunit (Source Term)	Modal Diameter (mm)	PM_{10} Emissions ($g/s/m^2$)	TSP Emissions ($g/s/m^2$)	Settling Velocity (m/s)	Reflection Coefficient
Active Flyash Pile (Current and Future)	0.038	8.0E-06	3.8E-05	0.115	0.45
Inactive Flyash Pile (Current and Future)	0.022	1.0E-06	4.0E-06	0.038	0.65
North Lime Sludge Pond (Current and Future)	0.021	8.0E-06	2.5E-04	0.038	0.65
South Lime Sludge Pond (Current and Future)	0.021	1.0E-06	4.0E-05	0.038	0.65
South Field (Current)	0.014	1.0E-06	3.0E-06	0.032	0.66
South Field (Future)	0.014	3.6E-05	8.5E-05	0.032	0.66
Solid Waste Landfill (Current)	0.021	1.0E-06	6.0E-06	0.038	0.65
Solid Waste Landfill (Future)	0.021	3.0E-05	1.4E-04	0.038	0.65

(in pCi/g) to Rn-222 fluxes (in pCi/s/m^2). The basic equations are presented in the RAWPA (DOE 1992). The porosity and moisture content values used in the groundwater transport analysis were also used in the RAECOM model.

The RAECOM model input parameters as well as the current and future Rn-222 fluxes from each emission source are presented in Table A.3-6. The RAECOM model output is presented in Attachment A.3.III. No changes were assumed to occur between the current and future conditions for the basic soil parameters (porosity, moisture content, density, and Ra-226 concentration) used in the RAECOM model. Therefore, the current and future Rn-222 source terms were the same for each subunit.

A.3.5.4 Receptor data

A receptor is defined as a user-selected point at a given distance from a source or origin. ISCLT2 estimates the location of maximum on property and off property concentrations and deposition rates at receptors from sources (EPA 1992a). On-subunit, on-property, and off-property receptors were determined by boundaries of individual Operable Unit 2 subunits and the FEMP boundary. A series of receptors around a source is commonly referred to as a "receptor grid" and may be expressed in polar or Cartesian coordinates.

The air pathways analysis for Operable Unit 2 used an 86 x 61 receptor grid (i.e. number of receptors along the north-south axis and the number of receptors along the east-west axis), with 50 meter spacing between each receptor. Origin of the receptor grid was located at State Planer Coordinates; 482,752.690 feet (North) and 1,376,778.760 feet (East) and 578.941 feet (elevation). See Figure A.3-11.

Discrete receptors were used in the air transport analysis to account for concentrations and deposition rates at sensitive locations. Discrete receptors consisted of Crosby Elementary School, Morgan Elementary School, Elda Elementary School, Ross Middle and High School, St. Johns Elementary and Ross County Day Nursery. Discrete receptors and corresponding Cartesian coordinate locations from the origin are listed in Table A.3-7.

A.3.6 AIR DISPERSION MODELING RESULTS

The objective of the analysis was to determine maximum annual concentration and deposition rate estimates at receptors located within the boundary of the individual subunits (on-subunit), between the

FIGURE A.3-11

OPERABLE UNIT 2 RECEPTOR GRID

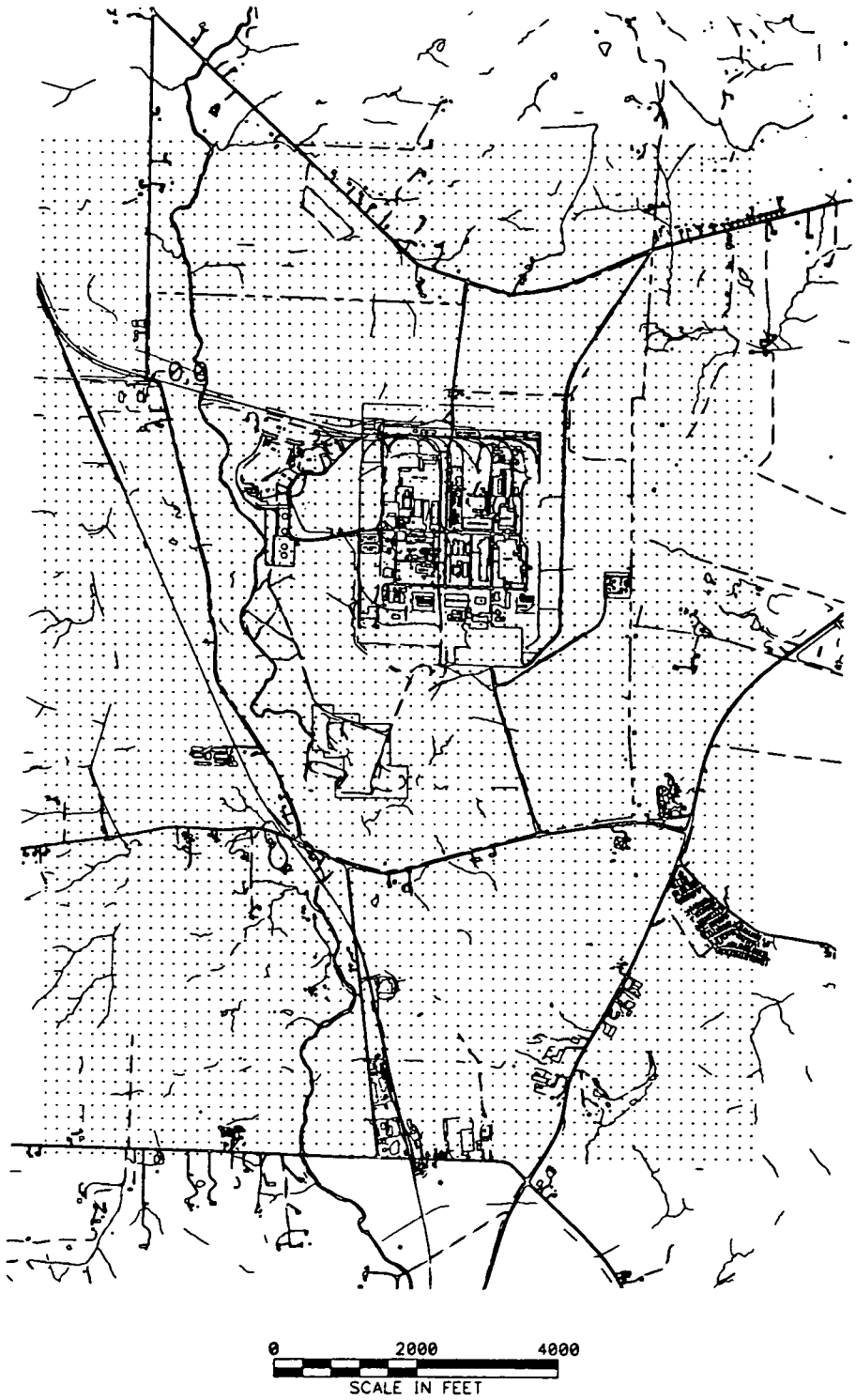

TABLE A.3-6

RAECOM MODEL INPUT PARAMETERS AND RN-222 EMISSION RATES
OPERABLE UNIT 2 REMEDIAL INVESTIGATION
FERNALD ENVIRONMENTAL MANAGEMENT PROJECT

Subunit (Media)	Ra-226 Conc. (pCi/g)	Soil Bulk Density (g/cm^3)	Soil Porosity (Percent)	Moisture Content (Wt %)	Radon source term ($pCi/cm^3/s$)	Rn-222 Emission Rate ($pCi/s/m^2$)
Active Flyash Pile						
(Surface soil)	4.60	1.70	52.0	28.6	6.32E-06	1.52
(Subsurface soil)	5.24	1.85	41.0	20.0	9.93E-06	
Inactive Flyash Pile						
(Surface soil)	1.98	1.70	52.0	29.8	2.71E-06	0.68
(Subsurface soil)	2.92	1.85	41.0	20.0	5.53E-06	
Lime Sludge Ponds						
(Surface soil)	1.92	1.70	52.0	84.2	2.63E-06	0.09
(Subsurface soil)	1.42	1.73	41.0	20.0	2.52E-06	
South Field						
(Surface soil)	30.8	1.70	52.0	18.2	4.25E-05	6.80
(Subsurface soil)	2.92	1.85	41.0	20.0	5.53E-06	
Solid Waste Landfill						
(Surface soil)	1.40	1.83	52.0	18.7	2.06E-06	0.53
(Subsurface soil)	1.55	1.89	41.0	21.7	3.00E-06	
Background						
(Surface soil)	1.23	1.70	52.0	29.8	1.69E-06	0.30
(Subsurface soil)	0.78	1.85	41.0	20.0	1.48E-06	

TABLE A.3-7

DISCRETE RECEPTORS AND DISTANCE FROM ORIGIN*
OPERABLE UNIT 2 REMEDIAL INVESTIGATION
FERNALD ENVIRONMENTAL MANAGEMENT PROJECT

Discrete Receptors	X-Coordinate (meters)	Y-Coordinate (meters)
Crosby Elementary	-1180	-3140
Morgan Elementary	-3200	3150
Elda Elementary	5360	1780
St. John Elementary	7130	-4650
Ross Middle/High School	6145	3300
Ross County Day Nursery	5575	2225

*Origin located at State Planer Coordinates, 482,752.690 feet North and 1,376,778.760 feet East.

subunit boundary and the FEMP boundary (on-property), at or beyond the FEMP boundary (off-property) and at sensitive receptors (i.e. elementary schools and daycare centers) within the vicinity of FEMP. Deposition rate estimations were determined at ground level and not at a 1.5 meter height as suggested in FEMP Air Modeling Protocol. Ground level was chosen in lieu of 1.5 meter height because it suggests that contaminated plants would be more accessible to a larger variety of animals for ingestion if they were at ground level than at an elevated distance. The maximum annual concentrations and deposition rates were taken from the worst case annual meteorological period.

A.3.6.1 Current Scenario - Concentrations Estimations

The highest annual concentration calculated for an on-subunit receptor was 26 $\mu g/m^3$ and occurred as a result of emissions from the Lime Sludge Ponds. This concentration was calculated for an on-subunit receptor located in the southeast corner of the North Lime Sludge Pond.

The highest annual concentration calculated for an on-property receptor was 15 $\mu g/m^3$ and occurred from emissions from the Lime Sludge Ponds. This concentration was calculated for a receptor located in the extreme western end of the Production Area.

The highest annual concentration calculated for an off-property receptor was 0.748 $\mu g/m^3$ and occurred from emissions from the Active Flyash Pile. This concentration was calculated for a receptor located 430 meters west-southwest of the Active Flyash Pile center.

A.3.6.2 Current Scenario - Deposition Rate Estimations

The highest annual deposition rate calculated for an on-subunit receptor was 55.7 g/m^2 and was the result of emissions from the Active Flyash Pile. This receptor was located on the Active Flyash Pile approximately 20 meters north of its center.

The highest annual deposition rate calculated at an on-property receptor was 29.7 g/m^2 and resulted from emissions from the Active Flyash Pile. This receptor was located 70 meters north of the center of the Active Flyash Pile center.

The highest annual deposition rate calculated at an off-property receptor was 0.98 g/m^2 and resulted from emissions from the Active Flyash Pile. This receptor was located 430 meters west-southwest of the Active Flyash Pile center.

A.3.6.3 Future Scenario - Concentration Estimations

Highest annual concentrations calculated at receptors located on-subunit, on-property and off-property were 410 $\mu g/m^3$, 358 $\mu g/m^3$ and 26 $\mu g/m^3$, respectively. All these concentrations estimations originated from emissions from the South Field.

A.3.6.4 Future Scenario - Deposition Rate Estimations

Highest annual deposition rate calculated at on-subunit and on-property receptors was 55.7 g/m^2 and 29.7 g/m^2, respectively. These estimations were a result of emissions from the Active Flyash Pile. The highest annual deposition rate calculated at an off-property receptor was 1.063 g/m^2 from emissions from the South Field. This particular receptor was located approximately 350 meters southwest of the center of South Field.

A summation of maximum concentrations and deposition rates for current and future scenarios at on-subunit, on-property and off-property receptors for Operable Unit 2 subunits are listed in Tables A.3-8 through A.3-11. Likewise, a summation of concentrations and deposition rate at sensitive receptors are listed in Tables A.3-12 through A.3-15.

Tables A.3-16 through A.3-29 illustrate maximum annual concentration and deposition rate estimations of each contaminant of concern (COC) inherent to each subunit as a function of air modeling and current and future scenarios.

TABLE A.3-8

MAXIMUM ANNUAL CONCENTRATIONS AND LOCATIONS OF ON-SUBUNIT, ON-PROPERTY AND OFF-PROPERTY RECEPTORS FOR OPERABLE UNIT 2 SUBUNITS CURRENT SCENARIO OPERABLE UNIT 2 REMEDIAL INVESTIGATION FERNALD ENVIRONMENTAL MANAGEMENT PROJECT

	Maximum Annual Concentrations ($\mu g/m^3$)				
Sensitive Receptors	Active Flyash Pile	South Field	Inactive Flyash Pile	Solid Waste Landfill	Lime Sludge Ponds
On-Subunit	10.3 (1000,-1650)	9.9 (950,-1500)	6.0 (750,-1500)	3.0 (950,-200)	26 (950,-650)
On-Property	7.5 (1000,-1600)	8.9 (1000,-1500)	7.0 (750,-1450)	3.0 (1000,-150)	15 (1000,-650)
Off-Property	0.748 (600,-1800)	0.7316 (550,-1700)	0.36 (500,-1600)	0.0494 (1150,350)	0.1771 (250,-850)

TABLE A.3-9

MAXIMUM ANNUAL DEPOSITION RATES AND LOCATIONS OF ON-SUBUNIT, ON-PROPERTY AND OFF-PROPERTY RECEPTORS FOR OPERABLE UNIT 2 SUBUNITS CURRENT SCENARIO OPERABLE UNIT 2 REMEDIAL INVESTIGATION FERNALD ENVIRONMENTAL MANAGEMENT PROJECT

	Maximum Annual Deposition Rates (g/m^2)				
Sensitive Receptors	Active Flyash Pile	South Field	Inactive Flyash Pile	Solid Waste Landfill	Lime Sludge Ponds
On-Subunit	55.7 (1000,-1650)	0.3091 (950,-1500)	0.3417 (750,-1400)	0.4195 (950,-200)	18 (950,-650)
On-Property	29.7 (1000,-1600)	0.3235 (1000,-1500)	0.3755 (750,-1450)	0.3678 (1000,-150)	11 (1000,-650)
Off-Property	0.98 (600,-1800)	0.0375 (550,-1700)	0.0284 (500,-1600)	0.0061 (1150,350)	0.1249 (250,-900)

DRAFT

TABLE A.3-10

MAXIMUM ANNUAL CONCENTRATIONS AND LOCATIONS OF ON-SUBUNIT, ON-PROPERTY AND OFF-PROPERTY RECEPTORS FOR OPERABLE UNIT 2 SUBUNITS FUTURE SCENARIO OPERABLE UNIT 2 REMEDIAL INVESTIGATION FERNALD ENVIRONMENTAL MANAGEMENT PROJECT

	Maximum Annual Concentrations ($\mu g/m^3$)				
Sensitive Receptors	Active Flyash Pile	South Field	Inactive Flyash Pile	Solid Waste Landfill	Lime Sludge Ponds
On-Subunit	10.3 (1000,-1650)	410 (950,-1500)	6.0 (750,-1400)	91 (950,-200)	26 (950,-650)
On-Property	7.5 (1000,-1600)	358 (1000,-1500)	7.0 (750,-1450)	91 (1000,-150)	15 (1000,-650)
Off-Property	0.748 (600,-1800)	26 (550,-1700)	0.36 (500,-1600)	1.5 (1150,350)	0.1771 (250,-850)

TABLE A.3-11

MAXIMUM ANNUAL DEPOSITION RATES AND LOCATIONS OF ON-SUBUNIT, ON-PROPERTY AND OFF-PROPERTY RECEPTORS FOR OPERABLE UNIT 2 SUBUNITS FUTURE SCENARIO OPERABLE UNIT 2 REMEDIAL INVESTIGATION FERNALD ENVIRONMENTAL MANAGEMENT PROJECT

	Maximum Annual Deposition Rates (g/m^2)				
Sensitive Receptors	Active Flyash Pile	South Field	Inactive Flyash Pile	Solid Waste Landfill	Lime Sludge Ponds
On-Subunit	55.7 (1000,-1650)	8.8 (950,-1500)	0.3417 (750,-1400)	9.8 (950,-200)	18 (950,-650)
On-Property	29.7 (1000,-1600)	9.2 (1000,-1500)	0.3755 (750,-1450)	8.6 (1000,-150)	11 (1000,-650)
Off-Property	0.98 (600,-1800)	1.063 (550,-1700)	0.0284 (500,-1600)	0.1417 (1150,350)	0.1249 (250,-900)

TABLE A.3-12

MAXIMUM CONCENTRATIONS* ($\mu g/m^3$) AT SENSITIVE RECEPTORS CURRENT SCENARIO OPERABLE UNIT 2 SUBUNITS OPERABLE UNIT 2 REMEDIAL INVESTIGATION FERNALD ENVIRONMENTAL MANAGEMENT PROJECT

Sensitive Receptors	Active Flyash Pile	South Field	Inactive Flyash Pile	Solid Waste Landfill	Lime Sludge Ponds
Crosby Elementary	0.039	0.0232	0.0057	0.0009	0.0067
Morgan Elementary	0.005	0.0035	0.001	0.0005	0.0025
Elda Elementary	0.028	0.0182	0.0048	0.0024	0.0134
St. Johns Elementary	0.020	0.0109	0.0028	0.0008	0.0056
Ross Middle High School	0.019	0.0129	0.0032	0.0016	0.0088
Ross County Day Nursery	0.024	0.0161	0.0042	0.0021	0.0119

*Calculated at flagpole receptor height of 1.5 meters.

TABLE A.3-13

MAXIMUM DEPOSITION RATES* (g/m^2)
AT SENSITIVE RECEPTORS
CURRENT SCENARIO
OPERABLE UNIT 2 SUBUNITS
OPERABLE UNIT 2 REMEDIAL INVESTIGATION
FERNALD ENVIRONMENTAL MANAGEMENT PROJECT

Sensitive Receptors	Active Flyash Pile	South Field	Inactive Flyash Pile	Solid Waste Landfill	Lime Sludge Ponds
Crosby Elementary	0.0165	0.0058	0.0019	0.0006	0.0254
Morgan Elementary	0.0003	0.0003	0.0001	0.0001	0.0026
Elda Elementary	0.0042	0.0031	0.0011	0.0008	0.0255
St. Johns Elementary	0.0011	0.0009	0.0003	0.0001	0.0042
Ross Middle High School	0.0017	0.0016	0.0005	0.0005	0.0133
Ross County Day Nursery	0.0032	0.0026	0.0009	0.0007	0.0214

*Calculated at ground level.

TABLE A.3-14

MAXIMUM CONCENTRATIONS* ($\mu g/m^3$) AT SENSITIVE RECEPTORS FUTURE SCENARIO OPERABLE UNIT 2 SUBUNITS OPERABLE UNIT 2 REMEDIAL INVESTIGATION FERNALD ENVIRONMENTAL MANAGEMENT PROJECT

Sensitive Receptors	Active Flyash Pile	South Field	Inactive Flyash Pile	Solid Waste Landfill	Lime Sludge Ponds
Crosby Elementary	0.039	0.8342	0.0057	0.0274	0.0067
Morgan Elementary	0.005	0.1259	0.001	0.0146	0.0025
Elda Elementary	0.028	0.6545	0.0048	0.0725	0.0134
St. Johns Elementary	0.020	0.3938	0.0028	0.0251	0.0056
Ross Middle High School	0.019	0.4375	0.0032	0.0477	0.0088
Ross County Day Nursery	0.024	0.5780	0.0042	0.0640	0.0119

*Calculated at flagpole receptor height of 1.5 meters.

TABLE A.3-15

MAXIMUM DEPOSITION RATES*(g/m²) AT SENSITIVE RECEPTORS FUTURE SCENARIO OPERABLE UNIT 2 SUBUNITS OPERABLE UNIT 2 REMEDIAL INVESTIGATION FERNALD ENVIRONMENTAL MANAGEMENT PROJECT

Sensitive Receptors	Active Flyash Pile	South Field	Inactive Flyash Pile	Solid Waste Landfill	Lime Sludge Ponds
Crosby Elementary	0.0165	0.1654	0.0019	0.0140	0.0254
Morgan Elementary	0.0003	0.0085	0.0001	0.0024	0.0026
Elda Elementary	0.0042	0.0888	0.0011	0.0197	0.0255
St. Johns Elementary	0.0011	0.0252	0.0003	0.0025	0.0042
Ross Middle High School	0.0017	0.0025	0.0005	0.0107	0.0133
Ross County Day Nursery	0.032	0.0042	0.0009	0.0168	0.0214

*Calculated at flagpole receptor height of 1.5 meters.

TABLE A.3-16

PRELIMINARY EXPOSURE POINT CONCENTRATIONS FOR THE ACTIVE FLYASH PILE OPERABLE UNIT 2 REMEDIAL INVESTIGATION FERNALD ENVIRONMENTAL MANAGEMENT PROJECT

Parameter	Concentration Term	Maximum Exposure Point Concentrations[a]		
		On-subunit[b]	On-site[c]	Off-site[d]
RADIOLOGICAL	(pCi/g)	(pCi/m³)	(pCi/m³)	(pCi/m³)
Neptunium 237	5.5	5.67e-05	4.13e-05	4.11e-06
Plutonium 238	0.7	7.21e-06	5.25e-06	5.24e-07
Plutonium 239/240	0.3	3.09e-06	2.25e-06	2.24e-07
Radium 226	4.6	4.74e-05	3.45e-05	3.44e-06
Radium 228	3.2	3.30e-05	2.40e-05	2.39e-06
Strontium 90	4.5	4.64e-05	3.38e-05	3.37e-06
Thorium 228	3.8	3.91e-05	2.85e-05	2.84e-06
Thorium 230	3.7	3.81e-05	2.78e-05	2.77e-06
Thorium 232	2.7	2.78e-05	2.03e-05	2.02e-06
Uranium 234	3.6	3.71e-05	2.70e-05	2.69e-06
Uranium 235/236	0.2	2.06e-06	1.50e-06	1.50e-07
Uranium 238	3.6	3.71e-05	2.70e-05	2.69e-06
INORGANICS/ORGANICS	(mg/kg)	(mg/m³)	(mg/m³)	(mg/m³)
Arsenic	89.8	9.25e-07	6.74e-07	6.72e-08
Barium	253.9	2.62e-06	1.90e-06	1.90e-07
Beryllium	4.7	4.84e-08	3.53e-08	3.52e-09
Chromium	13.3	1.37e-07	9.98e-08	9.95e-09
Cobalt	18.8	1.94e-07	1.41e-07	1.41e-08
Copper	73.8	7.60e-07	5.54e-07	5.52e-08
Cyanide	0.3	3.09e-09	2.25e-09	2.24e-10
Lead	55.4	5.71e-07	4.16e-07	4.14e-08
Molybdenum	8.6	8.86e-08	6.45e-08	6.43e-09
Nickel	40.1	4.13e-07	3.01e-07	3.00e-08
Selenium	5.9	6.08e-08	4.43e-08	4.41e-09
Thallium	2.7	2.78e-08	2.03e-08	2.02e-09
Toluene	0.1	1.03e-09	7.50e-10	7.48e-11
Vanadium	50.2	5.17e-07	3.77e-07	3.75e-08
Zinc	78.3	8.06e-07	5.87e-07	5.86e-08

[a]Maximum concentrations from ISCLT modeling

[b]Within the subunit itself, 10.3 ug/m3, approximately 20 meters north of Active Flyash Pile center

[c]Area from subunit boundary to FEMP boundary, 7.5 ug/m3, approximately 70 meters north of Active Flyash Pile center

[d]Area beyond the FEMP boundary, 0.748 ug/m3, approximately 430 meters west-southwest of Active Flyash Pile center

TABLE A.3-17

PRELIMINARY ANNUAL EXPOSURE POINT DEPOSITION RATES FOR THE ACTIVE FLYASH PILE OPERABLE UNIT 2 REMEDIAL INVESTIGATION FERNALD ENVIRONMENTAL MANAGEMENT PROJECT

Parameter	Concentration Term	Maximum Exposure Point Concentrations[a]		
		On-subunit[b]	On-site[c]	Off-site[d]
RADIOLOGICAL	(pCi/g)	(pCi/m^2)	(pCi/m^2)	(pCi/m^2)
Neptunium 237	5.5	3.06e+02	1.63e+02	5.39e+00
Plutonium 238	0.7	3.90e+01	2.08e+01	6.86e-01
Plutonium 239/240	0.3	1.67e+01	8.91e+00	2.94e-01
Radium 226	4.6	2.56e+02	1.37e+02	4.51e+00
Radium 228	3.2	1.78e+02	9.50e+01	3.14e+00
Strontium 90	4.5	2.51e+02	1.34e+02	4.41e+00
Thorium 228	3.8	2.12e+02	1.13e+02	3.72e+00
Thorium 230	3.7	2.06e+02	1.10e+02	3.63e+00
Thorium 232	2.7	1.50e+02	8.02e+01	2.65e+00
Uranium 234	3.6	2.01e+02	1.07e+02	3.53e+00
Uranium 235/236	0.2	1.11e+01	5.94e+00	1.96e-01
Uranium 238	3.6	2.01e+02	1.07e+02	3.53e+00
INORGANICS/ORGANICS	(mg/kg)	(mg/m^2)	(mg/m^2)	(mg/m^2)
Arsenic	89.8	5.00e+00	2.67e+00	8.80e-02
Barium	253.9	1.41e+01	7.54e+00	2.49e-01
Beryllium	4.7	2.62e-01	1.40e-01	4.61e-03
Chromium	13.3	7.41e-01	3.95e-01	1.30e-02
Cobalt	18.8	1.05e+00	5.58e-01	1.84e-02
Copper	73.8	4.11e+00	2.19e+00	7.23e-02
Cyanide	0.3	1.67e-02	8.91e-03	2.94e-04
Lead	55.4	3.09e+00	1.65e+00	5.43e-02
Molybdenum	8.6	4.79e-01	2.55e-01	8.43e-03
Nickel	40.1	2.23e+00	1.19e+00	3.93e-02
Selenium	5.9	3.29e-01	1.75e-01	5.78e-03
Thallium	2.7	1.50e-01	8.02e-02	2.65e-03
Toluene	0.1	5.57e-03	2.97e-03	9.80e-05
Vanadium	50.2	2.80e+00	1.49e+00	4.92e-02
Zinc	78.3	4.36e+00	2.33e+00	7.67e-02

[a]Maximum annual deposition rates from ISCLT modeling

[b]Within the subunit itself, 55.7 g/m2, approximately 20 meters north of Active Flyash Pile center

[c]Area from subunit boundary to FEMP boundary, 29.7 g/m2, approximately 70 meters north of Active Flyash Pile center

[d]Area beyond the FEMP boundary, 0.98 g/m2, approximately 430 meters west-southwest of Active Flyash Pile center

TABLE A.3-18

PRELIMINARY MAXIMUM CONCENTRATIONS FROM AIR DISPERSION MODELING SOUTH FIELD - CURRENT SCENARIO OPERABLE UNIT 2 REMEDIAL INVESTIGATION FERNALD ENVIRONMENTAL MANAGEMENT PROJECT

Parameter	Concentration Term	Maximum Annual Exposure Point Concentrations[a]		
		On-subunit[b]	On-site[c]	Off-site[d]
RADIOLOGICAL	(pCi/g)	(pCi/m^3)	(pCi/m^3)	(pCi/m^3)
Cesium 137	4.99e-01	4.94e-06	4.44e-06	3.65e-07
Neptunium 237	2.28e-01	2.26e-06	2.03e-06	1.67e-07
Plutonium 238	1.20e-01	1.19e-06	1.07e-06	8.78e-08
Plutonium 239/240	5.10e-02	5.05e-07	4.54e-07	3.73e-08
Radium 226	3.08e+01	3.05e-04	2.74e-04	2.25e-05
Radium 228	3.88e+00	3.84e-05	3.45e-05	2.84e-06
Strontium 90	1.00e+00	9.90e-06	8.90e-06	7.32e-07
Technecium 99	1.42e+02	1.41e-03	1.26e-03	1.04e-04
Thorium 228	4.41e+00	4.37e-05	3.92e-05	3.23e-06
Thorium 230	1.38e+01	1.37e-04	1.23e-04	1.01e-05
Thorium 232	3.99e+00	3.95e-05	3.55e-05	2.92e-06
Uranium 234	8.66e+00	8.57e-05	7.71e-05	6.33e-06
Uranium 235/236	4.19e-01	4.15e-06	3.73e-06	3.07e-07
Uranium 238	9.31e+00	9.22e-05	8.29e-05	6.81e-06
INORGANICS	(mg/kg)	(mg/m^3)	(mg/m^3)	(mg/m^3)
Arsenic	7.27e+00	7.20e-08	6.47e-08	5.32e-09
Beryllium	9.42e-01	9.33e-09	8.38e-09	6.89e-10
Chromium	1.39e+01	1.38e-07	1.24e-07	1.02e-08
Lead	2.46e+01	2.43e-07	2.19e-07	1.80e-08
ORGANICS	(mg/kg)	(mg/m^3)	(mg/m^3)	(mg/m^3)
Aroclor-1254	8.90e-02	8.81e-10	7.92e-10	6.51e-11
Aroclor-1260	5.20e-02	5.15e-10	4.63e-10	3.80e-11
Dieldrin	1.00e-02	9.90e-11	8.90e-11	7.32e-12
Benzo(a)anthracene	5.50e+00	5.45e-08	4.90e-08	4.02e-09
Benzo(a)pyrene	9.40e+00	9.31e-08	8.37e-08	6.88e-09
Benzo(b)fluoranthene	6.20e+00	6.14e-08	5.52e-08	4.54e-09
Benzo(k)fluoranthene	7.30e+00	7.23e-08	6.50e-08	5.34e-09
Carbazole	1.70e-01	1.68e-09	1.51e-09	1.24e-10
Chrysene	6.00e+00	5.94e-08	5.34e-08	4.39e-09
Dibenzo(a,h)anthracene	1.90e+00	1.88e-08	1.69e-08	1.39e-09
Indeno(1,2,3-cd)pyrene	6.00e+00	5.94e-08	5.34e-08	4.39e-09
bis(2-Ethylhexyl)phthalate	1.10e-01	1.09e-09	9.79e-10	8.05e-11
Methylene chloride	5.00e-03	4.95e-11	4.45e-11	3.66e-12
OTHER	(mg/kg)	(mg/m^3)	(mg/m^3)	(mg/m^3)
Total Uranium	2.96e+01	2.93e-07	2.63e-07	2.16e-08

[a]Maximum annual average concentrations from ISCLT modeling
[b]Within the boundary of the subunit itself, 9.9 ug/m3, approximately 100 meters northwest from the center of South Field
[c]Between the subunit boundary and the FEMP boundary, 8.9 ug/m3, approximately 125 meters northwest from the center of South Field
[d]At or beyond the FEMP boundary, 0.7316 ug/m3, approximately 350 meters southwest of the center of South Field

TABLE A.3-19

PRELIMINARY ANNUAL DEPOSITION RATES FROM AIR DISPERSION MODELING SOUTH FIELD - CURRENT SCENARIO OPERABLE UNIT 2 REMEDIAL INVESTIGATION FERNALD ENVIRONMENTAL MANAGEMENT PROJECT

Parameter	Concentration Term	Maximum Annual Exposure Point Concentrations[a]		
		On-subunit[b]	On-site[c]	Off-site[d]
RADIOLOGICAL	(pCi/g)	(pCi/m²)	(pCi/m²)	(pCi/m²)
Cesium 137	4.99e-01	1.54e-01	1.61e-01	1.87e-02
Neptunium 237	2.28e-01	7.05e-02	7.38e-02	8.55e-03
Plutonium 238	1.20e-01	3.71e-02	3.88e-02	4.50e-03
Plutonium 239/240	5.10e-02	1.58e-02	1.65e-02	1.91e-03
Radium 226	3.08e+01	9.52e+00	9.96e+00	1.16e+00
Radium 228	3.88e+00	1.20e+00	1.26e+00	1.46e-01
Strontium 90	1.00e+00	3.09e-01	3.24e-01	3.75e-02
Technecium 99	1.42e+02	4.39e+01	4.59e+01	5.33e+00
Thorium 228	4.41e+00	1.36e+00	1.43e+00	1.65e-01
Thorium 230	1.38e+01	4.27e+00	4.46e+00	5.18e-01
Thorium 232	3.99e+00	1.23e+00	1.29e+00	1.50e-01
Uranium 234	8.66e+00	2.68e+00	2.80e+00	3.25e-01
Uranium 235/236	4.19e-01	1.30e-01	1.36e-01	1.57e-02
Uranium 238	9.31e+00	2.88e+00	3.01e+00	3.49e-01
INORGANICS	(mg/kg)	(mg/m²)	(mg/m²)	(mg/m²)
Arsenic	7.27e+00	2.25e-03	2.35e-03	2.73e-04
Beryllium	9.42e-01	2.91e-04	3.05e-04	3.53e-05
Chromium	1.39e+01	4.30e-03	4.50e-03	5.21e-04
Lead	2.46e+01	7.60e-03	7.95e-03	9.22e-04
ORGANICS	(mg/kg)	(mg/m²)	(mg/m²)	(mg/m²)
Aroclor-1254	8.90e-02	2.75e-05	2.88e-05	3.34e-06
Aroclor-1260	5.20e-02	1.61e-05	1.68e-05	1.95e-06
Dieldrin	1.00e-02	3.09e-06	3.24e-06	3.75e-07
Benzo(a)anthracene	5.50e+00	1.70e-03	1.78e-03	2.06e-04
Benzo(a)pyrene	9.40e+00	2.91e-03	3.04e-03	3.53e-04
Benzo(b)fluoranthene	6.20e+00	1.92e-03	2.01e-03	2.33e-04
Benzo(k)fluoranthene	7.30e+00	2.26e-03	2.36e-03	2.74e-04
Carbazole	1.70e-01	5.25e-05	5.50e-05	6.38e-06
Chrysene	6.00e+00	1.85e-03	1.94e-03	2.25e-04
Dibenzo(a,h)anthracene	1.90e+00	5.87e-04	6.15e-04	7.13e-05
Indeno(1,2,3-cd)pyrene	6.00e+00	1.85e-03	1.94e-03	2.25e-04
bis(2-Ethylhexyl)phthalate	1.10e-01	3.40e-05	3.56e-05	4.13e-06
Methylene chloride	5.00e-03	1.55e-06	1.62e-06	1.88e-07
OTHER	(mg/kg)	(mg/m²)	(mg/m²)	(mg/m²)
Total Uranium	2.96e+01	9.14e-03	9.57e-03	1.11e-03

[a]Maximum annual deposition rates from ISCLT modeling
[b]Within the boundary of the subunit itself, 0.3091 g/m2, approximately 100 meters northwest from the center of South Field
[c]Between the subunit boundary and the FEMP boundary, 0.3235 g/m2, approximately 125 meters northwest from the center of South Field
[d]At or beyond the FEMP boundary, 0.0375 g/m2, approximately 350 meters southwest of the center of South Field

TABLE A.3-20

PRELIMINARY MAXIMUM CONCENTRATIONS FROM AIR DISPERSION MODELING SOUTH FIELD - FUTURE SCENARIO OPERABLE UNIT 2 REMEDIAL INVESTIGATION FERNALD ENVIRONMENTAL MANAGEMENT PROJECT

Parameter	Concentration Term	Maximum Annual Exposure Point Concentrations[a]		
		On-subunit[b]	On-site[c]	Off-site[d]
RADIOLOGICAL	(pCi/g)	(pCi/m³)	(pCi/m³)	(pCi/m³)
Cesium 137	4.99e-01	2.05e-04	1.79e-04	1.30e-05
Neptunium 237	2.28e-01	9.35e-05	8.16e-05	5.93e-06
Plutonium 238	1.20e-01	4.92e-05	4.30e-05	3.12e-06
Plutonium 239/240	5.10e-02	2.09e-05	1.83e-05	1.33e-06
Radium 226	3.08e+01	1.26e-02	1.10e-02	8.01e-04
Radium 228	3.88e+00	1.59e-03	1.39e-03	1.01e-04
Strontium 90	1.00e+00	4.10e-04	3.58e-04	2.60e-05
Technecium 99	1.42e+02	5.82e-02	5.08e-02	3.69e-03
Thorium 228	4.41e+00	1.81e-03	1.58e-03	1.15e-04
Thorium 230	1.38e+01	5.66e-03	4.94e-03	3.59e-04
Thorium 232	3.99e+00	1.64e-03	1.43e-03	1.04e-04
Uranium 234	8.66e+00	3.55e-03	3.10e-03	2.25e-04
Uranium 235/236	4.19e-01	1.72e-04	1.50e-04	1.09e-05
Uranium 238	9.31e+00	3.82e-03	3.33e-03	2.42e-04
INORGANICS	(mg/kg)	(mg/m³)	(mg/m³)	(mg/m³)
Arsenic	7.27e+00	2.98e-06	2.60e-06	1.89e-07
Beryllium	9.42e-01	3.86e-07	3.37e-07	2.45e-08
Chromium	1.39e+01	5.70e-06	4.98e-06	3.61e-07
Lead	2.46e+01	1.01e-05	8.80e-06	6.39e-07
ORGANICS	(mg/kg)	(mg/m³)	(mg/m³)	(mg/m³)
Aroclor-1254	8.90e-02	3.65e-08	3.19e-08	2.31e-09
Aroclor-1260	5.20e-02	2.13e-08	1.86e-08	1.35e-09
Dieldrin	1.00e-02	4.10e-09	3.58e-09	2.60e-10
Benzo(a)anthracene	5.50e+00	2.26e-06	1.97e-06	1.43e-07
Benzo(a)pyrene	9.40e+00	3.85e-06	3.37e-06	2.44e-07
Benzo(b)fluoranthene	6.20e+00	2.54e-06	2.22e-06	1.61e-07
Benzo(k)fluoranthene	7.30e+00	2.99e-06	2.61e-06	1.90e-07
Carbazole	1.70e-01	6.97e-08	6.09e-08	4.42e-09
Chrysene	6.00e+00	2.46e-06	2.15e-06	1.56e-07
Dibenzo(a,h)anthracene	1.90e+00	7.79e-07	6.80e-07	4.94e-08
Indeno(1,2,3-cd)pyrene	6.00e+00	2.46e-06	2.15e-06	1.56e-07
bis(2-Ethylhexyl)phthalate	1.10e-01	4.51e-08	3.94e-08	2.86e-09
Methylene chloride	5.00e-03	2.05e-09	1.79e-09	1.30e-10
OTHER	(mg/kg)	(mg/m³)	(mg/m³)	(mg/m³)
Total Uranium	2.96e+01	1.21e-05	1.06e-05	7.69e-07

[a]Maximum annual average concentrations from ISCLT modelinG
[b]Within the boundary of the subunit itself, 410 ug/m3, approximately 100 meters northwest from the center of South Field
[c]Between the subunit boundary and the FEMP boundary, 358 ug/m3, approximately 125 meters northwest from the center of South Field
[d]At or beyond the FEMP boundary, 26 ug/m3, approximately 350 meters southwest of the center of South Field

TABLE A.3-21

PRELIMINARY ANNUAL DEPOSITION RATES FROM AIR DISPERSION MODELING SOUTH FIELD - FUTURE SCENARIO OPERABLE UNIT 2 REMEDIAL INVESTIGATION FERNALD ENVIRONMENTAL MANAGEMENT PROJECT

Parameter	Concentration Term	Maximum Annual Exposure Point Concentrations[a]		
		On-subunit[b]	On-site[c]	Off-site[d]
RADIOLOGICAL	(pCi/g)	(pCi/m²)	(pCi/m²)	(pCi/m²)
Cesium 137	4.99e-01	4.39e+00	4.59e+00	5.30e-01
Neptunium 237	2.28e-01	2.01e+00	2.10e+00	2.42e-01
Plutonium 238	1.20e-01	1.06e+00	1.10e+00	1.28e-01
Plutonium 239/240	5.10e-02	4.49e-01	4.69e-01	5.42e-02
Radium 226	3.08e+01	2.71e+02	2.83e+02	3.27e+01
Radium 228	3.88e+00	3.41e+01	3.57e+01	4.12e+00
Strontium 90	1.00e+00	8.80e+00	9.20e+00	1.06e+00
Technecium 99	1.42e+02	1.25e+03	1.31e+03	1.51e+02
Thorium 228	4.41e+00	3.88e+01	4.06e+01	4.69e+00
Thorium 230	1.38e+01	1.21e+02	1.27e+02	1.47e+01
Thorium 232	3.99e+00	3.51e+01	3.67e+01	4.24e+00
Uranium 234	8.66e+00	7.62e+01	7.97e+01	9.20e+00
Uranium 235/236	4.19e-01	3.69e+00	3.85e+00	4.45e-01
Uranium 238	9.31e+00	8.19e+01	8.57e+01	9.90e+00
INORGANICS	(mg/kg)	(mg/m²)	(mg/m²)	(mg/m²)
Arsenic	7.27e+00	6.40e-02	6.69e-02	7.73e-03
Beryllium	9.42e-01	8.29e-03	8.67e-03	1.00e-03
Chromium	1.39e+01	1.22e-01	1.28e-01	1.48e-02
Lead	2.46e+01	2.16e-01	2.26e-01	2.61e-02
ORGANICS	(mg/kg)	(mg/m²)	(mg/m²)	(mg/m²)
Aroclor-1254	8.90e-02	7.83e-04	8.19e-04	9.46e-05
Aroclor-1260	5.20e-02	4.58e-04	4.78e-04	5.53e-05
Dieldrin	1.00e-02	8.80e-05	9.20e-05	1.06e-05
Benzo(a)anthracene	5.50e+00	4.84e-02	5.06e-02	5.85e-03
Benzo(a)pyrene	9.40e+00	8.27e-02	8.65e-02	9.99e-03
Benzo(b)fluoranthene	6.20e+00	5.46e-02	5.70e-02	6.59e-03
Benzo(k)fluoranthene	7.30e+00	6.42e-02	6.72e-02	7.76e-03
Carbazole	1.70e-01	1.50e-03	1.56e-03	1.81e-04
Chrysene	6.00e+00	5.28e-02	5.52e-02	6.38e-03
Dibenzo(a,h)anthracene	1.90e+00	1.67e-02	1.75e-02	2.02e-03
Indeno(1,2,3-cd)pyrene	6.00e+00	5.28e-02	5.52e-02	6.38e-03
bis(2-Ethylhexyl)phthalate	1.10e-01	9.68e-04	1.01e-03	1.17e-04
Methylene chloride	5.00e-03	4.40e-05	4.60e-05	5.32e-06
OTHER	(mg/kg)	(mg/m²)	(mg/m²)	(mg/m²)
Total Uranium	2.96e+01	2.60e-01	2.72e-01	3.14e-02

[a]Maximum annual deposition rates from ISCLT modeling
[b]Within the boundary of the subunit itself, 8.8 g/m2, approximately 100 meters northwest from the center of South Field
[c]Between the subunit boundary and the FEMP boundary, 9.2 g/m2, approximately 125 meters northwest from the center of South Field
[d]At or beyond the FEMP boundary, 1.063 g/m2, approximately 350 meters southwest of the center of South Field

TABLE A.3-22

PRELIMINARY MAXIMUM CONCENTRATIONS FROM AIR DISPERSION MODELING INACTIVE FLYASH PILE - (CURRENT AND FUTURE SCENARIOS) OPERABLE UNIT 2 REMEDIAL INVESTIGATION FERNALD ENVIRONMENTAL MANAGEMENT PROJECT

Parameter	Concentration Term	Maximum Annual Exposure Point Concentrations[a]		
		On-subunit[b]	On-site[c]	Off-site[d]
RADIOLOGICAL	(pCi/g)	(pCi/m^3)	(pCi/m^3)	(pCi/m^3)
Cesium 137	4.62e-01	2.77e-06	3.23e-06	1.66e-07
Neptunium 237	7.97e-01	4.78e-06	5.58e-06	2.87e-07
Plutonium 238	8.10e-02	4.86e-07	5.67e-07	2.92e-08
Plutonium 239/240	2.10e-02	1.26e-07	1.47e-07	7.56e-09
Radium 226	1.98e+00	1.19e-05	1.38e-05	7.11e-07
Radium 228	2.24e+00	1.35e-05	1.57e-05	8.07e-07
Strontium 90	8.70e-01	5.22e-06	6.09e-06	3.13e-07
Thorium 228	2.71e+00	1.63e-05	1.90e-05	9.76e-07
Thorium 230	2.77e+00	1.66e-05	1.94e-05	9.97e-07
Thorium 232	2.33e+00	1.40e-05	1.63e-05	8.39e-07
Uranium 234	8.65e+00	5.19e-05	6.05e-05	3.11e-06
Uranium 235/236	4.20e-01	2.52e-06	2.94e-06	1.51e-07
Uranium 238	8.87e+00	5.32e-05	6.21e-05	3.19e-06
INORGANICS	(mg/kg)	(mg/m^3)	(mg/m^3)	(mg/m^3)
Arsenic	3.32e+01	1.99e-07	2.32e-07	1.20e-08
Beryllium	2.27e+00	1.36e-08	1.59e-08	8.18e-10
Cadmium	3.10e+00	1.86e-08	2.17e-08	1.12e-09
Chromium	1.14e+01	6.82e-08	7.95e-08	4.09e-09
Lead	2.39e+01	1.44e-07	1.68e-07	8.61e-09
ORGANICS	(mg/kg)	(mg/m^3)	(mg/m^3)	(mg/m^3)
Carbazole	5.10e-01	3.06e-09	3.57e-09	1.84e-10
Dibenzo(a,h)anthracene	2.20e+00	1.32e-08	1.54e-08	7.92e-10
OTHER	(mg/kg)	(mg/m^3)	(mg/m^3)	(mg/m^3)
Total Uranium	2.62e+01	1.57e-07	1.83e-07	9.43e-09

[a]Maximum concentrations from ISCLT modeling

[b]Within the subunit itself, 6.0 ug/m3, approximately 25 meters east-southeast of Inactive Flyash Pile center

[c]Area from subunit boundary to FEMP boundary, 7.0 ug/m3, approximately 50 meters north-northeast of Inactive Flyash Pile center

[d]Area beyond the FEMP boundary, 0.36 ug/m3, approximately 250 meters southwest of Inactive Flyash Pile center

TABLE A.3-23

PRELIMINARY MAXIMUM DEPOSITION RATES FROM AIR DISPERSION MODELING INACTIVE FLYASH PILE - (CURRENT AND FUTURE SCENARIOS) OPERABLE UNIT 2 REMEDIAL INVESTIGATION FERNALD ENVIRONMENTAL MANAGEMENT PROJECT

Parameter	Concentration Term	Maximum Annual Exposure Point Concentrations[a]		
		On-subunit[b]	On-site[c]	Off-site[d]
RADIOLOGICAL	(pCi/g)	(pCi/m^2)	(pCi/m^2)	(pCi/m^2)
Cesium 137	4.62e-01	1.58e-01	1.73e-01	1.31e-02
Neptunium 237	7.97e-01	2.72e-01	2.99e-01	2.26e-02
Plutonium 238	8.10e-02	2.77e-02	3.04e-02	2.30e-03
Plutonium 239/240	2.10e-02	7.18e-03	7.89e-03	5.96e-04
Radium 226	1.98e+00	6.75e-01	7.42e-01	5.61e-02
Radium 228	2.24e+00	7.66e-01	8.42e-01	6.37e-02
Strontium 90	8.70e-01	2.97e-01	3.27e-01	2.47e-02
Thorium 228	2.71e+00	9.26e-01	1.02e+00	7.70e-02
Thorium 230	2.77e+00	9.47e-01	1.04e+00	7.87e-02
Thorium 232	2.33e+00	7.96e-01	8.75e-01	6.62e-02
Uranium 234	8.65e+00	2.96e+00	3.25e+00	2.46e-01
Uranium 235/236	4.20e-01	1.44e-01	1.58e-01	1.19e-02
Uranium 238	8.87e+00	3.03e+00	3.33e+00	2.52e-01
INORGANICS	(mg/kg)	(mg/m^2)	(mg/m^2)	(mg/m^2)
Arsenic	3.32e+01	1.13e-02	1.25e-02	9.43e-04
Beryllium	2.27e+00	7.77e-04	8.54e-04	6.46e-05
Cadmium	3.10e+00	1.06e-03	1.16e-03	8.80e-05
Chromium	1.14e+01	3.88e-03	4.27e-03	3.23e-04
Lead	2.39e+01	8.18e-03	8.99e-03	6.80e-04
ORGANICS	(mg/kg)	(mg/m^2)	(mg/m^2)	(mg/m^2)
Carbazole	5.10e-01	1.74e-04	1.92e-04	1.45e-05
Dibenzo(a,h)anthracene	2.20e+00	7.52e-04	8.26e-04	6.25e-05
OTHER	(mg/kg)	(mg/m^2)	(mg/m^2)	(mg/m^2)
Total Uranium	2.62e+01	8.95e-03	9.84e-03	7.44e-04

[a]Maximum deposition rates from ISCLT modeling

[b]Within the subunit itself, .3417 g/m2, approximately 90 meters north of Inactive Flyash Pile center

[c]Area from subunit boundary to FEMP boundary, .3755 g/m2, approximately 50 meters northeast of Inactive Flyash Pile center

[d]Area beyond the FEMP boundary, 0.0284 g/m2, approximately 250 meters southwest of Inactive Flyash Pile center

TABLE A.3-24

PRELIMINARY MAXIMUM CONCENTRATIONS FROM AIR DISPERSION MODELING - SOLID WASTE LANDFILL - CURRENT SCENARIO OPERABLE UNIT 2 REMEDIAL INVESTIGATION FERNALD ENVIRONMENTAL MANAGEMENT PROJECT

Parameter	Concentration Term	Maximum Annual Exposure Point Concentrations[a]		
		On-subunit[b]	On-site[c]	Off-site[d]
RADIOLOGICAL	(pCi/g)	(pCi/m^3)	(pCi/m^3)	(pCi/m^3)
Cesium 137	2.67e-01	8.01e-07	8.01e-07	1.32e-08
Neptunium 237	1.19e+00	3.57e-06	3.57e-06	5.87e-08
Plutonium 238	7.72e-01	2.32e-06	2.32e-06	3.81e-08
Plutonium 239/240	8.20e-02	2.46e-07	2.46e-07	4.05e-09
Radium 226	1.90e+00	5.69e-06	5.69e-06	9.37e-08
Radium 228	1.68e+00	5.04e-06	5.04e-06	8.30e-08
Strontium 90	9.55e-01	2.87e-06	2.87e-06	4.72e-08
Thorium 228	1.63e+00	4.88e-06	4.88e-06	8.03e-08
Thorium 230	6.48e+00	1.94e+05	1.94e+05	3.20e-07
Thorium 232	1.51e+00	4.53e-06	4.53e-06	7.46e-08
Uranium 234	4.21e+01	1.26e+04	1.26e+04	2.08e-06
Uranium 235/236	2.84e+00	8.51e+06	8.51e+06	1.40e-07
Uranium 238	7.72e+01	2.31e+04	2.31e+04	3.81e-06
INORGANICS	(mg/kg)	(mg/m^3)	(mg/m^3)	(mg/m^3)
Arsenic	6.67e+00	2.00e-08	2.00e-08	3.29e-10
Beryllium	6.98e-01	2.09e-09	2.09e-09	3.45e-11
Cadmium	8.50e-01	2.55e-09	2.55e-09	4.20e-11
Chromium	1.55e+01	4.64e-08	4.64e-08	7.64e-10
Lead	1.90e+01	5.70e-08	5.70e-08	9.39e-10
ORGANICS	(mg/kg)	(mg/m^3)	(mg/m^3)	(mg/m^3)
4,4-DDE	1.20e-02	3.60e-11	3.60e-11	5.93e-13
Benzo(a)anthracene	3.86e-01	1.16e-09	1.16e-09	1.91e-11
Benzo(a)pyrene	3.40e-01	1.02e-09	1.02e-09	1.68e-11
Benzo(b)fluoranthene	7.10e-01	2.13e-09	2.13e-09	3.51e-11
Benzo(k)fluoranthene	8.85e-01	2.66e-09	2.66e-09	4.37e-11
bis(2-Ethylhexyl)phthalate	4.80e-02	1.44e-10	1.44e-10	2.37e-12
Carbazole	7.70e-02	2.31e-10	2.31e-10	3.80e-12
Chrysene	4.53e-01	1.36e-09	1.36e-09	2.24e-11
Dibenzo(a,h)anthracene	2.00e-01	6.00e-10	6.00e-10	9.88e-12
Indeno(1,2,3-cd)pyrene	4.80e-01	1.44e-09	1.44e-09	2.37e-11
OTHER	(mg/kg)	(mg/m^3)	(mg/m^3)	(mg/m^3)
Total Uranium	2.25e+02	6.76e-02	6.76e-07	1.11e-08

[a]Maximum annual average deposition rates from ISCLT modeling
[b]Within the boundary of the subunit itself, 3.0 μg/m3, approximately 30 meters southeast from the center of Solid Waste Landfill
[c]Between the subunit boundary and the FEMP boundary, 3.0 μg/m3, approximately 75 meters east-northeast from the center of Solid Waste Landfill
[d]At or beyond the FEMP boundary, 0.0494 μg/m3, approximately 600 meters north-northeast from the center of the Solid Waste Landfill

TABLE A.3-25

PRELIMINARY MAXIMUM ANNUAL DEPOSITION RATES FROM AIR DISPERSION MODELING - SOLID WASTE LANDFILL - CURRENT SCENARIOS OPERABLE UNIT 2 REMEDIAL INVESTIGATION FERNALD ENVIRONMENTAL MANAGEMENT PROJECT

Parameter	Concentration Term	Maximum Annual Exposure Point Concentrations[a]		
		On-subunit[b]	On-site[c]	Off-site[d]
RADIOLOGICAL	(pCi/g)	(pCi/m²)	(pCi/m²)	(pCi/m²)
Cesium 137	2.67e-01	1.12e-01	9.82e-02	1.63e-03
Neptunium 237	1.19e+00	4.99e-01	4.37e-01	7.25e-03
Plutonium 238	7.72e-01	3.24e-01	2.84e-01	4.71e-03
Plutonium 239/240	8.20e-02	3.44e-02	3.02e-02	5.00e-04
Radium 226	1.90e+00	7.96e-01	6.98e-01	1.16e-02
Radium 228	1.68e+00	7.05e-01	6.18e-01	1.03e-02
Strontium 90	9.55e-01	4.01e-01	3.51e-01	5.83e-03
Thorium 228	1.63e+00	6.82e-01	5.98e-01	9.92e-03
Thorium 230	6.48e+00	2.72e+00	2.38e+00	3.95e-02
Thorium 232	1.51e+00	6.34e-01	5.56e-01	9.22e-03
Uranium 234	4.21e+01	1.77e+01	1.55e+01	2.57e-01
Uranium 235/236	2.84e+00	1.19e+00	1.04e+00	1.73e-02
Uranium 238	7.72e+01	3.24e+01	2.84e+01	4.71e-01
INORGANICS	(mg/kg)	(mg/m²)	(mg/m²)	(mg/m²)
Arsenic	6.67e+00	2.80e-03	2.45e-03	4.07e-05
Beryllium	6.98e-01	2.93e-04	2.57e-04	4.26e-06
Cadmium	8.50e-01	3.57e-04	3.13e-04	5.19e-06
Chromium	1.55e+01	6.49e-03	5.69e-03	9.43e-05
Lead	1.90e+01	7.97e-03	6.99e-03	1.16e-04
ORGANICS	(mg/kg)	(mg/m²)	(mg/m²)	(mg/m²)
4,4-DDE	1.20e-02	5.03e-06	4.41e-06	7.32e-08
Benzo(a)anthracene	3.86e-01	1.62e-04	1.42e-04	2.35e-06
Benzo(a)pyrene	3.40e-01	1.43e-04	1.25e-04	2.07e-06
Benzo(b)fluoranthene	7.10e-01	2.98e-04	2.61e-04	4.33e-06
Benzo(k)fluoranthene	8.85e-01	3.71e-04	3.26e-04	5.40e-06
bis(2-Ethylhexyl)phthalate	4.80e-02	2.01e-05	1.77e-05	2.93e-07
Carbazole	7.70e-02	3.23e-05	2.83e-05	4.70e-07
Chrysene	4.53e-01	1.90e-04	1.67e-04	2.76e-06
Dibenzo(a,h)anthracene	2.00e-01	8.39e-05	7.36e-05	1.22e-06
Indeno(1,2,3-cd)pyrene	4.80e-01	2.01e-04	1.77e-04	2.93e-06
OTHER	(mg/kg)	(mg/m²)	(mg/m²)	(mg/m²)
Total Uranium	2.25e+02	9.45e-02	8.28e-02	1.37e-03

[a]Maximum annual average deposition rates from ISCLT modeling
[b]Within the boundary of the subunit itself, 0.4195 g/m2, approximately 30 meters southeast from the center of Solid Waste Landfill
[c]Between the subunit boundary and the FEMP boundary, 0.3678 g/m2, approximately 75 meters east-northeast from the center of Solid Waste Landfill
[d]At or beyond the FEMP boundary, 0.0061 g/m2, approximately 600 meters north-northeast from the center of the Solid Waste Landfill

TABLE A.3-26

PRELIMINARY MAXIMUM CONCENTRATIONS FROM AIR DISPERSION MODELING SOLID WASTE LANDFILL - FUTURE SCENARIOS OPERABLE UNIT 2 REMEDIAL INVESTIGATION FERNALD ENVIRONMENTAL MANAGEMENT PROJECT

Parameter	Concentration Term	Maximum Annual Exposure Point Concentrations[a]		
		On-subunit[b]	On-site[c]	Off-site[d]
RADIOLOGICAL	(pCi/g)	(pCi/m^3)	(pCi/m^3)	(pCi/m^3)
Cesium 137	2.67e-01	2.43e-05	2.43e-05	4.01e-07
Neptunium 237	1.19e+00	1.08e-04	1.08e-04	1.78e-06
Plutonium 238	7.72e-01	7.03e-05	7.03e-05	1.16e-06
Plutonium 239/240	8.20e-02	7.46e-06	7.46e-06	1.23e-07
Radium 226	1.90e+00	1.73e-04	1.73e-04	2.85e-06
Radium 228	1.68e+00	1.53e-04	1.53e-04	2.52e-06
Strontium 90	9.55e-01	8.69e-05	8.69e-05	1.43e-06
Thorium 228	1.63e+00	1.48e-04	1.48e-04	2.44e-06
Thorium 230	6.48e+00	5.89e-04	5.89e-04	9.71e-06
Thorium 232	1.51e+00	1.38e-04	1.38e-04	2.27e-06
Uranium 234	4.21e+01	3.83e-03	3.83e-03	6.32e-05
Uranium 235/236	2.84e+00	2.58e-04	2.58e-04	4.26e-06
Uranium 238	7.72e+01	7.02e-03	7.02e-03	1.16e-04
INORGANICS	(mg/kg)	(mg/m^3)	(mg/m^3)	(mg/m^3)
Arsenic	6.67e+00	6.07e-07	6.07e-07	1.00e-08
Beryllium	6.98e-01	6.35e-08	6.35e-08	1.05e-09
Cadmium	8.50e-01	7.74e-08	7.74e-08	1.28e-09
Chromium	1.55e+01	1.41e-06	1.41e-06	2.32e-08
Lead	1.90e+01	1.73e-06	1.73e-06	2.85e-08
ORGANICS	(mg/kg)	(mg/m^3)	(mg/m^3)	(mg/m^3)
4,4-DDE	1.20e-02	1.09e-09	1.09e-09	1.80e-11
Benzo(a)anthracene	3.86e-01	3.51e-08	3.51e-08	5.79e-10
Benzo(a)pyrene	3.40e-01	3.09e-08	3.09e-08	5.10e-10
Benzo(b)fluoranthene	7.10e-01	6.46e-08	6.46e-08	1.07e-09
Benzo(k)fluoranthene	8.85e-01	8.05e-08	8.05e-08	1.33e-09
bis(2-Ethylhexyl)phthalate	4.80e-02	4.37e-09	4.37e-09	7.20e-11
Carbazole	7.70e-02	7.01e-09	7.01e-09	1.16e-10
Chrysene	4.53e-01	4.12e-08	4.12e-08	6.80e-10
Dibenzo(a,h)anthracene	2.00e-01	1.82e-08	1.82e-08	3.00e-10
Indeno(1,2,3-cd)pyrene	4.80e-01	4.37e-08	4.37e-08	7.20e-10
OTHER	(mg/kg)	(mg/m^3)	(mg/m^3)	(mg/m^3)
Total Uranium	2.25e+02	2.05e-05	2.05e-05	3.38e-07

[a]Maximum annual average concentrations from ISCLT modeling
[b]Within the boundary of the subunit itself, 91 ug/m3, approximately 30 meters southeast from the center of Solid Waste Landfill
[c]Between the subunit boundary and the FEMP boundary, 91 ug/m3, approximately 75 meters east-northeast from the center of Solid Waste Landfill
[d]At or beyond the FEMP boundary, 1.5 ug/m3, approximately 600 meters north-northeast from the center of the Solid Waste Landfill

TABLE A.3-27

PRELIMINARY MAXIMUM ANNUAL DEPOSITION RATES FROM AIR DISPERSION MODELING - SOLID WASTE LANDFILL - FUTURE SCENARIOS OPERABLE UNIT 2 REMEDIAL INVESTIGATION FERNALD ENVIRONMENTAL MANAGEMENT PROJECT

Parameter	Concentration Term	Maximum Annual Exposure Point Concentrations[a]		
		On-subunit[b]	On-site[c]	Off-site[d]
RADIOLOGICAL	(pCi/g)	(pCi/m²)	(pCi/m²)	(pCi/m²)
Cesium 137	2.67e-01	2.62e+00	2.30e+00	3.78e-02
Neptunium 237	1.19e+00	1.17e+01	1.02e+01	1.68e-01
Plutonium 238	7.72e-01	7.57e+00	6.64e+00	1.09e-01
Plutonium 239/240	8.20e-02	8.04e-01	7.05e-01	1.16e-02
Radium 226	1.90e+00	1.86e+01	1.63e+01	2.69e-01
Radium 228	1.68e+00	1.65e+01	1.45e+01	2.38e-01
Strontium 90	9.55e-01	9.36e+00	8.21e+00	1.35e-01
Thorium 228	1.63e+00	1.59e+01	1.40e+01	2.30e-01
Thorium 230	6.48e+00	6.35e+01	5.57e+01	9.18e-01
Thorium 232	1.51e+00	1.48e+01	1.30e+01	2.14e-01
Uranium 234	4.21e+01	4.13e+02	3.62e+02	5.97e+00
Uranium 235/236	2.84e+00	2.78e+01	2.44e+01	4.02e-01
Uranium 238	7.72e+01	7.56e+02	6.63e+02	1.09e+01
INORGANICS	(mg/kg)	(mg/m²)	(mg/m²)	(mg/m²)
Arsenic	6.67e+00	6.53e-02	5.73e-02	9.45e-04
Beryllium	6.98e-01	6.84e-03	6.00e-03	9.89e-05
Cadmium	8.50e-01	8.33e-03	7.31e-03	1.20e-04
Chromium	1.55e+01	1.52e-01	1.33e-01	2.19e-03
Lead	1.90e+01	1.86e-01	1.63e-01	2.69e-03
ORGANICS	(mg/kg)	(mg/m²)	(mg/m²)	(mg/m²)
4,4-DDE	1.20e-02	1.18e-04	1.03e-04	1.70e-06
Benzo(a)anthracene	3.86e-01	3.78e-03	3.32e-03	5.47e-05
Benzo(a)pyrene	3.40e-01	3.33e-03	2.92e-03	4.82e-05
Benzo(b)fluoranthene	7.10e-01	6.96e-03	6.11e-03	1.01e-04
Benzo(k)fluoranthene	8.85e-01	8.67e-03	7.61e-03	1.25e-04
bis(2-Ethylhexyl)phthalate	4.80e-02	4.70e-04	4.13e-04	6.80e-06
Carbazole	7.70e-02	7.55e-04	6.62e-04	1.09e-05
Chrysene	4.53e-01	4.44e-03	3.90e-03	6.42e-05
Dibenzo(a,h)anthracene	2.00e-01	1.96e-03	1.72e-03	2.83e-05
Indeno(1,2,3-cd)pyrene	4.80e-01	4.70e-03	4.13e-03	6.80e-05
OTHER	(mg/kg)	(mg/m²)	(mg/m²)	(mg/m²)
Total Uranium	2.25e+02	2.21e+00	1.94e+00	3.19e-02

[a]Maximum annual average deposition rates from ISCLT modeling
[b]Within the boundary of the subunit itself, 9.8 g/m2, approximately 30 meters southeast from the center of Solid Waste Landfill
[c]Between the subunit boundary and the FEMP boundary, 8.6 g/m2, approximately 75 meters east-northeast from the center of Solid Waste Landfill
[d]At or beyond the FEMP boundary, 0.1417 g/m2, approximately 600 meters north-northeast from the center of the Solid Waste Landfill

TABLE A.3-28

PRELIMINARY MAXIMUM CONCENTRATIONS FROM AIR DISPERSION MODELING LIME SLUDGE PONDS - CURRENT AND FUTURE SCENARIOS OPERABLE UNIT 2 REMEDIAL INVESTIGATION FERNALD ENVIRONMENTAL MANAGEMENT PROJECT

Parameter	Concentration Term	Maximum Annual Exposure Point Concentrations[a]		
		On-subunit[b]	On-site[c]	Off-site[d]
RADIOLOGICAL	(pCi/g)	(pCi/m^3)	(pCi/m^3)	(pCi/m^3)
Cesium 137	7.02e-01	1.83e-05	1.05e-05	1.24e-07
Neptunium 237	7.20e-01	1.87e-05	1.08e-05	1.28e-07
Plutonium 238	5.76e-01	1.50e-05	8.64e-06	1.02e-07
Plutonium 239/240	1.35e-01	3.51e-06	2.03e-06	2.39e-08
Radium 226	1.92e+00	4.99e-05	2.88e-05	3.40e-07
Radium 228	1.64e+00	4.26e-05	2.46e-05	2.90e-07
Strontium 90	7.85e-01	2.04e-05	1.18e-05	1.39e-07
Thorium 228	2.91e+00	7.57e-05	4.37e-05	5.15e-07
Thorium 230	4.48e+01	1.16e-03	6.72e-04	7.93e-06
Thorium 232	1.31e+00	3.40e-05	1.96e-05	2.31e-07
Uranium 234	2.10e+01	5.46e-04	3.15e-04	3.72e-06
Uranium 235/236	1.74e+00	4.53e-05	2.61e-05	3.09e-07
Uranium 238	7.14e+01	1.86e-03	1.07e-03	1.26e-05
INORGANICS	(mg/kg)	(mg/m^3)	(mg/m^3)	(mg/m^3)
Arsenic	7.19e+00	1.87e-07	1.08e-07	1.27e-09
Beryllium	1.52e+00	3.95e-08	2.28e-08	2.69e-10
Cadmium	1.20e+00	3.12e-08	1.80e-08	2.13e-10
Chromium	1.66e+01	4.31e-07	2.49e-07	2.94e-09
Lead	2.76e+01	7.17e-07	4.13e-07	4.88e-09
ORGANICS	(mg/kg)	(mg/m^3)	(mg/m^3)	(mg/m^3)
Aroclor-1254	5.90e+02	1.53e-05	8.85e-06	1.04e-07
Benzo(a)anthracene	9.10e-01	2.37e-08	1.37e-08	1.61e-10
Benzo(a)pyrene	1.10e+00	2.86e-08	1.65e-08	1.95e-10
Benzo(b)fluoranthene	1.00e+00	2.60e-08	1.50e-08	1.77e-10
Benzo(k)fluoranthene	8.00e-01	2.08e-08	1.20e-08	1.42e-10
bis(2-Ethylhexyl)phthalate	1.00e+01	2.60e-07	1.50e-07	1.77e-09
Carbazole	1.40e-01	3.64e-09	2.10e-09	2.48e-11
Chrysene	1.10e+00	2.86e-08	1.65e-08	1.95e-10
Dibenzo(a,h)anthracene	3.20e-01	8.32e-09	4.80e-09	5.67e-11
Indeno(1,2,3-cd)pyrene	7.20e-01	1.87e-08	1.08e-08	1.28e-10
OTHER	(mg/kg)	(mg/m^3)	(mg/m^3)	(mg/m^3)
Total Uranium	2.14e+02	5.57e-06	3.21e-06	3.80e-08

[a]Maximum annual average concentrations from ISCLT modeling
[b]Within the boundary of the subunit itself, 26 ug/m3, approximately 25 meters east-northeast from the center of the Sludge Ponds
[c]Between the subunit boundary and the FEMP boundary, 15 ug/m3, approximately 75 meters east-northeast from the center of the Sludge Ponds
[d]At or beyond the FEMP boundary, 0.1771 ug/m3, approximately 700 meters west-southwest from the center of the Sludge Ponds

TABLE A.3-29

PRELIMINARY MAXIMUM ANNUAL DEPOSITION RATES FROM AIR DISPERSION MODELING - LIME SLUDGE PONDS - CURRENT AND FUTURE SCENARIOS OPERABLE UNIT 2 REMEDIAL INVESTIGATION FERNALD ENVIRONMENTAL MANAGEMENT PROJECT

Parameter	Concentration Term	Maximum Annual Exposure Point Concentrations[a]		
		On-subunit[b]	On-site[c]	Off-site[d]
RADIOLOGICAL	(pCi/g)	(pCi/m²)	(pCi/m²)	(pCi/m²)
Cesium 137	7.02e-01	1.26e+01	7.72e+00	8.77e-02
Neptunium 237	7.20e-01	1.30e+01	7.92e+00	8.99e-02
Plutonium 238	5.76e-01	1.04e+01	6.34e+00	7.19e-02
Plutonium 239/240	1.35e-01	2.43e+00	1.49e+00	1.69e-02
Radium 226	1.92e+00	3.45e+01	2.11e+01	2.40e-01
Radium 228	1.64e+00	2.95e+01	1.80e+01	2.05e-01
Strontium 90	7.85e-01	1.41e+01	8.64e+00	9.80e-02
Thorium 228	2.91e+00	5.24e+01	3.20e+01	3.63e-01
Thorium 230	4.48e+01	8.06e+02	4.93e+02	5.60e+00
Thorium 232	1.31e+00	2.35e+01	1.44e+01	1.63e-01
Uranium 234	2.10e+01	3.78e+02	2.31e+02	2.62e+00
Uranium 235/236	1.74e+00	3.14e+01	1.92e+01	2.18e-01
Uranium 238	7.14e+01	1.28e+03	7.85e+02	8.92e+00
INORGANICS	(mg/kg)	(mg/m²)	(mg/m²)	(mg/m²)
Arsenic	7.19e+00	1.29e-01	7.91e-02	8.98e-04
Beryllium	1.52e+00	2.73e-02	1.67e-02	1.90e-04
Cadmium	1.20e+00	2.16e-02	1.32e-02	1.50e-04
Chromium	1.66e+01	2.98e-01	1.82e-01	2.07e-03
Lead	2.76e+01	4.96e-01	3.03e-01	3.44e-03
ORGANICS	(mg/kg)	(mg/m²)	(mg/m²)	(mg/m²)
Aroclor-1254	5.90e+02	1.06e+01	6.49e+00	7.37e-02
Benzo(a)anthracene	9.10e-01	1.64e-02	1.00e-02	1.14e-04
Benzo(a)pyrene	1.10e+00	1.98e-02	1.21e-02	1.37e-04
Benzo(b)fluoranthene	1.00e+00	1.80e-02	1.10e-02	1.25e-04
Benzo(k)fluoranthene	8.00e-01	1.44e-02	8.80e-03	9.99e-05
bis(2-Ethylhexyl)phthalate	1.00e+01	1.80e-01	1.10e-01	1.25e-03
Carbazole	1.40e-01	2.52e-03	1.54e-03	1.75e-05
Chrysene	1.10e+00	1.98e-02	1.21e-02	1.37e-04
Dibenzo(a,h)anthracene	3.20e-01	5.76e-03	3.52e-03	4.00e-05
Indeno(1,2,3-cd)pyrene	7.20e-01			
OTHER	(mg/kg)	(mg/m²)	(mg/m²)	(mg/m²)
Total Uranium	2.14e+02	3.86e+00	2.36e+00	2.68e-02

[a]Maximum annual average deposition rates from ISCLT modeling
[b]Within the boundary of the subunit itself, 18 g/m2, approximately 25 meters east-northeast from the center of the Sludge Ponds
[c]Between the subunit boundary and the FEMP boundary, 11 g/m2, approximately 75 meters east-northeast from the center of the Sludge Ponds
[d]At or beyond the FEMP boundary, 0.1249 g/m2, approximately 700 meters west-southwest from the center of the Sludge Ponds

ATTACHMENT A.3.II

Sample Calculations for Determining Unlimited and Limited Erosion Potential, Settling Velocity and Reflection Coefficient Used in the Air Transport Analysis for Operable Unit 2 Fernald Environmental Management Project

FEMP-OU02-5 DRAFT
June 15, 1994

ATTACHMENT A.3.I

1987-1989, 1991, and 1992 Meteorological Statistical Array Data Used in the Air Transport Analysis for Operable Unit 2 Fernald Environmental Management Project

1987 METEOROLOGICAL STATISTICAL ARRAY FOR FEMP

.000000.000000.000000.000000.000000.000000
.000138.000000.000138.000138.000000.000000
.000138.000000.000138.000138.000000.000000
.000138.000276.000828.000000.000000.000000
.000000.000552.000690.000138.000000.000000
.000138.000276.000276.000000.000000.000000
.000000.000000.000000.000000.000000.000000
.000000.000000.000000.000000.000000.000000
.000000.000000.000138.000000.000000.000000
.000000.000414.001517.000000.000000.000000
.000000.001241.003447.000414.000000.000000
.000000.000966.002344.000000.000000.000000
.000000.000828.001379.000000.000000.000000
.000000.000276.000690.000414.000000.000000
.000138.000138.000276.000552.000000.000000
.000000.000000.000414.000414.000138.000000
.000000.000414.000138.000000.000000.000000
.000000.000276.000552.000000.000000.000000
.000000.000828.002344.000138.000000.000000
.000276.000828.000276.000690.000000.000000
.000276.000690.000276.000138.000000.000000
.000000.000828.000000.000000.000000.000000
.000000.000138.000000.000000.000000.000000
.000138.000276.000138.000138.000000.000000
.000138.000138.000138.000000.000000.000000
.000138.000966.002069.000276.000000.000000
.000276.001241.002758.000138.000000.000000
.000552.001103.002069.000000.000000.000000
.000138.000966.001379.000138.000000.000000
.000000.000690.000828.000276.000000.000000
.000276.001103.000828.000552.000000.000000
.000000.000138.000414.000000.000000.000000
.000276.000690.000828.000000.000000.000000
.000138.000690.000966.000000.000000.000000
.000276.001241.001379.000414.000000.000000
.000690.002069.000552.001241.000000.000000
.000414.001241.000276.000138.000000.000000
.000552.000690.000000.000000.000000.000000
.000276.000276.000000.000000.000000.000000
.000138.000276.000138.000000.000000.000000
.000414.000828.000414.000000.000000.000000
.000414.001517.000828.000138.000000.000000
.001379.003861.001931.000276.000000.000000
.001103.003723.001379.000414.000000.000000
.000414.001241.001103.000414.000000.000000
.000414.001241.001241.000276.000000.000000
.000276.000966.000828.000276.000138.000000
.000276.001379.001103.000000.000000.000000
.002925.005653.009790.000828.000000.000000
.002386.009790.010893.004137.000000.000000
.004759.015856.010893.001931.000000.000000
.008523.024266.017648.005240.000000.000000
.006661.005791.001517.000138.000000.000000
.003883.002620.000000.000000.000000.000000
.003053.002482.000552.000000.000000.000000

DRAFT

.002777.002896.001517.000552.000000.000000
.004307.005102.002069.000276.000000.000000
.005162.012271.004137.001655.000000.000000
.006155.019441.000238.000828.000552.000000
.007242.013650.006756.003861.000276.000000
.005719.013512.014477.003723.000000.000000
.004335.013374.007997.001517.000000.000000
.002940.009927.007997.001655.000414.000000
.004596.008824.006067.002482.000276.000000
.003487.005240.000690.000138.000000.000000
.002508.003172.001793.000276.000000.000000
.003203.003723.000828.000000.000000.000000
.012519.011996.001931.000000.000000.000000
.011648.003172.000276.000000.000000.000000
.006381.002069.000138.000000.000000.000000
.004860.002620.000966.000000.000000.000000
.006661.002896.001241.000552.000000.000000
.006945.004412.002620.000138.000000.000000
.009055.011582.004412.000414.000000.000000
.014228.022336.006205.001103.000138.000000
.021367.008411.004137.001103.000000.000000
.013201.009652.003999.000276.000000.000000
.007369.006343.002344.000138.000000.000000
.009712.003723.001931.000276.000000.000000
.008185.002896.001379.000138.000000.000000
.006570.000138.000000.000000.000138.000138
.005994.000000.000138.000000.000000.000000
.006280.000000.000000.000000.000000.000000
.012646.002482.000000.000000.000000.000000
.017288.000552.000000.000000.000000.000000
.013558.000000.000000.000000.000000.000000
.006860.000276.000000.000000.000000.000000
.004287.000138.000000.000000.000000.000000
.005709.000000.000000.000000.000000.000000
.010019.000828.000000.000000.000000.000000
.020476.001931.000000.000000.000000.000000
.026874.001241.000000.000000.000000.000000
.028415.000414.000000.000000.000000.000000
.025413.000276.000000.000000.000000.000000
.022554.000138.000000.000000.000000.000000
.014281.000276.000000.000000.000000.000000

DRAFT

1988 METEOROLOGICAL-STATISTICAL ARRAY FOR FEMP

.000137.000775.000646.000259.000000.000000
.000658.000775.002453.001162.000000.000000
.000790.001033.001421.000775.000000.000000
.000002.000130.000388.000000.000000.000000
.000000.000000.000000.000000.000000.000130
.000000.000000.000000.000000.000000.000000
.000000.000000.000000.000000.000000.000130
.000000.000000.000259.000130.000000.000000
.000522.000130.000000.000000.000000.000000
.001045.000388.001162.000130.000000.000000
.000532.001291.003615.000259.000000.000000
.000145.001808.002712.000000.000000.000000
.000536.001808.003615.000517.000000.000000
.000787.000646.002066.000646.000000.000000
.000395.000517.001033.000000.000000.000000
.000396.000646.000646.000000.000000.000000
.000130.001033.000388.000000.000000.000000
.000130.000259.001162.000517.000000.000000
.000130.001033.000775.000000.000000.000000
.000000.000517.000517.000000.000000.000000
.000388.000259.000388.000000.000000.000000
.000130.000000.000000.000000.000000.000000
.000000.000000.000000.000000.000000.000000
.000259.000000.000000.000000.000000.000000
.000130.000000.000130.000000.000000.000000
.000388.001033.001550.000259.000000.000000
.000775.001550.002066.000130.000000.000000
.000517.001550.001550.000259.000000.000000
.000130.000904.002324.000259.000000.000000
.000517.000904.002324.000388.000000.000000
.000517.000388.001162.000130.000000.000000
.000646.000904.001033.000000.000000.000000
.000388.001033.000775.000517.000000.000000
.000388.001162.001421.000259.000000.000000
.000000.001937.000646.000259.000000.000000
.000259.001421.000646.000000.000000.000000
.000388.000646.000388.000000.000000.000000
.000646.000259.000130.000000.000000.000000
.000130.000388.000000.000000.000000.000000
.000259.000517.000388.000000.000000.000000
.000388.000775.000388.000000.000000.000000
.000517.001550.000904.000259.000130.000000
.000517.003228.001679.000259.000000.000000
.001162.003228.001679.000259.000000.000000
.000259.001550.001937.000259.000000.000000
.000646.001421.002712.000517.000000.000000
.000517.001162.001550.000130.000000.000000
.000130.001033.000904.000000.000000.000000
.001814.008134.004132.000517.000000.000000
.002718.007359.006843.000517.000000.000000
.003624.011748.005810.000388.000000.000000
.005952.016654.004906.000130.000000.000000
.005687.004906.001162.000130.000000.000000
.004265.002195.000130.000130.000000.000000
.002715.002841.000388.000000.000000.000000

DRAFT

.004266.004132.002324.000000.000000.000000
.004136.004003.002324.000000.000000.000000
.006981.008908.007617.004390.000000.000000
.009309.013863.009812.002841.000259.000000
.011635.014460.008385.001033.000000.000000
.008404.012136.011490.001808.000000.000000
.004398.009812.012781.002066.000000.000000
.004783.005681.006197.000517.000000.000000
.003363.007359.005164.000388.000000.000000
.003498.003357.001291.000130.000000.000000
.003366.002066.001291.000130.000000.000000
.002852.003873.000517.000000.000000.000000
.008552.009683.002582.000000.000000.000000
.006341.002195.000259.000000.000000.000000
.004012.001679.000000.000000.000000.000000
.004528.001033.000000.000000.000000.000000
.005695.002712.001421.000000.000000.000000
.005054.006068.006197.001937.000000.000000
.010625.011490.013169.003615.000000.000000
.014386.018074.009296.001291.000000.000000
.015540.012523.006455.001421.000000.000000
.013607.016009.005035.000259.000000.000000
.008809.008650.002970.000388.000000.000000
.006862.004390.001550.000130.000000.000000
.004921.003486.001162.000259.000000.000000
.006109.000000.000000.000000.000000.000130
.005850.000130.000000.000000.000000.000000
.005719.000000.000000.000000.000000.000000
.008846.001162.000000.000000.000000.000000
.015468.000259.000000.000000.000000.000000
.008968.000000.000000.000000.000130.000000
.007410.000130.000000.000000.000000.000000
.005851.000259.000000.000000.000000.000000
.010141.000388.000000.000000.000000.000000
.016906.001421.000000.000130.000000.000000
.028615.003228.000000.000000.000000.000000
.034336.003615.000000.000000.000000.000000
.034318.000904.000000.000000.000000.000000
.035742.000000.000130.000000.000000.000000
.021966.000130.000130.000000.000000.000000
.011832.000646.000000.000000.000000.000000

DRAFT

1989 METEOROLOGICAL STATISTICAL ARRAY FOR FEMP

.000000.000479.000598.000240.000000.000000
.000000.000359.000000.000000.000000.000000
.000000.000837.000240.000000.000000.000000
.000120.001435.001077.000000.000000.000000
.000000.001077.000000.000000.000000.000000
.000120.000000.000000.000000.000000.000000
.000000.000000.000000.000000.000000.000000
.000000.000000.000000.000000.000000.000000
.000000.000000.000000.000000.000000.000000
.000000.000837.001794.000120.000000.000000
.000000.002631.002272.000240.000000.000000
.000000.002990.002392.000000.000000.000000
.000120.001435.002511.000120.000000.000000
.000240.000837.000359.000359.000000.000000
.000479.000957.000120.000000.000000.000000
.000120.000240.001196.000000.000000.000000
.000120.000598.001077.000359.000000.000000
.000000.000479.000120.000000.000000.000000
.000359.000598.000000.000000.000000.000000
.000240.002153.000598.000000.000000.000000
.000718.000240.000000.000000.000000.000000
.000120.000000.000000.000000.000000.000000
.000000.000000.000120.000000.000000.000000
.000240.000000.000000.000000.000000.000000
.000000.000359.000120.000000.000000.000000
.000359.001435.001077.000000.000000.000000
.000718.001674.001913.000120.000000.000000
.000120.003109.001196.000120.000000.000000
.000598.001196.000718.000000.000000.000000
.000359.000718.000000.000000.000000.000000
.000240.000598.000240.000000.000000.000000
.000240.000479.000718.000120.000000.000000
.000000.001077.001196.000359.000000.000000
.000479.000837.000479.000120.000000.000000
.000359.001674.001316.000000.000000.000000
.001316.002153.000120.000000.000000.000000
.001316.000957.000000.000000.000000.000000
.000479.000598.000000.000000.000000.000000
.000359.000718.000240.000000.000000.000000
.000000.000359.000000.000000.000000.000000
.000000.001077.000359.000120.000000.000000
.000479.001674.001196.000000.000000.000000
.000837.003229.002033.000120.000000.000000
.001077.002750.001316.000000.000000.000000
.000598.001435.000837.000120.000000.000000
.000240.001316.000718.000000.000000.000000
.000359.001196.000718.000000.000000.000000
.000240.001196.000718.000000.000000.000000
.003468.012674.011359.001794.000000.000000
.006218.014587.011957.000598.000000.000000
.007772.016858.009207.000000.000000.000000
.009326.021880.006696.000120.000000.000000
.006815.006337.000479.000000.000000.000000
.005620.002392.000000.000000.000000.000000
.004066.002392.000120.000000.000000.000000

DRAFT

.003707.001674.000479.000120.000000.000000
.004305.007294.002392.000240.000000.000000
.007772.014348.006337.000479.000000.000000
.011120.015065.006218.000718.000000.000000
.010761.008609.005381.000240.000000.000000
.008609.007294.005500.000479.000000.000000
.004066.009207.007294.001077.000000.000000
.005739.008848.007772.000837.000000.000000
.004185.008968.003826.000479.000000.000000
.004916.005022.000837.000000.000000.000000
.004076.003826.000359.000240.000000.000000
.004674.003229.000240.000000.000000.000000
.011264.006815.000598.000000.000000.000000
.008025.001913.000120.000000.000000.000000
.003233.000120.000000.000000.000000.000000
.004551.000957.000000.000000.000000.000000
.006350.003348.000359.000000.000000.000000
.007790.005381.002153.000240.000000.000000
.015102.011478.007055.001674.000000.000000
.025648.019608.006696.000359.000000.000000
.023479.009087.001794.000000.000000.000000
.015100.010044.004663.000000.000000.000000
.011508.010163.005859.000957.000000.000000
.009466.005381.001674.000120.000000.000000
.006590.003229.000718.000359.000000.000000
.001871.000000.000000.000000.000000.000000
.002869.000000.000000.000000.000000.000000
.003617.000000.000000.000000.000000.000000
.005269.000718.000000.000000.000000.000000
.010226.000000.000000.000000.000000.000000
.008355.000000.000000.000000.000000.000000
.005487.000000.000000.000000.000000.000000
.006360.000000.000000.000000.000000.000000
.007488.000120.000000.000000.000000.000000
.013115.000479.000000.000000.000000.000000
.025979.000957.000000.000000.000000.000000
.040429.000598.000000.000000.000000.000000
.044155.000240.000000.000000.000000.000000
.038912.000120.000000.000000.000000.000000
.022956.000240.000000.000000.000000.000000
.008735.000120.000000.000000.000000.000000

DRAFT

1991 METEOROLOGICAL STATISTICAL ARRAY FOR FEMP

.000987.002838.001851.000000.000000.000000
.000741.003824.000741.000000.000000.000000
.002838.007402.002221.000000.000000.000000
.008142.010855.004071.000247.000000.000000
.004811.003824.000371.000124.000000.000000
.003208.001851.000000.000000.000000.000000
.001851.000864.000000.000000.000000.000000
.002591.001111.000000.000000.000000.000000
.002961.003084.002344.000000.000000.000000
.004811.011595.006291.000124.000000.000000
.006785.011595.005181.000371.000000.000000
.007895.009128.004811.000124.000000.000000
.004071.010979.004935.000617.000000.000000
.002714.004688.005798.000494.000000.000000
.002591.002591.001851.000000.000000.000000
.001481.003208.001481.000124.000000.000000
.000247.001111.000987.000000.000000.000000
.000371.000371.000617.000124.000000.000000
.000494.000864.000494.000000.000000.000000
.000987.001234.000494.000000.000000.000000
.000864.000741.000000.000000.000000.000000
.000741.000371.000000.000000.000000.000000
.000247.000247.000000.000000.000000.000000
.000741.000124.000247.000000.000000.000000
.001727.001481.000371.000000.000000.000000
.001481.002097.000864.000000.000000.000000
.001604.002591.001234.000000.000000.000000
.001604.000987.001481.000000.000000.000000
.001851.001727.000864.000247.000000.000000
.000741.000617.000494.000124.000000.000000
.000617.000864.000741.000000.000000.000000
.000494.000864.000987.000000.000000.000000
.000741.000987.000987.000124.000000.000000
.000247.001604.000371.000000.000000.000000
.000371.001357.000494.000000.000000.000000
.001357.000987.000124.000000.000000.000000
.001727.000864.000000.000124.000000.000000
.001481.000617.000000.000000.000000.000000
.000864.000247.000000.000000.000000.000000
.000371.000247.000000.000124.000000.000000
.000494.001234.000371.000000.000000.000000
.000494.001974.001974.000000.000000.000000
.001974.002714.000987.000000.000000.000000
.000864.001604.000741.000124.000000.000000
.002097.001234.000741.000124.000000.000000
.000617.001974.000371.000124.000000.000000
.000494.001481.000494.000000.000000.000000
.000617.000124.001111.000000.000000.000000
.002678.009869.007155.000247.000000.000000
.004653.008142.002714.000247.000000.000000
.006752.006291.002344.000124.000000.000000
.007986.005181.007031.001357.000000.000000
.004735.002097.000494.000000.000000.000000
.002736.000371.000000.000000.000000.000000
.002247.001481.000000.000000.000000.000000

DRAFT

.002996.002097.000864.000000.000000.000000
.003520.006045.002838.000247.000000.000000
.010789.015296.007772.000494.000000.000000
.014497.012582.003948.000000.000000.000000
.011602.007135.004935.000741.000000.000000
.007674.013816.006882.000987.000000.000000
.008996.007525.005756.000987.000000.000000
.005014.006538.001974.000124.000000.000000
.004405.008142.003578.000247.000000.000000
.004311.001111.000247.000000.000000.000000
.002417.000987.000124.000000.000000.000000
.003187.001604.000000.000000.000000.000000
.009926.004194.000124.000000.000000.000000
.007586.000987.000000.000000.000000.000000
.004289.000124.000000.000000.000000.000000
.005314.000864.000000.000000.000000.000000
.004461.002221.000864.000000.000000.000000
.010342.005921.002468.000124.000000.000000
.013744.011595.004318.000987.000000.000000
.026036.008758.002344.000124.000000.000000
.024452.005551.001111.000247.000000.000000
.015464.003824.001357.000000.000000.000000
.010153.003084.000741.000124.000000.000000
.009732.001111.000371.000000.000000.000000
.007961.000864.000617.000000.000000.000000
.005192.000000.000000.000000.000000.000000
.004919.000000.000000.000000.000000.000000
.004373.000000.000000.000000.000000.000000
.007718.000617.000000.000000.000000.000000
.011204.000000.000000.000000.000000.000000
.007105.000000.000000.000000.000000.000000
.004099.000000.000000.000000.000000.000000
.006012.000000.000000.000000.000000.000000
.007118.000124.000000.000000.000000.000000
.013690.000247.000000.000000.000000.000000
.018049.000124.000000.000000.000000.000000
.023774.000000.000000.000000.000000.000000
.025700.000124.000000.000000.000000.000000
.028692.000000.000000.000000.000000.000000
.030209.000124.000000.000000.000000.000000
.015056.000247.000000.000000.000000.000000

DRAFT

5659

1992 METEOROLOGICAL STATISTICAL ARRAY FOR FEMP

.000252.000828.000709.000000.000000.000000
.000995.002482.001300.000000.000000.000000
.002100.004254.008891.000000.000000.000000
.001143.004372.001773.000000.000000.000000
.001463.001655.000237.000119.000000.000000
.000963.000237.000000.000000.000000.000000
.000370.000709.000000.000000.000000.000000
.000725.000355.000000.000000.000000.000000
.001478.002718.001891.000000.000000.000000
.001882.005790.003545.000000.000000.000000
.002848.006262.004018.000000.000000.000000
.002129.006262.001891.000000.000000.000000
.001485.003190.002482.000237.000000.000000
.000869.002009.001418.000355.000000.000000
.000875.002482.002718.000119.000000.000000
.000516.002482.001064.000000.000000.000000
.000119.000946.000591.000000.000000.000000
.000237.001064.000473.000000.000000.000000
.001064.001536.000000.000000.000000.000000
.000709.001891.000591.000000.000000.000000
.001182.000591.000000.000000.000000.000000
.000473.000237.000000.000000.000000.000000
.000946.000237.000000.000000.000000.000000
.000828.000709.000000.000000.000000.000000
.000709.002482.000355.000000.000000.000000
.001418.002127.000473.000000.000000.000000
.001536.002482.001418.000119.000000.000000
.001182.001182.000119.000000.000000.000000
.001182.001064.000473.000000.000000.000000
.000591.001182.000237.000000.000000.000000
.000591.001418.001300.000000.000000.000000
.000591.000591.000709.000000.000000.000000
.000473.000591.000709.000000.000000.000000
.000709.001064.000355.000000.000000.000000
.001418.001536.000237.000000.000000.000000
.000946.001536.000355.000000.000000.000000
.001418.000237.000119.000000.000000.000000
.000828.000237.000000.000000.000000.000000
.000591.000237.000000.000000.000000.000000
.000473.000828.000237.000000.000000.000000
.001182.001773.000828.000000.000000.000000
.002009.002718.000591.000000.000000.000000
.002127.001064.000946.000119.000000.000000
.001773.001064.000119.000000.000000.000000
.001064.001064.000709.000119.000000.000000
.000709.001536.000591.000119.000000.000000
.000946.001064.001655.000237.000000.000000
.000709.000946.000709.000000.000000.000000
.003960.009098.005435.000000.000000.000000
.005161.011933.003545.000000.000000.000000
.008607.012760.000709.000000.000000.000000
.014433.014887.003545.000000.000000.000000
.005605.005435.000591.000000.000000.000000
.004523.002600.000000.000000.000000.000000
.004402.002009.000000.000000.000000.000000

DRAFT

5659

.006190.003663.000237.000119.000000.000000
.006560.006617.002600.000000.000000.000000
.009921.014651.003663.000000.000000.000000
.009914.012997.003663.000355.000000.000000
.011921.010752.002364.000119.000000.000000
.014057.010634.005672.000119.000000.000000
.007911.016187.008307.000000.000000.000000
.007527.018397.005971.000709.000000.000000
.005262.008271.004136.000237.000000.000000
.004909.001773.000000.000119.000000.000946
.003228.002482.000709.000000.000000.000000
.004538.001536.000000.000000.000000.000000
.011159.003781.000237.000000.000000.000000
.008792.001655.000000.000000.000000.000000
.006330.000473.000000.000000.000000.000000
.007196.001064.000591.000000.000000.000000
.007995.003545.001182.000355.000000.000000
.011243.011106.001655.000000.000000.000000
.020584.015005.001773.000000.000000.000000
.028202.013824.002127.000119.000000.000000
.020312.005317.000709.000119.000000.000000
.015106.005908.001182.000119.000000.000000
.013523.005790.001064.000237.000000.000000
.010279.002718.000119.000119.000000.000000
.008205.002363.000946.000000.000000.000000
.006913.000119.000000.000000.000000.000000
.005377.000000.000000.000000.000000.000000
.004412.000000.000000.000000.000000.000000
.009315.000473.000237.000000.000000.000000
.009985.000355.000000.000000.000000.000000
.006775.000119.000000.000000.000000.000000
.006598.000709.000000.000000.000000.000000
.003762.000237.000000.000000.000000.000000
.007051.000946.000000.000000.000000.000000
.013175.002127.000591.000000.000000.000000
.019260.001418.000000.000000.000000.000000
.024046.000355.000000.000000.000000.000000
.026645.000237.000119.000000.000000.000000
.026606.000000.000000.000000.000000.000000
.026547.000473.000237.000000.000000.000000
.013136.000237.000237.000000.000000.000000

DRAFT

ATTACHMENT A.3.II

Sample Calculations for Determining Unlimited and Limited Erosion Potential, Settling Velocity and Reflection Coefficient Used in the Air Transport Analysis for Operable Unit 2 Fernald Environmental Management Project

CALCULATION WORKSHEET Order No. 19118 (01-611)

CLIENT FEMP CU2	JOB NUMBER 5659
SUBJECT Calculation of wind erosion emission rate (Landfill)	
BASED ON Current Scenario	DRAWING NUMBER
BY Wagner	CHECKED BY Loger
APPROVED BY	DATE

Current Scenario

*Use Equation 4-1 Limited erosion potential due to wind erosion.

$$E_{10} = 0.83 \frac{f(P(u^t))(1-V)}{(PE/50)^2} \quad (mg/m^2\text{-}hr)$$

where f = disturbances/month = 1
V = vegetative cover = 85%
u^t = 24 m/s from Table 4-1*
$P(u^t)$ = 6.7 (u^t - u_t)
PE = 103 from Fig 4-2*

From surface soil analysis of Landfill, majority of particles < 75μ with diameters between 30μ - 13μ, yielding an average diameter of 31μm. From Figure 3-4* the Threshold Friction Velocity (u_t) = 10.3 cm/s or .103 m/s

$$P(u^t) = 6.7(24\,m/s - .103\,m/s)$$
$$= 160.1\,m/s$$

$$E_{10} = 0.83 \frac{(1)(160.1)(1-.85)}{(103/50)^2}$$

$$= \frac{19.93}{4.24} = (4.70\,mg/m^2\text{-}hr)\frac{hr}{3600\,s}$$

$$= 1.31 \times 10^{-3}\,mg/m^2\text{-}s$$

* EPA Publication 600/8-85/002

CALCULATION WORKSHEET Order No. 19116 (01-91)

CLIENT FEMP CU2		JOB NUMBER 5659	
SUBJECT Calculation of wind erosion emission rate (Landfill)			
BASED ON Current Scenario		DRAWING NUMBER	
BY Wagner	CHECKED BY Lege	APPROVED BY	DATE

$$E_{10} = \left(1.31 \times 10^{-3}\ mg/m^2\text{-}s\right)\left(10^{-3}\ g/mg\right)$$

$$E_{10} = 1.31 \times 10^{-6}\ g\,PM_{10}/m^2\text{-}s$$

wind erosion PM emission rate based on limited erosion potential

$$a \begin{cases} \%\,TSP & 0.742 \\ \%\,PM_{10} & 0.174 \end{cases} \qquad \left(1.31 \times 10^{-6}\ g\,PM_{10}/m^2\text{-}s\right)$$

$$E_{TSP} = 5.6 \times 10^{-6}\ g\,TSP/m^2\text{-}s$$

wind erosion (TSP) emission rate based on limited erosion potential

a: from "Particle Size Analysis" of Surface Soils from the Solid Waste Landfill

D

PARTICLE SIZE ANALYSIS
ASTM D 422

Project Name: FERNALD OU2 | Client Number: 111499

Project Number: 483500.075.01 | ETDC Number: ETDC- 3473

Specific Gravity = 2.600 Assumed

Moisture Content = 23.1%

SIEVE ANALYSIS

COARSE Sieve No.	Diameter mm	Percent Finer	
3"	75.000	100.0%	
1.5"	37.500	100.0%	1.2
0.75"	19.000	98.8%	1.3
0.375"	9.500	97.3%	0.8
#4	4.750	96.5%	2.7
#10	2.000	93.8%	

FINE Sieve No.	Diameter mm	Percent Finer	
#20	0.850	88.9%	4.9
#40	0.425	84.7%	4.2
#60	0.250	80.9%	3.8
#100	0.149	77.3%	3.6
#140	0.106	75.5%	1.8
#200	0.075	74.2%	1.3

HYDROMETER ANALYSIS

HYDROMETER Diameter mm	Percent Finer	
0.05782	73.4%	0.8
0.04188	67.6%	5.8
0.03014	64.7%	2.9
0.02106	38.6%	26.1
0.01288	21.2%	17.4
0.00921	17.4%	3.8
0.00650	13.5%	3.9
0.00463	11.6%	1.9
0.00328	10.6%	1.0
0.00140	7.7%	2.9

Majority of particles fall bet. 30μ-12μ

Mean Particle Diameter 21μm

%TSP ≤75μm = 74.2%

%PM10 ≤ 10μm = 17.4%

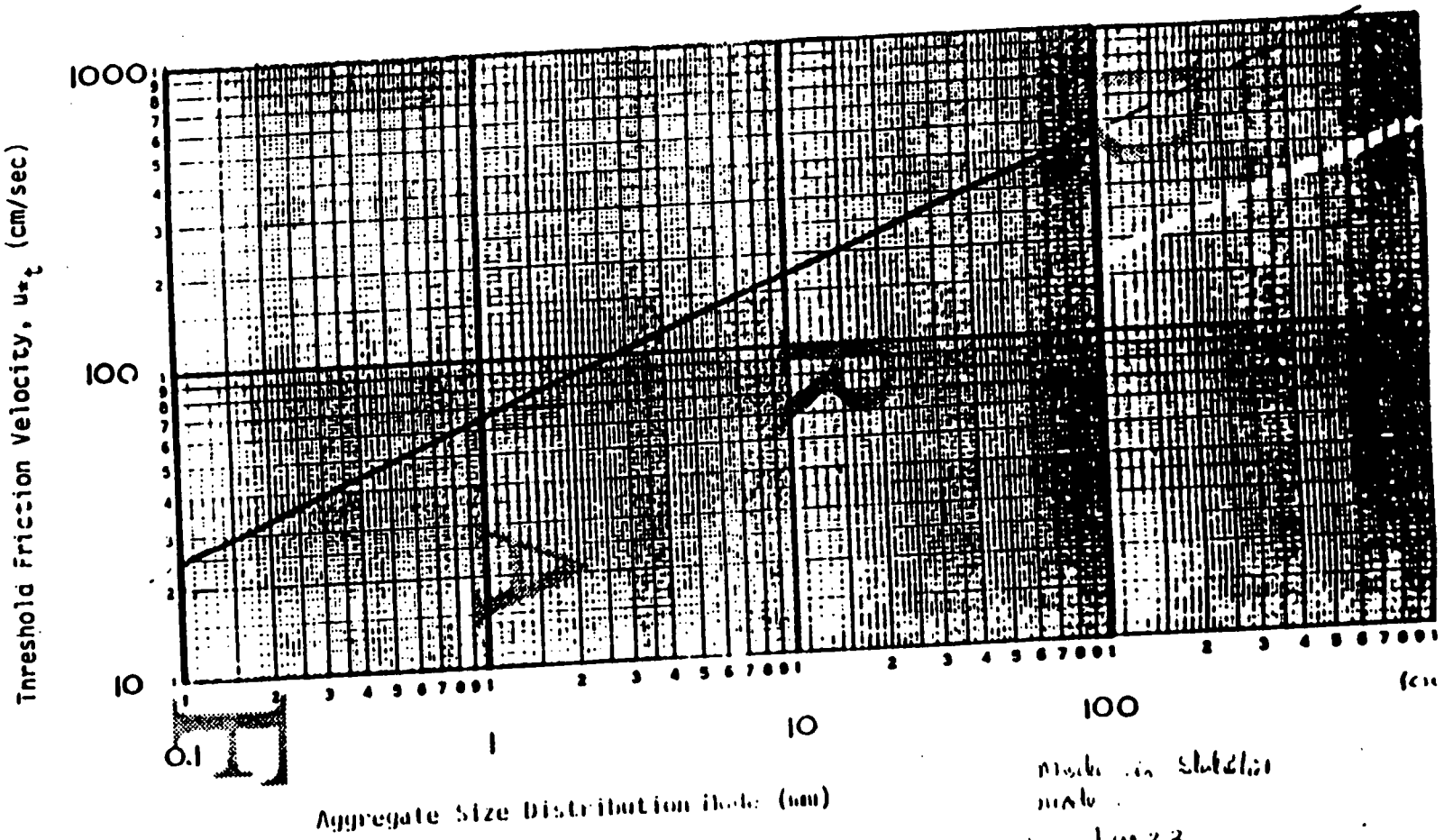

Figure 3.4. Relationship of Threshold Friction Veloc
to Size Distribution Mode

000376

TABLE 4-1. FASTEST MILE[a] [u^+] AND MEAN WIND SPEED[b] [u] FOR SELECTED UNITED STATES STATIONS

Station	State	[u^+] (m/s)	[u] (m/s)	Station	State	[u^+] (m/s)	[u] (m/s)
Birmingham	AL	20.8	3.3	Detroit	MI	21.8	4.6
Montgomery	AL	20.2	3.0	Grand Rapids	MI	21.6	4.5
Tucson	AZ	23.0	3.7	Lansing	MI	23.7	4.6
Yuma	AZ	21.8	3.5	Sault St. Marie	MI	21.6	4.3
Fort Smith	AR	20.8	3.4	Duluth	MN	22.8	5.1
Little Rock	AR	[illegible]	3.6	Minneapolis	MN	22.0	4.7
Fresno	CA	[illegible]	2.3	Jackson	MS	20.5	3.4
Red Bluff	CA	[illegible]	3.9	Columbia	MO	22.4	4.4
Sacramento	CA	[illegible]	3.7	Kansas City	MO	22.6	4.6
San Diego	CA	15.4	3.0	St. Louis	MO	21.2	4.2
Denver	CO	22.0	[illegible]	Springfield	MO	22.4	3.0
Grand Junction	CO	23.6	[illegible]	Billings	MT	25.6	5.1
Pueblo	CO	28.1	3.9	Great Falls	MT	26.4	5.9
Hartford	CT	20.2	4.0	Havre	MT	25.9	4.5
Washington	DC	21.6	3.4	Helena	MT	24.7	3.5
Jacksonville	FL	21.7	3.3	Missoula	MT	21.6	2.7
Tampa	FL	22.2	3.9	North Platte	NE	27.7	4.6
Atlanta	GA	21.2	[illegible]	Omaha	NE	24.6	4.8
Macon	GA	20.1	3.5	Valentine	NE	27.1	4.8
Savannah	GA	21.3	3.9	Ely	NV	23.6	4.7
Boise	ID	21.4	4.0	Las Vegas	NV	24.4	4.0
Pocatello	ID	23.8	[illegible]	Reno	NV	25.2	2.9
Chicago	IL	21.0	[illegible]	Winnemucca	NV	22.4	3.5
Moline	IL	24.5	[illegible]	Concord	NH	19.2	3.0
Peoria	IL	23.2	[illegible]	Albuquerque	NM	25.6	4.0
Springfield	IL	24.2	[illegible]	Roswell	NM	26.0	4.1
Evansville	IN	20.9	3.7	Albany	NY	21.4	4.0
Fort Wayne	IN	23.7	4.6	Binghamton	NY	22.0	4.6
Indianapolis	IN	24.8	[illegible]	Buffalo	NY	24.1	5.5
Burlington	IA	25.0	[illegible]	New York	NY	22.5	5.5
Des Moines	IA	25.8	5.0	Rochester	NY	23.9	4.3
Sioux City	IA	25.9	[illegible]	Syracuse	NY	22.5	4.4
Concordia	KS	25.7	5.4	Cape Hatteros	NC	25.9	5.1
Dodge City	KS	27.1	6.3	Charlotte	NC	20.0	3.4
Topeka	KS	24.4	4.6	Greensboro	NC	18.9	3.4
Wichita	KS	26.0	5.6	Wilmington	NC	22.3	4.0
Louisville	KY	22.0	3.8	Bismarck	ND	26.1	4.7
Shreveport	LA	19.9	3.9	Fargo	ND	26.6	5.7
Portland	ME	21.7	3.9	Cleveland	OH	23.6	4.8
Baltimore	MD	25.0	4.2	Columbus	OH	[illegible]	3.9
Boston	MA	25.2	5.6	Dayton	OH	[illegible]	4.6

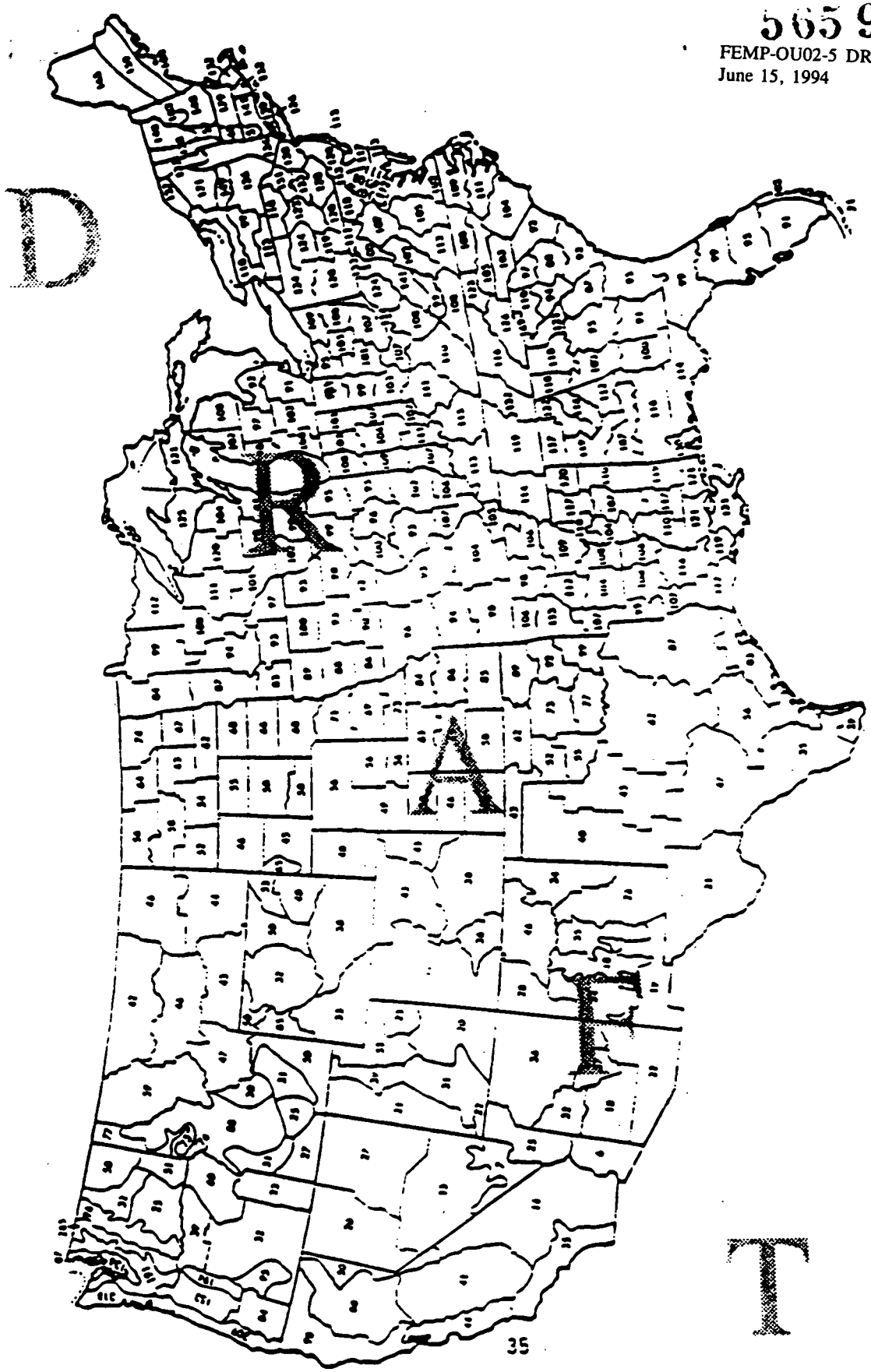

Figure 4-2. Map of P-E Index for State Climatic Divisions

DRAFT

CLIENT FEMP OU2		JOB NUMBER 5659	
SUBJECT Calculation of wind erosion emission rate			
BASED ON Future Scenario		DRAWING NUMBER	
BY Wagner	CHECKED BY Leyr	APPROVED BY	DATE

Future Scenario

*Use Equation 4-4 Unlimited erosion potential due to wind erosion. Crops are assumed to grow on the Landfill 6 months of the year. Use 50% annual vegetative cover.

$$E_{10} = 0.036(1-V)\left(\frac{[u]}{u_t}\right)^3 F(x) \qquad (Eq\ 4\text{-}4)$$

where
V = vegetative cover
[u] = mean wind speed
u_t = Threshold Friction Velocity @ 7meters
F(x) = See Figure 4-3*
E_{10} = PM$_{10}$ Emission Factor (gpm_{10}/m^2-hr)

[u] = 2.28 m/s Highest annual average wind speed from 6 years of on-site data, (See RI 00-4)

V = 50%

Calculate:

$$u(z) = \frac{u_*}{0.4}\ln\left(\frac{z}{z_0}\right)$$

where z = 7 meters
z_0 = 0.02 meters
$u_* = u_t$ = .103 m/s

$$u(z) = \frac{.103\ m/s}{0.4}\ln\left(\frac{7m}{0.02m}\right)$$

u(z) = 1.51 m/s ✓ Subsitute u(z) for u_t in Eq 4-4. This is to correct the TFV from 7meters to ground level (where erosion occurs)

Eq 4-4 becomes →

*EPA Publication EPA/8-88/002

CALCULATION WORKSHEET Order No. 10116 (01-01)

CLIENT FEMP OU2		JOB NUMBER 5559	
SUBJECT Calculation of wind erosion emission rate (Landfill			
BASED ON Future Scenario		DRAWING NUMBER	
BY Wagner	CHECKED BY Lazor	APPROVED BY	DATE

$$E_{10} = 0.036(1-V)\left(\frac{[u]}{u(z)}\right)^3 F(x)$$

$$= 0.036(1-.50)\left(\frac{2.28\ m/s}{1.51\ m/s}\right)^3 (F(x))$$

$F(x) = ?$ where $x = 0.886\,(u_t/[u])$

$= 0.886\,(.103/2.28)$

$= 0.04$

when $x = 0.04$ $F(x) = 1.91$ From Figure 4-2

$$E_{10} = 0.036(1-.50)\left(\frac{2.28\ m/s}{1.51\ m/s}\right)^3 1.91$$

$$= (0.12\ g\,pm/m^2\text{-}s)\left(\frac{hr}{3600\ s}\right)$$

$= \underline{\underline{3.29\times10^{-5}\ g\,pm_{10}/m^2\text{-}s}}$ wind erosion em rate based o unlimited erosio potential

$$\frac{\%\ TSP\ 0.742}{\%\ pm_{10}\ 0.174}\left(3.29\times10^{-5}\ g\,pm_{10}/m^2\text{-}s\right)$$

$\underline{\underline{1.40\times10^{-4}\ g_{TSP}/m^2\text{-}s}}$ wind erosion emission r of TSP based on erosion potential

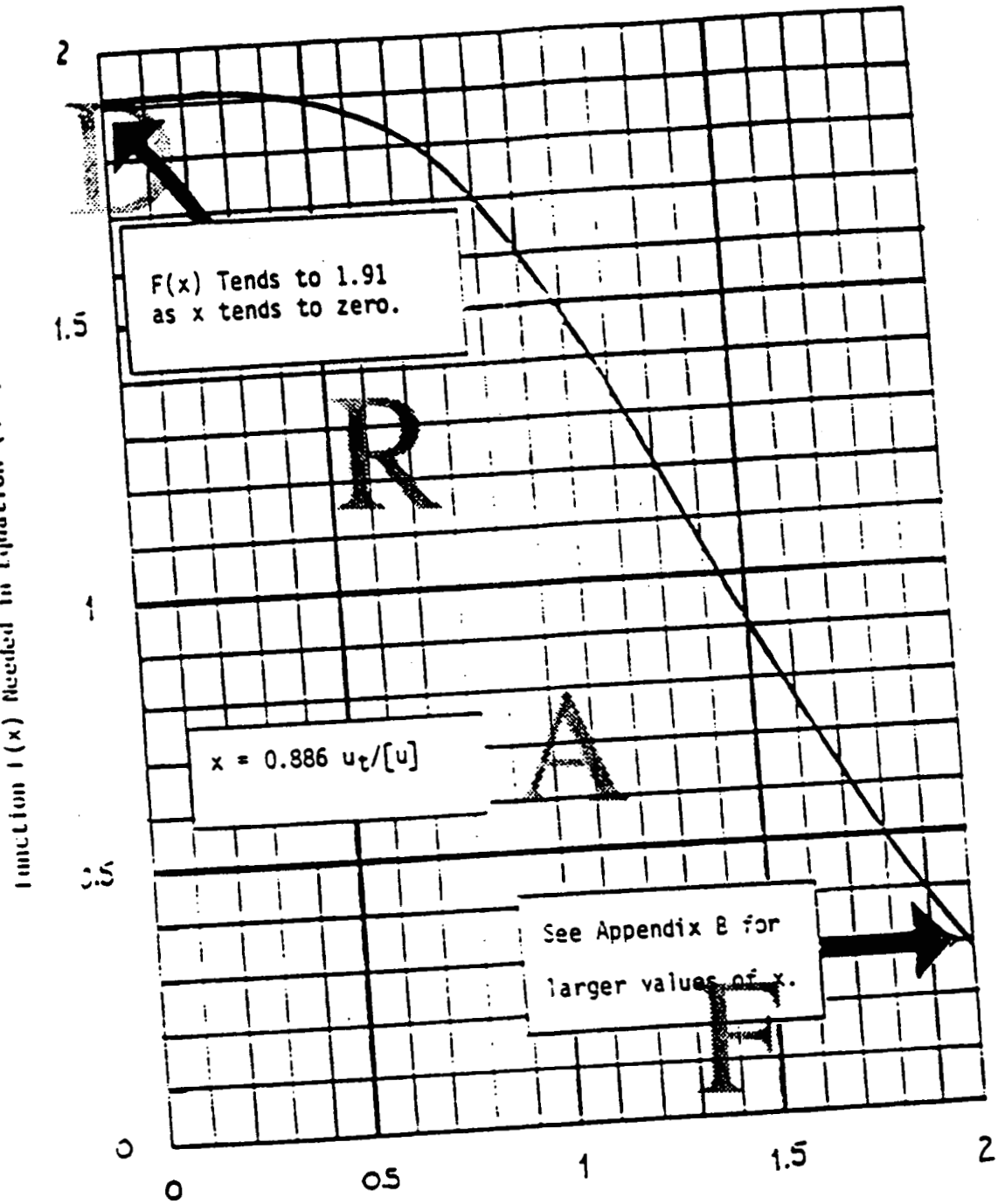

Figure 4-3. Graph of Function F(X) Needed to Estimate Unlimited Erosion

CALCULATION WORKSHEET Order No. 10116 (91-01)

CLIENT FEMP OU2	JOB NUMBER
SUBJECT Calculation of Deposition modeling input 1	DRAWING NUMBER
BASED ON Surface Soil Data	APPROVED BY / DATE
BY Wagner / CHECKED BY Leger	

From current scenario use average particle diameter of 21 μm.

Calculate Settling velocity

$$V_{sn}^{*} = \frac{2 \rho g r^2}{9 \mu}$$

*from ISC Users Guide Vol page 1-35.

where $\rho = 2.65\ g/cm^3$ (from sfc soil analysis of Landfill)
$g = 980\ cm/s^2$
$r = 1.1 \times 10^{-3}\ cm$
$\mu = 1.83 \times 10^{-4}\ g/cm\text{-}s$

$$V_{sn} = \frac{2(2.65\ g/cm^3)(980\ cm/s^2)(1.1 \times 10^{-3}\ cm)^2}{9(1.83 \times 10^{-4}\ g/cm/s)}$$

$$= 3.82\ cm/s \text{ or } 0.0382\ m/s$$

From Figure 1-7 ISC Users Guide Vol. 2, calculate "Reflection Coefficent" (γ)

$\gamma = 0.65$

In Summation

Particle diameter (μm)	mass Fraction	Settling velocity (cm/s)	Reflection Coefficent
21	100%	3.82	0.65

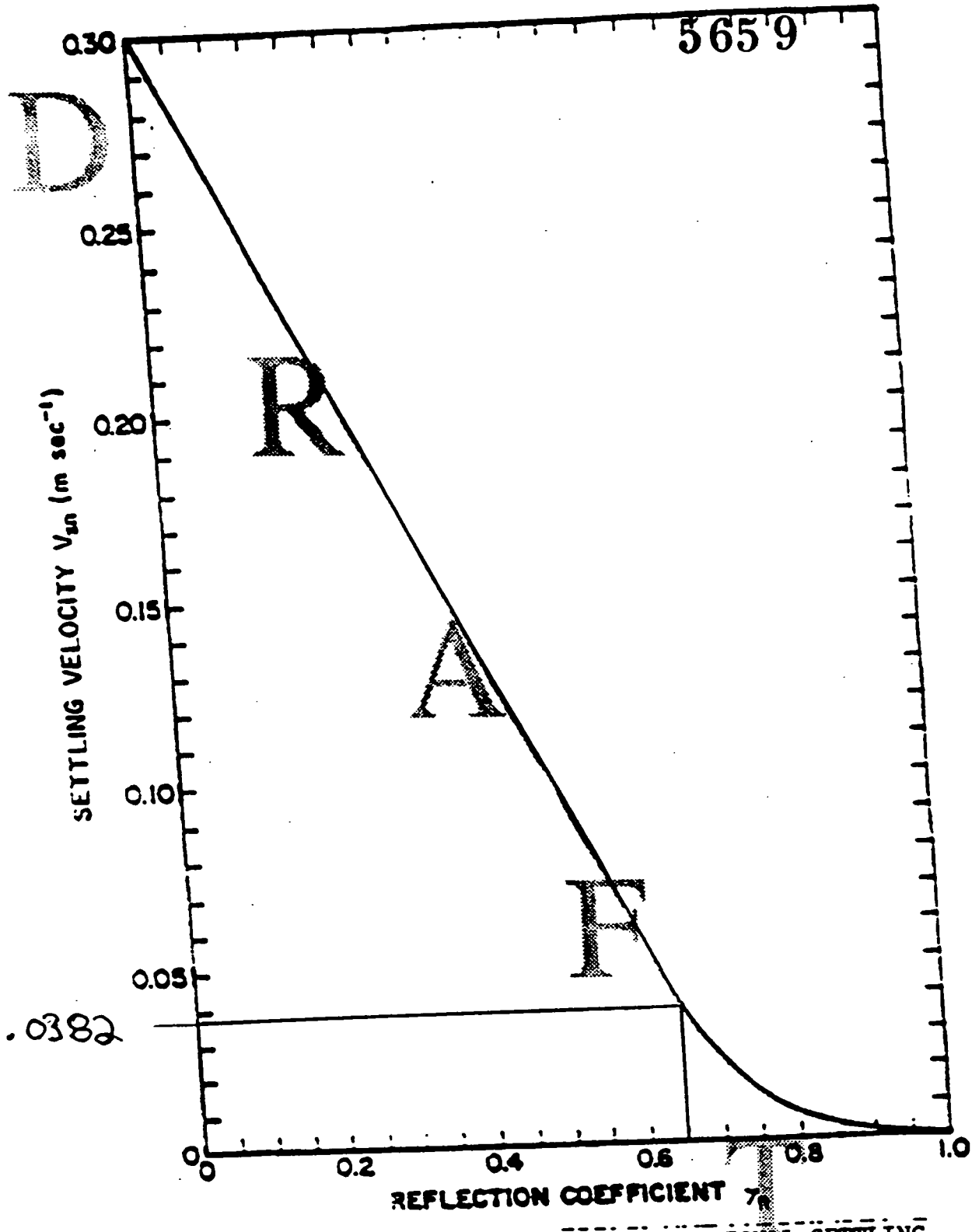

FIGURE 1-7. RELATIONSHIP BETWEEN THE GRAVITATIONAL SETTLING VELOCITY, V_{sn} AND THE REFLECTION COEFFICIENT, γ_N, SUGGESTED BY DUMBAULD, et al. (1976)

U.S. GOVERNMENT PRINTING OFFICE: 1994-550-232/80149

ATTACHMENT A.3.III

RAECOM Model Output for Each Operable Unit 2 Subunit

12/14/93

000385

OU2 ACTIVE FLYASH PILE: COMBINED SURFACE AND SUBSURFACE CONTRIBUTION

********** INPUT PARAMETERS **********

NUMBER OF LAYERS:	2	
RADON FLUX INTO LAYER 1:	.000	pCi/m2/sec
SURFACE RADON CONCENTRATION:	.000	pCi/LITER
BARE SOURCE FLUX (Jo) FROM LAYER 1:	1.154	pCi/m2/sec

LAYER	THICKNESS (cm)	DIFF COEFF (cm2/SEC)	POROSITY	SOURCE (pCi/cm3/sec)	MOISTURE (dry wt. %)
1	570.	.1698E-02	.4100	.9900E-05	20.00
2	30.	.4188E-02	.5200	.6300E-05	28.60

***** RESULTS OF RADON DIFFUSION CALCULATION*****

LAYER	THICKNESS (cm)	EXIT FLUX (pCi/m2/sec)	EXIT CONC. (pCi/liter)	MIC
1	570.	.8134E+00	.1391E+05	.4250
2	30.	.1517E+01	.0000E+00	.4725

12/14/93

OU2 LIME SLUDGE PONDS: COMBINED SURFACE AND SUBSURFACE CONTRIBUTION

********** INPUT PARAMETERS **********

NUMBER OF LAYERS: 2
RADON FLUX INTO LAYER 1: .000 pCi/m2/sec
SURFACE RADON CONCENTRATION: .000 pCi/LITER

LAYER 2 EXCEEDS SATURATION. MOISTURE CHANGED FROM .842 TO .397

BARE SOURCE FLUX (Jo) FROM LAYER 1: .2914 pCi/m2/sec

LAYER	THICKNESS (cm)	DIFF COEFF (cm2/SEC)	POROSITY	SOURCE (pCi/cm3/sec)	MOISTURE (dry wt. %)
1	570.	.1698E-02	.4100	.2500E-05	20.00
2	30.	.8675E-04	.5200	.2600E-05	39.72

***** RESULTS OF RADON DIFFUSION CALCULATION*****

LAYER	THICKNESS (cm)	EXIT FLUX (pCi/m2/sec)	EXIT CONC. (pCi/liter)	MIC
1	570.	-.2770E-01	.1304E+05	.4250
2	30.	.8636E-01	.0000E+00	.2674

12/14/93

OU2 SOUTH FIELD: COMBINED SURFACE AND SUBSURFACE CONTRIBUTION

********** INPUT PARAMETERS **********

NUMBER OF LAYERS:	2	
RADON FLUX INTO LAYER 1:	.000	pCi/m2/sec
SURFACE RADON CONCENTRATION:	.000	pCi/LITER
BARE SOURCE FLUX (Jo) FROM LAYER 1:	.6412	pCi/m2/sec

LAYER	THICKNESS (cm)	DIFF COEFF (cm2/SEC)	POROSITY	SOURCE (pCi/cm3/sec)	MOISTURE (dry wt. %)
1	570.	.1698E-02	.4100	.5500E-05	20.00
2	30.	.1725E-01	.5200	.4230E-04	18.20

***** RESULTS OF RADON DIFFUSION CALCULATION*****

LAYER	THICKNESS (cm)	EXIT FLUX (pCi/m2/sec)	EXIT CONC. (pCi/liter)	MIC
1	570.	.4530E+00	.7685E+04	.4250
2	30.	.6797E+01	.0000E+00	.6643

5659

12/14/93

OU2 SOLID WASTE LANDFILL: COMBINED SURFACE AND SUBSURFACE CONTRIBUTION

********** INPUT PARAMETERS **********

NUMBER OF LAYERS:	2	
RADON FLUX INTO LAYER 1:	.000	pCi/m2/sec
SURFACE RADON CONCENTRATION:	.000	pCi/LITER
BARE SOURCE FLUX (Jo) FROM LAYER 1:	.2355	pCi/m2/sec

LAYER	THICKNESS (cm)	DIFF COEFF (cm2/SEC)	POROSITY	SOURCE (pCi/cm3/sec)	MOISTURE (dry wt. %)
1	570.	.7701E-03	.4100	.3000E-05	21.70
2	30.	.1645E-01	.5200	.2100E-05	18.70

***** RESULTS OF RADON DIFFUSION CALCULATION*****

LAYER	THICKNESS (cm)	EXIT FLUX (pCi/m2/sec)	EXIT CONC. (pCi/liter)	MIC
1	570.	.2232E+00	.7475E+03	.3761
2	30.	.5265E+00	.0000E+00	.6551

REFERENCES

ASI/IT, Advanced Sciences, Inc./International Technologies Corporation, October 1992. Work Plan Addendum. Fernald, OH.

Atlantic Environmental Services (AES), 1988, "Management of Manufactured Gas Plant Sites," Vol. III, Risk Assessment, Gas Research Institute, Chicago, IL, GRI-87/0260.3.

Barari, A. and L. S. Hedges, 1985. "Movement of Water in Glacial Till." International Association of Hydrogeologists, Memoirs, Vol. XVII, Part 1. Proceedings, Hydrogeology of Rocks of Low Permeability. Tucson, AZ.

Batu, V., 1989. "A Generalized Two-Dimensional Analytical Solution for Hydrodynamic Dispersion in Bounded Media with the First-Type Boundary Condition at the Source," Water Resources Research, Vol. 25, No. 6, pp. 1125-1132.

Biggar, J. W. and D. R. Nielsen, 1976. "Spatial Variability of the Leaching Characteristics of a Field Soil." Water Resources Research, Vol 12, No. 1.

Bowers, T. S., K.L. Von Damm, and J.M. Edmond, 1985, "Chemical Evolution of Mid-Ocean Ridge Hot Springs," Geochemical et Cosmochimica Acta, Vol. 49, pp. 2239-2252.

Brenner, H., 1962. "The Diffusion Model of Longitudinal Mixing in Beds of Finite Length Numerical Values." Chemical Engineering Science, Vol. 17, pp. 229-243.

Brockman, S. C., 1988. "Glacial Geologic Mapping in Hamilton County, Ohio, Report of Progress on the Final Phase." Ohio Department of Natural Resources, Division of Geological Survey.

Cravens, S. J. and L. C. Ruedisili, 1987. "Water Movement in Till of East-Central South Dakota." Groundwater, Vol. 25, No. 5.

Dames and Moore, 1985. Groundwater Task C Report, Department of Energy Feed Materials Production Center, prepared for National Lead of Ohio, Inc., Cincinnati, OH.

Daveler, S. A. and T. J. Wolery, 1992, EQPT, A Data File Preprocessor for the EQ3/6 Software Package: User's Guide and Related Documentation (Version 7.0), UCRL-MA-110662-PT-II (Draft 1.1), Lawrence Livermore National Laboratory, Livermore, CA.

Dove, G. D. and S. E. Norris, 1951. "Conditions Governing the Occurrence of Groundwater in the Fernald Area, Ohio, with Reference to the Possibilities of Contamination by Disposal of Chemical Wastes." U.S. Geological Survey, Groundwater Branch. Columbus, OH.

Fetter, C. W., 1989. Applied Hydrogeology, Second Ed. Columbus, OH: Charles E. Merrill Publishing Company.

Freeze, R. A. and J. A. Cherry, 1979. Groundwater. New York: Prentice-Hall.

Geotrans, Inc., 1987. "The Sandia Waste-Isolation Flow and Transport Model for Fractured Media, SWIFT III, Release 2.32." Herndon, VA.

Grisak, G. E., J. A. Cherry, J. A. Vonhof, and J. P. Blumele, 1976. "Hydrogeologic and Hydrochemical Properties of Fractured Till in the Interior Plains Region: in Glacial Till, An Interdisciplinary Study." The Royal Society of Canada, Special Publications, No. 12, Robert F. Legget, ed. Ottawa, Ontario.

Haith, D. A., 1980, "A Mathematical Model for Estimating Pesticide Losses in Runoff," Journal of Environmental Quality, Vol 9, No.3, pp. 428-433.

Heath, R. C., 1983. "Basic Groundwater Hydrology." U.S. Geological Survey, Water Supply Paper 2220. Reston, VA.

Helgeson, 1969, "Thermodynamics of Hydrothermal systems at Elevated Temperatures and Pressures," American Journal of Science, Vol. 267, pp. 729-804.

Hendry, M. J., 1988. "Hydrogeology of Clay Till in a Prairie Region of Canada." Groundwater, Vol. 26, No. 5.

Hershfield, D. M., 1961, "Rainfall Frequency Atlas of the United States: For Durations from 30 Minutes to 24 Hours and Retain Periods From 1 to 100 Years," U.S. Department of Commerce, Washington, D.C., Technical Paper No. 40.

Howard, P. H., R. S. Boethling, W. F. Jarvis, W. M. Meylan and E. M. Michalenko, 1991. Environmental Degradation Rates. Chelsea, MI: Lewis Publishers, Inc.

INTERA, 1983, "Geochemical Models Suitable for Performance Assessment of Nuclear Waste Storage: Comparison of PHREEQE and EQ3/EQ6," ONWI-473, INTERA Environmental Consultants, Houston, TX.

IT Corporation, 1990a. "Flow and Solute Transport Computer Code Verification." Prepared for U.S. Department of Energy, Oak Ridge Operations Office, Oak Ridge, TN.

IT Corporation, 1990b. "FMPC Groundwater Report." Prepared for U.S. Department of Energy, Oak Ridge Operations Office, Oak Ridge, TN.

IT Corporation, November 7, 1990c. Memorandum from Sirous H. Djafari of IT for distribution, Subject - "Determination of Hydraulic Conductivity of Till and Unsaturated Great Miami Aquifer Units."

IT Corporation, 1989. "Geochemical Program : Issues 3 and 5." Prepared for U.S. Department of Energy, Oak Ridge Operations Office, Oak Ridge, TN.

Jackson, K. J., 1988, "Verification and Validation Studies of the Addition of Areazer's Equations to the EQ3/6 Brine Model," UCRL-53841, Lawrence Livermore National Laboratory, Livermore, CA.

Javandel, I., C. Doughty, and C. F. Tsang, 1984. "Groundwater Transport: Handbook of Mathematical Models." American Geophysical Union Water Resources Monograph Series 10. Washington, DC.

Kerrisk, J. F., 1981, "Chemical Equilibrium Calculations for Aqueous Geothermal Brines," LA-8851-MS, Los Alamos National Laboratory, Los Alamos, NM.

Kincaid, C. T. and J.R. Morey, 1984,"Geohydrochemical Model for Solute Migration , Volume 2: Preliminary Evaluation of Selected Computer Codes," EPRI EA-3417, Electric Power Research Institute, Palo Alto, CA.

Mills, W. B., J. D. Dean, D. B. Porcella, S. A. Gherini, R. J. M. Hudson, W. E. Frick, G. L. Rupp, and G. L. Bowie, 1982, "Water Quality Assessment: A Screening Procedure for Toxic and Conventional Pollutants: Parts 1, 2, and 3," EPA-6001 6-82-004 a,b,c, U.S. Environmental Protection Agency, Environmental Research Laboratory, Office of Research and Development, Athens, GA.

Mills, W. B., D. B. Porcella, M. J. Ungs, S. A. Ghevini, K. V. Summers, Lingfung Mok, G. L. Rupp, G. L. Bowie, and D. A. Haith, 1985, "Water Quality Assessment: A Screening Procedure for Toxic and Conventional Pollutants in Surface and Groundwater," EPA/600/6-85/002a, U.S. Environmental Protection Agency, Environmental Research Laboratory, Office of Research and Development, Athens, GA.

Mills, W. B., J. D. Dean, D. B. Porcella, S. A. Gherini, R. J. M. Hudson, W. E. Frick, G. L. Rupp, and G. L. Bowie, 1982. "Water Quality Assessment: A Screening Procedure for Toxic and Conventional Pollutants: Parts 1, 2, and 3." U.S. EPA Environmental Research Laboratory, Office of Research and Development. Athens, GA, EPA-6001 6-82-004 a, b, c.

Mills, W.B., D.B. Porcella, M.J. Ungs, S.A. Gherini, K.V. Summers, Lingfung Mok, G.L. Rupp, G.L. Bowie, and D.A Haith, 1985. Water Quality Assessment: A Screening Procedure for Toxic and Conventional Pollutants in Surface and Groundwater. US EPA Environmental Research Laboratory, Office of Research and Development. EPA/600/6-85/002a. Athens, GA.

Mockus, J., 1972, "Estimation of Direct Runoff from Storm Rainfall," In National Engineering Handbook, Section 4, U.S. Department of Agriculture, Soil Conservation Service, Washington, D.C.

Morris, D. A. and A. I. Johnson, 1967. "Summary of Hydrologic and Physical Properties of Rock and Soil Materials, as Analyzed by the Hydrologic Laboratory of the U.S. Geological Survey." U.S. Geological Survey, Water-Supply Paper 1839-D.

Nordstrom, D. K., 1979, "A Comparison of Computerized Chemical Models for Equilibrium Calculations on Aqueous Systems," ACS Symposium Series, American Chemical Society, Washington, D.C., Vol. 93, pp 857-892.

Ogata, A. and R. B. Banks, 1961. "A Solution of the Differential Equation of Longitudinal Dispersion in Porous Media." U.S. Geological Survey, Professional Paper 411-A, Reston, VA.

Parsons, 1993. "South Plume Removal Action Pumping Test Report, Operable Unit 5, Project Order 37." Fernald Environmental Management Project, Fairfield, Ohio.

Rajendran, R., J. B. Patro, A. K. Sridharan, and M. Sampath, 1979. "Solvent Extraction of Uranyl Nitrate with Tributyl Phosphate," in Symposium on Solvent Extraction of Metals. Bombay, India: Department of Atomic Energy.

Solebello, L. P., 1991, "Mineralogy of Soil Core Sample, Feed Materials Production Center," Technical report issued by McCrone Associates, Inc., Fernald, OH.

U.S. Environmental Protection Agency, 1993, "Risk-Based Concentration Table, Second Quarter for 1993," U.S. Environmental Protection Agency, Region III Memorandum dated May 10, 1993, Philadelphia, PA.

U.S. Environmental Protection Agency (EPA), 1992a, "User's Guide for the Industrial Source Complex (ISC2) Dispersion Model, Volume I - User Instructions," including Addendum A, September 1992, EPA/540/4-92/008a, Office of Air Quality Planning and Standards, U.S. EPA, Research Triangle Park, NC.

U.S. Environmental Protection Agency (EPA), 1992b, "User's Guide for the Industrial Source Complex (ISC2) Dispersion Model, Volume II - Description of Model Algorithms," including Addendum A, September 1992, EPA/540/4-92/008b, Office of Air Quality Planning and Standards, U.S. EPA, Research Triangle Park, NC.

U.S. Environmental Protection Agency (EPA), 1989, "Air/Superfund National Technical Guidance Study Series, Volume IV - Procedures for Dispersion Modeling and Air Monitoring for Superfund Air Pathway Analysis," EPA/450/1-89/004, Office of Air Quality Planning and Standards, U.S. EPA, Research Triangle Park, NC.

U.S. Environmental Protection Agency, 1988, "Superfund Exposure Assessment Manual," EPA/540/1-88/001, Office of Remedial Response, U.S. EPA, Washington, D.C.

U.S. Environmental Protection Agency, 1987. "Low-Level and NARM Radioactive Wastes, Model Documentation PRESTO-EPA-POP, Volume 1, Methodology Manual; Volume II, Users Manual." EPA/520/1-87-024-1 and 2. Washington, DC: EPA, Office of Radiation Programs.

U.S. Environmental Protection Agency (EPA), 1987b, "On Site Meteorological Program Guidance for Regulatory Modeling Applications," EPA/450/1-87-013, Office of Air Quality Planning and Standards, U.S. EPA, Research Triangle Park, NC.

U.S. Environmental Protection Agency, 1985. "Water Quality Assessment," EPA/600/6-85/002b. Athens, Georgia: Office of Research and Development.

U.S. Environmental Protection Agency (EPA), 1985b, "Rapid Assessment of Exposure to Particulate Emissions from Surface Contamination Sites, "EPA/600/8-85/002, Office of Health and Environmental Assessment, U.S. EPA, Washington, DC.

U.S. Environmental Protection Agency, 1984. "The Hydrologic Evaluation of Landfill Performance (HELP) Model." EPA/530-SW-84-009. Washington, DC: US EPA, Office of Solid Waste and Emergency Response.

U.S. Department of Energy, 1993, "Remedial Investigation Report for Operable Unit 2", Fernald Environmental Management Project, Remedial Investigation and Feasibility Study, Fernald, OH.

U.S. Department of Energy, 1993a. Groundwater Modeling Report - Summary of Model Development. Fernald, OH.

U.S. Department of Energy, March 1993b. "Sitewide Characterization Report." FEMP, SWCR-6, Final.

U.S. Department of Energy, May 1993c. "Characterization of Background Water Quality for Streams and Groundwater." Fernald, OH, Draft.

U.S. Department of Energy, 1993d. "Paddys Run Flow and Infiltration Model Report: Description and Results," prepared for the U.S. Department of Energy Fernald Field Office by IT Corporation.

U.S. Department of Energy, 1993e. "Remedial Investigation for Operable Unit 4," Fernald Environmental Management Project, Fernald, OH.

No. 5-3 U.S. Department of Energy (DOE), 1993f "Surface Water Flow and Infiltration Model Summary Report, Draft Final, "U.S. DOE, Fernald Field Office, Fernald, OH.

U.S. Department of Energy, 1992. "Final Risk Assessment Work Plan Addendum." Fernald Environmental Management Project, Remedial Investigation and Feasibility Studies, Fernald, OH.

U.S. Department of Energy, 1992a. "Work Plan Addendum for Excavation of Trenches in the Operable Unit 2 Solid Waste Landfill."

U.S. Department of Energy, 1990. "Groundwater Report - Draft." Prepared for U.S. Department of Energy, Oak Ridge Operations Office, Oak Ridge, TN.

U.S. Department of Energy, 1990a, "Engineering Evaluation/Cost Analysis, South Plume, FMPC, Fernald, Ohio," DOE, Oak Ridge Operations Office, Oak Ridge, TN.

U.S. Department of Energy, 1990b, "Groundwater Report - Draft," prepared for U.S. Department of Energy, Oak Ridge Operations Office, Oak Ridge, TN.

U.S. Nuclear Regulatory Commission (NRC), 1984, "Radon Attenuation Handbook for Uranium Mill Tailing Cover Design," NUREG/CR-3533, Office of Nuclear Regulatory Research, U.S. NRC, Washington, DC.

Walton, W. C., 1970. Groundwater Resource Evaluation. McGraw-Hill.

Walton, W. C., 1984. Practical Aspects of Groundwater Modeling - 2nd Edition. Worthington, OH: National Water Well Association.

Wolery, T. J., 1983, EQ3NR, A Computer Program for Geochemical Aqueous Speciation-Solubility Calculations: User's Guide and Documentation, UCRL-53414, Lawrence Livermore National Laboratory, Livermore, California.

Wolery, T. J, 1992a, EQ3/6: A Software Package for Geochemical Modeling of Aqueous Systems: Package Overview and Installation Guide (Version 7.0), UCRL-MA-110662-PT-I (Draft), Lawrence Livermore National Laboratory, Livermore, CA.

Wolery, T. J, 1992b, EQ3NR: A Computer Program for Geochemical Aqueous Speciation-Solubility Calculations: Theoretical Manual, User's Guide, and Related Documentation (Version 7.0), UCRL-MA-110662-PT-III (Draft 1.1), Lawrence Livermore National Laboratory, Livermore, CA.

Wolery, T. J, 1992c, EQ6: A Computer Program for Reaction Pathway Modeling of Aqueous Geochemical Systems: Theoretical Manual, User's Guide, and Related Documentation (Version 7.0), UCRL-MA-110662-PT-IV (Draft 1.1), Lawrence Livermore National Laboratory, Livermore, CA.

Wolery, T. J. and S. A. Daveler, 1989, "EQ6, A Computer Program for Reaction-Path Modeling of Aqueous Geochemical Systems: User's Guide and Documentation," Draft, Distribution Category UC-70, Lawrence Livermore National Laboratory, Livermore, CA.

☆ U.S. GOVERNMENT PRINTING OFFICE: 1994-550-232/80240

LEGEND

- ELEVATION CONTOURS
- ROADS
- STREAM
- FENCE
- 1000 MONITORING WELLS
- 2000 MONITORING WELLS
- 3000 MONITORING WELLS
- 4000 MONITORING WELLS
- SOIL BORING
- HYDROPUNCH
- SURFACE SAMPLE
- TRENCH

NOTE:
Coordinates are in State Planar NAD 1927.
Surface contours based on 1992 flyover.

SCALE (FT)
0 80 160

000002

FIGURE 2-12
SURFACE AND SUBSURFACE SOIL SAMPLE LOCATIONS
SOUTH FIELD / FLYASH PILES AREA

fig0213.dgn

110707_1

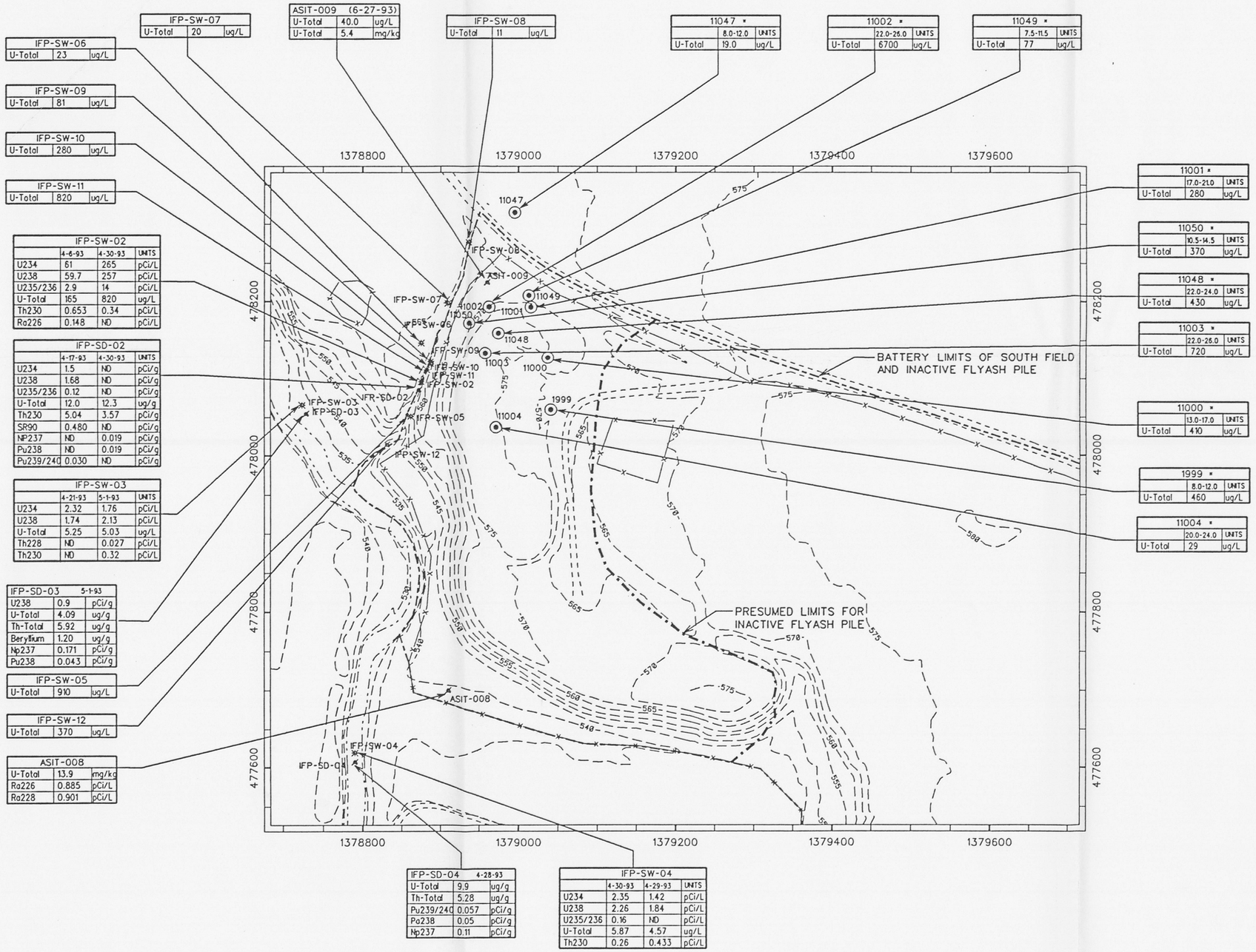

LEGEND

- ELEVATION CONTOURS
- ROADS
- STREAM
- DRAINAGE
- FENCE
- SEDIMENT SAMPLE
- SURFACE WATER SAMPLE
- HYDROPUNCH

ND = INDICATES NOT DETECTED ABOVE BACKGROUND CONCENTRATIONS.

* INDICATES RESULTS OF ON-SITE LABORATORY SCREENING FOR TOTAL URANIUM

NOTE:
Coordinates are in State Planar NAD 1927.
Surface contours based on 1992 flyover.

SCALE (FT)
0 50 100 200

FIGURE 4-16 000011
RADIONUCLIDES IN SURFACE WATER, SEDIMENT, AND SELECTED HYDROPUNCH SAMPLES DETECTED ABOVE BACKGROUND IN THE INACTIVE FLYASH PILE

fig0492.dgn

116707_9

SF-SS-21 (03/18/93)	0.0'-0.5'	
Np237	0.056	pCi/g
U234	7.93	pCi/g
U235/236	0.458	pCi/g
U238	9.32	pCi/g
U-Total	24.5	ug/g
Ra226	3.24	pCi/g
Ra228	1.29	pCi/g
Beryllium	1	mg/kg

SF-SS-19 (03/22/93)	0.0'-0.5'	
Np237	0.11	pCi/g
Pu238	0.06	pCi/g
U234	4.26	pCi/g
U235/236	0.166	pCi/g
U238	5.46	pCi/g
U-Total	16.3	ug/g
Th230	2.33	pCi/g
Ra226	1.43	pCi/g
Ra228	1.16	pCi/g

1046 (02/06/88)	0.0'-1.5'	
U234	1.7	pCi/g
U238	2.1	pCi/g
Th228	1.1	pCi/g
Th230	1.3	pCi/g
Ra226	1.3	pCi/g
Ra228	1.3	pCi/g

SF-SS-17 (03/18/93)	0.0'-0.5'	
U234	4.94	pCi/g
U235/236	0.258	pCi/g
U238	5.99	pCi/g
U-Total	28.4	ug/g
Ra226	1.92	pCi/g
Ra228	1.31	pCi/g
Beryllium	1.9	mg/kg
Chromium	21.5	mg/kg

1972 (03/19/93)	0.0'-0.5'	
Pu238	0.341	pCi/g
U234	6.18	pCi/g
U235/236	0.299	pCi/g
U238	6.88	pCi/g
U-Total	28.3	ug/g
Ra226	21.6	pCi/g
Ra228	1.17	pCi/g
Chromium	17.3	mg/kg

11186 (03/19/93)	0.0'-0.5'	
Np237	0.23	pCi/g
Pu238	0.05	pCi/g
U234	8.01	pCi/g
U235/236	0.346	pCi/g
U238	9.06	pCi/g
U-Total	36.0	ug/g
Th228	1.25	pCi/g
Th230	13.8	pCi/g
Th232	1.2	pCi/g
Th-Total	11.04	ug/g
Ra226	30.8	pCi/g
Ra228	1.65	pCi/g
Beryllium	0.83	mg/kg

11188 (03/22/93)	0.0'-0.5'	
U234	3.2	pCi/g
U235/236	0.226	pCi/g
U238	3.54	pCi/g
U-Total	10.4	ug/g
Th230	1.70	pCi/g
Th232	0.927	pCi/g
Ra226	1.44	pCi/g

11187 (03/19/93)	0.0'-0.5'	
U234	13.7	pCi/g
U235/236	0.771	pCi/g
U238	15.1	pCi/g
U-Total	50.6	ug/g
Th228	1.71	pCi/g
Th230	2.22	pCi/g
Th232	1.42	pCi/g
Th-Total	13.1	ug/g
Ra226	1.16	pCi/g
Ra228	1.92	pCi/g

SF-SS-20 (03/19/93)	0.0'-0.5'	
U234	11.56	pCi/g
U235/236	0.47	pCi/g
U238	11.68	pCi/g
U-Total	36.4	ug/g
Ra226	1.06	pCi/g
Ra228	1.26	pCi/g

SF-SS-18 (03/18/93)	0.0'-0.5'	
Pu238	0.125	pCi/g
U234	2.73	pCi/g
U235/236	0.149	pCi/g
U238	2.87	pCi/g
U-Total	17.2	ug/g
Th230	1.53	pCi/g
Ra226	1.04	pCi/g
Ra228	0.917	pCi/g

1977 (03/19/93)	0.0'-0.5'	
Np237	0.34	pCi/g
Pu238	0.035	pCi/g
U234	3.32	pCi/g
U235/236	0.17	pCi/g
U238	4.15	pCi/g
U-Total	19.0	ug/g
Th228	1.06	pCi/g
Th230	1.92	pCi/g
Ra226	1.12	pCi/g
Ra228	1.18	pCi/g
Beryllium	0.63	mg/kg

SF-SS-16 (03/22/93)	0.0'-0.5'	
Np237	0.09	pCi/g
U234	6.44	pCi/g
U235/236	0.285	pCi/g
U238	6.53	pCi/g
U-Total	1.86	ug/g
Th228	1.08	pCi/g
Th230	2.06	pCi/g
Ra226	1.33	pCi/g
Ra228	1.2	pCi/g
Beryllium	0.84	mg/kg

1970 (03/22/93)	0.0'-0.5'	
U234	7.44	pCi/g
U235/236	0.315	pCi/g
U238	7.72	pCi/g
U-Total	27.4	ug/g
Th228	1.03	pCi/g
Th230	2.21	pCi/g
Ra226	1.14	pCi/g
Ra228	1.05	pCi/g
Beryllium	0.68	mg/kg

1964 (03/22/93)	0.0'-0.5'	
Np237	0.18	pCi/g
Pu238	0.019	pCi/g
U234	3.43	pCi/g
U235/236	0.157	pCi/g
U238	3.47	pCi/g
U-Total	10.5	ug/g
Th228	0.911	pCi/g
Th230	1.35	pCi/g
Ra226	1.22	pCi/g
Ra228	1.07	pCi/g
Beryllium	0.86	mg/kg

1975 (03/22/93)	0.0'-0.5'	
Np237	0.11	pCi/g
Pu238	0.019	pCi/g
U234	6.62	pCi/g
U235/236	0.35	pCi/g
U238	6.92	pCi/g
U-Total	23.8	ug/g
Th228	0.980	pCi/g
Th230	3.52	pCi/g
Tc99	14.2	pCi/g
Beryllium	0.61	mg/kg

1971 (03/22/93)	0.0'-0.5'	
U234	6.04	pCi/g
U235/236	0.344	pCi/g
U238	6.48	pCi/g
U-Total	25.5	ug/g
Beryllium	0.75	mg/kg

1969 (03/22/93)	0.0'-0.5'	
Np237	0.136	pCi/g
Pu238	0.044	pCi/g
U234	3.58	pCi/g
U235/236	0.197	pCi/g
U238	3.79	pCi/g
U-Total	16.7	ug/g
Beryllium	1.5	mg/kg

1978 (03/22/93)	0.0'-0.5'	
Np237	0.18	pCi/g
Pu238	0.058	pCi/g
U234	4.98	pCi/g
U235/236	0.21	pCi/g
U238	5.35	pCi/g
U-Total	18.8	ug/g
Th228	1.02	ug/g
Th230	1.81	ug/g
Ra226	1.22	pCi/g
Beryllium	0.86	mg/kg

1967 (03/22/93)	0.0'-0.5'	
Pu238	0.13	pCi/g
U234	4.46	pCi/g
U235/236	0.198	pCi/g
U238	4.41	pCi/g
U-Total	12.5	ug/g
Ra226	0.95	pCi/g
Ra228	1.05	pCi/g
Beryllium	0.71	mg/kg

1965 (03/22/93)	0.0'-0.5'	
Np237	0.48	pCi/g
Pu238	0.019	pCi/g
U234	16.3	pCi/g
U235/236	0.887	pCi/g
U238	16.6	pCi/g
U-Total	49.0	ug/g
Ra226	1.8	pCi/g
Ra228	1.21	pCi/g
Beryllium	0.98	mg/kg

1966 (03/22/93)	0.0'-0.5'	
Np237	0.214	pCi/g
Pu238	0.116	pCi/g
U234	10.0	pCi/g
U235/236	0.515	pCi/g
U238	11.3	pCi/g
U-Total	38.1	ug/g
Th228	4.41	pCi/g
Th230	12.1	pCi/g
Th232	3.99	pCi/g
Th-Total	36.7	ug/g
Ra226	1.74	pCi/g
Ra228	3.88	pCi/g
Beryllium	0.91	mg/kg

1516 (05/19/90)	0.0'-0.5'	
U234	4.64	pCi/g
U235/236	0.6	pCi/g
U238	7.0	pCi/g
Th228	1.01	pCi/g
Th230	5.59	pCi/g
Th232	1.11	pCi/g
Th-Total	10.0	ug/g
Tc99	0.9	pCi/g

1518 (05/20/90)	0.0'-0.5'	
U234	1.20	pCi/g
U235/236	0.6	pCi/g
U238	1.24	pCi/g
U-Total	6.2	ug/g
Th228	1.23	pCi/g
Th230	1.63	pCi/g
Tc99	0.9	pCi/g

1517 (05/20/90)	0.0'-0.5'	
U234	1.09	pCi/g
U235/236	0.6	pCi/g
U238	1.45	pCi/g
U-Total	2.95	ug/g
Tc99	0.9	pCi/g

1968 (03/22/93)	0.0'-0.5'	
Np237	0.185	pCi/g
Pu238	0.072	pCi/g
U234	9.71	pCi/g
U235/236	0.303	pCi/g
U238	9.84	pCi/g
U-Total	31.2	ug/g
Th230	1.98	pCi/g
Th232	1.07	pCi/g
Th-Total	9.84	ug/g

LEGEND

- 575 ELEVATION CONTOURS
- ROADS
- STREAM
- DRAINAGE
- FENCE
- 1000 MONITORING WELLS
- SOIL BORING
- SURFACE SAMPLE

NOTE:
Coordinates are in State Planar NAD 1927.
Surface contours based on 1992 flyover.

N

SCALE (FT)
0 150 300

000012

FIGURE 4-17
RADIONUCLIDES, AND METALS OF CONCERN IN SURFACE SAMPLES DETECTED ABOVE BACKGROUND IN THE SOUTH FIELD

fig0421.dgn

110707_11

SF-SS-21	(03/18/93)	
	0.0-0.5	UNITS
Acetone	7	ug/kg

SF-SS-20	(03/19/93)	
	0.0-0.5	UNITS
Acetone	9	ug/kg
Benzo(a)anthracene	46	ug/kg
Benzo(a)pyrene	79	ug/kg
Benzo(b)fluoranthene	65	ug/kg
Benzo(g,h,i)perylene	79	ug/kg
Benzo(k)fluoranthene	57	ug/kg
bis(2-Ethylhexyl) pht	71	ug/kg
Chrysene	65	ug/kg
Fluoranthene	68	ug/kg
Indeno(1,2,3-cd)pyren	45	ug/kg
Pyrene	62	ug/kg

SF-SS-18	(03/18/93)	
	0.0-0.5	UNITS
Acenaphthylene	120	ug/kg
Anthracene	110	ug/kg
Aroclor-1260	38	ug/kg
Benzo(a)anthracene	530	ug/kg
Benzo(a)pyrene	750	ug/kg
Benzo(b)fluoranthene	700	ug/kg
Benzo(g,h,i)perylene	560	ug/kg
Benzo(k)fluoranthene	670	ug/kg
bis(2-Ethylhexyl) pht	72	ug/kg
Carbazole	48	ug/kg
Chrysene	670	ug/kg
Dibenzo(a,h)anthracen	180	ug/kg
Fluoranthene	1100	ug/kg
Indeno(1,2,3-cd)pyren	520	ug/kg
Phenanthrene	400	ug/kg
Pyrene	850	ug/kg

1977	(03/19/93)	
	0.0-0.5	UNITS
Acenaphthylene	130	ug/kg
Anthracene	130	ug/kg
Aroclor-1254	89	ug/kg
Benzo(a)anthracene	630	ug/kg
Benzo(a)pyrene	800	ug/kg
Benzo(b)fluoranthene	670	ug/kg
Benzo(g,h,i)perylene	650	ug/kg
Benzo(k)fluoranthene	710	ug/kg
bis(2-Ethylhexyl) pht	66	ug/kg
Carbazole	67	ug/kg
Chrysene	750	ug/kg
Dibenzo(a,h)anthracen	230	ug/kg
Fluoranthene	1000	ug/kg
Indeno(1,2,3-cd)pyren	620	ug/kg
Phenanthrene	380	ug/kg
Pyrene	930	ug/kg

1970	(03/22/93)	
	0.0-0.5	UNITS
Acetone	68	ug/kg
Benzoic acid	63	ug/kg
Benzo(a)anthracene	58	ug/kg
Benzo(a)pyrene	67	ug/kg
Benzo(b)fluoranthene	74	ug/kg
Benzo(g,h,i)perylene	51	ug/kg
Benzo(k)fluoranthene	69	ug/kg
bis(2-Ethylhexyl) pht	91	ug/kg
Chrysene	83	ug/kg
Fluoranthene	130	ug/kg
Indeno(1,2,3-cd)pyren	52	ug/kg
Phenanthrene	48	ug/kg
Pyrene	100	ug/kg

1964	(03/22/93)	
	0.0-0.5	UNITS
Benzoic acid	270	ug/kg
bis(2-Ethylhexyl) pht	91	ug/kg
Fluoranthene	45	ug/kg

SF-SS-19	(03/22/93)	
	0.0-0.5	UNITS
Aroclor-1260	52	ug/kg
Benzoic acid	72	ug/kg
Benzo(a)anthracene	54	ug/kg
Benzo(a)pyrene	59	ug/kg
Benzo(b)fluoranthene	66	ug/kg
Benzo(g,h,i)perylene	62	ug/kg
Benzo(k)fluoranthene	71	ug/kg
bis(2-Ethylhexyl) pht	83	ug/kg
Chrysene	77	ug/kg
Fluoranthene	87	ug/kg
Indeno(1,2,3-cd)pyren	51	ug/kg
Pyrene	80	ug/kg

1972	(03/19/93)	
	0.0-0.5	UNITS
Acenaphthylene	1200	ug/kg
Anthracene	730	ug/kg
Benzo(a)anthracene	5500	ug/kg
Benzo(a)pyrene	9400	ug/kg
Benzo(b)fluoranthene	6200	ug/kg
Benzo(g,h,i)perylene	6200	ug/kg
Benzo(k)fluoranthene	7300	ug/kg
Chrysene	6000	ug/kg
Dibenzo(a,h)anthracen	1900	ug/kg
Dieldrin	9.7	ug/kg
Fluoranthene	9200	ug/kg
Indeno(1,2,3-cd)pyren	6000	ug/kg
Phenanthrene	1200	ug/kg
Pyrene	8200	ug/kg

11186	(03/19/93)	
	0.0-0.5	UNITS
Anthracene	87	ug/kg
Benzo(a)anthracene	250	ug/kg
Benzo(a)pyrene	270	ug/kg
Benzo(g,h,i)perylene	150	ug/kg
Benzo(k)fluoranthene	240	ug/kg
bis(2-Ethylhexyl) pht	91	ug/kg
Chrysene	310	ug/kg
Dibenzo(a,h)anthracen	66	ug/kg
Fluoranthene	640	ug/kg
Indeno(1,2,3-cd)pyren	150	ug/kg
Phenanthrene	410	ug/kg
Pyrene	480	ug/kg

11187	(03/19/93)	
	0.0-0.5	UNITS
Benzo(a)pyrene	51	ug/kg
Benzo(b)fluoranthene	46	ug/kg
Benzo(g,h,i)perylene	53	ug/kg
Benzo(k)fluoranthene	49	ug/kg
bis(2-Ethylhexyl) pht	65	ug/kg
Chrysene	60	ug/kg
Dimethyl phthalate	62	ug/kg
Fluoranthene	73	ug/kg
Pyrene	11	ug/kg

1975	(03/22/93)	
	0.0-0.5	UNITS
Acetone	19	ug/kg
bis(2-Ethylhexyl) pht	64	ug/kg
Fluoranthene	48	ug/kg

SF-SS-17	(03/22/93)	
	0.0-0.5	UNITS
Acenaphthene	140	ug/kg
Acenaphthylene	590	ug/kg
Anthracene	560	ug/kg
Benzoic acid	52	ug/kg
Benzo(a)anthracene	2500	ug/kg
Benzo(a)pyrene	4700	ug/kg
Benzo(b)fluoranthene	3900	ug/kg
Benzo(g,h,i)perylene	3100	ug/kg
Benzo(k)fluoranthene	3300	ug/kg
bis(2-Ethylhexyl) pht	100	ug/kg
Carbazole	170	ug/kg
Chrysene	3200	ug/kg
Dibenzofuran	130	ug/kg
Dibenzo(a,h)anthracen	1100	ug/kg
Fluoranthene	4300	ug/kg
Fluorene	220	ug/kg
Indeno(1,2,3-cd)pyren	3000	ug/kg
Phenanthrene	2300	ug/kg
Pyrene	3500	ug/kg

11188	(03/22/93)	
	0.0-0.5	UNITS
Acenaphthylene	55	ug/kg
Benzoic acid	56	ug/kg
Benzo(a)anthracene	180	ug/kg
Benzo(a)pyrene	280	ug/kg
Benzo(b)fluoranthene	240	ug/kg
Benzo(g,h,i)perylene	210	ug/kg
Benzo(k)fluoranthene	290	ug/kg
bis(2-Ethylhexyl) pht	80	ug/kg
Chrysene	240	ug/kg
Dibenzo(a,h)anthracen	69	ug/kg
Endrin ketone	5.9	ug/kg
Fluoranthene	320	ug/kg
Indeno(1,2,3-cd)pyren	210	ug/kg
Phenanthrene	81	ug/kg
Pyrene	270	ug/kg

1969	(03/22/93)	
	0.0-0.5	UNITS
Benzoic acid	62	ug/kg
Benzo(g,h,i)perylene	160	ug/kg
bis(2-Ethylhexyl) pht	89	ug/kg
Fluoranthene	53	ug/kg

1971	(03/22/93)	
	0.0-0.5	UNITS
Benzo(a)anthracene	44	ug/kg
Benzo(k)fluoranthene	52	ug/kg
bis(2-Ethylhexyl) pht	80	ug/kg
Chrysene	63	ug/kg
Fluoranthene	120	ug/kg
Phenanthrene	67	ug/kg
Pyrene	93	ug/kg

1967	(03/22/93)	
	0.0-0.5	UNITS
Benzoic acid	72	ug/kg
bis(2-Ethylhexyl) pht	73	ug/kg

1965	(03/22/93)	
	0.0-0.5	UNITS
Benzoic acid	95	ug/kg
bis(2-Ethylhexyl) pht	110	ug/kg

1966	(03/22/93)	
	0.0-0.5	UNITS
bis(2-Ethylhexyl) pht	91	ug/kg

SF-SS-16	(05/22/93)	
	0.0-0.5	UNITS
Anthracene	59	ug/kg
Benzoic acid	78	ug/kg
Benzo(a)anthracene	160	ug/kg
Benzo(a)pyrene	170	ug/kg
Benzo(b)fluoranthene	160	ug/kg
Benzo(g,h,i)perylene	100	ug/kg
Benzo(k)fluoranthene	180	ug/kg
bis(2-Ethylhexyl) pht	95	ug/kg
Chrysene	200	ug/kg
Dibenzo(a,h)anthracen	43	ug/kg
Fluoranthene	340	ug/kg
Indeno(1,2,3-cd)pyren	110	ug/kg
Phenanthrene	200	ug/kg
Pyrene	270	ug/kg

1978	(03/22/93)	
	0.0-0.5	UNITS
bis(2-Ethylhexyl) pht	82	ug/kg

1968	(03/22/93)	
	0.0-0.5	UNITS
Acetone	19	ug/kg
Benzoic acid	60	ug/kg
Benzo(a)anthracene	51	ug/kg
Benzo(a)pyrene	55	ug/kg
Benzo(b)fluoranthene	62	ug/kg
Benzo(k)fluoranthene	53	ug/kg
bis(2-Ethylhexyl) pht	87	ug/kg
Chrysene	70	ug/kg
Fluoranthene	110	ug/kg
Pyrene	86	ug/kg

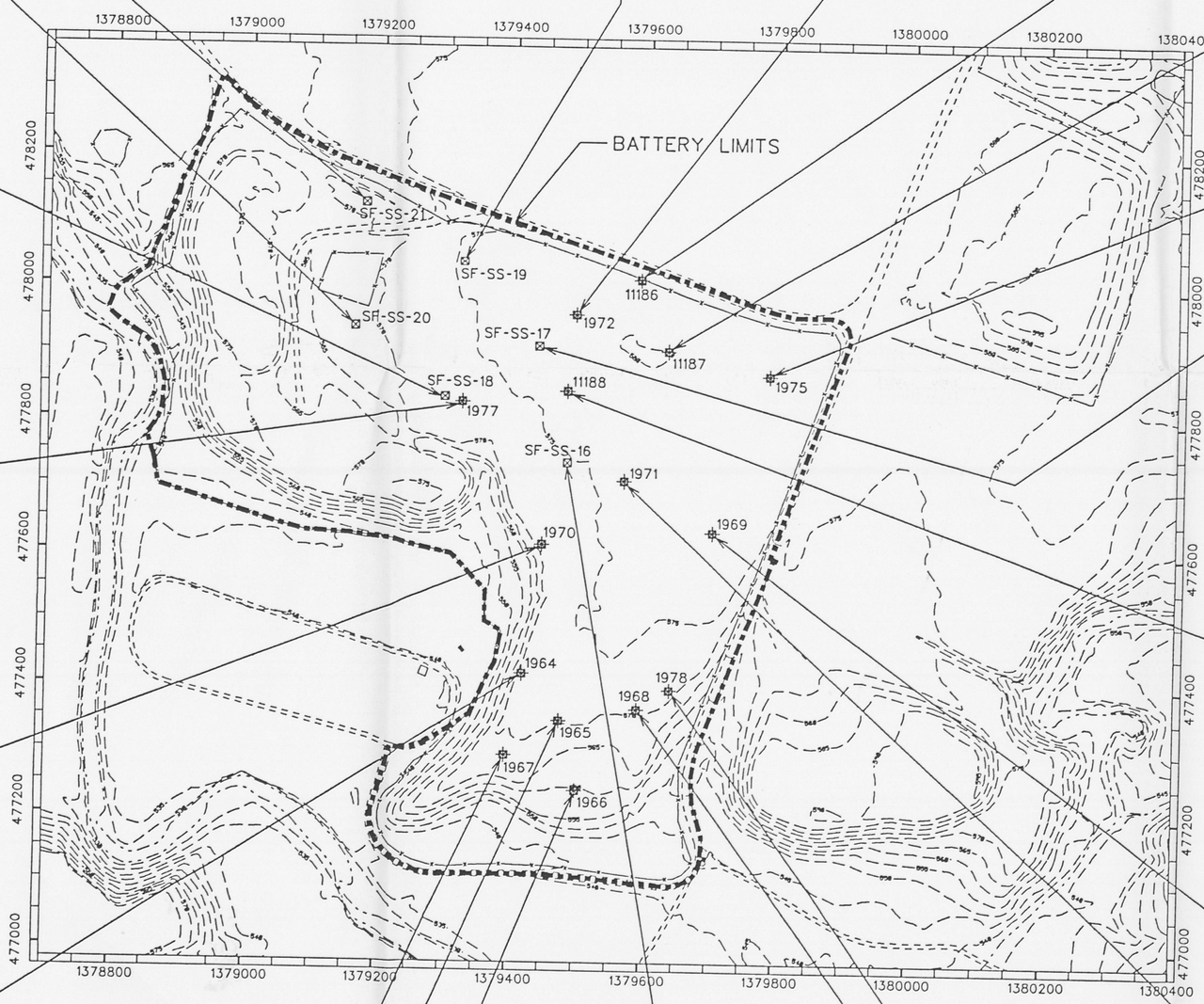

LEGEND

- ELEVATION CONTOURS
- ROADS
- STREAM
- DRAINAGE
- FENCE
- SOIL BORING
- SURFACE SAMPLE

NOTE:
Coordinates are in State Planar NAD 1927.
Surface contours based on 1992 flyover.

SCALE (FT)
0 150 300

000013

FIGURE 4-18
ORGANICS IN
SURFACE SOIL SAMPLES
DETECTED ABOVE BACKGROUND
SOUTH FIELD

fig0442.dgn

110701_12

1794	08/13/91		
	1-1.5 ft	2-2.5 ft	UNITS
Acetone	5	10	ug/kg
Benzo(a)anthracene	100	78	ug/kg
Benzo(a)pyrene	46	ND	ug/kg
Benzo(b)fluoranthene	140	88	ug/kg
Benzo(a)perylene	45	ND	ug/kg
Benzoic acid	66	ND	ug/kg
Chrysene	82	70	ug/kg
Fluoranthene	170	150	ug/kg
Octachlorodibenzo-p-dioxin	0.6	1.5	ug/kg
Phenanthrene	96	93	ug/kg
Pyrene	170	140	ug/kg

SF-SS-19	03/22/93	
	0.5-1 ft	UNITS
Aroclor-1260	89	ug/kg
Benzo(a)anthracene	97	ug/kg
Benzo(a)pyrene	110	ug/kg
Benzo(b)fluoranthene	110	ug/kg
Benzo(g,h,i)perylene	79	ug/kg
Benzo(k)fluoranthene	110	ug/kg
Fluoranthene	210	ug/kg
Indeno(1,2,3-cd)pyrene	77	ug/kg
Phenanthrene	80	ug/kg
Pyrene	170	ug/kg
bis(2-Ethylhexyl)phthalate	88	ug/kg

1456	11/05/89	
	3.75 ft	UNITS
Aroclor-1254	130	ug/kg
Chloroform	3	ug/kg
Fluoranthene	39	ug/kg
Pyrene	43	ug/kg

11188	11/02/93		
	5-6 ft	10-10 ft	UNITS
Acetone	4	45	ug/kg
Toluene	41	8	ug/kg
2-Butanone	ND	6	ug/kg

1046	02/08/88	
	15-16.5 ft	UNITS
Acetone	8	ug/l
Chloroform	3	ug/l
Methylene chloride	2	ug/l

1972	03/19/93			
	0.5-1 ft	2.5-4 ft	7.5-9 ft	UNITS
Acenaphthylene	410	ND	ND	ug/kg
Acetone	ND	6	ND	ug/kg
Anthracene	250	ND	ND	ug/kg
Aroclor-1254	85	ND	ND	ug/kg
Benzo(a)anthracene	1100	ND	ND	ug/kg
Benzo(a)pyrene	1800	ND	ND	ug/kg
Benzo(b)fluoranthene	1600	ND	ND	ug/kg
Benzo(g,h,i)perylene	1200	ND	ND	ug/kg
Benzo(k)fluoranthene	1600	ND	ND	ug/kg
Carbazole	51	ND	ND	ug/kg
Chrysene	1400	ND	ND	ug/kg
Dibenzo(a,h)anthracene	440	ND	ND	ug/kg
Fluoranthene	1800	ND	ND	ug/kg
Indeno(1,2,3-cd)pyrene	210	ND	ND	ug/kg
Phenanthrene	350	ND	ND	ug/kg
Pyrene	1400	ND	ND	ug/kg
bis(2-Ethylhexyl) phthalate	87	ND	ND	ug/kg
Toluene	ND	11	3	ug/kg

1795	08/23/91		
	1-1.5 ft	3-4 ft	UNITS
Acetone	5	5	ug/kg
Anthracene	58	ND	ug/kg
Benzo(a)anthracene	270	ND	ug/kg
Benzo(a)pyrene	120	ND	ug/kg
Benzo(b)fluoranthene	360	ND	ug/kg
Benzo(g,h,i)perylene	100	ND	ug/kg
Chrysene	300	ND	ug/kg
Fluoranthene	610	ND	ug/kg
Indeno(1,2,3-cd)pyrene	84	ND	ug/kg
Octachlorodibenzo-p-dioxin	2.9	3.6	ug/kg
Phenanthrene	370	ND	ug/kg
Pyrene	500	ND	ug/kg

11187	03/24/93	04/13/93	
	0.5-1 ft	4-6 ft	UNITS
Aroclor-1254	58	86	ug/kg
Benzo(a)pyrene	41	ND	ug/kg
Benzo(k)fluoranthene	48	ND	ug/kg
Fluoranthene	83	110	ug/kg
bis(2-Ethylhexyl) phthalate	55	ND	ug/kg

TRENCH 1	06/03/93	
	7.0 ft	UNITS
Anthracene	62	ug/kg
Aroclor-1254	170	ug/kg
Benzo(a)anthracene	60	ug/kg
Benzo(a)pyrene	59	ug/kg
Benzo(b)fluoranthene	58	ug/kg
Benzo(g,h,i)perylene	52	ug/kg
Benzo(k)fluoranthene	58	ug/kg
Di-n-buthylphthalate	49	ug/kg
Fluoranthene	140	ug/kg
Indeno(1,2,3-cd)pyrene	42	ug/kg
Phenanthrene	62	ug/kg
Pyrene	110	ug/kg
Tributylphosphate	170	ug/kg
bis(2-Ethyhexyl) phthalate	340	ug/kg

11186	04/24/93	
	0.5-1 ft	UNITS
Aroclor-1254	82	ug/kg
Benzo(a)anthracene	57	ug/kg
Benzo(a)pyrene	51	ug/kg
Benzo(k)fluoranthene	57	ug/kg
Fluoranthene	130	ug/kg
Phenanthrene	61	ug/kg
Pyrene	120	ug/kg

1459	11/06/89	
	5 ft	UNITS
Aroclor-1254	1100	ug/kg
Benzo(a)anthracene	170	ug/kg
Benzo(a)pyrene	230	ug/kg
Benzo(b)fluoranthene	290	ug/kg
Chrysene	170	ug/kg
Fluoranthene	300	ug/kg
Phenanthrene	110	ug/kg
Pyrene	270	ug/kg

1975	03/22/93		
	0.5-1 ft	4-5 ft	UNITS
Aroclor-1254	140	41	ug/kg
bis(2-Ethylhexy) phthalate	51	71	ug/kg

1977	04/06/93		
	8.5-10 ft	16.5-18.5 ft	UNITS
Acetone	8	14	ug/kg
2-Butanone	ND	2	ug/kg
Toluene	2	31	ug/kg

1462	11/07/89	
	4 ft	UNITS
Aroclor-1254	690	ug/kg
Benzo(a)anthracene	130	ug/kg
Benzo(b)fluoranthene	140	ug/kg
Chloroform	7	ug/kg
Chrysene	150	ug/kg
Fluoranthene	300	ug/kg
Methylene chloride	6	ug/kg
Phenanthrene	240	ug/kg
Pyrene	400	ug/kg

TRENCH 4	06/03/93	
	3.5 ft	UNITS
Aroclor-1254	430	ug/kg

1465	11/08/89	
	3.5 ft	UNITS
Pyrene	44	ug/kg

1971	03/22/93		
	0.5-1 ft	9.5-11 ft	UNITS
Acetone	ND	3	ug/kg
bis(2-Ethylhexyl) phthalate	100	ND	ug/kg
Toluene	ND	3	ug/kg

1970	04/18/93		
	4-5.5 ft	9-10.5 ft	UNITS
Benzoic acid	46	ND	ug/kg
bis(2-Ethylhexyl) phthalate	56	5	ug/kg
Toluene	1	ND	ug/kg

1468	11/14/89	
	2.5 ft	UNITS
Methylene chloride	2	ug/kg
bis(2-Ethyhexyl) phthalate	40	ug/kg

1793	08/15/91	
	3-4.5 ft	UNITS
Aroclor-1254	740	ug/kg
Benzoic acid	150	ug/kg
octanchlorodibenzo-p-dioxin	0.65	ng/g

1969	03/22/93		
	0.5-1 ft	9-10.5 ft	UNITS
Aroclor-1254	54	ND	ug/kg
Benzoic acid	57	ND	ug/kg
bis(2-Ethylhexyl) phthalate	110	ND	ug/kg
Toluene	ND	17	ug/kg

1964	04/17/93		
	5-6.5 ft	29-30.5 ft	UNITS
2-Butanone	3	1	ug/kg
Toluene	ND	20	ug/kg
bis(2-Ethylhexyl) phthalate	ND	68	ug/kg

1471	11/16/89	
	4 ft	UNITS
Methylene chloride	57	ug/kg

1965	04/20/93		
	4-6 ft	26.5-28 ft	UNITS
Aroclor-1254	43	ND	ug/kg
Toluene	3	1	ug/kg
bis(2-Ethylhexy) phthalate	44	ND	ug/kg

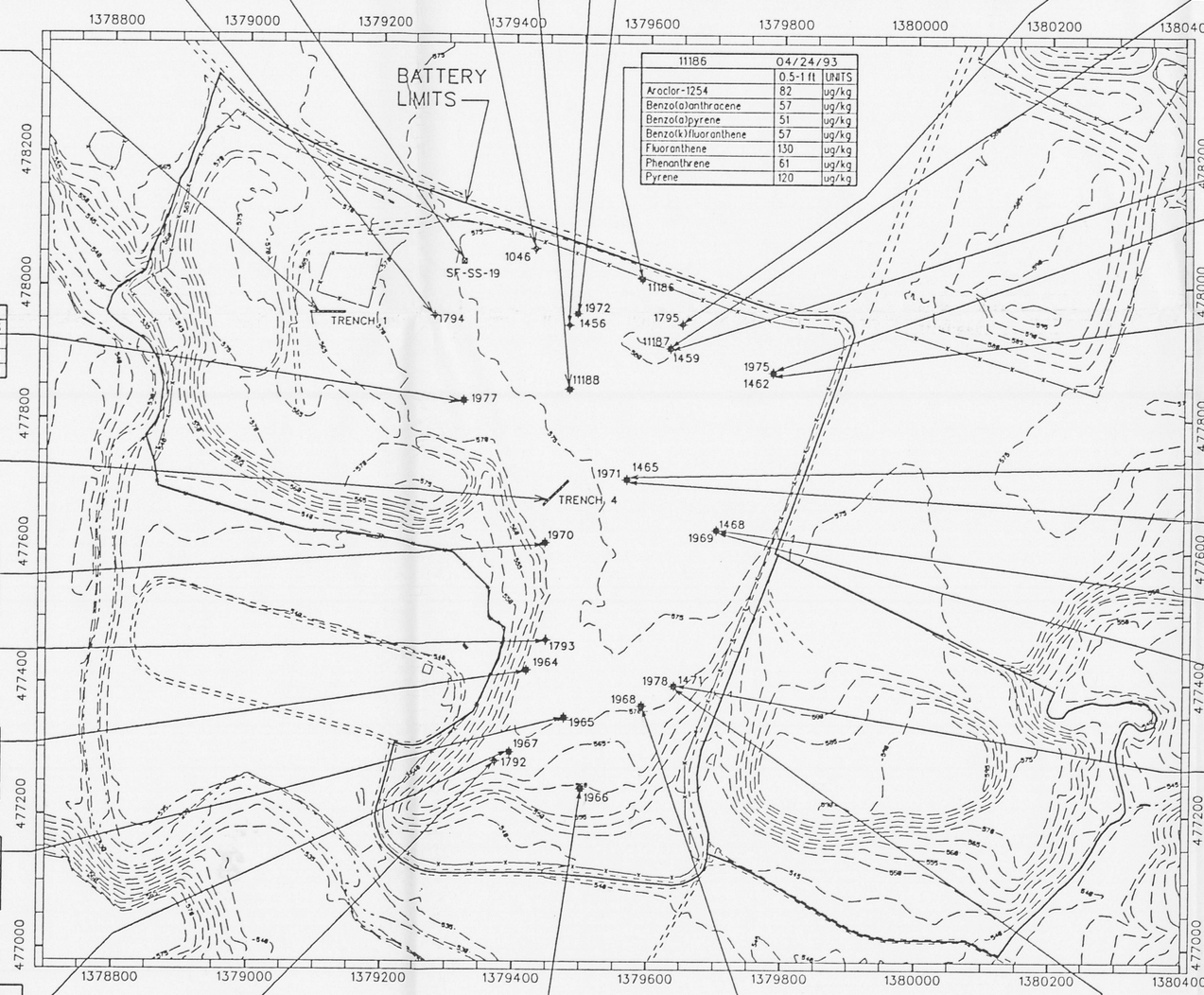

1967	04/18/93			
	0.5-1 ft	4.5-7.5 ft	29.5-31 ft	UNITS
Benzoic acid	45	ND	ND	ug/kg
bis(2-Ethylhexy) phthalate	96	49	ND	ug/kg
Aroclor-1254	ND	85	ND	ug/kg
Toluene	ND	39	2	ug/kg

1966	03/24/93		
	0.5-1 ft	4.5-6.5 ft	UNITS
2-Methylnaphthalene	91	ND	ug/kg
Chrysene	53	ND	ug/kg
Naphthalene	61	ND	ug/kg
Phenanthrene	85	ND	ug/kg
Pyrene	44	ND	ug/kg
Tokuenen	ND	11	ug/kg

1968	03/22/93			
	0.0-1 ft	4.5-6.5 ft	15.5-16.5 ft	UNITS
Benzo(a)anthracene	44	ND	ND	ug/kg
Benzo(b)fluoranthene	42	ND	ND	ug/kg
Dieldrin	16	ND	ND	ug/kg
Endrin ketone	5.3	ND	ND	ug/kg
Fluoranthene	96	ND	ND	ug/kg
Phenanthrene	52	ND	ND	ug/kg
Pyrene	76	ND	ND	ug/kg
alpha-Chlordane	8	ND	ND	ug/kg
bis(2-Ethylhexyl) phthalate	51	ND	ND	ug/kg
gamma-Chlordand	7.2	ND	ND	ug/kg
2-Butanone	ND	11	ND	ug/kg
Acetone	ND	56	3	ug/kg
Toluene	ND	4	ND	ug/kg

1978	03/24/93			
	0.5-1 ft	9.5-11 ft	13.5-15 ft	UNITS
Aroclor-1254	47	ND	ND	ug/kg
Acetone	ND	5	3	ug/kg
Benzo(a)pyrene	3	ND	ND	ug/kg
Benzo(g,h,i)perylene	ND	76	ND	ug/kg
Toluene	1	ND	ND	ug/kg
bis(2-Ethylhexyl)phthalate	46	ND	ND	ug/kg

1792	08/21/91				
	1.5-3 ft	12-13.5 ft	16.5-18 ft	21.5-23 ft	UNITS
Aroclor-1254	ND	32	ND	ND	ug/kg
Benzoic acid	ND	47	57	110	ug/kg
Fluoranthene	ND	42	ND	ND	ug/kg
Pyrene	ND	48	ND	ND	ug/kg
Tetrachlorodibenzofuran	ND	0.018	ND	ND	ug/kg
2-Methylnaphthalene	ND	56	ND	ND	ug/kg
Aroclor-1254	ND	100	ND	ND	ug/kg
Di-n-octylphthalate	ND	210	ND	ND	ug/kg
Octachlorodibenzo-p-dioxin	0.18	0.75	1.1	0.12	ug/kg
Pyrene	ND	51	57	ND	ug/kg
Xylenes, Total	ND	2	1	ND	ug/kg
4-Methyl-2-pentanone	ND	ND	1	3	ug/kg
Acetone	ND	ND	36	56	ug/kg
Diethylphthalate	ND	ND	ND	84	ug/kg

LEGEND

- ELEVATION CONTOURS
- ROADS
- STREAM
- DRAINAGE
- FENCE
- 1000 MONITORING WELLS
- 2000 MONITORING WELLS
- SOIL BORING
- TRENCH
- SURFACE SAMPLE

ND - NOT DETECTED ABOVE BACKGROUND CONCENTRATIONS

NOTE:
Coordinates are in State Planar NAD 1927.
Surface contours based on 1992 flyover.

SCALE (FT)
0 150 300

000014

FIGURE 4-20
ORGANICS IN SUBSURFACE SAMPLES DETECTED ABOVE BACKGROUND IN THE SOUTH FIELD

fig0443.dgn

110707_13

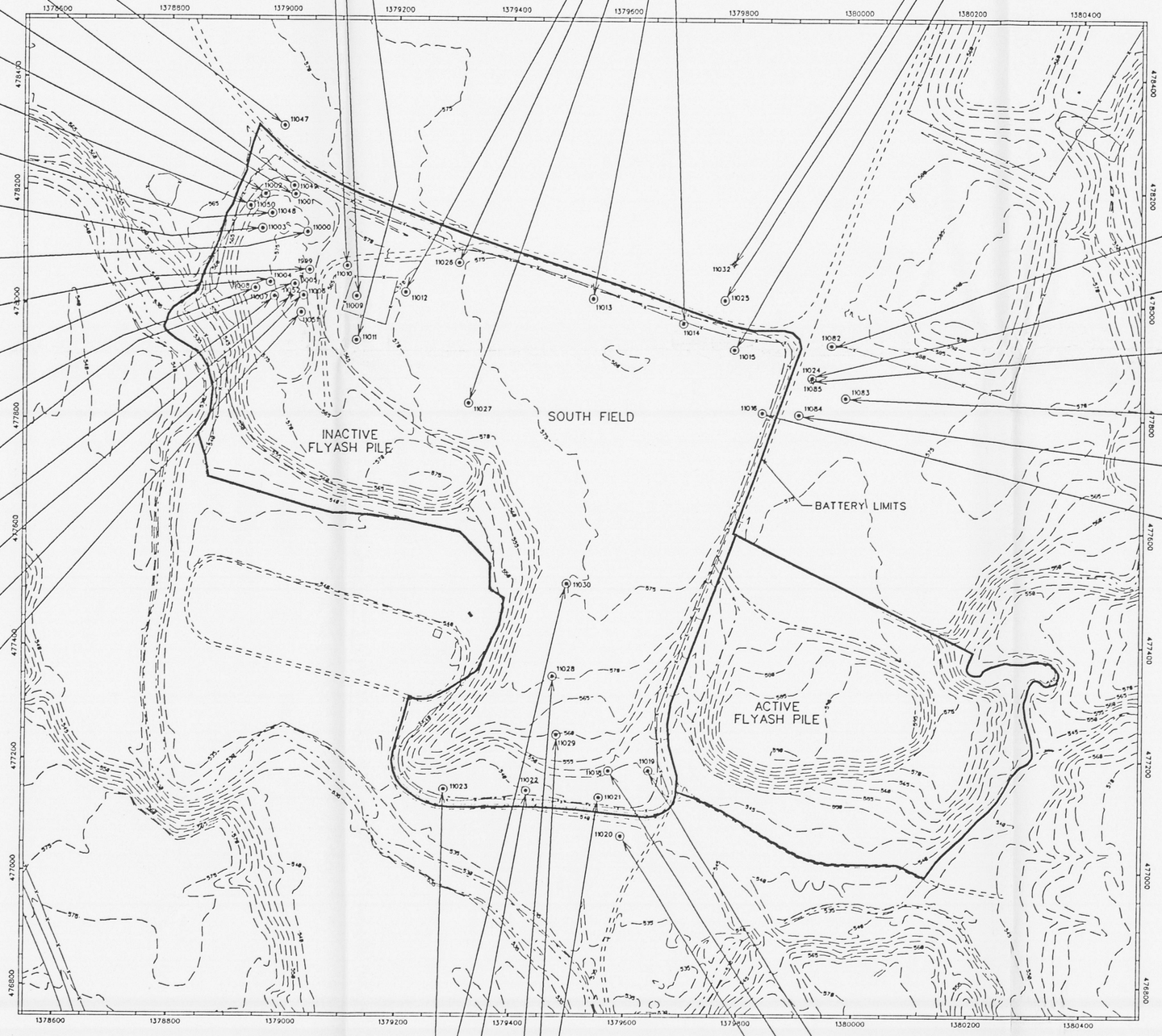

11011	(04/08/93)	(04/08/93)	
	10.5'-11.0'	18.0'-18.5'	
U-Total Soil	165	26	ug/kg

11009	(04/06/93)		
	9.0'-14.0'	3.5'-4.0'	
U-Total Water	110	NC	ug/L
U-Total Soil	NC	69	ug/kg

11010	(04/05/93)	
	9.0'-13.0'	
U-Total Water	14	ug/L

11027	(05/14/93)	
	12.0'-16.0'	
U-Total Water	87	ug/L

11026	(05/15/93)	
	10.0'-14.5'	
U-Total Water	7.8	ug/L

11012	(04/08/93)	
	10.0'-14.0'	
U-Total Water	360	ug/L

11013	(04/17/93)	
	5.5'-9.5'	
U-Total Water	22	ug/L

11014	(03/30/93)	(04/06/93)	
	5.0'-9.0'	1.0'-1.5'	
U-Total Water	580	NC	ug/L
U-Total Soil	NC	14	ug/kg

11032	(06/24/93)	
	8.0'-12.0'	
U-Total Water	17	ug/L

11025	(05/15/93)	
	6.5'-10.5'	
U-Total Water	32	ug/L

11015	(03/25/93)	
	8.0'	
U-Total Water	270	ug/L

11047	(05/16/93)	
	8.0'	
U-Total Water	19	ug/L

11049	(05/27/93)	
	11.5'-12.5'	
U-Total Water	77	ug/L

11001	(04/13/93)	
	21.5'-22.0'	
U-Total Water	280	ug/L

11002	(05/05/93)	
	16.5'	
U-Total Water	6700	ug/L

11050	(06/27/93)	
	16.0'-18.0'	
U-Total Water	370	ug/L

11048	(05/25/93)	
	21.0'-22.0'	
U-Total Water	430	ug/L

11003	(04/17/93)	
	25.5'-26.0'	
U-Total Water	720	ug/L
U-Total Soil	378	ug/kg

11000	(04/15/93)	
	16.5'-18.0'	
U-Total Water	410	ug/L

1999	(04/19/93)	
	12.0'-13.0'	
U-Total Water	460	ug/L

11004	(04/18/93)	
	24.0'-25.0'	
U-Total Water	29	ug/L

11008	(05/02/93)
	21.0'-21.5'
	DRY

11005	(04/29/93)	
	10.5'-11.0'	
U-Total Soil	165	ug/kg

11007	(04/21/93)	
	22.5'-23.0'	
U-Total Water	9.5	ug/L

11052	(05/25/93)	
	19.0'-21.0'	
U-Total Soil	1000	ug/kg

11006	(04/26/93)	
	22.5'-24'	
U-Total Soil	3300	ug/kg

11051		(05/27/93)	
	21.0'-22.0'	22.0'-24.0'	
U-Total Water	720	74	ug/L
U-Total Soil	1010	1470	ug/kg

11082	(06/03/93)	
	9.0'-13.0'	
U-Total Water	26	ug/L

11024	(05/15/93)	
	6.5'-10.5'	
U-Total Water	540	ug/L

MONITORING WELL SAMPLE		
11085	(06/16/93)	
	NA	
U-Total Water	5000*	ug/L

11083	(06/02/93)	
	9.0'-13.0'	
U-Total Water	<2	ug/L

11084	(06/01/93)	
	10.5'-14.5'	
U-Total Water	19	ug/L

11016	(04/18/93)	
	5.5'-9.5'	
U-Total Water	20	ug/L

11023	(05/14/93)	
	21.0'-25.0'	
U-Total Water	12	ug/L

11030	(06/01/93)	
	62.0'-67.0'	
U-Total Water	54	ug/L

11022	(05/13/93)	
	21.0'-25.0'	
U-Total Water	4.2	ug/L

11021	(05/13/93)	
	21.0'-25.0'	
U-Total Water	120	ug/L

11029	(05/06/93)	
	40.0'-42.0'	
U-Total Water	93	ug/L

11028	(05/25/93)	
	55.0'	
U-Total Water	210	ug/L

11019	(05/12/93)	
	21.0'-25.0'	
U-Total Water	150	ug/L

11018	(04/17/93)	
	21.0'-24.0'	
U-Total Water	700	ug/L

11020	(05/11/93)	
	19.0'-23.0'	
U-Total Water	75	ug/L

LEGEND

- ELEVATION CONTOURS
- ROADS
- STREAM
- DRAINAGE
- BATTERY LIMITS
- FENCE
- 1000 MONITORING WELLS
- HYDROPUNCH
- SOIL BORING

NC = NOT COLLECTED

* VALUE IS QUESTIONABLE SINCE IT IS ONE ORDER OF MAGNITUDE HIGHER THAN HYDROPUNCH 11024 AND TWO ORDERS HIGHER THAN THE WELL SAMPLE FOR THE SAME LOCATION (SEE FIGURE 4-23a).

NOTE:
Coordinates are in State Planar NAD 1927.
Surface contours based on 1992 flyover.

SCALE (FT)
0 150 300

FIGURE 4-23
SCREENING RESULTS FOR TOTAL URANIUM IN HYDROPUNCH SAMPLES IN THE SOUTH FIELD AND INACTIVE FLYASH PILE AREA

000015

fig0483.dgn

110707_14

2047						
	01/22/89	05/02/89	07/28/89	04/03/90	04/27/93	UNITS
U234	5.1	3.2	3.7	4.72	3.74	pci/L
U235/236	ND	ND	ND	ND	0.15	pci/L
U238	4.5	3.4	3.8	4.66	3.38	pci/L
U-Total	15	10	9	13.8	9.51	ug/L

2955	06/22/93	
		UNITS
U234	2.99	pci/L
U235/236	0.698	pci/L
U238	3.01	pci/L
U-Total	8.19	ug/L

2402			
	01/28/92	05/05/93	UNITS
U234	7.73	4.54	pci/L
U235/236	ND	0.16	pci/L
U238	9.97	5.89	pci/L
U-Total	27.3	15.2	ug/L
Np237	ND	0.30	pci/L
Pu239/240	ND	0.05	pci/L

2945			
	04/28/93	05/26/93	UNITS
Np237	0.796	0.962	pci/L
U234	662	ND	pci/L
U235/236	31.7	ND	pci/L
U238	707	ND	pci/L
U-Total	2070	1820	ug/L
Th232	0.044	ND	pCi/L

21190 (1016)		
	02/26/89	UNITS
U234	2.5	pci/L
U238	2.6	pci/L
U-Total	9	ug/L

2401	05/11/93	
		UNITS
Np237	0.841	pci/L
U234	1.59	pci/L
U238	1.44	pci/L
U-Total	5.13	ug/L

2046						
	02/02/89	05/10/85	07/28/89	04/03/90	05/11/93	UNITS
Np237	ND	ND	ND	ND	0.71	pci/L
U234	93.8	219	86.9	199	160	pci/L
U235/236	4.3	9.7	3.8	11.5	8.72	pci/L
U238	102	231	87.7	206	172	pci/L
U-Total	309	851	232	907	423	ug/L

2954	06/21/93	
		UNITS
Np237	0.698	pci/L
U234	372	pci/L
U235/236	15.7	pci/L
U238	384	pci/L
U-Total	1167	ug/L

2065								
	04/19/88	08/04/88	02/02/89	11/08/88	07/30/89	04/09/90	05/03/93	UNITS
U234	5.1	4.8	6	4.7	5.5	3.89	5.43	pci/L
U235/236	ND	ND	ND	ND	ND	ND	0.311	pci/L
U238	3.3	4.1	3.9	3.9	5.3	3.78	3.64	pci/L
U-Total	3	10	13	12	12	11.4	9.96	ug/L
Th228	ND	ND	2.3	ND	ND	ND	ND	pCi/L
Th230	1.2	ND	1.6	ND	ND	ND	ND	pci/L
Th232	ND	ND	1.4	ND	ND	ND	ND	pCi/L
Th-Total	ND	ND	13	ND	ND	ND	ND	ug/L

2385				
	05/06/90	07/10/90	02/25/93	UNITS
U234	51.4	34.8	33.7	pci/L
U235/236	1.78	1.81	1.69	pci/L
U238	51.4	36.2	37.1	pci/L
U-Total	204	108	98.7	ug/L
Th230	1.78	ND	ND	pCi/L
Th232	1.49	ND	ND	pCi/L
Th-Total	13.5	ND	ND	ug/L

2048			
	04/01/90	04/27/93	UNITS
U234	3.4	ND	pci/L
U238	3.02	ND	pci/L
U-Total	2.07	ND	ug/L

2943			
	05/05/93	05/27/93	UNITS
Np237	0.15	ND	pci/L
U234	ND	1.23	pci/L
U238	1.31	1.25	pci/L
U235/236	0.71	0.757	pci/L
U-Total	2.93	3.2	ug/L
Th230	2.06	ND	ug/L

21033	06/17/93	
		UNITS
U234	13.1	pci/L
U235/236	0.673	pci/L
U238	16.1	pci/L
U-Total	43.2	ug/L
Ra226	0.502	pci/L

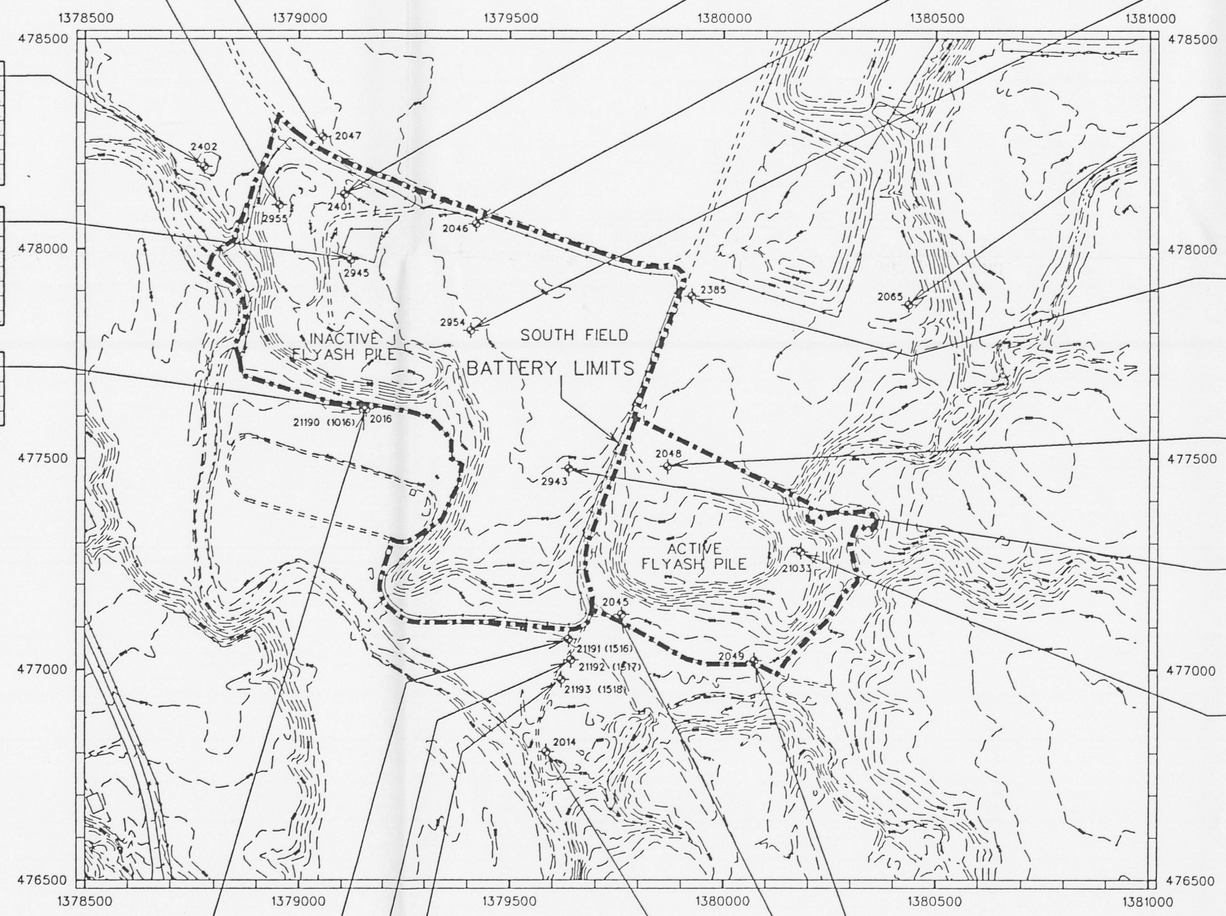

LEGEND

- ELEVATION CONTOURS
- ROADS
- STREAM
- DRAINAGE
- FENCE
- 2000 MONITORING WELLS

ND = NOT DETECTED ABOVE BACKGROUND CONCENTRATIONS

2016								
	03/28/88	08/03/88	11/04/88	02/07/89	07/26/89	03/04/90	04/30/93	UNITS
U234	7.7	5.3	4.6	6.6	5.1	4.28	6.02	pci/L
U235/236	ND	ND	ND	ND	ND	ND	.046	pci/L
U238	6.2	6.4	ND	8	5.8	5.03	6.5	pci/L
U-Total	ND	18	17	22	17	29.4	17.1	ug/L
Np237	ND	ND	ND	ND	ND	ND	0.710	pci/L
Pu238	ND	ND	ND	ND	NDF	ND	0.160	pci/L

21193 (1518)			
	07/17/90	08/21/90	UNITS
U-Total	139	64	ug/L

21192 (1517)			
	07/17/90	08/21/90	UNITS
U-Total	966	29.9	ug/L
Th-Total	3.72	ND	ug/L

21191 (1516)			
	07/17/90	08/21/90	UNITS
U-Total	293	687	ug/L

2049										
	08/03/88	12/06/88	12/06/88	02/07/89	05/10/89	07/30/89	04/03/90	04/08/90	05/10/93	UNITS
U234	3.1	ND	1.3	2.3	42.9	83.2	ND	50.8	41.5	pci/L
U235/236	ND	ND	ND	ND	1.8	1.4	ND	2.3	1.86	pci/L
U238	2.8	ND	ND	2.1	47.5	89.9	ND	51.4	46.4	pci/L
U-Total	8	2	3	6	175	147	43.3	130	111	ug/L

2045										
	01/23/89	05/01/89	05/01/89	07/25/89	12/03/89	04/01/90	04/01/90	04/28/93	UNITS
U234	ND	77.6	74.7	104.	78.9	97.	95.3	131.	pci/L
U238	ND	4.4	3.2	4.7	3.5	4.55	3.56	5.46	pci/L
U235/236	ND	85.5	87.5	119.	92.3	104.	103.	144.	pci/L
U-Total	ND	291.	265.	341.	283.	461.	462.	364.	ug/L
Th-Total	5	ND	ND	ND	ND	9.47	ND	ND	ug/L
Ra226	ND	ND	ND	ND	ND	ND	ND	ND	pci/L

2014									
	03/28/88	07/28/88	11/06/88	01/31/89	07/26/89	04/01/90	04/30/93	UNITS
U234	9.5	7.7	1.2	4.2	7	7.15	3.49	pci/L
U238	13.1	9.9	13.5	5.7	9	8.95	3.29	pci/L
U235/236	1.6	ND	ND	119.	ND	ND	.22	pci/L
Ra226	ND	ND	1.2	1.4	ND	ND	ND	pci/L
U-Total		33	35	17	33	36	9.05	ug/L

NOTE:
Coordinates are in State Planar NAD 1927.
Surface contours based on 1992 flyover.

SCALE (FT)
0 125 250 500

FIGURE 4-25 000016
RADIONUCLIDES IN 2000-SERIES WELLS DETECTED ABOVE BACKGROUND IN THE SOUTH FIELD /FLYASH PILES AREA

fig0494.dgn

110701_15

AFP-SS-06 (05/14/93)		UNITS
Pu238	0.127	pCi/g
U234	4.43	pCi/g
U238	3.9	pCi/g
U-Total	14.2	ug/g
Th228	2.41	pCi/g
Th230	3.31	pCi/g
Th232	2.53	pCi/g
Th-Total	23.3	ug/g
Ra226	3.8	pCi/g
Ra228	2.8	pCi/g
Arsenic	53.1	mg/kg
Beryllium	5.7	mg/kg

1981 (05/13/93)		UNITS
1,1,1-Trichloroethane	8	ug/kg
Benzoic acid	80	ug/kg
Di-n-butylphthalate	58	ug/kg
Methylene Chloride	63	ug/kg
Toluene	51	ug/kg

1981 (05/13/93)		UNITS
Np237	0.3	pCi/g
Pu238	0.30	pCi/g
Pu239/240	0.12	pCi/g
Th228	3.81	pCi/g
Th230	6.74	pCi/g
Th232	3.74	pCi/g
Th-Total	34.1	ug/g
U234	3.37	pCi/g
U235/236	0.19	pCi/g
U238	3.67	pCi/g
U-Total	13.3	ug/g
Ra226	4.61	pCi/g
Ra228	3.17	pCi/g
Arsenic	115	mg/kg
Beryllium	5.8	mg/kg
SR90	0.76	pCi/g

AFP-SS-05 (05/14/93)		UNITS
Pu239/240	0.022	pCi/g
U234	3.7	pCi/g
U235/236	0.159	pCi/g
U238	3.37	pCi/g
U-Total	12.7	ug/g
Th228	2.23	pCi/g
Th230	2.87	pCi/g
Th232	2.1	pCi/g
Th-Total	19.3	ug/g
Ra226	3.53	pCi/g
Ra228	2.75	pCi/g
Arsenic	82.8	mg/kg
Beryllium	4.6	mg/kg

AFP-SW-02 (05/13/93)		
U234	1.5	pCi/L
U238	1.69	pCi/L
U235/236	0.102	pCi/L
U-Total	4.18	ug/L
Ra228	1.7	pCi/L
Np237	0.264	pCi/L
Pu238	0.108	pCi/L
Arsenic	0.005	pCi/L

AFP-SD-06 (05/13/93)		
U234	2.77	pCi/g
U238	2.9	pCi/g
U-Total	11.3	ug/g
U235/236	0.163	pCi/g
Pu238	0.024	pCi/g
Np237	0.038	pCi/g

AFP-SD-06 (05/13/93)		
4-Methylphenol	1700	ug/kg
Benzoic acid	680	ug/kg
Di-n-butylphthalate	64	ug/kg
Phenol	230	ug/kg

ASIT-006 (06/27/88) (03-30-89)				
U-Total	22.9	ug/g	14	ug/L

AFP-SD-05 (5-13-93)		UNITS
Benzo(a)pyrene	70	ug/kg
Fluoranthene	180	ug/kg
Benzo(b)fluoranthene	100	ug/kg
bis(2-ethylhexyl)phthalate	1400	ug/kg
Pyrene	120	ug/kg
Phenanthrene	120	ug/kg
Chrysene	72	ug/kg
Toluene	62	ug/kg

AFP-SD-05 (5-13-93)		UNITS
Np237	0.058	pCi/g
Pu238	0.036	pCi/g
Pu239/240	0.011	pCi/g
Sr90	0.214	pCi/g
Th228	1.78	pCi/g
Th230	2.66	pCi/g
Th232	1.81	pCi/g
Th-Total	16.5	mg/kg
U234	3.25	pCi/g
U235/236	0.152	pCi/g
U238	3.62	pCi/g
U-Total	12.5	mg/kg
Ra226	2.75	pCi/g
Ra228	2.48	pCi/g
Arsenic	50.4	mg/kg
Beryllium	3.1	mg/kg

AFP-SS-05 (5-14-93)		UNITS
Toluene	52.0	ug/kg
Methylene Chloride	44.0	ug/kg

ASIT-004 (06/27/88) (03-21-89)				
U-Total	38.9	ug/g	318	ug/L
Ra226	1.24	pCi/g	ND	pCi/L
Ra228	1.08	pCi/g	ND	pCi/L

ASIT-007 (06/28/88) (03-30-89)				
U-Total	4.53	ug/g	24	ug/L

1980 (05/12/93)		UNITS
Np237	0.083	pCi/g
Pu238	0.057	pCi/g
U234	3.43	pCi/g
U238	3.47	pCi/g
U-Total	7.86	ug/g
Th228	2.39	pCi/g
Th230	2.89	pCi/g
Th232	2.44	pCi/g
Th-Total	22.4	ug/g
Ra226	3.45	pCi/g
Ra228	2.69	pCi/g
Arsenic	94.8	mg/kg
Beryllium	6.4	mg/kg

AFP-SD-04 (5-13-93)		UNITS
Np237	0.124	pCi/g
Pu238	0.035	pCi/g
Pu239/240	0.03	pCi/g
Th232	1.61	pCi/g
Th-Total	14.7	mg/kg
U234	2.37	pCi/g
U235/236	0.173	pCi/g
U238	3.05	pCi/g
U-Total	10.2	mg/kg
Ra226	1.96	pCi/g
Ra228	1.67	pCi/g
Arsenic	27.2	mg/kg
Beryllium	2.1	mg/kg
Benzo(a)anthracene	110	ug/kg
Pyrene	230	ug/kg
Phenanthrene	210	ug/kg
Indeno(1,2,3-cd)pyrene	74	ug/kg
Fluoranthene	390	ug/kg
Chrysene	150	ug/kg
Benzoic acid	120	ug/kg
Benzo(a)pyrene	120	ug/kg
Benzo(k)fluoranthene	73	ug/kg
Benzo(b)fluoranthene	180	ug/kg

AFP-SS-06 (05/14/93)		UNITS
Methylene Chloride	110	ug/kg

1979 (05/10/93)		UNITS
U234	2.94	pCi/g
U238	2.88	pCi/g
U-Total	10.78	ug/g
Th228	2.35	pCi/g
Th230	2.43	pCi/g
Th232	2.0	pCi/g
Th-Total	18.4	ug/g
Ra226	3.32	pCi/g
Ra228	2.86	pCi/g
Arsenic	145	mg/kg
Beryllium	5.4	mg/kg

ASIT-005 (06/27/88) (03-21-89)				
U-Total	51.8	ug/g	1829	ug/L

1980 (05/12/93)		UNITS
bis(Ethylhexyl) phthalate	45	ug/kg

AFP-SS-04 (05/14/93)		UNITS
Pu238	0.043	pCi/g
Sr90	1.73	pCi/g
U234	3.4	pCi/g
U235/236	0.151	pCi/g
U238	3.5	pCi/g
U-Total	10.4	ug/g
Th228	2.51	pCi/g
Th230	3.03	pCi/g
Th232	2.55	pCi/g
Th-Total	23.5	ug/g
Ra226	3.73	pCi/g
Ra228	2.98	pCi/g
Arsenic	69.1	mg/kg
Beryllium	4.3	mg/kg

AFP-SS-01 (5-13-93)		UNITS
Di-n-butylphthalate	98.0	ug/kg
Toluene	21.0	ug/kg

AFP-SS-01 (05/14/93)		UNITS
Pu238	0.29	pCi/g
Pu239/240	0.12	pCi/g
Sr90	4.24	pCi/g
U238	3.36	pCi/g
U234	3.06	pCi/g
U-Total	13.1	ug/g
Th228	2.56	pCi/g
Th230	3.01	pCi/g
Th232	2.45	pCi/g
Th-Total	22.3	ug/g
Ra226	3.29	pCi/g
Ra228	2.9	pCi/g
Arsenic	64.2	mg/kg
Beryllium	3.0	mg/kg

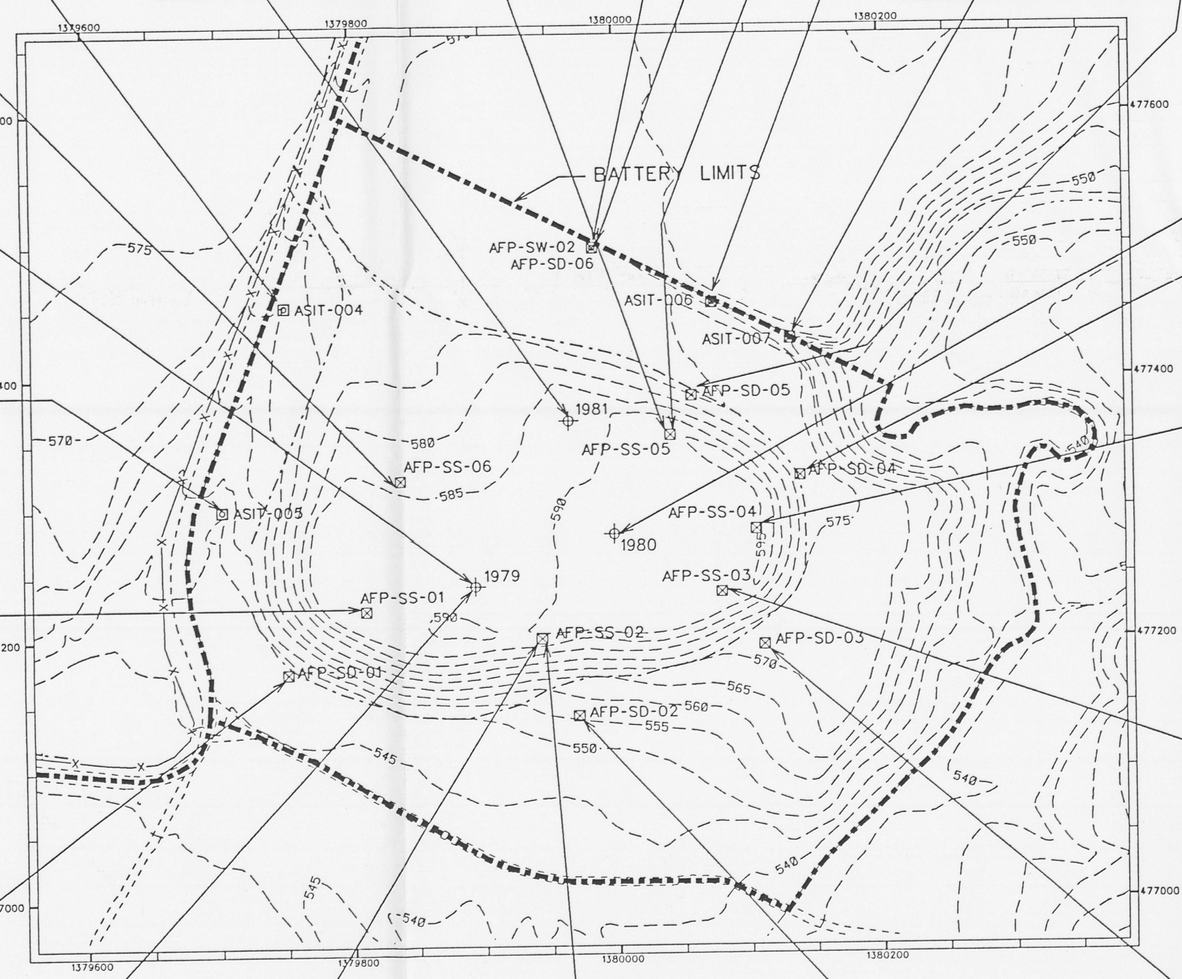

AFP-SS-04 (5-14-93)		UNITS
Butylbenzylphthalate	180.0	ug/kg
Toluene	88.0	ug/kg

AFP-SS-03 (5-13-93)		UNITS
2-Methylnaphthalene	55.0	ug/kg
Toluene	62.0	ug/kg
Pheranthrene	47.0	ug/kg

AFP-SS-03 (05/14/93)		UNITS
Pu238	1.29	pCi/g
Ra226	3.6	pCi/g
Sr90	0.386	pCi/g
U234	3.21	pCi/g
U235/236	0.178	pCi/g
U238	3.11	pCi/g
U-Total	10.0	ug/g
Th228	2.38	pCi/g
Th230	2.93	pCi/g
Th232	2.13	pCi/g
Th-Total	19.6	ug/g
Ra228	2.92	pCi/g
Arsenic	89.4	mg/kg
Beryllium	4.5	mg/kg

LEGEND

- 575 ELEVATION CONTOURS
- ROADS
- STREAM
- DRAINAGE
- FENCE
- SOIL BORING
- SURFACE SOIL SAMPLE
- SURFACE WATER SAMPLE
- SURFACE SEDIMENT SAMPLE

NOTE:
Coordinates are in State Planar NAD 1927.
Surface contours based on 1992 flyover.

SCALE (FT)
0 80 160

AFP-SD-01 (5-15-93)		UNITS
Pu238	0.173	pCi/g
Pu239/240	0.075	pCi/g
Th228	2.38	pCi/g
Th230	3.09	pCi/g
Th232	2.41	pCi/g
Th-Total	22.2	mg/kg
U234	3.39	pCi/g
U235/236	0.199	pCi/g
U238	3.42	pCi/g
U-Total	14.8	mg/kg
Ra226	3.53	pCi/g
Ra228	2.92	pCi/g
Arsenic	37	mg/kg
Beryllium	2	mg/kg
2-Methylnaphtalene	56	ug/kg
Pyrene	100	ug/kg
Fluoranthene	130	ug/kg
Benzo(a)anthracene	53	ug/kg
Chrysene	69	ug/kg
Phenanthrene	99	ug/kg
Naphthalene	51	ug/kg
Benzo(b)fluoranthene	100	ug/kg
Benzo(k)fluoranthene	54	ug/kg
Toluene	4	ug/kg

AFP-SS-02 (5-14-93)		UNITS
Di-n-butylphthalate	130.0	ug/kg
Fluoranthene	160.0	ug/kg
Phenanthrene	100.0	ug/kg
Pyrene	120.0	ug/kg
Methylene Chloride	65	ug/kg

1979 (05/10/93)		UNITS
Benzoic acid	76	ug/kg
Methylene Chloride	5	ug/kg
Toluene	160	ug/kg

AFP-SS-02 (05/14/93)		UNITS
Pu238	0.06	pCi/g
Sr90	4.47	pCi/g
U234	3.09	pCi/g
U235/236	0.16	pCi/g
U238	2.95	pCi/g
U-Total	8.44	ug/g
Th228	2.34	pCi/g
Th230	2.83	pCi/g
Th232	2.34	pCi/g
Th-Total	21.3	ug/g
Ra226	3.28	pCi/g
Ra228	2.58	pCi/g
Arsenic	129	mg/kg
Beryllium	4.3	mg/kg

AFP-SD-02 (5-12-93)		UNITS
Cs137	0.919	pCi/g
Np237	0.120	pCi/g
Sr90	0.227	pCi/g
Pu238	0.071	pCi/g
Pu239/240	0.099	pCi/g
U234	4.14	pCi/g
U235/236	0.196	pCi/g
U238	4.39	pCi/g
U-Total	13.6	mg/kg
Arsenic	10.4	mg/kg
Beryllium	1.9	mg/kg
bis(2-ethylhexyl)phthalate	150	ug/kg

AFP-SD-03 (5-13-93)		UNITS
Np237	0.057	pCi/g
Pu238	0.032	pCi/g
Pu239/240	0.041	pCi/g
Th-Total	11.2	mg/kg
U234	2.83	pCi/g
U238	3.11	pCi/g
U-Total	10.7	mg/kg
Ra228	1.29	pCi/g
Arsenic	13.2	mg/kg
Beryllium	1.5	mg/kg
Tetrachloroethene	2	ug/kg

000017

FIGURE 4-28
RADIONUCLIDES, METALS OF CONCERN, AND ORGANICS IN SURFACE SAMPLES DETECTED ABOVE SOIL BACKGROUND IN THE ACTIVE FLYASH PILE

fig0498.dgn

110707-16

1846	02/22/92		
	6-7.5 ft	13.5-15 ft	UNITS
1,1,1-Trichloroethane	240	120	ug/kg
2-Methylnaphthalene	94	49	ug/kg
Benzene	2	ND	ug/kg
Benzoic acid	62	68	ug/kg
Di-n-butylphthalate	69	47	ug/kg
Naphthalene	52	ND	ug/kg
Toluene	130	110	ug/kg
bis(2-Ethylhexyl) phthalate	120	ND	ug/kg
4-Methyl-2-pentanone	ND	25	ug/kg
Phenanthrene	ND	43	ug/kg

1820	10/16/91		
	1.5-3 ft	6-7.5 ft	UNITS
1,1,1-Trichloroethane	28	32	ug/kg
Di-n-butylphthalate	49	ND	ug/kg
Toluene	13	21	ug/kg
Di-n-octylphthate	ND	3000	ug/kg

1048	10/13/87	
U238	2.4	pCi/g
U235/236	ND	pCi/g
Th228	1.6	pCi/g
Th230	1.9	pCi/g

1981	05/13/93				
	2-4 ft	8-10 ft	17-19 ft	19-21 ft	UNITS
1, 1, 1-Trichloroethane	ND	740	ND	ND	ug/kg
2-Hexanone	ND	10	ND	ND	ug/kg
Acetone	ND	37	ND	ND	ug/kg
Benzoic acid	2	100	ND	56	ug/kg
Di-n-butylphthalate	ND	86	ND	ND	ug/kg
Toluene	130	76	ND	ND	ug/kg
bis(2-Ethylhexyl) phthalate	ND	48	ND	ND	ug/kg
Methylene chloride	ND	ND	25	ND	ug/kg

1820	10/16/91			
	1.5-3 ft	6-7.5 ft	9.5-12 ft	UNITS
U234	3.68	3.08	ND	pCi/g
U238	ND	7.23	ND	pCi/g
U-Total	9.08	20.7	ND	ug/g
Th228	3.18	3.44	ND	pCi/g
Th230	3	4.01	ND	pCi/g
Th232	ND	2.82	ND	pCi/g
Th-Total	17	25.4	3.38	ug/g
Ra226	3.16	ND	ND	pCi/g
Ra228	2.4	ND	ND	pCi/g
SR90	1.4	ND	ND	pCi/g

1981	05/14/93				
	2-4 ft	8-10 ft	17-19 ft	19-21 ft	UNITS
Np237	0.3	0.45	ND	ND	pCi/g
U234	3.43	3.23	1.01	0.87	pCi/g
U238	ND	ND	1.2	ND	pCi/g
U235/236	ND	0.22	ND	ND	pCi/g
U-Total	14.1	15.7	4.15	3.3	ug/g
Th228	3.27	3.12	1.37	ND	pCi/g
Th230	5.52	5.01	3.6	2.67	pCi/g
Th232	3.12	2.17	1.35	ND	pCi/g
Th-Total	28.4	20	12.4	6.62	ug/g
Ra226	3.55	3.27	1.73	ND	pCi/g
Ra228	3.07	2.42	1.33	ND	pCi/g
Arsenic	ND	ND	18.7	14.0	mg/kg
Beryllium	ND	ND	1.1	1.1	mg/kg
Pu238	0.47	0.320	ND	ND	pCi/g
SR90	0.65	ND	ND	ND	pCi/g
Pu239/240	0.86	0.110	ND	ND	pCi/g

1723	07/11/91				
	3-6.0 ft	12-15.0 ft	26-27.5 ft	29-30.5 ft	UNITS
U234	4.77	4.34	ND	ND	pCi/g
U238	4.92	7.96	ND	ND	pCi/g
U-Total	11.7	31.3	2.72	ND	ug/g
Th228	3.46	2.99	1.76	ND	pCi/g
Th230	3.55	3.02	ND	ND	pCi/g
Th232	2.84	1.93	ND	ND	pCi/g
Th-Total	25.6	17.4	ND	ND	ug/g
Ra226	4.12	4.05	ND	ND	pCi/g
Ra228	3.89	2.83	ND	ND	pCi/g
Beryllium	3.9	4.6	ND	0.75	mg/kg
Arsenic	51.1	ND	ND	ND	mg/kg
SR90	1.010	1.090	ND	ND	pCi/g

1726	06/29/91					
	4.5-6 ft	7.5-9 ft	15-16.5 ft	16.5-18 ft	19.5-21 ft	UNITS
U234	17.3	3.9	12.3	5.7	0.932	pCi/g
U235	0.6	ND	ND	ND	ND	pCi/g
U238	12.6	ND	6.55	ND	ND	pCi/g
U235/236	4.12	ND	3.42	ND	ND	pCi/g
U-Total	28.1	18.5	27.7	28.1	3.08	ug/g
Th228	2.91	3.46	2.93	4.47	2.09	pCi/g
Th230	5.92	3.7	3.8	3.62	1.97	pCi/g
Th232	2.91	2.8	2.37	2.8	ND	pCi/g
Th-Total	26.2	25.3	21.4	25.3	ND	ug/g
Ra224	3.44	ND	3.74	ND	ND	pCi/g
Ra226	3.04	4.51	3.76	4.52	ND	pCi/g
Ra228	2.91	3.61	2.85	3.45	1.45	pCi/g
Pb210	1.52	ND	1.630	ND	ND	pCi/g
SR90	ND	1.370	ND	1.160	ND	pCi/g

1979	05/11/93				
	2.0-4.0 ft	20.0-22.0ft	25.5-27.5ft	29.5-31.5ft	UNITS
Np237	ND	0.059	ND	ND	pCi/g
U234	3.08	5.02	ND	ND	pCi/g
U238	ND	7.12	ND	ND	pCi/g
U235/236	1.25	0.326	ND	ND	pCi/g
U-Total	9.34	22.1	4.49	4.27	ug/g
Th228	3.2	2.88	ND	ND	pCi/g
Th230	3.3	3.52	ND	ND	pCi/g
Th232	2.9	3.14	ND	ND	pCi/g
Th-Total	26.7	28.9	ND	ND	ug/g
Ra226	3.51	4.02	ND	ND	pCi/g
Ra228	2.91	3.69	ND	ND	pCi/g
Arsenic	ND	ND	11	ND	mg/kg
Beryllium	2.4	2.5	ND	ND	mg/kg
SR90	0.705	ND	ND	ND	pCi/g
Pu238	0.081	0.062	ND	ND	pCi/g
Np237	0.122	0.059	ND	ND	pCi/g
Pu239/240	ND	0.012	ND	ND	pCi/g

1726	07/01/91		
	9-10.5 ft	18-19.5 ft	UNITS
1,1,1-Trichloroethane	69	ND	ug/kg
Methylene chloride	73	ND	ug/kg
bis(2-Ethylhexyl) phthalate	480	2700	ug/kg
2-Butanone	ND	4	ug/kg
2-Chlorophenol	ND	48	ug/kg
4-Chloro-3-methylphenol	ND	58	ug/kg
4-Nitrophenol	ND	48	ug/kg
Benzoic acid	ND	73	ug/kg
Phenanthrene	ND	48	ug/kg
Phenol	ND	58	ug/kg
Toluene	13	ND	ug/kg

1980	05/12/93				
	2-4 ft	13-15 ft	20-22 ft	24-26 ft	UNITS
1, 1, 1-Trichloroethane	12	600	4	ND	ug/kg
Toluene	12	ND	2	ND	ug/kg
Xylenes, Total	53	ND	ND	5600	ug/kg
bis(2-Ethylhexyl) phthalate	300	780	4200	98	ug/kg

1980	05/12/93				
	2.0-4.0 ft	13.0-15.0ft	20.0-22.0ft	24.0-26.0ft	UNITS
Np237	0.11	ND	ND	ND	pCi/g
U234	3.58	3.04	0.917	0.952	pCi/g
U238	3.46	3.94	1.19	1.21	pCi/g
U235/236	0.19	0.179	ND	ND	pCi/g
U-Total	12.9	13	3.34	4.534	ug/g
Th228	2.44	1.8	ND	ND	pCi/g
Th230	3.32	2.4	1.25	ND	pCi/g
Th232	2.36	2.05	ND	ND	pCi/g
Th-Total	21.7	18.9	9.29	ND	ug/g
Ra226	3.97	2.96	ND	ND	pCi/g
Ra228	2.84	2.23	ND	ND	pCi/g
Arsenic	ND	ND	ND	10.6	mg/kg
Beryllium	ND	ND	1.4	1.4	mg/kg
Pu259/240	0.048	ND	ND	ND	pCi/g
Pu238	0.082	0.123	ND	ND	pCi/g

1724	07/13/91				
	3-4.5 ft	14.5-16 ft	40-41.5 ft	41.5-43 ft	UNITS
U234	4.75	4.01	1.27	ND	pCi/g
U238	4.96	5.53	2.04	ND	pCi/g
U-Total	18.4	16.4	7.17	ND	ug/g
Th228	5.79	3.21	ND	ND	pCi/g
Th230	6.08	3.45	ND	ND	pCi/g
Th232	5.08	ND	ND	ND	pCi/g
Th-Total	45.8	21.9	ND	ND	ug/g
Ra226	6.22	3.6	ND	ND	pCi/g
Ra228	5.32	2.76	ND	ND	pCi/g
Beryllium	ND	ND	ND	0.74	mg/kg
SR90	1.53	1.270	ND	ND	pCi/g

3045	05/09/93	
	105-106.5ft	UNITS
U-Total	2.85	ug/g
Th230	1.42	pCi/g

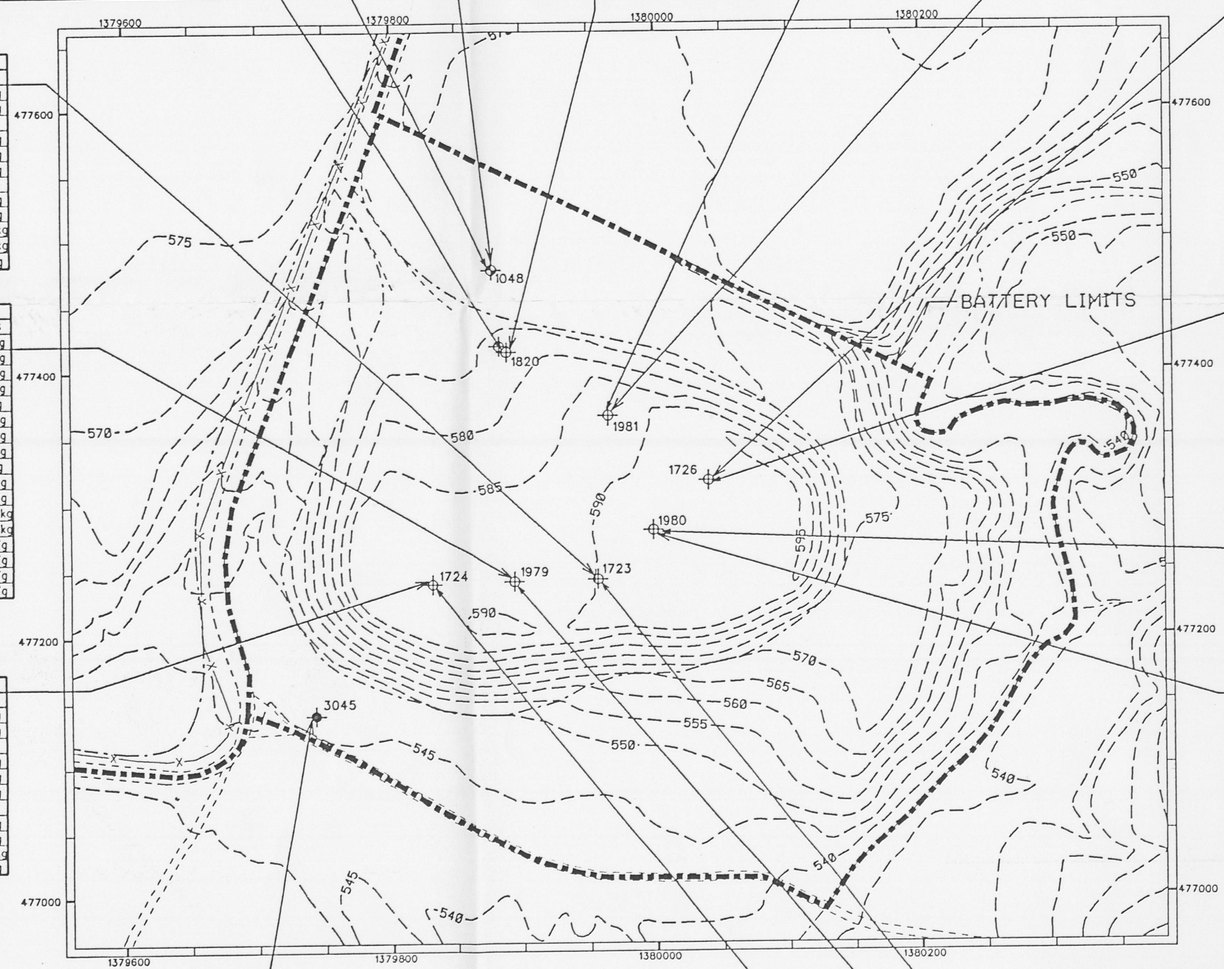

1723	07/11/91			
	4.5-6 ft	13.5-15 ft	29-30.5 ft	UNITS
1,1,1-Trichloroethane	80	ND	25	ug/kg
1,1-Dichloroethene	ND	2	ND	ug/kg
bis(2-Ethylhexyl) phthalate	ND	ND	42	ug/kg
Carbon disulfide	ND	7	ND	ug/kg
Methylene chloride	37	65	ND	ug/kg

1979	05/10/93			
	2-4 ft	20-22 ft	25.5-27.5ft	UNITS
Pentachlorophenol	56	ND	ND	ug/kg
Benzoic acid	ND	95	ND	ug/kg
Toluene	ND	140	ND	ug/kg
Di-n-octylphthalate	ND	ND	46	ug/kg

1724	07/13/91			
	4.5-6 ft	16-17.5 ft	41.5-43 ft	UNITS
1,1,1-Trichloroethane	1300	40	ND	ug/kg
2-Methylnaphthalene	160	ND	ND	ug/kg
Benzoic acid	52	ND	ND	ug/kg
Phenanthrene	72	ND	ND	ug/kg
4-Methyl-2-pentanone	ND	11	ND	ug/kg
Methylene chloride	ND	34	ND	ug/kg
2-Butanone	ND	ND	3	ug/kg
Naphthalene	82	ND	ND	ug/kg

LEGEND

- 575 ELEVATION CONTOURS
- ROADS
- STREAM
- DRAINAGE
- FENCE
- 1000 MONITORING WELLS
- 3000 MONITORING WELLS
- SOIL BORING

ND - NOT DETECTED ABOVE BACKGROUND CONCENTRATIONS

NOTE:
Coordinates are in State Planar NAD 1927.
Surface contours based on 1992 flyover.

SCALE (FT)
0 80 160

FIGURE 4-29 000018
RADIONUCLIDES, METALS OF CONCERN AND ORGANICS IN SUBSURFACE SOILS DETECTED ABOVE SOIL BACKGROUND IN THE ACTIVE FLYASH PILE

fig0495.dgn

110707-17

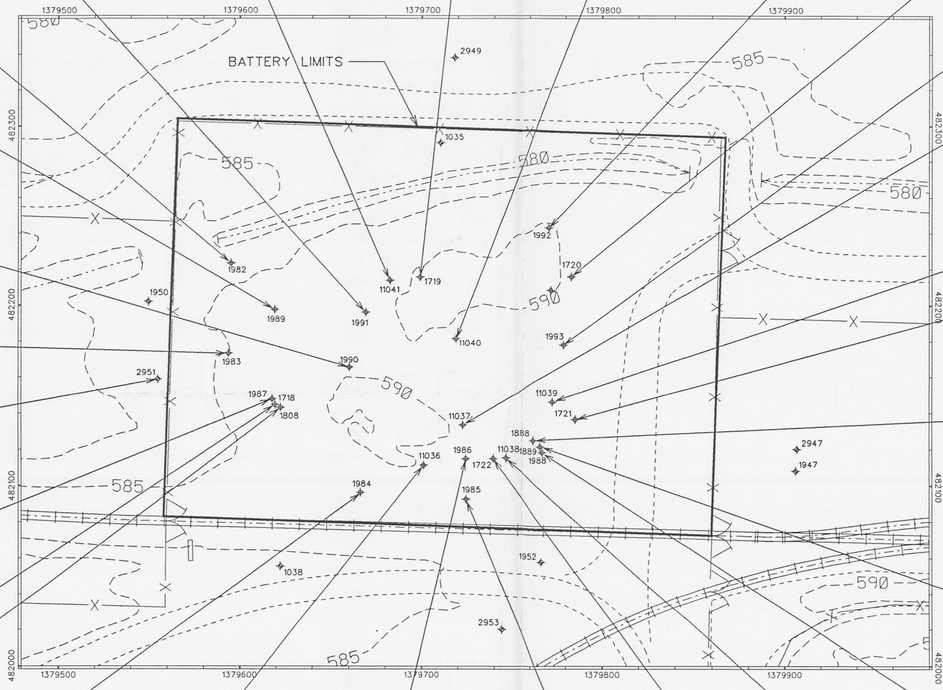

1982 (5-6-93)	0.0-2.5	7.5-10.0	UNITS
Acenaphthene	55	ND	ug/kg
Anthracene	77	ND	ug/kg
Aroclor-1254	48	ND	ug/kg
Benzo(a)anthracene	170	ND	ug/kg
Benzo(a)pyrene	120	ND	ug/kg
Benzo(b)fluoranthene	180	ND	ug/kg
Benzo(g,h,i)perylene	86	ND	ug/kg
Benzo(k)fluoranthene	120	ND	ug/kg
Chrysene	200	ND	ug/kg
Dibenzo(a,h)anthracene	40	ND	ug/kg
Fluoranthene	480	ND	ug/kg
Fluorene	46	ND	ug/kg
Indeno(1,2,3-cd)pyrene	91	ND	ug/kg
Phenanthrene	410	ND	ug/kg
Pyrene	350	ND	ug/kg
bis(2-Ethylhexyl) phthalate	260	250	ug/kg
Toluene	2	1	ug/kg

1991 (5-6-93)	7.5-10.0	12.5-15.0	UNITS
Acenaphthene	180	ND	ug/kg
Anthracene	300	ND	ug/kg
Benzo(a)anthracene	560	ND	ug/kg
Benzo(a)pyrene	470	ND	ug/kg
Benzo(b)fluoranthene	540	ND	ug/kg
Benzo(g,h,i)perylene	320	ND	ug/kg
Benzo(k)fluoranthene	410	ND	ug/kg
Carbazole	98	ND	ug/kg
Chrysene	640	ND	ug/kg
Dibenzo(a,h)anthracene	140	ND	ug/kg
Dibenzofuran	130	ND	ug/kg
Endosulfan II	6.2	ND	ug/kg
Fluoranthene	1800	ND	ug/kg
Fluorene	190	ND	ug/kg
Indeno(1,2,3-cd)pyrene	320	ND	ug/kg
Naphthalene	84	ND	ug/kg
Phenanthrene	1500	ND	ug/kg
Pyrene	1300	ND	ug/kg
bis(2-Ethylhexyl) phthalate	300	810	ug/kg

11041 (5-19-93)	0.0-2.5	12.5-15.0	UNITS
4,4'-DDD	4.3	ND	ug/kg
Acenaphthene	5800	ND	ug/kg
Anthracene	9700	ND	ug/kg
Benzo(a)anthracene	18000	ND	ug/kg
Benzo(a)pyrene	13000	ND	ug/kg
Benzo(g,h,i)perylene	5800	ND	ug/kg
Benzo(k)fluoranthene	25000	ND	ug/kg
Carbazole	4200	ND	ug/kg
Chrysene	18000	ND	ug/kg
Dibenzo(a,h)anthracene	3000	ND	ug/kg
Dibenzofuran	3000	ND	ug/kg
Dieldrin	13	ND	ug/kg
Endrin aldehyde	190	ND	ug/kg
Fluoranthene	48000	ND	ug/kg
Fluorene	6000	ND	ug/kg
Indeno(1,2,3-cd)pyrene	6500	ND	ug/kg
Naphthalene	1700	ND	ug/kg
Phenanthrene	48000	ND	ug/kg
Pyrene	38000	ND	ug/kg
Toluene	2	2	ug/kg

1719 (8-7-91)	3.0-4.5	15.0-16.5	18.0-19.5	UNITS
1,2,3,4,6,7,8-Heptachlorodibenzofu	0.073	ND	ND	ug/kg
1,2-Dichloroethane	6	ND	ND	ug/kg
2-Methylnaphthalene	93	ND	ND	ug/kg
Acenaphthene	840	ND	ND	ug/kg
4-Methyl-2-pentanone	ND	1	ND	ug/kg
Acetone	7	10	10	ug/kg
Anthracene	1000	130	30	ug/kg
Benzo(a)anthracene	7500	290	72	ug/kg
Benzo(a)pyrene	8200	290	ND	ug/kg
Benzo(b)fluoranthene	15000	260	150	ug/kg
Benzo(g,h,i)perylene	ND	300	ND	ug/kg
Benzo(k)fluoranthene	ND	300	ND	ug/kg
Benzoic acid	ND	110	ND	ug/kg
Chlorobenzene	2	6	ND	ug/kg
Chrysene	5600	370	74	ug/kg
Di-n-butylphthalate	ND	120	ND	ug/kg
Dibenzo(a,h)anthracene	49	110	ND	ug/kg
Ethylbenzene	ND	18	ND	ug/kg
Dibenzofuran	340	ND	ND	ug/kg
Fluoranthene	12000	720	150	ug/kg
Fluorene	640	ND	ND	ug/kg
Heptachlorodibenzo-p-dioxin	0.65	ND	ND	ug/kg
Heptachlorodibenzofuran	0.25	ND	ND	ug/kg
Indeno(1,2,3-cd)pyrene	5500	210	ND	ug/kg
Naphthalene	140	ND	ND	ug/kg
Octachlorodibenzo-p-dioxin	7.1	0.71	0.063	ug/kg
Phenanthrene	4800	620	83	ug/kg
Pyrene	12000	610	140	ug/kg
Toluene	ND	8	ND	ug/kg
Trichlorofluoromethane	ND	640	ND	ug/kg
Xylenes, Total	ND	100	ND	ug/kg
bis(2-Ethylhexyl) phthalate	ND	1200	40	ug/kg
2-Hexanone	ND	1	ND	ug/kg

11040 (5-20-93)	2.5-5.0	UNITS
Anthracene	100	ug/kg
Benzo(a)anthracene	350	ug/kg
Benzo(a)pyrene	320	ug/kg
Benzo(b)fluoranthene	290	ug/kg
Benzo(g,h,i)perylene	190	ug/kg
Benzo(k)fluoranthene	290	ug/kg
Carbazole	58	ug/kg
Chrysene	370	ug/kg
Dibenzo(a,h)anthracene	96	ug/kg
Fluoranthene	770	ug/kg
Indeno(1,2,3-cd)pyrene	200	ug/kg
Phenanthrene	440	ug/kg
Pyrene	640	ug/kg
bis(2-Ethylhexyl) phthalate	48	ug/kg

1992 (5-11-93)	7.5-10.0	17.5-20.0	UNITS
Acenaphthene	47	ND	ug/kg
Anthracene	70	ND	ug/kg
Benzo(a)anthracene	380	ND	ug/kg
Benzo(a)pyrene	510	ND	ug/kg
Benzo(b)fluoranthene	1200	ND	ug/kg
Benzo(g,h,i)perylene	420	ND	ug/kg
Carbazole	62	ND	ug/kg
Chrysene	560	ND	ug/kg
Fluoranthene	870	ND	ug/kg
Indeno(1,2,3-cd)pyrene	260	ND	ug/kg
Phenanthrene	490	ND	ug/kg
Pyrene	790	ND	ug/kg
Tetrachloroethene	1	ND	ug/kg
bis(2-Ethylhexyl) phthalate	340	310	ug/kg

1720 (8-10-91)	3.0-4.5	7.5-9.0	9.0-10.5	UNITS
2-Chlorophenol	49	ND	ND	ug/kg
4-Chloro-3-methylphenol	55	ND	ND	ug/kg
Acenaphthene	53	ND	ND	ug/kg
Benzo(a)anthracene	130	43	ND	ug/kg
Benzo(a)pyrene	69	ND	ND	ug/kg
Benzo(b)fluoranthene	190	54	ND	ug/kg
Chrysene	140	47	ND	ug/kg
Diethylphthalate	ND	ND	750	ug/kg
Fluoranthene	250	94	ND	ug/kg
Methylene chloride	ND	6	ND	ug/kg
Octachlorodibenzo-p-dioxin	7.8	7.2	0.86	ug/kg
Phenanthrene	160	53	ND	ug/kg
Phenol	61	ND	ND	ug/kg
Pyrene	270	73	ND	ug/kg
1,2-Dichloroethene	ND	12	ND	ug/kg

1993 (5-11-93)	2.5-5.0	15.0-17.5	UNITS
2-Methylnaphthalene	160	ND	ug/kg
Acenaphthene	290	ND	ug/kg
Anthracene	440	ND	ug/kg
Benzo(a)anthracene	570	ND	ug/kg
Benzo(a)pyrene	510	ND	ug/kg
Benzo(b)fluoranthene	630	ND	ug/kg
Benzo(g,h,i)perylene	150	ND	ug/kg
Benzo(k)fluoranthene	220	ND	ug/kg
Carbazole	200	ND	ug/kg
Chrysene	530	ND	ug/kg
Dibenzofuran	240	ND	ug/kg
Fluoranthene	1200	ND	ug/kg
Fluorene	370	ND	ug/kg
Indeno(1,2,3-cd)pyrene	320	ND	ug/kg
Naphthalene	290	ND	ug/kg
Phenanthrene	1400	ND	ug/kg
Pyrene	890	ND	ug/kg
bis(2-Ethylhexyl) phthalate	800	470	ug/kg

1989 (5-14-93)	2.5-5.0	12.5-15.0	UNITS
4-Methylphenol	140	ND	ug/kg
Acenaphthene	90	ND	ug/kg
Benzo(a)anthracene	170	ND	ug/kg
Benzo(a)pyrene	110	ND	ug/kg
Benzo(b)fluoranthene	220	ND	ug/kg
Benzo(g,h,i)perylene	64	ND	ug/kg
Chrysene	140	ND	ug/kg
Di-n-butylphthalate	170	71	ug/kg
Fluoranthene	340	ND	ug/kg
Indeno(1,2,3-cd)pyrene	67	ND	ug/kg
Phenanthrene	260	ND	ug/kg
Pyrene	270	ND	ug/kg
Toluene	ND	3	ug/kg

11037 (5-15-93)	5.0-7.0	17.5-20.0	UNITS
Benzo(a)anthracene	48	ND	ug/kg
Benzo(b)fluoranthene	67	ND	ug/kg
Chrysene	48	ND	ug/kg
Fluoranthene	89	ND	ug/kg
Pyrene	72	ND	ug/kg
2-Hexanone	ND	2	ug/kg
4-Methyl-2-pentanone	ND	20	ug/kg
Acetone	ND	6	ug/kg
Di-n-octylphthalate	ND	55	ug/kg
Ethylbenzene	ND	7	ug/kg
Toluene	ND	4	ug/kg
Xylenes, Total	ND	23	ug/kg

11039 (5-19-93)	2.5-5.0	12.0-14.0	UNITS
2-Butanone	110	ND	ug/kg
2-Hexanone	1	ND	ug/kg
2-Methylnaphthalene	46000	100	ug/kg
Acenaphthene	140000	370	ug/kg
Acetone	88	ND	ug/kg
Anthracene	250000	580	ug/kg
Benzo(a)anthracene	310000	1000	ug/kg
Benzo(a)pyrene	260000	760	ug/kg
Benzo(b)fluoranthene	220000	1200	ug/kg
Benzo(g,h,i)perylene	150000	380	ug/kg
Benzo(k)fluoranthene	140000	740	ug/kg
Carbazole	89000	210	ug/kg
Chrysene	310000	920	ug/kg
Dibenzo(a,h)anthracene	79000	180	ug/kg
Dibenzofuran	120000	260	ug/kg
Ethylbenzene	2	ND	ug/kg
Fluoranthene	790000	2400	ug/kg
Fluorene	180000	430	ug/kg
Indeno(1,2,3-cd)pyrene	150000	410	ug/kg
Phenanthrene	900000	2600	ug/kg
Pyrene	690000	1900	ug/kg
Toluene	1	54	ug/kg
Naphthalene	96000	320	ug/kg
Acenaphthylene	2500	ND	ug/kg

1990 (5-10-93)	6.0-9.0	17.5-20.0	UNITS
Acenaphthene	260	ND	ug/kg
Anthracene	260	ND	ug/kg
Benzo(a)anthracene	460	ND	ug/kg
Benzo(a)pyrene	420	ND	ug/kg
Benzo(b)fluoranthene	530	ND	ug/kg
Benzo(g,h,i)perylene	170	ND	ug/kg
Benzo(k)fluoranthene	210	ND	ug/kg
Carbazole	180	ND	ug/kg
Chrysene	460	ND	ug/kg
Dibenzo(a,h)anthracene	68	ND	ug/kg
Dibenzofuran	170	ND	ug/kg
Endosulfan sulfate	9.4	ND	ug/kg
Endrin ketone	5.7	ND	ug/kg
Fluoranthene	1200	ND	ug/kg
Fluorene	210	ND	ug/kg
Indeno(1,2,3-cd)pyrene	280	ND	ug/kg
Naphthalene	46	ND	ug/kg
Phenanthrene	1200	ND	ug/kg
Pyrene	900	ND	ug/kg
bis(2-Ethylhexyl) phthalate	1100	490	ug/kg
Toluene	ND	5	ug/kg

1721 (7-6-91)	9.0-10.5	13.5-15.0	UNITS
1,1-Dichloroethane	16	ND	ug/kg
1,2-Dichloroethene	ND	2	ug/g
1,4-Dioxane	12900	ND	ug/kg
Acetone	39	ND	ug/kg
Aroclor-1260	610	ND	ug/kg
Chloromethane	6	ND	ug/kg
Dichlorodifluoromethane	576	ND	ug/kg
Methylene chloride	8	ND	ug/kg
Octachlorodibenzo-p-dioxin	0.31	0.05	ug/g

1983 (5-3-93)	1.5-2.5	2.5-5.0	17.5-20.0	UNITS
Benzo(a)anthracene	49	78	ND	ug/kg
Benzo(a)pyrene	47	64	ND	ug/kg
Benzo(b)fluoranthene	49	66	ND	ug/kg
Benzo(k)fluoranthene	56	97	ND	ug/kg
Carbon disulfide	ND	ND	2	ug/kg
Chrysene	130	99	ND	ug/kg
Fluoranthene	130	190	ND	ug/kg
Indeno(1,2,3-cd)pyrene	ND	45	ND	ug/kg
Phenanthrene	66	120	ND	ug/kg
Pyrene	120	170	ND	ug/kg
Toluene	ND	2	ND	ug/kg
bis(2-Ethylhexyl) phthalate	3200	67	ND	ug/kg

2951 (4-21-93)	0.0-5.0	UNITS
Acetone	15	ug/kg

1888 (2-23-92)	0.0-1.5	3.0-6.0	UNITS
Octachlorodibenzo-p-dioxin	1	3.8	ug/kg
1,2-Dichloroethene	ND	3	ug/kg
Acetone	ND	7	ug/kg
Chrysene	ND	47	ug/kg
Diethylphthalate	ND	45	ug/kg
Methylene chloride	6	6	ug/kg
Phenanthrene	ND	160	ug/kg
Pyrene	ND	81	ug/kg
bis(2-Ethylhexyl) phthalate	ND	920	ug/kg
Toluene	2	ND	ug/kg

1987 (5-13-93)	5.0-7.5	12.5-15.0	UNITS
2-Methylnaphthalene	97	ND	ug/kg
Anthracene	450	ND	ug/kg
Benzo(a)anthracene	730	ND	ug/kg
Benzo(a)pyrene	700	ND	ug/kg
Benzo(b)fluoranthene	910	ND	ug/kg
Benzo(g,h,i)perylene	170	ND	ug/kg
Benzo(k)fluoranthene	320	ND	ug/kg
Carbazole	240	ND	ug/kg
Chrysene	740	ND	ug/kg
Dibenzo(a,h)anthracene	110	ND	ug/kg
Dibenzofuran	160	ND	ug/kg
Endosulfan sulfate	10	ND	ug/kg
Endrin ketone	7.1	ND	ug/kg
Fluoranthene	1900	ND	ug/kg
Fluorene	280	ND	ug/kg
Indeno(1,2,3-cd)pyrene	440	ND	ug/kg
Naphthalene	120	ND	ug/kg
Phenanthrene	1700	ND	ug/kg
Pyrene	1300	ND	ug/kg
bis(2-Ethylhexyl) phthalate	710	460	ug/kg

1889 (2-25-92)	15.5-17.5	UNITS
Methylene chloride	13	ug/kg

1718 (7-31-91)	3.0-4.5	7.5-9.0	13.5-15.0	UNITS
Octachlorodibenzo-p-dioxin	13.7	0.44	0.11	ug/kg

1984 (5-1-93)	2.5-5.0	12.-15.0	UNITS
Fluoranthene	46	ND	ug/kg
Pyrene	44	ND	ug/kg
Toluene	2	2	ug/kg
bis(2-Ethylhexyl) phthalate	700	1000	ug/kg

1722 (7-29-91)	1.5-3.0	14.0-16.5	UNITS
1,1-Dichloroethane	130	ND	ug/kg
Octachlorodibenzo-p-dioxin	0.05	ND	ug/kg
2-Butanone	ND	3	ug/kg

1988 (5-12-93)	0.0-1.5	2.5-5.0	17.5-20.0	UNITS
1,2-Dichloroethene	ND	2	ND	ug/kg
4-Methyl-2-pentanone	ND	3	ND	ug/kg
Benzene	ND	3	ND	ug/kg
Ethylbenzene	ND	76	ND	ug/kg
Fluoranthene	ND	160	ND	ug/kg
Phenanthrene	ND	82	ND	ug/kg
Pyrene	ND	100	ND	ug/kg
Xylenes, Total	ND	260	1	ug/kg
bis(2-Ethylhexyl) phthalate	ND	ND	410	ug/kg

1808 (8-27-91)	3.0-4.5	7.5-9.0	15.0-16.5	UNITS
1,4-Dioxane	ND	66	ND	ug/kg
4-Methyl-2-pentanone	ND	1	ND	ug/kg
Acenaphthene	250	240	ND	ug/kg
Anthracene	270	390	ND	ug/kg
Aroclor-1254	150	ND	ND	ug/kg
Benzo(a)anthracene	910	1100	ND	ug/kg
Benzo(a)pyrene	700	1000	ND	ug/kg
Benzo(b)fluoranthene	1500	560	ND	ug/kg
Benzo(g,h,i)perylene	490	650	ND	ug/kg
Benzo(k)fluoranthene	ND	1800	ND	ug/kg
Chrysene	1100	1400	ND	ug/kg
Dibenzo(a,h)anthracene	92	250	ND	ug/kg
Dibenzofuran	160	ND	ND	ug/kg
Diethylphthalate	ND	680	ND	ug/kg
Fluoranthene	2200	3300	ND	ug/kg
Fluorene	250	250	ND	ug/kg
Heptachlorodibenzo-p-dioxin	ND	0.9	ND	ug/g
Indeno(1,2,3-cd)pyrene	440	620	ND	ug/kg
Naphthalene	41	ND	ND	ug/kg
Octachlorodibenzo-p-dioxin	0.31	2.7	0.085	ug/g
Phenanthrene	1900	2700	ND	ug/kg
Pyrene	1800	2500	ND	ug/kg
Pyridine	ND	3	ND	ug/kg
Toluene	ND	ND	1	ug/kg
Tetrachloroethene	30	ND	ND	ug/kg
Styrene			2	ug/kg

110.36 (5-17-93)	2.0-5.0	17.0-19.0	UNITS
1,1-Dichloroethane	55	1	ug/kg
2-Butanone	13	ND	ug/kg
4,4'-DDD	4.5	ND	ug/kg
Acetone	64	ND	ug/kg
Anthracene	80	ND	ug/kg
Aroclor-1260	26	ND	ug/kg
Benzene	4	ND	ug/kg
Benzo(a)anthracene	280	ND	ug/kg
Benzo(a)pyrene	230	ND	ug/kg
Benzo(b)fluoranthene	340	ND	ug/kg
Benzo(g,h,i)perylene	130	ND	ug/kg
Ethylbenzene	15	ND	ug/kg
Fluoranthene	630	ND	ug/kg
Phenanthrene	340	ND	ug/kg
Pyrene	490	ND	ug/kg
Tetrachloroethene	2	ND	ug/kg
Toluene	4	13	ug/kg
Vinyl chloride	2	ND	ug/kg
Xylenes, Total	54	ND	ug/kg
bis(2-Ethylhexyl) phthalate	ND	1600	ug/kg
Chrysene	350	ND	ug/kg
Indeno(1,2,3-cd)pyrene	130	ND	ug/kg

1986 (4-28-93)	2.5-5.0	12.5-15.0	UNITS
Acenaphthene	83	ND	ug/kg
Anthracene	140	ND	ug/kg
Aroclor-1260	70	ND	ug/kg
Benzo(a)anthracene	490	ND	ug/kg
Benzo(a)pyrene	320	ND	ug/kg
Benzo(b)fluoranthene	480	ND	ug/kg
Benzo(g,h,i)perylene	90	ND	ug/kg
Benzo(k)fluoranthene	370	ND	ug/kg
Carbazole	68	ND	ug/kg
Chrysene	550	ND	ug/kg
Dibenzo(a,h)anthracene	120	ND	ug/kg
Dibenzofuran	39	ND	ug/kg
Fluoranthene	1300	ND	ug/kg
Fluorene	80	ND	ug/kg
Indeno(1,2,3-cd)pyrene	230	ND	ug/kg
Phenanthrene	1100	ND	ug/kg
Toluene	1	ND	ug/kg
Acetone	ND	9	ug/kg
bis(2-Ethylhexyl) phthalate	ND	950	ug/kg
Pyrene	1100	ND	ug/kg

1985 (4-26-93)	2.0-4.0	15.0-17.0	UNITS
4,4'-DDD	5	ND	ug/kg
Acenaphthene	93	ND	ug/kg
Anthracene	180	ND	ug/kg
Aroclor-1260	77	ND	ug/kg
Benzo(a)anthracene	1100	ND	ug/kg
Benzo(a)pyrene	790	ND	ug/kg
Benzo(b)fluoranthene	1100	ND	ug/kg
Benzo(g,h,i)perylene	420	ND	ug/kg
Benzo(k)fluoranthene	700	ND	ug/kg
Carbazole	67	ND	ug/kg
Chrysene	940	ND	ug/kg
Dibenzo(a,h)anthracene	250	ND	ug/kg
Dibenzofuran	38	ND	ug/kg
Endosulfan sulfate	6.2	ND	ug/kg
Fluoranthene	1700	ND	ug/kg
Fluorene	83	ND	ug/kg
Indeno(1,2,3-cd)pyrene	520	ND	ug/kg
Phenanthrene	970	ND	ug/kg
Pyrene	1500	ND	ug/kg
bis(2-Ethylhexyl) phthalate	2500	1700	ug/kg

110.38 (5-16-93)	0.0-2.5	12.5-15.0	UNITS
Anthracene	73	ND	ug/kg
Aroclor-1260	170	ND	ug/kg
Benzo(a)anthracene	300	ND	ug/kg
Benzo(a)pyrene	300	ND	ug/kg
Benzo(b)fluoranthene	300	ND	ug/kg
Benzo(g,h,i)perylene	200	ND	ug/kg
Benzo(k)fluoranthene	360	ND	ug/kg
Chrysene	400	ND	ug/kg
Dibenzo(a,h)anthracene	96	ND	ug/kg
Fluoranthene	780	ND	ug/kg
Indeno(1,2,3-cd)pyrene	210	ND	ug/kg
Phenanthrene	400	ND	ug/kg
Pyrene	630	ND	ug/kg
Toluene	ND	5	ug/kg

LEGEND

- ELEVATION CONTOURS
- ROADS
- DRAINAGE
- FENCE
- RAILROAD
- 1000 MONITORING WELLS
- 2000 MONITORING WELLS
- SOIL BORING

NOTE: ORGANICS NOT DETECTED IN WELLS 1035, 1038, 1947, 1950, 1952, 2947, 2949, AND 2953.

NOTE:
Coordinates are in State Planar NAD 1927.
Surface contours based on 1992 flyover.

SCALE (FT)
0 20 40 60

000003

FIGURE 4-4
ORGANICS IN SUBSURFACE SOILS DETECTED ABOVE BACKGROUND IN THE SOLID WASTE LANDFILL

fig0487.dgn

110707-2

1455 (11/04/89)	3.0-3.2	3.75-3.95	UNITS
U234	12.6	2.44	pCi/g
U235/236	0.748	ND	pCi/g
U238	14.6	3.1	pCi/g
U-Total	42.6	10.3	ug/g
Th228	1.52	1.42	pCi/g
Th230	10.3	2.12	pCi/g
Th232	1.29	1.19	pCi/g
Th-Total	11.6	10.7	ug/g
Ra226	5.96	1.3	pCi/g
Ra228	1.27	1.58	pCi/g

1456 (11/04/89)	3.75-3.9	4.25-4.4	UNITS
U234	9.36	22.1	pCi/g
U235/236	0.655	1.12	pCi/g
U238	10.6	22.6	pCi/g
U-Total	27.7	ND	ug/g
Th228	1.07	1.25	pCi/g
Th230	1.37	1.78	pCi/g
Th232	1.03	1.05	pCi/g
Th-Total	9.33	9.44	ug/g
Ra226	0.94	1.18	pCi/g
Ra228	0.90	1.30	pCi/g
Beryllium	1.5	ND	mg/kg
Chromium	24.9	ND	mg/kg

1457 (11/04/89)	4.0-4.2	4.4-4.6	UNITS
U234	26.4	4.06	pCi/g
U235/236	1.66	ND	pCi/g
U238	28.1	4.41	pCi/g
U-Total	71.4	11.9	ug/g
Th228	2.63	1.3	pCi/g
Th230	57.3	2.16	pCi/g
Th232	3.44	1.29	pCi/g
Th-Total	31.0	11.6	ug/g
Ra226	15.7	1.44	pCi/g
Ra228	2.46	1.56	pCi/g

3046 (09/29/87)	100.0-101.5	UNITS
U234	4.33	pCi/g
U238	4.23	pCi/g
U-Total	12.7	ug/g
Th-Total	3.93	ug/g
Tc99	1.1	pCi/g

1972 (03/19/93)	0.5-1.0	2.5-4.0	7.5-9.0	UNITS
Cs137	0.547	ND	ND	pCi/g
Np237	ND	0.37	0.291	pCi/g
Pu239/240	ND	ND	0.030	pCi/g
Pu238	0.059	ND	0.03	pCi/g
U234	7.486	15.2	4.48	pCi/g
U235/236	0.287	0.83	0.26	pCi/g
U238	8.090	15.7	5.0	pCi/g
U-Total	36.2	47.6	14.4	ug/g
Th228	ND	0.94	ND	pCi/g
Th230	ND	4.18	ND	pCi/g
Th232	ND	1.00	ND	pCi/g
Th-Total	ND	9.1	5.43	ug/g
Sr90	ND	1.28	ND	pCi/g
Ra226	31.2	5.14	0.87	pCi/g
Ra228	2.070	1.14	0.93	pCi/g
Arsenic	14.1	10.2	ND	mg/kg

11188 (03/22/93)	5.0-6.0	10.0-10.5	UNITS
Np237	0.077	0.037	pCi/g
Pu238	0.025	ND	pCi/g
Pu239/240	0.015	ND	pCi/g
U234	1.75	ND	pCi/g
U235/236	0.146	ND	pCi/g
U238	1.86	ND	pCi/g
U-Total	6.68	ND	ug/g
Th228	0.979	ND	pCi/g
Th230	1.46	ND	pCi/g
Th232	0.975	ND	pCi/g
Th-Total	8.88	4.99	ug/g
Sr90	2.39	0.789	pCi/g
Ra226	1.42	ND	pCi/g
Ra228	1.31	ND	pCi/g

11186 (03/19/93)	0.5-1.0	4.5-6.5	9.5-11.5	UNITS
Np237	0.167	0.553	0.267	pCi/g
Pu238	0.042	0.044	0.025	pCi/g
Pu239/240	0.031	0.042	ND	pCi/g
U234	9.220	6.05	2.31	pCi/g
U235/236	0.428	0.30	0.153	pCi/g
U238	9.320	6.61	2.73	pCi/g
U-Total	29.0	1.80	17.5	ug/g
Th228	ND	0.991	ND	pCi/g
Th230	3.19	2.00	ND	pCi/g
Th232	ND	0.985	ND	pCi/g
Th-Total	ND	8.98	7.22	ug/g
Sr90	ND	0.815	0.889	pCi/g
Ra226	3.010	1.99	0.948	pCi/g
Ra228	ND	1.10	0.876	pCi/g
Arsenic	9.8	ND	ND	mg/kg
Beryllium	0.820	0.83	ND	mg/kg

1460 (11/06/89)	3.5-3.7	4.25-4.45	UNITS
U234	119.0	75.7	pCi/g
U235/236	20.6	3.77	pCi/g
U238	131.0	78.8	pCi/g
U-Total	394.0	230.0	ug/g
Th228	1.28	1.26	pCi/g
Th230	1.73	3.22	pCi/g
Th232	0.959	1.12	pCi/g
Th-Total	8.65	10.1	ug/g
Ra226	1.06	1.15	pCi/g
Ra228	0.94	ND	pCi/g

11187 (03/19/93)	0.5-1.0	4.0-6.0	9.0-10.5	UNITS
Cs137	0.165	ND	ND	pCi/g
Np237	0.142	0.316	6.53	pCi/g
Pu238	0.042	0.023	0.024	pCi/g
Pu239/240	8.028	0.016	0.034	pCi/g
U234	29.7	ND	3.51	pCi/g
U235/236	1.450	ND	0.113	pCi/g
U238	29.30	ND	4.55	pCi/g
U-Total	91.5	297.0	12.3	ug/g
Th228	2.590	1.28	ND	pCi/g
Th230	3.010	2.61	ND	pCi/g
Th232	1.52	1.29	ND	pCi/g
Th-Total	13.8	11.8	6.53	ug/g
Sr90	ND	ND	0.892	pCi/g
Ra226	1.640	1.21	0.971	pCi/g
Ra228	2.230	1.54	0.934	pCi/g
Beryllium	ND	ND	0.65	mg/kg

1459 (11/06/89)	5.0-5.2	6.0-6.2	UNITS
U234	76.3	57.2	pCi/g
U235/236	4.05	2.73	pCi/g
U238	82.7	60.7	pCi/g
U-Total	228.0	189.0	ug/g
Th228	1.52	1.62	pCi/g
Th230	1.56	2.16	pCi/g
Th232	1.31	1.33	pCi/g
Th-Total	11.8	12.0	ug/g
Ra226	1.6	1.31	pCi/g
Ra228	1.37	1.25	pCi/g
Beryllium	1.4	ND	mg/kg
Chromium	23.8	ND	mg/kg

14.33 (07/29/92)	2.0-2.5	UNITS
U234	41.2	pCi/g
U235/236	2.24	pCi/g
U238	2.24	pCi/g
U-Total	128.0	ug/g
Th228	20.3	pCi/g
Th230	5.86	pCi/g
Th232	17.5	pCi/g
Th-Total	158.0	ug/g
Ra226	7.67	pCi/g
Ra228	19.0	pCi/g
SR90	1.910	pCi/g

TRENCH 1 (06/03/93)	2.9'	UNITS
U-Total	14.3	ug/kg

TRENCH 2 (06/09/93)	5.5'	6.0'	UNITS
U-Total	724	34	ug/kg
Th-Total	ND	3540	ug/kg
Ra226	12	9.3	pCi/g
Ra228	ND	85	pCi/g

1977 (03/19/93)	8.5-10.0	16.5-18.5	UNITS
Cs137	0.07	ND	pCi/g
Np237	0.44	0.112	pCi/g
Pu238	0.05	0.023	pCi/g
Pu239/240	0.030	ND	pCi/g
U234	9.37	1.09	pCi/g
U235/236	0.58	ND	pCi/g
U238	10.4	0.98	pCi/g
U-Total	35.9	3.50	ug/g
Th228	0.91	ND	pCi/g
Th230	1.38	ND	pCi/g
Th232	0.82	0.82	pCi/g
Th-Total	7.43	7.50	ug/g
Ra226	1.16	0.81	pCi/g
Ra228	0.97	0.87	pCi/g
SR90	ND	0.59	pCi/g
Beryllium	0.77	ND	mg/kg

1463 (11/07/89)	3.5-3.7	4.5-4.7	UNITS
U234	19.7	1.15	pCi/g
U235/236	2.55	ND	pCi/g
U238	61.4	1.46	pCi/g
U-Total	121.0	5.52	ug/g
Th228	5.32	1.22	pCi/g
Th230	4.39	2.01	pCi/g
Th232	ND	1.16	pCi/g
Th-Total	6.62	10.4	ug/g
Ra226	0.94	1.51	pCi/g
Ra228	ND	1.26	pCi/g
Arsenic	ND	1.26	mg/kg

1458 (11/06/89)	3.8-4.0	4.5-4.7	UNITS
U234	24.2	22.4	pCi/g
U235/236	1.58	1.18	pCi/g
U238	23.7	23.6	pCi/g
U-Total	76.1	59.8	ug/g
Th228	1.78	2.06	pCi/g
Th230	3.18	4.41	pCi/g
Th232	1.74	1.87	pCi/g
Th-Total	15.7	16.9	ug/g
Ra226	1.48	1.41	pCi/g
Ra228	ND	1.95	pCi/g

2385 (04/20/90)	4.5-6.0	43.0-46.5	UNITS
U234	0.981	ND	pCi/g
U-Total	ND	4.63	ug/g
Th-Total	5.88	ND	ug/g
Sr90	1.34	ND	pCi/g

1975 (03/19/93)	0.5-1.0	4.0-5.0	8.5-10.5	UNITS
Np237	ND	0.269	0.167	pCi/g
Pu238	0.050	0.048	0.306	pCi/g
Pu239/240	ND	0.021	ND	pCi/g
U234	9.86	2.49	0.977	pCi/g
U235/236	0.440	ND	ND	pCi/g
U238	10.2	2.74	1.04	pCi/g
U-Total	29.7	11.6	4.82	ug/g
Th228	ND	1.2	ND	pCi/g
Th230	4.060	1.69	ND	pCi/g
Th232	ND	1.17	ND	pCi/g
Th-Total	ND	10.7	7.16	ug/g
Ra226	1.510	1.26	1.12	pCi/g
Ra228	ND	1.42	1.08	pCi/g
Sr90	ND	7.57	ND	pCi/g
Beryllium	ND	0.85	ND	mg/kg

1464 (11/08/89)	3.75-3.95	4.5-4.7	UNITS
U234	1.09	1.96	pCi/g
U238	1.37	1.76	pCi/g
U-Total	ND	5.03	ug/g
Th228	0.983	1.48	pCi/g
Th230	1.46	1.82	pCi/g
Th232	0.833	1.23	pCi/g
Th-Total	7.51	11.1	ug/g
Ra226	ND	1.44	pCi/g
Ra228	ND	1.26	pCi/g

2065 (09/29/87)	13.5-15.0	UNITS
U234	1.2	pCi/g
U238	1.3	pCi/g
Th228	1.0	pCi/g
Th230	1.6	pCi/g

1971 (03/22/93)	0.5-1.0	4.5-6.5	9.5-11.0	UNITS
Np237	0.077	ND	ND	ND
Pu238	0.016	0.034	ND	pCi/g
Pu239/240	0.021	ND	0.021	ND
U234	5.05	1.07	0.949	pCi/g
U235/236	0.261	ND	ND	ND
U238	4.84	1.34	1.04	pCi/g
U-Total	16.7	2.58	5.68	ug/g
Ra226	ND	1.25	0.90	pCi/g
Ra228	ND	1.54	0.965	pCi/g
Beryllium	0.780	ND	ND	pCi/g
SR90	ND	ND	1.78	pCi/g

1462 (11/07/89)	4.25-4.4	5.0-5.2	UNITS
U234	5.04	4.71	pCi/g
U238	6.21	4.70	pCi/g
U-Total	19.4	14.8	ug/g
Th228	0.982	1.27	pCi/g
Th230	3.33	2.06	pCi/g
Th232	1.05	1.27	pCi/g
Th-Total	9.45	11.5	ug/g
Ra226	1.3	1.38	pCi/g
Ra228	ND	1.37	pCi/g
Chromium	24	ND	mg/kg

1461 (11/07/89)	4.0-4.2	5.0-5.2	UNITS
U234	4.74	1.49	pCi/g
U238	5.58	1.42	pCi/g
U-Total	19.1	5.17	ug/g
Th228	1.27	1.72	pCi/g
Th230	4.12	2.13	pCi/g
Th232	1.05	1.40	pCi/g
Th-Total	9.46	12.6	ug/g
Ra226	1.23	1.65	pCi/g
Ra228	1.06	1.41	pCi/g

1465 (11/04/89)	3.5-3.7	4.5-4.7	UNITS
U234	1.68	3.27	pCi/g
U235/236	0.757	ND	pCi/g
U238	1.09	3.5	pCi/g
U-Total	ND	4.26	ug/g
Th228	1.12	1.22	pCi/g
Th230	1.3	1.41	pCi/g
Th232	0.969	0.856	pCi/g
Th-Total	8.75	7.73	ug/g
Ra226	ND	1.3	pCi/g
Ra228	ND	1.31	pCi/g
Beryllium	1.3	ND	mg/kg
Chromium	25.3	ND	mg/kg

TRENCH 4 (06/16/93)	3.5'	UNITS
U-Total	951	ug/kg

1466 (11/08/89)	3.0-3.2	4.5-4.7	UNITS
U234	1.13	4.71	pCi/g
U238	1.26	5.36	pCi/g
U-Total	ND	4.72	ug/g
Th228	ND	1.35	pCi/g
Th230	1.3	1.44	pCi/g
Th232	0.84	1.14	pCi/g
Th-Total	7.58	10.3	ug/g
Ra226	ND	1.56	pCi/g
Ra228	ND	1.46	pCi/g
SR90	ND	0.920	pCi/g

1467 (11/14/89)	2.5-2.7	3.5-3.7	UNITS
U234	13.82	0.965	pCi/g
U238	4.14	1.32	pCi/g
U-Total	11.38	8.59	ug/g
Th228	0.983	1.12	pCi/g
Th230	1.7	1.99	pCi/g
Th232	ND	1.18	pCi/g
Th-Total	6.35	10.6	ug/g
Ra226	ND	1.56	pCi/g
Ra228	1.05	1.35	pCi/g

1468 (11/14/89)	2.5-2.7	3.5-3.7	UNITS
U234	3.42	1.31	pCi/g
U238	3.56	1.32	pCi/g
U-Total	12.26	ND	ug/g
Th228	0.909	1.19	pCi/g
Th230	1.61	1.82	pCi/g
Th232	ND	1.13	pCi/g
Th-Total	6.97	10.2	ug/g
Ra226	0.94	1.58	pCi/g
Ra228	0.9	ND	pCi/g

1969 (03/22/93)	0.5-1.0	4.5-6.0	9.0-10.5	UNITS
Np237	0.356	0.034	0.034	pCi/g
Pu238	0.068	ND	0.058	pCi/g
Pu239/240	0.083	ND	ND	pCi/g
U234	3.24	1.44	ND	pCi/g
U235/236	0.241	0.766	ND	pCi/g
U238	3.7	1.76	ND	pCi/g
U-Total	9.85	4.82	3.47	ug/g
Ra226	ND	0.918	0.927	pCi/g
Ra228	1.320	ND	ND	pCi/g
Beryllium	ND	ND	0.66	mg/kg
Sr90	ND	0.650	0.666	pCi/g

1964 (03/22/93)	5.0-6.5	29.0-30.5	UNITS
Np237	0.07	ND	pCi/g
U234	2.59	ND	pCi/g
U238	2.91	ND	pCi/g
U-Total	16.7	10.3	ug/g
Th228	0.9	ND	pCi/g
Th230	1.77	1.37	pCi/g
Th-Total	6.92	3.0	ug/g
Ra226	1.23	ND	pCi/g
Ra228	0.86	ND	pCi/g
Beryllium	1.23	ND	mg/kg
Chromium	0.86	ND	mg/kg
SR90	0.789	ND	pCi/g
Pu239/240	0.030	ND	pCi/g

1967 (03/22/93)	0.5-1.0	4.5-5.5	29.5-31.0	UNITS
Cs137	0.237	ND	ND	pCi/g
Np237	0.166	ND	ND	pCi/g
Pu238	0.096	ND	ND	pCi/g
U234	2.350	2.5	ND	pCi/g
U235/236	ND	0.16	ND	pCi/g
U238	2.360	2.56	0.859	pCi/g
U-Total	7.340	15.3	9.17	ug/g
Th228	ND	ND	0.995	pCi/g
Th230	1.7	4.35	1.96	pCi/g
Th232	ND	0.84	ND	pCi/g
Th-Total	ND	7.66	7.32	ug/g
Ra226	ND	1.07	1.02	pCi/g
Ra228	ND	1.04	0.899	pCi/g

1965 (03/22/93)	4.0-6.0	26.5-28.0	UNITS
Np237	0.032	ND	pCi/g
Pu238	0.097	ND	pCi/g
U234	3.07	ND	pCi/g
U235/236	0.0996	ND	pCi/g
U238	3.04	ND	pCi/g
U-Total	20.6	9.81	ug/g
Th230	2.01	ND	pCi/g
Th-Total	7.53	ND	ug/g
Ra226	1.12	ND	pCi/g
Ra228	1.12	ND	pCi/g

1968 (03/22/93)	0.5-1.0	4.5-6.5	15.5-16.5	UNITS
Cs137	0.311	ND	ND	pCi/g
Np237	0.116	0.075	0.119	pCi/g
Pu238	ND	0.103	ND	pCi/g
U234	9.130	1.36	0.959	pCi/g
U235/236	0.474	ND	ND	pCi/g
U238	9.41	1.71	0.993	pCi/g
U-Total	30.0	14.9	12.2	ug/g
Th228	ND	0.915	ND	pCi/g
Th230	1.930	1.25	ND	pCi/g
Th232	ND	0.967	ND	pCi/g
Th-Total	ND	8.9	5.23	ug/g
Ra226	ND	1.17	0.863	pCi/g
Ra228	ND	0.959	ND	pCi/g
Beryllium	ND	1.6	ND	mg/kg
Chromium		21.3	ND	mg/kg

1966 (03/22/93)	0.5-1.0	4.5-6.5	24.0-25.0	UNITS
Cs137	0.301	ND	ND	pCi/g
Pu238	0.052	ND	ND	pCi/g
Pu239/240	0.045	ND	ND	pCi/g
Np237	0.283	ND	0.07	pCi/g
U234	8.05	1.78	0.884	pCi/g
U235/236	0.473	ND	ND	pCi/g
U238	10.6	1.9	1.01	pCi/g
U-Total	31.72	13.9	12.6	ug/g
Th228	2.86	ND	ND	pCi/g
Th230	4.65	ND	ND	pCi/g
Th232	2.86	ND	ND	pCi/g
Th-Total	26.0	ND	ND	ug/g
Ra226	ND	1.84	1.26	pCi/g
Ra228	3.38	1.15	0.913	pCi/g
Beryllium	ND	0.74	0.73	mg/kg
Sr90	ND	0.861	0.963	pCi/g

1978 (03/22/93)	0.5-1.0	9.5-11.0	13.5-15.0	UNITS
Np237	0.219	0.046	ND	pCi/g
Pu238	0.047	0.74	ND	pCi/g
U234	3.190	ND	0.971	pCi/g
U235/236	0.169	ND	ND	pCi/g
U238	3.46	ND	0.897	pCi/g
U-Total	10.70	5.76	4.74	ug/g
Ra226	1.510	1.12	0.872	pCi/g
Ra228	ND	1.41	0.984	pCi/g
Sr90	0.57	ND	ND	pCi/g
Beryllium	ND	1	ND	mg/kg

1470 (11/16/89)	3.0-3.2	4.2-4.4	UNITS
U234	3.79	1.51	pCi/g
U238	4.04	1.61	pCi/g
U-Total	11.6	5.06	ug/g
Th228	1.1	1.05	pCi/g
Th230	1.94	1.63	pCi/g
Th232	1.08	0.903	pCi/g
Th-Total	9.7	8.15	ug/g
Tc99	ND	0.9	pCi/g
Sr90	ND	0.66	pCi/g

1471 (11/16/89)	4.25-4.4	5.5-5.7	UNITS
U234	1.52	1.04	pCi/g
U238	2.12	1.35	pCi/g
U-Total	6.89	5.24	ug/g
Th228	ND	1.24	pCi/g
Th230	ND	1.9	pCi/g
Th232	0.85	1.0	pCi/g
Th-Total	7.67	9.05	ug/g
Ra226	1.24	ND	pCi/g
Ra228	0.994	1.09	pCi/g
Tc99	0.9	ND	pCi/g

2045 (12/05/88)	21.5-23.0	UNITS
U-Total	2.0	ug/g

1472 (11/16/89)	4.25-4.4	5.0-5.2	UNITS
U234	3.46	2.13	pCi/g
U238	3.64	2.06	pCi/g
U-Total	10.2	9.9	ug/g
Th228	0.999	1.07	pCi/g
Th230	2.85	1.65	pCi/g
Th232	0.895	1.05	pCi/g
Th-Total	8.08	9.49	ug/g
Ra226	1.33	ND	pCi/g
Ra228	0.961	ND	pCi/g

1469 (11/14/89)	2.5-2.7	3.5-3.7	UNITS
U234	2.59	1.14	pCi/g
U238	3.18	1.38	pCi/g
U-Total	10.89	4.96	ug/g
Th228	ND	0.954	pCi/g
Th230	ND	1.19	pCi/g
Th232	ND	0.865	pCi/g
Th-Total	4.88	7.99	ug/g
Ra226	0.9	1.27	pCi/g
Ra228	0.74	1.39	pCi/g

LEGEND

- 575 — ELEVATION CONTOURS
- ROADS
- STREAM
- DRAINAGE
- FENCE
- 1000 MONITORING WELLS
- 2000 MONITORING WELLS
- 3000 MONITORING WELLS
- SOIL BORING
- SOIL BORING

ND = NOT DETECTED ABOVE BACKGROUND CONCENTRATIONS

NOTE:
Coordinates are in State Planar NAD 1927.
Surface contours based on 1992 flyover.

N

SCALE (FT)
0 100 200

000004

FIGURE 4-19
RADIONUCLIDES, AND METALS OF CONCERN IN SUBSURFACE SOIL DETECTED ABOVE BACKGROUND IN THE SOUTH FIELD

fig0422.dgn

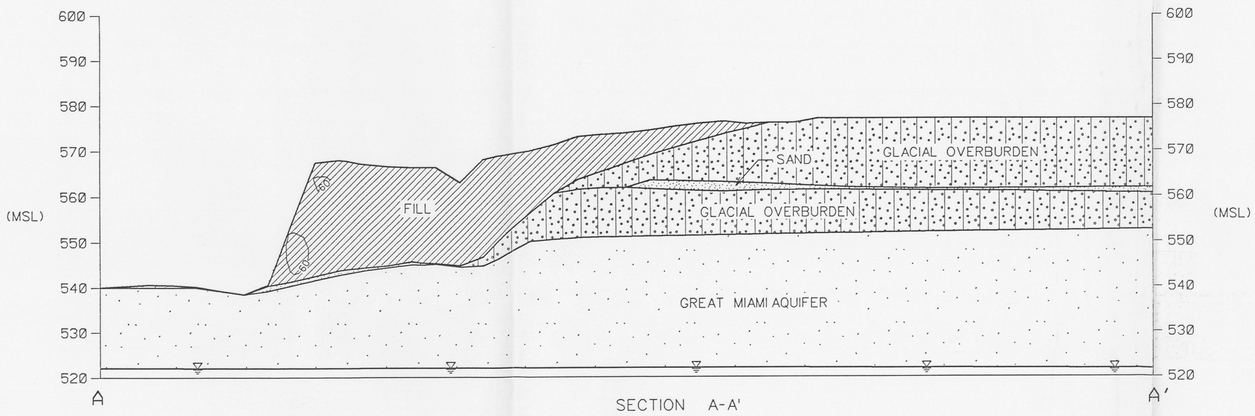

SECTION A-A'

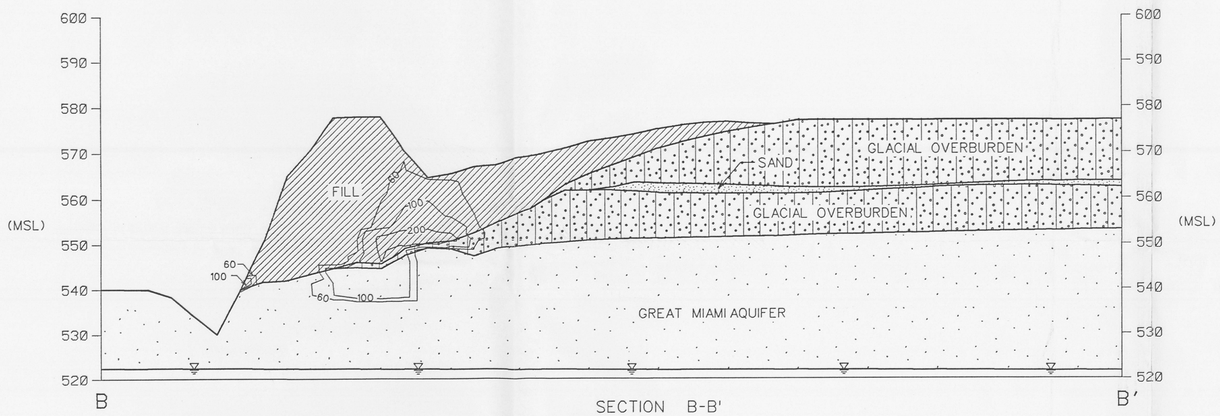

SECTION B-B'

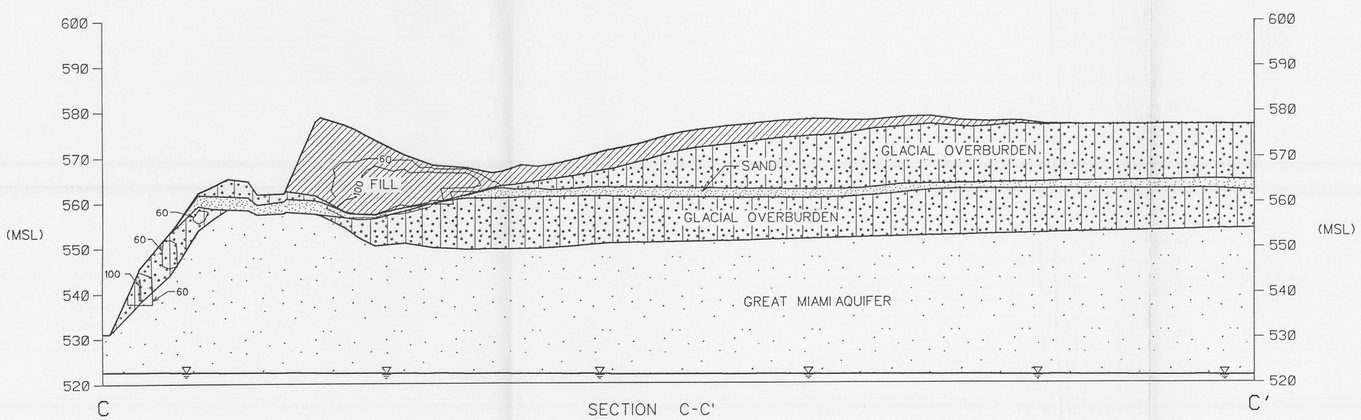

SECTION C-C'

NOTE: (MSL) INDICATES MEAN SEA LEVEL ELEVATIONS

0 80 160
SCALE, SECTIONS (FT)
Vertical Exaggeration = 5 to 1

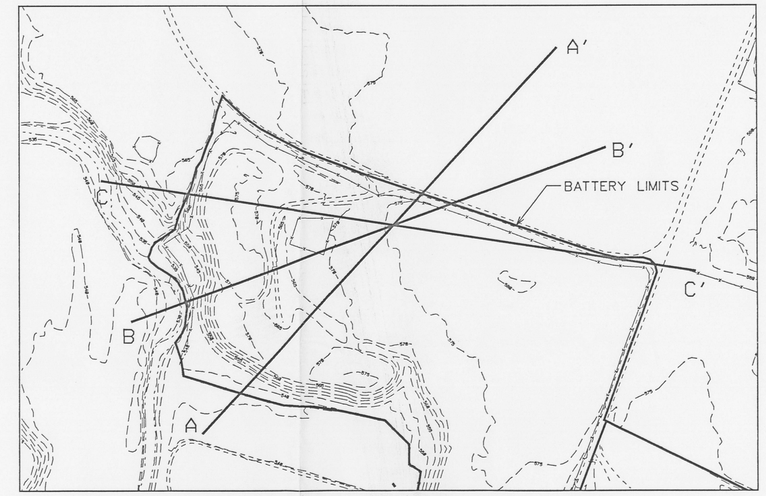

CROSS SECTION LOCATION KEY (1"=160')

MODEL LEVEL	FROM	TO	15 pCi/g		60 pCi/g		200 pCi/g		500 pCi/g	
			VOLUME	AVG U-238	VOLUME	AVG U-238	VOLUME	AVG U-238	VOLUME	AVG U-238
			Cu. ft.	pCi/g	Cu. ft.	pCi/g	Cu. ft.	pCi/g	Cu. ft.	pCi/g
25	532.5	535.0	3125	140.9	1563	257.2	1563	257.2		
24	535.0	537.5	14063	147.8	4063	147.8				
23	537.5	540.0	60938	126.4	57813	131.7				
22	540.0	542.5	78125	111.1	62500	132.8	1563	208.5		
21	542.5	545.0	89063	97.2	57813	132.3				
20	545.0	547.5	109375	85.0	65625	123.0	4688	333.9	1563	560.4
19	547.5	550.0	110938	114.0	64063	172.1	12500	449.8	4688	761.0
18	550.0	552.5	212500	107.0	92188	207.5	26563	465.8	9375	773.3
17	552.5	555.0	260938	87.8	93750	197.6	25000	443.7	7813	726.9
16	555.0	557.5	270313	93.3	82813	246.2	37500	421.1	10938	668.6
15	557.5	560.0	462500	71.8	01250	270.3	50000	372.1	10938	616.2
14	560.0	562.5	229688	102.4	78125	247.1	39063	374.9	9375	610.8
13	562.5	565.0	229688	98.5	82813	223.9	35938	364.8	7813	586.4
12	565.0	567.5	214063	88.3	65625	226.3	29688	363.8	4688	589.7
11	567.5	570.0	185938	73.4	45313	217.2	21875	324.6	1563	564.1
10	570.0	572.5	150000	67.2	23438	288.5	17188	343.8	1563	538.1
9	572.5	575.0	157813	25.1	1563	60.5				
8	575.0	577.5	176563	36.0	28125	81.1				
7	577.5	580.0	67188	48.8	23438	75.2				
			3082813	83.0	1021875	194.3	303125	387.1	70313	661.0

LEGEND
- ELEVATION CONTOURS
- ROADS
- STREAM
- DRAINAGE
- FENCE
- AVERAGE GROUNDWATER ELEVATION
- 60 CONTAMINATION LEVELS OF U-238 (pCi/g)

N

NOTE:
Coordinates are in State Planar NAD 1927.
Surface contours based on 1992 flyover.

000005

FIGURE 4-21
CONCEPTUAL MODEL FOR SUBSURFACE DISTRIBUTION OF U-238 CONTAMINATION SOUTH FIELD/ INACTIVE FLYASH PILE

fig0420.dgn

110707_4

SWL-SS-09	04/02/93	
		UNITS
Np237	0.064	pCi/g
Pu238	0.019	pCi/g
U234	6.7	pCi/g
U235/236	0.398	pCi/g
U238	8.21	pCi/g
U-Total	27.5	ug/g
Th230	3.88	pCi/g
Ra226	2.26	pCi/g
SR90	1.440	pCi/g
Beryllium	0.85	mg/kg
Pyrene	49	ug/kg
Pu239/240	0.032	pCi/g

SWL-SS-10	04/02/93	
		UNITS
Np237	0.046	pCi/g
Pu238	0.097	pCi/g
U234	2.28	pCi/g
U238	2.90	pCi/g
U-Total	10.5	ug/g
Ra228	1.21	pCi/g
SR90	0.527	pCi/g
Acetone	3	ug/kg
Beryllium	0.97	mg/kg
Pu239/240	0.026	pCi/g

ASIT-021				
	SAMPLE 8100 07/11/88	SAMPLE 1160 02/21/89	SAMPLE 1161 02/21/89	UNITS
U234	ND	7.3	6.1	pCi/L
U238	ND	13.7	9.7	pCi/L
U-Total	24.0	42.0	26.0	ug/L

SWL-SS-11	04/02/93	
		UNITS
U234	4.97	pCi/g
U235/236	0.288	pCi/g
U238	6.68	pCi/g
U-Total	19.5	ug/g
Acetone	5	ug/kg
bis(2-Ethylhexyl) phthalate	43	ug/kg
Pu239/240	0.023	pCi/g

SWL-SS-12	04/02/93	
		UNITS
Np237	3.11	pCi/g
Pu238	0.33	pCi/g
U234	5.46	pCi/g
U235/236	0.346	pCi/g
U238	5.58	pCi/g
U-Total	18.7	ug/g
Ra228	2.07	pCi/g
SR90	1.070	pCi/g
Beryllium	0.63	mg/kg

SWL-SW-01	04/07/93	
		UNITS
U234	17.2	pCi/L
U235/236	1.3	pCi/L
U238	18.7	pCi/L
U-Total	46.1	ug/L
bis(2-Ethylhexyl) phthalate	1.0	ug/L

SWL-SD-01	04/08/93	
		UNITS
SR90	0.990	pCi/g
U234	3.66	pCi/g
U235/236	0.250	pCi/g
U238	4.56	pCi/g
U-Total	14.7	ug/g
Pyrene	58	ug/kg
Pu239/240	0.039	pCi/g
Pu238	0.036	pCi/g
Np237	0.62	pCi/g

SWL-SW-02	04/06/93	
		UNITS
U234	17.1	pCi/L
U235/236	0.846	pCi/L
U238	20.2	pCi/L
U-Total	59.3	ug/L

SWL-SD-02	04/06/93	
		UNITS
SR90	0.590	pCi/g
U234	4.18	pCi/g
U238	6.80	pCi/g
U-Total	22.6	ug/g
Acenophthene	98	ug/kg
Anthracene	240	ug/kg
Benzo(a)anthracene	500	ug/kg
Benzo(a)pyrene	550	ug/kg
Benzo(b)fluoranthene	730	ug/kg
Benzo(g,h,i)perylene	240	ug/kg
Benzo(k)fluoranthene	270	ug/kg
Carbazole	120	ug/kg
Chrysene	510	ug/kg
Fluoranthene	1400	ug/kg
Indeno(1,2,3-cd)pyrene	310	ug/kg
Phenanthrene	1000	ug/kg
Pyrene	990	ug/kg
bis(2-Ethylhexyl) phthalate	53	ug/kg

SWL-SS-08	04/19/93	
		UNITS
Np237	0.075	pCi/g
Pu238	0.902	pCi/g
U234	12.4	pCi/g
U235/236	0.809	pCi/g
U238	26.9	pCi/g
U-Total	97.0	ug/g
Th230	3.13	pCi/g
Ra228	1.45	pCi/g
Benzo(a)anthracene	79	ug/kg
Benzo(a)pyrene	67	ug/kg
Benzo(b)fluoranthene	64	ug/kg
Benzo(k)fluoranthene	75	ug/kg
Chrysene	94	ug/kg
Fluoranthene	200	ug/kg
Indeno(1,2,3-cd)pyrene	46	ug/kg
Phenanthrene	120	ug/kg
Pyrene	170	ug/kg
Pu239/240	0.113	pCi/g

SWL-SS-06	04/01/93	
		UNITS
Pu238	0.049	pCi/g
U234	1.83	pCi/g
U238	2.43	pCi/g
U-Total	9.77	pCi/g
SR90	0.789	pCi/g
4,4'-DDE	12	ug/kg
Acenophthene	49	ug/kg
Anthracene	120	ug/kg
Benzo(a)anthracene	220	ug/kg
Benzo(a)pyrene	190	ug/kg
Benzo(b)fluoranthene	150	ug/kg
Benzo(g,h,i)perylene	100	ug/kg
Benzo(k)fluoranthene	210	ug/kg
Chrysene	250	ug/kg
Dibenzo(a,h)anthracene	56	ug/kg
Fluoranthene	530	ug/kg
Fluorene	56	ug/kg
Indeno(1,2,3-cd)pyrene	100	ug/kg
Phenanthrene	470	ug/kg
Pyrene	660	ug/kg
bis(2-Ethylhexyl) phthalate	43	ug/kg

SWL-SS-04	04/01/93	
		UNITS
Pu238	0.207	pCi/g
U234	22.2	pCi/g
U235/236	1.26	pCi/g
U238	29.4	pCi/g
U-Total	90.8	ug/g
Th228	2.33	pCi/g
Th230	2.14	pCi/g
Th232	2.5	pCi/g
Th-Total	22.8	ug/g
Ra228	2.99	pCi/g
SR90	1.09	pCi/g
Benzo(a)anthracene	140	ug/kg
Benzo(a)pyrene	140	ug/kg
Benzo(b)fluoranthene	140	ug/kg
Benzo(g,h,i)perylene	93	ug/kg
Benzo(k)fluoranthene	140	ug/kg
Beryllium	0.72	mg/kg
Chrysene	180	ug/kg
Di-n-butylphthalate	55	ug/kg
Fluoranthene	300	ug/kg
Indeno(1,2,3-cd)pyrene	91	ug/kg
Phenanthrene	150	ug/kg
Pyrene	300	ug/kg

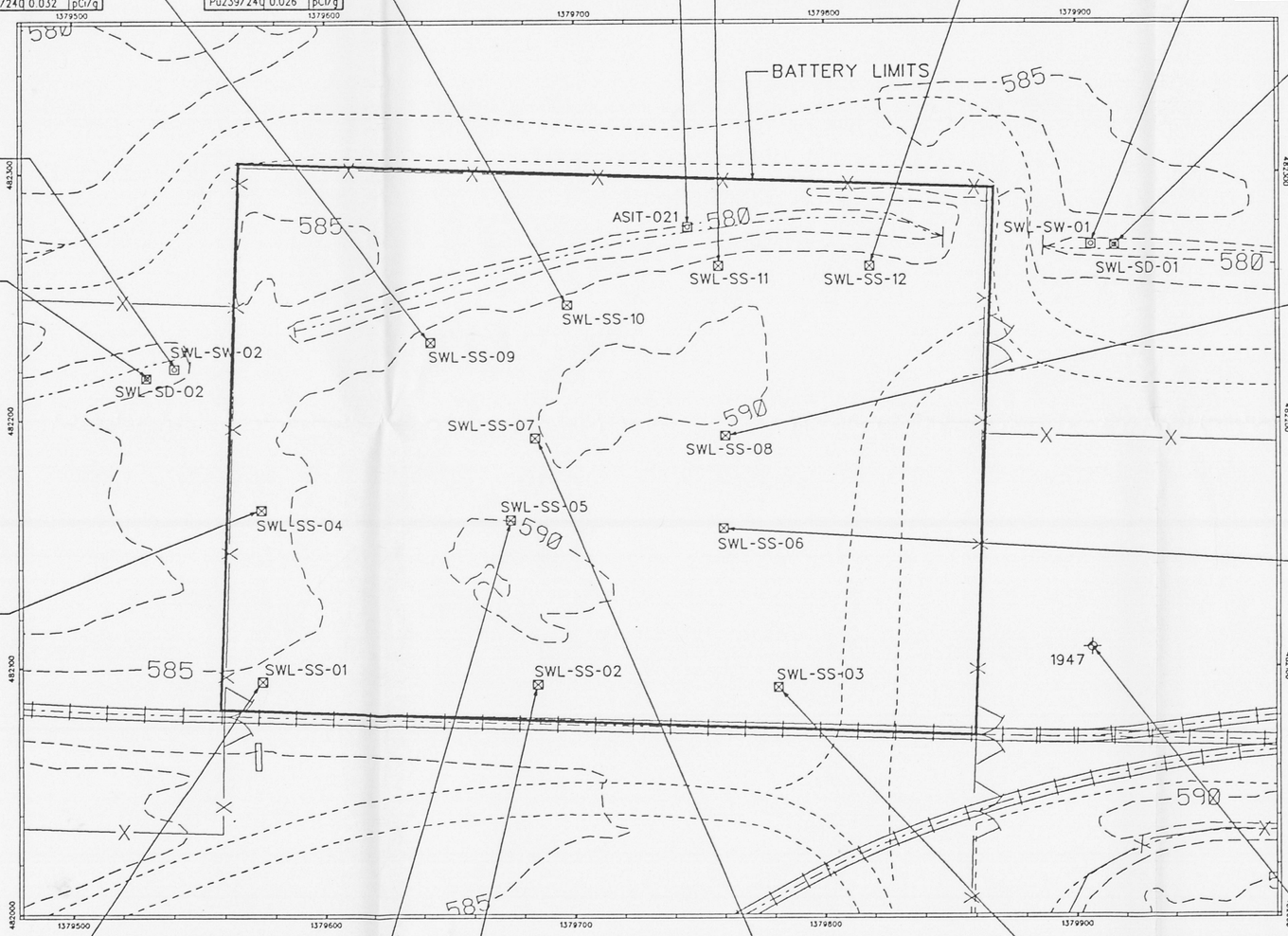

SWL-SS-01	04/01/93	
		UNITS
U234	5.94	pCi/g
U235/236	0.512	pCi/g
U238	13.6	pCi/g
U-Total	39.8	ug/g
Th230	2.21	pCi/g
SR90	0.580	pCi/g
2-Butanone	1	ug/kg
Acenophthene	120	ug/kg
Acetone	1	ug/kg
Anthracene	230	ug/kg
Benzo(a)anthracene	880	ug/kg
Benzo(a)pyrene	760	ug/kg
Benzo(b)fluoranthene	710	ug/kg
Benzo(g,h,i)perylene	500	ug/kg
Benzo(k)fluoranthene	880	ug/kg
Carbazole	77	ug/kg
Chrysene	1100	ug/kg
Dibenzo(a,h)anthracene	200	ug/kg
Dibenzofuran	56	ug/kg
Fluoranthene	1900	ug/kg
Fluorene	100	ug/kg
Indeno(1,2,3-cd)pyrene	480	ug/kg
Phenanthrene	1500	ug/kg
Pyrene	2100	ug/kg

SWL-SS-05	04/01/93	
		UNITS
Np237	0.194	pCi/g
Pu238	0.072	pCi/g
U234	48.9	pCi/g
U235/236	3.33	pCi/g
U238	49.4	pCi/g
U-Total	143	ug/g
Th230	9.61	pCi/g
Th-Total	11.4	ug/g
Ra226	1.59	pCi/g
Benzo(a)anthracene	55	ug/kg
Benzo(a)pyrene	59	ug/kg
Benzo(k)fluoranthene	78	ug/kg
Chrysene	77	ug/kg
Fluoranthene	130	ug/kg
Phenanthrene	90	ug/kg
Pyrene	130	ug/kg
bis(2-Ethylhexyl) phthalate	48	ug/kg
Ra228	1.3	pCi/g
Pu239/240	0.126	pCi/g
Arsenic	8.3	mg/kg

SWL-SS-02	04/01/93	
		UNITS
Np237	0.115	pCi/g
Pu238	0.0573	pCi/g
U234	13.5	pCi/g
U235/236	0.816	pCi/g
U238	34.6	pCi/g
U-Total	114	ug/g
Th230	3.74	pCi/g
SR90	1.230	pCi/g
Acetone	2	ug/kg
Chrysene	45	ug/kg
Fluoranthene	57	ug/kg
Pyrene	55	ug/kg
Pu239/240	0.019	pCi/g

SWL-SS-07	04/02/93	
		UNITS
Np237	0.0457	pCi/g
Pu238	0.023	pCi/g
SR90	1.050	pCi/g
U234	1.43	pCi/g
U238	2.34	pCi/g
U-Total	6.86	ug/g
Benzo(k)fluoranthene	42	ug/kg
Chrysene	49	ug/kg
Fluoranthene	85	ug/kg
Phenanthrene	59	ug/kg
Pyrene	130	ug/kg
bis(2-Ethylhexyl) phthalate	40	ug/kg

SWL-SS-03	04/01/93	
		UNITS
Np237	0.147	pCi/g
Pu238	0.095	pCi/g
U234	33.1	pCi/g
U235/236	1.92	pCi/g
U238	63.8	pCi/g
U-Total	194	ug/g
Th230	3.24	pCi/g
Ra228	1.28	pCi/g
Benzo(a)anthracene	110	ug/kg
Benzo(a)pyrene	110	ug/kg
Benzo(b)fluoranthene	96	ug/kg
Benzo(g,h,i)perylene	82	ug/kg
Benzo(k)fluoranthene	150	ug/kg
Bromomethane	2	ug/kg
Chloromethane	2	ug/kg
Chrysene	150	ug/kg
Fluoranthene	260	ug/kg
Indeno(1,2,3-cd)pyrene	73	ug/kg
Phenanthrene	150	ug/kg
Pyrene	260	ug/kg
Pu239/240	0.085	pCi/g

1947	04/28/93	
		UNITS
U-Total	70 *	ug/L

LEGEND

- 575 — ELEVATION CONTOURS
- ROADS
- DRAINAGE
- FENCE
- RAILROAD
- 1000 MONITORING WELLS
- SURFACE SAMPLE
- SURFACE WATER SAMPLE
- SEDIMENT SAMPLE

ND = NOT DETECTED ABOVE BACKGROUND CONCENTRATIONS

* INDICATES RESULTS OF ON-SITE LABORATORY SCREENING FOR TOTAL URANIUM

NOTE:
Coordinates are in State Planar NAD 1927.
Surface contours based on 1992 flyover.

SCALE (FT)
0 40 80

000006

FIGURE 4-2
RADIONUCLIDES, METALS OF CONCERN, AND ORGANICS IN SURFACE WATER, SEDIMENT AND SURFACE SOIL SAMPLES DETECTED ABOVE BACKGROUND IN THE SOLID WASTE LANDFILL

fig0405.dgn

110707_5

1991	05/06/93		
	7.5-10.0	12.5-15.0	UNITS
U234	2.61	ND	pCi/g
U238	6.27	0.95	pCi/g
U235/236	0.2	ND	pCi/g
U-Total	25.4	3.24	ug/g
Th232	0.96	ND	pCi/g
Th-Total	8.83	ND	ug/g
Ra226	1.14	1.04	pCi/g
Ra228	1.05	0.86	pCi/g
Np237	0.25	0.30	pCi/g
Pu238	0.06	0.070	pCi/g
Pu239/240	0.03	0.070	pCi/g
Arsenic	13.9	ND	pCi/g
Beryllium	0.69	0.84	mg/kg

11041	05/19/93		
	0.0-2.5	12.5-15.0	UNITS
U234	8.27	ND	pCi/g
U238	12.5	ND	pCi/g
U235/236	0.382	ND	pCi/g
U-Total	40.7	4.71	ug/g
Th228	2.09	ND	pCi/g
Th230	1.74	ND	pCi/g
Th232	1.75	ND	pCi/g
Th-Total	16	ND	ug/g
Ra226	1.16	1.15	pCi/g
Ra228	2.14	ND	pCi/g
TC-99	0.754	ND	pCi/g
Np237	0.34	1.10	pCi/g
Pu238	0.10	0.040	pCi/g
Pu239/240	0.060	0.038	pCi/g

1719	08/07/91				
	1.5-3.0	10.5-12.0	16.5-18.0	12.5-14.0	UNITS
Np237	ND	0.6	ND	ND	pCi/g
Pu238	ND	0.6	ND	ND	pCi/g
U234	5.53	20.5	0.91	ND	pCi/g
U238	8.66	141.0	1.59	ND	pCi/g
U235/236	1.23	0.6	ND	ND	pCi/g
U-Total	10.6	393.0	19.7	ND	ug/g
Th228	1.24	ND	1.12	ND	pCi/g
Th230	1.88	ND	ND	ND	pCi/g
Ra226	1.24	ND	ND	ND	pCi/g
Ra228	1.1	ND	ND	ND	ug/g
Beryllium	ND	ND	ND	0.71	mg/kg
SR90	0.860	1.10	1.16	ND	pCi/g

11040	05/20/93		
	2.5-5.0	12.5-15.0	UNITS
U234	1.32	ND	pCi/g
U238	1.84	0.9	pCi/g
U235/236	0.1	ND	pCi/g
U-Total	8.49	ND	ug/g
Ra226	1.22	0.92	pCi/g
Ra228	1.13	0.9	pCi/g
Beryllium	0.69	0.65	mg/kg
Arsenic	ND	10.4	mg/kg

1992	05/11/93		
	7.5-10.0	17.5-20.0	UNITS
U234	18.2	0.901	pCi/g
U238	60.4	1.17	pCi/g
U-Total	191	3.5	ug/g
Th228	1.51	ND	pCi/g
Th230	2.05	ND	pCi/g
Th232	1.32	0.877	pCi/g
Th-Total	12.0	8.07	ug/g
Ra226	1.19	0.899	pCi/g
Ra228	1.39	1.01	pCi/g
Beryllium	1.5	1.4	mg/kg
Np237	0.117	0.351	pCi/g
Pu239/240	0.36	0.112	pCi/g
Pu238	0.106	ND	pCi/g
Cs137	0.101	ND	pCi/g

1720	08/10/91				
	1.5-3.0	3.0-4.5	7.5-9.0	9.0-10.5	UNITS
U234	18.5	ND	1.35	1.24	pCi/g
U238	45.2	ND	3.54	1.81	pCi/g
U235/236	1.27	ND	ND	ND	pCi/g
U-Total	150	ND	13	5.83	ug/g
SR90	1.58	ND	3.090	ND	pCi/g
Th228	2.1	ND	1.17	2.02	pCi/g
Th230	3.46	ND	2.51	1.89	pCi/g
Ra226	1.06	ND	1.01	1.55	pCi/g
Ra228	1.35	ND	1.07	1.48	pCi/g
Arsenic	ND	ND	ND	15.4	pCi/g
Beryllium	ND	0.99	0.84	0.95	mg/kg

1993	05/11/93		
	2.5-5.0	15.0-17.5	UNITS
Np237	0.252	0.087	pCi/g
Pu238	0.023	0.034	pCi/g
Pu239/240	0.023	ND	pCi/g
U234	7.33	0.906	pCi/g
U238	15.3	0.973	pCi/g
U235/236	0.382	ND	pCi/g
U-Total	38.9	3.02	ug/g
Th228	0.904	ND	pCi/g
Th230	6.72	ND	pCi/g
Th232	0.88	ND	pCi/g
Th-Total	8.1	ND	ug/g
Ra226	1.165	0.944	pCi/g
Ra228	1.21	0.884	pCi/g
Beryllium	0.72	ND	mg/kg

11039	05/19/93		
	2.5-5.0	12.0-14.0	UNITS
U234	97	1.1	pCi/g
U238	119	1.18	pCi/g
U235/236	5.72	ND	pCi/g
U-Total	375	6.08	ug/g
Th228	1.02	2.98	pCi/g
Th230	4.3	4.7	pCi/g
Th232	ND	5.16	pCi/g
TC-99	0.84	ND	pCi/g
Th-Total	ND	47.0	ug/g
Ra226	0.824	0.824	pCi/g
Ra228	1.06	ND	pCi/g
Pu239/240	0.080	ND	pCi/g
Pu238	0.14	ND	pCi/g
Cs137	0.38	ND	pCi/g
Np237	0.19	ND	pCi/g
TC-99	0.84	ND	pCi/g
Arsenic	ND	11.5	mg/kg

1982	05/06/93		
	10.0-2.5	7.0-7.5	UNITS
U234	11.3	ND	pCi/g
U238	20.3	ND	pCi/g
U-Total	64.8	4.83	ug/g
Th228	1.19	ND	pCi/g
Th230	1.76	ND	pCi/g
Th232	1.02	ND	pCi/g
Th-Total	9.31	ND	ug/g
Ra226	1.3	0.93	pCi/g
Ra228	1.19	ND	pCi/g
Np237	ND	0.310	pCi/g
Pu238	ND	0.09	pCi/g
Pu239/240	ND	0.97	pCi/g
Beryllium	0.96	ND	ug/g

1035	03/27/88	
	21.0-22.5	UNITS
U234	5.2	pCi/g
U238	18.1	pCi/g
Ra226	0.8	pCi/g

3037	02/23/92	
	22.5-24.0	UNITS
U238	0.9	pCi/g
Th228	1.2	pCi/g
Th230	1.3	pCi/g

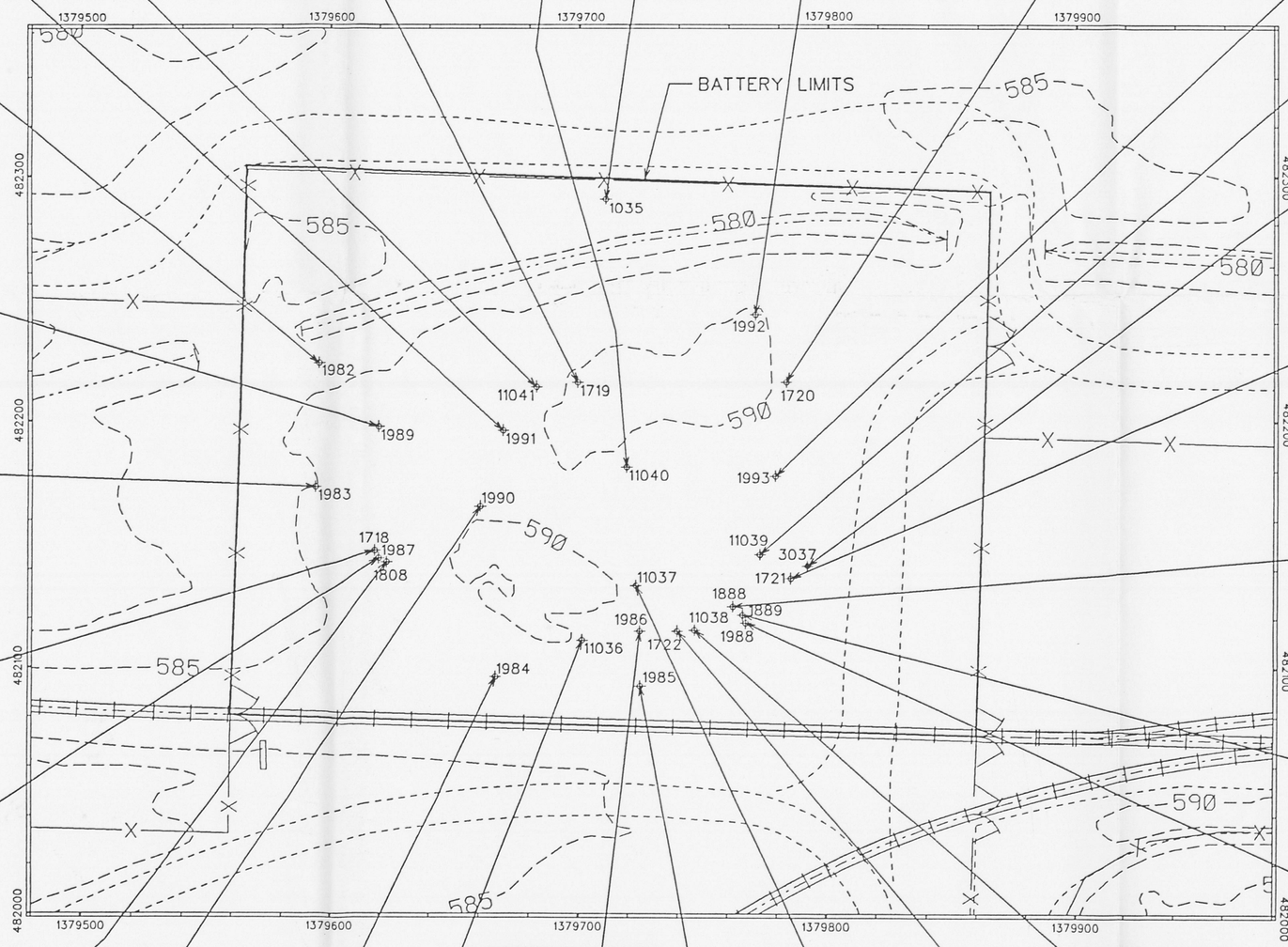

1989	05/14/93		
	2.5-5.0	12.5-15.0	UNITS
U234	5.66	0.91	pCi/g
U238	10.6	ND	pCi/g
U235/236	0.37	ND	pCi/g
U-Total	33.5	5.15	ug/g
Ra226	0.97	1.03	pCi/g
Ra228	1.22	1.07	pCi/g

1721	07/28/91					
	3.0-4.5	7.5-9.0	9.0-10.5	13.5-15.0	15.0-16.5	UNITS
U234	1.39	1.64	ND	ND	1.76	pCi/g
U238	2.33	3.0	ND	ND	3.61	pCi/g
U235/236	ND	ND	ND	ND	0.126	pCi/g
U-Total	6.7	8.9	ND	ND	11.2	ug/g
SR90	0.80	8.9	ND	ND	0.730	pCi/g
Th228	1.57	1.02	ND	ND	1.4	pCi/g
Th230	1.37	ND	ND	ND	1.74	pCi/g
Th232	ND	0.94	ND	ND	0.931	pCi/g
Th-Total	ND	8.51	ND	ND	8.4	ug/g
Ra226	0.89	0.88	ND	ND	0.98	pCi/g
Ra228	ND	1.04	ND	ND	ND	pCi/g
Ra224	ND	1.24	ND	ND	ND	mg/kg
Arsenic	ND	ND	0.92	0.93	ND	mg/kg
Beryllium	ND	ND	20.2	21.9	ND	mg/kg

1983	05/03/93			
	1.5-2.5	2.5-5.0	17.5-20.0	UNITS
U234	32	3.7	ND	pCi/g
U238	30.3	10.9	ND	pCi/g
U235/236	1.66	0.22	ND	pCi/g
U-Total	94.3	36.8	3.18	ug/g
Th228	2.69	1.11	ND	pCi/g
Th230	3.47	4.26	ND	pCi/g
Th232	2.07	0.87	ND	pCi/g
Th-Total	18.8	7.93	5.47	ug/g
Ra226	1.35	1.17	0.94	pCi/g
Ra228	2.39	1.02	ND	pCi/g
Cs137	0.16	ND	ND	pCi/g
Np237	0.237	0.185	0.280	pCi/g
Pu238	0.433	0.033	0.040	pCi/g
Pu239/240	0.068	ND	0.080	pCi/g
Beryllium	1.7	1.8	ND	mg/g

1888	02/23/92			
	0.0-1.5	5.0-6.0	6.0-7.5	UNITS
Pb210	ND	ND	1.030	pCi/g
U234	ND	ND	4.1	pCi/g
U235	ND	ND	0.27	pCi/g
U238	ND	ND	5.3	ug/g
U-Total	ND	ND	19	pCi/g
SR90	ND	ND	1.01	pCi/g
Th228	ND	ND	1.37	pCi/g
Th230	ND	ND	2.3	ug/g
Th232	ND	ND	1.58	pCi/g
Th-Total	ND	ND	14.3	pCi/g
Ra224	ND	ND	2.14	pCi/g
Ra226	ND	ND	1.12	pCi/g
Ra228	ND	ND	1.57	pCi/g
Arsenic	9.9	12.5	ND	mg/kg
Beryllium	1.6	1.6	ND	mg/kg

1718	07/31/91			
	1.5-3.0	9.0-10.5	15.0-16.5	UNITS
U234	23.3	8.7	0.89	pCi/g
U238	22.1	40.8	1.11	pCi/g
U235/236	1.65	1.13	ND	pCi/g
U-Total	67.2	124	3.05	ug/g
Th228	3.39	2.29	0.96	pCi/g
Th230	2.3	1.74	ND	pCi/g
Th232	2.22	1.25	ND	pCi/g
Th-Total	20	11.3	3.96	ug/g
Ra226	1.41	1.15	1.03	pCi/g
Ra228	3.15	1.13	ND	pCi/g

1889	02/25/92			
	2.5-5.0	12.5-15.0	15.0-17.5	UNITS
Pu238	0.06	ND	ND	pCi/g
SR90	ND	0.710	ND	pCi/g
Beryllium	ND	ND	5.32	mg/kg

LEGEND

575 ELEVATION CONTOURS
ROADS
BATTERY LIMITS
FENCE
RAILROAD
SOIL BORING
3000 MONITORING WELL

ND - NOT DETECTED ABOVE BACKGROUND CONCENTRATIONS

NOTE: RADIONUCLIDES WERE NOT DETECTED OUTSIDE OF THE LANDFILL

NOTE:
Coordinates are in State Planar NAD 1927.
Surface contours based on 1992 flyover.

1987	05/13/93		
	5.0-7.5	12.0-15.0	UNITS
U234	3.56	ND	pCi/g
U238	9.35	ND	pCi/g
U235/236	0.301	ND	pCi/g
U-Total	28.8	3.94	ug/g
Th228	0.978	ND	pCi/g
Th230	1.69	ND	pCi/g
Th232	1.07	ND	pCi/g
Th-Total	9.75	ND	ug/g
Pu238	0.019	ND	pCi/g
Np237	0.116	ND	pCi/g
Ra226	1.21	0.885	pCi/g
Ra228	1.37	ND	pCi/g
Beryllium	1.3	0.36	pCi/g

1988	05/12/93		
	2.5-5.0	17.5-20.0	UNITS
U234	24.6	0.991	pCi/g
U238	37.8	0.961	pCi/g
U235/236	1.43	0.077	pCi/g
U-Total	109	3.62	ug/g
Th228	1.92	ND	pCi/g
Th230	2.33	ND	pCi/g
Th232	1.96	0.832	pCi/g
Th-Total	17.8	7.58	ug/g
Ra226	1.15	0.98	pCi/g
Ra228	2.56	1	pCi/g
Beryllium	1.5	1.1	mg/kg
Cs137	0.091	ND	pCi/g
Pu239/240	ND	0.015	pCi/g
Pu238	ND	0.015	pCi/g

1986	04/30/93		
	12.5-15.0	2.5-5.0	UNITS
U-Total	11.4	ND	pCi/g
Th232	0.81	ND	pCi/g
Ra226	0.84	ND	pCi/g
Ra228	0.92	ND	pCi/g
Beryllium	1.4	1.6	ug/g

11038	05/16/93	
	12.5-15.0	UNITS
U-Total	5.32	ug/g
Ra226	0.94	pCi/g
Ra228	0.88	pCi/g
Pu238	0.021	pCi/g

1808	08/27/91					
	1.5-3.0	3.0-4.5	7.5-9.0	10.5-12.0	13.5-15.0	15.0-16.5	UNITS
U234	17.6	ND	ND	6.26	0.924	ND	pCi/g
U238	17.3	ND	ND	21	1.08	ND	pCi/g
U235/236	1.17	ND	ND	0.606	ND	ND	pCi/g
U-Total	ND	ND	ND	66.8	3.21	ND	ug/g
Th228	4.01	ND	ND	1.17	1.17	ND	pCi/g
Th230	2.76	ND	ND	2.42	1.92	ND	pCi/g
Th232	3.59	ND	ND	1.12	ND	ND	pCi/g
Th-Total	32.4	ND	ND	10.1	ND	ND	pCi/g
Ra226	ND	ND	ND	1.05	ND	ND	pCi/g
Ra228	ND	ND	ND	1.16	ND	ND	pCi/g
Beryllium	ND	0.71	0.88	ND	ND	0.75	mg/g

1990	05/10/93		
	6.0-9.0	17.5-20.0	UNITS
U234	71.2	ND	pCi/g
U238	170	ND	pCi/g
U235/236	8.04	ND	pCi/g
U-Total	446	3.06	ug/g
Th228	1.4	ND	pCi/g
Th230	3.42	ND	pCi/g
Th232	1.37	ND	pCi/g
Th-Total	12.6	ND	ug/g
Ra226	0.879	0.883	pCi/g
Ra228	1.35	ND	pCi/g
Beryllium	ND	1.0	ug/g
Np237	0.14	0.116	pCi/g
Pu239/240	0.055	0.666	pCi/g
Pu238	0.232	0.043	pCi/g

1984	04/26/93		
	2.5-5.0	12.5-15.0	UNITS
U234	1.639	1.11	pCi/g
U238	1.73	1.24	pCi/g
U235/236	0.093	ND	pCi/g
U-Total	13.3	12.7	ug/g
Th228	0.93	0.92	pCi/g
Th230	1.51	1.3	pCi/g
Ra226	1.11	0.79	pCi/g
Ra228	1.06	0.99	pCi/g
Beryllium	1.3	1.4	ug/g
Np237	0.050	ND	pCi/g
Pu239/240	0.110	ND	pCi/g
Pu238	0.027	0.040	pCi/g

11036	05/17/93		
	17.0-19.0	2.5-5.0	UNITS
U234	1	553	pCi/g
U238	1.08	577	pCi/g
U235/236	0.75	28.9	pCi/g
U-Total	3.1	1770	ug/g
Th228	0.94	9.36	pCi/g
Th230	1.44	720	pCi/g
Th232	ND	8.22	pCi/g
Th-Total	ND	75.6	ug/g
Ra226	1.05	113	pCi/g
Ra228	0.86	6.65	pCi/g
Cs137	ND	0.522	pCi/g
SR90	ND	1.99	pCi/g
Pu239/240	ND	0.022	pCi/g
Pu238	ND	0.337	pCi/g
Np237	ND	1.67	pCi/g

1985	04/26/93		
	2.0-4.0	15.0-17.0	UNITS
U234	11.57	1.21	pCi/g
U238	19.77	1.52	pCi/g
U235/236	0.68	ND	pCi/g
U-Total	62.3	5.91	ug/g
Th230	15.36	3.06	pCi/g
Th232	ND	0.93	pCi/g
Th-Total	ND	8.52	ug/g
Ra226	1.87	1.23	pCi/g
Ra228	1.19	0.98	pCi/g
Beryllium	1.3	1.3	ug/g
Pu239/240	0.049	ND	pCi/g
Pu238	ND	0.032	pCi/g
SR90	ND	0.67	pCi/g
Np237	ND	0.099	pCi/g

11037	05/15/93		
	5.0-7.5	17.5-20.0	UNITS
U234	0.95	1.47	pCi/g
U238	1.19	1.56	pCi/g
U235/236	ND	0.09	pCi/g
U-Total	5.01	5.5	ug/g
Th228	0.92J	ND	pCi/g
Th230	1.5J	ND	pCi/g
Th232	1J	ND	pCi/g
Th-Total	9.12J	ND	ug/g
Ra226	1.18	0.9	pCi/g
Ra228	1.16	7.19	pCi/g
Beryllium	0.73	ND	ug/g

1722	07/30/91				
	3.0-4.5	11.0-12.5	12.5-14.0	12.5-14.0	UNITS
U234	334	4.51	30.6	ND	pCi/g
U235	ND	ND	1.89	ND	pCi/g
U238	420	6.53	47.7	ND	pCi/g
U235/236	22.4	ND	2.47	ND	pCi/g
U-Total	940	17.5	146	ND	pCi/g
SR90	ND	1.420	ND	ND	ug/g
Th228	1.61	1.09	0.96	ND	pCi/g
Th230	12.3	2.4	3.81	ND	pCi/g
Th232	ND	1.2	0.85	ND	pCi/g
Th-Total	8.99	10.8	ND	ND	ug/g
Ra226	1.5	1.01	0.87	ND	pCi/g
Ra228	1.03	1.32	0.98	ND	pCi/g
Ra224	ND	1.49	1.11	ND	pCi/g
Beryllium	ND	ND	ND	0.63	mg/kg

N

SCALE (FT)
0 20 40 60

000007

FIGURE 4-3
RADIONUCLIDES, AND METALS OF CONCERN IN SUBSURFACE SOILS DETECTED ABOVE BACKGROUND IN THE SOLID WASTE LANDFILL

fig0404.dgn

W0707-6

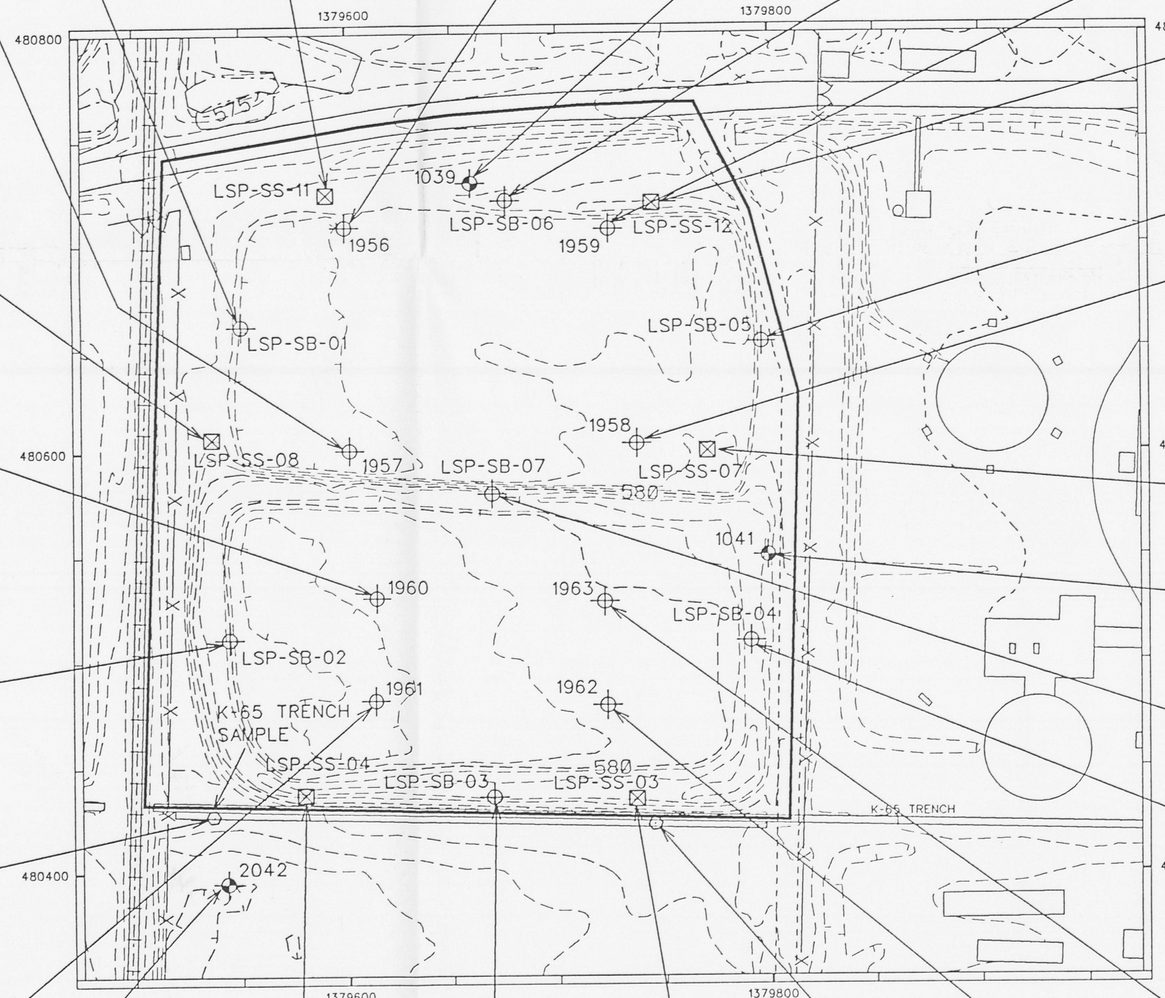

1957	06/07/93)		
	0.5-2.0	4.0-5.0	UNITS
U234	2.44	1.15	pCi/g
U238	2.84	1.14	pCi/g
U235/236	0.130	ND	pCi/g
U-Total	9.73	11.1	ug/g
Th228	ND	1.27	pCi/g
Th230	1.37	1.51	pCi/g
Th232	ND	1.12	pCi/g
Th-Total	ND	12.3	ug/g
Ra226	0.880	1.37	pCi/g
Ra228	ND	1.44	pCi/g
Arsenic	ND	14.6	mg/kg
Beryllium	ND	0.85	mg/kg
Pu238	0.06	0.065	pCi/g
Pu239/240	0.035	0.035	pCi/g
Np237	0.130	0.077	pCi/g
Cs137	0.06	ND	pCi/g

LSP-SB-01	(05/05/93)	
	0.5-1.0	UNITS
U234	1.60	pCi/g
U238	1.99	pCi/g
U235/236	0.080	pCi/g
U-Total	6.91	ug/g
Ra226	1.05	pCi/g
Pu238	0.03	pCi/g
Np237	0.110	pCi/g
Pu239/240	0.03	pCi/g

LSP-SS-11	(05/04/93)	
	0.5-1.0	UNITS
U234	3.66	pCi/g
U238	4.05	pCi/g
U235/236	0.204	pCi/g
U-Total	11.2	ug/g
Th228	0.898	pCi/g
Th230	1.15	pCi/g
Th232	ND	pCi/g
Th-Total	7.75	ug/g
Ra226	1.14	pCi/g
Ra228	1.08	pCi/g
Beryllium	1.6	mg/kg
Pu238	0.079	pCi/g
Pu239/240	0.020	pCi/g
Np237	0.128	pCi/g

1956	(06/08/93)		
	0.0-4.0	6.0-7.0	UNITS
U234	3.37	0.890	pCi/g
U238	3.17	0.970	pCi/g
U235/236	0.140	ND	pCi/g
U-Total	16.8	13.7	ug/g
Th230	ND	1.24	pCi/g
Th232	ND	1.00	pCi/g
Th-Total	ND	9.08	ug/g
Ra226	ND	1.25	pCi/g
Ra228	ND	0.900	pCi/g
Tc99	0.890	ND	pCi/g
Arsenic	11.2	ND	mg/kg
Beryllium	0.72	0.79	mg/kg
Cs137	0.088	ND	pCi/g
Pu239/240	0.046	0.040	pCi/g
Pu238	0.536	0.107	pCi/g
Np237	0.086	ND	pCi/g

1039	(04/08/88)	
	12.0-13.5	UNITS
Th230	1.5	pCi/g
Th232	0.9	pCi/g
Ra226	0.9	pCi/g

LSP-SB-06	(05/10/93)	
	0.5-1.0	UNITS
U234	2.67	pCi/g
U238	2.75	pCi/g
U235/236	0.143	pCi/g
U-Total	18.5	ug/g
Th230	1.53	pCi/g
Ra226	0.970	pCi/g
Ra228	1.16	pCi/g
Beryllium	0.96	mg/kg
Np237	0.354	pCi/g

1959	(06/05/93)			
	3.0-5.0	8.0-8.5	11.0-13.5	UNITS
U234	2.55	1.08	1.14	pCi/g
U238	2.47	1.15	1.15	pCi/g
U235/236	0.199	0.117	ND	pCi/g
U-Total	15.0	12.3	11.3	ug/g
Th228	ND	1.02	ND	pCi/g
Th230	ND	1.28	ND	pCi/g
Th232	ND	1.26	ND	pCi/g
Th-Total	ND	11.5	ND	ug/g
Ra226	ND	1.17	1.22	pCi/g
Ra228	ND	1.06	1.05	pCi/g
Beryllium	ND	ND	1.5	mg/kg
Np237	ND	0.071	0.054	pCi/g
Pu239/240	0.133	0.016	0.020	pCi/g
Pu238	0.133	0.034	0.016	pCi/g

LSP-SS-12	(05/04/93)	
	0.5-1.0	UNITS
U234	3.58	pCi/g
U238	4.10	pCi/g
U235/236	0.197	pCi/g
U-Total	13.7	ug/g
Th230	2.02	pCi/g
Th-Total	7.46	ug/g
Ra226	1.15	pCi/g
Ra228	0.983	pCi/g
Beryllium	1.8	mg/kg
Cs137	0.130	pCi/g
Np237	0.045	pCi/g

LSP-SB-05	(05/10/93)	
	0.5-1.0	UNITS
U234	3.46	pCi/g
U238	3.78	pCi/g
U235/236	0.181	pCi/g
U-Total	19.1	ug/g
Th228	0.911	pCi/g
Th230	5.02	pCi/g
Th232	0.947	pCi/g
Th-Total	8.71	ug/g
Ra226	0.953	pCi/g
Ra228	1.08	pCi/g
Beryllium	0.79	mg/kg
Np237	0.289	pCi/g

LSP-SS-08	(05/03/93)	
	0.5-1.0	UNITS
U234	3.75	pCi/g
U238	4.68	pCi/g
U235/236	0.290	pCi/g
U-Total	22.7	ug/g
Th228	0.960	pCi/g
Th230	2.90	pCi/g
Th232	0.940	pCi/g
Th-Total	8.55	ug/g
Ra226	1.12	pCi/g
Ra228	1.33	pCi/g
Beryllium	2.2	mg/kg
Np237	0.040	pCi/g
Pu238	0.040	pCi/g
Pu239/240	0.011	pCi/g

1958	(06/06/93)		
	0.5-2.5	4.5-5.0	UNITS
U234	1.91	1.29	pCi/g
U238	1.84	1.37	pCi/g
U235/236	0.144	0.079	pCi/g
U-Total	14.0	13.1	ug/g
Th228	ND	1.07	pCi/g
Th230	ND	1.35	pCi/g
Th232	ND	1.21	pCi/g
Th-Total	ND	11.0	ug/g
Ra226	ND	1.26	pCi/g
Ra228	ND	1.18	pCi/g
Arsenic	ND	13.8	mg/kg

1960	(05/27/93)	(05/28/93)	
	5.0-6.0	13.0-13.5	UNITS
U234	1.47	ND	pCi/g
U238	1.59	ND	pCi/g
U-Total	3.72	12.3	ug/g
Th230	1.88	4.51	pCi/g
Ra226	ND	0.880	pCi/g
Pu238	0.104	0.020	pCi/g
Pu239/240	0.044	ND	pCi/g
Np237	ND	0.050	pCi/g

LSP-SS-07	(05/02/93)	
	0.5-1.0	UNITS
U234	4.50	pCi/g
U238	5.61	pCi/g
U235/236	0.209	pCi/g
U-Total	17.6	ug/g
Th228	1.09	pCi/g
Th230	32.2	pCi/g
Th232	1.34	pCi/g
Th-Total	12.2	ug/g
Ra226	2.36	pCi/g
Ra228	1.37	pCi/g
Beryllium	1.5	mg/kg
Cs137	0.130	pCi/g
Np237	0.190	pCi/g
SR90	0.860	pCi/g
Pu239/240	0.043	pCi/g
Pu238	0.067	pCi/g

1041	(04/10/88)	
	0.0-1.5	UNITS
U234	3.8	pCi/g
U238	5.9	pCi/g
Th228	1.3	pCi/g
Th230	3.8	pCi/g
Th232	1.5	pCi/g
Ra226	1.1	pCi/g
Ra228	0.9	pCi/g

LSP-SB-02	(05/05/93	
	0.5-1.0	UNITS
U234	3.71	pCi/g
U238	3.93	pCi/g
U235/236	0.203	pCi/g
U-Total	15.1	ug/g
Ra226	1.33	pCi/g
Ra228	1.24	pCi/g
Beryllium	1.8	mg/kg
Np237	0.111	pCi/g
Pu239/240	0.042	pCi/g
SR90	0.959	pCi/g
Pu238	0.042	pCi/g

LSP-SB-07	(05/06/93)	
	0.5-1.0	UNITS
U234	4.49	pCi/g
U238	5.09	pCi/g
U235/236	0.220	pCi/g
U-Total	26.4	ug/g
Th228	1.27	pCi/g
Th230	5.19	pCi/g
Th232	1.07	pCi/g
Th-Total	9.84	ug/g
Ra226	1.26	pCi/g
Ra228	1.32	pCi/g
Cs137	0.116	pCi/g
Pu239/240	0.089	pCi/g
Pu238	0.098	pCi/g
Np237	0.541	pCi/g

LSP-SB-04	(05/06/93)	
	0.5-1.0	UNITS
U234	5.45	pCi/g
U238	6.47	pCi/g
U235/236	0.260	pCi/g
U-Total	25.2	ug/g
Th228	1.15	pCi/g
Th230	4.74	pCi/g
Th-Total	8.10	ug/g
Ra226	1.14	pCi/g
Ra228	1.43	pCi/g
Beryllium	0.88	mg/kg
Cs137	0.100	pCi/g
Np237	0.48	pCi/g
Pu239/240	0.090	pCi/g
Pu238	0.110	pCi/g

114767	(05/01/93)	
	0.0-6.0	UNITS
U234	3.64	pCi/g
U238	3.91	pCi/g
U235/236	0.277	pCi/g
U-Total	11.5	ug/g
Th228	1.30	pCi/g
Th230	5.34	pCi/g
Th232	0.912	pCi/g
Th-Total	8.31	ug/g
Ra226	5.93	pCi/g
Ra228	1.02	pCi/g
Beryllium	1.0	mg/kg
Cs137	0.113	pCi/g
Pu239/240	0.056	pCi/g
Pu238	0.344	pCi/g
Np237	0.103	pCi/g

1961	(06/01/93)		
	2.0-4.0	12.0-13.0	UNITS
U234	1.85	1.05	pCi/g
U238	1.86	1.17	pCi/g
U235/236	0.960	0.080	pCi/g
U-Total	13.5	14.3	ug/g
Th230	2.70	ND	pCi/g
Th232	ND	0.860	pCi/g
Th-Total	ND	7.84	ug/g
Ra226	ND	1.03	pCi/g
Ra228	ND	0.960	pCi/g

2042	(04/11/88)	(04/12/88)	
	3.0-4.5	45.0-46.0	UNITS
U238	0.9	ND	pCi/g
Th228	1.0	ND	pCi/g
Th230	2.3	1.3	pCi/g
Th232	1.3	ND	pCi/g
Ra226	1.0	ND	pCi/g
Ra228	1.2	ND	pCi/g
SR90	6.0	ND	pCi/g

LSP-SS-04	(05/02/93)	
	0.5-1.0	UNITS
U234	3.83	pCi/g
U238	4.52	pCi/g
U235/236	0.220	pCi/g
U-Total	20.7	ug/g
Th228	0.960	pCi/g
Th230	1.80	pCi/g
Th232	0.940	pCi/g
Th-Total	8.54	ug/g
Ra226	1.06	pCi/g
Ra228	1.12	pCi/g
Beryllium	1.6	mg/kg
Pu239/240	0.051	pCi/g
Pu238	0.082	pCi/g
Np237	0.03	pCi/g

LSP-SB-03	(05/05/93)	
	0.5-1.0	UNITS
U234	4.28	pCi/g
U238	8.75	pCi/g
U235/236	0.204	pCi/g
U-Total	23.5	ug/g
Th228	1.06	pCi/g
Th230	1.94	pCi/g
Th232	1.05	pCi/g
Th-Total	7.57	ug/g
Ra226	1.06	pCi/g
Ra228	1.21	pCi/g
Beryllium	1.8	mg/kg
Cs137	0.094	pCi/g
SR90	0.841	pCi/g
Pu239/240	0.013	pCi/g
Np237	0.044	pCi/g

LSP-SS-03	05/01/93)	
	0.5-1.0	UNITS
U234	4.40	pCi/g
U238	4.69	pCi/g
U235/236	0.200	pCi/g
U-Total	24.0	ug/g
Th228	1.07	pCi/g
Th230	2.00	pCi/g
Th232	1.03	pCi/g
Th-Total	9.4	ug/g
Ra226	1.08	pCi/g
Ra228	1.33	pCi/g
Beryllium	1.4	mg/kg
Np237	0.080	pCi/g
Pu239/240	0.039	pCi/g
Pu238	0.06	pCi/g

114776	(06/07/93)	
	0.5-1.0	UNITS
U234	5.33	pCi/g
U238	5.5	pCi/g
U235/236	0.26	pCi/g
U-Total	24.8	ug/g
Th230	20.3	pCi/g
Th232	1.43	pCi/g
Th-Total	13.0	ug/g
Ra226	2.32	pCi/g
Ra228	1.72	pCi/g
Cs137	0.092	pCi/g
Np237	0.305	pCi/g
Pu238	0.036	pCi/g
Pu239/240	0.046	pCi/g

1962	(05/20/93)	(05/25/93)	
	4.5-7.0	12.5-14.0	UNITS
U234	3.31	ND	pCi/g
U238	3.33	ND	pCi/g
U235/236	0.233	ND	pCi/g
U-Total	6.76	2.17	ug/g
Th230	3.06	2.47	pCi/g
Ra226	ND	0.842	pCi/g
Cs137	0.029	ND	pCi/g
Pu238	0.144	0.043	pCi/g

1963	(06/03/93)	(06/03/93)	(06/11/93)	
	2.0-4.0	13.5-15.5	17.0-18.0	UNITS
U234	0.900	5.33	1.01	pCi/g
U238	0.870	5.50	1.02	pCi/g
U235/236	0.080	0.260	ND	pCi/g
U-Total	10.6	24.8	4.01	ug/g
Th228	ND	1.75	0.919	pCi/g
Th230	ND	20.3	1.34	pCi/g
Th232	ND	1.43	0.939	pCi/g
Th-Total	ND	13.0	8.56	ug/g
Ra226	ND	2.32	1.04	pCi/g
Ra228	ND	1.72	0.890	pCi/g
Beryllium	ND	ND	0.68	mg/kg
Np237	ND	0.05	0.129	pCi/g

LEGEND

- ELEVATION CONTOURS
- ROADS
- DRAINAGE
- FENCE
- RAILROAD
- 1000 MONITORING WELLS
- 2000 MONITORING WELLS
- SOIL BORING
- SURFACE SAMPLE
- TRENCH SAMPLE

ND - NOT DETECTED ABOVE BACKGROUND CONCENTRATIONS

NOTE:
Coordinates are in State Planar NAD 1927.
Surface contours based on 1992 flyover.

SCALE (FT)
0 50 100

000008

FIGURE 4-9
RADIONUCLIDES, AND METALS OF CONCERN IN SUBSURFACE SAMPLES DETECTED ABOVE BACKGROUND IN THE LIME SLUDGE PONDS

fig0484.dgn

11070_1

1711				(05/29/91)		
	1.5-3 ft	4.5-6 ft	7.5-9 ft	13.5-15 ft	18.0-19.5 ft	UNITS
U234	42	ND	5.93	4.95	ND	pCi/g
U235	2.42	ND	ND	ND	ND	pCi/g
U238	40.1	ND	5.61	4.54	ND	pCi/g
U235/236	5.34	ND	0.87	ND	ND	pCi/g
U-Total	123	ND	18.2	18	ND	ug/g
Th228	0.79	ND	3.34	1.56	ND	pCi/g
Th230	1.41	ND	6.09	2.14	ND	pCi/g
Th232	0.8	ND	3.1	1.1	ND	pCi/g
Th-Total	ND	ND	28	9.89	ND	ug/g
Ra224	2.94	ND	3.22	1.71	ND	pCi/g
Ra226	2.74	ND	4.11	1.48	ND	pCi/g
Ra228	2.16	ND	2.67	1.27	ND	pCi/g
Arsenic	ND	28	35.4	ND	ND	mg/kg
Beryllium	ND	3	2.5	ND	0.79	mg/kg
Pb210	1.24	ND	1.870	ND	ND	pCi/g

1998				(04/29/93)	
	2-3.5 ft	8-9.5 ft	10-11.5 ft	17-18.5 ft	UNITS
U234	4.23	4.14	8.6	ND	pCi/g
U238	4.46	4.78	9.22	0.85	pCi/g
U235/236	0.19	0.21	0.4	ND	pCi/g
U-Total	14.3	14.9	31.7	4.39	ug/g
Th228	ND	1.17	1.3	ND	pCi/g
Th230	ND	2.8	4.17	ND	pCi/g
Th232	ND	0.979	1.35	ND	pCi/g
Th-Total	ND	8.92	12.3	ND	ug/g
Ra226	3.44	1.46	2.07	0.79	pCi/g
Ra228	2.51	1.18	1.59	ND	pCi/g
Pu238	0.115	ND	0.133	0.066	pCi/g
Pu239/240	0.069	ND	0.100	ND	pCi/g
Np237	0.113	0.165	0.490	0.160	pCi/g
Cs137	ND	0.088	0.105	ND	pCi/g

11006	(04/26/93)	
	22.5-24ft	UNITS
U234	771	pCi/g
U238	803	pCi/g
U235/236	49.1	pCi/g
U-Total	1714	ug/g
Th228	1.03	pCi/g
Th230	1.11	pCi/g
Th232	1.12	pCi/g
Th-Total	10.3	ug/g

11052	(05/25/93)	
	19-21 ft	UNITS
U234	106.5	pCi/g
U238	115.8	pCi/g
U235/236	5.76	pCi/g
U-Total	294	ug/g
Th228	1.41	pCi/g
Th230	8.02	pCi/g
Th232	1.35	pCi/g
Th-Total	12.3	ug/g
Ra226	4.06	pCi/g
Ra228	1.6	pCi/g
Pu239/240	0.038	pCi/g
Np237	0.310	pCi/g

1047	(10/16/87)	
	9-10.5 ft	UNITS
Tc99	1.5	pCi/g
Th230	1.4	pCi/g

2047	(12/20/88)	
	25-26.5 ft	UNITS
SR90	0.70	pCi/g

11051	(05/27/93)		
	21-22 ft	22-24 ft	UNITS
U234	1380	726	pCi/g
U238	1570	763	pCi/g
U235/236	68.8	35.5	pCi/g
U-Total	3580	2280	ug/g
Th228	2.44	1.38	pCi/g
Th230	121	74.9	pCi/g
Th232	2.54	1.77	pCi/g
Th-Total	23.1	16.1	ug/g
Ra226	37.8	42.3	pCi/g
Ra228	3.04	2.29	pCi/g
Beryllium	ND	1.1	mg/kg
Np237	37.3	1.91	pCi/g
SR90	0.86	ND	pCi/g
Pu238	1.85	0.430	pCi/g
Pu239/240	0.380	ND	pCi/g

1710				(06/01/91)		
	3-4.5 ft	4.5-5 ft	9-10.5 ft	22.5-23 ft	27-28.5 ft	UNITS
Np237	ND	ND	ND	ND	0.6	pCi/g
U234	11.4	ND	ND	51.4	187	pCi/g
U235	.057	ND	ND	2.04	12.7	pCi/g
U238	11.8	ND	ND	54.2	191	pCi/g
U235/236	0.88	ND	ND	3.29	18.5	pCi/g
U-Total	38.2	ND	ND	128	660	ug/g
Tc99	ND	ND	ND	ND	0.9	pCi/g
Th228	2.64	ND	ND	4.1	3.03	pCi/g
Th230	3.31	ND	ND	12.8	54.6	pCi/g
Th232	2.47	ND	ND	4	3.28	pCi/g
Th-Total	22.2	ND	ND	36.1	29.6	ug/g
Ra224	3.05	ND	ND	3.11	3.49	pCi/g
Ra226	2.35	ND	ND	6.36	ND	pCi/g
Ra228	2.46	ND	ND	2.88	3.12	pCi/g
Arsenic	ND	31.7	20.7	ND	ND	mg/kg
Beryllium	ND	6.7	2.4	ND	ND	mg/kg
Pb210	1.180	ND	ND	16.80	0.60	pCi/g
SR90	ND	ND	ND	ND	3.120	pCi/g

1997				(05/02/93)		
	0-1.5 ft	10-11.5 ft	28.5-30 ft	34-35.5 ft	38-39 ft	UNITS
U234	23.4	3.91	ND	ND	1.29	pCi/g
U238	23.7	4.19	0.98	0.91	1.44	pCi/g
U235/236	1.28	0.21	0.04	0.04	0.08	pCi/g
U-Total	69.8	10.9	5.62	2.62	5.86	ug/g
Th228	1.16	2.36	0.63	0.74	ND	pCi/g
Th230	1.89	3.05	ND	ND	ND	pCi/g
Th232	1	2.34	0.85	0.87	ND	pCi/g
Th-Total	9.2	21.3	7.76	7.95	3.28	ug/g
Ra226	1.3	2.85	1.26	1.22	0.78	pCi/g
Ra228	1.29	2.22	0.91	0.99	ND	pCi/g
Cs137	0.55	ND	ND	ND	ND	pCi/g
Pu239/240	0.090	0.040	0.060	0.050	0.180	pCi/g
Pu238	0.060	0.270	0.040	0.040	0.040	pCi/g
Np237	0.30	0.160	0.180	0.260	0.040	pCi/g

1709			(06/11/93)	
	4.5-6 ft	15-16.5 ft	28.5-30 ft	UNITS
Np237	ND	0.78	ND	pCi/g
U234	4.4	4.63	3.52	pCi/g
U235	1.1	4.4	ND	pCi/g
U238	11	5.09	3.8	pCi/g
U235/236	0.96	ND	ND	pCi/g
U-Total	67	14.5	14.4	ug/g
Th228	2.08	2.78	2.51	pCi/g
Th230	3.74	4.5	3.07	pCi/g
Th232	2.02	2.65	2.21	pCi/g
Th-Total	18.3	23.9	20	ug/g
Ra224	2.29	2.96	3.05	pCi/g
Ra226	1.96	2.79	2.13	pCi/g
Ra228	1.66	2.2	2.19	pCi/g
Arsenic	16.3	74.8	ND	mg/kg
Beryllium	3.9	4.3	ND	mg/kg
Pb210	ND	1.25	1.170	pCi/g

1996				(04/29/93)	
	2-4 ft	8-9.5 ft	13-13.5 ft	20-21.5 ft	UNITS
U234	14.55	9.48	2.65	ND	pCi/g
U238	14.56	9.9	2.84	0.86	pCi/g
U235/236	0.74	0.73	0.16	0.043	pCi/g
U-Total	48.3	38.5	31.7	3.62	ug/g
Th228	2.09	2.24	2.65	ND	pCi/g
Th230	4.07	8.8	4.7	2.03	pCi/g
Th232	1.9	1.84	2.6	ND	pCi/g
Th-Total	17.3	16.7	23.7	ND	ug/g
Ra226	2.86	2.78	2.54	0.87	pCi/g
Ra228	2.34	2.36	1.96	ND	pCi/g
Np237	0.490	0.480	0.27	ND	pCi/g
Pu239/240	0.130	0.120	0.160	ND	pCi/g
Pu238	0.260	0.200	0.31	ND	pCi/g

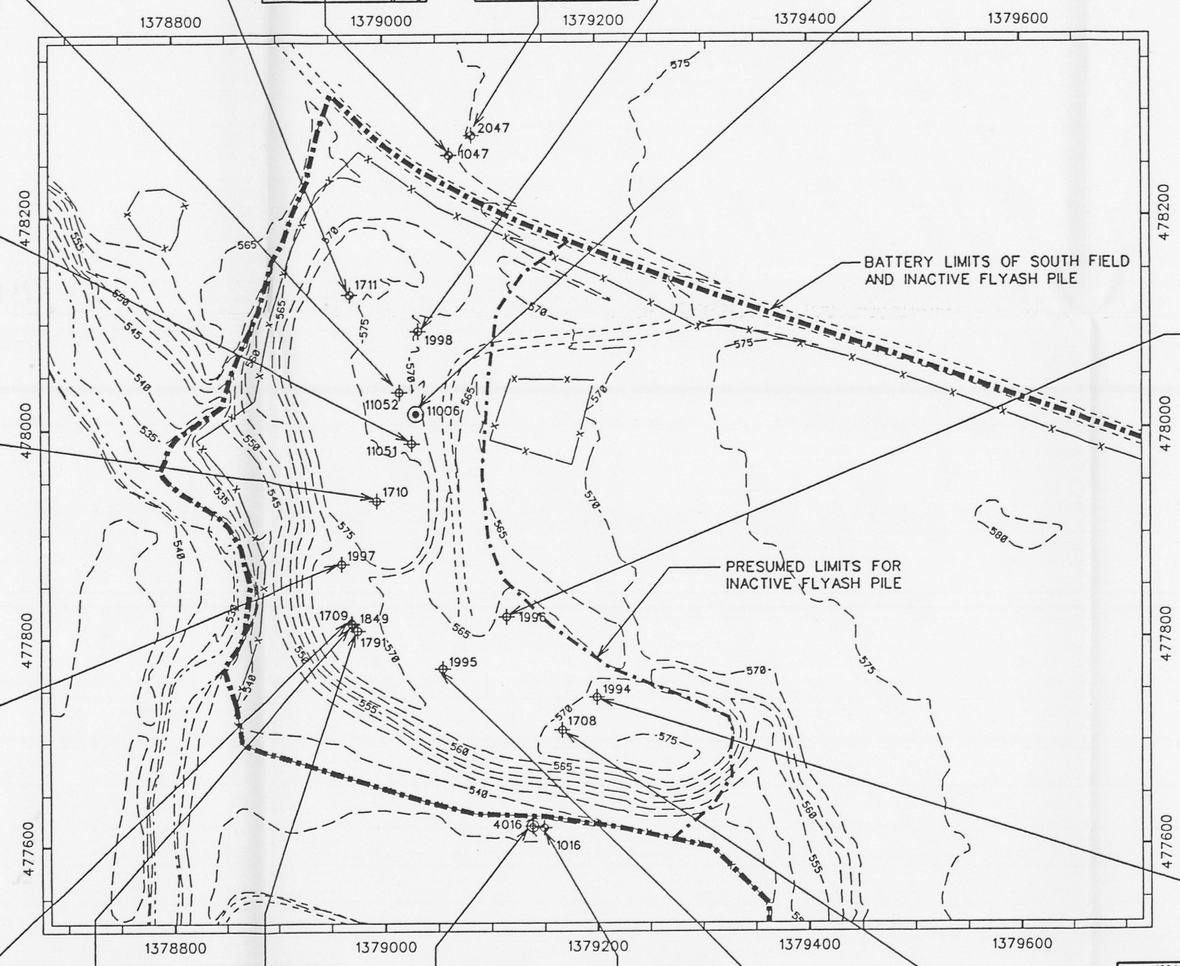

1849	(02/22/92)	
	28.5-30ft	UNITS
U234	1.73	pCi/g
U238	1.76	pCi/g
U-Total	6.93	ug/g
Th228	1.44	pCi/g
Th230	1.69	pCi/g
Th232	0.91	pCi/g
Th-Total	8.21	ug/g
Ra224	1.02	pCi/g
Ra226	0.95	pCi/g
SR90	6.930	pCi/g

1791	(06/25/91)	
	27-28.5ft	UNITS
U-Total	873	ug/g
Th228	1.11	pCi/g
Th230	1.73	pCi/g
Th232	0.95	pCi/g
Th-Total	8.58	ug/g
Ra226	1.39	pCi/g
Ra228	1.03	pCi/g

4016	(12/20/88)	
	95-96.5 ft	UNITS
U234	0.7	pCi/g
U238	0.8	pCi/g
SR90	4.0	pCi/g

1016	(10/15/87)	
	1.5-3 ft	UNITS
U234	10.7	pCi/g
U238	11.4	pCi/g

1995	(05/02/93)			
	2-3.5 ft	8-9 ft	30-31.5 ft	UNITS
U234	61.9	2.63	ND	pCi/g
U238	62.7	2.6	ND	pCi/g
U235/236	2.91	0.13	ND	pCi/g
U-Total	187	8.61	3.41	ug/g
Th228	2.61	2.26	ND	pCi/g
Th230	5.17	4.14	1.62	pCi/g
Th232	2.51	1.94	ND	pCi/g
Th-Total	22.9	17.7	ND	ug/g
Ra226	1.71	3.18	1.01	pCi/g
Ra228	2.72	2.59	0.72	pCi/g
Cs237	0.079	ND	ND	pCi/g
Pu239/240	0.103	ND	0.165	pCi/g
Np237	0.502	ND	0.137	pCi/g
Pu238	ND	ND	0.031	pCi/g

1708	(06/16/93)			
	6-7.5 ft	15-16.5 ft	30-31.5 ft	UNITS
Np237	ND	ND	0.6	pCi/g
U234	3.65	2.88	20.64	pCi/g
U238	3.94	2.97	21.94	pCi/g
U235/236	ND	ND	0.687	pCi/g
U-Total	15.6	11.1	68.2	ug/g
Th228	3.14	2.7	1.59	pCi/g
Th230	2.98	2.73	2.93	pCi/g
Th232	2.42	1.81	1.17	pCi/g
Th-Total	21.8	16.3	10.6	ug/g
Ra226	3.07	2.66	1.72	pCi/g
Ra228	3.13	2.46	1.09	pCi/g
Beryllium	1.8	2	ND	mg/kg
SR90	1.230	1.25	ND	pCi/g
Cs137	ND	ND	0.20	pCi/g
Ru106	ND	ND	0.60	pCi/g
Pu238	ND	ND	0.60	pCi/g

1994	(05/13/93)				
	2-3.5 ft	14-15.5 ft	26-27.5 ft	36-37.5 ft	UNITS
U234	3.95	1.33	17.9	ND	pCi/g
U238	3.86	1.54	20.7	ND	pCi/g
U235/236	0.162	ND	1.05	ND	pCi/g
U-Total	12.8	13.3	50.7	3.44	ug/g
Th228	3.08	2.62	1.32	ND	pCi/g
Th230	2.95	2.91	5.19	ND	pCi/g
Th232	2.65	2.54	1.14	ND	pCi/g
Th-Total	24.1	23.1	10.4	ND	ug/g
Ra226	2.96	ND	3.15	ND	pCi/g
Ra228	2.97	ND	1.8	ND	pCi/g
Np237	ND	ND	0.228	ND	pCi/g
Pu238	ND	ND	0.082	0.122	pCi/g
Pu239/240	ND	ND	ND	0.035	pCi/g

LEGEND

- ELEVATION CONTOURS
- ROADS
- STREAM
- DRAINAGE
- FENCE
- 1000 MONITORING WELLS
- 2000 MONITORING WELLS
- 3000 MONITORING WELLS
- 4000 MONITORING WELLS
- SOIL BORING
- HYDROPUNCH

ND- NOT DETECTED ABOVE BACKGROUND CONCENTRATIONS

NOTE:
Coordinates are in State Planar NAD 1927.
Surface contours based on 1992 flyover.

SCALE (FT)
0 50 100 200

000009

FIGURE 4-14
RADIONUCLIDES, AND METALS OF CONCERN IN SUBSURFACE SOILS DETECTED ABOVE BACKGROUND IN THE INACTIVE FLYASH PILE

fig0416.dgn

110707_8

1711	05/29/91			
	4.5-6.0	9.0-10.5	18.0-19.5	UNITS
1,1,1-Trichloroethane	51	35	ND	ug/kg
Toluene	ND	3	ND	ug/kg
2-Hexanone	ND	ND	3	ug/kg
Acetone	ND	ND	68	ug/kg
Aroclor-1254	ND	ND	210	ug/kg
Benzoic acid	ND	ND	150	ug/kg
Cargon Disulade	ND	20	ND	ug/kg

1998	04/28/93				
	2.0-3.5	8.0-9.5	10.0-11.5	17.0-18.5	UNITS
1,1,1-Trichloroethane	16	2	ND	ND	ug/kg
Toluene	150	ND	ND	59	ug/kg
bis(2-Ethylhexyl) phthalate	150	87	130	840	ug/kg

11052	05/25/93	
	19.0-21.0	UNITS
Acetone	6	ug/kg
bis(2-Ethylhexyl) phthalate	52	ug/kg

11006	04/26/93	
	22.5-24.0	UNITS
4-Methylphenol	10	ug/kg
Anthracene	3	ug/kg
Aroclor-1254	570	ug/kg
Benzo(a) anthracene	8	ug/kg
Benzo(a) pyrene	7	ug/kg
Benzo(b) fluoranthene	5	ug/kg
Benzo(g,h,i) perylene	4	ug/kg
Benzo(k) fluoranthene	6	ug/kg
Dibenzo(a,h) anthracene	2	ug/kg
Fluoranthene	16	ug/kg
Indeno(1,2,3-cd) pyrene	4	ug/kg
Isophorone	4	ug/kg
Phenanthrene	10	ug/kg
Phenol	2	ug/kg
Pyrene	14	ug/kg
Tributylphosphate	2	ug/kg
bis(2-Ethylhexyl) phthalate	2	ug/kg

11051	05/27/93	
	22.0-24.0	UNITS
4-Methylphenol	54	ug/kg
Aroclor-1254	180	ug/kg
Benzo(a) anthracene	100	ug/kg
Benzo(a) pyrene	88	ug/kg
Benzo(b) fluoranthene	81	ug/kg
Benzo(g,h,i) perylene	57	ug/kg
Benzo(k) fluoranthene	84	ug/kg
Chrysene	110	ug/kg
Di-n-butylphthalate	55	ug/kg
Fluoranthene	260	ug/kg
Indeno(1,2,3-cd) pyrene	46	ug/kg
Phenanthrene	210	ug/kg
Pyrene	220	ug/kg
Tributylphosphate	200	ug/kg
bis(2-Ethylhexyl) phthalate	160	ug/kg

1850	02/23/92		
	6.0-7.5	13.5-15.0	UNITS
2-Methylnaphthalene	89	66	ug/kg
Anthracene	49	ND	ug/kg
Naphthalene	53	ND	ug/kg
Phenanthrene	49	41	ug/kg
Styrene	2	ND	ug/kg
Toluene	38	110	ug/kg
1,1,1-Trichloroethane	37	ND	ug/kg

1997	05/05/93					
	0.0-1.5	10.0-11.5	28.5-30.0	34.0-35.5	38.0-39.0	UNITS
Toluene	14	ND	ND	ND	16	ug/kg
Chlorobenzene	ND	14	ND	ND	ND	ug/kg
Diethyl phthalate	ND	52	ND	ND	ND	ug/kg
2-Butanone	ND	ND	ND	3	ND	ug/kg
Acetone	ND	ND	11	16	ND	ug/kg

1709	06/06/91		
	7.5-9.0	13.5-15.0	UNITS
1,1,1-Trichloroethane	150	50	ug/kg
Acetone	13	10	ug/kg
Vinyl Acetate	ND	2	ug/kg

11057	05/20/93	
	18.0	UNITS
Toluene	1	ug/kg

1995	05/01/93			
	2.0-3.5	8.0-9.0	30.0-31.5	UNITS
1,1,1-Trichloroethane	ND	920	1	ug/kg
Aroclor-1254	120	ND	ND	ug/kg
Benzo(a) anthracene	39	ND	ND	ug/kg
Benzo(k) fluoranthene	43	ND	ND	ug/kg
Chrysene	48	ND	ND	ug/kg
Fluoranthene	99	ND	ND	ug/kg
Phenanthrene	56	ND	ND	ug/kg
Pyrene	96	ND	ND	ug/kg
Toluene	14	1800	ND	ug/kg
alpha-Chlordane	3.3	ND	ND	ug/kg
bis(2-Ethylhexyl) phthalate	2600	1600	58	ug/kg
Methylene chloride	ND	180	ND	ug/kg
Acetone	ND	10	ND	ug/kg
Trichloroethene	ND	2	ND	ug/kg
Diethyl phthalate	ND	ND	180	ug/kg

1994	05/12/93				
	2.0-3.5	14.0-15.5	26.0-27.5	36.0-37.5	UNITS
1,1,-Trichloroethane	18	35	5	ND	ug/kg
Acetone	12	ND	3	12	ug/kg
Anthracene	49	ND	ND	ND	ug/kg
Benzo(a) anthracene	130	ND	ND	ND	ug/kg
Benzo(a) pyrene	98	ND	ND	ND	ug/kg
Benzo(b) fluoranthene	140	ND	ND	ND	ug/kg
Benzo(g,h,i) perylene	59	ND	ND	ND	ug/kg
Benzo(k) fluoranthene	190	ND	ND	ND	ug/kg
Chrysene	150	ND	ND	ND	ug/kg
Fluoranthene	340	ND	ND	ND	ug/kg
Indeno(1,2,3-cd) pyrene	63	ND	ND	ND	ug/kg
Methylene chloride	54	110	ND	53	ug/kg
Phenanthrene	280	ND	ND	ND	ug/kg
Toluene	4	22	97	4	ug/kg
bis(2-Ethylhexyl) phthalate	500	860	990	48	ug/kg
4-Methyl-2-pentanone	3	ND	ND	ND	ug/kg
Chloromethane	52	ND	ND	ND	ug/kg

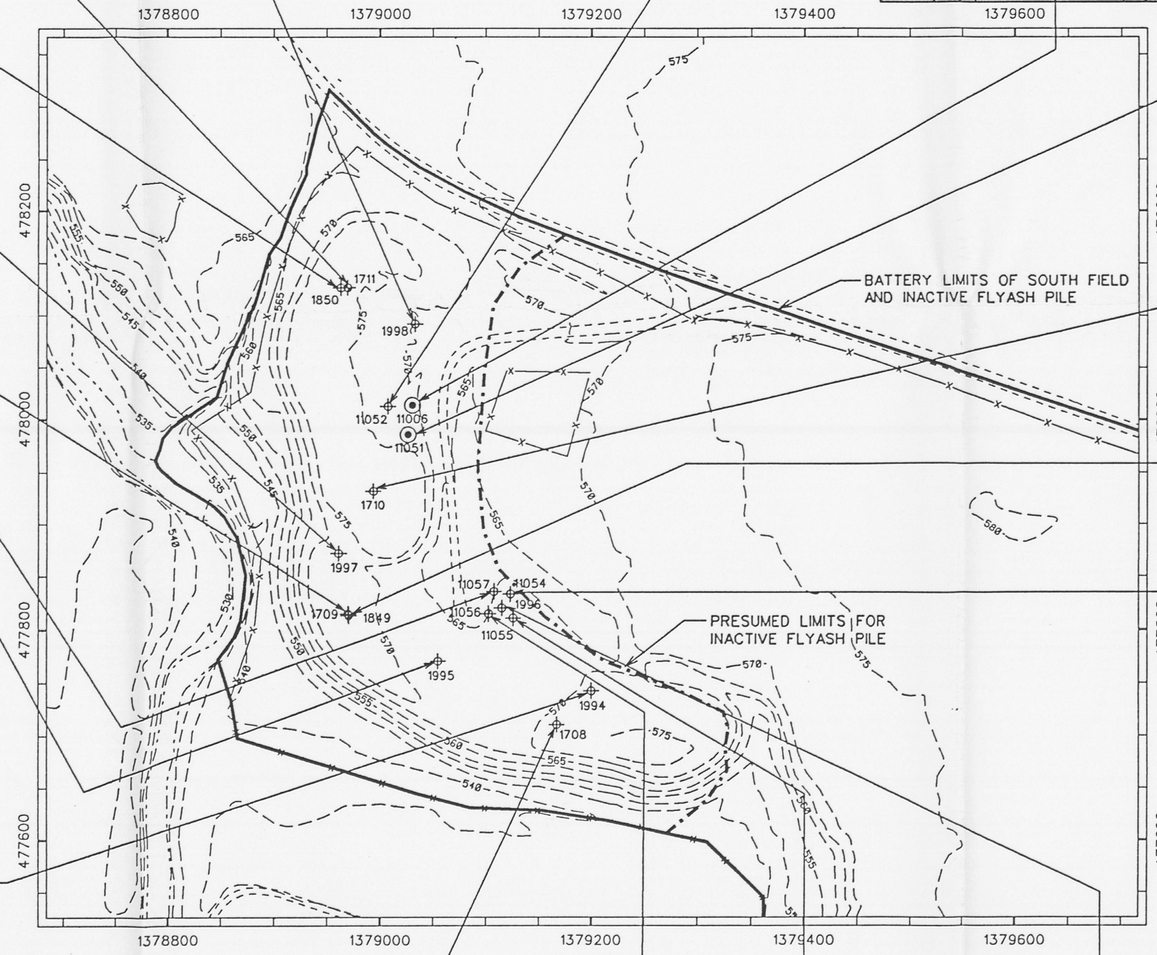

1710	05/31/91		
	4.5-5.0	9.0-10.5	28.5-30.0	UNITS
4-Methyl-2-pentanone	2	ND	1	ug/kg
1,1,1-Trichloroethane	ND	74	ND	ug/kg
Acetone	ND	75	ND	ug/kg
Aroclor-1260	ND	ND	390	ug/kg
bis(2-Ethylhexyl) phthalate	ND	ND	620	ug/kg

1849	02/22/92		
	6.0-7.5	13.5-15.0	UNITS
1,1,1-Trichloroethane	18	170	ug/kg
2-Methylnapthalene	50	79	ug/kg
Toluene	20	13	ug/kg
Di-n-butylphthalate	ND	46	ug/kg
Naphthalene	ND	53	ug/kg

11054	05/21/93		
	16.0-17.0	23.0-24.0	UNITS
Toluene	2	1	ug/kg
bis(2-Ethylhexyl) phthalate	54	46	ug/kg

1996	04/29/93			
	8.0-9.5	14.0-15.0	20.0-21.5	UNITS
2-Methylnaphthalene	74	ND	ND	ug/kg
Di-n-butylphthalate	110	ND	ND	ug/kg
Naphthalene	81	ND	ND	ug/kg
Phenanthrene	60	ND	ND	ug/kg
Toluene	180	1000	78	ug/kg
bis(2-Ethylhexyl) phthalate	260	2800	130	ug/kg
4-Methyl-2-pentanone	ND	ND	6	ug/kg

1708	06/14/91			
	7.5-9.0	16.5-18.0	31.5-33.0	UNITS
Benzo(a) anthracene	110	ND	ND	ug/kg
Benzo(a) pyrene	130	ND	ND	ug/kg
Benzo(b) fluoranthene	360	ND	ND	ug/kg
Benzo(k) fluoranthene	260	ND	ND	ug/kg
Chrysene	150	ND	ND	ug/kg
Fluoranthene	94	ND	ND	ug/kg
Pyrene	120	ND	ND	ug/kg
Toluene	3	ND	ND	ug/kg
1,1,1-Trichloroethane	ND	4	ND	ug/kg
Benzoic acid	ND	97	ND	ug/kg
Acetone	ND	ND	190	ug/kg

11056	05/20/93	
	16.0-18.0	UNITS
1,1,1-Trichloroethane	8	ug/kg
Toluene	23	ug/kg

11055	05/19/93		
	16.0-18.0	23.5-25.0	UNITS
1,1,1-Trichloroethane	8	ND	ug/kg
Acetone	23	11	ug/kg
Di-n-butylphthalate	59	75	ug/kg
Tetrachloroethene	1	ND	ug/kg
bis(2-Ethylhexyl) phthalate	48	36	ug/kg
Toluene	ND	37	ug/kg

LEGEND

- ELEVATION CONTOURS
- ROADS
- STREAM
- DRAINAGE
- FENCE
- 1000 MONITORING WELLS
- SOIL BORING

ND = NOT DETECTED ABOVE BACKGROUND CONCENTRATIONS

NOTE:
Coordinates are in State Planar NAD 1927.
Surface contours based on 1992 flyover.

SCALE (FT)
0 50 100 200

000020

FIGURE 4-15
ORGANICS IN SUBSURFACE SOILS DETECTED ABOVE BACKGROUND IN THE INACTIVE FLYASH PILE

fig0491.dgn

110702_9